



A Report to the U.S. Congress and the Secretary of Energy

**Evaluation of the Department of Energy's
Research Program to Examine
the Performance of Commercial High
Burnup Spent Nuclear Fuel During
Extended Storage and Transportation**

U.S. Nuclear Waste Technical Review Board

July 2021



UNITED STATES
NUCLEAR WASTE TECHNICAL REVIEW BOARD
2300 Clarendon Boulevard, Suite 1300
Arlington, VA 22201-3367

July 2021

The Honorable Nancy Pelosi
Speaker
United States House of Representatives
Washington, DC 20515

The Honorable Patrick J. Leahy
President Pro Tempore
United States Senate
Washington, DC 20510

The Honorable Jennifer Granholm
Secretary
U.S. Department of Energy
Washington, DC 20585

Dear Speaker Pelosi, Senator Leahy, and Secretary Granholm:

Congress created the U.S. Nuclear Waste Technical Review Board in the 1987 Nuclear Waste Policy Amendments Act (NWPAA) (Public Law 100-203) to evaluate the technical and scientific validity of activities undertaken by the Secretary of Energy to manage and dispose of the nation's spent nuclear fuel (SNF) and high-level radioactive waste (HLW). In fulfilling this mandate, the Board has completed an evaluation of Department of Energy (DOE) research related to the storage and transportation of a type of commercial SNF termed high burnup fuel.¹ The Board's conclusions, findings, and recommendations are documented in a report to Congress and the Secretary of Energy titled *Evaluation of the Department of Energy's Research Program to Examine the Performance of Commercial High Burnup Spent Nuclear Fuel during Extended Storage and Transportation*.

DOE is responsible not only for managing and eventually disposing of DOE-managed SNF and HLW, but it is also responsible for taking possession and disposing of commercial SNF that is discharged from commercial nuclear power plants throughout the United States. Although DOE has taken possession of small quantities of commercial SNF, most commercial SNF remains in storage at nuclear power plant sites and, eventually, will have to be transported away from the sites for possible interim storage and for disposal.

¹ Fuel burnup is a measure of the thermal energy generated in a nuclear reactor per unit mass of nuclear fuel initially loaded in the reactor and is typically expressed in units of gigawatt-days per metric ton of uranium (GWd/MTU). In the U.S., nuclear fuel utilized beyond 45 GWd/MTU is defined by the U.S. Nuclear Regulatory Commission as high burnup fuel. Most spent nuclear fuel currently stored in the U.S. is low burnup fuel, while future spent nuclear fuel is expected to be mainly high burnup fuel.

Telephone: 703-235-4473 Fax: 703-235-4495 www.nwtrb.gov

Extensive research has provided confidence that low burnup fuel can be stored for extended periods and transported in accordance with the U.S. Nuclear Regulatory Commission (NRC) requirements. Similar research to improve the understanding of the performance of high burnup fuel has been started but is not yet complete. DOE is conducting several research activities with the aim of obtaining data that can enhance the understanding of the performance of high burnup fuel in extended storage and transportation conditions and during subsequent operations expected to occur at a geologic repository site, which could include repackaging of SNF. The Board commends DOE for undertaking this research to improve the understanding of the characteristics and performance of high burnup fuel. This report provides the Board's assessment of DOE's high burnup fuel research program and makes recommendations that, if implemented, will improve DOE's program and its ability to provide data that will enhance the understanding of high burnup fuel.

Based on the information developed in the report, the Board provides the following recommendations:²

1. *General Recommendations*

- a. *The Board recommends that, following the completion of HDRP sister rod examinations and drop testing of surrogate SNF assemblies, DOE prepare a document that compiles the results of DOE research on extended storage and transportation of HBF, with the purpose of providing the technical bases for conclusions reached regarding HBF performance during extended storage and transportation.*
- b. *The Board recommends that DOE continue to review the results of the Electric Power Research Institute's Extended Storage Collaboration Program and research in other countries to determine if the results of ongoing HBF studies either change the priorities for DOE's planned research or add technical information needs requiring new research.*
- c. *The Board recommends that DOE indicate how its tests and models do or do not apply to the broad range of HBF types and storage and transportation system designs for which information is still needed and take steps to meet those remaining technical information needs.*

2. *Spent Nuclear Fuel Drying*

- a. *The Board recommends that DOE evaluate the extent to which chemisorbed water remains after the drying process is completed and whether this water could affect the ability of SNF cask or canister systems and their contents to continue to meet storage and transportation requirements.*
- b. *The Board recommends that DOE further explore the possibility of monitoring the moisture content and gas composition of dry cask storage systems loaded by nuclear*

² Due to the nature of the issues to be addressed, specialized technical terminology is necessary and is used to properly and fully convey the recommendations. The technical terminology is explained in the main body of the report, the appendices, and the glossary. However, explanations of these technical terms have been omitted from this letter to preserve its brevity and readability.

utilities with HBF for an extended period. DOE should improve and validate gas sampling methods, with a particular focus on water vapor sampling and measurement, before the next samples are obtained.

3. Hydrogen Effects in High Burnup Fuel Cladding

- a. *The Board recommends that, as the need for new testing of HBF cladding is identified, DOE's research efforts make use of irradiated samples rather than unirradiated samples to avoid the large uncertainties and difficulties in interpreting test results that arise from using unirradiated samples.*
- b. *The Board recommends that DOE define a standard set of test parameters (e.g., fuel burnup, test temperatures, rod internal pressures) and results, where possible, that must be recorded for all DOE-funded research related to hydride reorientation. This will allow DOE managers, computer model developers, and nuclear industry practitioners to better use the data to make scientifically meaningful comparisons of experimental results from various research sources, even when the data were not collected for that purpose.*
- c. *The Board recommends that DOE gather into one database all relevant information that is publicly available on hydride-related testing of zirconium-based alloys to provide the basis for (1) evaluating the effects of variables that influence hydride reorientation; (2) supporting the ongoing development of new standards for inducing hydride reorientation in test samples and quantifying hydride reorientation and its effects; (3) explaining the differences in hydride reorientation and its effects among cladding types; and (4) developing computer models to predict hydride formation and reorientation in all zirconium-based cladding types, including those that have not been tested.*

4. High Burnup Fuel Performance under Normal Conditions of Dry Storage

High Burnup Dry Storage Research Project

- a. *The Board recommends that the test plan for the HDRP sister rods should (a) link each proposed test to one or more of the technical information needs identified in the most recent DOE report on technical information needs and (b) explain how the results of each proposed test will be used to meet the technical information needs or support modeling of HBF performance during dry storage.*
- b. *The Board recommends that DOE preserve selected sister rods (or rod segments and components) for future use in follow-up studies to the HDRP, if needed, or in support of other programs.*

Thermal Modeling

- c. *The Board recommends that DOE continue its activities to ensure its thermal models are rigorously validated, including industry-standard uncertainty quantification, for use on SNF storage or transport systems. Important factors to consider during validation are the various designs of cask and canister systems, inclusion of new fuel designs like*

accident tolerant fuel, and inclusion of SNF assemblies with other components, such as control rod assemblies or discrete burnable absorber rods.

5. *High Burnup Fuel Performance under Normal Conditions of Transport*

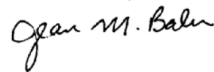
The Board recommends that DOE quantify the uncertainties introduced by the use of unirradiated assembly components and surrogate components, such as concrete mock-SNF assemblies, in experiments being used to benchmark the DOE structural model. The structural model should also be exercised to evaluate HBF cladding strains for different cask and canister types, fuel types, and degree of pellet-cladding bonding.

6. *Fuel Performance Modeling*

The Board recommends that DOE continue to develop fuel performance models (e.g., BISON) that are validated utilizing experimental data. In so doing, DOE-sponsored fuel performance model developers should clearly identify the data they need to develop and validate models to DOE-sponsored experimentalists. Experimentalists should clearly explain the capabilities and limitations of their experimental equipment and facilities to model developers. This close collaboration is needed to ensure optimal experimental setup and collection of data needed to improve the models and achieve a better understanding of HBF characteristics and performance.

The Board trusts that Congress and the Secretary will find the information in this report useful and looks forward to continuing its ongoing technical and scientific review of DOE activities related to nuclear waste management and disposal.

Sincerely,



Jean M. Bahr
Chair

U.S. NUCLEAR WASTE TECHNICAL REVIEW BOARD

Jean M. Bahr, Ph.D., Chair

University of Wisconsin, Madison, Wisconsin

Steven M. Becker, Ph.D.

Old Dominion University, Norfolk, Virginia

Susan L. Brantley, Ph.D.

Pennsylvania State University, University Park, Pennsylvania

Allen G. Croff, Nuclear Engineer, M.B.A.

Vanderbilt University, Nashville, Tennessee

Tissa Illangasekare, Ph.D., P.E.

Colorado School of Mines, Golden, Colorado

Kenneth Lee Peddicord, Ph.D., P.E.

Texas A&M University, College Station, Texas

Paul J. Turinsky, Ph.D., Deputy Chair

North Carolina State University, Raleigh, North Carolina

Note: Dr. Gerald Frankel served as a Board member from September 12, 2012, to August 15, 2016. Dr. Rodney Ewing served as a Board member from July 28, 2011, to January 5, 2017, and as Chair from September 12, 2012, to January 5, 2017. Dr. Linda Nozick served as a Board member from July 28, 2011 to May 9, 2019. Dr. Mary Lou Zoback served as a Board member from September 25, 2012, to May 17, 2021. Dr. Efi Foufoula-Georgiou served as a Board member from September 25, 2012, to May 17, 2021. During their time at the Board, they played roles in developing this report.

U.S. NUCLEAR WASTE TECHNICAL REVIEW BOARD STAFF

EXECUTIVE STAFF

Nigel Mote, Executive Director

Neysa Slater-Chandler, Director of Administration

SENIOR PROFESSIONAL STAFF

Hundal (Andy) Jung, Materials Engineering, Corrosion

Bret Leslie, Geoscience, External Affairs

Chandrika Manepally, Hydrogeology

Daniel Ogg, Nuclear Engineering, Operations

Roberto Pabalan, Geochemistry, Physical Chemistry

PROFESSIONAL STAFF

Yoonjo (Jo Jo) Lee, Nuclear Engineering, Corrosion

ADMINISTRATIVE & SUPPORT STAFF

Davonya Barnes, Information Technology Systems Specialist

Jayson Bright, Systems Administrator

Sonya Townsend, Secretary

Casey Waithe, Financial Manager

Note: The following Senior Professional Staff members contributed to this report but retired before publication: Ms. Karyn Severson retired March 2019 and Dr. Robert Einziger retired June 2019.

CONTENTS

U.S. NUCLEAR WASTE TECHNICAL REVIEW BOARD	v
U.S. NUCLEAR WASTE TECHNICAL REVIEW BOARD STAFF	vi
CONTENTS.....	vii
EXECUTIVE SUMMARY	xix
1. INTRODUCTION.....	1
1.1 Operations Affecting Spent Nuclear Fuel.....	2
1.2 Regulations and Guidance for Spent Nuclear Fuel Storage and Transportation	3
1.3 DOE Research on the Characteristics of High Burnup Fuel	5
1.4 Board Evaluation Activities.....	7
2. BACKGROUND.....	9
2.1 Spent Nuclear Fuel Generation and Management.....	9
2.1.1 Nuclear Power Plant Operation	9
2.1.2 Spent Nuclear Fuel Packaging and Storage	10
2.1.3 Spent Nuclear Fuel Transportation, Possible Interim Storage, and Disposal ...	13
2.2 Characteristics of High Burnup Spent Nuclear Fuel	15
2.2.1 General Description of Spent Nuclear Fuel.....	15
2.2.2 Characteristics of High Burnup Spent Nuclear Fuel Compared to Low Burnup Spent Nuclear Fuel.....	19
2.3 Research on Spent Nuclear Fuel Storage Prior to Current DOE Studies	25
2.4 Technical Information Needs for Spent Nuclear Fuel Storage and Transportation.	26
2.4.1 Technical Information Needs Identified by DOE	27
2.4.2 Board Assessment of DOE Technical Information Needs	27
2.5 Research and Analyses of the Consequences of a Release of Radioactive Material from High Burnup Fuel in a Postulated Accident	29
2.6 Implications of High Burnup Fuel on the Geologic Disposal of Spent Nuclear Fuel	29
2.6.1 Thermal Effects	29
2.6.2 Thermal Management.....	31
3. EVALUATION OF DOE RESEARCH ON HIGH BURNUP FUEL PERFORMANCE DURING EXTENDED STORAGE AND TRANSPORTATION	33
3.1 Spent Nuclear Fuel Drying	33
3.1.1 Nuclear Regulatory Commission Guidance on Spent Nuclear Fuel Drying.....	34
3.1.2 Drying Research.....	35

3.1.3	Evaluation and Findings	37
3.1.4	Recommendations for Spent Nuclear Fuel Drying	39
3.2	Hydrogen Effects in High Burnup Fuel Cladding.....	39
3.2.1	Hydride Reorientation.....	40
3.2.2	Evaluation and Findings	46
3.2.3	Recommendations for Hydrogen Effects in High Burnup Fuel Cladding	48
3.3	High Burnup Fuel Performance under Normal Conditions of Dry Storage.....	49
3.3.1	High Burnup Dry Storage Research Project	49
3.3.2	Modeling Temperature Profiles in Spent Nuclear Fuel and Spent Nuclear Fuel Cask Systems.....	52
3.3.3	Evaluation and Findings	54
3.3.4	Recommendations for High Burnup Fuel Performance under Normal Conditions of Dry Storage	59
3.4	High Burnup Fuel Performance under Normal Conditions of Transport.....	60
3.4.1	Research Program Description.....	60
3.4.2	Modeling Structural Behavior of Spent Nuclear Fuel and Spent Nuclear Fuel Cask Systems.....	65
3.4.3	Evaluation and Findings	65
3.4.4	Recommendations for High Burnup Fuel Performance under Normal Conditions of Transport.....	68
3.5	Fuel Performance Modeling	68
3.5.1	Background and Discussion	68
3.5.2	Evaluation and Findings	70
3.5.3	Recommendations for Fuel Performance Modeling.....	71
4.	CONCLUSIONS, FINDINGS, AND RECOMMENDATIONS	73
4.1	Conclusions	73
4.2	Summary Findings and Recommendations	74
	REFERENCES	79
	GLOSSARY	91
	APPENDICES	A-i
	Appendix A Characteristics of High Burnup Spent Nuclear Fuel	A-1
A.1	General Description of Spent Nuclear Fuel Rods and Assemblies.....	A-1
A.2	Characteristics of High Burnup Fuel Compared to Low Burnup Fuel.....	A-8
A.3	References	A-25
	Appendix B Technical Information Needs for the Management of High Burnup Fuel	B-1
B.1	DOE-Identified Technical Information Needs and Priorities	B-2

B.2	NRC-Identified Technical Information Needs and Priorities	B-6
B.3	EPRI/ESCP-Identified Technical Information Needs and Priorities.....	B-7
B.4	International Technical Information Needs and Priorities	B-8
B.5	Board Evaluation of Technical Information Needs.....	B-11
B.6	Conclusion	B-11
B.7	References.....	B-12
Appendix C Regulations and Guidance Applicable to Spent Nuclear Fuel.....		C-1
C.1	Introduction	C-1
C.2	Nuclear Regulatory Commission Regulations	C-1
C.3	Nuclear Regulatory Commission Guidance	C-6
C.4	References.....	C-10
Appendix D Implications of the Trend toward High Fuel Burnups for Geologic Disposal of Spent Nuclear Fuel.....		D-1
D.1	Thermal Effects.....	D-1
D.2	Thermal Management	D-4
D.3	References.....	D-5
Appendix E Spent Nuclear Fuel Drying		E-1
E.1	Introduction	E-1
E.2	Drying Commercial Spent Nuclear Fuel.....	E-2
E.3	Potential Effects of Residual Water Remaining in a Spent Nuclear Fuel Cask or Canister	E-5
E.4	Research on Spent Nuclear Fuel Drying	E-6
E.5	Current State of Drying Research.....	E-18
E.6	References.....	E-19
Appendix F Hydrogen Effects in Spent Nuclear Fuel Cladding.....		F-1
F.1	Introduction	F1
F.2	Hydrogen Accumulation and Hydride Formation in Nuclear Fuel Cladding	F-2
F.3	Hydride Reorientation	F-6
F.4	Delayed Hydride Cracking	F-41
F.5	Louhan Recommendations White Paper.....	F-43
F.6	References.....	F-55
Appendix G Spent Nuclear Fuel Performance under Normal Conditions of Dry Storage		G-1
G.1	Background.....	G-1
G.2	Department of Energy High Burnup Dry Storage Research Project.....	G-2

G.3	Modeling of Temperature Profiles in Spent Nuclear Fuel and Spent Nuclear Fuel Cask Systems.....	G-12
G.4	Past Spent Nuclear Fuel Demonstration Programs.....	G-23
G.5	Planned or Ongoing International Demonstration Programs.....	G-26
G.6	Comparison of Demonstrations.....	G-27
G.7	References	G-28
Appendix H Spent Nuclear Fuel Performance under Normal Conditions of Transport...		H-1
H.1	Introduction.....	H-1
H.2	Department of Energy (DOE) Research Related to Spent Nuclear Fuel Transportation.....	H-2
H.3	Measuring High Burnup Fuel Cladding Properties Relevant to Normal Conditions of Transport.....	H-4
H.4	Determining the Fatigue Lifetime of High Burnup Fuel	H-6
H.5	30 cm Drop Tests	H-21
H.6	Structural Modeling.....	H-25
H.7	References	H-27
Appendix I Fuel Performance Modeling.....		I-1
I.1	Overview.....	I-1
I.2	Evaluation.....	I-5
I.3	References	I-8

LIST OF FIGURES

FIGURE ES-1. SIMPLIFIED FIGURE OF A BOILING WATER REACTOR (BWR) FUEL ROD.	XXII
FIGURE 2-1. SIMPLIFIED SCHEMATIC OF A NUCLEAR FUEL ROD AND FUEL ASSEMBLY.	9
FIGURE 2-2. TN-68 BOLTED-LID STORAGE/TRANSPORT CASK BWR SNF.	11
FIGURE 2-3. NUHOMS HORIZONTAL STORAGE MODULES AND CANISTER FOR COMMERCIAL SNF.	12
FIGURE 2-4. CROSS SECTION OF THE HI-STORM 100 DRY CASK STORAGE SYSTEM.	13
FIGURE 2-5. SCHEMATICS OF PWR (A) AND BWR (B) FUEL ASSEMBLIES.	17
FIGURE 2-6. EXAGGERATED DEPICTION OF “BAMBOOING” DEFORMATION OF SNF CLADDING.	18
FIGURE 2-7. CROSS SECTIONS OF PWR FUEL PELLETS.	19
FIGURE 2-8. HYDRIDE DISTRIBUTION AND ORIENTATION IN HIGH BURNUP (~70 GWD/MTU) PWR ZIRLO® CLADDING ABOUT 1.1 METERS ABOVE THE FUEL MID-PLANE.	23
FIGURE 3-1. RESULTS OF THE HDRP CASK DRYNESS TEST.	35
FIGURE 3-2. CIRCUMFERENTIAL AND RADIAL HYDRIDE ORIENTATIONS.	40
FIGURE 3-3. EFFECT OF STRESS ON HYDRIDE REORIENTATION.	41
FIGURE 3-4. PINCH LOAD, P, ON A CROSS-SECTION OF CLADDING CAUSED BY A HYPOTHETICAL TRANSPORTATION SIDE DROP ACCIDENT.	44
FIGURE 3-5. AREVA (NOW ORANO) TN®32 CASK.	50
FIGURE 3-6. MULTIMODAL TRANSPORTATION TEST CASK ON A RAILCAR.	64
FIGURE A-1. A SIMPLIFIED FIGURE OF ONE TYPE OF BWR FUEL ROD.	A-2
FIGURE A-2. CROSS SECTION OF A FUEL ROD SHOWING DISHED FUEL PELLETS INSIDE THE FUEL CLADDING.	A-3
FIGURE A-3. SCHEMATIC OF A GENERIC LWR FUEL ROD.	A-3
FIGURE A-4. SCHEMATICS OF (A) PRESSURIZED WATER REACTOR AND (B) BOILING WATER REACTOR FUEL ASSEMBLIES.	A-5
FIGURE A-5. EXAMPLE OF A SPACER GRID.	A-6
FIGURE A-6. SIMPLIFIED SCHEMATIC OF A PWR NUCLEAR FUEL ROD AND FUEL ASSEMBLY.	A-7
FIGURE A-7. CONTROL ROD GUIDE TUBE IN A PWR ASSEMBLY SHOWING INSERTION OF A CONTROL ROD.	A-8
FIGURE A-8. PERCENTAGE RADIOACTIVE COMPOSITION OF LOW BURNUP SNF AS A FUNCTION OF IRRADIATION TIME.	A-10
FIGURE A-9. SPENT NUCLEAR FUEL (A) RADIOACTIVITY AND (B) DECAY POWER.	A-11
FIGURE A-10. CROSS SECTIONS OF PWR FUEL PELLETS.	A-12
FIGURE A-11. EXAGGERATED DEPICTION OF “BAMBOOING” DEFORMATION OF SNF CLADDING.	A-12
FIGURE A-12. ETCHED FUEL PELLETS OF H.B. ROBINSON FUEL AT A ROD AVERAGE BURNUP OF 67 GWD/MTU.	A-14

FIGURE A-13. POROSITY AT THE PELLETT CENTER (LEFT) AND RIM REGION (RIGHT) OF H.B. ROBINSON FUEL AT ROD AVERAGE BURNUP OF 67 GWD/MTU.....	A-15
FIGURE A-14. FRACTION OF FISSION GAS CREATED THAT MIGRATES TO THE FREE VOLUME IN THE FUEL ROD IN U.S. PWRs.....	A-16
FIGURE A-15. PROFIOMETRY SCAN OF THE OUTER SNF ROD SURFACE SHOWING LOCALIZED RIDGING AT PELLETT-PELETT INTERFACES.....	A-17
FIGURE A-16. EXAMPLE OF A HYDRIDE BLISTER AT THE OUTER DIAMETER OF FUEL CLADDING.	A-22
FIGURE A-17. SIMPLIFIED DEPICTION OF A BWR CONTROL BLADE BETWEEN FOUR BWR FUEL ASSEMBLIES.....	A-24
FIGURE D-1. CALCULATED TEMPERATURES VERSUS TIME AT THE SURFACE OF WASTE PACKAGES CONTAINING 32 PRESSURIZED WATER REACTOR FUEL ASSEMBLIES AND AT THE DRIFT WALL OF A REPOSITORY IN SEDIMENTARY (CLAY-RICH) ROCK.	D-3
FIGURE D-2. CALCULATED THERMAL POWER VERSUS AGE FOR A WASTE PACKAGE CONTAINING 32 ASSEMBLIES OF PRESSURIZED WATER REACTOR SNF.....	D-5
FIGURE E-1. RESULTS OF THE HDRP CASK DRYNESS TEST (PRESSURE REBOUND TEST).....	E-3
FIGURE E-2. PRESSURE VERSUS TIME DURING VACUUM DRYING OF A CASTOR IB SNF CASK.....	E-7
FIGURE E-3. UNIVERSITY OF SOUTH CAROLINA SNF DRYING TEST CHAMBER.....	E-12
FIGURE E-4. EXAMPLE OF A CONTROL ROD GUIDE TUBE SHOWING THE DRAIN HOLES NEAR THE BOTTOM.....	E-13
FIGURE E-5. ILLUSTRATION OF THE MOCK FUEL ASSEMBLY USED IN THE UNIVERSITY OF SOUTH CAROLINA EXPERIMENTS.	E-14
FIGURE E-6. VIEW OF THE SURROGATE SNF BASKET AND THERMOCOUPLE THROUGH A VIEWPORT.....	E-15
FIGURE F-1. OXIDE LAYER THICKNESS ON ZIRCALOY-4 AND M5® CLADDING.....	F-3
FIGURE F-2. HYDRIDE DISTRIBUTION AND ORIENTATION IN HBF (APPROXIMATELY 70 GWD/MTU) WITH ZIRLO® CLADDING.....	F-4
FIGURE F-3. BWR ZIRCALOY-2 CLADDING CONTAINING PRECIPITATED HYDRIDES.....	F-5
FIGURE F-4. INFLUENCE OF APPLIED STRESS ON THE EXTENT OF HYDRIDE REORIENTATION.....	F-6
FIGURE F-5. HYDRIDE REORIENTATION IN IRRADIATED ZIRCALOY-4 CLADDING AT APPROXIMATELY 35 GWD/MTU.	F-6
FIGURE F-6. FUEL CLADDING SEGMENT DISPLAYING INTERNAL PRESSURE AND HOOP STRESS.	F-7
FIGURE F-7. STEADY-STATE SOLUBILITY OF HYDROGEN IN ZIRCONIUM AND ZIRCALOY.....	F-11
FIGURE F-8. AN EARLY COMPILATION OF HYDRIDE REORIENTATION DATA TAKEN ON A VARIETY OF ZIRCALOY CLADDING TYPES.	F-13
FIGURE F-9. PINCH LOAD, P, ON A CROSS-SECTION OF CLADDING CAUSED BY A HYPOTHETICAL TRANSPORTATION SIDE DROP ACCIDENT.	F-17
FIGURE F-10. RING COMPRESSION TEST APPARATUS.....	F-18
FIGURE F-11. EXAMPLE OF A CLADDING SAMPLE THAT CRACKED DURING A RING COMPRESSION TEST.....	F-19

FIGURE F-12. LOAD–DISPLACEMENT CURVES FROM RCTs ON ZIRCALOY-4 RODLETS.	F-21
FIGURE F-13. EFFECT OF MAXIMUM CLADDING HOOP STRESS ON CLADDING DUCTILITY.....	F-22
FIGURE F-14. MICROGRAPH OF RADIAL HYDRIDES IN M5® CLADDING.....	F-33
FIGURE F-15. RCT DUCTILITY CURVES FOR HIGH BURNUP M5® CLADDING.	F-34
FIGURE F-16. MICROGRAPHS OF IRRADIATED BWR SNF CLADDING WITH A ZIRCONIUM LINER.....	F-35
FIGURE F-17. MICROGRAPHS OF CLADDING AFTER HRT SHOWING THE ORIENTATION OF HYDRIDES. ...	F-40
FIGURE G-1. TN®-32 CASK MANUFACTURED BY AREVA (NOW ORANO).	G-3
FIGURE G-2. PENETRATION LOCATIONS FOR THERMOCOUPLE LANCES IN THE MODIFIED LID FOR THE AREVA TN®-32 HDRP STORAGE CASK.....	G-4
FIGURE G-3. AXIAL LOCATIONS FOR THERMOCOUPLES IN THE HDRP STORAGE CASK.	G-5
FIGURE G-4. FINAL LOADING MAP FOR THE HDRP CASK.	G-6
FIGURE G-5. MEASURED TEMPERATURES IN THE HOTTEST ASSEMBLY DURING AND AFTER DRYING OF THE HDRP CASK.....	G-7
FIGURE G-6. GENERAL LAYOUT OF THE SNL DRY CASK SIMULATOR.....	G-17
FIGURE G-7. PEAK TEMPERATURE MEASUREMENTS DURING THE HDRP DRYING PROCESS.....	G-19
FIGURE G-8. MODEL-PREDICTED TEMPERATURES, MEASURED TEMPERATURES, AND TEMPERATURE DIFFERENCES (ΔT) IN THREE LOCATIONS IN THE HDRP CASK.	G-20
FIGURE G-9. COBRA-SFS SIMULATION OF THE TEMPERATURE TIME-HISTORY COMPARED TO THERMOCOUPLE DATA FOR ASSEMBLY 14 (CELL 14) IN THE HDRP TEST CASK.	G-21
FIGURE H-1. MODEL OF AN SNF ASSEMBLY IN A HORIZONTAL POSITION DURING TRANSPORT.	H-2
FIGURE H-2. SCHEMATIC OF AN SNF TRANSPORTATION CASK AND CASK CRADLE.	H-4
FIGURE H-3. THE CYCLIC INTEGRATED REVERSIBLE-BENDING FATIGUE TESTER, OR CIRFT.....	H-5
FIGURE H-4. FATIGUE CURVES FOR SEVERAL AS-IRRADIATED HBF SAMPLES.....	H-8
FIGURE H-5. EQUIVALENT STRAIN AMPLITUDES ($\Delta \epsilon / 2$; A MEASURE OF STRAIN) AS A FUNCTION OF THE NUMBER OF CYCLES TO FAILURE.	H-9
FIGURE H-6. EXAMPLE OF AN HBF TEST SPECIMEN AFTER FAILURE IN THE CIRFT.	H-11
FIGURE H-7. FATIGUE CURVES FOR HBF ROD SPECIMENS FOLLOWING TRANSIENT SHOCKS.....	H-12
FIGURE H-8. TRUCK, SURROGATE CASK COMPONENTS, AND SURROGATE ASSEMBLY USED DURING MEASUREMENTS OF THE VIBRATION AND SHOCK SPECTRUM FOR TRUCK TRANSPORT.....	H-14
FIGURE H-9. SNL SHAKER TABLE AND TRUCK TRANSPORT TEST COMPARISON. (McCONNELL 2016)	H-16
FIGURE H-10. MAXIMUM STRAINS MEASURED BY SNL DURING TRANSPORT TESTING OF SURROGATE ZIRCALOY-4 RODS.	H-17
FIGURE H-11. INSTRUMENTATION CONFIGURATION ON THE SNL ASSEMBLY FOR THE MMTT.....	H-18
FIGURE H-12. ACCUMULATED FATIGUE DAMAGE FOR EACH STRAIN GAGE DURING THE MMTT.....	H-21
FIGURE H-13. PHOTO OF THE 1/3 SCALE ENSA ENUN-32 CASK WITH IMPACT LIMITERS.	H-23
FIGURE H-14. FULL-SCALE DUMMY ASSEMBLY AND BASKET TUBE FOR SNL DROP TESTS.	H-24

FIGURE H-15. FULL-SCALE DUMMY ASSEMBLY DROP TEST SETUP.H-24
FIGURE I-1. DESIRED ATTRIBUTES OF A FUEL PERFORMANCE MODEL..... I-4

LIST OF TABLES

TABLE ES-1 TECHNICAL INFORMATION NEEDS AND RELATED RESEARCH AREAS.	XXIII
TABLE 2-1 CHANGES IN KEY CHARACTERISTICS OF SNF AND THEIR POTENTIAL EFFECTS AS SNF BURNUP INCREASES.....	20
TABLE 2-2 HIGH OR MEDIUM PRIORITY DOE TECHNICAL INFORMATION NEEDS RELATED TO SNF AND SNF CLADDING.....	28
TABLE A-1 COMPOSITIONS OF ALLOYS USED AS NUCLEAR FUEL CLADDING.	A-4
TABLE A-2 OXIDE GROWTH IN MICROMETERS (MM) ON PWR CLADDING AS A FUNCTION OF BURNUP.	A-20
TABLE B-1 DOE SUMMARY OF CROSS-CUTTING TECHNICAL INFORMATION NEEDS FOR HBF CLADDING.	B-4
TABLE B-2 DOE-IDENTIFIED DEGRADATION MECHANISMS THAT COULD IMPACT THE CHARACTERISTICS AND/OR THE PERFORMANCE OF FUEL PELLETS.....	B-5
TABLE B-3 DOE-IDENTIFIED DEGRADATION MECHANISMS THAT COULD IMPACT THE CHARACTERISTICS AND/OR PERFORMANCE OF SNF CLADDING.....	B-5
TABLE B-4 NRC-IDENTIFIED HIGH RANKING TECHNICAL INFORMATION NEEDS.....	B-6
TABLE B-5 EPRI-IDENTIFIED TECHNICAL INFORMATION NEEDS AND PRIORITIES.....	B-9
TABLE B-6 TECHNICAL INFORMATION NEEDS AND PRIORITIES IDENTIFIED BY OTHER COUNTRIES.....	B-10
TABLE I-1 PHYSICAL AND MATERIAL MODELS IN THE BISON FUEL PERFORMANCE MODEL.....	I-3

ABBREVIATIONS AND ACRONYMS

ANL	Argonne National Laboratory
BWR	boiling water reactor
CFR	Code of Federal Regulations
CIRFT	Cyclic Integrated Reversible-Bending Fatigue Tester
CRUD	Chalk River unidentified deposits
DHC	delayed hydride cracking
DOE	U.S. Department of Energy
DTT	ductile transition temperature
ENSA	Equipos Nucleares S.A. (Sociedad Anónima)
EPRI	Electric Power Research Institute
ESCP	Extended Storage Collaboration Program
FGR	fission gas release
GWd/MTU	gigawatt days/metric ton uranium
HBF	high burnup fuel
HDRP	High Burnup Dry Storage Research Project ¹
HLW	high level radioactive waste
HRT	hydride reorientation treatment
INL	Idaho National Laboratory
IRP	Integrated Research Project
ISG	Interim Staff Guidance
LBF	low burnup fuel
LWR	light water reactor
NCT	normal conditions of transport
NRC	U.S. Nuclear Regulatory Commission

¹ This project is also known as the High Burnup Demo Project, the High Burnup Spent Fuel Data Project, and the High Burnup Dry Storage Cask Research and Development Project.

NWTRB	U.S. Nuclear Waste Technical Review Board (Board)
ORNL	Oak Ridge National Laboratory
PNNL	Pacific Northwest National Laboratory
PSI	pounds per square inch
PWR	pressurized water reactor
R&D	research and development
RHCF	radial hydride continuity factor
SNF	spent nuclear fuel
SNL	Sandia National Laboratories
SRP	Standard Review Plan
WPPM	weight parts per million

ACKNOWLEDGMENTS

The Board wishes to express its appreciation to Robert E. Einziger, Ph.D., formerly of the Board's staff, whose expertise and many years of experience working with spent nuclear fuel were the foundation for this report.

The Board also wishes to thank John Kessler, Ph.D., of J. Kessler and Associates, for his technical review of this report.

EXECUTIVE SUMMARY

Congress established the U.S. Nuclear Waste Technical Review Board (Board) in the 1987 Nuclear Waste Policy Amendments Act and charged it to “evaluate the technical and scientific validity of activities undertaken by the Secretary [of Energy] ... including ... activities relating to the packaging or transportation of high-level radioactive waste [HLW] or spent nuclear fuel [SNF]” (Public Law 100–203). In fulfilling its mandate, the Board also evaluates plans to dispose of SNF and HLW as well as issues arising from on-site storage of SNF and HLW that could affect subsequent transportation and disposal. The Board reports its findings, conclusions, and recommendations to Congress and to the Secretary of Energy.

The U.S. Department of Energy (DOE) is responsible not only for managing and eventually disposing of DOE-managed SNF and HLW, but it is also responsible for taking possession and disposing of commercial SNF that is discharged from commercial nuclear power plants throughout the U.S. Although DOE has taken possession of small quantities of commercial SNF, most commercial SNF remains in storage at nuclear power plant sites and, eventually, will have to be transported away from the sites (e.g., for disposal). For many years, DOE has conducted research to understand better the characteristics of commercial SNF. DOE has also been planning for the eventual transportation and disposal of those wastes.

The Board has evaluated DOE’s activities related to the packaging, transportation, and eventual disposal of SNF for many years. In 2005, the Board reviewed DOE plans for SNF packaging and transportation as part of DOE’s Total System Model for the Yucca Mountain Project.² Later, as the focus of the nuclear industry and DOE shifted to extended dry-storage of SNF, including high burnup SNF (HBF; see the text box on this page), the Board published the report, *Evaluation of the Technical Basis for Extended Dry Storage and Transportation of Used Nuclear Fuel* (December 2010).

More recently, the Board held public meetings in February 2016³ and October 2018,⁴ to examine

High Burnup Fuel

Fuel burnup is a measure of the thermal energy generated in a nuclear reactor per unit mass of nuclear fuel as initially loaded in the reactor and is typically expressed in units of gigawatt-days per metric ton of uranium (GWd/MTU).

The average burnup of spent nuclear fuel has increased from 35 GWd/MTU in the 1990s to over 45 GWd/MTU in 2018. In the U.S., nuclear fuel utilized beyond 45 GWd/MTU is defined by the U.S. Nuclear Regulatory Commission as high burnup fuel. Most spent nuclear fuel currently stored in the U.S. is low burnup fuel.

² The Board’s comments can be found in the letter from B. John Garrick, Chairman, U.S. Nuclear Waste Technical Review Board, to Mr. Paul M. Golan, Acting Director of the Office of Civilian Radioactive Waste Management, December 19, 2005.

³ Information about the February 2016 Board meeting, including presentations made during the meeting, can be found on the Board’s website at [Winter 2016 Board meeting](#).

⁴ Information about the October 2018 Board meeting, including presentations made during the meeting, can be found on the Board’s website at [Fall 2018 Board meeting](#).

and discuss DOE research and development programs focused on performance of HBF during extended storage and transportation.⁵

The Board continues to evaluate DOE research on SNF, including HBF, through reviews of DOE reports and other documents, and through interactions between the Board and DOE, including phone calls, fact-finding meetings, and the Board's public meetings. These efforts, as well as relevant technical expertise within the Board, have contributed to the evaluations, findings, and recommendations of this report.

Extensive research has provided confidence that storing and transporting low burnup fuel (LBF; see the text box on the preceding page) complies with U.S. Nuclear Regulatory Commission (NRC) regulations.⁶ Similar research for HBF has started but will take time to complete. In the meantime, the inventory of HBF continues to grow. Based on data collected by DOE in 2019, HBF comprises approximately 25 percent of all commercial SNF currently stored in the U.S.⁷ DOE has sponsored several research activities with the aim of obtaining data to enhance the understanding of the performance (i.e., chemical, physical, and radiological behavior) of HBF in extended storage and transportation conditions, and during subsequent operations at a geologic repository site, which could include repackaging of SNF from currently-used casks and canisters⁸ to new canisters designed for disposal. This report provides the Board's assessment of DOE's HBF research program and offers recommendations that, if implemented, will improve the program and support obtaining information that will be useful to utilities, DOE, and the NRC in their respective activities to manage and regulate the storage and transportation of HBF.

The characteristics or condition of SNF (including HBF) may or may not have implications for public and worker safety during storage, transportation, and repository operations depending on the specific details of the associated application for NRC approval of storage⁹

⁵ Board observations and recommendations from the February 2016 meeting are recorded in a Board letter from Ewing to Kotek, dated May 23, 2016, [May 2016 Board letter](#). Observations and recommendations from the October 2018 meeting are recorded in a Board letter from Bahr to McGinnis, dated November 27, 2018, [Nov. 2018 Board letter](#).

⁶ For example, see the discussions in the NRC's NUREG-2215, Standard Review Plan for Spent Fuel Dry Storage Systems and Facilities and NUREG-2216, Standard Review Plan for Transportation Packages for Spent Fuel and Radioactive Material.

⁷ See the DOE-sponsored report, *Spent Nuclear Fuel and Reprocessing Waste Inventory*, FCRD-NFST-2013-000263, Rev. 7, September 2020.

⁸ SNF may be packaged into a welded stainless-steel canister that is then placed into a shielded overpack for storage and, for some designs, transportation. Alternatively, SNF may be packaged into a bolted-lid cask (sometimes called a bare fuel cask) that does not use an internal canister and includes its own shielding. These packaging systems are explained in more detail in section 2.1.2 of this report. For storage applications, some literature refers to both of these types of systems as "dry cask storage systems" and this report uses the same terminology. This report also may use the terms "cask" and "canister" when it is necessary to distinguish between specific types of storage or transportation systems.

⁹ The NRC regulations for SNF storage are provided in Title 10, Code of Federal Regulations [CFR], Part 72, Licensing Requirements for the Independent Storage of Spent Nuclear Fuel, High-Level Radioactive Waste, and Reactor-Related Greater than Class C Waste.

of cask systems or for transportation¹⁰ of cask systems. In most cases (e.g., for undamaged SNF),¹¹ the condition of the SNF (Figure ES-1) is important for preventing the release of radioactive materials. It may also be necessary for the SNF to maintain its configuration to avoid criticality. In these cases, the utility (or applicant) relies on the integrity of the SNF only in a secondary role (a “defense-in-depth” role).

However, if the integrity of the SNF is not relied on for safety (e.g., in the case of SNF that is known to be damaged), then only limited details about its condition are needed to be included in the storage or transportation safety documentation because other SNF cask or canister system components are designed to meet the regulatory requirements. Similarly, the condition of the SNF may or may not have implications for the ability to retrieve SNF assemblies from SNF casks or canisters for repackaging. Once DOE takes possession of the SNF and transports it to another facility, it may need to retrieve the SNF from its existing package and repackage it into another container. For example, in DOE’s license application for the Yucca Mountain, Nevada geologic repository,¹² DOE assumed that approximately 10% of the commercial SNF that arrived at the repository would have to be repackaged at the repository’s surface handling facilities.

The expected need for repackaging was based on an assumption that some SNF would arrive at the repository facility packaged in casks or canisters not designed for disposal and the SNF would have to be repackaged into canisters suitable for disposal. If the SNF is undamaged and is relied on to provide a secondary safety function, the applicants and DOE (when it takes title to commercial SNF) need to know the condition of the SNF when it is loaded into a storage or transportation cask system. The applicants (and DOE) also need to have confidence, based on experimental data or technically sound analyses and computer modeling, that the condition of the SNF will not change substantially during storage and transportation so that the SNF can meet the requirements for subsequent storage, if needed, and for disposal. This need for information has motivated DOE to sponsor research

¹⁰ The NRC regulations for SNF transportation are found in *Packaging and Transportation of Radioactive Material*, 10 CFR Part 71.

¹¹ Damaged SNF is defined as “[a]ny fuel rod or fuel assembly that cannot fulfill its fuel-specific or system-related functions.” See NRC Division of Spent Fuel Storage and Transportation, Interim Staff Guidance-1, Revision 2 (ISG-1, Rev. 2), *Classifying the Condition of Spent Nuclear Fuel for Interim Storage and Transportation Based on Function*.

¹² Yucca Mountain Repository License Application Safety Analysis Report. DOE/RW-0573, Rev. 1. February 2009.

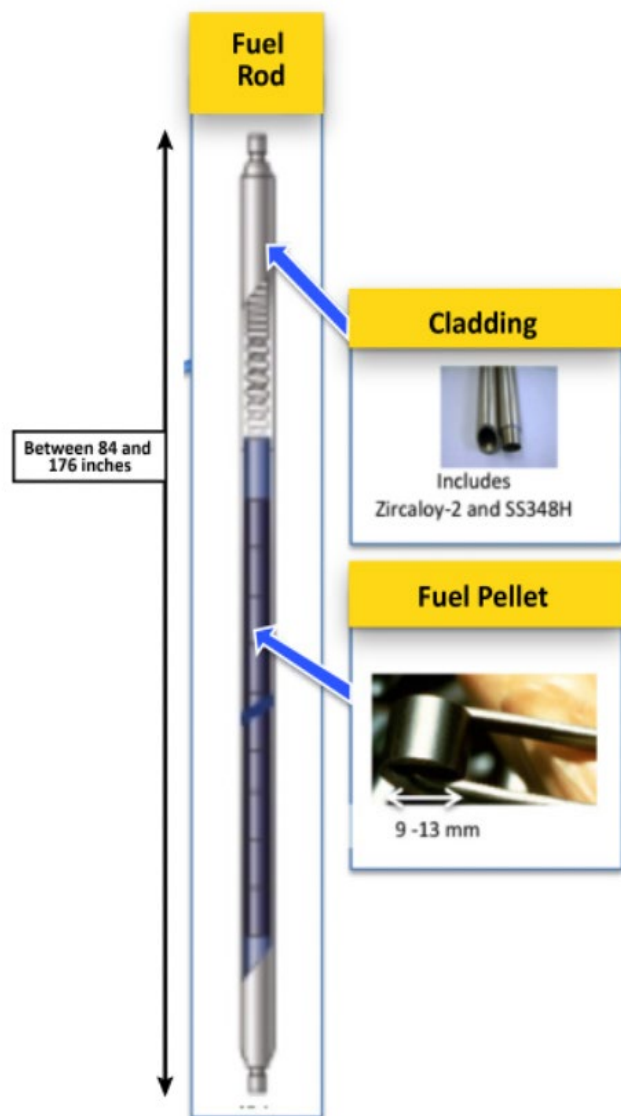


Figure ES-1. Simplified figure of a boiling water reactor (BWR) fuel rod. The range of lengths of the fuel, widths of cylindric fuel pellet, and thickness of cladding used for BWR fuel is depicted. The general arrangement of a pressurized water reactor (PWR) fuel rod is similar (modified from Wagner et al. 2012)

to better understand the characteristics and performance of SNF, including HBF, and how the condition of SNF may change during extended storage and transportation.¹³

DOE has completed several evaluations (also called “gap analyses”) to determine what technical information is needed to improve the understanding of the characteristics and performance of SNF, including HBF, during storage and transportation.¹⁴ DOE’s evaluations cover components and characteristics of SNF rods and SNF dry cask storage systems and include a priority ranking of the technical information needs. Meeting the higher priority technical information needs is a key consideration for DOE as it decides which research efforts to support. Table ES-1 provides a listing of DOE’s priority technical information needs that apply to SNF (including HBF) and cladding, aligned to DOE’s research focus areas and the corresponding sections of this report. The table also includes the cross-cutting research area of fuel performance modeling that the Board considers to be important. When fully developed, a fuel performance model will provide valuable computer-based tools for predicting the characteristics and behavior of HBF, including HBF with operating histories and/or cladding types that have not been fully studied and characterized.

¹³ Categorization of Used Nuclear Fuel Inventory in Support of a Comprehensive National Nuclear Fuel Cycle Strategy. ORNL/TM-2012/308. FCRD-FCT-2012-000232. December 2012.

¹⁴ The most recent DOE evaluation of technical information needs can be found in the document *Gap Analysis to Guide DOE R&D in Supporting Extended Storage and Transportation of Spent Nuclear Fuel: An FY2019 Assessment*. SAND2019-15479R. December 23, 2019.

Table ES-1 Technical information needs and related research areas.

Priority Technical Information Needs ^a	DOE Research Area (corresponding report section)
1. Drying Issues	SNF drying (Section 3.1)
2. Hydrogen effects in SNF cladding	Hydrogen effects in HBF cladding (section 3.2)
Hydride reorientation	Hydride reorientation in HBF cladding (section 3.2.1)
3. Thermal profiles for SNF (during drying and storage)	HBF performance under normal conditions of dry storage and thermal modeling (section 3.3)
4. Stress profiles for SNF (during normal conditions of transport)	HBF performance under normal conditions of transport and structural modeling (section 3.4)
Crosscutting Research ^b	DOE Research Area (corresponding report section)
5. Predictions of fuel behavior	Fuel performance modeling (section 3.5)

^a The numbering of the technical information needs is intended to aid in the organization of this report and does not represent another level of prioritization.

^b In its 2014 R&D plan,¹⁵ DOE considered fuel performance modeling to be part of the effort to study hydrogen effects in SNF cladding and DOE provided funding for its development. However, it was not assigned a high priority by itself. The Board believes it is an important effort to include in ongoing research.

The four main research efforts that align with DOE’s priority technical information needs and the cross-cutting research topic of fuel performance modeling are summarized below.

Spent Nuclear Fuel Drying. After drying SNF, including HBF, some water may remain inside an SNF cask or canister, including water inside breached SNF rods.¹⁶ This water can undergo radiolytic decomposition, generating hydrogen and oxygen gases, which can lead to pressure buildup inside the cask or canister and corrosion of the SNF cladding and the internal components of the cask or canister. It is necessary to understand the location, chemical form, and amount of water remaining in the cask or canister after drying in order to assess the importance of these effects. Therefore, DOE has sponsored research to investigate drying processes.

Hydrogen Effects in High Burnup Fuel Cladding. Hydrogen is generated during cladding oxidation in a nuclear reactor. When absorbed into nuclear fuel cladding, the hydrogen can have different chemical forms and physical orientations. Under certain conditions, higher hydrogen levels can potentially be available in HBF cladding and can lead to embrittlement of the cladding as it cools after drying and during extended storage. This embrittlement can increase the probability of a breach if the cladding is subjected to sufficiently high physical shocks or stresses. DOE continues to sponsor research to investigate the concentration and impact of hydrogen compounds in HBF cladding.

High Burnup Fuel Performance under Normal Conditions of Dry Storage. Better knowledge of HBF storage environments (e.g., temperatures) and HBF characteristics (e.g., yield strength) and how they change over time is important for enhancing the technical bases for extended

¹⁵ See Stockman et al., Used Nuclear Fuel Extended Storage and Transportation Research and Development Review And Plan, FCRD-UFD-2014-0000050, August 4, 2014.

¹⁶ According to the NRC, breached SNF can include SNF with pinholes or hairline cracks in the cladding. A subset of breached SNF is SNF with grossly breached cladding. Grossly breached cladding includes cladding with defects that could allow the release of fuel pellet fragments. See footnote 10 above.

storage and transportation of HBF. DOE, in cooperation with the Electric Power Research Institute (EPRI), is sponsoring the High Burnup Dry Storage Research Project (HDRP, see Appendix G) where HBF assemblies have been loaded into a dry cask storage system and will be stored for a period of at least ten years. The project includes detailed examinations of selected HBF rods (called “sister rods” or “sibling pins”) withdrawn from both HDRP test assemblies and similar (sister) assemblies before the dry storage period (i.e., while the assemblies were in the spent fuel pool). The project also includes examinations of additional HBF rods that will be withdrawn from the HDRP test assemblies after storage and transportation to a facility with the capabilities to handle HBF assemblies and rods. This will allow DOE to gain a better understanding of the changes in HBF characteristics that may occur during storage and transportation. The effort also provides data that can be used to test and validate computer-based fuel performance models (see #5 below) and thermal models that are used to predict SNF dry cask storage system temperatures.

High Burnup Fuel Performance under Normal Conditions of Transport. During NCT, SNF, including HBF, is subjected to a variety of stresses that can strain the SNF cladding. These strains must be evaluated to assess the probability of a cladding breach that would prevent the SNF from performing its intended functions as specified in the NRC-approved certificate of compliance. DOE has cosponsored research on transporting surrogate SNF by truck, ship, and rail to measure the shock and vibration loads experienced by the SNF and other system components. This effort is accompanied by the development of computer models that can be used to predict the stresses and strains on the SNF and system components during transportation. DOE has also sponsored laboratory testing to measure how actual SNF responds (i.e., measure the strain levels in the SNF) when subjected to a range of vibration amplitudes and frequencies and when subjected to certain drop loads. The results of the laboratory testing (i.e., the loads the SNF can withstand) can be compared to the results of the transport testing (i.e., the loads to which the SNF will be subjected) to support assessing the probability of a cladding breach. The testing results also allow for validation of computer model predictions of structural response.

Fuel Performance Modeling. Because it is not practical to obtain measurements of the changes in SNF characteristics for the entire range of SNF types subjected to all reactor operating conditions and storage conditions, validated computer models must be utilized to predict changes in SNF characteristics and performance (i.e., the chemical, physical, and radiological behavior of SNF during drying, storage, and transportation). DOE is sponsoring several efforts to develop sophisticated computer models with the goal of using the models to predict the characteristics and performance of SNF, including HBF, in a variety of storage and transportation conditions.

The Board agrees with the DOE-identified technical information needs and priorities that apply to extended storage and subsequent transportation of HBF, with one exception. As noted above, the Board believes that fuel performance modeling should be included among the priority research efforts. Although DOE’s technical information needs appear to be appropriate, the various DOE reports on technical information needs do not provide a clear indication of how the results of the DOE research projects will be used to meet or “close” the technical information needs. The Board’s evaluation of the appropriateness of the DOE projects to address the technical information needs and whether the scope of these projects will adequately bound all HBF types is the focus of this report.

Much of the DOE research summarized above has been completed but some is still in progress, including HBF rod examinations as part of the HDRP and drop tests of surrogate SNF assemblies to examine shock loads that may occur during NCT. As a result of the testing completed as of late 2019, DOE reached the following conclusion regarding the integrity of HBF in conditions of extended storage and transportation: “Results of the [DOE-sponsored testing] examined as integrated effects from actual temperature, actual hoop stress, and realistic external loads, indicate that risks associated with [hydrogen] embrittlement to cladding integrity of SNF are low for current fuel designs, burnups, and reactor operational limits [in] the United States.”¹⁷

The Board notes that the results cited above are based on testing primarily PWR HBF, with only limited study of BWR HBF and no testing of HBF that incorporates integral burnable absorber rods used to absorb neutrons and assist in reactor reactivity control. HBF rods that contain boron as the absorber material may have higher internal gas pressures, resulting in higher hoop stress in the cladding. This may cause the HBF cladding to be more susceptible to brittle fracture under certain load conditions, such as in the event of a transportation accident.

The HDRP has provided, and will continue to provide, useful data regarding the characteristics and performance of PWR HBF in a bolted-lid cask system. The Board encourages the continuation of the project, including completion of the tests included in EPRI’s Final Test Plan¹⁸ that are scheduled to be performed following storage of the cask for ten years. Ongoing tests of high interest include drop testing of surrogate SNF assemblies and testing of HBF cladding ductility using fueled cladding specimens (i.e., cladding that still contains the fuel pellets). The latter testing should provide valuable information about amount of strength added by the fuel pellets to the pellet-cladding composite structure and whether the cladding can be pinched enough to cause fracturing when impacted in the event of an accident.

Summary Findings and Recommendations

Although the DOE testing to date has provided some assurance that the characteristics and performance of HBF are understood sufficiently to support NRC approval of HBF extended storage and transportation, the testing has been limited mostly to PWR HBF. Based on the Board’s evaluation of recent DOE research on HBF, as well as its review of historical DOE and industry research on LBF, the Board makes the following summary findings and recommendations.

A note about the summary findings and recommendations:

Due to the nature of the issues to be addressed, specialized technical terminology is necessary and is used below to properly and fully convey the findings and recommendations. The technical terminology is explained in the main body of the report, the appendices, and the glossary. However, explanations of these technical terms have been omitted from the earlier parts of this executive summary to preserve its brevity and

¹⁷ Teague et al. Gap Analysis to Guide DOE R&D in Supporting Extended Storage and Transportation of Spent Nuclear Fuel: An FY2019 Assessment. SAND2019-15479R. December 2019.

¹⁸ See “High Burnup Dry Storage Cask Research and Development Project: Final Test Plan,” EPRI, Palo Alto, California. DE-NE-0000593. February 2014.

readability. Readers who are unfamiliar with the terminology, but would like to know more, should refer to the glossary or the sections of the report indicated in the parentheses following each summary finding below.

1. General Recommendations

- a. *Summary Finding: The Board finds that the results of DOE-sponsored research on HBF have been reported by a variety of organizations and in a variety of formats but there is no compendium that contains the results of all DOE research related to extended storage and transportation of HBF. (general finding; report section not applicable)*

Recommendation: The Board recommends that, following the completion of HDRP sister rod examinations and drop testing of surrogate SNF assemblies, DOE prepare a document that compiles the results of DOE research on extended storage and transportation of HBF, with the purpose of providing the technical bases for conclusions reached regarding HBF performance during extended storage and transportation.

- b. *Summary Finding: The Board finds that important research relevant to extended storage and transportation of HBF is being sponsored by organizations outside of DOE, both in the U.S. and in other countries. (See section 2.3 and Appendices A, F, and G)*

Recommendation: The Board recommends that DOE continue to review the results of the Electric Power Research Institute's Extended Storage Collaboration Program and research in other countries to determine if the results of ongoing HBF studies either change the priorities for DOE's planned research or add technical information needs requiring new research.

- c. *Summary Finding: The Board finds that many of the tests and models used to determine the performance of HBF have been completed for a relatively narrow range of fuel and cladding types, burnup levels, temperatures, storage and transportation system designs, etc. The limitations of the tests and models are not always clear with respect to their applicability to a wider range of HBF types, storage and transportation system designs, and storage and transportation conditions. (See sections 3.1–3.5)*

Recommendation: The Board recommends that DOE indicate how its tests and models do or do not apply to the broad range of HBF types and storage and transportation system designs for which information is still needed and take steps to meet those remaining technical information needs.

2. Spent Nuclear Fuel Drying

- a. *Summary Finding: The Board finds that water remaining inside SNF dry cask storage systems may cause corrosion of SNF cladding or the internal components of the system and significant uncertainty remains regarding the quantities of hydrogen and oxygen gases that can be generated due to*

radiolysis of the remaining water. While the SNF drying process used by industry removes most of the water, including water physically adsorbed on metal surfaces, some of the more tightly bound chemisorbed water is likely to remain. (See section 3.1 and Appendix E)

Recommendation: The Board recommends that DOE evaluate the extent to which chemisorbed water remains after the drying process is completed and whether this water could affect the ability of SNF cask or canister systems and their contents to continue to meet storage and transportation requirements.

- b. Summary Finding: The Board finds that few gas samples have been obtained from inside dry cask storage systems containing commercial SNF. (See section 3.1 and Appendix E)*

Recommendation: The Board recommends that DOE further explore the possibility of monitoring the moisture content and gas composition of dry cask storage systems loaded by nuclear utilities with HBF for an extended period. DOE should improve and validate gas sampling methods, with a particular focus on water vapor sampling and measurement, before the next samples are obtained.

3. Hydrogen Effects in High Burnup Fuel Cladding

- a. Summary Finding: The Board finds that data obtained from testing of unirradiated cladding does not replicate data obtained from testing of irradiated cladding. (See section 3.2. and Appendix F)*

Recommendation: The Board recommends that, as the need for new testing of HBF cladding is identified, DOE's research efforts make use of irradiated samples rather than unirradiated samples to avoid the large uncertainties and difficulties in interpreting test results that arise from using unirradiated samples.

- b. Summary Finding: The Board finds that there are a variety of test methods for examining hydride reorientation in HBF cladding and that the results of the testing are reported with significant format variations that make comparison of results difficult. (See section 3.2 and Appendix F)*

Recommendation: The Board recommends that DOE define a standard set of test parameters (e.g., fuel burnup, test temperatures, rod internal pressures) and results, where possible, that must be recorded for all DOE-funded research related to hydride reorientation. This will allow DOE managers, computer model developers, and nuclear industry practitioners to better use the data to make scientifically meaningful comparisons of experimental results from various research sources, even when the data were not collected for that purpose.

- c. Summary Finding: The Board finds that data on the characteristics of HBF (e.g., HBF rod internal pressures) and results of research on hydride formation and hydride reorientation in zirconium-based alloys are reported by a variety of*

organizations and saved in a variety of information archives. (See section 3.2 and Appendix F)

Recommendation: The Board recommends that DOE gather into one database all relevant information that is publicly available on hydride-related testing of zirconium-based alloys to provide the basis for (1) evaluating the effects of variables that influence hydride reorientation; (2) supporting the ongoing development of new standards for inducing hydride reorientation in test samples and quantifying hydride reorientation and its effects; (3) explaining the differences in hydride reorientation and its effects among cladding types; and (4) developing computer models to predict hydride formation and reorientation in all zirconium-based cladding types, including those that have not been tested.

4. High Burnup Fuel Performance under Normal Conditions of Dry Storage

High Burnup Dry Storage Research Project

- a. *Summary Finding: The Board finds that DOE has not clearly indicated how the data obtained from the HDRP and related sister rod testing will be used to meet the DOE-identified technical information needs or support modeling of HBF performance during dry storage and transportation. (See section 3.3 and Appendix G)*

Recommendation: The Board recommends that the test plan for the HDRP sister rods should (a) link each proposed test to one or more of the technical information needs identified in the most recent DOE report on technical information needs and (b) explain how the results of each proposed test will be used to meet the technical information needs or support modeling of HBF performance during dry storage.

- b. *Summary Finding: The Board finds that obtaining and characterizing the sister rods has been a worthwhile undertaking but has required the expenditure of extensive time and resources. These rods constitute a valuable asset for future research and development. (See section 3.3 and Appendix G)*

Recommendation: The Board recommends that DOE preserve selected sister rods (or rod segments and components) for future use in follow-up studies to the HDRP, if needed, or in support of other programs.

Thermal Modeling

- c. *Summary Finding: The Board finds that DOE-sponsored thermal models will be valuable tools for calculating realistic SNF cladding temperatures during drying and storage in dry cask storage systems if realistic input data are used and if the predicted temperature uncertainty due to all sources of uncertainty can be quantified and defensibly bounded. (See section 3.3 and Appendix G)*

Recommendation: The Board recommends that DOE continue its activities to ensure its thermal models are rigorously validated, including industry-standard uncertainty quantification, for use on SNF storage or transport systems. Important factors to consider during validation are the various designs of cask and canister systems, inclusion of new fuel designs like accident tolerant fuel, and inclusion of SNF assemblies with other components, such as control rod assemblies or discrete burnable absorber rods.

5. High Burnup Fuel Performance under Normal Conditions of Transport

- a. *Summary Finding: The Board notes that DOE continues to develop a structural model that can be used to predict the structural response of SNF, SNF cask or canister systems, and SNF transport vehicles under normal conditions of transport. The Board finds that the DOE structural model development and validation efforts include a number of uncertainties stemming from the use of dummy or surrogate fuel assemblies and unirradiated fuel material properties. (See section 3.4 and Appendix H)*

Recommendation: The Board recommends that DOE quantify the uncertainties introduced by the use of unirradiated assembly components and surrogate components, such as concrete mock-SNF assemblies, in experiments being used to benchmark the DOE structural model. The structural model should also be exercised to evaluate HBF cladding strains for different cask and canister types, fuel types, and degree of pellet-cladding bonding.

6. Fuel Performance Modeling

- a. *Summary Finding: The Board finds that the limited testing of irradiated HBF provides a potentially insufficient database of mechanical properties and other HBF characteristics required to develop accurate fuel performance models. (See section 3.5 and Appendix I)*

Recommendation: The Board recommends that DOE continue to develop fuel performance models (e.g., BISON) that are validated utilizing experimental data. In so doing, DOE-sponsored fuel performance model developers should clearly identify the data they need to develop and validate models to DOE-sponsored experimentalists. Experimentalists should clearly explain the capabilities and limitations of their experimental equipment and facilities to model developers. This close collaboration is needed to ensure optimal experimental setup and collection of data needed to improve the models and achieve a better understanding of HBF characteristics and performance.

1. INTRODUCTION

This report documents the U.S. Nuclear Waste Technical Review Board's (Board) evaluation of the U.S. Department of Energy's (DOE) research program to examine the performance of the portion of the commercial spent nuclear fuel (SNF)¹⁹ inventory termed high burnup fuel (HBF; see the text box on this page). In the U.S., HBF comprises approximately 25 percent of all SNF in storage (Peters, Vinson, and Carter 2020). The Secretary of Energy has the responsibility for transporting commercial SNF, including HBF, from nuclear power plant sites to a nuclear waste repository or to a monitored retrievable storage facility and then to a repository for disposal (U.S. Congress 1987). DOE's research program with respect to HBF is designed to investigate how the characteristics of HBF may change during extended dry storage or transportation. Specifically, the research program endeavors to determine whether HBF experiences physical or chemical changes that may cause it to respond differently from what is known or what is expected for low burnup fuel (LBF) under storage conditions, normal conditions of transport (NCT), and certain postulated transport accident conditions (i.e., accidents that can cause a pinch load on a fuel rod).

Extensive research has provided confidence that LBF can be stored and transported in accordance with the U.S. Nuclear Regulatory Commission (NRC) requirements.²⁰ Similar research to improve the understanding of the performance of HBF has been started but is not yet complete. DOE is conducting several research activities with the aim of obtaining data that can enhance the understanding of the performance of HBF in extended storage and transportation conditions and during subsequent operations at a geologic repository site, which could include the repackaging of SNF. This report provides the Board's assessment of DOE's HBF research program and makes recommendations that, if implemented, will improve DOE's program and its ability to provide data that will enhance the understanding of HBF.

High Burnup Fuel

Fuel burnup is a measure of the thermal energy generated in a nuclear reactor per unit mass of nuclear fuel as initially loaded in the reactor and is typically expressed in units of gigawatt-days per metric ton of uranium (GWd/MTU).

The average burnup of spent nuclear fuel has increased from 35 GWd/MTU in the 1990s to over 45 GWd/MTU in 2018. In the U.S., nuclear fuel utilized beyond 45 GWd/MTU is defined by the U.S. Nuclear Regulatory Commission as high burnup fuel (NRC 2014a). Most spent nuclear fuel currently stored in the U.S. is low burnup fuel.

¹⁹ The Nuclear Waste Policy Act defines spent nuclear fuel as fuel that has been withdrawn from a nuclear reactor following irradiation, the constituent elements of which have not been separated by reprocessing. Spent nuclear fuel is sometimes called used nuclear fuel.

²⁰ For example, see the discussions in the NRC's NUREG-2215, Standard Review Plan for Spent Fuel Dry Storage Systems and Facilities (NRC 2020a) and NUREG-2216, Standard Review Plan for Transportation Packages for Spent Fuel and Radioactive Material (NRC 2020b).

1.1 Operations Affecting Spent Nuclear Fuel

Having an improved technical knowledge of the characteristics and performance of HBF, as the fuel experiences a range of operations and conditions, will be useful in demonstrating that the fuel will meet the NRC regulations (see section 1.2). SNF, including HBF, will experience several operations during its lifetime, including transfers during spent fuel pool operations, cask or canister²¹ loading, drying, storage, transportation, and disposal. These operations will subject the SNF to a range of mechanical, chemical, radiological, and thermal conditions, which may affect the characteristics of the SNF and its performance during subsequent operations. Examples of the conditions to which SNF may be subjected during these operations are noted below.

Heating and cooling SNF: SNF assemblies experience a wide range of temperatures over their lifetimes, and some SNF operations include large temperature variations within a short period. Sometimes the temperature variation can be more than 150°C (302°F); e.g., during the vacuum drying process after SNF is loaded into a cask or canister (Fort et al. 2019a). The temperature variations can influence corrosion processes on the surface of SNF rods, chemical processes inside the fuel pellets and the fuel cladding, and internal pressures (and thus, stresses) on the fuel cladding. Operations that subject the fuel to large temperature variations include but are not limited to changes in reactor operating conditions ranging from full power to zero power and drying SNF in a cask or canister followed by backfilling the cask or canister with an inert gas (e.g., helium).

Lifting and handling SNF assemblies: A crane or hoist is used to lift an SNF assembly during certain operations (examples listed below). During these operations, the SNF assembly may be subjected to both vertical and horizontal loads (slight bumps), and the outside surface of the SNF assembly may be subjected to touching or rubbing against other components, such as SNF basket cells inside an SNF cask. SNF assembly lifting operations include, but are not limited to:

- transfer from the nuclear reactor core to the spent fuel pool,
- transfer from the spent fuel pool into an SNF cask or canister (see section 2.1.2 for a description of the different types of SNF casks and canisters), and
- transfer from one cask or canister to another (if SNF repackaging is needed—see section 2.1.3).

Lifting and handling SNF casks or canisters: A transporter or crane is used to handle or lift a cask or canister loaded with SNF in a number of operations. During these operations, the

²¹ SNF may be packaged into a welded stainless-steel canister that is then placed into a shielded overpack for storage and, for some designs, transportation. Alternatively, SNF may be packaged into a bolted-lid cask (sometimes called a bare fuel cask) that does not use an internal canister and includes its own shielding. These packaging systems are explained in more detail in section 2.1.2 of this report. For storage applications, some literature refers to both of these types of systems as “dry cask storage systems” and this report uses the same terminology. This report also may use the terms “cask” and “canister” when it is necessary to distinguish between specific types of storage or transportation systems.

cask or canister and its contents may be subjected to both vertical and horizontal loads. SNF cask or canister lifting operations include, but are not limited to:

- Transfer from the spent fuel pool into an onsite transport overpack and movement by an onsite transporter to a dry storage facility;
- Transfer from a dry storage facility to a truck, railcar, or barge for inter-site transport; and
- Unloading from the transport conveyance to SNF storage facilities at an away-from-reactor interim storage site or a waste repository site.

Transporting SNF: SNF assemblies, inside SNF transportation casks, are subjected to a range of vibrations and bumps during transportation operations. These operations will subject the SNF assemblies to both horizontal and vertical accelerations that will vary depending on the design of the cask or canister system and the nature of the vibrations and bumps.

1.2 Regulations and Guidance for Spent Nuclear Fuel Storage and Transportation

To understand the objectives of the DOE HBF research program, it is first necessary to understand the regulatory framework in which SNF dry storage and transportation activities are approved by the NRC. A brief discussion of the regulatory requirements is provided below. For more detail, see Appendix C.

General Requirements and the Importance of the Condition of the SNF.

Commercial SNF must be stored and transported in cask or canister systems approved by the NRC. Specifically, these systems are designed to satisfy NRC storage regulations (Title 10, Code of Federal Regulations [CFR] Part 72,²² transportation regulations (10 CFR Part 71),²³ or, in some cases, both. To obtain NRC approval of a license or a certificate of compliance for a specific storage or transportation cask system, detailed descriptions of the physical, chemical, and radiological characteristics of the SNF, the physical arrangement of the cask system components, and the operating conditions and limitations of the overall system are required as part of a comprehensive application. The operating conditions and limitations include restrictions on certain parameters, such as maximum SNF cladding temperature, external cask system temperatures, and external dose rates.

The condition of the SNF (including HBF) may or may not have a key role in protecting public and worker safety during storage and transportation operations, depending on the specific details in the application and in the subsequent NRC-approved license or certificate of compliance. In some cases, credit is taken for the SNF (i.e., the fuel rod cladding and certain fuel assembly components, such as the assembly spacer grids [see section 2.2.1]) to provide a barrier against the release of radioactive materials or for preventing criticality.

²² Licensing Requirements for the Independent Storage of Spent Nuclear Fuel, High-Level Radioactive Waste, and Reactor-Related Greater Than Class C Waste (10 CFR Part 72).

²³ Packaging and Transportation of Radioactive Material (10 CFR Part 71).

However, if the integrity of the SNF is not relied on for safety, then less information about the condition of the SNF will be needed to support the license or certificate of compliance because other cask system components will provide the needed protection.

Retrieval and Recovery of SNF from Cask or Canister Systems.

In certain storage situations, SNF assemblies will have to retain sufficient structural integrity to allow retrieval or recovery from dry cask storage systems. The NRC requires that “[s]torage systems must be designed to allow ready retrieval of spent fuel ... for further processing or disposal” (10 CFR 72.122(l)). In accordance with additional NRC guidance (NRC 2016a), SNF retrieval from a dry cask storage system can occur as SNF assemblies, SNF in a welded canister, or SNF in a cask. Therefore, the ability to retrieve individual SNF assemblies will depend on the specific design of the dry cask storage system. In the event of an accident involving an SNF dry cask storage system, the NRC guidance states that the retrievability requirement for SNF does not apply and that, instead, the focus should be on “post-accident recovery.”²⁴

In the case of SNF transport (i.e., after storage), the NRC does not specifically require that SNF be retrievable or recoverable during NCT or following transportation accidents. However, the NRC requires that certificate of compliance applicants must include in their applications structural analyses demonstrating that the “geometric form of the package contents [i.e., the SNF] would not be substantially altered” following operational events during NCT (10 CFR 71.55(d)(2)) and therefore, the SNF would be recoverable from the transportation cask.

Robustness of SNF Storage and Transportation Cask Systems.

The NRC regulatory requirements and guidance for SNF dry storage and transportation allow the applicant some flexibility in designating the components of the cask system that meet the regulations, but the cask components are specifically required to meet the defined standards for structural integrity. For example, the NRC transportation regulation (10 CFR Part 71) requires the applicant to demonstrate through analyses or testing that the transportation cask system can withstand each of four challenging accidents scenarios in sequence (drop, puncture, fire, and water immersion). The applicant must demonstrate that the cask system continues to meet criticality safety requirements following these accident scenarios. Furthermore, during and after the postulated accidents, the transportation cask system must continue to meet regulatory requirements that specify maximum allowed values for structural deformation of the cask, cask system temperatures, release of radioactive material, and radiation doses (10 CFR Part 71). Similarly, dry cask storage systems must meet the regulatory requirements of 10 CFR Part 72.²⁵ As stated earlier, the applicant may choose to assign the SNF no safety role or only a secondary safety role (a role often referred to as “defense in depth” in the nuclear industry).

²⁴ Recovery only applies to accidents, but recovery is not defined in NRC Spent Fuel Project Office, Interim Staff Guidance-3 (ISG-3), *Post Accident Recovery and Compliance with 10 CFR 72.122(l)* (NRC No Date).

²⁵ While 10 CFR Part 71 specifies the types of transportation accidents that a cask system must endure, 10 CFR Part 72 does not explicitly list the accidents that a cask system must endure while in storage.

SNF that is Known to be Damaged.

If an SNF assembly is known or suspected to contain a damaged SNF rod (i.e., an SNF rod that is grossly breached or that cannot perform the functions required of it), it is placed in an additional container (sometimes called a damaged fuel can) or an acceptable alternative prior to being loaded into an SNF dry cask storage system.²⁶ The damaged fuel can restricts the SNF assembly to a known, fixed location inside the SNF cask or canister and allows the SNF assembly to be moved without subjecting the assembly to lifting stresses. In the case of SNF placed inside a damaged fuel can, the applicant takes no credit for the SNF or SNF cladding to meet regulatory requirements and relies entirely on the damaged fuel can and cask system structural components for this purpose.

Determining whether HBF Retains Sufficient Integrity to Meet Regulatory Requirements.

In cases where the integrity of HBF is relied on to meet the regulatory requirements for storage or transportation, or to facilitate HBF retrieval or recovery, the applicants (and DOE, when it takes title to commercial SNF) need to know the condition of the HBF when it is loaded into a storage or transportation cask system. DOE also needs to be able to predict, based on experimental data and technically sound analyses, any changes in the condition of the HBF during and after extended storage and in subsequent transportation, repackaging, and disposal operations. It is this need for information that led DOE to sponsor research to better understand the characteristics and performance of HBF. The Board notes that after DOE began its HBF research program, the NRC published guidance for the implementation of aging management programs that may assist applicants to better manage the condition of SNF and SNF dry cask storage systems during extended storage (NRC 2019).

1.3 DOE Research on the Characteristics of High Burnup Fuel

For LBF storage and transport, fuel characteristics and expected performance are well understood. Although HBF has been approved by the NRC for storage, there remains some uncertainty about changes that may occur in the condition of HBF, especially during extended periods of dry storage and in transportation conditions after extended storage. Therefore, DOE updated its research objectives for extended storage and transportation of SNF, with a focus on HBF (Alsaed and Hanson 2017, Teague et al. 2019):

- “Support the enhancement of the technical bases for continued safe and secure storage of SNF for extended periods;
- Support the enhancement of the technical bases for [SNF cask systems] and SNF retrievability to facilitate extended storage, transportation, and disposal, which may include repackaging of the SNF assemblies;
- Support the enhancement of the technical bases for transportation of SNF.”

The Board agrees with the DOE research objectives that apply to extended storage and subsequent transportation of HBF, with one exception. The Board believes that fuel performance modeling should be included among the priority research efforts. The full details of DOE’s research efforts and the Board’s evaluation of those efforts are explained in section 2.4 and in the Appendices of this report. The DOE-identified research efforts and the

²⁶ The guidance pertaining to damaged SNF can be found in the NRC Division of Spent Fuel Storage and Transportation, Interim Staff Guidance-1, Revision 2 (ISG-1, Rev. 2), *Classifying the Condition of Spent Nuclear Fuel for Interim Storage and Transportation Based on Function* (NRC 2007).

Board-identified topic of fuel performance modeling can be grouped into five main focus areas and are summarized below.

- 1) *Spent Nuclear Fuel Drying.* After drying SNF, including HBF, some water may remain inside an SNF cask or canister, including water inside breached SNF rods.²⁷ This water can undergo radiolytic decomposition, generating hydrogen and oxygen gases, which can lead to pressure buildup inside the cask or canister and corrosion of the SNF cladding and the internal components of the cask or canister. It is necessary to understand the location, chemical form, and amount of water remaining in the cask or canister after drying in order to assess the importance of these effects. Therefore, DOE has sponsored research to investigate drying processes. (See section 3.1 and Appendix G for more detail.)
- 2) *Hydrogen Effects in High Burnup Fuel Cladding.* Hydrogen is generated during cladding oxidation in a nuclear reactor. When absorbed into nuclear fuel cladding, the hydrogen can have different chemical forms and physical orientations. Under certain conditions, higher hydrogen levels can potentially be available in HBF cladding and can lead to embrittlement of the cladding as it cools after drying and during extended storage. This embrittlement can increase the probability of a breach if the cladding is subjected to sufficiently high physical shocks or stresses. DOE continues to sponsor research to investigate the concentration and impact of hydrogen compounds in HBF cladding. (See section 3.2 and Appendix F for more detail.)
- 3) *High Burnup Fuel Performance under Normal Conditions of Dry Storage.* Better knowledge of HBF storage environments (e.g., temperatures) and HBF characteristics (e.g., yield strength) and how they change over time is important for enhancing the technical bases for extended storage and transportation of HBF. DOE, in cooperation with the Electric Power Research Institute (EPRI), is sponsoring the High Burnup Dry Storage Research Project (HDRP, see Appendix G) where HBF assemblies have been loaded into a dry cask storage system and will be stored for a period of at least ten years. The project includes detailed examinations of selected HBF rods (called “sister rods” or “sibling pins”) withdrawn from both HDRP test assemblies and similar (sister) assemblies before the dry storage period (i.e., while the assemblies were in the spent fuel pool). The project also includes examinations of additional HBF rods that will be withdrawn from the HDRP test assemblies after storage and transportation to a facility with the capabilities to handle HBF assemblies and rods. This will allow DOE to gain a better understanding of the changes in HBF characteristics that may occur during storage and transportation. The effort also provides data that can be used to test and validate computer-based fuel performance models (see #5 below) and thermal models that are used to predict SNF dry cask storage system temperatures.
- 4) *High Burnup Fuel Performance under Normal Conditions of Transport.* During NCT, SNF, including HBF, is subjected to a variety of stresses that can strain the SNF

²⁷ According to the NRC, breached SNF can include SNF with pinholes or hairline cracks in the cladding. A subset of breached SNF is SNF with grossly breached cladding. Grossly breached cladding includes cladding with defects that could allow the release of fuel pellet fragments.

cladding. These strains must be evaluated to assess the probability of a cladding breach that would prevent the SNF from performing its intended functions as specified in the NRC-approved certificate of compliance. DOE has cosponsored research on transporting surrogate SNF by truck, ship, and rail to measure the shock and vibration loads experienced by the SNF and other system components. This effort is accompanied by the development of computer models that can be used to predict the stresses and strains on the SNF and system components during transportation. DOE has also sponsored laboratory testing to measure how actual SNF responds (i.e., measure the strain levels in the SNF) when subjected to a range of vibration amplitudes and frequencies and when subjected to certain drop loads. The results of the laboratory testing (i.e., the loads the SNF can withstand) can be compared to the results of the transport testing (i.e., the loads to which the SNF will be subjected) to support assessing the probability of a cladding breach. The testing results also allow for validation of computer model predictions of structural response. (See section 3.4 and Appendix H for more detail.)

- 5) *Fuel Performance Modeling.* Because it is not practical to obtain measurements of the changes in SNF characteristics for the entire range of SNF types subjected to all reactor operating conditions and storage conditions, validated computer models must be utilized to predict changes in SNF characteristics and performance (i.e., the chemical, physical, and radiological behavior of SNF during drying, storage, and transportation). DOE is sponsoring several efforts to develop sophisticated computer models with the goal of using the models to predict the characteristics and performance of SNF, including HBF, in a variety of storage and transportation conditions. (See section 3.5 and Appendix I for more detail.)

1.4 Board Evaluation Activities

As specified in its enabling legislation, the Board shall “evaluate the technical and scientific validity of activities undertaken by the Secretary [of Energy] ... including ... activities relating to the packaging or transportation of high-level radioactive waste [HLW] or spent nuclear fuel [SNF]” (Public Law 100–203, U.S. Congress 1987). In fulfilling its mandate, the Board also evaluates DOE plans to dispose of SNF and HLW as well as issues arising from on-site storage of SNF and HLW that could affect subsequent transportation and disposal. In 2005, the Board reviewed the DOE plans for SNF packaging, transportation, and disposal as part of DOE’s Total System Model for the Yucca Mountain Project (Garrick 2005). In 2010, the Board completed a review and issued a report on the technical basis for long-term storage and transportation of SNF, including HBF (NWTRB 2010). More recent review efforts related to HBF include three public Board meetings, fact-finding meetings with DOE and laboratory scientists, and several other communications with DOE as summarized below.

The Board held a public meeting in February 2016, in Knoxville, Tennessee, to examine and discuss DOE research and development (R&D) programs focused on HBF performance during storage and transportation. The meeting featured presentations by representatives of DOE, Oak Ridge National Laboratory (ORNL), Argonne National Laboratory (ANL), Pacific Northwest National Laboratory (PNL), the NRC, and other SNF experts from the nuclear industry. Following the meeting, the Board issued a letter to DOE offering recommendations to improve DOE research programs (Ewing 2016a).

The Board continued its review of HBF R&D by conducting fact-finding meetings with DOE and SNF researchers at the University of South Carolina in February 2016, the Board offices in May 2016, the DOE Nevada Field Office in July 2016 and August 2018, and the Idaho National Laboratory (INL) in October 2016. Further interactions between the Board and DOE included phone calls, video conferencing, staff-to-staff meetings, and document reviews. Board letters to DOE reflecting these efforts and offering additional Board recommendations on DOE research programs were issued on June 3, 2016, (Ewing 2016b), December 7, 2016 (Ewing 2016c), and August 25, 2017 (Bahr 2017).

Most recently, the Board held public meetings in October 2018, in Albuquerque, New Mexico, and November 2019, in Alexandria, Virginia, to discuss DOE R&D activities related to managing and disposing of commercial SNF, including updates on research focused on HBF performance during extended storage and transportation. Following the meetings, the Board sent letters to DOE offering observations and recommendations to improve DOE research (Bahr 2018, Bahr 2020).

2. BACKGROUND

2.1 Spent Nuclear Fuel Generation and Management

2.1.1 Nuclear Power Plant Operation

Large-scale commercial nuclear power production began in the U.S. in the 1950s. As of December 2020, 94 commercial nuclear reactors were operating in the U.S.; the two types of nuclear reactors used to generate electricity in the U.S. are pressurized water reactors (PWRs) and boiling water reactors (BWRs) (NRC 2020c).

As nuclear fuel (see Figure 2-1) is irradiated with neutrons (i.e., “burned”) in a reactor, the fuel generates a large amount of heat, mainly due to fission of “fissile” radionuclides (primarily uranium-235 (U-235)). The heat is then used to generate electricity. The amount of thermal (or heat) energy generated due to fission in the fuel divided by the initial mass of uranium in the fuel is called the fuel “burnup” and has units of gigawatt-days per metric ton of uranium (GWd/MTU). In the U.S., the NRC defines SNF having an assembly average burnup greater than 45 GWd/MTU as “high burnup” SNF (HBF). Although other factors affect the economics of nuclear power plant operations, in general, increasing the burnup of the fuel reduces the fuel costs. Consequently, there is a trend towards using fuel that can achieve higher burnups and, in the future, it is expected that the proportion of SNF discharged as HBF in the U.S. will continue to increase.

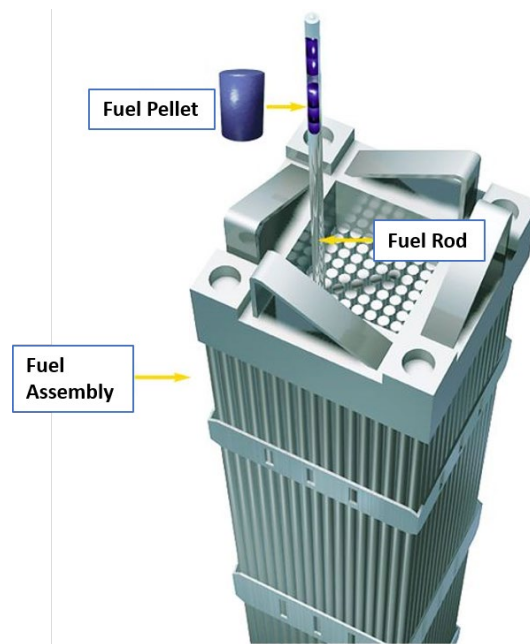


Figure 2-1. Simplified schematic of a nuclear fuel rod and fuel assembly.
(adapted from Duke Energy 2016).

During the fission process, many different radioactive isotopes are generated, and these can be grouped into two major classes:

- 1) "Fission products" from the fission process. Some of the fission products are gaseous (termed "fission gas").
- 2) "Actinides," formed when heavy elements, such as uranium, absorb neutrons or undergo radioactive decay. Actinides are chemical elements with atomic numbers from 89 to 103 (actinium through lawrencium).

Many of these fission products and actinides undergo radioactive decay, generating considerable radiation and "decay heat"²⁸ long after the fuel is removed from the reactor. Consequently, the cask or canister systems (explained below) used for storing and transporting SNF must provide radiation shielding and heat removal for the SNF they contain.

Immediately after removal from the reactor, the SNF is intensely radioactive and thermally hot and is stored underwater, in a nearby spent fuel pool. The pool provides at least 6 m (20 ft) of water above the top of the SNF to shield facility workers and equipment from receiving a radiation dose above acceptable limits. The water also removes the decay heat generated by SNF. Radiation protection and decay heat management are central safety criteria in the NRC regulations for storage and transportation (Appendix C).

2.1.2 Spent Nuclear Fuel Packaging and Storage

In 1977, President Carter halted the reprocessing of SNF from commercial nuclear power reactors.²⁹ Although this decision was subsequently reversed, reprocessing of commercial SNF was not restarted in the U.S. Because there are neither significant off-site storage facilities nor a permanent disposal facility currently available, SNF has been stored at nuclear power plant sites. Initially, the SNF is stored in the spent fuel pools on site but, over time, many spent fuel pools have reached their maximum allowed capacity and the utilities have had to make other arrangements for storing the SNF.³⁰ Except for a relatively small quantity of SNF that is moved from one spent fuel pool to another, SNF being moved out of the pools is being loaded into dry cask storage systems that are kept at the nuclear power plant sites in facilities called Independent Spent Fuel Storage Installations (ISFSIs).

As of December 2020, the commercial nuclear industry in the U.S. had placed 3,379 dry cask storage systems, holding approximately 144,000 SNF assemblies into dry storage (UxC 2020). The utilities continue to move SNF into dry storage at a pace of approximately 220 dry cask storage systems per year. In the U.S., two predominant styles of dry cask storage systems have been used. These are the bolted-lid (or bare fuel) cask system and the

²⁸ The heat produced by the decay of radioactive fission products and actinides after a reactor has been shut down.

²⁹ Reprocessing generally refers to the processes used to separate spent nuclear fuel into nuclear materials that may be recycled for use in new fuel and material that would be discarded as waste.

³⁰ Relatively small amounts of SNF have been moved from the spent fuel pools at certain nuclear power plant sites to the spent fuel pools at another nuclear power plant sites. Other small amounts reside in a spent fuel pool at a storage facility in Morris, IL. Some SNF generated decades ago has been reprocessed.

welded-lid (canistered) system, which has two configurations, horizontal or vertical, depending on the vendor's design.

Bolted-lid dry cask storage systems

In the bolted-lid dry cask storage systems, SNF is placed in a fuel basket inside a heavily shielded metal cask that is closed and sealed with gaskets and a bolted lid to provide containment of radioactive material. The basket designs include neutron poisons for criticality safety purposes. The bolted-lid cask shell provides the radiation shielding necessary to protect workers and the environment using thick layers of metals such as steel and lead, and allows for decay heat removal, primarily by conduction and eventually by natural convection air flow at the cask outer surface. In the U.S., bolted-lid cask systems for commercial SNF have capacities ranging from 21 to 40 assemblies for PWR SNF and 68 assemblies (one design only) for BWR SNF³¹ (UxC 2020). Figure 2-2 shows a typical bolted-lid dry cask storage system.

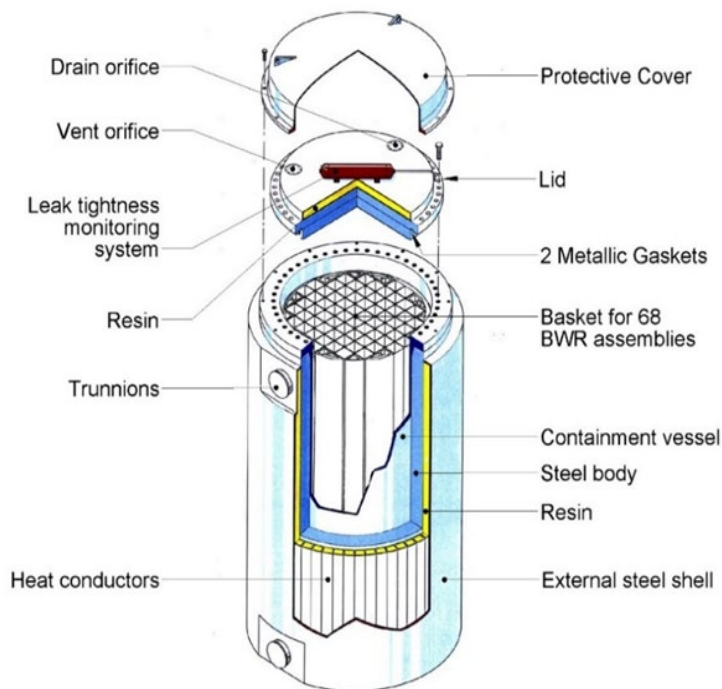


Figure 2-2. TN-68 bolted-lid storage/transport cask BWR SNF.
(adapted from Hunter 2004).

Canistered dry cask storage systems

In a canistered dry cask storage system, the SNF is placed in a metal fuel basket inside a stainless steel canister that is sealed by a welded stainless steel lid. The baskets include internal design features (e.g., neutron absorbers) for criticality safety purposes. The walls of the canister range in thickness from 1.3 to 2.5 cm (0.5 to 1.0 in), depending on canister design. Unlike bolted-lid systems, which have radiation shielding materials integrated into the cask, canistered systems make use of a thick storage overpack (sometimes called a

³¹ There is only one currently-approved bolted-lid cask system for BWR SNF—the Orano TN-68 (see Figure 2-2).

storage module) that includes shielding to provide radiation protection. The storage overpack or module allows air flow around the canister to aid in decay heat removal by natural convective heat transfer, as the heat is conducted and radiated from the SNF to the outer surface of the canister. In a horizontal system like that shown in Figure 2-3, the SNF canister is stored horizontally. Alternatively, the SNF canister may be stored vertically (see Figure 2-4) in an overpack that is part of an above-ground or below-ground design. Canistered dry cask storage systems for commercial SNF in the U.S. have capacities ranging from 7 to 37 assemblies for PWR SNF and 52 to 89 assemblies for BWR SNF (UxC 2020).

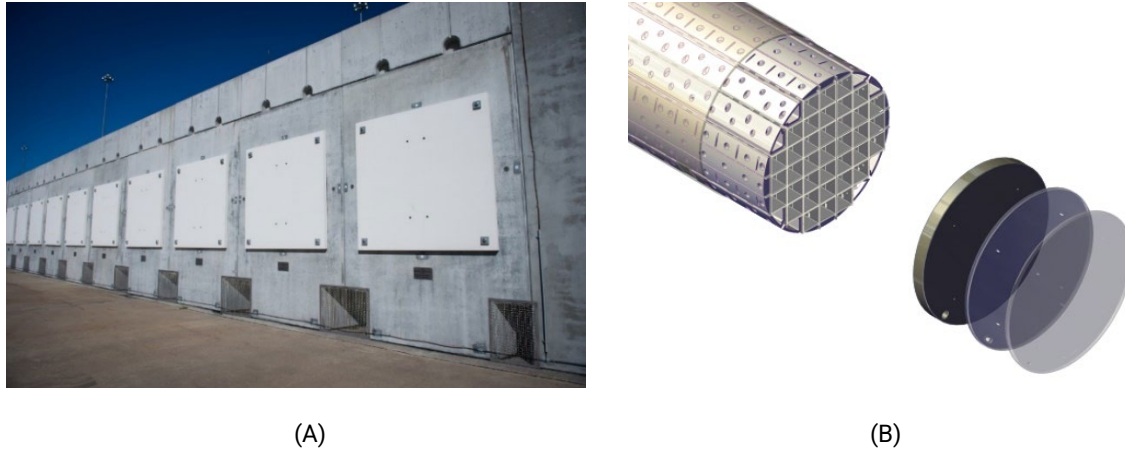


Figure 2-3. NUHOMS Horizontal Storage Modules and canister for commercial SNF.

(A) Photo of NUHOMS horizontal storage modules; (B) schematic of NUHOMS 37PTH Dry Shielded Canister

(Images: copyright Orano, with permission).

HBF is stored in the same manner as LBF. However, over time, larger capacity SNF dry cask storage systems have been introduced and more HBF versus LBF is being discharged from nuclear power plants; both trends combine to raise temperatures in the dry cask storage systems. NRC guidance suggests a maximum temperature of 400°C [752°F] that SNF cladding is allowed to reach in a dry cask storage system to limit adverse effects in the cladding.

Therefore, it is necessary to understand how HBF characteristics and performance may change when subjected to temperatures as high as 400°C [752°F] during drying or while in storage and how these changes may affect the subsequent transportation of HBF. This has prompted the nuclear industry and DOE to identify “technical information needs” related to HBF that need to be addressed through research (see section 2.4 for a discussion of technical information needs) to achieve the necessary understanding. DOE research efforts related to storing HBF are discussed in section 3.3 and Appendix G.

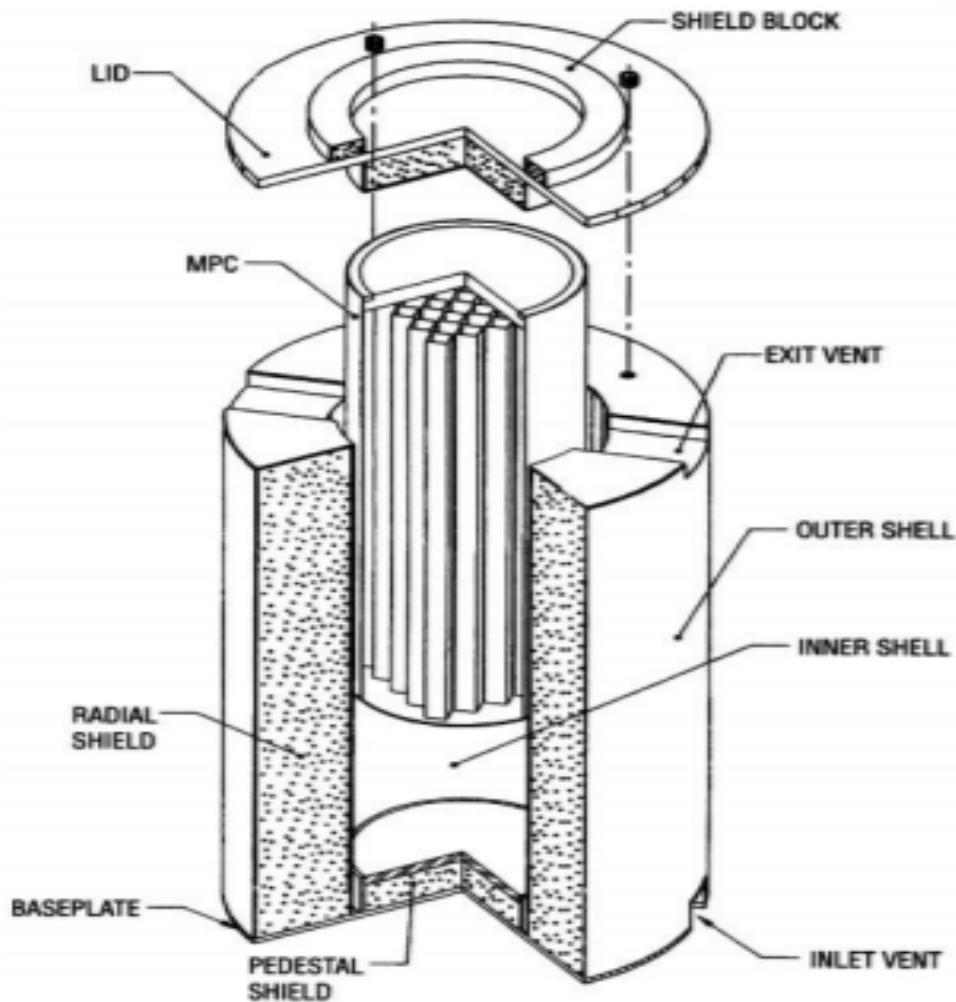


Figure 2-4. Cross section of the HI-STORM 100 dry cask storage system.
(Holtec International 2016).

2.1.3 Spent Nuclear Fuel Transportation, Possible Interim Storage, and Disposal

Transportation

In the U.S., commercial SNF is not currently being transported away from nuclear power plant sites, except in small quantities for research purposes. Past shipments of commercial SNF were conducted for SNF reprocessing to alleviate spent fuel pool capacity issues and as part of the decommissioning of the Three Mile Island Unit 2 nuclear reactor. Other types of SNF, such as naval and research reactor SNF, are transported to DOE sites for storage, pending final disposition. More information on these and other shipments can be found in a DOE-sponsored evaluation of the worldwide experience in transporting SNF (Connolly and Pope 2016). All modern designs of SNF dry cask storage systems and approximately 95% of all systems loaded in the U.S. are “dual-purpose” systems; i.e., they are also designed for transporting SNF (Greene, Medford, and Macy 2013; UxC 2020).

Dual-purpose bolted-lid systems can be transported after the requirements of the NRC-approved transportation certificate of compliance are met and impact limiters are installed. Concurrently, transportation vehicles and associated equipment must be made ready, and the transport routes must be planned and approved. For all canistered systems except the Holtec International HI-STAR 100 system, the SNF canister must be removed from the storage overpack and placed into a transportation cask for transport. The HI-STAR 100 system storage cask is transportable as-is with the SNF canister inside. Again, all certificate of compliance requirements must be met, impact limiters installed, and transportation route planning completed. A report containing a description of many of the technical issues to be addressed in preparing for SNF transport was issued by the Board in 2019 (NWTRB 2019a).

Although there is some experience in the U.S. with transporting LBF, there is little experience with transporting HBF. Until recently, when the NRC and DOE began conducting research focused on HBF, it was not clear whether HBF would behave in the same manner as LBF during transportation. This uncertainty led DOE to accord a higher priority to research on HBF and its performance during transportation (Teague et al. 2019). See section 3.4 and Appendix H for details about DOE research on the effects of transporting HBF.

*Away-from-reactor interim storage*³²

Away-from-reactor interim storage of commercial SNF entails the shipment of SNF to an interim storage facility as an intermediate step on the path to disposal of the SNF.³³ Away-from-reactor interim storage, using dry-storage systems, has not yet been implemented in the U.S. but recently, two commercial entities have begun design and licensing activities for such facilities; one in southeastern New Mexico and one in western Texas. At these sites, the SNF would be stored in canistered dry cask storage systems, similar to storage at ISFSIs at many nuclear power plant sites. The need to move HBF from dry storage at nuclear power plant sites to an interim storage facility, if needed, and later, to a storage facility at a repository site, highlights the importance of understanding the cumulative effects of the handling, transportation, and storage on the condition of the HBF.

Disposal

Because no disposal facility for SNF and HLW is licensed to operate in the U.S., considerable uncertainty remains about the final design of such a facility and its capability to receive SNF casks and canisters and dispose of them without the need to remove the SNF and repackage it into disposal packages. This is important because repackaging is another operation, along with repository emplacement, that may have an impact on the characteristics of the SNF. Although DOE considered the potential impact of disposal operations on HBF characteristics during its prioritization of technical information needs (Teague et al. 2019), there were no research activities focused specifically on this issue at the time this report was prepared.

³² Interim storage in this context is different from storage of SNF at an ISFSI at a nuclear power plant site.

³³ In the Nuclear Waste Policy Act, interim storage, which would be managed by DOE, is called monitored retrievable storage (U.S. Congress 1982).

Conversely, it is expected that the disposal of HBF will have some impact on the design and performance of a deep geologic repository. For more details about the potential implications of disposing of HBF, see section 2.6 and Appendix D.

2.2 Characteristics of High Burnup Spent Nuclear Fuel

Older SNF had assembly average burnup levels at or below 45 GWd/MTU. As improvements in fuel designs and reactor operations have been made over the decades, assembly average burnup levels have increased beyond 45 GWd/MTU, with individual fuel rod average burnup allowed by the NRC to be as high as 62 GWd/MTU. The characteristics of the fuel pellets and cladding that constitute fuel rods change as the fuel is irradiated in a reactor. For some characteristics of HBF, such as hydrogen absorption in the cladding, the rate of change starts to increase for burnups in the range of 45-50 GWd/MTU, which are relevant to HBF. For some newer fuel designs, such as fuels with M5[®] cladding, these effects are less pronounced because fuel vendors have modified the cladding to accommodate higher burnups. As discussed later in this section, some of the characteristics that change with higher burnup may affect HBF performance during storage and transportation.

This section focuses on the following three topics:

- 1) A description of PWR and BWR fuel rods and assembly designs. Except for changes in the concentration of radionuclides and the amount of decay heat, the condition of the SNF at the time it is placed in a cask or canister for drying and dry storage is expected to be the same as when it was placed initially in the spent fuel pool after irradiation.³⁴ The chemical and physical condition of SNF at the time of placement in a storage or transportation cask is a key factor in determining if and how much SNF characteristics will change during the storage or transportation process.
- 2) Differences in the characteristics of HBF and LBF.
- 3) How SNF characteristics, as a function of burnup, affect storage, transportation, and disposal.

A more extensive review of HBF characteristics is provided in Appendix A.

2.2.1 General Description of Spent Nuclear Fuel

A commercial nuclear fuel rod, such as that shown in Figure 2-1, is comprised of a column of ceramic pellets composed of sintered³⁵ uranium dioxide grains containing uranium that is isotopically enriched to levels up to 5% by weight U-235. The pellets, which are sometimes

³⁴ See Appendix A for reasons that the condition of SNF at the time of dry storage has not changed appreciably since the SNF was placed into the spent fuel pool for 5 to 25 years of cooling. This is important because almost all SNF characterization is done immediately after irradiation as part of fuel qualification programs.

³⁵ Sintering is the process in which the particles of a powder are pressed into “green” pellets (in the case of nuclear fuel pellets), bonded together through heating to a high temperature but below the melting point, and then ground to the precise diameter desired.

dished³⁶ on the ends to allow space for growth and deformation caused by irradiation and thermal expansion (see Appendix A, Figure A-1), are sealed inside zirconium-alloy metal tubes, referred to as cladding. Sufficient space is left at the top and/or bottom of the column of fuel pellets to accommodate fuel pellet expansion and fission gas that is released from the pellets, both of which occur during irradiation. PWR and BWR fuels were originally clad in stainless steel but the cladding used on PWR and BWR fuels manufactured in the 1970s and later has been primarily Zircaloy-4 and Zircaloy-2, respectively. While these zirconium alloys are still used, some newer fuel cladding is fabricated using other similar zirconium alloys, including ZIRLO[®], Optimized ZIRLO[™], and M5[®] for PWRs and variations of the Zircaloy-2 composition and Ziron (zirconium plus 1% iron) for BWRs. There is a small gap between the fuel pellets and cladding in as-manufactured fuel and the size of this gap decreases (initially) during irradiation, affecting the structural strength of the fuel rod and the volume available to accommodate fission gases (see section 2.2.2.4). The fuel rods are generally about 4 m (13 ft) long and are held in a square array by spacer grids (generally made from a zirconium alloy). The entire structure of rods, grids, and top and bottom nozzles (in PWRs) or tie plates (in BWRs)³⁷ is referred to as a fuel assembly or bundle (see Figures 2-1 and 2-5).

Rods in a PWR fuel assembly (Figure 2-5A) are arranged in a square array ranging from 14 by 14 rods to 17 by 17 rods, with smaller diameter rods with reduced cladding thicknesses used as the array size increases to retain the same assembly size. All fuel rods pass through short metal spacer grids (also called spacers) that have an egg-crate-like configuration and are positioned at several locations along the length of the assembly. The spacer grids serve to position the rods radially.

PWR HBF generally has an array size of 16 by 16 rods or 17 by 17 rods. After the pellets are inserted into the cladding, rods are flushed with and then pressurized with helium. The initial pressure in PWR fuel rods at ambient temperature generally ranges from 2.0 to 3.4 MPa (290 to 490 pounds per square inch [psi]). Approximately 20 of the fuel rods in a PWR fuel assembly are replaced by control rod guide tubes that normally contain only water during reactor operation, and which serve to connect the upper and lower nozzles of the assembly. Most control rod guide tubes are closed at the bottom but include small holes in the tube wall, referred to as drain holes, located approximately 15 cm (6 in) above the bottom to allow water to be displaced when the control rods are inserted during reactor operation.³⁸

The drain holes in some guide tube designs are closer to the bottom (see Appendix E, Figure E-4). The location of the drain hole is important in determining how much water might remain in an SNF assembly after the draining and drying process. To mitigate damage to the

³⁶ Pellet dimensions range anywhere from 1.0 to 1.5 cm (0.39 to 0.59 in) long. The ends of some pellets are concave (dished) to allow space for axial swelling of the pellet, and some pellets have a chamfered edge to reduce mechanical interactions between the pellets and the cladding.

³⁷ The nozzles on the ends of PWR fuel assemblies and the tie plates on the ends of BWR fuel assemblies have similar functions, such as providing paths for coolant flow and connection points at the top for lifting the assemblies. In some literature, nozzles are also called end bells and the lower tie plate is called a nose piece.

³⁸ The exact location of the drain hole varies from design to design.

rods due to debris in the coolant water flowing through the reactor core, most assemblies also include a debris filter as part of the bottom nozzle.

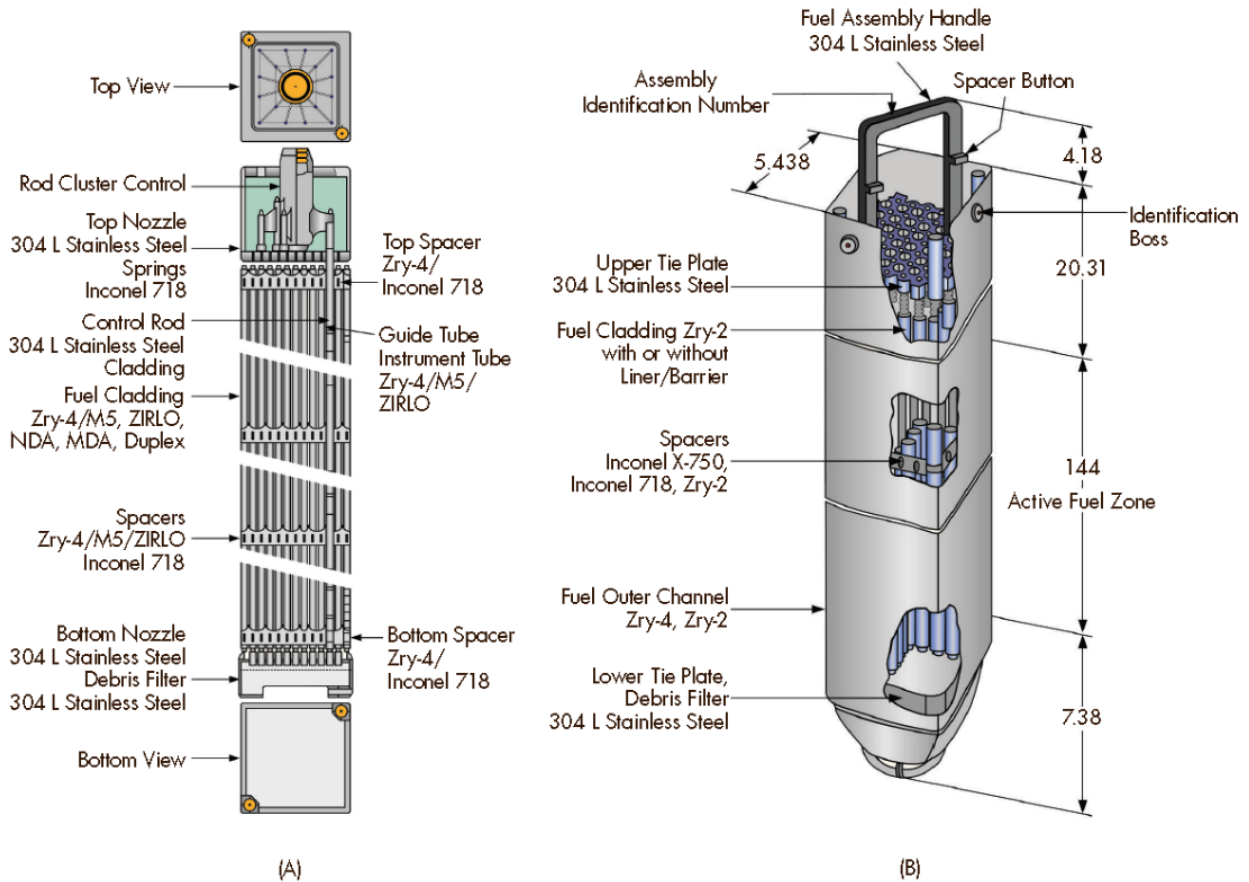


Figure 2-5. Schematics of PWR (A) and BWR (B) fuel assemblies.

Dimensions in (B) are inches

(Provided courtesy of Advanced Nuclear Technology International, see Strasser, Rudling, and Patterson 2014).

Rods in a BWR fuel assembly such as that shown in Figure 2-5B, are arranged in square arrays ranging from 6 by 6 rods to 11 by 11 rods, again with decreasing rod diameter as the number of rods in the array increases. Like PWR fuel, BWR fuel designs include spacer grids. BWR HBF generally comprises fuel assemblies with higher numbers of rods in the array. The cladding of BWR fuel rods is typically thicker than that of PWR fuel rods. Newer BWR fuel cladding usually has an inner surface liner of pure zirconium or other material to reduce potential pellet-cladding mechanical interaction in the reactor. This layer also acts as a sink for hydrogen during the drying process and reduces the quantity of hydrogen available to form zirconium hydrides in the Zircaloy-2 cladding during cooldown (see Appendix F for a detailed discussion). Similar to PWR fuel rods, BWR fuel rods are flushed with, and then pressurized with helium. The typical initial helium pressure in BWR fuel rods ranges from 0.7 to 1.4 MPa (100 to 200 psi), which is lower than in PWR fuel rods. PWR fuel rod pressure is higher to counterbalance the PWR coolant pressure, which is higher than that of a BWR. BWR assemblies are held together by fuel rods that have threaded connectors at each end

(called tie rods), which are bolted to the top and bottom tie plates. There are usually 4 to 8 tie rods per assembly. A zirconium alloy wrapper (sometimes called a channel or shroud) surrounds the assembly from top to bottom to guide the control rod blades outside the assemblies and to limit the lateral flow of water and steam. In both PWR and BWR assemblies, all of the fuel rods will grow due to irradiation creep and fuel pellet swelling. Some of the fuel rods will lengthen as much as a few centimeters during irradiation.³⁹

During PWR operation, fuel cladding tends to “creep down” or shrink onto the fuel pellets due to the force of the high-pressure cooling water outside of the cladding. As a result, the fuel cladding can attain a slight bamboo-like shape (not visible to the human eye) to conform to the deformed fuel pellets, with larger diameters and larger stresses occurring at pellet-pellet interfaces inside the cladding (see Figure 2-6).

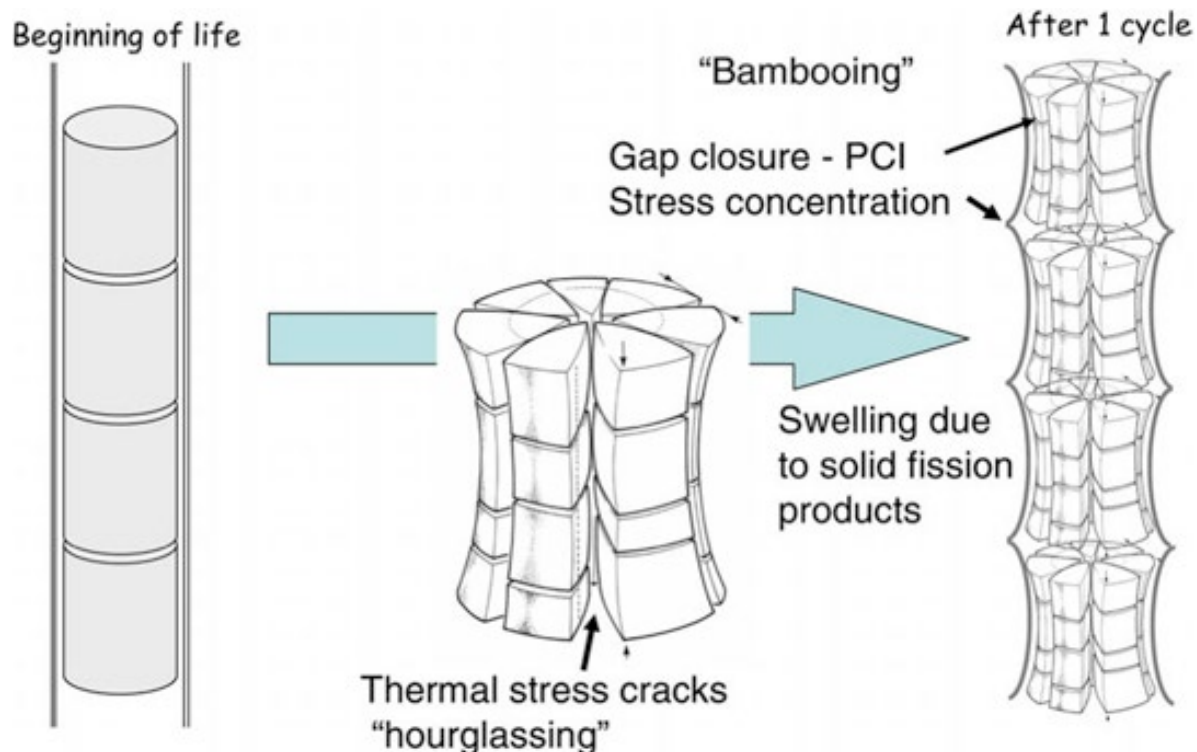


Figure 2-6. Exaggerated depiction of “bambooing” deformation of SNF cladding.

“Hourglassing” of fuel pellets and bambooing of SNF cladding are not usually visible to the human eye (Olander 2009).

Notes: PCI = pellet cladding interaction

Over time, the cladding outer surface will oxidize by reacting with the coolant water. A portion of the hydrogen generated by the oxidation of the cladding will migrate into the cladding and can lead to “hydriding” (see Appendix A). The reactor coolant water also slowly corrodes the surface of some components in the reactor that are in contact with the water. Some of the resulting corrosion products will dissolve in the water and eventually become

³⁹ The reason for the difference in rod-length growth is not clear, but it is probably due to the small variations in temperature, irradiation level, and position of the various fuel rods with respect to the control rods.

deposited on the surface of the fuel rods. These corrosion products deposits are called CRUD (Chalk River Unidentified Deposits)⁴⁰ and, like the oxide layer on the outer surface of the cladding, the CRUD layer on the cladding reduces the cladding's ability to transfer heat to the coolant water. In some cases, the behavior of the CRUD (i.e., CRUD spalling from the cladding) can lead to greater cladding oxidation rates, which, in turn, can eventually lead to embrittlement of the cladding (see Appendix A for details).

The fission process produces heat, fission products, activation products, and actinides in the fuel pellets. Many of these materials are radioactive isotopes. Most of the isotopes produced are contained in the fuel pellet uranium dioxide matrix (the crystalline lattice of the fuel) but some are released to the free volume of the fuel rod. The high temperatures inside the fuel pellets plus the generation and retention of most of the isotopes within the pellets causes pellet swelling. The thermal gradients across the pellets can lead to pellet cracking, which is normal and accommodated in the fuel design. As assembly average burnup increases beyond approximately 45 GWd/MTU, a more-densely cracked and fine-grained region, called the "rim region"⁴¹ forms near the outer circumference of some fuel pellets (see Figure 2-7).

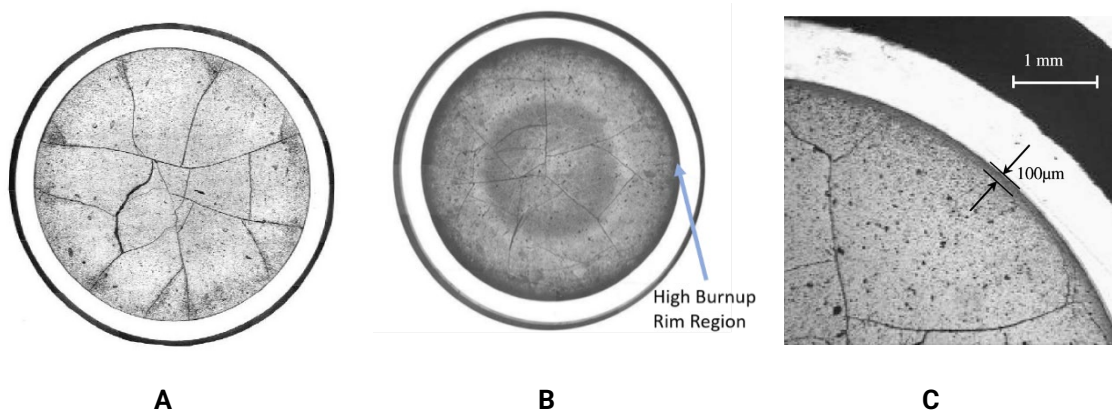


Figure 2-7. Cross sections of PWR fuel pellets.

Images of (A) a 35 GWd/MTU (average) PWR fuel pellet (Tsai Billone 2003); (B) a 67 GWd/MTU (average) PWR fuel pellet, indicating the high burnup rim region near the outer circumference of the fuel pellet (Tsai and Billone 2003); and (C) a 59 GWd/MTU (average) PWR fuel pellet, indicating the high burnup rim region within 100 μm of the outer circumference of the fuel pellet (Fors et al. 2009).

2.2.2 Characteristics of High Burnup Spent Nuclear Fuel Compared to Low Burnup Spent Nuclear Fuel

While the chemical and physical characteristics of nuclear fuel gradually change during irradiation, some of the changes in fuel pellets, fuel rods, and fuel assemblies tend to accelerate as irradiation proceeds beyond 45–50 GWd/MTU (IAEA 2011). Two examples are

⁴⁰ CRUD is a porous, metal oxide deposit that impedes heat flow from the rod to the coolant. Its chemical composition and crystalline structure depend on the type of reactor, the reactor coolant water impurities, and the construction materials of the reactor's primary cooling system (Sandoval et al. 1991).

⁴¹ In some literature, the rim region is called the "high burnup structure."

the extent, or depth, of the high burnup rim region at the outer surface of the fuel pellet and the rate of fission gas release (FGR) from the fuel pellets. These changes can affect HBF performance during storage, transportation, and disposal. Key changes in HBF and the potential effects of these changes on the performance of the fuel during storage, transportation, and disposal are summarized in Table 2-1 and discussed in the following sections and in Appendix A (see also Lovasic and Einziger [2009]).

Table 2-1 Changes in key characteristics of SNF and their potential effects as SNF burnup increases

Component	Change as fuel burnup increases (report section where discussed)	Potential Effects During Storage (S), Transportation (T), and Disposal (D) ^a
Fuel pellet	Increased fission product and actinide content (section 2.2.2.1)	<ol style="list-style-type: none"> 1. Higher radiation dose (S, T, D) 2. Higher fuel and cladding temperatures (S, T, D) 3. Longer cooling time in the pool or higher heat transfer capability of the cask (S, T, D) 4. Larger number of radionuclides ("source term") (S, T, D) 5. More pellet cracking (S, T, D)
	Increased fission gas release and rod internal pressure (section 2.2.2.2)	<ol style="list-style-type: none"> 1. Higher cladding stress (S, T, D) 2. Higher potential cladding failure and fission gas release if cask containment breaches (S, T) 3. Higher instant release fraction (D)^b
	Pellet rim formation (section 2.2.2.3)	<ol style="list-style-type: none"> 1. Higher airborne release fraction (S, T)^c 2. Different leach rate (D)
Cladding	Irradiation induced cladding alterations (Appendix A)	<ol style="list-style-type: none"> 1. Rod growth affects the structural response of the SNF rod during an accident (T) 2. Hardening changes the mechanical properties such as the yield strength (S, T)
	Pellet to cladding gap closure (section 2.2.2.4)	<ol style="list-style-type: none"> 1. Stress on the cladding due to increased internal rod gas pressure and pellet swelling (T)^d 2. Rod stiffness can increase (S, T)
	Increased cladding corrosion (section 2.2.2.5)	<ol style="list-style-type: none"> 1. Thinner cladding wall resulting in higher cladding stress and potential rod breach (S, T) 2. Increased hydrogen pickup during reactor operations (S, T, D)
	Higher hydride content (section 2.2.2.5)	<ol style="list-style-type: none"> 1. Changes to the mechanical properties such as the yield strength (S, T) 2. May lead to hydride reorientation and degradation of mechanical properties (S, T)
Assembly	BWR channel and assembly deformation (section 2.2.2.6)	Loss of assembly structural configuration that could complicate retrieval (S, T)
	Spacer grid embrittlement (Appendix A)	Potential to change the rod spacing (T)

^a A more complete description of SNF changes and their effects can be found in Appendix A.

^b The instant release fraction is the fraction of fission products and actinides present in the pellet-cladding gap that are expected to be released rapidly when water breaches the disposal package and SNF cladding in a geological repository.

^c In accident analyses involving radioactive materials, the airborne release fraction “is the fraction of [radioactive material released in an accident] that can be suspended to become available for airborne transport following a specific set of induced physical stresses” (SAIC 1998).

^d The pellet-cladding gap in PWR fuel rods tends to close during reactor operations due to the pressure of the reactor coolant causing the cladding to creep down onto the fuel pellets. In low burnup fuel, the gap will open again due to differential thermal expansion as the fuel cools. At higher burnups, the fuel pellets swell more and the pellets and cladding become chemically bonded during reactor operation. This tends to prevent the cladding from pulling away from the fuel pellets after the fuel is discharged from the reactor.

A key point of interest, and the focus of much of the DOE research effort, is determining whether the characteristics of the HBF can change in unexpected ways or rates during extended dry storage and transportation. The DOE research aims to gather data about the characteristics and performance of HBF to ensure that storage and transportation cask systems, when loaded with HBF, will be able to meet NRC safety requirements for retrieval from storage, potential repackaging, transportation, potential centralized storage followed by more transportation, and finally, disposal.

The changes in HBF characteristics, as fuel burnup increases, are discussed below in the order they appear in Table 2-1, except for “irradiation induced cladding alterations,” and “spacer grid embrittlement” which are discussed in Appendix A.

2.2.2.1 Increased Fission Product and Actinide Content

Increased burnup results in SNF with increased concentrations of fission products and actinides other than uranium (primarily plutonium) (Lovasic and Einziger 2009). Changes in the radionuclide distribution occur in both the fuel pellet matrix (the uranium dioxide grains) and at the grain boundaries. This, in turn, can affect the behavior of the gaseous fission product inventory that is available to be released to the fuel rod free volume, which is the volume comprised of the pellet-cladding gap and the fuel rod plenum. As fission product and actinide concentrations increase, the SNF becomes more radioactive, and the decay heat increases (per unit mass).

2.2.2.2 Increased Fission Gas Release and Rod Internal Pressure

Only a few of the fission products generated during reactor operation are gases at fuel operating temperatures. Two of these, xenon and krypton, are noble gases. The FGR⁴² of xenon and krypton to the rod free volume during reactor operation can vary slightly within a batch of fuel discharged from a reactor. The FGR increases with burnup⁴³ and leads to higher rod internal pressure, which increases the hoop stress on the cladding. This may also

⁴² FGR is the fraction of fission gas generated in the fuel pellets that is released to the pellet-cladding gap and the fuel rod plenum.

⁴³ When discussing FGR, one needs to distinguish between the average rod burnup that is relevant when determining the FGR by puncturing a rod, and the localized burnup that is determined by measuring the FGR from a small sample cut from the fuel pellet. A fuel rod with an average burnup in the range of 60 GWd/MTU may contain fuel pellets that have experienced substantially higher localized burnup if located axially away from the ends of the rod and at the outer circumference of the fuel pellet (the rim region).

contribute to a greater release of radioactive materials in the event that SNF cladding and the SNF cask or canister are breached in the event of an accident during storage, transport, or disposal operations.

2.2.2.3 Pellet Rim Formation

The isotope concentrations within fuel pellets change during irradiation in a reactor. Neutron capture is higher at the fuel pellet surface, which leads to higher concentrations of isotopes at the pellet surface as compared to the center of the pellet (Jernkvist and Massih 2002).

The non-uniform buildup of plutonium is important because it is the underlying cause of the rim region that develops near the circumferential surface of the pellet (see Figure 2-7B and Appendix A). This may add to the total amount of fission gas that can be released from the pellet to the free volume of the fuel rod. It could also add to the proportion of small, respirable particulates of radioactive material that could be released if a fuel rod were to experience a gross breach and the SNF cask system also experiences a breach in the event of an accident during storage or transportation. This latter effect is mitigated to a variable extent by the reduction in the size of the pellet-cladding gap that occurs in HBF, creating a greater resistance to gas flow that leads to slower depressurization and fewer entrained particles.⁴⁴

After disposal, the larger concentration of small fuel particles in the rim region of HBF compared to LBF may contribute to a faster release of radioactive material to the repository environment. This would occur because the smaller fuel particles may experience a greater leach rate when groundwater eventually reaches the fuel after corrosion and failure of the waste package, the SNF cask or canister, and the SNF cladding.

2.2.2.4 Pellet to Cladding Gap Closure

PWR and BWR fuel is manufactured with a small pellet-cladding gap that is flushed and filled with helium to remove moisture, minimize the pressure differential across the cladding during reactor operations, and increase the thermal conductance from the fuel pellets to the cladding (see Appendix A, Figures A-2 and A-3). This gap closes as the fuel pellets swell and the cladding deforms down onto the fuel pellet surface under the pressure of the reactor coolant. This phenomenon is more prevalent in PWR fuel rods than BWR fuel rods and the gap closes earlier in PWR fuel than in BWR fuel due to higher coolant pressures and thinner PWR cladding. Decreases in the gap size and increased chemical bonding of the fuel to the cladding at higher burnup increases the stiffness of the rods (Wang and Wang 2017), which could improve HBF rod fatigue life and reduce the potential for cladding damage in the event of a transportation accident if the bond remains intact (NRC 2020d).

2.2.2.5 Increased Cladding Corrosion and Higher Hydride Content

During irradiation in a water-cooled reactor, fuel cladding walls can thin by up to 10% because of oxidation by the reactor coolant water. In this process, some of the water

⁴⁴ Since radioactive particulate release will have a strong influence on the potential source term for contamination analysis, the effect of the fuel pellet rim region on the release fraction of fuel particulate was studied by Rondinella et al. (2015). Gas transmission inside fuel rods was also studied by Montgomery et al. (2018) during the decompression studies of the HDRP sister rods. For more detail, see section 3.3 and Appendix G of this report.

molecules are broken down into oxygen and hydrogen. The extent of oxidation depends on the metallurgical properties and chemical composition of the cladding and the coolant water chemistry and temperature. As a result of the oxidation process, the cladding thickness decreases and layers of zirconium oxide begin to grow on the outer surface. Some newer zirconium-based alloys, such as M5[®], have been designed to be more resistant to this oxidation. For the older Zircaloy cladding types, such as Zircaloy-4, the layers of zirconium oxide start to grow more rapidly beyond a burnup of about 40 GWd/MTU (Motta, Couet, and Comstock 2015). High burnup PWR rods with Zircaloy-4 cladding have been observed with oxide thicknesses of 80–100 μm ⁴⁵ and higher (Sabol et al. 1997). Since this oxide is porous, no credit is taken⁴⁶ for its strength in modeling the potential response of irradiated cladding to transportation accidents (NRC 2003).

During the cladding oxidation process, between 15 and 20% of the hydrogen produced diffuses through the oxide layer and into the cladding (for details, see Appendices A and F). The percentage of generated hydrogen that diffuses into the cladding decreases as the burnup increases. When the hydrogen concentration in the cladding reaches its solubility limit, any hydrogen beyond the limit combines with zirconium and precipitates within the cladding alloy as zirconium hydride (often called simply “hydride”). Multiple zirconium hydride precipitates (or platelets) can combine to form a brittle hydride-rich layer within the cladding, as shown in Figure 2-8. Because hydrogen that is dissolved in the Zircaloy cladding migrates to regions of lower temperature, the hydrogen tends to collect (and precipitate) near the outer, cooler surface of the cladding. With the exception of some new alloy designs, such as M5[®], at burnups greater than about 40 GWd/MTU, a brittle hydride-rich layer forms at the outer surface of the cladding, just beneath the zirconium oxide layers.

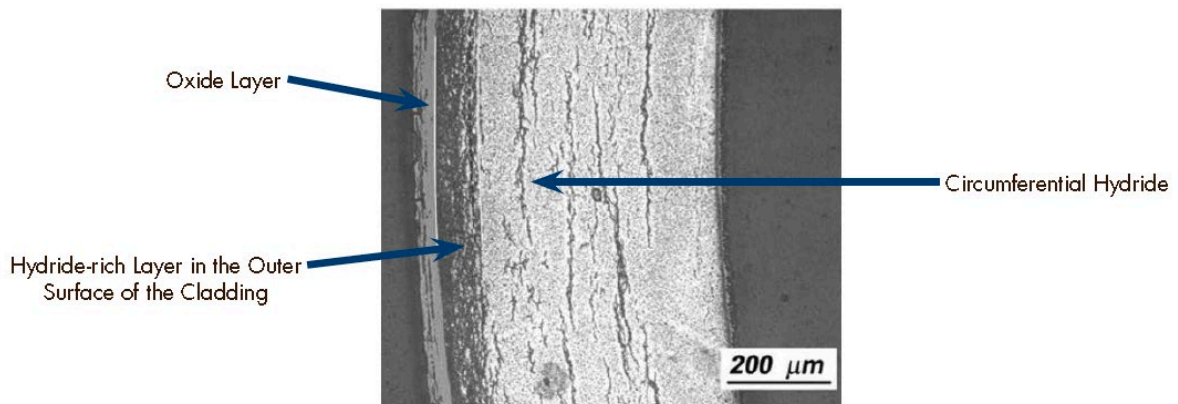


Figure 2-8. Hydride distribution and orientation in high burnup (~70 GWd/MTU) PWR ZIRLO™ cladding about 1.1 meters above the fuel mid-plane. The hydrogen content of the hydride-rich layer is 660 weight parts per million (wppm) (Billone, Burtseva, and Einziger 2013). The hydrides form in the circumferential direction due to the orientation of the cladding grains (texture) developed during the manufacturing process.

⁴⁵ The cladding thickness of PWR fuel rods is approximately 600 μm (Billone, Burtseva, and Einziger 2013) and therefore, the oxide thickness can be as large as 17% of the cladding thickness. Note that this value varies with fuel assembly design and cladding material type.

⁴⁶ When calculating the stress in the cladding tube, the thickness of the cladding is reduced by the thickness of the metal that has corroded. Hence, no credit is taken for the corrosion layer.

In radial cross-sections of the cladding, these hydride platelets are observed as parts of rings, or arcs, aligned parallel to the cladding surface (see Figure 2-8), and in axial cross-sections they are observed as linear features parallel to the cladding axis (not shown). Because their orientation is parallel to the outer circumference of the cladding, these hydrides are sometimes called circumferential hydrides. Most of the hydride precipitation occurs after SNF is removed from the reactor and is stored in the spent fuel pool at temperatures of ~30-40°C (86–104°F) (Billone et al. 2008). As long as the cladding temperature remains below approximately 200°C (392°F), the hydrides remain fixed within the alloy structure of the cladding.

The orientation of hydride precipitates tends to be different in BWR fuel cladding compared to PWR fuel cladding. The BWR fuel cladding is formed by a recrystallization and annealing process not used for PWR fuel cladding. This process results in equiaxed grains⁴⁷ in the cladding. Because of this grain structure, the hydrides in BWR SNF tend to precipitate in random orientations (Cook et al. 1991).

New cladding designs and materials developed for both PWRs and BWRs have improved oxidation resistance resulting in less hydrogen absorption in the cladding compared to older cladding types and therefore, less hydride precipitation. For more detailed discussions of hydride precipitation, hydride orientation, and the effects of hydrides, see section 3.2.1, and Appendices A and F.

The mechanical properties of cladding change during reactor operation due to oxidation of the outer surface of the cladding and the dissolution of hydrogen in the zirconium alloy (Appendix F). The oxide layer gets thicker with increasing burnup (Motta and Chen 2012) and causes most cladding to absorb more hydrogen, which eventually may precipitate as zirconium hydrides and lead to reduced cladding ductility. Reduction in cladding ductility would lead to a higher probability of cladding breaches in the event of a transportation accident (compared to cladding with greater ductility). The average hydrogen content of LBF cladding is approximately 100–200 wppm. At this concentration, the hydrogen and any precipitated hydrides have little effect on the mechanical properties of the cladding (Appendix F) (Yagnik et al. 2004; Yagnik, Hermann, and Kuo 2005). At higher burnups, depending on the alloy type, cladding has been measured to absorb 500-1000 wppm hydrogen in certain locations. Only at the very upper end of this range will hydrides in the circumferential orientation affect the ductile behavior of the cladding.

2.2.2.6 Boiling Water Reactor Channel and Assembly Deformation

Due to damage from the neutron flux and temperature gradients in the reactor, BWR channels are subject to several types of deformation, including slight bending or “bowing.” The deformation tends to increase with burnup but is physically constrained by the available space in the core. Assemblies can be difficult to place into or remove from the baskets inside storage and transportation canisters or casks if they are too deformed to fit properly. In addition, any deformation must be accounted for in structural analyses, either to

⁴⁷ Equiaxed grains of zirconium alloy metal are grains having axes of equal length in all three dimensions.

determine the potential rod damage during a drop accident or for precise heat-transfer calculations to predict cladding temperatures.

2.3 Research on Spent Nuclear Fuel Storage Prior to Current DOE Studies

The initial characterization and performance testing of SNF to support the design of a waste repository, which started in the mid-1970s, was not intended to support dry storage and transportation of SNF. Prior to that time, little commercial SNF was transported and when it was, it was transported in small-capacity, water-filled casks holding one or two assemblies (Anderson and Meyer 1980). In the early 1980s, spent fuel pools at operating reactors began to reach their NRC-licensed capacity and the nuclear utilities began to consider options to alleviate the pool storage limitations. Hanford Engineering Development Laboratory at the Pacific Northwest Laboratory (now PNNL) in the U.S., as well as programs in Canada and Germany, began to support major research efforts on storing and transporting SNF (Boase and Vandergraaf 1977; Davis 1979; Peehs, Bokelmann, and Fleisch 1986).

At that time, regulations for storing and transporting SNF were being written by the NRC (Appendix C). A primary concern was the potential for SNF cladding to deform under a sustained applied stress such as that from fission gas pressure inside the fuel rod (i.e., “cladding creep”). Based on German criteria for cladding creep in the reactor, storage conditions (e.g. temperature, gaseous atmosphere, and rod stress) were set so the maximum cladding creep did not exceed 1%. Subsequently, studies conducted in Germany evaluated the types of cladding degradation mechanisms that might occur during dry storage (Peehs, Kaspar, and Steinberg 1986) and concluded that cladding creep is a self-limiting mechanism because, as cladding creeps, the rod volume increases and the cladding stress drops. The 1% creep limit became generally accepted.

In the late 1970s, Hanford Engineering Development Laboratory started a program to characterize and test whole rod performance (cladding creep, failure lifetime, gas release, etc.) for the Basalt Waste Isolation Project repository program (Davis 1979; Einziger et al. 1982; Einziger and Kohli 1984). This work was also applicable to SNF dry storage. During one test, sponsored by Hanford Engineering Development Laboratory, pressure was lost in an SNF rod because of a faulty brazed joint near the rod end cap, and the stress on the cladding was significantly reduced. In post-test examinations, it was observed that cladding hydrides had reoriented to an unfavorable radial orientation in the test rods that did not lose internal pressure but remained in the circumferential orientation (i.e., did not reorient) in the depressurized rod (Einziger and Kohli 1984). See section 3.2.1 and Appendix F for more detailed descriptions of hydride reorientation. Hydride reorientation was a surprise because it was observed in cladding that had been textured to preclude reorientation in the reactor.⁴⁸ Although hydride reorientation is a concern because it could eventually lead to reduced ductility in the cladding under certain conditions, the potential for hydride reorientation to pose an unacceptable safety risk in dry storage was not investigated at the time.

⁴⁸ While it was discovered by Louthan and Marshall (1963) that hydride reorientation could happen in the reactor, it was thought to have been prevented by controlling the texture of the cladding during manufacturing so that all the precipitation would occur in the circumferential direction.

Detailed analyses of cladding creep mechanisms that might occur during dry storage were conducted later at Pacific Northwest Laboratory and then PNNL (Tarn, Madsen, and Chin 1986; Simonen and Gilbert 1988; Gilbert et al. 2002). Based on the data available, NRC set a maximum cladding temperature limit for drying and storing SNF of all burnups at 400°C (752°F) (NRC 2003). According to the NRC, this criterion, among others, “will limit cladding hoop stresses and limit the amount of soluble hydrogen available to form radial hydrides” (NRC 2003).

The Pacific Northwest Laboratory also sponsored a demonstration test at the Idaho National Engineering Laboratory (now INL) to benchmark the thermal models developed to predict the temperatures and radiation doses in dry cask storage systems using data from LBF in dry cask storage systems on a storage pad at the Idaho site (McKinnon and DeLoach 1993). One of these systems, the Castor V/21, was opened after 15 years to examine the fuel. The non-destructive examination and destructive examination at ANL revealed that—within experimental uncertainty—the condition of the LBF was the same as when it was loaded into the cask (Einzigler et al. 2003). This demonstration is described in more detail in Appendix G.

By the mid-1980s, dry storage was an NRC-approved method for utilities to store SNF as reactor spent fuel pools reached their maximum allowed storage capacity.⁴⁹ At the time, the maximum assembly average burnup was approximately 45 GWd/MTU. When it became clear that DOE would not begin accepting fuel in 1998 for transportation to a repository as planned, utilities recognized that more SNF would need to be placed in dry storage when spent fuel pools reached their maximum allowed capacity. At the same time, the reactors were irradiating the fuel longer to reduce costs, causing fuel burnups to increase beyond 45 GWd/MTU. Doing so required changes to the design of the fuel and resulted in changes in the characteristics of the SNF after it was irradiated in the reactor (see section 2.2 and Appendix A).

During a 2008 Board meeting (Garrick 2009), it became apparent that some SNF would remain in temporary storage facilities for considerably longer than the initial 20-year term approved by the NRC. This highlighted the need to gather information on fuel performance during extended storage and subsequent transportation. That meeting, among other drivers, prompted the Electric Power Research Institute (EPRI) to set up the Extended Storage Collaboration Program (ESCP) in 2009 to assess the implications of extended storage followed by transportation of HBF. Clearly identifying the technical information needs to be met by ongoing storage and transportation research is a key focus of the ESCP effort.

2.4 Technical Information Needs for Spent Nuclear Fuel Storage and Transportation

The NRC, DOE, EPRI ESCP (which included participation by DOE), and organizations in other countries have developed lists of prioritized technical information needs related to SNF storage and transportation. Some organizations also refer to technical information needs as “data gaps” and call their evaluations “gap reports.” Meeting the HBF technical information needs is intended to provide a better understanding of the performance of HBF during

⁴⁹ The Surry nuclear power plant site received its first dry storage license in 1986.

extended storage as the basis for predicting the changes in characteristics that may occur during subsequent transportation and interim storage, if used. This EPRI ESCP effort, taking account of gap reports by DOE, NRC, and the Board, was based on knowledge, testing, modeling, and operational experience gained from previous studies of LBF (Appendix B). Detailed tables providing each organization's listing of technical information needs, rankings, and priorities, and a short reason for each technical information need are provided in Appendix B. DOE distinguishes between rankings and priorities. Rankings that are high, medium, or low, refer to the importance of obtaining the data. Priority refers to the order in which the data will be obtained, given the availability of funding, SNF samples, and hot cells, among other things.

2.4.1 Technical Information Needs Identified by DOE

DOE published its first report on technical information needs for SNF storage and transportation in 2012 (Hanson et al. 2012) and has updated various aspects of the report several times, most recently in 2019 (Teague et al. 2019). DOE's technical information needs are similar to those discussed by the Board (NWTRB 2010) and those identified by EPRI, the NRC, and the international community (see Appendix B). The DOE technical information needs reports and the need to support aging management programs for SNF storage systems⁵⁰ form the basis for the DOE research agenda. Table 2-2 provides a summary of DOE's efforts to list and prioritize technical information needs that formed the basis for its HBF R&D program. One key effort in the DOE R&D program is the High Burnup Dry Storage Cask Research and Development Project (HDRP), which is co-sponsored by EPRI.⁵¹ The HDRP includes activities to examine HBF rods, and to monitor HBF under actual storage conditions to gather temperature data and confirm predictions of expected HBF performance (see Appendix G).

2.4.2 Board Assessment of DOE Technical Information Needs

The Board notes that several organizations have identified technical information needs for the storage and transportation of SNF. However, the priority given to meeting the technical information needs varied significantly from group to group due to the different situations each organization faced and the urgency for needing the data. For example, DOE originally prioritized the technical information needs based on two criteria: (1) how urgently the information was needed to support the renewal of licenses and certificates of compliance for HBF dry storage, and (2) the time required to accomplish the work. The NRC, however, prioritized the technical information needs based on what information was needed to determine if any technical issues had regulatory implications (NRC 2014b).

⁵⁰ Aging management programs are programs to identify degradation mechanisms for a material, component, or facility; perform periodic re-examination; and plan and implement any remediation or replacement that may be necessary. An extensive discussion of aging management programs can be found in NRC (2016b).

⁵¹ The HDRP acronym has different meanings depending on the organization using the term: for example, for DOE, it is the High Burnup Spent Fuel Data Project.

Table 2-2 High or medium^a priority DOE technical information needs related to SNF and SNF cladding.

Component Affected	Technical Information Need (Alsaed and Hanson 2017; Teague et al 2019)	Recent and Ongoing Work by DOE and others to satisfy the Technical Information Need
Cladding	Hydrogen Effects	
	Delayed hydride cracking	No work. This previous high-priority issue (Hanson et al. 2012) was downgraded to medium priority (Alsaed and Hanson 2017) due to an NRC determination that this was not an active mechanism (Raynaud and Einziger 2015)
	Hydride reorientation	Testing at ANL, ORNL, and PNNL; ASTM International review; and computer model development
Cross-Cutting	Drying	SNF drying tests at the University of South Carolina, revision of the ASTM standard guide on SNF drying (ASTM International 2016), modeling of radiolysis effects, and HDRP testing
	Stress Profile Measurement and modeling ^b	Bend tests, road tests, shaker table tests, Multi-modal Transportation Test, and PNNL model development
	Temperature profile measurement and modeling	Developing computer models to predict HDRP test Cask thermal conditions and benchmarking the models against measured temperatures

^a All priorities are high except delayed hydride cracking, which has a medium priority.

^b Stresses in SNF cladding arise from various sources, including rod internal pressure, temperature gradients, fabrication, vibration, and handling.

The Board reviewed the most recent DOE report on technical information needs (Teague et al. 2019), including the DOE ranking of technical information needs for the study of HBF. The Board finds that the DOE listing of priority technical information needs is largely consistent with the Board’s previously-published “recommended research needs” for extended storage and transportation of SNF (NWTRB 2010). The Board agrees with the DOE-identified technical information needs and priorities, with one exception; the Board believes the cross-cutting research area of fuel performance modeling should be pursued as a priority effort. The Board considers fuel performance modeling to be an important effort that, when fully developed, will provide valuable computer-based tools for predicting the characteristics and performance of HBF, including HBF with operating histories and/or cladding types that have not been fully studied and characterized.

The Board finds that the EPRI ESCP effort supports the conclusion that the technical information needs identified by DOE are appropriate because the DOE technical information needs are comparable to the ESCP technical information needs (EPRI 2012), which were identified through a deliberative process that included input from several U.S. and overseas

SNF experts. For a detailed discussion of the HBF technical information needs identified by other organizations in the U.S. and other countries, see Appendix B.

Although the technical information needs appear to be appropriate, the various DOE reports on technical information needs do not provide a clear indication of how the results of the DOE research projects will be used to meet the technical information needs. As decisions are made concerning the path that the SNF will take from the reactor to eventual disposal, it may be necessary to revise the technical information needs, both in character and priority. The Board's evaluation of the appropriateness of the DOE projects to address the technical information needs and the scope of these projects to adequately bound all HBF types and operating conditions are the focus of this report.

2.5 Research and Analyses of the Consequences of a Release of Radioactive Material from High Burnup Fuel in a Postulated Accident

DOE prioritized its technical information needs related to HBF based on the need to support future management of HBF storage and transportation including obtaining NRC approval of transportation certificates of compliance. DOE's research efforts to-date have focused on issues related to whether the SNF cladding could be grossly breached (i.e., the probability of gross breach) under the conditions to which it is expected to be exposed (e.g., normal conditions of transport). However, DOE's research efforts are still in the early stages of examining the potential for release of radioactive material, criticality, and radiation exposure to workers and the public (i.e., the consequences of a gross breach) that may result from the degradation of HBF cladding. Other organizations such as EPRI (EPRI 2017) are also studying the potential consequences of a gross breach in HBF cladding that may occur during transportation. EPRI also sponsored research to study the amount of radioactive material (source term) available to be released from a grossly breached SNF rod (EPRI 2018). The Board notes that DOE contributes funding for and participates in the EPRI ESCP effort and is aware of the ongoing studies related to consequence analysis.

2.6 Implications of High Burnup Fuel on the Geologic Disposal of Spent Nuclear Fuel

As summarized in Table 2-1, HBF has several characteristics that make it different from LBF, including higher decay heat, higher radioactivity, and higher concentrations of fission products and actinides. However, as discussed in Appendix D, only the higher decay heat of HBF could have a significant effect on geologic disposal of SNF.

2.6.1 Thermal Effects

At any given decay time, HBF generates more decay heat per unit mass, on average, than LBF, so disposal of HBF would increase the temperature in the near field⁵² of a geologic repository more so than disposal of LBF, with the extent of the increase depending on

⁵² "Near field" is the excavated area of a repository near or in contact with the waste packages, including filling or sealing materials, and those parts of the host medium/rock whose characteristics have been or could be altered by the repository or its content (IAEA 2003).

several factors. These factors include the waste package loading (i.e., the number of SNF assemblies in the waste package), the characteristics (e.g., thermal conductivity) of the host rock and engineered barrier (i.e., buffer, backfill), the repository design (e.g., spacing of waste packages and disposal drifts, backfilled or unbackfilled drifts), SNF storage time for decay, disposal drift ventilation period, and, of course, fuel burnup. For example, Liljenfeldt et al. (2017) presented calculated temperatures at the waste package surface and at the drift wall of a repository in sedimentary (clay-rich) rock resulting from the emplacement of a waste package that contains 32 PWR SNF assemblies. The results reported by Liljenfeldt et al. (2017) show that, if the backfill has a thermal conductivity of 0.6 W/m-K, the peak waste package surface temperature can reach approximately 150, 260, and 350°C for SNF burnup levels of 20, 40, and 60 GWd/MTU, respectively. Similarly, the peak drift wall temperature can reach approximately 70, 105, and 135°C from disposal of SNF with burnup levels of 20, 40, and 60 GWd/MTU, respectively.

Because temperature is an important driver for many thermal, hydrological, mechanical, and chemical processes, the higher temperatures resulting from disposal of HBF will increase the degree, extent, and significance of coupled thermal–hydrological–mechanical–chemical processes in the repository near field. These coupled processes could, for example, affect the performance of the bentonite buffer that is used in some repository concepts to protect and isolate the waste canisters and to retain and retard radionuclides once the canisters have breached. Bentonite is a clay with a high content of minerals that swell when wetted to impede water flow and retard radionuclide transport. However, elevated temperatures can alter its mineralogical, hydraulic, and geomechanical properties, which degrade its safety functions.

The rates of engineered material (e.g., waste package) corrosion and waste form dissolution also tend to increase with temperature. Thus, higher temperatures that may result from geologic disposal of HBF could lead to higher waste package corrosion and SNF degradation rates.

High temperatures also could affect the properties of the geologic host rock in the near field. In the case of repositories with clay-rich host rocks, heating can modify the structure and composition of the clay mineral components that are considered to be important for retarding radionuclide transport. In a salt repository, high temperatures could affect the local deformation rate of the salt body, which may cause changes in the salt porosity and permeability in the near field and facilitate the movement of water (liquid and vapor) around the waste package. Also, hydrous clay and sulfate minerals that may be present in bedded salt formations can dehydrate and release water upon heating, and the resulting brines potentially can contact the waste package and cause its corrosion. In crystalline host rocks such as granite, higher temperatures due to geologic disposal of HBF are unlikely to cause significant chemical alteration of the host rock, but thermally induced microcracking may degrade near-field in-situ mechanical properties or create flow paths for water movement and radionuclide transport through the geologic barrier. If the host rock is volcanic tuff, higher temperatures could facilitate the alteration of the volcanic glass in the tuff to zeolites and clay minerals. This alteration could enhance or impede radionuclide transport depending on the resulting changes in the porosity, permeability, and radionuclide sorption characteristics of the volcanic host rock.

Although thermal effects on host rocks can be significant in the disposal drifts of a repository, these effects will decrease as distance from the heat source increases. Thus, the performance of the natural barrier—the host rock in the far-field—should not be significantly affected.

2.6.2 Thermal Management

Because of concerns about temperature effects on repository performance, maximum temperature limits are imposed on various features of repository designs. For example, for the Finnish repository under construction and for the proposed Swedish repository, it is required that the temperature at the canister surface must not exceed 100°C to avoid mineral transformations in the buffer that could degrade its safety functions (SKB and Posiva Oy 2017). If HBF were to be emplaced in a repository with a similar temperature limit, the heat output of HBF waste packages could be reduced by decreasing the waste package loading, increasing the time the HBF is allowed to cool by radioactive decay during storage at a surface facility, or by ventilating the repository during the preclosure period after HBF emplacement. The potential thermal effects also could be reduced by increasing the waste package spacing in the disposal drifts or by increasing the spacing between the repository drifts, both of which would decrease the temperatures within the repository (Hardin et al. 2012).

3. EVALUATION OF DOE RESEARCH ON HIGH BURNUP FUEL PERFORMANCE DURING EXTENDED STORAGE AND TRANSPORTATION

This section provides the Board’s evaluation of five programmatic research areas in which DOE has sponsored work to address technical information needs or to advance cross-cutting research (in the case of fuel performance modeling) related to extended storage and transportation of HBF. Each sub-section below provides a brief discussion of the research area and a description of the relevant DOE activities. Each sub-section also contains the Board’s evaluation of the research, including test methods, completeness of the data reported, uncertainties in the data, utilization of the data to develop and validate predictive models, and applicability of the research to loaded HBF systems. Based on these evaluations, the Board’s findings and recommendations regarding the DOE research programs are presented. More extensive information on each of the research areas can be found in the appendices.

The five programmatic research areas are:

1. SNF Drying
2. Hydrogen Effects in HBF Cladding
3. HBF Performance under Normal Conditions of Dry Storage
4. HBF Performance under Normal Conditions of Transport
5. Fuel Performance Modeling

In some research areas, such as “SNF Performance under Normal Conditions of Dry Storage” and “SNF Performance under Normal Conditions of Transport,” there are multiple sub-parts to the research, and they are often interrelated. These interrelationships are noted where appropriate. Recommendations are made to improve the quality of the information obtained or to expand the usefulness of the data from the specific SNF types tested to other types of SNF that will be stored or transported but that have not been specifically tested.

3.1 Spent Nuclear Fuel Drying

At nuclear power plant sites, SNF, including HBF, is loaded into a cask (or canister) underwater. The water in the cask or canister is then drained and the inside is dried and backfilled with an inert gas (e.g., helium) to improve heat transfer and to reduce corrosion rates. However, little information is available about the quantity and form of water remaining inside an SNF cask or canister after drying because very few moisture samples have been obtained from loaded systems. In 2018, the Board highlighted to DOE the need for additional research on drying: “More work also is needed to quantify the amount and form of moisture that remains in a dry storage cask following drying performed according to typical industry practices” (Bahr 2018). This section (and Appendix E) will address drying and residual moisture in more detail.

3.1.1 Nuclear Regulatory Commission Guidance on Spent Nuclear Fuel Drying

NRC's NUREG-2216, *Standard Review Plan for Transportation Packages for Spent Fuel and Radioactive Material*, (NRC 2020b) provides guidance that there should be no more than 5% by volume of flammable gases, such as hydrogen, inside SNF transportation packages. Since SNF casks and canisters are backfilled with an inert gas (e.g., helium), the process by which hydrogen gas is generated would be primarily through radiolysis of any water remaining inside the cask or canister. Hydrogen gas could also be generated, to a lesser degree, by certain cladding corrosion processes caused by residual water in the cask (Jung et al. 2013). Therefore, the method by which the casks and canisters are dried should be designed to remove enough water to preclude the generation of 5% hydrogen by volume, which could be flammable if a sufficient concentration of oxygen were to be present. Oxygen is also generated by radiolysis, but its buildup is limited by consumption by oxidative corrosion of SNF cladding and internal components and surfaces of the cask or canister.

Some of the water inside the cask or canister is in the form of water vapor or liquid water (henceforth free water) which can be readily removed given sufficient drying time. Temperatures reached during vacuum drying are usually high enough to desorb water that is physically bound to SNF or internal components of an SNF cask or canister (i.e., physisorbed water⁵³); however, the temperature is not high enough to remove water that is chemically bound to SNF or internal components in the cask or canister (i.e., chemisorbed water⁵⁴). The oxide and CRUD layers on SNF are common adsorption points for chemisorbed water and HBF will typically have thicker oxide and CRUD layers than LBF of the same cladding type⁵⁵ because of its longer irradiation times.

One NRC-accepted dryness test (called the pressure rebound test) (Knoll and Gilbert 1987; ASTM International 2016) is conducted after an SNF cask or canister has been drained of water and vacuum dried. In the test, as implemented by the nuclear utilities, the SNF cask or canister is pumped down to a vacuum below 400 Pa (3 Torr, $\sim 6 \times 10^{-2}$ psi), isolated from the vacuum pump, and then the pressure in the cask or canister is monitored for 30 minutes. If the pressure in the cask does not rise above 3 Torr ($\sim 6 \times 10^{-2}$ psi), the cask passes the test. It is assumed that there is no significant amount of water in the cask or canister because the presence of water would lead to the formation of water vapor under vacuum conditions, creating a significant pressure rise in the cask. The results of the pressure rebound test conducted on the HDRP test cask, using this routine industry procedure, is shown in Figure 3-1 (EPRI 2019).

This dryness test does not specify the level (below 3 Torr [$\sim 6 \times 10^{-2}$ psi]) to which the pressure should be lowered in the system just before the vacuum pump is isolated. If the system is evacuated to a sufficiently low pressure, the pressure could remain below 3 Torr

⁵³ Physisorbed water (adsorbed water) is “water that is physically bound as an adsorbate (by weak forces) to internal or external surfaces of solid material” (ASTM International 2016).

⁵⁴ Chemisorbed water is “water that is bound to other species by forces whose energy levels approximate those of a chemical bond” (ASTM International 2016).

⁵⁵ The growth of oxide layers and CRUD layers has been reduced by the use of new-design fuels such as those with M5[®] cladding and by adjusting the placement of the fuel assemblies within the reactor core. However, much of the existing, older SNF will be adversely affected by the oxide and CRUD layers.

($\sim 6 \times 10^{-2}$ psi) during the 30-minute isolation period but could continue to rise and eventually exceed 3 Torr ($\sim 6 \times 10^{-2}$ psi) during a longer isolation period.

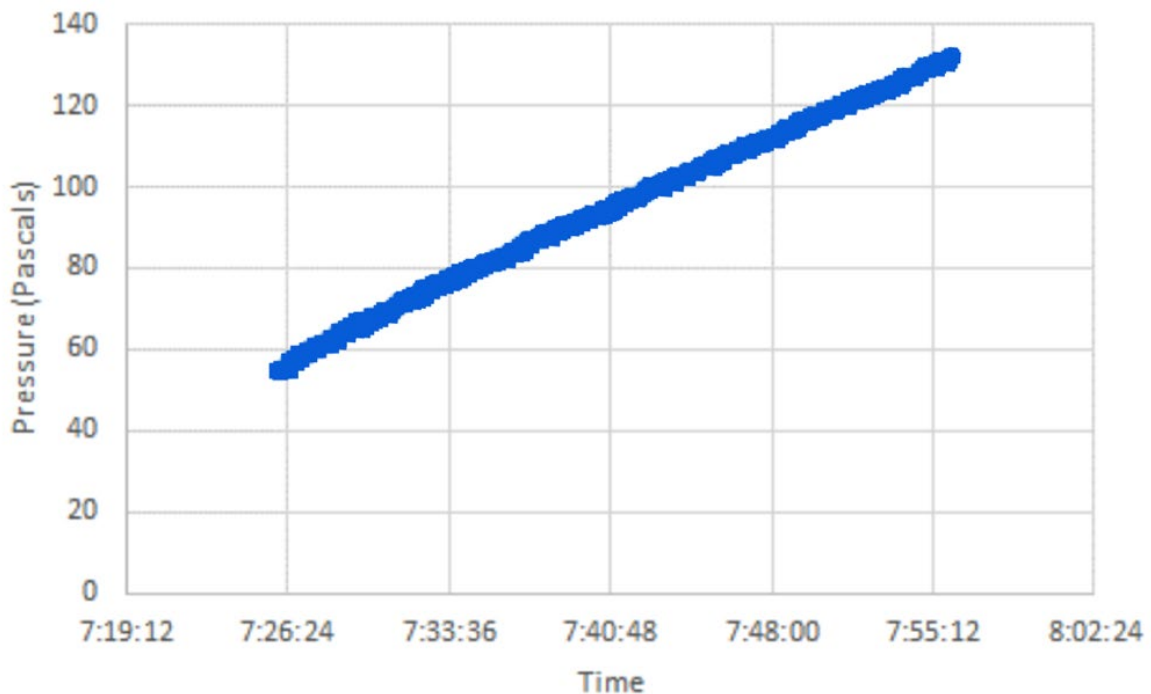


Figure 3-1. Results of the HDRP cask dryness test.

For reference, 140 Pa = 1.05 Torr (0.02 psi) (adapted from EPRI 2019).

3.1.2 Drying Research

As noted above, both free water and physisorbed water are expected to be removed from the cask or canister during the standard drying process. However, the chemisorbed water is not expected to be removed at temperatures lower than 500°C (932°F) (ASTM International 2016). Several reports examine the behavior of water, particularly chemisorbed water, remaining in an SNF cask or canister after drying and evaluate the release of that water through thermal or radiolytic means (e.g., see Jung et al. 2013; Wittman 2013; ASTM International 2016).

However, uncertainties remain regarding the behavior of the chemisorbed water and the behavior of any hydrogen and oxygen liberated due to radiolysis. Some of the reports provide significantly different results depending on the assumption that are made in the analyses. For example, Jung et al. (2013) concluded that, for most cases analyzed, the oxygen generated by radiolysis is consumed by oxidation of the SNF cladding and other metal surfaces in the dry cask storage system. However, in other cases analyzed, some oxygen remains in the cask. For example, assuming linear decomposition of water by radiolysis in about 72 years, low cladding initial temperatures (102–302°C [215– 575°F]), and a cladding failure rate of 0.01%, the amount of oxygen remaining after 300 years would be 21.8 moles (Jung et al. 2013).

In 2015, DOE sponsored an Integrated Research Program (IRP) that was jointly conducted by the University of South Carolina, the University of Florida, and Orano to evaluate how well two SNF drying processes, vacuum drying and forced helium dehydration (see ASTM International 2016 or Appendix E for more detail), remove free water from casks containing undamaged SNF or damaged SNF (Knight 2016). The program also began work to develop a computer model that can predict SNF drying processes for use by utilities, vendors, and regulators.

The IRP team built a mock cask system holding a surrogate fuel assembly that allowed the team to introduce known amounts of water into the system and evaluate different vacuum drying processes (Appendix E). Because the test rods in the IRP test did not include oxide or CRUD layers on their outer surfaces and no physisorbed or chemisorbed water, the IRP testing was limited to measuring the effectiveness of the drying processes on removing free water from the system. Results from the IRP testing are discussed in section 3.1.3. Additional details about the testing are included in Appendix E.

A second DOE research effort with relevance to HBF drying is the HDRP (see Appendix G for a description of the HDRP). In November 2017, the HDRP team completed an NRC-accepted vacuum drying process on an SNF storage cask loaded with 32 PWR HBF assemblies (the HDRP test cask). Because the HDRP cask was loaded with HBF, it has the potential to provide information about the amount of physisorbed and chemisorbed water in the oxide and CRUD layers of the fuel (EPRI 2014).

Three gas samples were obtained from the HDRP cask in the two-week period after drying to determine the amount of water vapor, hydrogen, and other gases in the cask. The sampling results for water vapor, reported by SNL, were ~17,400 ppm by volume \pm 10% (equivalent to ~100 ml [3.4 oz] of water) within the entire cask gas phase (Bryan et al. 2019). For comparison, it is assumed that if an SNF cask or canister passes the dryness test accepted by the NRC, then the quantity of water remaining should be no more than 7.74 ml (0.26 oz) (NRC 2020a). For the HDRP test cask, SNL noted that measuring water content “proved challenging.” However, given the relatively high temperatures in the cask, SNL concluded that “[i]f the cask gas phase is compositionally homogeneous, then liquid water is not present within the cask, unless trapped in inaccessible locations” (Bryan et al. 2019). Details of the gas sampling are included in Appendix E. DOE plans to obtain more gas samples from the HDRP cask just before or after transporting the cask to a facility where it can be opened to allow more rods to be removed for R&D at the end of the 10-year storage period (NWTRB 2019b).

DOE has continued to fund analyses of the potential consequences of water remaining in an SNF cask or canister after drying, including estimates of the quantities of hydrogen and oxygen generated due to radiolysis of water. For example, d’Entremont, Kesterson, and Sindelar (2020) estimated the generation of hydrogen and oxygen inside the HDRP cask after drying. In this study, it was assumed that no liquid water remained in the HDRP cask and that only water in the form of water vapor, physisorbed water, and chemisorbed water was available and subject to radiolysis. d’Entremont, Kesterson, and Sindelar (2020) evaluated several different gas generation scenarios, based on different assumptions about the locations of residual water and the possible “replenishment” of surface-adsorbed water from the water vapor in the cask. However, the results for the total hydrogen gas generation (at 12 days after drying) were highly variable, ranging from approximately 500 ppmv to

approximately 16,000 ppmv hydrogen, depending on the assumptions about residual water. For comparison, SNL measured approximately 500 ppmv hydrogen in a vapor sample obtained from the HDRP cask 12 days after drying (Bryan et al. 2019).

Regarding oxygen gas generation, d'Entremont, Kesterson, and Sindelar (2020) concluded that oxygen from radiolytic breakdown of free and surface water is not built up in the canister, and rather is assumed to be consumed by oxidation reactions. Overall, the study found that “[t]hese results illustrate the need for testing to refine understanding of radiolysis rates, etc., in systems closely resembling the SNF-in-canister materials system. ... A laboratory-scale test involving surrogate specimens to represent the materials in the canister is suggested” (d'Entremont, Kesterson, and Sindelar 2020).

DOE also sponsored work to develop a new sensor technology to detect and measure the amount of liquid water inside a dry cask storage system (Meyer et al. 2019). PNNL conducted a feasibility study utilizing ultrasonic sensors mounted on the exterior of the system. Through several scoping tests on a mock cask system, PNNL demonstrated the efficacy of the proposed sensing approach. Additional work is proposed to optimize the sensor design.

3.1.3 Evaluation and Findings

The goal of the IRP at University of South Carolina was to determine the effectiveness of different drying processes in removing residual free water from a cask with a variety of cask heat loadings and locations of residual water. In tests with no simulated failed rods, post-test inspections revealed “complete dryness of the chamber was achieved in every type of [forced helium dehydration] and vacuum test” (Knight et al. 2019). One notable result is that, in some tests that included a simulated grossly breached rod, free water remained in the rod even after the system passed the NRC-approved dryness test. The final report (Knight et al. 2019) does not include a detailed description of the specific test conditions used when drying the test cask with a simulated grossly breached rod. Therefore, an independent evaluation of the test results cannot be made, and some uncertainty remains regarding the amount of water that may be retained in occluded areas of an SNF cask or canister after drying.

Following drying of the HDRP test cask, the NRC dryness criterion was met. Sampling and analyses of the three gas samples taken over the two-week period after the cask was backfilled with helium proved to be difficult and, in some cases, the results were inconsistent or inconclusive as noted above (Bryan et al. 2019; EPRI 2020a). Due to the limited quantity of data obtained from the HDRP test cask regarding the amount of water vapor remaining in the cask after drying, DOE is planning additional testing to obtain more data (Hanson 2018). Bryan et al. (2019) described several lessons learned that can be applied to future water vapor sampling efforts. For example, the researchers noted “it is essential that the sample bottles be heated to desorb water adsorbed onto the interior of the bottles” (Bryan et al. 2019). The Board encourages DOE to validate gas sampling methods before attempting to obtain the next set of samples.

The Board notes that if further testing or further moisture measurements do not provide greater detail regarding the amount of moisture remaining in SNF casks and canisters, other drying processes that may be more effective (e.g., forced helium dehydration) and other

methods to evaluate the degree of dryness (e.g., falling rate method)⁵⁶ may need to be considered.

If all free water and physisorbed water is removed during draining and vacuum drying, the amount of chemisorbed water in the system determines the amount of hydrogen that can be generated by radiolysis. Hydrogen generated by radiolysis may accumulate in a cask or canister and it may be absorbed by the SNF cladding. Detailed analyses of the radiation effects on decomposition of water are available in the literature (Jung et al. 2013; Wittman 2013). Since radiolytic decomposition of chemisorbed water occurs over long time periods (years), even more effective dryness test methods (e.g., falling rate method) may not resolve outstanding issues with detecting chemisorbed water remaining in the cask. DOE planned “small scale tests” to examine further the implications of water remaining in an SNF cask after drying (Hanson 2018). However, as of December 2020, only preliminary analyses and development had been completed (e.g., see d’Entremont, Kesterson, and Sindelar 2020). DOE has also discussed a plan to obtain additional gas samples from of an SNF cask (Larson 2019) but, as of December 2020, the details of the plan have not been published.

The Board finds that:

- The 3-Torr ($\sim 6 \times 10^{-2}$ psi) pressure rebound test for dryness in an SNF cask or canister leads to some uncertainty about the quantity of water remaining after drying because the cask or canister pressure may still be rising when the test is deemed to have been completed successfully. The quantity of water remaining may be greater than intended following performance of the NRC-accepted drying processes.
- Chemisorbed water in the CRUD, oxide layers, or inside breached fuel rods might eventually undergo radiolysis, releasing oxygen and hydrogen to the gas space inside the cask or canister. Recent testing indicates little concern related to the generation of hydrogen or oxygen gases immediately after drying and early in the dry storage period. However, over extended storage periods, the significance of the presence of chemisorbed water, the subsequent release of oxygen and hydrogen to the inside of an SNF cask or canister, and the effect of metal corrosion in consuming radiolytic oxygen is not fully understood.
- There has been limited gas sampling, including sampling of water vapor, from SNF casks and canisters after long periods of dry storage. Additional gas sampling of the vapor space of commercial SNF casks or canisters would provide valuable information that may reduce uncertainties about the amount of water remaining after drying. Furthermore, there is a need to improve and validate gas sampling methods, with a focus on water vapor sampling and measurement.

⁵⁶ The falling rate method of dryness test is a method where the system is pumped down to an acceptable vacuum and the pressure in the system is allowed to rise. The time to reach a pre-determined (higher) pressure is measured. The system is subsequently pumped down again, and the process is repeated. The time to reach the predetermined upper pressure is plotted against the number of drying cycles. When the time required to reach the higher pressure is constant, the system is deemed dry (Christensen and Wendt 2001).

3.1.4 Recommendations for Spent Nuclear Fuel Drying.

- a. Recommendation: The Board recommends that DOE evaluate the extent to which chemisorbed water remains after the drying process is completed and whether this water could affect the ability of SNF cask or canister systems and their contents to continue to meet storage and transportation requirements.
- b. Recommendation: The Board recommends that DOE further explore the possibility of monitoring the moisture content and gas composition of dry cask storage systems loaded by nuclear utilities with HBF for an extended period. DOE should improve and validate gas sampling methods, with a particular focus on water vapor sampling and measurement, before the next samples are obtained.

3.2 Hydrogen Effects in High Burnup Fuel Cladding

Hydrogen produced during cladding oxidation in a nuclear reactor, when absorbed into HBF cladding, can have different chemical and physical forms. In certain temperature and stress conditions following discharge from the reactor, high hydrogen levels in SNF cladding can lead to embrittlement of the cladding and increase the probability of a gross breach when the cladding is subjected to sufficiently large physical shocks or stresses, such as those occurring in a pinch-mode of loading. DOE continues to sponsor research to understand better the behavior of hydrogen and zirconium hydride in HBF cladding and their potential adverse effects.

As discussed in Appendix F, one of the requirements of 10 CFR Part 71 is that the transportation package (i.e., a bolted-lid cask containing bare SNF assemblies or a transportation overpack with SNF assemblies inside a welded steel canister) must remain subcritical in the event of a transportation accident. If the SNF cladding experiences a fracture during a transportation accident, the fissile material (i.e., the fuel) might possibly change its location inside the cask or canister in a manner that would increase the possibility of criticality. To evaluate the potential for criticality under hypothetical accident conditions, it is necessary to perform criticality calculations assuming the cladding is damaged and the SNF is in a geometry that would maximize the potential for criticality. Furthermore, if there is a gross breach, more fission gas and particulates could be released to the cask or canister interior. If the cask or canister leaks after an accident, there could be unacceptable quantities of radioactive gases and particulates released to the environment.

The primary SNF cladding characteristic governing the potential for cladding fracture during a transportation accident is the cladding ductility. More ductile cladding will be better able to withstand large stresses without fracturing; more brittle (less ductile) cladding would be more susceptible to fracture. The main phenomenon affecting the ductility of SNF cladding is the formation within the cladding of relatively brittle zirconium hydrides in certain orientations that disrupt the relatively ductile zirconium alloy. This phenomenon is more prevalent in SNF with higher fuel burnup and in certain zirconium cladding alloys.

Understanding the ramifications of the potential adverse effects of zirconium hydrides on retrieving and transporting SNF after extended dry storage is a high priority. This high

priority has been independently determined by many organizations (NRC, DOE, EPRI, and groups in other countries) during their evaluations of technical information needs related to SNF extended storage and transportation (see Appendix B). Brief descriptions of the phenomena of hydrogen uptake, zirconium hydride formation, and hydride reorientation are provided below. More detailed descriptions of these phenomena can be found in Appendix F as well as Motta et al. (2019), EPRI (2020c), and NRC (2020).

3.2.1 Hydride Reorientation

3.2.1.1 What is Hydride Reorientation?

During irradiation in a nuclear reactor, the outside surface of all nuclear fuel cladding experiences some degree of oxidation. In the oxidation process, water molecules from the reactor coolant react with the zirconium alloy cladding of the fuel, thereby producing hydrogen and oxygen. The oxygen from the water forms zirconium oxides that build up on the outer surface of the fuel cladding, and a portion of the hydrogen from the water diffuses into solid solution in the zirconium alloy crystalline structure. At concentrations exceeding the solubility limit, some of the hydrogen combines with zirconium and precipitates as a chemical compound, zirconium hydride. Too much zirconium hydride in the cladding combined with an adverse orientation of the hydride precipitates can cause cladding embrittlement, potentially making the cladding more susceptible to fracture during handling and transportation. The amount of zirconium hydride that precipitates depends on the type of cladding, the cladding manufacturing process, the fuel operating history, and the temperature of the cladding. HBF generally contains more hydride precipitate than LBF, for any given cladding type.

At the time of discharge from the reactor, SNF cladding contains some zirconium hydride precipitates in the physical form of platelets that are predominately oriented around the circumference of the cladding (i.e., platelets aligned parallel to the cladding surface, like the rim of a bicycle wheel) (Figure 3-2). These zirconium hydride precipitates, or platelets, are often called “circumferential hydrides.”

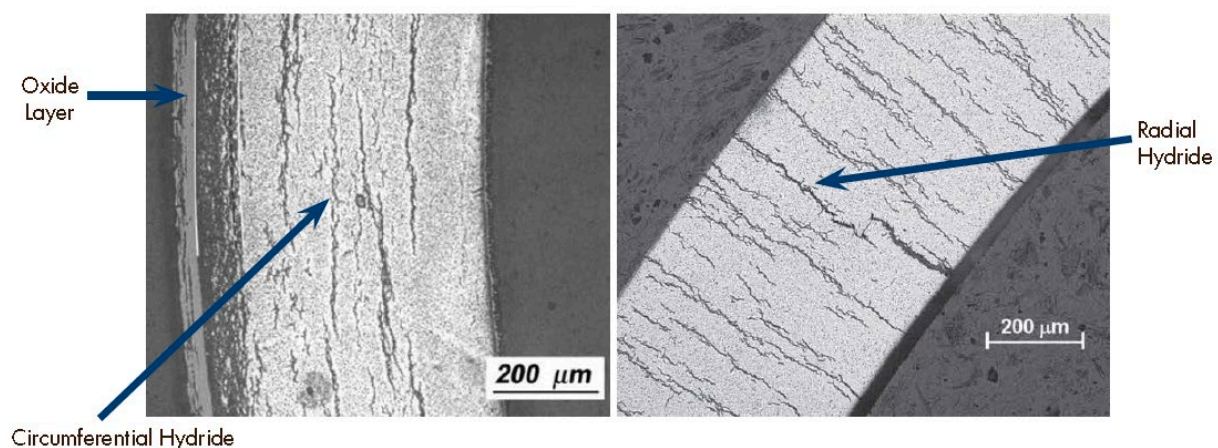


Figure 3-2. Circumferential and radial hydride orientations.

(A) depicts circumferential hydrides in zirconium-alloy cladding, and (B) depicts radial hydrides (Billone, Burtseva, and Einziger 2013).

When SNF is removed from wet storage and placed in a cask or canister, a drying process (e.g., vacuum drying, see section 3.1) is used to dry the SNF. During vacuum drying, SNF temperature increases due to the decay heat of the SNF coupled with reduced heat-transfer efficiency as water is drained from the SNF cask or canister and is replaced by a vacuum, which is a poor conductor of heat. When the temperature of SNF increases during the drying process, some of the hydrogen from zirconium hydrides goes back into solution in the zirconium alloy cladding in an amount up to the solubility limit at the local drying temperature. After the drying process is finished and verified, the cask or canister is backfilled with an inert gas (e.g., helium).

The helium gas increases heat transfer, thereby cooling the SNF. As the temperature drops during the storage period, the solubility of hydrogen in the cladding decreases causing some of the hydrogen to reprecipitate as zirconium hydride platelets. Some of these reprecipitated hydrides may form in a radial direction (i.e., platelets aligned perpendicular to the cladding surface, like the spokes of a bicycle wheel) when there is a sufficiently high tensile hoop stress on the cladding (Figure 3-3) from either rod internal pressure or swelling of fuel pellet fragments in contact with the cladding.

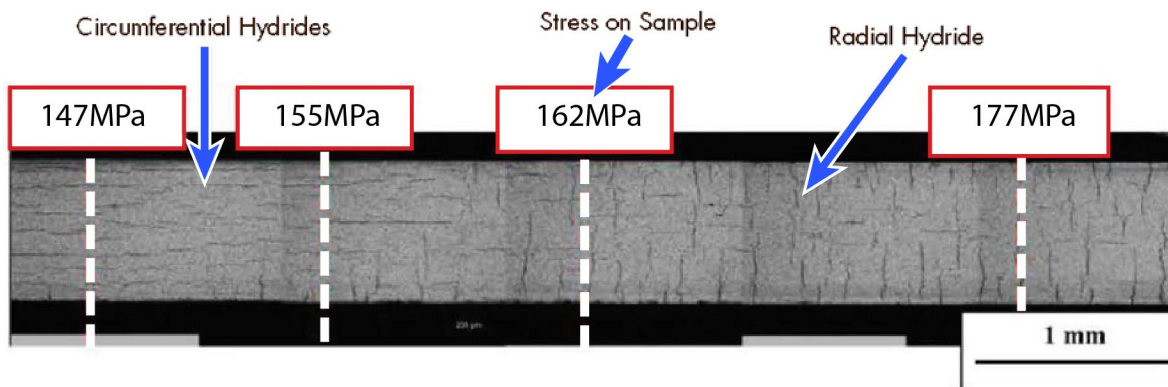


Figure 3-3. Effect of stress on hydride reorientation.

In this testing, Zircaloy-4 flat-plate test specimens were subjected to a tensile stress, simulating a hoop stress in tubular cladding. Note that the orientation of the hydrides in the sample depends on the stress to which the sample is subjected (*adapted from Cinbiz, Koss, and Motta 2016*).

This process of hydrides changing from a circumferential orientation to a radial orientation is known as hydride reorientation. It should be noted that this phenomenon does not occur during reactor operation because the high coolant pressure outside the cladding offsets the rod internal pressure and results in either a compressive stress or mild tensile stress on the cladding.

3.2.1.2 Potential Effects of Hydride Reorientation

Circumferential hydrides formed at cladding hydrogen concentrations typical of irradiated fuel cladding⁵⁷ are not of concern because the hydrides are always parallel to any expected

⁵⁷ Yagnik et al. (2004) found that dense circumferential hydrides, formed when cladding hydrogen concentrations exceeded approximately 900 ppm (depending on the cladding type), could cause a reduction in cladding ductility. However, a hydrogen concentration of 900 ppm is much higher than that found in irradiated fuel cladding.

external stresses and therefore, do not make the cladding more susceptible to fracture (Yagnik et al. 2004). As discussed in Appendix F, the presence of radial hydrides, however, may make the cladding more susceptible to fracture (i.e., the radial hydrides may reduce the cladding ductility) when an external stress is applied perpendicular to the cladding surface, as may occur during a fuel handling accident or a transportation accident.

Based on data compiled by ANL⁵⁸ (Appendix F, Chung 2004) and examinations of LBF from the 15-year demonstration test using PWR SNF with a burnup of ~34 GWd/MTU (Appendix G, Einziger et al. 2003), the NRC determined:

“The following acceptance criteria and review procedures are designed to provide reasonable assurance that the spent fuel is maintained in the configuration that is analyzed in the storage SARs [Safety Analysis Reports]. These criteria are applicable to all commercial spent fuel burnup levels and cladding materials.

In order to assure integrity of the cladding material, the following criteria should be met:

1. For all fuel burnups (low and high), the maximum calculated fuel cladding temperature should not exceed 400°C (752°F) for normal conditions of storage and short-term loading operations (e.g., drying, backfilling with inert gas, and transfer of the cask to the storage pad. ...”⁵⁹ (NRC 2003).

The Board notes that the NRC criteria listed in NRC (2003) were based on data obtained from LBF and with no data available from HBF.

In recent years, nuclear utilities have been operating nuclear fuel to an industry-wide average burnup of approximately 45 GWd/MTU (Peters, Vinson, and Carter 2020), which is higher than historical averages. For any given cladding type, higher burnups lead to higher hydrogen concentrations in cladding. Some new cladding types, such as M5[®], have been designed to reduce corrosion and hydrogen pick-up compared to the older Zircaloy-2 and Zircaloy-4 cladding types. However, for most older cladding types, higher burnups have led to more cladding corrosion, leading to increased thinning of the cladding, and slightly higher rod internal pressures due to increased FGR from the fuel pellets. As a result of this increased thinning and higher rod internal pressure, HBF experiences higher cladding stress. Uncertainties introduced by these new conditions led NRC and EPRI to fund ANL to conduct research to gather more information on the potential for hydride reorientation to occur and its ramifications (Billone, Burtseva, and Einziger 2013). This work is being continued with funding from DOE (Saltzstein et al. 2017a).

⁵⁸ As indicated in Appendix F, these data covered a broad range of fuel types and conditions, including irradiated and unirradiated cladding, various zirconium-based cladding alloys, different hydrogen levels in the cladding, and a large range of temperatures and stresses.

⁵⁹ The NRC cites two other criteria, related to thermal cycling and accident conditions, but this report is focused on the temperature limitation cited in criterion 1.

3.2.1.3 Inducing and Measuring Hydride Reorientation in the Laboratory

Zirconium hydrides reorient in SNF cladding when there is sufficiently high hydride concentrations and sufficiently high hoop stress from either rod internal pressure or swelling of the fuel pellets during storage. In the laboratory, hydride reorientation is induced using either a section of irradiated cladding that contains a measured hydride concentration or un-irradiated cladding infused with hydrogen. A hoop stress is applied to the cladding while increasing the temperature to dissolve the hydrogen from a portion of the hydrides—once the sample reaches the intended temperature, it is maintained at that temperature for a known length of time and subsequently cooled slowly while under either decreasing or constant stress. This process is called hydride reorientation treatment (HRT). After the sample is cool, it is examined metallurgically to determine if and to what degree reorientation occurred.

The NRC sponsored ANL to conduct testing on sections of unirradiated cladding infused with hydrogen and sections of irradiated HBF cladding. Both unirradiated and irradiated cladding were tested at a range of temperatures up to 400°C (752°F) and at a range of cladding hoop stresses up to the maximum expected in dry storage (see Appendix F). Key conclusions from the ANL study are summarized below (Billone, Burtseva, and Einziger 2013; Billone and Liu 2013).

1. Several factors influence the extent of hydride reorientation including the cladding composition, how it was manufactured, the maximum temperature experienced by the cladding, the maximum stress applied to the cladding, the rate at which the cladding cooled, and the number of drying cycles required to adequately dry the fuel.
2. Unirradiated cladding charged with hydrogen is a poor surrogate for irradiated cladding when trying to determine hydride reorientation effects.⁶⁰
3. As explained in detail in Appendix F, the conventional measure of hydride reorientation (the ratio of radial hydrides to total hydrides) can easily be misinterpreted depending on the amount of hydrogen in the cladding relative to the hydrogen solubility limit at the maximum cladding temperature.⁶¹

DOE has continued the ANL testing program but focused on lower cladding hoop stresses and lower maximum temperatures to reflect values closer to those found in recent DOE-sponsored research. DOE has also funded ANL to evaluate a range of cladding types, such as ZIRLO®, Zircaloy-4, and M5® (see Appendix F).

3.2.1.4 Ring Compression Tests of Cladding to Simulate Hypothetical Accident Conditions during Transportation

Hydride reorientation, if it occurs, happens either during the drying process or in the early stages of storage, but its ramifications may not be evident unless an accident occurs later in the lifetime of the HBF. Specifically, a side drop or side impact accident while the HBF is

⁶⁰ See Appendix F for details on this issue.

⁶¹ This is the maximum temperature the cladding reaches once it is placed in a storage cask and the cask has been drained, irrespective of whether this occurs during drying or after the cask is backfilled with an inert gas.

being transported can cause exterior stress to the cladding that is perpendicular to the orientation of the radial hydrides (like two fingers pinching a straw; see Figure 3-4) and may cause the cladding to fracture. Determining the ramifications of hydride reorientation requires knowledge of the ductility of the cladding across the range of potential temperatures of HBF cladding during transportation.

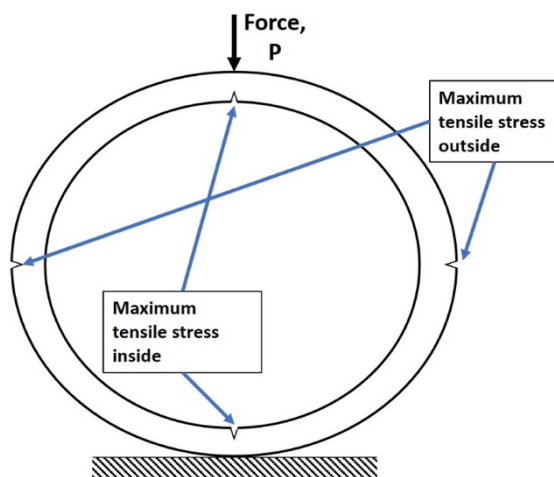


Figure 3-4. Pinch load, P, on a cross-section of cladding caused by a hypothetical transportation side drop accident.

The figure shows the locations of the maximum tensile stresses in the cladding.

There is a significant quantity of cladding ductility data at higher temperatures (Yagnik et al. 2004) but little data on the ductility of irradiated cladding with reoriented hydrides at the lower temperatures that cladding may experience during transportation. A testing program at ANL was started by the NRC (Billone et al. 2008) and continued by DOE (Billone, Burtseva, and Liu 2012) to determine the extent to which the ductility of HBF cladding is reduced under various conditions, such as lower temperature.

A common way to test cladding ductility is to cut a ring from a cladding sample and subject it to an external load in a series of ring compression tests until a cladding crack develops. Details of this test method can be found in Appendix F. ANL has conducted several sets of ring compression tests since the late 2000s (e.g., see Billone, Burtseva, and Einziger 2013; Billone and Liu 2013; Billone 2019; and Billone and Burtseva 2020). For each test, a load versus displacement (amount of deformation) curve was generated and this curve was used to determine changes in the ductility of the cladding sample (see Appendix F, Figure F-12).

ANL conducted ring compression tests on cladding samples that were “as-irradiated” (i.e., with no HRT) as well as cladding samples subjected to HRT under various temperature and hoop stress conditions to induce hydride reorientation. In some cases, the conditions of temperature and hoop stress applied during the ANL testing were significantly higher than those expected in the majority of SNF storage systems (Billone et al. 2013).⁶² ANL

⁶² At the time the ANL and NRC tests were conducted, the hoop stress on the cladding during the drying process was thought to be much larger than is now believed based on temperature measurements from the HDRP tests described in Appendix G.

continues to conduct ring compression tests on cladding samples from the HDRP sister rods (Billone and Burtseva 2020; see section 3.3.1.2, Appendix G).

Several observations have been made by researchers as a result of ANL ring compression tests and testing on the HDRP sister rods. The published observations and conclusions have evolved over time as more data have been collected:

- For the cladding types tested at ANL, the ring compression tests confirmed that the presence of radial hydrides, in sufficient concentrations, can reduce the ductility of the cladding. Furthermore, higher hydrogen concentrations in the cladding (above certain thresholds that depend on cladding type) and higher drying/storage temperatures and internal rod pressures (above certain thresholds that depend on cladding type) result in greater concentrations of radial hydrides in the cladding. (Billone, Burtseva, and Einziger 2013; Billone, Burtseva, and Martin-Rengel 2015; Billone, Burtseva, and Garcia-Infanta 2017).
- There is scatter in some of the ring compression data. Test results for high burnup ZIRLO[®] following ring compression tests at 350°C (662°F) appeared to have more scatter than test results conducted on the same material following ring compression tests at 400°C (752°F). Some of this scatter may have been due to the difficulty in interpreting load-displacement curves from the ring compression tests. The determination of cladding ductility could be improved by conducting repeat tests. (Billone, Burtseva, and Martin-Rengel 2015).
- Based on a limited series of ring compression tests on irradiated ZIRLO[®] samples that experienced a maximum cladding temperature of 350°C (662°F) during HRT, it appears that the cladding ductility began to decrease when temperatures decreased to approximately 120°C (248°F) during cooling. This temperature is higher than the temperature at which ductility began to decrease in specimens subjected to HRT with a maximum cladding temperature of 400°C (752°F). This was unexpected and opposite of behavior observed in other cladding specimens (i.e., the ZIRLO[®] cladding was more brittle rather than less brittle when the HRT temperature was changed from 400°C [752°F] to 350°C [662°F]) (Billone, Burtseva, and Martin-Rengel 2015). Later testing revealed that the ductility of ZIRLO[®] cladding is very sensitive to the maximum hoop stress experienced, especially in the range of 90±5 MPa (~13,000±725 psi) at 350°C (662°F) during HRT (Billone 2019).
- Data collected during 2014–2018 suggest that radial hydride-induced embrittlement may not occur in PWR fuel rod cladding because end-of-life rod internal pressures (<5 MPa [725 psi] at 25°C [77°F]), maximum cladding temperatures (≤400°C [752°F]), and average assembly discharge burnups (<50 GWd/MTU) are all lower than previously anticipated. The low rod internal pressures result in hoop stresses too low to induce significant radial hydride precipitation even if more hydrogen were available for precipitation (Billone and Burtseva 2018). These results do not

necessarily apply to HBF integral burnable absorber rods containing boron,⁶³ which typically have higher rod internal pressures.

3.2.1.5 Interpreting Hydride Test Results

In 2014, ASTM International convened the 2nd International Workshop on Hydrides in Zirconium Alloy Cladding and Assembly Components to discuss the results and implications of recent hydride research. A white paper,⁶⁴ sponsored by DOE, summarizing the consensus findings of the workshop was reviewed by the Board at its February 2016 meeting⁶⁵ and one of the coauthors of the white paper provided an overview of the findings (Louthan 2016). Later, Louthan provided additional detail on this topic to the Board (see Appendix F). In that meeting, Louthan emphasized several observations, including:

- The general processes associated with hydride reorientation have been extensively studied and are well known; however, applying results obtained from testing on unirradiated cladding samples to a specific assembly having a specific irradiation history⁶⁶ and dried under a specific set of conditions is difficult because of the large number of variables involved (see Appendix F).
- Standards are needed for inducing hydride reorientation in cladding samples, testing the effects of the reorientation, and quantifying the results to resolve difficulties in comparing often-contradictory results.
- Testing on several cladding types under different potential storage conditions has shown that the temperature below which zirconium-based cladding begins to lose ductility can increase significantly under certain conditions due to hydride reorientation.

3.2.2 Evaluation and Findings

It is well known that there is a temperature below which hydrided zirconium alloys become brittle. This temperature was not known for highly irradiated alloys containing hydrogen that had precipitated as radial hydrides. Previous studies (Yagnik et al. 2004) had shown that, for typical HBF cladding, the hydrogen that precipitated in cladding as circumferential hydrides did not affect the cladding ductility at room temperature. However, there was little or no information available to determine if the presence of radial hydrides caused the cladding to become less ductile at lower temperatures. This is important because the cladding

⁶³ Certain fuel rods in a PWR fuel assembly contain both uranium dioxide fuel pellets and a burnable neutron absorber material used to control the reactivity level in the reactor. Some of these rods contain a boron compound for neutron absorption and generate helium gas via an (n, alpha) reaction with boron-10, increasing the rod internal pressure. Integral burnable absorbers rods, like the Westinghouse Integral Fuel Burnable Absorber (IFBA) rods, are to be distinguished from discrete burnable absorber rods that contain neutron absorber materials but no fuel.

⁶⁴ Robert Sindelar of Savannah River National Laboratory was funded by DOE to develop a white paper summarizing the consensus findings of the workshop (Sindelar, Louthan, and Hanson 2015).

⁶⁵ February 17, 2016, in Knoxville, Tennessee.

⁶⁶ Irradiation history refers to the in-reactor operation of the fuel/cladding and includes factors such as power and temperature time-histories and the overall burnup of the fuel.

temperature at the time of transportation could be lower than the temperature at which the cladding ductility begins to decrease, depending on the cladding type, the length of time in storage, and the ambient temperatures during transport. In certain hypothetical accident conditions (e.g., a side impact, or side drop accident), the cladding may experience a high pinch load that is perpendicular to the radial hydrides in the cladding, potentially resulting in cladding fracture.

DOE, together with other national and international partners, has spent considerable time and effort conducting research to determine whether hydride reorientation in zirconium alloy cladding can make the cladding susceptible to fracture when exposed to sufficiently high loads that might occur when SNF is stored for long periods, transported, and then either placed into storage again or disposed of.

Based on the data collected in the NRC and DOE research programs to study HBF storage and transportation, DOE reached the following conclusion regarding the hydride reorientation technical information need (or knowledge gap):

- “With the exception of confirmatory testing being conducted under the Sister Rod test program, this gap is essentially closed. ... Results of [ring compression tests, cyclic fatigue tests, HDRP tests, and SNF cask transport tests], examined as integrated effects from actual temperature, actual hoop stress, and realistic external loads, indicate that risks associated with hydride reorientation and embrittlement to cladding integrity of SNF are low for current fuel designs, burnups, and reactor operational limits [in] the United States.” (Teague et al. 2019)

Based on its research to date, DOE has gained confidence that hydride reorientation will not adversely affect most PWR SNF types that do not include integral burnable absorber rods. However, the Board notes that many uncertainties remain about hydride formation and hydride reorientation and the Board makes the following findings and observations:

1. **Many Variables Affect Hydride Formation and Reorientation.** There are numerous variables affecting the formation of hydrides in SNF cladding and the extent of hydride reorientation. These variables fall into two major groups: 1) inherent fuel and cladding properties, including those properties imparted to the cladding during manufacturing (cold working, annealing, etc.), and 2) conditions or environments to which the fuel and cladding are exposed (e.g., maximum cladding temperature during drying). See Appendix F for a full listing of these variables. Although some correlations and generalizations have been made concerning hydride formation and reorientation in certain cladding types, the lack of testing on all cladding types precludes making broad conclusions about which variables might exert the most influence on hydride formation and hydride reorientation as it relates to the performance of HBF during storage and transportation.
2. **Unirradiated Cladding Materials Are Poor Surrogates for Irradiated Cladding.** Experiments conducted at ANL and PNNL with unirradiated cladding samples have shown that data obtained from testing of unirradiated cladding does not replicate data obtained from testing of irradiated cladding, even under the same test conditions. DOE and others have documented these findings (Billone, Burtseva, and Einziger 2013; Sindelar, Louthan, and Hanson 2015).

3. **Variations in Test Methods Make Comparison of Results Difficult.** Different treatment protocols may be used to cause circumferential hydrides in SNF cladding to reorient as radial hydrides. Furthermore, different methods of quantifying the degree of hydride reorientation exist. The differences in these treatment protocols and quantification methods make it difficult to compare results obtained from different testing programs. The Board notes that DOE is involved in the development of a new industry standard, through ASTM International, that is expected to address these issues.
4. **Comprehensive Data on HBF Rod Internal Pressures Are Not Readily Available.** Rod internal pressure is an important parameter needed to predict the existence and extent of hydride reorientation. Most measurements of rod internal pressure are obtained by fuel manufacturers in their fuel qualification programs. However, most of this information is proprietary and not available for use by DOE (NRC 2020d). Data that have been obtained by DOE and NRC programs are publicly available but are limited in extent.
5. **Extrapolation of Testing Results is Subject to Many Assumptions and Large Uncertainties.** Hydride reorientation tests have been conducted on samples representing a limited range of cladding types, manufacturing processes, burnups, cladding stresses, cooling rates, and maximum cladding temperatures reached during the drying process. Using mathematical models to extrapolate the results of these tests to other SNF types and SNF with other histories requires assumptions to be made and introduces large uncertainties. (Louthan 2016) (Appendix F.3).

3.2.3 Recommendations for Hydrogen Effects in High Burnup Fuel Cladding

- a. Recommendation: The Board recommends that, as the need for new testing of HBF cladding is identified, DOE's research efforts make use of irradiated samples rather than unirradiated samples to avoid the large uncertainties and difficulties in interpreting test results that arise from using unirradiated samples.
- b. Recommendation: The Board recommends that DOE define a standard set of test parameters (e.g., fuel burnup, test temperatures, rod internal pressures) and results, where possible, that must be recorded for all DOE-funded research related to hydride reorientation. This will allow DOE managers, computer model developers, and nuclear industry practitioners to better use the data to make scientifically meaningful comparisons of experimental results from various research sources, even when the data were not collected for that purpose.
- c. Recommendation: The Board recommends that DOE gather into one database all relevant information that is publicly available on hydride-related testing of zirconium-based alloys to provide the basis for (1) evaluating the effects of variables that influence hydride reorientation; (2) supporting the ongoing development of new standards for inducing hydride reorientation in test samples and quantifying hydride reorientation and its effects; (3) explaining the differences in hydride reorientation and its effects among cladding types; and (4) developing computer models to predict hydride formation and reorientation in all zirconium-based cladding types, including those that have not been tested.

3.3 High Burnup Fuel Performance under Normal Conditions of Dry Storage

Maintaining fuel integrity during storage is an important factor in ensuring that the safety functions of the SNF dry cask storage system are met in accordance with 10 CFR Part 72. The NRC expected that cladding damage (gross breaches) would not occur in the initial 20-year period of dry storage⁶⁷ if the recommendations in NRC ISG-11, Rev. 3, were followed (NRC 2003). Due to the lack of a permanent geological repository for SNF, storage of SNF beyond 20 years has been and will be needed. To renew storage licenses, an aging management program is required (10 CFR Part 72). While data to support aging management programs for storage of LBF have been available (Appendix G), fewer data have been documented to support aging management programs for the storage of HBF.

A long-term demonstration to obtain data and confirm the predicted performance of HBF during dry storage, based on ISG-11 Rev. 3 (NRC 2003), was not identified in any of the original reports identifying technical information needs (NWTRB 2010; Hanson et al. 2012); however, it was added to the DOE Used Fuel Storage Program when the NRC indicated, in ISG-24, Rev 0, that a long-term prototypical demonstration is a useful method to support aging management program for a license extension for storage of SNF (NRC 2014a).

In 2014, DOE, in coordination with EPRI, began the HDRP, a long-term demonstration of HBF dry storage performance under actual storage conditions, which would allow any degradation mechanisms to be identified and evaluated (see Appendix G). The major goals include (EPRI 2014) the following:

- 1) provide confirmatory data for models, enhance future SNF dry storage cask design, and support HBF storage license renewals; and
- 2) use modeling, separate effects tests, and small-scale tests to extend the applicability of the data collected during the HDRP to evaluate the integrity of HBF over longer storage periods and to evaluate a wider set of fuel designs and storage environmental conditions.

See Appendix G for a detailed description of previous relevant U.S. and international SNF demonstrations and the lessons learned from these efforts that may be applied to the HDRP.

3.3.1 High Burnup Dry Storage Research Project

There are uncertainties with extrapolating test data from short-term accelerated tests designed to measure a single effect to long periods of dry storage where multiple mechanisms might be operating synergistically. In the NUREG-1927, *Standard Review Plan for Renewal of Specific Licenses and Certificates of Compliance for Dry Storage of Spent Nuclear Fuel*, the NRC identified that a dry storage demonstration to support aging management programs for HBF, similar to the one conducted for LBF (Appendix G; NRC

⁶⁷ The allowed licensing and renewal periods were 20 years each when the NRC first promulgated 10 CFR Part 72. Subsequently, the NRC revised 10 CFR Part 72 to permit an initial licensing period of up to 40 years and renewals of licenses up to 40 years.

2016b), is one acceptable method to confirm that the HBF configuration is maintained during the period of extended storage. Per NUREG-1927, Rev. 1 (NRC 2016b), any demonstration must include representative HBF types such that the data obtained from the demonstration will be applicable to the HBF content and conditions of storage specified for the associated NRC-approved SNF storage system.

3.3.1.1 High Burnup Dry Storage Research Project Cask and Operation

In 2014, DOE selected 32 PWR HBF assemblies from the spent fuel pool that serves reactor Units 1 and 2 at the North Anna Nuclear Generating Station to be loaded into an Orano TN[®]32 cask (also called the test cask; Figure 3-5). The test cask closure lid was modified to allow diagnostic monitoring of the fuel temperature and internal cask gas composition. The burnup of the fuel in the 32 assemblies ranges between an assembly average of 50 and 55.5 GWd/MTU. The fuel was cooled in the reactor spent fuel pool anywhere from 5 to 30 years (EPRI 2019; for more details, see Appendix G).



Figure 3-5. AREVA (now Orano) TN[®]32 cask.
(EPRI 2019).

Based on early thermal calculations by PNNL, the maximum fuel cladding temperature during storage was not expected to exceed 270°C (518°F) (Hanson 2016).⁶⁸ A license amendment request to allow the modified system to be used to contain HBF was submitted to the NRC in August 2015⁶⁹ and subsequently approved. Loading of the Orano TN[®]32 cask

⁶⁸ The HDRP was planned to allow the maximum cladding temperature to reach as close as possible to the NRC recommended maximum cladding temperature of 400°C (752°F) (NRC 2003). For this reason, the program originally planned to use fuel assemblies that had cooled for a shorter period after discharge from the reactor. However, this would have resulted in the maximum temperature allowed (149°C [300°F]) for the neutron shield in the cask shell to be exceeded, so the plan was changed to use longer-cooled fuel in the test cask (Fort et al. 2019).

⁶⁹ NRC Docket number 71-9377.

started November 14, 2017, and the cask was placed on the storage pad in early December 2017.

While the HDRP cask was being vacuum dried and during a two-week “soak period” for temperature equilibration, the cask internal temperatures were continuously monitored (see section 3.3.2 and Appendix G for temperature results). During the soak period, operators obtained three gas samples from the cask and the samples were analyzed for fission product gases, hydrogen, oxygen, and water vapor. No krypton-85 was detected, confirming that none of the fuel rods had through wall cladding penetrations that allowed FGR⁷⁰ (see Appendix E for more detailed gas sample results).

The HDRP is planned to include HBF storage for a minimum of ten years and then transport of the TN[®]32 cask to a facility where some of the HBF assemblies will be extracted from the cask. Selected HBF rods would then be characterized in a hot cell facility for comparison with the sister rods (EPRI 2014), whose purpose is described below. The results of the examinations of the sister rods and test rods will be compared and will allow DOE to determine if (and how much) cladding creep, hydride reorientation, or other changes in cladding characteristics occurred during storage and transportation. DOE has identified the CPP-603 facility at INL to receive the HDRP cask for removal of HBF assemblies and rods for further examination (Larson 2019).

The CPP-603 facility is not equipped to conduct SNF examinations, but DOE expects the HBF to be transferred to the Hot Fuels Examination Facility at INL for further testing (NWTRB 2019b).

3.3.1.2 Sister Rods

A sister rod is a fuel rod that has characteristics similar to a fuel rod that is stored in the HDRP cask. There were two potential donor fuel assembly sources for sister rods and both types of sources were used: (1) assemblies having similar operating histories to those assemblies chosen for storage in the HDRP cask; or (2) actual fuel assemblies selected for storage in the cask. To be considered a sister rod, the fuel rod must have a similar fuel type, cladding (e.g., Zircaloy-4, ZIRLO[®], M5[®]), initial enrichment, relative reactor core location, and reactor operating history as an HBF rod in the HDRP cask (EPRI 2014).

The HDRP project team selected 25 sister rods from reactor Units 1 and 2 at the North Anna Nuclear Generating Station. The sister rods are being characterized to establish a baseline against which the test rods removed following the ten-year storage period can be compared to identify any potential changes during storage and transportation. Non-destructive examination has been completed on the sister rods and included visual examination, profilometry (measurement of the rod diameter along the length of the rod), length measurements, eddy current measurements of the thickness of oxide layers on the outer surface of the fuel rod cladding (and, by inference, the hydrogen content), and gamma-scanning to determine the pellet-pellet interfaces, the location of the spacer grids relative to the bottom of the rods, and a relative burnup profile. Detailed descriptions of the plans for characterizing the sister rods can be found in Hanson et al. (2016) and in Saltzstein et al.

⁷⁰ It should be noted that it is possible for SNF cladding to have a through-wall crack that has resealed due to corrosion such that fission gases cannot be released.

(2017a). The non-destructive examinations were completed and nothing unexpected was observed (Montgomery et al. 2017; Saltzstein 2017).

The next step of characterization for the sister rods was destructive examination, including two phases of work. Phase 1 destructive examinations included puncturing several of the sister rods and capturing the gas released to determine the internal void volume and rod internal pressure. The examinations also included gas communication tests (to measure how freely gases flow axially through the SNF rod) (Saltzstein et al. 2017a; Montgomery et al. 2019). Initial measurements from ORNL indicated that rod pressures and internal rod void volumes were within the publicly available database envelope (Montgomery et al. 2019). Ten sister rods were shipped to PNNL for destructive examinations including gas communication tests, burst tests, and metallurgical testing. Shimskey et al. (2019) reported preliminary results of gas communication tests that are in line with measurements from earlier test programs reported in Hanson et al. (2008). Some sister rods have been segmented, defueled, and sent to ANL for ring compression tests. Follow-on work, in Phase 2, to address all the outstanding HBF technical information needs will depend on the results of the Phase 1 testing. A complete description of the HDRP long-term HBF testing program and the sister rod examination program can be found in Appendix G.

3.3.2 Modeling Temperature Profiles in Spent Nuclear Fuel and Spent Nuclear Fuel Cask Systems

The temperature history of SNF cladding is a critical variable used to determine many cladding characteristics and the rate of cladding degradation for almost all degradation mechanisms. Computer models simulating the temperature profiles and temperature histories in SNF assemblies and rods (sometimes called thermal models or thermal codes) are used by utilities and cask manufacturers to predict SNF cladding temperatures for fuel assemblies that are planned to be loaded into a cask or canister. This modeling is completed in order to demonstrate cladding temperatures remain below the suggested maximum (or peak) cladding temperature specified by the NRC (NRC 2003).⁷¹ In addition, the model predictions must show that other components, such as neutron shielding materials and lid seals, stay within their approved temperature ranges. To provide a sufficient, or conservative, margin of safety, the thermal models are intentionally biased by the nuclear industry to assure the regulators that they do not underestimate SNF dry cask storage system temperatures, including cladding temperatures.

Several notable efforts to develop thermal models to predict cladding temperatures in the public domain in the U.S. are those by the NRC (Das, Basu, and Walter 2014; Solis and Zigh 2016), PNNL for DOE (McKinnon and DeLoach 1993; Adkins et al. 2013; Cuta et al. 2013; Michener et al. 2015), and the University of Nevada-Reno (Hadj-Nacer et al. 2015). These thermal models are discussed in more detail in Appendix G. One of the models developed at

⁷¹ Later guidance is provided in NUREG-2215, section 5.4.4, Analytical Methods, Models, and Calculations, which states, "The computer codes used in the thermal evaluation should be well-verified and validated. ... The applicant should provide acceptable basis (e.g., benchmark efforts that mimic heat transfer and flow characteristics for the proposed design and that includes well defined boundary conditions and high-quality data for validation purposes, published results that include the range of applicability of the computer codes and highlight the specific features relevant to storage container design) for the accuracy of the selected computer code or codes and justification for the code's use in the proposed evaluation" (NRC 2020a).

PNNL—the COBRA-SFS model—is being used by DOE as the primary means of estimating temperature profiles in the HDRP test cask.

Due to the detail and accuracy of the COBRA-SFS model and the planned use of best-estimate input parameters, DOE’s temperature predictions are intended to be more realistic and less conservative than those typically used by the nuclear industry to plan fuel loading into dry storage cask and canisters. In COBRA-SFS, PNNL specifically removed conservative inputs and assumptions from the model that are typically used by industry for the purposes of licensing. The PNNL changes were (Fort et al. 2019a):

- 1) using more realistic ambient temperatures instead of maximums;
- 2) using measured drying times and profiles instead of maximums;
- 3) using the characteristics of the SNF actually loaded into the cask, instead of design-basis loadings; and,
- 4) using “best estimate” decay heat calculations.

The effects of making these changes are discussed in Appendix G.

3.3.2.1 Benchmarking the Temperature Models

To determine the ability of COBRA-SFS to predict cladding temperatures accurately, it was benchmarked against the temperatures measured just after the HDRP cask was vacuum dried, backfilled with helium, and in a steady-state condition (see Appendix G). Under EPRI coordination, four thermal models, including COBRA-SFS, were used to predict the HDRP cask system temperatures after drying in a “blind” round robin exercise (EPRI 2020a), where the modelers did not have access to measured data. A particular focus was placed on predicting the maximum cladding temperature, because the NRC suggests a maximum cladding temperature of 400°C (752°F) for SNF cladding (NRC 2003). The range of steady-state maximum cladding temperatures predicted by the four thermal models was 254–288°C (489–550°F), while the measured, steady-state maximum cladding temperature in the HDRP cask was 229°C (444°F) (EPRI 2020a).

The thermal modelers believe the temperature overprediction was due to uncertainties in one or more input parameters. Based on a review of the cask’s design drawings, the analysts believe a major contributor to the overprediction was uncertainty in the size of the physical gap between the SNF basket and the cask rails centering the basket, which differed from the design basis value due to thermal expansion and manufacturing variations. When the models were adjusted to account for the variation in gap size, the agreement between the model predictions and measured temperatures became much closer⁷² (Hanson 2018; Richmond and Fort 2018; Hall Zigh, and Solis 2019). The benchmarking is discussed in more detail in Appendix G.

DOE also sponsored testing at Sandia National Laboratories (SNL) to develop a surrogate SNF assembly and cask system to do detailed benchmarking of thermal models for dry cask storage systems of different designs (Lindgren et al. 2019; Pulido et al. 2020). The

⁷² Reducing the modeled physical gap from 2.54 to 1.27 mm (0.1 to 0.05 in) reduced the over-prediction of the cladding temperature by 5–20°C (9–36°F) depending on the assembly location in the cask and the axial elevation of the temperature measurement.

surrogate SNF assembly included electrically-heated rods to allow for adjustment of the system temperatures. The testing has allowed the COBRA-SFS model to be applied to surrogate BWR fuel assemblies, including the BWR assembly channel, in both vertical and horizontal surrogate dry storage systems. Once full validation is complete, the model can be used to generate time- and space-dependent temperature profiles for use in conjunction with other models to predict hydride formation, corrosion rates, creep rates, and other factors that affect the integrity of the fuel and its packaging. The SNL testing includes features not included in the HDRP, like a surrogate BWR assembly and a surrogate welded SNF canister. However, the SNL testing does not include other SNF assembly components such as control rod assemblies or discrete burnable absorber rods,⁷³ which could affect conductive and convective heat transfer inside the SNF cask or canister.

3.3.3 Evaluation and Findings

The HDRP represents a significant improvement over demonstrations for LBF, the results of which were accepted by the NRC to support approval of extended storage of LBF. For example, the HBF assemblies were loaded into the cask in the reactor spent fuel pool, so the loading and drying operations were more representative of typical operations at a nuclear power plant and could be monitored. In addition, there is substantial characterization of the HBF rods being done in the sister rod examination program to determine the pre-storage condition of the rods. Finally, the HDRP includes monitoring of cask temperatures and sampling of gas from the cask. Given this unique opportunity to examine HBF rod specimens, the Board encourages DOE to continue to collect useful characterization data, such as data on gaseous and particulate radionuclides released during rod depressurization tests.

The HDRP was designed to generate useful data to address many of the outstanding questions surrounding extended storage of HBF. The characteristics of the rods in the cask at the start of the test are well known because the sister rods are well characterized. Multiple existing cladding types, representative of those used in PWRs in the U.S., are included. Despite these positive attributes, there are limitations in the project that lead to uncertainties about the applicability of the test results to the full inventory of stored commercial HBF.

Limitations of the HDRP

- 1) **Limited Number of Fuel Types.** The first limitation of the HDRP is that only SNF from PWRs is being used even though BWR SNF represents approximately one third of the U.S. inventory of SNF on a mass basis. PWR and BWR fuels have different cladding types and the Zircaloy-2 cladding that is common in BWR fuel is not included in the HDRP. New advanced nuclear fuels and accident tolerant fuels being developed and tested now in nuclear power reactors are also not represented in the HDRP. While

⁷³ Control rod assemblies (also called rod cluster control assemblies or rod control cluster assemblies), comprise several rods containing neutron absorbers connected by a common structure or “spider.” The control rods are used for core reactivity and axial power shape control by insertion of the rods into some of the control rod guide tubes in some of the fuel assemblies. Similarly, a bank of connected discrete burnable absorber rods, which contain neutron absorber materials but no fuel, may be inserted into some of the guide tubes in some fuel assemblies to control the reactivity of the reactor core.

there is reason to believe BWR fuel is less prone to degradation than PWR fuel because of lower stress on the cladding, recent changes in BWR fuel design may challenge this assumption (Marschman and Winston 2015). As the industry transitions from BWR assemblies with 7 x 7 fuel rod arrays to 11 x 11 fuel rod arrays or larger, the assemblies still need to contain the same total mass of fissile uranium and have the same overall dimensions. Therefore, the fuel rods in those assemblies may have thinner cladding and a smaller diameter. According to the thin-walled formula for cladding stress,⁷⁴ a smaller cladding thickness will result in a higher stress, but a smaller diameter will result in a lower stress. Given these competing effects, one cannot draw a broad conclusion about whether the stress will be higher or lower in newer BWR fuel designs compared to older BWR designs. If the cladding stress is higher, it would increase the probability of hydride reorientation. However, recent research on BWR cladding that has an internal liner⁷⁵ indicates that hydrogen in the cladding tends to diffuse into the liner rather than remaining in the bulk of the cladding where it can form radial hydrides (Valance et al. 2015). The liner acts to decrease the probability of hydride reorientation.

If it is not possible to demonstrate through testing and computer modeling that the performance of PWR fuel bounds the expected performance of BWR fuel types and other new fuel types, a demonstration and/or further testing using these fuel types may be necessary.

- 2) **Maximum Cladding Temperature.** As noted in section 3.3.2.1, a second limitation of the HDRP is that the maximum steady-state cladding temperature measured just following the drying process was 229°C (444°F),⁷⁶ which was well below the target temperature (near 400°C [752°F]). This is likely lower than the temperatures reached by some SNF already loaded into dry cask storage systems and SNF that will be loaded at commercial nuclear power plant sites in the future. This may make it difficult to extrapolate accurately the results of this demonstration to systems where hydride reorientation may occur. To re-create conditions required to assess the effects of hydride formation and hydride reorientation during long-term storage, the HDRP test plan was altered to include heating some HDRP sister rods to 400°C (752°F). While these new heater tests will provide some additional data about the extent of hydride reorientation in SNF that is subjected to higher temperatures, the tests included some artificialities that may limit the value of the data. For example, the heater tests included a cooldown rate of approximately 4°C (7.2°F) per hour, while some SNF experiences a much slower cooldown rate (less than 1°C [1.8°F] per hour), depending on the axial and radial location in the SNF cask. These different

⁷⁴ The formula for cladding hoop stress is $\sigma = P D/t$, where σ is cladding hoop stress, P = the internal SNF rod pressure, t = the thickness of the cladding, and D is the diameter of the cladding.

⁷⁵ To reduce the interaction of the fuel pellets with the cladding in BWR fuel rods, the industry lines the inside of the Zircaloy-2 cladding with a thin layer of pure zirconium, which is called a liner.

⁷⁶ During the relatively brief period in which a vacuum was applied to the HDRP cask, the measured maximum cladding temperature was 237°C (459°F).

cooldown rates can affect the annealing of the cladding⁷⁷ and the formation of hydrides in different ways. As stated above and previously noted by the Board,⁷⁸ a methodology to extrapolate the HDRP results to HBF that is subjected to higher maximum cladding temperatures is needed.

- 3) **Gas Sampling.** The third limitation of the HDRP is that only a limited number of gas samples were obtained over a relatively short period of time following cask loading. Furthermore, the efforts to collect and analyze the gas samples “proved challenging” and were accompanied by some uncertainty (Bryan et al. 2019). The Board observes that obtaining additional gas samples from the HDRP cask, over longer periods of time, would improve the understanding of the quantity of moisture remaining in an SNF cask after drying and the generation of hydrogen and oxygen gases due to radiolysis. The Board’s findings and recommendations on this topic can be found in section 3.1.
- 4) **Damaged SNF and SNF with Integral Burnable Absorber Rods Containing Boron.** The fourth limitation of the HDRP is that the test cask includes no damaged (grossly breached) and waterlogged SNF rods or SNF assemblies with integral burnable absorber rods containing boron. The Board notes that shortcomings of the LBF demonstration at Idaho were that it did not include grossly breached fuel, the fuel was not loaded into the casks in a spent fuel pool, and the cask did not go through a drying process. SNF with grossly breached cladding may become waterlogged during storage in the spent fuel pool and then not have all of the water removed during the drying process. This retained water could eventually produce hydrogen and oxygen gases via radiolysis and these gases could contribute to pressure buildup and, in the case of oxygen, corrosion inside the dry cask storage system. Results from a new Canadian demonstration with grossly breached SNF rods in a moist atmosphere may provide information about the potential impacts of storing grossly breached SNF with water inside the cladding for extended periods (see Appendix G).

Because integral burnable absorber rods containing boron generate helium in the fuel pellets during irradiation, the internal rod pressure and thus the cladding hoop stress will be higher in these rods. The higher hoop stress in integral burnable absorber rods may make hydride reorientation more likely. If hydride reorientation occurs in the cladding of these rods during storage, their susceptibility to degradation during transport will be higher than that of normal HBF rods.

- 5) **Applicability of Results.** A fifth limitation of the HDRP is that it includes just one type of dry cask storage system (the Orano TN[®]32 cask). The TN[®]32 cask does not include an SNF canister, which is used in approximately 80% of all loaded SNF dry cask storage systems in the U.S. and may have an impact on the thermal behavior of

⁷⁷ Annealing removes stresses and allows metals to become more ductile via heating to higher temperatures. Annealing typically requires an extended time at an elevated temperature to be effective.

⁷⁸ Letter from Jean M. Bahr, NWTRB Chair to Mr. Edward McGinnis, Principal Deputy Assistant Secretary for Nuclear Energy, U.S. Department of Energy, November 27, 2018 (Bahr 2018).

the cask system, the mechanical response of the system during transportation, and the quantity of water that remains in the system following drying operations. DOE (or future SNF licensees) will have to do considerable work to extrapolate the results from the HDRP cask to other SNF dry cask storage systems being used in the U.S.

While the HDRP is providing valuable data on the characteristics and performance of certain PWR HBF types that can be used in support of NRC licensing or certification of the storage or transportation of those fuel types, the extent to which these data can be extended to other HBF types is unclear. Generally, to support licenses or certificates for the extended storage of HBF, the NRC has proposed two approaches to address age-related uncertainties associated with HBF: (1) a confirmatory demonstration (like the HDRP), or (2) supplemental safety analyses “that demonstrate the [dry cask storage system] can still meet the pertinent regulatory requirements by assuming hypothetical reconfiguration of the [HBF] contents into justified geometric forms”⁷⁹ (NRC 2020d). The use of a confirmatory demonstration requires the results to conform to the guidance of NUREG-1927, Rev. 1 (NRC 2016b). There are also a number of qualifiers on an acceptable demonstration detailed in ISG-24, Rev. 0 (NRC 2014a). If the characteristics of the SNF that the applicant is storing (e.g., cladding type, manufacturing technique, burnup) are different from those of the demonstration SNF, or if the conditions of actual storage (e.g., maximum temperature) are different from those in the demonstration, then using demonstration results requires additional experimental and/or modeling justification.

The Board notes that a new SNF storage demonstration in Japan (Fukuda et al. 2015) includes PWR SNF with Zircaloy-4 and ZIRLO® cladding. Data from this demonstration will be used for benchmarking a computer model to predict the performance of other SNF types and cask types during SNF storage (see Appendix G for more details).

The Board finds that:

- The HDRP has provided, and will continue to provide, useful data regarding the characteristics and performance of PWR HBF in a bolted-lid cask system. The Board encourages the continuation of the project, including transportation of the HDRP cask to a facility where further gas samples can be obtained from the cask and where HBF test rods can be extracted and moved to a hot cell facility for characterization.
- The HDRP demonstration, as constituted, has a number of limitations that make applying the HDRP results to the extended storage of much of the commercial SNF in the U.S. inventory challenging. It contains no BWR fuel, integral burnable absorber rods, grossly breached rods, or accident tolerant fuel; and it does not include a welded SNF canister.

⁷⁹ In this approach, “justified geometric form” of the HBF is not defined, but the guidance implies that the licensee would need to provide a sound technical basis for the geometric form of the HBF assumed in the analyses.

Sister Rod Test Program

The sister rod test program continues to be refined based on results from the early stages of sister rod examinations (Saltzstein et al. 2017a). All non-destructive examination and sister rod gas analyses are complete and nothing unexpected was found (Appendix G). The destructive examinations are being conducted in two stages with the plans for the second stage accounting for the results obtained in the first stage. Early in the formulation of the sister rod test program, the Board made a number of points to DOE and national laboratory representatives (Ewing 2016b; Bahr 2017). Among the points made were that the sister rod test program did not clearly show how the data collected during sister rod examinations would be used to support computer modeling or meet the technical information needs related to HBF that DOE identified in its technical information need reports. The Board also pointed out to DOE that the segments of sister rods that remain untested are valuable resources and should be preserved for future possible use.

The Board finds that:

- Based on the results to date, the HDRP sister rod examinations should be adequate to establish the necessary baseline HBF characteristics (before storage and transport) for comparison with the characteristics of the test rods that will be withdrawn from HBF in the HDRP cask (after storage and transport).
- DOE has not clearly indicated how the data obtained from the sister rod testing will be used to meet the technical information needs or support modeling of HBF performance during dry storage and transportation.
- Segments of sister rods that have not been tested are valuable resources and should be preserved for future possible use.

Thermal Modeling

Prior to the HDRP, PNNL's COBRA-SFS model had only been benchmarked against LBF and smaller-size, bolted-lid (bare fuel) SNF packages. The temperature measurements obtained in the HDRP were used to improve the PNNL model predictions (Hanson 2018). This showed that the COBRA-SFS model and a second model used by PNNL (STAR-CCM+) over-predicted the temperatures in the HDRP cask, compared to the measured temperatures, by as much as 40°C (72°F) (Fort et al. 2019a). The NRC team that participated in the blind round robin exercise noted that its model (ANSYS FLUENT) "over-predicted the experimental measurements everywhere, and by more than 60°C (110°F) in some locations." (Hall, Zigh, and Solis 2019).

The HDRP modeling teams conducted sensitivity studies and postulated that the temperature over-prediction was due to the closure of the physical gap between the SNF basket and the cask rails that center the basket, which improved the conductive heat transfer, and was not accounted for in the models (Fort et al. 2019a; Hall, Zigh, and Solis 2019). The Board observes that this type of physical variation or change in dimensions, which is not shown in design drawings, is likely to exist to varying degrees in all SNF dry cask storage systems and will be a source of irreducible uncertainty in the modeling that needs to be addressed.

All modeling teams involved in the HDRP blind round robin exercise recognized that the uncertainty in predicting temperatures of a real SNF dry cask storage system is an issue that needs to be addressed. DOE, EPRI, NRC, and international groups collaborating within the ESCP Thermal Subcommittee are working together to understand and address these uncertainties (EPRI 2020b).

The Board finds that:

- The PNNL COBRA-SFS model will be a valuable tool for calculating realistic SNF cladding temperatures in dry cask storage systems if realistic input data are used and if the predicted temperature uncertainty due to all sources of uncertainty can be quantified.

The Board notes that the COBRA-SFS model is also being calibrated against the highly controlled dry cask simulator at SNL. This effort has allowed the model to be adapted and tested against a surrogate canister-based system and against a surrogate BWR assembly that includes the fuel channel, neither of which is included in the HDRP test cask. However, the Board observes that such a controlled experiment is not likely to uncover the types of biases and uncertainties that were found during modeling of the HDRP cask or that may be found in other real-world SNF dry cask storage systems deployed at nuclear power plant sites. These biases and uncertainties arise from physical sources such as dimensional variations (that fall within the design specification) introduced during manufacturing and dimensional changes that are caused by thermal expansion and gravitational loads. Other biases and uncertainties arise from computation sources such as the governing equations and associated closure relationships and by the numerical methods applied, which do not completely represent the system being modeled.

The Board finds that:

- The PNNL COBRA-SFS model has not been validated against dry cask storage systems holding new fuel designs, such as accident tolerant fuels, or SNF assemblies equipped with other components such as control rod assemblies or discrete burnable absorber rods, which could affect conductive and convective heat transfer in dry cask storage systems.

3.3.4 Recommendations for High Burnup Fuel Performance under Normal Conditions of Dry Storage

HDRP and Sister Rods

- a. Recommendation: The Board recommends that the test plan for the HDRP sister rods should (a) link each proposed test to one or more of the technical information needs identified in the most recent DOE report on technical information needs and (b) explain how the results of each proposed test will be used to meet the technical information needs or support modeling of HBF performance during dry storage.*
- b. Recommendation: The Board recommends that DOE preserve selected sister rods (or rod segments and components) for future use in follow-up studies to the HDRP, if needed, or in support of other programs.*

Thermal Modeling

- c. *Recommendation: The Board recommends that DOE continue its activities to ensure its thermal models are rigorously validated, including industry-standard uncertainty quantification, for use on SNF storage or transport systems. Important factors to consider during validation are the various designs of cask and canister systems, inclusion of new fuel designs like accident tolerant fuel, and inclusion of SNF assemblies with other components, such as control rod assemblies or discrete burnable absorber rods.*

3.4 High Burnup Fuel Performance under Normal Conditions of Transport

The NRC regulation 10 CFR 71.55, “General requirements for fissile material packages,” requires that, during NCT, “the geometric form of the package contents [i.e., the SNF] would not be substantially altered.” This requirement is to ensure that criticality is prevented. Transportation vibrations and bumps are considered to be the primary sources of stress that may affect the structural integrity of SNF during NCT. Vibrations cause the cladding to flex a small amount, but over many cycles. If there are enough vibration cycles, at high enough stress levels, the vibrations could eventually cause cladding failure. This is called fatigue failure. DOE has sponsored both laboratory and “over the road” testing to gather data for computer models of the structural behavior of the fuel and cladding. This DOE-sponsored work includes:

- Laboratory testing to examine failure conditions for relatively large static loads and for relatively small loads applied many times (cyclic loads);
- Over the road testing to measure cladding strains versus number of vibration cycles for different transportation options (truck, rail, and ship); and
- Modeling that incorporates the laboratory data and the over the road strain data to assess the probability of cladding fatigue failure.

In practice, LBF casks or canisters that have been shipped are rarely opened for examination of the LBF condition after transportation. NRC accepts the many historical shipments of LBF for testing purposes with no reported fuel rod breaches as evidence that the transportation regulations are met consistently. As one example, several LBF shipments were made from the Turkey Point nuclear power plant site in Florida, to Columbus, Ohio, where the rods were examined and found to be intact (Einziger et al. 1982).⁸⁰

3.4.1 Research Program Description

Although there have been some shipments of small quantities of HBF for research purposes, there have been no shipments of HBF in large casks in the U.S. where the cask

⁸⁰ The assemblies were then shipped to the Nevada Test Site where the transportation casks were opened and the SNF was transferred into storage casks for the Climax Mine Test. Eventually, the SNF was shipped to INL to be included in thermal testing of SNF in dry storage casks, where no evidence of failed fuel was reported (Appendix G).

was opened to ensure that the HBF was not “substantially altered,” as required by 10 CFR Part 71.⁸¹ There have been many shipments of HBF in Europe to reprocessing plants, and there have been no reported incidents of fuel that was substantially altered,⁸² although it should be noted this fuel had not been dried in line with the practice used by utilities in the U.S. The European HBF that is transported to reprocessing plants experiences an elevated cladding temperature during transport due to the short cooling time of the HBF in the reactor spent fuel pool. Because of the higher temperatures, this operational experience is of limited relevance to transporting HBF today in the U.S.

For HBF in the U.S., the cladding temperature will have decreased significantly after an extended period in dry storage compared to when the HBF was put into dry storage. For example, computer modeling of the cladding temperatures of HBF in a dry cask storage system at the Catawba Nuclear Station predicted the maximum cladding temperature would decrease by approximately 50°C (90°F) after ten years in dry storage and by approximately 190°C (342°F) after 100 years in dry storage (Fort et al. 2016). As a consequence, the cladding temperature may be below the temperature at which the ductility of the cladding begins to decrease at the time of transportation.

To evaluate if “the geometric form of the package contents [i.e., SNF] would not be substantially altered”⁸³ under NCT, as required by the NRC, DOE has undertaken several projects (see Appendix H) that, taken together, have the following objectives:

- 1) Determine the fatigue lifetime (number of cycles to cladding breakage at a specified vibration load on the SNF cladding) of HBF rods as a function of the cladding composition, irradiation condition, vibration frequency, load, and previous storage conditions;
- 2) Determine the magnitude and frequency of realistic vibration loads (cyclic loading due to road vibrations and intermittent bumps during transportation) expected to be experienced by HBF rods and assemblies during loading and transportation via road, ship, and rail;

⁸¹ All the fuel shipped to the Morris Interim Storage Facility was in a bolted-lid cask (no canister) with a dry air atmosphere. None of the fuel was HBF. The SNF could be visually inspected as it was placed in the storage pool but other than CRUD spallation, especially from the BWR fuel, no inspection results have been reported.

⁸² Following a period of storage, these fuel assemblies were reprocessed and are not available for further examination.

⁸³ If the fuel is substantially altered such that it physically reconfigures in the cask or canister, it is not expected that there would be a release of radioactive material because the cask or canister is designed by the vendor and certified by the NRC to provide the primary barrier against radiological release. SNF that is substantially altered may affect the radiological source term if the cask or canister is breached in an extreme (highly unlikely) accident. Altered or reconfigured SNF may also affect the ability of the cask or canister to prevent a criticality accident in the event the cask or canister becomes flooded with water. Finally, altered SNF may present operational dose hazards if the SNF alteration is unknown and the cask or canister is opened.

- 3) Determine the magnitude of instantaneous strains due to assembly and canister/cask handing and due to bumps during NCT;
- 4) Determine if the pellet-cladding bonding, which occurs in HBF in the reactor, will change the response of the cladding to applied vibration and drop loads experienced during NCT; and
- 5) Develop and benchmark a computer model for predicting the transmission of the mechanical loads experienced by the truck or railcar to the HBF as a function of the type of transportation cask, basket, and cradle.⁸⁴

Bend Testing and Cyclic Fatigue Testing at ORNL. Among the first research efforts initiated to meet these objectives was a cyclic fatigue testing program for HBF that was funded by the NRC at ORNL. This testing included static bend testing to failure and cyclic bend testing to failure (fatigue testing) of segments of real HBF with fuel pellets to determine the ultimate yield strength and fatigue strength of the fuel (Wang and Wang 2017). The testing provided a baseline set of data for HBF, including stress-strain curves indicating yield strength and curves of strain (at failure) versus number of cycles indicating the fatigue strength for different HBF types (see Appendix H for more details). Key observations from this testing and follow-on testing sponsored by DOE include (Wang et al. 2016a; Wang et al. 2016b; Wang and Wang 2017):

- Considering the complexity and non-uniformity of the fuel pellet and cladding composite system, it is significant that the strain-to-failure data for HBF rods were characterized by strain-to-failure curves that would be obtained for standard uniform materials [i.e., simple metal samples].
- Fractures in the HBF cladding occur primarily at locations corresponding to a pellet-pellet interface.
- The fuel pellets provide strength (flexural rigidity) to the fuel pellet and cladding composite system. The additional strength depends on the extent of mechanical bonding between the pellets and the cladding.
- One HBF cladding specimen was subjected to a transient shock, equivalent to a 30 cm (1 ft) drop⁸⁵ prior to fatigue testing. It was found that this drop load shortened the fatigue lifetime of the specimen by approximately 50%.

Testing sponsored by DOE (Wang et al. 2016a; Wang et al. 2016b) included HBF segments with hydride reorientation induced in the cladding, for comparison to HBF without hydride reorientation (see section 3.2.1 and Appendix F for a description of hydride reorientation). The results of this testing showed that the fatigue strength of HBF samples with hydride reorientation was not statistically different from the fatigue strength of HBF without hydride

⁸⁴ A cradle is the physical support for an SNF transport cask and the cradle is mounted to the bed of a truck trailer or railcar. Each SNF transport cask type will have its own specially designed cradle.

⁸⁵ In its requirements applicable to transport packages containing commercial SNF (10 CFR Part 71), the NRC specifies a 30 cm (1 ft) drop as the maximum shock to be expected and evaluated for NCT.

reorientation.⁸⁶ This is unexpected given that radial hydrides, at a sufficiently high concentration, will cause a reduction in ductility compared to HBF with no radial hydrides. However, this result was based on tests of only three samples with hydride reorientation (Wang and Wang 2017).

As part of the HDRP (see section 3.3.1) sponsored by DOE and EPRI, 25 HBF sister rods were retrieved for non-destructive examination and destructive examination to obtain a baseline dataset for the characteristics of the HBF before drying, extended dry storage, and transportation. The destructive examination test plan includes several tests, including bend testing and fatigue testing of selected sister rod segments (see Appendix G). The first of the destructive examinations were conducted in 2019, with preliminary results published in Montgomery et al. (2019) and Shimskey et al. (2019). Fatigue tests of sister rods continued in 2020 and ORNL reported that “the preliminary results indicate that the baseline sister rod’s fatigue lifetime is consistent with other rods of the same type that were tested in the past” (Montgomery and Bevard 2020). Additional destructive examinations of sister rods continue at ORNL, PNNL, and SNL.

Road Testing and Shaker Table Testing. In addition to the lab testing at ORNL, DOE sponsored a demonstration of truck transportation using a surrogate SNF assembly that included accelerometers to measure the transport vibrations (McConnell et al. 2014). This demonstration, conducted by SNL, measured the vibration spectrum that was transmitted from the truck tires to the truck bed to the surrogate fuel assembly (Appendix H). The test employed an unirradiated 17 x 17 PWR assembly containing rods with copper cladding, except for one rod with Zircaloy-4 cladding. The rods were filled with lead rope weighing nearly the same as uranium dioxide fuel pellets and the assembly was placed in a surrogate PWR basket with the same internal dimensions as an actual truck cask PWR basket. SNL analysts also performed shaker table tests⁸⁷ on a surrogate SNF assembly to expand the vibration spectrum and evaluate the impact of some of the surrogate components that were used in the truck transportation test (McConnell et al. 2015). SNL reported that “[t]he strains measured on three Zircaloy-4 rods for all tests were in the micro-strain levels—well below the elastic limit for either unirradiated or irradiated Zircaloy-4,” and “[f]atigue failures are unlikely, too, due to the low magnitude of cyclic stresses imposed during rail transport” (McConnell et al. 2015).

DOE also developed a computer-based structural model to predict the stresses and strains that an SNF rod and assembly would experience for a wide variety of transportation conditions (Adkins et al. 2013). The DOE structural modeling effort is described in more detail in section 3.4.2 and in Appendix H.

Multimodal Transportation Test. In 2017, DOE, in cooperation with ENUSA Industrias Avanzadas, S.A., of Spain and the Korea Atomic Energy Research Institute, completed a multimodal transportation test using surrogate SNF assemblies in a commercial SNF

⁸⁶ Although the HBF rods that had undergone HRT exhibited longer fatigue lifetimes, on average, than as-irradiated rods, the fatigue lifetimes were within the range of testing uncertainty.

⁸⁷ In shaker table testing, an assembly is placed on a table that can be shaken in 3–6 directions (including rotational directions) with a given input vibration frequency to measure the strain responses of the fuel rods.

transport cask to measure and evaluate the vibration spectrum and shocks experienced by the SNF during rail, road, and ship transportation (Figure 3-6) (Saltzstein et al. 2017b).



Figure 3-6. Multimodal Transportation Test cask on a railcar.

The ENSA [Equipos Nucleares S.A.] test cask is shown on a 12-axle railcar for delivery to and testing at the Transportation Technology Center in Pueblo, Colorado. Note that for an actual SNF shipment, the cask would have impact limiters installed at both ends (McConnell et al. 2018).

Accelerometers were attached to the transport vehicles, the cask cradle, cask, and surrogate fuel assemblies to record accelerations and shocks throughout the transportation test (see Appendix H for more details). SNL concluded that “[t]he test results provide a compelling technical basis for the safe transport of spent fuel under normal conditions of transport” (Kalinina et al. 2018). This conclusion was supported by the statement:

“Data collected during the multimodal transportation test showed that the stresses fuel rods experience due to vibration and shock during normal transportation are far below the yield and fatigue limits ($\sim 9,000 \mu\text{m}/\text{m}$) for cladding. The maximum strains observed in this test were $99 \mu\text{m}/\text{m}$ in rail coupling at [the Transportation Technology Center] and $35 \mu\text{m}/\text{m}$ during 1,950 mi rail transport from the port of Baltimore to Pueblo, Colorado.” (Kalinina et al. 2018)

The results of this test were used to benchmark DOE’s structural model, with a focus on SNF performance during NCT (Klymyshyn et al. 2018). PNNL also conducted an analysis of the accumulated vibration damage in the cladding (see Appendix H) and found that cladding will not fail due to fatigue even when accounting for the cumulative miles traveled during a trip

with multiple transportation legs.⁸⁸ Further details about the DOE test programs and DOE's analysis of the resulting data are included in Appendix H.

30 cm (1 ft) Drop Tests. DOE has been conducting drop tests to measure accelerations and strains on surrogate fuel assemblies to determine whether the SNF rods can maintain their integrity inside a cask when dropped from a height of 30 cm (1 ft) (Kalinina et al. 2019, Kalinina et al. 2020). Due to cost considerations and limited availability of a full-scale cask with impact limiters, DOE began with drop tests using surrogate assemblies inside a 1/3-scale cask (Kalinina et al. 2019). Using the acceleration and strain data collected in the 1/3-scale drop test, DOE planned and conducted drop tests of a single, full-scale, surrogate SNF assembly inside a surrogate SNF basket cell. These latter drop tests were conducted in 2019 and 2020 at SNL, and the assembly accelerations and strains were measured. Based on the test results, SNL reported that “[t]he major conclusion that can be drawn from the 30 cm drop test is that the fuel rods will maintain their integrity after being dropped 30 cm or less” (Kalinina et al. 2020). Although some confidence is gained in the ability of HBF rods to maintain their integrity during NCT based on the 30 cm (1 ft) drop testing, the Board notes that these experiments did not account for any changes in mechanical behavior of the HBF cladding that would occur due to hydride reorientation or irradiation hardening in the cladding. These factors add some uncertainty to the testing results.

3.4.2 Modeling Structural Behavior of Spent Nuclear Fuel and Spent Nuclear Fuel Cask Systems

DOE funded PNNL to develop a computer-based structural model that can be used to predict the transmission of vibration and shock loads from a transport vehicle (e.g., a truck or railcar) through the cask system components and the SNF assembly components to the SNF rods. Based on the predicted vibration and shock loads, the model can then be used to predict the strains on the SNF rods. These transportation strains can then be compared against SNF rod yield strength and flexural rigidity measurements obtained in laboratory settings to determine the likelihood of the SNF rods fracturing during NCT.

PNNL first developed and adapted its SNF structural model using historical data from the NRC (Adkins et al. 2013). The model includes separate, detailed sub-models for SNF assemblies and rods, SNF baskets and casks, and for the SNF railcars (see Appendix H for details). PNNL further refined the model using data gathered during the SNL truck testing and shaker table testing. Then, in 2017, PNNL benchmarked the model against the vibration and shock loads measured on surrogate SNF assemblies during the multimodal transportation test described above (Klymyshyn et al. 2019).

3.4.3 Evaluation and Findings

DOE has sponsored considerable research to examine the characteristics of HBF, such as flexural rigidity and yield strength, which are directly relevant to the fuel's mechanical performance and its resistance to fracture during NCT. Further testing has measured actual vibration and shock loads using shaker tables and during transport by truck, barge, and rail.

⁸⁸ Vibration fatigue damage is cumulative. If an SNF assembly is transported to an interim storage facility, stored, and then transported to a repository, the cumulative effects of all vibrations during both legs of transportation must be considered when evaluating fatigue damage.

Comparing the strength of the HBF, particularly the HBF cladding, with the applied loads allows an assessment of the probability of cladding fracture during NCT.

Bend Testing and Cyclic Fatigue Testing at ORNL. The Board observes that ORNL efforts to conduct bend tests and fatigue tests of HBF cladding have provided valuable information regarding the characteristics of HBF, particularly mechanical property data that are needed to assess the performance of HBF in NCT. Early bend testing and fatigue testing was limited to just a few HBF cladding types, but continuing work with the HDRP sister rods has expanded the body of data to include more cladding types.

The Board finds that:

- The HBF cladding types, including cladding with radial hydrides, subjected to fatigue testing at ORNL can withstand vibration fatigue without fracturing for the duration of a cross-country trip. This finding is contingent on the loads and frequencies experienced during normal transportation (considering the method of transportation, cask designs, fuel designs, etc.) being bounded by the loads and frequencies used in the ORNL testing.
- The ORNL static bend tests demonstrate that the presence of fuel pellets adds strength to the pellet-cladding system (fuel rod). However, the amount of flexural rigidity and fatigue strength added by the pellets through pellet-cladding bonding are not well known, nor is the persistence of the bonding during HBF storage and transport operations. Continued testing of HDRP sister rods with pellet-pellet bonding and pellet-cladding bonding is encouraged and may provide additional data that can improve the understanding of this phenomenon.
- Because ORNL fatigue testing of HBF cladding specimens conducted after a 30 cm (1 ft) drop showed a 50% reduction in fatigue lifetime, further testing is advisable. However, based on the Multimodal Transportation Test data, if one applies the maximum number and amplitude of vibration loads measured on SNF cladding during NCT, the resultant fatigue loading is approximately 100 times lower than the loading needed to cause fatigue failure of the cladding (Larson 2019). Therefore, even after a 50% reduction in fatigue lifetime, there would still be a 50x safety margin. The Board acknowledges and encourages the DOE-sponsored drop testing of surrogate SNF assemblies to further evaluate the potential for reduced fatigue lifetime that may result from transient shocks during NCT.

Road Testing. The SNL road testing of SNF included several artificial features, including the use of lead rope instead of irradiated uranium dioxide pellets, which precluded investigation of any pellet-pellet interactions or pellet-cladding bonding effects. The Zircaloy-4 cladding used for one fuel rod was unirradiated and did not have circumferential or radial hydrides, irradiation damage, or partial annealing of the damage that may occur during the drying process—all of which could be present in irradiated cladding. Finally, the road tests used a concrete block to mimic the mass of an actual transportation cask, which might change the shock amplitude and frequency experienced by the fuel assembly during transportation. Some of these shortcomings were addressed by the shaker table testing and the multimodal transportation test.

Shaker Table Testing. The shaker table tests using the input vibration spectrum measured during the road tests showed that several of the compromises introduced by using surrogates in the road tests may not have affected the results. The shaker table test results indicate that the type of surrogate fuel pellet used in the test does not affect the strains on the cladding as long as there is no pellet-to-cladding bonding. The results also showed that strains experienced by the surrogate rods are similar for the different types of cladding surrogates used in the unirradiated state; however, there are variables that cannot be addressed in a shaker table test such as basket configuration, cask and canister design, and cladding strength in an irradiated state. The follow-on multimodal transportation test obtained more data about the effects of an SNF basket and cask on the vibration spectrum.

Multimodal Transportation Test. The multimodal transportation test was a major improvement over the road testing at SNL because all the components of the test were real except for the SNF assemblies (see Appendix H) (Sorenson et al. 2016; Kalinina et al. 2018). The SNF was represented by three instrumented but unirradiated surrogate assemblies of different designs. Some of the rods in each of the test assemblies had either Zircaloy-4 or ZIRLO® cladding, containing lead rope or lead or molybdenum pellets in lieu of uranium dioxide pellets. Concrete dummy assemblies, weighing the same as the fuel assemblies, were loaded in the other 29 positions of the 32-position SNF basket. An actual cask and basket were used, although the basket had not experienced the aging that might occur during extended storage. This might not be an issue if the HDRP results show minimal aging of the basket properties.

Unlike previous tests, the multimodal transportation test included three different modes of transportation and several monitored intermodal transfers. After the SNF cask arrived at the Transportation Technology Center, in Pueblo, Colorado, the cask and the railcar system were subjected to rigorous rail tests under extreme conditions. The full set of results from the strain gauges and accelerometers used during the test have been evaluated (Kalinina et al. 2018, Klymyshyn et al. 2019). The results indicated that there was less cladding strain experienced by the fuel in the railcar system than experienced by the fuel in the truck tests. In either case (rail or truck), the maximum strain measured was approximately 100 times smaller than the strain that would cause failure of HBF cladding (Klymyshyn et al. 2018), with or without reoriented hydrides, as reported in Wang et al. (2016b).

Structural Modeling. The Board observes that the DOE effort to develop a structural model to predict the structural behavior of HBF has advanced and the effort benefited from benchmarking against the data collected during the multimodal transportation test. However, uncertainties remain because the multimodal test did not include irradiated SNF assemblies and because it included dummy (concrete) assemblies in 29 of 32 basket positions. Irradiation effects can include more extensive pellet-cladding bonding, loosening of the retention force of the spacer grid springs on the rods, irradiation hardening of the spacer grid springs, embrittlement of the spacer grids, and embrittlement of PWR assembly guide tubes. These will impact the input data used in the models and therefore affect the predicted fuel cladding stresses and strains. These irradiation effects are not included in the model. The 29 concrete dummy assemblies create another source of uncertainty regarding the transmission of vibrations and shocks within the SNF basket, including the amount of resonant feedback from the rods to the assembly. Another limitation of the PNNL model is that it does not consider changes in the SNF rods or assembly hardware that may occur during extended storage or during transportation.

The Board finds that:

- The DOE structural modeling effort is good but does not fully account for some uncertainties stemming from the use of unirradiated materials and the use of surrogate SNF assemblies. Until DOE can accurately quantify the relationship between the behavior of surrogate components and the behavior of HBF—either by modeling or measurement—the results from the current projects will still have a degree of uncertainty when used to predict the structural behavior of real HBF during transport.
- DOE’s transportation testing and modeling efforts have been focused on PWR SNF transported in non-canistered storage and transport systems. The testing has not yet been expanded to include:
 - Canistered SNF systems;
 - Fuel types other than 17 x 17 PWR fuel; and
 - SNF rods that have significant flaws in the cladding, pellet-pellet gaps, or variability of the pellet-cladding bonding that may affect how the HBF responds to the vibrations and shocks that may be experienced during NCT.

3.4.4 Recommendations for High Burnup Fuel Performance under Normal Conditions of Transport

- a. *Recommendation: The Board recommends that DOE quantify the uncertainties introduced by the use of unirradiated assembly components and surrogate components, such as concrete mock-SNF assemblies, in experiments being used to benchmark the DOE structural model. The structural model should also be exercised to evaluate HBF cladding strains for different cask and canister types, fuel types, and degree of pellet-cladding bonding.*

3.5 Fuel Performance Modeling

3.5.1 Background and Discussion

Computational simulation or modeling, together with a focused experimental program and observations from the field, provide the only feasible approach to understanding and extrapolating the performance of HBF given the wide range of cladding materials and conditions that may affect the rods while in the reactor and during post-irradiation storage and transportation. Any computational simulation must include coupling of models for thermal-hydraulics, solid mechanics, structural analysis and material behaviors. Modeling of thermal profiles of SNF dry cask storage systems is discussed in section 3.3 and modeling of structural responses of the cask/canister and fuel rod to transportation shocks and vibrations is discussed in section 3.4. This section discusses fuel performance modeling, which couples a thermo-mechanical model with material-property models at the spatial level of the fuel rod (i.e., macro-scale). Fuel performance modeling focuses on the evolution of a fuel rod’s geometry, temperature profile, internal rod pressure, and material composition and microstructure over time as functions of irradiation and thermal-hydraulic history.

The complexity and feedbacks that are inherent in a fuel performance model present a challenge to modeling. The discussion below provides an overview of the development of fuel performance models and the associated challenges. Appendix I provides a detailed discussion of the complexity and feedbacks, and of DOE supported R&D to develop a fuel performance model with the capabilities to analyze fuel performance during reactor operations, drying, storage, and transportation.

BISON⁸⁹ (Hales et al. 2014) is a fuel performance model being developed by INL. As applied to light water reactors, the development of BISON has focused on predicting in-reactor fuel rod (i.e., pellets and cladding) performance for normal operations and under potential accident conditions. To date, the cladding material property models associated with BISON have been limited mainly to Zircaloy-4, for which experimental data are publicly available.

DOE also sponsored the Consortium for Advanced Simulation of Light Water Reactors with a goal to predict the performance of existing and next-generation commercial nuclear reactors through comprehensive, science-based modeling and simulation. Part of the Consortium effort included a Science Council as an independent body of subject-matter experts that periodically reviewed the Consortium's science and technology strategy, results, and R&D plans. The Science Council concluded that BISON's prediction capabilities for fuel with Zircaloy-4 cladding in normal, in-reactor conditions are comparable to those of other fuel performance models used in fuel design and licensing.⁹⁰ They also concluded that BISON has enhanced potential for performance improvements due to its 3-D capability and strong multi-physics coupling solution algorithm, both of which are lacking in other fuel performance models. Thus, BISON should be capable of providing the initial conditions required to evaluate post-irradiation fuel performance for HBF with Zircaloy-4 cladding. As the number of material-properties models increases for other cladding alloys due to an increase in publicly available experimental data, BISON should also be able to provide initial conditions required to evaluate post-irradiation fuel performance for HBF with these other alloys.

Focusing on fuel performance modeling of light water reactor fuel during post-irradiation operations, BISON contains material models for irradiated uranium dioxide fuel and Zircaloy-4 cladding; however, validation of these models for post-irradiation conditions is limited, and cladding material models and failure models are either non-existent or in need of improvement for many other materials (see Appendix I). Via limited efforts, which were supported by Nuclear Energy Advanced Modeling and Simulation and INL Laboratory Directed Research and Development, material models that are important for post-irradiation assessment have been developed for the BISON code. The material models assess zirconium hydride formation, which includes cladding corrosion, hydrogen retention, migration and redistribution of hydrogen, precipitation and dissolution of zirconium hydride

⁸⁹ BISON is a finite element-based nuclear fuel performance model applicable to a variety of fuel forms including PWR and BWR fuel rods, tri-structural isotropic particle fuel, and metallic fuel in both rod and plate forms. It is a multiphysics fuel analysis model that solves fully-coupled thermomechanical problems.

⁹⁰ Comparisons have been made against experimental data and with predictions from the FALCON model (Richmond and Geelhood 2017) and the PAD model (Crede et al. 2016) that were validated using proprietary data that EPRI and Westinghouse Electric Company collected. Comparisons against the proprietary models were done under Consortium funding and are not publicly available.

particles, and a very preliminary model for damage due to the presence of hydrides (Casagrande et al. 2017).

To further advance model development, DOE funded an IRP in 2017 led by Pennsylvania State University collaborating with several other universities, national laboratories, and industry. The focus of this research is to complete single physics experiments on unirradiated material and, when combined with existing experimental results on unirradiated and irradiated material, the effort will allow the development of predictive computer models. Specifically, the models to be developed are planned to improve the predictions of the migration and redistribution of hydrogen, precipitation and dissolution of zirconium hydride platelets, and the impact of hydride microstructure on mechanical properties of the cladding. A review paper summarizing recent research efforts, the current state of knowledge, and open questions about zirconium hydride formation and behavior has been published by Motta et al. (2019).

The material models being developed are planned to be incorporated into the DOE-supported BISON and NRC-supported FRAPCON fuel performance codes. This work will assist in further development of what is referred to as meso-scale models, such as incorporated in the DOE Office of Nuclear Energy MARMOT code (Tonks et al. 2012). Meso-scale models are being used to predict at a grain level the evolution of cladding microstructure, which in turn can be used to develop macro-scale models as used in BISON. This is of interest because the microstructure greatly affects the mechanical properties of the cladding which determines crack growth.

3.5.2 Evaluation and Findings

To obtain data that can improve the understanding of the characteristics and performance of HBF during extended storage and transportation, and to inform model development, DOE has been conducting a number of laboratory and field experiments with surrogate SNF and real HBF (Saltzstein et al. 2017a and 2017b). The data obtained from these experiments—plus modeling—will be used to extrapolate conclusions about HBF that has been tested to other HBF designs that were not included in tests. However, to be applicable to the entire anticipated inventory of commercial HBF, any model needs to account for several variables such as irradiation history, cladding type, fuel manufacturing processes, drying processes, and storage conditions. Under DOE's current testing program, it is not clear that a sufficient number of HBF samples, representing a sufficiently large range of these variables, have been examined. Although DOE's experimental efforts have been well-coordinated with thermal modeling and structural modeling efforts, much less coordination has been occurring between experimentalists and fuel performance model developers. To adequately predict how HBF will respond to the full range of conditions anticipated during storage and transportation, DOE will need to develop new fuel performance models or modify existing models (e.g., BISON), the development of which has been focused on in-reactor fuel performance (see Appendix I for more details).

The Board finds that:

- The limited testing of real HBF provides a limited, and possibly insufficient, database of mechanical properties and other HBF characteristics that can be used to develop and validate sufficiently accurate fuel performance models that can be used to predict the performance of HBF.

- DOE efforts to develop fuel performance models or modify existing models (e.g., BISON) have not yet advanced those models to a point where they can predict the performance of the full range of HBF types under the full range of storage and transportation operating conditions.

3.5.3 Recommendations for Fuel Performance Modeling

- a. Recommendation: The Board recommends that DOE continue to develop fuel performance models (e.g., BISON) that are validated utilizing experimental data. In so doing, DOE-sponsored fuel performance model developers should clearly identify the data they need to develop and validate models to DOE-sponsored experimentalists. Experimentalists should clearly explain the capabilities and limitations of their experimental equipment and facilities to model developers. This close collaboration is needed to ensure optimal experimental setup and collection of data needed to improve the models and achieve a better understanding of HBF characteristics and performance.*

4. CONCLUSIONS, FINDINGS, AND RECOMMENDATIONS

4.1 Conclusions

This report documents the Board's review and evaluation of the DOE R&D program related to understanding better the characteristics and performance of HBF during extended storage and transportation. Much of the DOE research continues and the Board recognizes that the results of this work could change its evaluation of the DOE program.

For the DOE work conducted to date, the Board agrees with the DOE-identified technical information needs and priorities (Teague et al. 2019) that apply to extended storage and subsequent transportation of HBF. DOE has implemented several research programs to obtain the data to resolve the technical information needs. The Board evaluated the DOE research programs to determine (1) if the research is likely to obtain the needed data; (2) whether computer models have been developed and validated to extrapolate the results of research on a few fuel types to all HBF that will be stored in the U.S. inventory; and (3) if the testing has been conducted in a technically defensible way.

As of December 2020, key DOE research efforts related to HBF, such as the HDRP, sister rod examinations, thermal modeling, and plans for obtaining additional SNF cask gas samples are continuing. Based on the research to date, the Board draws the following conclusions:

- DOE is to be commended for sponsoring the HDRP and Multimodal Transportation Test, both of which produced significant quantities of valuable information regarding the characteristics and performance of HBF.
- Nothing has been found to date in the DOE R&D program that indicates that safe long-term storage and subsequent transportation of commercial HBF cannot be accomplished while meeting all regulations.
- Based on laboratory experiments, HBF examinations, and results from thermal models, it does not appear that hydride reorientation will occur in currently-loaded PWR HBF during cask drying or storage. However, this conclusion may not apply if utilities start to load hotter HBF for dry storage to take advantage of the temperature margins identified by the improved modeling of SNF temperatures or if HBF containing integral burnable absorbers rods are loaded in the dry cask storage systems.
- For HBF already loaded into dry cask storage systems, maximum cladding temperatures that were reached during drying and helium backfill processes appear to have been well below 400°C, as found in the HDRP test cask. These relatively low temperatures may mean that, for this HBF, there is no need to perform additional testing to gather more data on cladding mechanical properties to support NRC licensing and certification activities; these NRC activities are adequately supported using currently-available cladding mechanical properties (i.e., without hydride reorientation). However, if utilities load hotter HBF for storage, the resulting higher

temperatures during drying and helium backfill may induce a greater degree of hydride reorientation and, in this case, additional testing may be warranted to gather data on cladding mechanical properties.

- The HDRP testing and associated thermal modeling have been conducted using a limited number of fuel types (from PWRs) and using just one type of dry cask storage system. Some uncertainty remains regarding the extrapolation of the results of this research to other types of fuel with other operating histories and to other types of dry cask storage systems.
- Laboratory testing of HBF specimens combined with field testing of SNF surrogate assemblies indicate that there should be no significant degradation or change in the characteristics of HBF cladding during NCT.
- Although nuclear industry drying processes remove water from SNF dry cask storage systems to a level that meets the NRC dryness criterion, it is not clear how much water remains in a dry cask storage system after drying. It has also not been determined how much water can remain in a dry cask storage system without causing an unacceptable amount of HBF degradation or hydrogen gas generation during extended storage periods. These issues continue to be addressed by DOE.

4.2 Summary Findings and Recommendations

The Board found that, generally, the ongoing DOE research programs are expected to provide the information needed to improve the understanding of HBF characteristics and performance during extended storage and transportation. However, efforts are still needed to reduce the uncertainties that remain in many research areas. Therefore, the Board offers the following summary findings and recommendations to improve the focus of the research and to address the uncertainties.

1. General Recommendations

- a. *Summary Finding: The Board finds that the results of DOE-sponsored research on HBF have been reported by a variety of organizations and in a variety of formats but there is no compendium that contains the results of all DOE research related to extended storage and transportation of HBF.*

Recommendation: The Board recommends that, following the completion of HDRP sister rod examinations and drop testing of surrogate SNF assemblies, DOE prepare a document that compiles the results of DOE research on extended storage and transportation of HBF, with the purpose of providing the technical bases for conclusions reached regarding HBF performance during extended storage and transportation.

- b. *Summary Finding: The Board finds that important research relevant to extended storage and transportation of HBF is being sponsored by organizations outside of DOE, both in the U.S. and in other countries.*

Recommendation: The Board recommends that DOE continue to review the results of the Electric Power Research Institute's Extended Storage Collaboration Program and research in other countries to determine if the results of ongoing HBF studies either change the priorities for DOE's planned research or add technical information needs requiring new research.

- c. *Summary Finding: The Board finds that many of the tests and models used to determine the performance of HBF have been completed for a relatively narrow range of fuel and cladding types, burnup levels, temperatures, storage and transportation system designs, etc. The limitations of the tests and models are not always clear with respect to their applicability to a wider range of HBF types, storage and transportation system designs, and storage and transportation conditions.*

Recommendation: The Board recommends that DOE indicate how its tests and models do or do not apply to the broad range of HBF types and storage and transportation system designs for which information is still needed and take steps to meet those remaining technical information needs.

2. Spent Nuclear Fuel Drying

- a. *Summary Finding: The Board finds that water remaining inside SNF dry cask storage systems may cause corrosion of SNF cladding or the internal components of the system and significant uncertainty remains regarding the quantities of hydrogen and oxygen gases that can be generated due to radiolysis of the remaining water. While the SNF drying process used by industry removes most of the water, including water physically adsorbed on metal surfaces, some of the more tightly bound chemisorbed water is likely to remain.*

Recommendation: The Board recommends that DOE evaluate the extent to which chemisorbed water remains after the drying process is completed and whether this water could affect the ability of SNF cask or canister systems and their contents to continue to meet storage and transportation requirements.

- b. *Summary Finding: The Board finds that few gas samples have been obtained from inside dry cask storage systems containing commercial SNF.*

Recommendation: The Board recommends that DOE further explore the possibility of monitoring the moisture content and gas composition of dry cask storage systems loaded by nuclear utilities with HBF for an extended period. DOE should improve and validate gas sampling methods, with a particular focus on water vapor sampling and measurement, before the next samples are obtained.

3. Hydrogen Effects in High Burnup Fuel Cladding

- a. *Summary Finding: The Board finds that data obtained from testing of unirradiated cladding does not replicate data obtained from testing of irradiated cladding.*

Recommendation: The Board recommends that, as the need for new testing of HBF cladding is identified, DOE's research efforts make use of irradiated samples rather than unirradiated samples to avoid the large uncertainties and difficulties in interpreting test results that arise from using unirradiated samples.

- b. *Summary Finding: The Board finds that there are a variety of test methods for examining hydride reorientation in HBF cladding and that the results of the testing are reported with significant format variations that make comparison of results difficult.*

Recommendation: The Board recommends that DOE define a standard set of test parameters (e.g., fuel burnup, test temperatures, rod internal pressures) and results, where possible, that must be recorded for all DOE-funded research related to hydride reorientation. This will allow DOE managers, computer model developers, and nuclear industry practitioners to better use the data to make scientifically meaningful comparisons of experimental results from various research sources, even when the data were not collected for that purpose.

- c. *Summary Finding: The Board finds that data on the characteristics of HBF (e.g., HBF rod internal pressures) and results of research on hydride formation and hydride reorientation in zirconium-based alloys are reported by a variety of organizations and saved in a variety of information archives.*

Recommendation: The Board recommends that DOE gather into one database all relevant information that is publicly available on hydride-related testing of zirconium-based alloys to provide the basis for (1) evaluating the effects of variables that influence hydride reorientation; (2) supporting the ongoing development of new standards for inducing hydride reorientation in test samples and quantifying hydride reorientation and its effects; (3) explaining the differences in hydride reorientation and its effects among cladding types; and (4) developing computer models to predict hydride formation and reorientation in all zirconium-based cladding types, including those that have not been tested.

4. High Burnup Fuel Performance under Normal Conditions of Dry Storage

High Burnup Dry Storage Research Project

- a. *Summary Finding: The Board finds that DOE has not clearly indicated how the data obtained from the HDRP and related sister rod testing will be used to*

meet the DOE-identified technical information needs or support modeling of HBF performance during dry storage and transportation.

Recommendation: The Board recommends that the test plan for the HDRP sister rods should (a) link each proposed test to one or more of the technical information needs identified in the most recent DOE report on technical information needs and (b) explain how the results of each proposed test will be used to meet the technical information needs or support modeling of HBF performance during dry storage.

- b. *Summary Finding: The Board finds that obtaining and characterizing the sister rods has been a worthwhile undertaking but has required the expenditure of extensive time and resources. These rods constitute a valuable asset for future research and development.*

Recommendation: The Board recommends that DOE preserve selected sister rods (or rod segments and components) for future use in follow-up studies to the HDRP, if needed, or in support of other programs.

Thermal Modeling

- c. *Summary Finding: The Board finds that DOE-sponsored thermal models will be valuable tools for calculating realistic SNF cladding temperatures during drying and storage in dry cask storage systems if realistic input data are used and if the predicted temperature uncertainty due to all sources of uncertainty can be quantified and defensibly bounded.*

Recommendation: The Board recommends that DOE continue its activities to ensure its thermal models are rigorously validated, including industry-standard uncertainty quantification, for use on SNF storage or transport systems. Important factors to consider during validation are the various designs of cask and canister systems, inclusion of new fuel designs like accident tolerant fuel, and inclusion of SNF assemblies with other components, such as control rod assemblies or discrete burnable absorber rods.

5. High Burnup Fuel Performance under Normal Conditions of Transport

- a. *Summary Finding: The Board notes that DOE continues to develop a structural model that can be used to predict the structural response of SNF, SNF cask or canister systems, and SNF transport vehicles under normal conditions of transport. The Board finds that the DOE structural model development and validation efforts include a number of uncertainties stemming from the use of dummy or surrogate fuel assemblies and unirradiated fuel material properties.*

Recommendation: The Board recommends that DOE quantify the uncertainties introduced by the use of unirradiated assembly components and surrogate components, such as concrete mock-SNF assemblies, in experiments being used to benchmark the DOE structural model. The structural model should also

be exercised to evaluate HBF cladding strains for different cask and canister types, fuel types, and degree of pellet-cladding bonding.

6. Fuel Performance Modeling

- a. *Summary Finding: The Board finds that the limited testing of irradiated HBF provides a potentially insufficient database of mechanical properties and other HBF characteristics required to develop accurate fuel performance models.*

Recommendation: The Board recommends that DOE continue to develop fuel performance models (e.g., BISON) that are validated utilizing experimental data. In so doing, DOE-sponsored fuel performance model developers should clearly identify the data they need to develop and validate models to DOE-sponsored experimentalists. Experimentalists should clearly explain the capabilities and limitations of their experimental equipment and facilities to model developers. This close collaboration is needed to ensure optimal experimental setup and collection of data needed to improve the models and achieve a better understanding of HBF characteristics and performance.

REFERENCES

- 10 CFR Part 71. "Packaging and Transportation of Radioactive Material." *Code of Federal Regulations*. Washington, DC: Government Printing Office.
- 10 CFR Part 72. "Licensing Requirements for the Independent Storage of Spent Nuclear Fuel, High-Level Radioactive Waste, and Reactor-Related Greater than Class C Waste." *Code of Federal Regulations*. Washington, DC: Government Printing Office.
- Adkins, H., K. Geelhood, B. Koepfel, J. Coleman, J. Bignell, G. Flores, J-A. Wang, S. Sanborn, R. Spears, N. Klymyshyn. 2013. *Used Nuclear Fuel Loading and Structural Performance Under Normal Conditions of Transport – Demonstration of Approach and Results on Used Fuel Performance Characterization*. FCRD-UFD-2013-000325. September 30.
- Alsaed, H. and B. Hanson. 2017. *Extended Storage and Transportation Gap Analysis Update—5 Year Delta*. Presentation at the Spent Fuel and Waste Science and Technology Annual Group Meeting. Las Vegas, Nevada. May 23.
- Anderson, P.A. and H.S. Meyer. 1980. *Dry Storage of Spent Nuclear Fuel*. NUREG/CR-1223. April.
- ASTM International. 2016. *Standard Guide for Drying Behavior of Spent Nuclear Fuel*. ASTM C1553-16.
- Bahr, J.M. 2017. Letter from Jean M. Bahr, Chair, U.S. Nuclear Waste Technical Review Board, to Mr. Edward McGinnis, Acting Assistant Secretary for Nuclear Energy, "Comments from the Board's review of the June 21, 2017, combined Post Irradiation Examination test plan *EPRI/DOE High Burnup Fuel Sister Pin Test Plan Simplification and Visualization (SAND2017-7597, July 2017)*". August 25.
- Bahr, J.M. 2018. Letter from Jean M. Bahr, Chair, U.S. Nuclear Waste Technical Review Board to Mr. Edward McGinnis, Acting Assistant Secretary for Nuclear Energy, "Comments and observations following the Board's October 24, 2018 meeting on research and development (R&D) activities related to managing and disposing of commercial spent nuclear fuel (SNF)". November 27.
- Bahr, J.M. 2020. Letter from Jean M. Bahr, Chair, U.S. Nuclear Waste Technical Review Board to The Honorable Rita Baranwal and Mr. William White, with comments following the Board's Fall 2019 meeting held on November 19, 2019. January 10.
- Billone, M.C. 2019. *Ductility of High-Burnup-Fuel ZIRLO™ following Drying and Storage*. ANL-19/14. Rev. 3. June 30.
- Billone, M.C. and T.A. Burtseva. 2020. *Preliminary Destructive Examination Results for Sibling Pin Cladding*. ANL-19/53, Rev. 2. Argonne National Laboratory. Lemont, Illinois. February 28.
- Billone, M. and Y. Liu. 2013. Ductile-to-Brittle Transition Temperatures for High-Burnup PWR Cladding Alloys. Presentation to the Nuclear Waste Technical Review Board at its November 20, 2013 meeting.

Billone, M., Y. Yan, T. Burtseva, and R. Daum. 2008. *Cladding Embrittlement During Postulated Loss-of-Coolant Accidents*. NUREG/CR-6967. July.

Billone, M.C., T.A. Burtseva, and R.E. Einziger. 2013. "Ductile-to-Brittle Transition Temperature for High-Burnup Cladding Alloys Exposed to Simulated Drying-Storage Conditions." *Journal of Nuclear Materials*. Vol. 433, pp. 431–448.

Billone, M.C., T.A. Burtseva, Z. Han, and Y.Y. Liu. 2013. *Embrittlement and DBTT of High-Burnup PWR Fuel Cladding Alloys*. FCRD-UFD-2013-000401. September 30.

Billone, M.C., T.A. Burtseva, and Y.Y. Liu. 2012. *Baseline Studies for Ring Compression Testing of High-Burnup Fuel Cladding*. FCRD-USED-2013-000040. November 23.

Billone, M.C., T.A. Burtseva, and M.A. Martin-Rengel. 2015. *Effects of Lower Drying-Storage Temperatures on the DBTT of High-Burnup PWR Cladding*. FCRD-UFD-2015-000008. August 28.

Billone, M.C., T.A. Burtseva, and J.M. Garcia-Infanta. 2017. *Effects of Radial Hydrides on PWR Cladding Ductility following Drying and Storage*. SFWD-SFWST-2017-000001. September 13.

Billone, M.C. and T.A. Burtseva. 2018. *Results of Ring Compression Tests*. SFWD-SFWST-2018-000510. September 28.

Boase, D.G. and T.T. Vandergraaf. 1977. "The Canadian Spent Fuel Storage Canister: Some Material Aspects." *Nuclear Technology*. Vol. 32, pp. 60–71.

Bryan, C.R., R.L. Jarek, C. Flores, and E. Leonard. 2019. *Analysis of Gas Samples Taken from the High Burnup Demonstration Cask*. SAND2019-2281. February.

Casagrande, A., D.S. Stafford, G. Pastore, R.L. Williamson, B.W. Spencer, and J.D. Hales. 2017. *UFD Proof-of-Concept Demonstration*. M2MS-17IN0201012. June.

Christensen, A.B. and K.M. Wendt. 2001. "Drying of Spent Nuclear Fuels and Fuel Debris Dried in a Vacuum Furnace." *Proceedings of the 8th International Conference on Radioactive Waste Management and Environmental Remediation*. Bruges, Belgium. September 30–October 4.

Chung, H.M. 2004. "Understanding Hydride- and Hydrogen-Related Processes in High-Burnup Cladding in Spent-Fuel-Storage and Accident Situations." *Proceedings of an International Topical Meeting on Light Water Reactor Fuel Performance*. Orlando, Florida. September 19-22.

Cinbiz, M.N., D.A. Koss, and A.T. Motta. 2016. "The Influence of Stress State on the Reorientation of Hydrides in a Zirconium Alloy." *Journal of Nuclear Materials*. Vol. 477, pp. 157–164.

Connolly, K.J. and R.B. Pope. 2016. *A Historical Review of the Safe Transport of Spent Nuclear Fuel*. FCRD-NFST-2016-000474, Rev. 1, ORNL/SR-2016/261, Rev. 1. August 31.

- Cook, C.S., G.P. Sabol, K.R. Sekera, and S.N. Randal. 1991. "Texture Control in Zircaloy Tubing Through Processing." *Zirconium in the Nuclear Industry: 9th International Symposium*. American Society for Testing and Materials STP 1132. pp. 80–95.
- Crede, T.M., P.J. Kersting, R.S. Lenahan, O. Linsuaín, Y. Long, G. Pan, and D.T. Rumschlag. 2016. *Westinghouse Performance Analysis and Design Model (PAD5)*. WCAP-17642-NP, Revision 1. May.
- Cuta, J.M., S.R. Suffield, J.A. Fort, and H.E. Adkins. 2013. *Thermal Performance Sensitivity Studies in Support of Material Modeling for Extended Storage of Used Nuclear Fuel*. FCRD-UFD-2013-000257. September 27.
- Das, K., D. Basu, and G. Walter. 2014. Thermal Analysis of Horizontal Storage Casks for Extended Storage Applications. NUREG/CR-7191. December.
- Davis, R.B. 1979. Data Report for the Nondestructive Examination of Turkey Point Spent Fuel Assemblies B02, B03, B17, B41, and B43. HEDL TC-1284. March.
- d'Entremont, A.L., R.L. Kesterson, and R.L. Sindelar. 2020. Evaluation of Hydrogen Generation in High Burnup Demonstration Dry Storage Cask. SRNL-STI-2020-00268, Revision 0. August 1.
- DOE (U.S. Department of Energy). 2009. Yucca Mountain Repository License Application Safety Analysis Report. DOE/RW-0573, Rev. 1. February.
- Duke Energy, Nuclear Information Center. 2016. The Facts About Used Nuclear Fuel. <https://nuclear.duke-energy.com/2016/10/05/the-facts-about-used-nuclear-fuel>. October 5.
- Einzig, R.E., S.D. Atkin, D.E. Stellrecht, and V. Pasupathi. 1982. "High Temperature Postirradiation Materials Performance of Spent Pressurized Water Reactor Fuel Rods under Dry Storage Conditions." *Nuclear Technology*. Vol. 57, pp. 65–80.
- Einzig, R.E. and R. Kohli. 1984. "Low-Temperature Rupture Behavior of Zircaloy-Clad Pressurized Water Reactor Spent Fuel Rods Under Dry Storage Conditions." *Nuclear Technology*. Vol. 67, pp. 107–123.
- Einzig, R.E., H. Tsai, M.C. Billone, and B.A. Hilton. 2003. "Examination of Spent Pressurized Water Reactor Fuel Rods After 15 Years in Dry Storage." *Nuclear Technology*. Vol. 144, pp. 186–200.
- EPRI (Electric Power Research Institute). 2012. *Extended Storage Collaboration Program International Subcommittee Report: International Perspectives on Technical Data Gaps Associated with Extended Storage and Transportation of Used Nuclear Fuel*. EPRI, Palo Alto, California. 1026481.
- EPRI. 2014. *High Burnup Dry Storage Cask Research and Development Project: Final Test Plan*. EPRI, Palo Alto, California. DE-NE-0000593.
- EPRI. 2017. *Dry Cask Storage Welded Stainless Steel Canister Breach Consequence Analysis Scoping Study*. EPRI, Palo Alto, California. 3002008192.

EPRI. 2018. *Development of Radionuclide Source Terms for Consequence Analysis of Canister Breach due to Through-Wall Chloride-Induced Stress Corrosion Cracking*. EPRI, Palo Alto, California. 3002014470.

EPRI. 2019. *High Burnup Dry Storage Research Project Cask Loading and Initial Results*. EPRI, Palo Alto, California. 3002015076.

EPRI. 2020a. *High-Burnup Used Fuel Dry Storage System Thermal Modeling Benchmark: Round Robin Results*. EPRI, Palo Alto, California. 3002013124.

EPRI. 2020b. *Phenomena Identification and Ranking Table (PIRT) for Thermal Modeling*. EPRI, Palo Alto, California. 3002018441.

EPRI. 2020c. *Effect of Hydride Reorientation in Spent Fuel Cladding—Status from Twenty Years of Research*. EPRI, Palo Alto, California. 3002016033.

Ewing, R.C. 2016a. Letter from Rodney C. Ewing, Chairman, U.S. Nuclear Waste Technical Review Board, to John F. Kotek, Acting Assistant Secretary for Nuclear Energy, Department of Energy, "Board letter to Acting Assistant Secretary John Kotek." May 23.

Ewing, R.C. 2016b. Letter from Rodney C. Ewing, Chairman, U.S. Nuclear Waste Technical Review Board, to John Kotek, Acting Assistant Secretary for Nuclear Energy, Department of Energy, "U.S. Nuclear Waste Technical Review Board Comments on *Post Irradiation Examination Plan for High Burnup Demonstration Project Sister Rods*." June 3.

Ewing, R.C. 2016c. Letter from Rodney C. Ewing, Chairman, U.S. Nuclear Waste Technical Review Board, to Dr. Monica Regalbuto, Assistant Secretary for Secretary for Environmental Management, and Mr. John Kotek, Acting Assistant Secretary for Nuclear Energy, "Comments from the August 2016 Board Meeting." December 7.

Fors, P., P. Carbol, S. Van Winckel, and K. Spahiu. 2009. "Corrosion of high burn-up structured UO₂ fuel in presence of dissolved H₂" *Journal of Nucl. Mater.* 394, 1–8. October.

Fort, J.A., T.E. Michener, S.R. Suffield, D.J. Richmond. 2016. *Thermal Modeling of a Loaded MAGNASTOR Storage System at Catawba Nuclear Station*. FCRD-UFD-2016-000068. PNNL-25871, Rev. 0. September 29.

Fort, J.A., D.J. Richmond, B.J. Cuta, and S.R. Suffield. 2019a. *Thermal Modeling of the TN-32B Cask for the High Burnup Spent Fuel Data Project*. PNNL-28915. July 30.

Fukuda, S., N. Irie, Y. Kawano, K. Nishi, and J. Kishimoto. 2015. "Demonstration Test Program for Long-term Dry Storage of PWR Spent Fuel." *Proceedings of the International Conference on Management of Spent Fuel from Nuclear Power Reactors—An Integrated Approach to the Back-End of the Fuel Cycle*. Vienna, Austria. June 17–19.

Garrick, B.J. 2005. Letter from B. John Garrick, Chairman, U.S. Nuclear Waste Technical Review Board, to Mr. Paul M. Golan, Acting Director of the Office of Civilian Radioactive Waste Management. December 19.

Garrick, B.J. 2009. Letter from B. John Garrick, Chairman, U.S. Nuclear Waste Technical Review Board, to the Honorable Steven Chu, Secretary, Department of Energy, "Feedback from the Board's June 2009 meeting." August 13.

Gilbert, E.R., C.E. Beyer, E.P. Simonen, and P.G. Medvedev. 2002. "Update of CSFM Creep and Creep Rupture Models for Determining Temperature Limits for Dry Storage of Spent Fuel." *Proceedings of the International Congress on Advanced Nuclear Power Plants: ICAPP; embedded topical meeting*. Hollywood, Florida. June 9–13.

Greene, S.R., J.S. Medford, and S.A. Macy. 2013. *Storage and Transport Cask Data for Used Commercial Nuclear Fuel (2013 US Edition)*. Report ATI-TR-13047. August 9.

Hadj-Nacer, M., T. Manzo, M. Ho, I. Graur, and M. Greiner. 2015. "Phenomena Affecting Used Nuclear Fuel Cladding Temperatures During Vacuum Drying Operations." *Proceedings of the 2015 International High-Level Radioactive Waste Management Meeting*. Charleston, South Carolina. April 12–16.

Hales, J.D., K.A. Gamble, B.W. Spencer, S.R. Novascone, G. Pastore, W. Liu, D.S. Stafford, R.L. Williamson, D.M. Perez, and R.J. Gardner. 2014. *BISON User's Manual: BISON Release 1.1*. INL/MIS-13-30307, Rev. 2. October.

Hall, K., G. Zigh, and J. Solis. 2019. *CFD Validation of Vertical Dry Cask Storage System*. NUREG/CR-7260. May.

Hanson, B.D., W. Wu, R.C. Daniel, P.J. MacFarlan, A.M. Casella, R.W. Shimskey, R.S. Wittman. 2008. *Fuel-In-Air FY07 Summary Report*. PNNL-17275, Rev. 1. September.

Hanson, B., H. Alsaed, C. Stockman, D. Enos, R. Meyer, and K. Sorenson. 2012. *Gap Analysis to Support Extended Storage of Used Nuclear Fuel*. FCRD-USED-2011-000136, Rev. 0. January.

Hanson, B. 2016. *Peak Cladding Temperatures: Conservative Licensing Approach vs. Actual*. Presentation at the 2016 Nuclear Energy Institute Used Fuel Management Conference. Orlando, Florida. May 3–5.

Hanson, B.D., S.C. Marschman, M.C. Billone, J. Scaglione, K.B. Sorenson, and S.J. Saltzstein. 2016. *High Burnup Spent Fuel Data Project Sister Rod Test Plan Overview*. FCRD-UFD-2016-000063. April 29.

Hanson, B. 2018. *High Burnup Spent Fuel Data Project & Thermal Modeling and Analysis*. Presentation to the Nuclear Waste Technical Review Board at its October 24, 2018, meeting.

Hardin, E., T. Hadgu, D. Clayton, R. Howard, H. Greenberg, J. Blink, M. Sharma, M. Sutton, J. Carter, M. Dupont, and P. Rodwell. 2012. *Repository Reference Disposal Concepts and Thermal Load Management Analysis*. FCRD-UFD-2012-000219 Rev. 2. November.

Holtec International. 2016. *Holtec International Final Safety Analysis Report for the HI-STORM 100 Cask System*. Non-proprietary, Rev. 13. March 31.

Hunter, I. 2004. "AREVA – Preparation of Waste Shipments, Cask Vendor Perspective." Presentation to the Nuclear Waste Technical Review Board at its January 21, 2004, meeting.

- IAEA (International Atomic Energy Agency). 2003. Radioactive Waste Management Glossary: 2003 Edition. STI/PUB/1155. July.
- IAEA. 2011. Impact of High Burnup Uranium Oxide and Mixed Uranium-Plutonium Oxide Water Reactor Fuel on Spent Fuel Management. IAEA Nuclear Energy Series No. NF-T-3.8. Vienna: International Atomic Energy Agency.
- Jernkvist, L.O. and A. Massih. 2002. Analysis of the Effect of UO₂ High Burnup Microstructure on Fission Gas Release. SKI Report 02:56. December.
- Jung, H., P. Shukla, T. Ahn, L. Tipton, K. Das, X. He, and D. Basu. 2013. Extended Storage and Transportation: Evaluation of Drying Adequacy. Center for Nuclear Waste Regulatory Analyses. ADAMS Accession No. ML13169A039.
- Kalinina, E.A., C. Wright, L. Lujan, N. Gordon, S.J. Saltzstein, and K.M. Norman. 2018. Data Analysis of ENSA/DOE Rail Cask Tests. SFWD-SFWST-2018-000494. November 19.
- Kalinina, E.A., D. Ammerman, C. Grey, M. Arviso, C. Wright, L. Lujan, G. Flores, and S. Saltzstein. 2019. 30 cm Drop Tests. SAND2019-15256 R, December 17.
- Kalinina, E., D. Ammerman, C. Grey, G. Flores, L. Lujan, S. Saltzstein, and D. Michel. 2020. Surrogate Assembly 30 cm Drop Test. SAND2020-10498R. September 28.
- Klymyshyn, N.A., P. Ivanusa, K. Kadooka, C. Spitz, P.J. Jensen, S.B. Ross, and B.D. Hanson, D. Garcia, J. Smith, S. Lewis. 2018. *Modeling and Analysis of the ENSA/DOE Multimodal Transportation Campaign*. PNNL-28088. September 28.
- Klymyshyn, N.A., P. Ivanusa, K. Kadooka, C. Spitz, E.D. Irick, P.J. Jensen, S.B. Ross, and B.D. Hanson. 2019. *Structural Dynamic Analysis of Spent Nuclear Fuel*. PNNL-29150. September 30.
- Knight, T.W. 2016. *Experimental Determination and Modeling of Used Fuel Drying by Vacuum and Gas Circulation for Dry Cask Storage*. Presentation to the Nuclear Waste Technical Review Board at its February 17, 2016 meeting.
- Knight, T.W., T. Farouk, J. Khal, E. Roberts, J. Tarbuton, J. Yulenko. 2019. *Experimental Determination and Modeling of Used Fuel Drying by Vacuum and Gas Circulation for Dry Cask Storage: Final Report*. Integrated Research Project Awards, Nuclear Energy University Program, U.S. Department of Energy.
- Larson, N. 2019. *DOE High Burnup Demonstration Project*. Presentation to the Nuclear Waste Technical Review Board at its November 19, 2019 meeting.
- Liljenfeldt, H., K. Banerjee, J. Clarity, J. Scaglione, R. Jubin, V. Sobes, R. Howard, E. Hardin, L. Price, E. Kalinina, T. Hadgu, A. Ilgen, C. Bryan, J. Carter, T. Severynse, and F. Perry. 2017. *Summary of Investigations on Technical Feasibility of Direct Disposal of Dual-Purpose Canisters*. SFWD-SFWST-2017-000045. September.
- Lindgren, E.R., S.G. Durbin, R.J.M. Pulido, and A. Salazar. 2019. *Update on the Thermal Hydraulic Investigations of a Horizontal Dry Cask Simulator*. SAND2019-11688R. September.

Louthan, M.R. Jr. and R.P. Marshall. 1963. "Control of Hydride Orientation in Zircaloy." *Journal of Nuclear Materials*. Vol. 9, pp. 170–184.

Louthan, M.R. Jr. 2016. *Hydride Reorientation Occurrence and Effects: Summary of the Findings of the June 2014 Jackson, WY Workshop Used Fuel Disposition Campaign Published in SRNL-STI-2015-00256*. Presentation to the Nuclear Waste Technical Review Board at its February 17, 2016, meeting.

Lovasic, Z. and R. Einziger. 2009. "International Atomic Energy Agency (IAEA) Activity on Technical Influence of High Burnup UOX and MOX Water Reactor Fuel on Spent Fuel Management—9065." *Proceedings of the WM2009 Conference*. Phoenix, Arizona. March 1–5.

Marschman, S.C. and P.L. Winston. 2015. *Concepts for Small-Scale Testing of Used Nuclear Fuel*. FCRD-UFD-2015-000767, Rev. 0. September 25.

McConnell, P., R. Wauneka, S. Saltzstein, and K. Sorenson. 2014. *Normal Conditions of Transport Truck Test of a Surrogate Fuel Assembly*. FCRD-UFD-2014-000066, Rev. 0.1. December 15.

McConnell, P., G. Koenig, W. Uncapher, C. Grey, C. Engelhardt, S. Saltzstein, and K. Sorenson. 2015. *Surrogate Fuel Assembly Multi-Axis Shaker Tests to Simulate Normal Conditions of Rail and Truck Transportation*. FCRD-UFD-2015-000128, Rev. 0. September 11.

McConnell, P., S. Ross, C. Grey, W. Uncapher, M. Arviso, R.G. Garmendia, I.F. Pérez, A. Palacio, G. Calleja, D. Garrido, A.R. Casas, L.G. García, W. Chilton, D. Ammerman, J. Walz, S. Gershon, S. Saltzstein, K. Sorenson, N. Klymyshyn, B. Hanson, R. Peña, and R. Walker. 2018. *Rail-Cask Tests: Normal-Conditions-of-Transport Tests of Surrogate PWR Fuel Assemblies in an ENSA ENUN 32P Cask*. SFSW-SFWST-2017-000004. January 16.

McKinnon, M.A. and V.A. DeLoach. 1993. *Spent Nuclear Fuel Storage—Performance Tests and Demonstrations*. PNL-8451. April.

Meyer, R., M.S. Good, J.D. Suter, F. Luzi, B. Glass, and C. Hutchinson. 2019. *Sensor Development for Liquid Water Detection in Dry Storage Casks: FY19 Status*. PNNL-29112. September 16.

Michener, T.E., J.M. Cuta, D.R. Rector, and H.E. Adkins, Jr. 2015. *COBRA-SFS: A Thermal-Hydraulic Analysis Code for Spent Fuel Storage and Transportation Casks, Cycle 4*. PNNL-24841. October.

Montgomery, R. and B. Bevard. 2020. *Sister Rod Destructive Examinations (FY20)*. ORNL/SPR-2020/1798. November 30.

Montgomery, R., B. Bevard, R.N. Morris, J. Goddard, Jr., S.K. Smith, J. Hu, J. Beale, and B. Yoon. 2017. *Sister Rod Nondestructive Examination Annual Report FY2017*. SFWD-SFWST-2017-000003. September 15.

Montgomery, R., B. Bevard, R.N. Morris, J. Goddard, Jr., S.K. Smith, J. Hu, J. Beale, and B. Yoon. 2018. *Sister Rod Nondestructive Examination Final Report*. SFWD-SFWST-2017-000003 Rev. 1. May 16.

Montgomery, R., R.N. Morris, R. Ilgner, B. Roach, J. Wang, Z. Burns, J.T. Dixon, and S.M. Curlin. 2019. *Sister Rod Destructive Examinations (FY19)*. ORNL/SPR-2019/1251, Rev. 1. September 27.

Motta, A.T. and L-Q. Chen. 2012. "Hydride Formation in Zirconium Alloys." *JOM*. Vol. 64, pp. 1403–1408.

Motta, A.T., A. Couet, and R.J. Comstock. 2015. "Corrosion of Zirconium Alloys Used for Nuclear Fuel Cladding." *Annu. Rev. Mater. Res.* 2015. 45:311-343.

Motta, A.T., L. Capolungo, L-Q. Chen, M.N. Cinbiz, M.R. Daymond, D.A. Koss, E. Lacroix, G. Pastore, P-C.A. Simon, M.R. Tonks, B.D. Wirth, and M.A. Zikry. 2019. "Hydrogen in Zirconium Alloys: A Review." *Journal of Nuclear Materials*. Vol. 518, pp. 440–460.

NRC (U.S. Nuclear Regulatory Commission). 2003. *Spent Fuel Project Office Interim Staff Guidance-11, Revision 3, Cladding Considerations for the Transportation and Storage of Spent Fuel*. November.

NRC. 2007. *Division of Spent Fuel Storage and Transportation Interim Staff Guidance-1, Revision 2, Classifying the Condition of Spent Nuclear Fuel for Interim Storage and Transportation Based on Function*. May.

NRC. 2014a. *Division of Spent Fuel Storage and Transportation Interim Staff Guidance-24, Revision 0, The Use of a Demonstration Program as a Surveillance Tool for Confirmation of Integrity for Continued Storage of High Burnup Fuel Beyond 20 Years*. July.

NRC. 2014b. *Identification and Prioritization of the Technical Information Needs Affecting Potential Regulation of Extended Storage and Transportation of Spent Nuclear Fuel*. May.

NRC. 2016a. *Division of Spent Fuel Management Interim Staff Guidance-2, Revision 2, Fuel Retrievability in Spent Fuel Storage Applications*. April.

NRC. 2016b. *Standard Review Plan for Renewal of Specific Licenses and Certificates of Compliance for Dry Storage of Spent Nuclear Fuel*. NUREG-1927, Rev. 1. June.

NRC. No Date. *Spent Fuel Project Office Interim Staff Guidance-3, Post Accident Recovery and Compliance with 10 CFR 72.122(l)*.

NRC. 2019. *Managing Aging Processes In Storage (MAPS) Report, Final Report*. NUREG-2214. July.

NRC. 2020a. *Standard Review Plan for Spent Fuel Dry Storage Systems and Facilities, Final Report*. NUREG-2215. April.

NRC. 2020b. *Standard Review Plan for Transportation Packages for Spent Fuel and Radioactive Material, Final Report*. NUREG-2216. August.

NRC. 2020c. *2020–2021 Information Digest*. NUREG-1350, Volume 32. August.

NRC. 2020d. *Dry Storage and Transportation of High Burnup Spent Nuclear Fuel, Final Report*. NUREG 2224. November.

- NWTRB (U.S. Nuclear Waste Technical Review Board). 2010. *Evaluation of the Technical Basis for Extended Dry Storage and Transportation of Used Nuclear Fuel*. December.
- NWTRB. 2019a. *Preparing for Nuclear Waste Transportation: Technical Issues that Need to Be Addressed in Preparing for a Nationwide Effort to Transport Spent Nuclear Fuel and High-Level Radioactive Waste*. September.
- NWTRB. 2019b. *Transcript of November 19, 2019, Nuclear Waste Technical Review Board Meeting*. pp. 1-350.
- Olander, D. 2009. "Nuclear fuels – Present and future." *Journal of Nuclear Materials*. Vol. 89. pp 1-22.
- Peehs, M., R. Bokelmann, and J. Fleisch. 1986. "Spent Fuel Dry Storage Performance in Inert Atmosphere." *Proceedings of the Third International Spent Fuel Storage Technology Symposium/Workshop*. Seattle, Washington. April 8–10.
- Peehs, M., G. Kaspar, and E. Steinberg. 1986. "Experimentally Based Spent Fuel Dry Storage Performance Criteria." *Proceedings of the Third International Spent Fuel Storage Technology Symposium/Workshop*. Seattle, Washington. April 8–10.
- Peters, S., D. Vinson, and J. T. Carter. 2020. *Spent Nuclear Fuel and Reprocessing Waste Inventory*, FCRD-NFST-2013-000263, Rev. 7. September.
- Pulido, R.J.M., E.R. Lindgren, S.G. Durbin, A. Zigh, J. Solis, S.R. Suffield, D.J. Richmond, J.A. Fort, L.E. Herranz, F. Feria, J. Penalva, M. Lloret, M. Galbán, J. Benavides, and G. Jiménez. 2020. *Modeling Validation Exercises Using the Dry Cask Simulator*. SAND2019-6079R. January.
- Raynaud, P.A.C. and R.E. Einziger. 2015. "Cladding Stress During Extended Storage of High Burnup Spent Nuclear Fuel." *Journal of Nuclear Materials*. Vol. 464, pp. 304–312.
- Richmond, D.J. and K.J. Geelhood. 2017. "FRAPCON Analysis of Cladding Performance during Dry Storage Operations." *2017 Water Reactor Fuel Performance Meeting*. Jeju Island, Korea. September 10–14.
- Richmond, D. and J. Fort. 2018. *HBU Demo Cask Thermal Modeling: COBRA-SFS and STAR-CCM+*. Presentation at the Spent Fuel and Waste Science and Technology Annual Group Meeting. Las Vegas, Nevada. May 23.
- Rondinella V.V., D Papaioannou, R. Nasyrow, W. Goll, and M. Rehm. 2015. "Measurement of Gas Permeability Along the Axis of a Spent Fuel Rod." *Proceedings of the 2015 TopFuel Reactor Fuel Performance Conference*. Zurich, Switzerland. September 13–17.
- Sabol, G.P., R.J. Comstock, G. Schoenberger, H. Kunishi, and D.L. Nuhfer. 1997. "In-Reactor Fuel Cladding Corrosion Performance at Higher Burnups and Higher Coolant Temperatures." *Proceedings of an International Topical Meeting on Light Water Reactor Fuel Performance*. Portland, Oregon. March 2–6.
- SAIC (Science Applications International Corp.). 1998. *Nuclear Fuel Cycle Facility Accident Analysis Handbook*. NUREG/CR-6410. SAIC. Reston, Virginia. March.

- Saltzstein, S.J. 2017. *High Burn-up Demo Sister Rod Test Program*. Presentation at the 2017 NRC Division of Spent Fuel Management Regulatory Conference. White Flint, Maryland. October 31.
- Saltzstein, S.J., K. Sorenson, B. Hanson, R. Shimskey, N. Klymyshyn, R. Webster, P. Jensen, P. MacFarlan, M. Billone, J. Scaglione, R. Montgomery, and B. Bevard. 2017a. *EPRI/DOE High Burnup Fuel Sister Rod Test Plan Simplification & Visualization*. SAND2017-1031R. September 15.
- Saltzstein, S.J., K. Sorenson, P. McConnell, and S. Ross. 2017b. *ENSA ENUN 32P Rail Cask Transport Tests*. Presentation at the 2017 NRC Division of Spent Fuel Management Regulatory Conference. White Flint, Maryland. October 31.
- Sandoval, R.P., R.E. Einziger, H. Jordan, A.P. Malinauskas, and W.J. Mings. 1991. *Estimate of CRUD Contribution to Shipping Cask Containment Requirements*. SAND88-1358. January.
- Shimskey, R.W., J.R. Allred, R.C. Daniel, M.K. Edwards, J. Geeting, P.J. MacFarlan, L.I. Richmond, T.S. Scott, and B.D. Hanson. 2019. *PNNL Phase 1 Update on Sibling Pin Destructive Examination Results*. PNNL-29179. September 27.
- Simonen, E.P. and E.R. Gilbert. 1988. *Dating—A Computer Code for Determining Allowable Temperatures for Dry Storage of Spent Fuel in Inert and Nitrogen Gases*. PNL-6639. December.
- Sindelar, R.L., M.R. Louthan, Jr., and B.D. Hanson. 2015. *White Paper Summary of 2nd ASTM International Workshop on Hydrides in Zirconium Alloy Cladding, June 10–12, 2014, Jackson, WY*. FCRD-UFD-2015-000533. May 29.
- Solis, J. and G. Zigh. 2016. *Impact of Variation in Environmental Conditions on the Thermal Performance of Dry Storage Casks: Final Report*. NUREG-2174. March.
- Sorenson, K., S. Saltzstein, P. McConnell, D. Ammerman, S. Ross, B. Hanson, N. Klymyshyn, P. Jensen, and J. England. 2016. *Full-scale Rail-Cask Tests with Surrogate PWR Assemblies*. Presentation at the 2016 EPRI Extended Storage Collaboration Program Meeting. Orlando, Florida. May 2.
- Strasser, A., P. Rudling, and C. Patterson. 2014. *Fuel Fabrication Process Handbook, Rev. 1*. Mölnlycke, Sweden: Advanced Nuclear Technology International. February.
- SKB (Svensk Kärnbränslehantering AB). 2010. *Spent Nuclear Fuel for Disposal in the KBS-3 Repository*. TR-10-13. December.
- SKB and Posiva Oy. 2017. *Safety Functions, Performance Targets and Technical Design Requirements for a KBS-3V Repository: Conclusions and Recommendations from a Joint SKB and Posiva Working Group*. Posiva SKB Report 01. January.
- Tarn, J.C.L., N.H. Madsen, and B.A. Chin. 1986. "Predictions of Dry Storage Behavior of Zircaloy Clad Spent Fuel Rods Using Deformation and Fracture Analysis." *Proceedings of the Third International Spent Fuel Storage Technology Symposium/Workshop*. Seattle, Washington. April 8–10.

Teague, M., S. Saltzstein, B. Hanson, K. Sorenson, and G. Freeze. 2019. *Gap Analysis to Guide DOE R&D in Supporting Extended Storage and Transportation of Spent Nuclear Fuel: An FY2019 Assessment*. SAND2019-15479R. December.

Tonks, M.R., D. Gaston, P.C. Millett, D. Anders, and P. Talbot. 2012. "An Object-Oriented Finite Element Framework for Multiphysics Phase Field Simulations." *Computational Materials Science*. Vol. 51, pp. 20–29.

Tsai, H. and M.C. Billone. 2003. "Characterization of High-Burnup PWR and BWR Rods, and PWR Rods after Extended Dry-Cask Storage." *Proceedings of the 2002 Nuclear Safety Research Conference*. NUREG/CP-0180. pp. 157–168.

U.S. Congress. 1982. Nuclear Waste Policy Act of 1982. 97th Congress, 1st Session. 1982. Washington, DC. Government Printing Office.

U.S. Congress. 1987. Nuclear Waste Policy Amendments Act of 1987. 100th Congress, 1st Session. 1987. Washington, DC. Government Printing Office.

UxC. 2020. *StoreFUEL and Decommissioning Report*. Vol. 22. May 5.

Valance, S., M. Zemek, J. Bertsch, and C. Hellwig. 2015. "Hydrogen Relocation Kinetics Within Zircaloy Cladding Tubes." *Proceedings of the 2015 TopFuel Reactor Fuel Performance Conference*. Zurich, Switzerland. September 13–17.

Wagner, J.C., J.L. Peterson, D.E. Mueller, J.C. Gehin, A. Worrall, T. Taiwo, M. Nutt, M.A. Williamson, M. Todosow, R. Wigeland, W.G. Halsey, R.P. Omberg, P.N. Swift, and J.T. Carter. 2012. *Categorization of Used Nuclear Fuel Inventory in Support of a Comprehensive National Nuclear Fuel Cycle Strategy*. ORNL/TM-2012/308. FCRD-FCT-2012-000232. December.

Wang, J.-A., H. Wang, B.B. Bevard, and J.M. Scaglione. 2016a. *FY 2016 Status Report: CIRFT Testing Data Analyses and Updated Curvature Measurements*. ORNL/SPR-2016/276. July 24.

Wang, J.-A., H. Wang, H. Jiang, Y. Yan, B.B. Bevard, and J.M. Scaglione. 2016b. *FY 2016 Status Report: Documentation of All CIRFT Data Including Hydride Reorientation Tests*. ORNL/SR-2016/424. September 14.

Wang, J. and H. Wang. 2017. *Mechanical Fatigue Testing of High-Burnup Fuel for Transportation Applications*. NUREG/CR-7198, Rev. 1. October.

Wittman, R. 2013. *Radiolysis Model Sensitivity Analysis for a Used Fuel Storage Container*. FCRD-UFD-2013-000357. September 20.

World Nuclear Association. 2019. *Nuclear Power in the USA*. <http://www.world-nuclear.org/information-library/country-profiles/countries-t-z/usa-nuclear-power.aspx>.

Yagnik, S.K., R-C Kuo, Y.R. Rashid, A.J. Machiels, and R.L. Yang. 2004. "Effect of Hydrides on the Mechanical Properties of Zircaloy-4." *Proceedings of the 2004 International Meeting on LWR Fuel Performance*. Orlando, Florida. September 19–22. pp. 191–199.

Yagnik, S.K., A. Hermann, and R-C. Kuo. 2005. "Ductility of Zircaloy-4 Fuel Cladding and Guide Tubes at High Fluences." *Journal of ASTM International*. Vol. 2, pp. 604–631.

GLOSSARY

aerosol A system of liquid or solid particles uniformly distributed in a finely-divided state through a gas, usually air.

aging management program A program for addressing aging effects in structures, systems, and components. The program may include prevention, mitigation, condition monitoring, and performance monitoring.

annealing A process that causes metals to become more ductile via heating to high temperatures. Annealing typically requires an extended time at an elevated temperature to be effective.

anoxic Generally, oxygen-free. An anoxic environment is one where there is no available or free oxygen; but there could be chemically bound oxygen.

argillite A compact rock derived from claystone, siltstone, or shale that has hardened via heat or pressure or introduction of a cementing material.

assembly nozzles Fixtures attached to the upper and bottom portions of fuel assemblies to allow handling of the assemblies and to properly locate the assemblies in the reactor core. See **fuel assembly**.

bare fuel Spent nuclear fuel assemblies that are unconfined or have not been packaged in a canister. Also referred to as “bare spent nuclear fuel assemblies.”

bentonite A soft, plastic, porous, light-colored rock composed of clay minerals formed by chemical alteration of volcanic ash. Compacted bentonite has been proposed for backfill and buffer material in many geologic repositories for nuclear waste because of its ability to prevent or substantially delay movement of water or radionuclides.

bound water Water that is chemically or physically bound to a material. See **chemisorbed water** and **physisorbed water**.

breached fuel A spent nuclear fuel rod with cladding defects that may permit the release of gases or solid fuel particulates from the interior of the fuel rod. Spent nuclear fuel rod breaches include pinhole leaks, hairline cracks, and gross ruptures.

brittle When a material is brittle, it cannot accommodate concentrations of stress because it lacks ductility, and therefore fractures easily. See **ductility**.

Brownian motion Any of various physical phenomena in which some quantity is constantly undergoing small, random fluctuations.

burnable absorber rod A rod in a nuclear fuel assembly, either fixed or movable, containing a burnable absorber used to control the reactivity level in a reactor. See **integral burnable absorber rod** and **discrete burnable absorber rod**.

burnup A measure of the amount of energy generated in a nuclear reactor per unit mass of nuclear fuel (e.g., uranium) initially loaded in the fuel, often measured in gigawatt-days per metric ton of uranium.

calorimetry The science or technology of measuring heat developed during a mechanical, electrical, or chemical reaction, and used for calculating the heat capacity of materials.

canning The placement of damaged spent nuclear fuel for storage into a can designed for damaged fuel or in an acceptable alternative. The purpose of a can designed for damaged fuel is to (1) confine gross fuel particles, debris, or damaged assemblies to a known volume within the cask; (2) to demonstrate that compliance with the criticality, shielding, thermal, and structural requirements are met; and (3) permit normal handling and retrieval from a spent nuclear fuel cask or canister.

ceramography The description or study of ceramics, often used during the post-irradiation examination of spent nuclear fuel.

certificate of compliance (CoC) (for a dry storage system) The certificate issued by the U.S. Nuclear Regulatory Commission that approves the design and operation of a spent nuclear fuel dry cask storage system in accordance with the provisions of 10 CFR Part 72, "Licensing Requirements for the Independent Storage of Spent Nuclear Fuel, High-Level Radioactive Waste, and Reactor-Related Greater Than Class C Waste," Subpart L, "Approval of Spent Fuel Storage Casks."

certificate of compliance (CoC) (for a transportation package) The certificate issued by the U.S. Nuclear Regulatory Commission that approves the design and operation of a package for the transportation of radioactive material in accordance with the provisions of 10 CFR Part 71, "Packaging and Transportation of Radioactive Material," Subpart D, "Application for Package Approval."

Chalk River Unidentified Deposits (CRUD) A colloquial term for corrosion and wear products (rust particles, etc.) that form in the primary coolant water of a nuclear reactor and can deposit on the surface of nuclear fuel.

chamfering The modification (removal) of the sharp edge of a nuclear fuel pellet where the cylindrical side of the fuel pellet meets the end face of the pellet. Chamfering reduces the local stress riser at the sharp corner of the pellet when the cladding creeps down on the pellet and it reduces the effects of pellet-cladding mechanical interactions. See **dished** and **stress riser**.

channel deformation Boiling water reactor (BWR) fuel assembly channels bow due to asymmetric placement of control rod blades that generate local neutron flux and temperature spatial gradients in the reactor. Furthermore, the pressure gradient

between the inside and the outside of a BWR channel might cause the assembly to bulge permanently in the reactor. Because the causes of channel deformation are related to irradiation in the reactor, higher burnup can lead to greater channel deformation. Also referred to as bow deformation.

chemisorbed water Water that is bound to other materials by forces whose energy levels approximate those of a chemical bond.

circumferential hydrides Zirconium hydride precipitates or platelets in zirconium-alloy cladding that lie in a plane formed by the axial direction and the circumferential (azimuthal) direction in cylindrical coordinates. See **radial hydrides**.

cladding The thin-walled metal tube that forms the outer jacket of a nuclear fuel rod. It prevents corrosion of the fuel by the coolant and the release of fission products into the coolant. Aluminum, stainless steel, and zirconium alloys are common cladding materials.

colloid Sub-micron particles found in groundwater that have a high surface area per unit mass and a high capacity for sorption of low-solubility or strongly-adsorbing contaminants. Typically, they are defined as being on the order of 1 to 1000 nanometers in diameter.

compressive strength The maximum load that a material can support without fracture when being compressed, divided by the original cross-sectional area of the material.

confinement (in a dry cask storage system for spent nuclear fuel) The ability to limit or prevent the release of radioactive substances into the environment.

confinement system In the context of nuclear systems licensed or approved by the U.S. Nuclear Regulatory Commission, a confinement system is a system, including a ventilation system, that acts as a barrier between areas containing radioactive substances and the environment.

containment system In the context of packaging systems approved by the U.S. Nuclear Regulatory Commission for the transportation of radioactive materials, a containment system is the assembly of components of the packaging that retains the radioactive material during transport.

control rod A rod, plate, or tube containing a neutron-absorbing material such as hafnium, boron, etc., used to control the reactivity and power level of a nuclear reactor. By absorbing neutrons, a control rod prevents the neutrons from causing further nuclear fissions.

control rod guide tube A component of a nuclear fuel assembly that constrains and directs the motion of a control rod as it is inserted into the reactor core to control reactivity.

cradle See **transport cradle**.

creep A time-dependent phenomenon by which material permanently deforms under stress and elevated temperatures.

critical crack size The depth of a crack in a material across the thickness, such as zirconium alloy cladding, beyond which a cracking mechanism can trigger failure (through-wall cracking) of the material.

criticality safety Evaluations, along with administrative and physical controls, that ensure a fissile material remains subcritical under normal and credible off-normal conditions.

Cyclic Integrated Reversible-Bending Fatigue Tester (CIRFT) A laboratory testing system at the Oak Ridge National Laboratory composed of a U-frame equipped with load cells to impose pure bending loads on spent nuclear fuel rod specimens and measure the in-situ curvature of the specimens during bending. The system was also designed to operate in a cyclic mode to measure the number of bending cycles to failure for spent nuclear fuel rod specimens, to determine the fatigue lifetime of the specimens. See **fatigue lifetime** and **fatigue failure**.

damage fraction A method of determining the fatigue lifetime of a material, such as spent nuclear fuel, by recording all shock and vibration loads that the material experiences during loading, handling, transportation, etc. and then calculating the amount of cladding damage each shock and vibration load causes. Each load is then summed over the lifetime of the cladding to determine the accumulated fatigue damage. When the accumulated fatigue damage is equal to or greater than 1.0, then, in theory, the cladding will fracture (breach).

damaged spent nuclear fuel Any spent nuclear fuel rod or spent nuclear fuel assembly that cannot meet the pertinent fuel-specific or system-related regulations specified by the U.S. Nuclear Regulatory Commission for dry storage or transportation of spent nuclear fuel.

dash pots A feature of pressurized water reactor assemblies that is located at the bottom of control rod guide tubes to slow the descent of a control rod during its last few centimeters of travel. This is one place where water may be retained after spent nuclear fuel is dried for storage.

decay heat Heat that is generated in a radioactive material, such as spent nuclear fuel, by radiation emitted from fission products and actinides undergoing radioactive decay.

delayed hydride cracking (DHC) A time-dependent mechanism generally thought to occur when hydrogen that is dissolved in spent nuclear fuel cladding diffuses to a crack tip and precipitates as zirconium hydride, which increases the probability of the cladding cracking.

Density Functional Theory A theory used to calculate the electronic structure of atoms, molecules, and solids. Its goal is the quantitative understanding of material properties from the fundamental laws of quantum mechanics.

destructive examination A broad group of analytical testing used in science and technology applications to evaluate the properties of a material or component; the examination process damages the material being examined. See **non-destructive examination**.

deviatoric stress A stress state with different magnitudes in different component directions.

discrete burnable absorber rod A burnable absorber rod that contains neutron absorber materials but no fuel and is part of a bank of connected rods that may be inserted into some of the guide tubes in some fuel assemblies to control the reactivity of the reactor core. See **burnable absorber rod**.

dished (pellet) In some nuclear fuel pellets, the circular ends of the pellet are hollowed out to accommodate thermal expansion and radiation-induced swelling. Also see **chamfering**.

dryness test A measurement or check made to ensure that a spent nuclear fuel cask or canister has been dried in accordance with guidance published by the U.S. Nuclear Regulatory Commission. A typical process used to conduct a dryness test is a “pressure rebound test” but other methods, such as the “falling rate method” may be used. See **pressure rebound test** and **falling rate method**.

dry storage The storage of spent nuclear fuel in a dry cask storage system that typically involves drying the spent nuclear fuel cask or canister, backfilling it with an inert gas (typically helium), and moving the cask or canister to a dry storage pad. See **dry cask storage system**.

dry cask storage system (DCSS) A system that uses a cask or canister to store spent nuclear fuel in a dry environment. A DCSS provides confinement, radiological shielding, criticality control, structural support, and passive cooling of the spent nuclear fuel during normal, off-normal, and accident conditions.

ductility transition temperature The temperature demarcating the transition between ductile and brittle behavior of spent nuclear fuel cladding in a “pinch mode” of loading, like that which may be experienced by high burnup fuel cladding in a side-drop accident during transportation.

ductility Capacity of a material to deform permanently without fracture (e.g., stretch, bend, or spread) in response to stress.

dummy assemblies Mock-up spent nuclear fuel assemblies used for testing purposes that simulate or mimic real spent nuclear fuel assemblies.

end-drop accident An accident scenario in which a spent nuclear fuel assembly is dropped on its end. An end drop accident can apply to an individual assembly or to a spent nuclear fuel cask or canister holding one or more assemblies.

engineered barrier system The designed or engineered components of a geologic repository, including waste packages and other features intended to prevent, or substantially delay, movement of water or radionuclides.

e-N curve A data plot or graph of strain versus the number of cycles to failure obtained from repeatedly bending or flexing a material at different stress levels. This type of curve is used for materials fatigue assessment. See **fatigue lifetime** and **fatigue curve**.

falling rate method A dryness test method where the system is pumped down to an acceptable vacuum, the vacuum pump is isolated, and the pressure in the system is allowed to rise. The time to reach a pre-determined (higher) pressure is measured. The system is subsequently pumped down again, and the process is repeated. The time to reach the predetermined higher pressure is plotted against the number of drying cycles. When the time required to reach the higher pressure is constant, the system is deemed dry. See also **dryness test**.

far field The geosphere beyond the near field. See **near field**.

fatigue curve A data plot is created from data collected by repeatedly bending or flexing a material to the same stress level until it fails, and recording the number of cycles at failure as a method of experimentally determining fatigue lifetime of a material. The test is repeated on specimens at different stress levels, and all the results are plotted on a graph of strain versus the number of cycles to failure (e-N curve) or stress versus the number of cycles to failure (S-N curve). See **fatigue lifetime**, **fatigue failure**, **S-N curve**, and **Cyclic Integrated Reversible-Bending Fatigue Tester**.

fatigue failure Material failure, such as through-wall cracking of a metal rod or plate, caused by repeated vibrations like those expected during normal conditions of transport. Fatigue failure is a function of the number of vibrations and the amount of deformation of the metal during each vibration.

fatigue lifetime The lifetime of a material expressed in number of cycles or vibrations to failure. See **fatigue failure** and **Cyclic Integrated Reversible-Bending Fatigue Tester**.

fission gas Gaseous fission products that are produced when a nuclear fuel material, such as uranium-235, fissions or splits after absorbing a neutron. In nuclear power reactors, fission gases are primarily the noble gases krypton and xenon. See **fission products**.

fission gas release The release of fission gases to the pellet-cladding gap and fuel rod plenum during steady-state reactor operation. The amount of fission gas release

typically increases with fuel burnup and can lead to higher rod internal pressure. See **fission gas** and **rod plenum**.

fission products The nuclei (fission fragments) formed by the fission of heavy elements, plus the nuclei formed by the fission fragments' radioactive decay.

flexural rigidity A measure of a structure's resistance to bending. For a cylindrical rod, flexural rigidity is $E \times I = \Delta M / \Delta \kappa$, where E is the elastic modulus, I is the area moment of inertia, M is bending moment, and κ is the curvature of the bending rod.

forced helium drying or **forced helium dehydration** A method of drying a spent nuclear fuel cask or canister where a heated inert gas, such as helium, is circulated in a closed system. Moisture is removed from the recirculating gas before it returns to the cask or canister.

fuel assembly A structured group of fuel rods (long, slender, metal tubes containing pellets of fissionable material, which provide fuel for nuclear reactors). Depending on the design, a nuclear reactor may have dozens of fuel assemblies (also known as fuel bundles), each of which may contain 200 or more fuel rods.

fuel fines Small fuel particles that can be released from a fuel pellet when a pellet fractures due to thermal stresses. Also fuel fines can collect at the pellet-pellet interfaces as the edges of the pellets are ground away when the pellets swell and press against each other.

galvanic corrosion An electrochemical process in which one metal corrodes preferentially when it is in electrical contact with another in the presence of an electrolyte.

gas transmission tests Also called gas communication tests. These are tests to determine the rate that the internal gas can flow from one end of a fuel rod to the other through or past the column of fuel pellets. This information is useful to determine the degassing flow rate immediately after a hypothetical cladding breach and then, the potential for entrainment of small fuel particles as they pass through the cladding breach.

grain boundaries Surface or area defects that constitute the interface between two single-crystal grains of different crystallographic orientation. The normal atomic bonding in grains terminates at the grain boundary.

grains Small, often microscopic, crystals of a material having a given and continuous crystal lattice orientation, interspersed with more randomly oriented atoms (termed the intergranular regions or grain boundaries).

gross breach Also called a gross rupture. A breach in spent nuclear fuel cladding that is larger than either a pinhole leak or a hairline crack that can allow the release of particulate matter from the spent nuclear fuel rod.

guillotine fractures A type of break in a rod or pipe that occurs in a plane that is perpendicular to the rod axis. See **breached fuel**.

hold-down spring A component that holds a column of fuel pellets in place within a fuel rod with sufficient space to accommodate gaseous fission products. The purpose of the hold-down spring is to ensure that the stack of pellets remain together and to allow for expansion of the fuel pellets during irradiation.

high burnup fuel Nuclear fuel with an assembly average burnup greater than 45 gigawatt-days per metric ton of uranium. See **burnup** and **low burnup fuel**.

high burnup structure See **rim region**.

hoop stress In the context of a nuclear fuel rod, hoop stress is a tensile stress in the fuel cladding that results from either rod internal pressure or swelling fuel pellets in contact with the cladding. Hoop stress is exerted circumferentially.

hydride reorientation A phenomenon in which hydrides that were initially precipitated in a circumferential orientation in pressurized water reactor fuel cladding, or in a random orientation in boiling water reactor fuel cladding, dissolve at high temperature (e.g., during and after spent nuclear fuel drying) in the zirconium-alloy matrix, and then reprecipitate upon cooling in a radial orientation. This phenomenon only occurs when both an adequate cladding hoop (circumferential) stress is present and the cladding temperature is high enough to dissolve the existing hydrides.

hydride reorientation treatment A treatment process for zirconium alloy cladding samples that causes the reorientation of zirconium hydrides from a circumferential to a radial orientation (in cladding that contained pre-existing hydrides) or the formation of radial hydrides (in cladding that did not contain pre-existing hydrides).

hydride rich layer A region near the outer surface of zirconium-alloy nuclear fuel cladding that contains high concentrations of zirconium hydrides. The hydride rich layer is most prominent in nuclear fuel that has achieved a high burnup, and thus, has been subjected to more extensive cladding corrosion, leading to hydrogen absorption in the cladding and the formation of hydrides.

hypothetical accident conditions, or accident conditions As applied to nuclear systems and components by the U.S. Nuclear Regulatory Commission, an accident condition is the extreme level of an event or condition, which exceeds off-normal events or conditions. Accident conditions include both design-basis accidents and conditions caused by natural or manmade phenomena.

illite A clay mineral of the muscovite mica group, with a lattice structure that does not expand on absorption of water.

illitization The transformation of smectite to illite which could compromise some beneficial features of bentonite, such as sorption and swelling capacity. See **bentonite** and **smectite**.

instant release fraction As applied to spent nuclear fuel in a geologic repository environment, the instant release fraction is the fraction of non-matrix-bound radionuclides in the spent nuclear fuel radionuclide inventory that is susceptible to prompt, or “instantaneous,” release upon breach of the waste package and first exposure of the spent nuclear fuel to groundwater (i.e., fission products and actinides present in the pellet-cladding gap).

integral burnable absorber rod One specific type of burnable absorber rod that contains nuclear fuel and neutron absorbers such as boron, which absorb neutrons during reactor operation and generate helium gas via an (n, alpha) reaction. The helium gas increases the rod internal pressure. See **burnable absorber rod**.

isobaric A condition or state of having constant pressure.

isothermal A condition or state of having constant temperature.

Jacobian-Free Newton-Krylov method (or approach) A synergistic combination of Newton-type methods for super linearly convergent solution of nonlinear equations and Krylov subspace methods for solving the Newton correction equations.

lattice defects An imperfection in the regular geometrical arrangement of the atoms in a crystalline solid. Also referred to as crystal defects.

linear heat rating The heat generated per unit length in a nuclear fuel element or pellet. Higher linear heat rate translates into higher fuel pellet internal stresses.

liner A material (e.g., pure zirconium) that is used to line the inner surface of some boiling water reactor fuel claddings. The purpose of the liner is to minimize pellet-cladding interaction defects in the cladding and the presence of a liner acts to decrease the probability of hydride reorientation.

low burnup fuel Nuclear fuel with an assembly average burnup lower than 45 gigawatt-days per metric ton of uranium. See **burnup** and **high burnup fuel**.

M5[®] AREVA-trademarked fuel cladding alloy, containing zirconium and niobium.

macro-scale models Computational models applicable to spatial scales larger than micro-scale and meso-scale (e.g., fuel rods and assemblies). See **meso-scale models** and **micro-scale models**.

macroscopic hydrides Collections of zirconium hydrides formed from stacking of small hydride platelets to form larger hydrides. Also referred to as “hydride stacks.”

material model A computational tool that simulates the physical, chemical, and metallurgical characteristics of a material and, when properly validated, can be

used to predict the behavior of the material in response to various environmental conditions. Material models can be combined with other models (like thermal models or mass diffusion models) in a multiphysics suite of models that can predict overall material performance, e.g., predicting the performance of spent nuclear fuel rods during reactor operation.

maximum cladding temperature limit A limit of 400°C provided as guidance by the U.S. Nuclear Regulatory Commission for the cladding of fuel of all burnups during drying and storage. This temperature limit was based on the assumption that “(t)he use of a 400°C temperature limit for normal conditions of storage and for short-term fuel loading and storage operations will simplify the calculations (Safety Analysis Reports) while assuring that hydride reorientation will be minimized.” See **safety analysis report**.

meso-scale models Computational models applicable to spatial scales larger than micro-scale and smaller than macro-scale (e.g., behavior of zirconium hydrides and crystalline grains). See **macro-scale models** and **micro-scale models**.

metallography The study of the structure of metals and alloys, particularly using microscopy (optical and electron) and X-ray diffraction techniques.

micro-scale models Computational models applicable to fine spatial scales, usually at a microscopic scale (e.g., electronic and atomic structure).

natural barriers In the context of geologic disposal of radioactive wastes, natural barriers are features of the natural setting that prevent or substantially delay movement of water or radionuclides.

near field The excavated area of a geologic repository near to or in contact with the waste packages, including filling or sealing materials, and those parts of the host medium/rock whose characteristics have been or could be altered by the repository or its contents. See **far field**.

neutron absorber A substance that has a large capacity for absorbing neutrons. Typically, an absorber material is used in certain nuclear reactors to decrease or control the initial reactivity of freshly loaded fuel. See **burnable absorber**.

neutron flux A measure of the rate of flow of neutrons. The neutron flux value is calculated as the neutron density (n) multiplied by neutron velocity (v), where n is the number of neutrons per cubic centimeter (expressed as neutrons/cm³) and v is the distance the neutrons travel in 1 second (expressed in centimeters per second, or cm/sec). Consequently, neutron flux is measured in neutrons/cm²/sec.

non-destructive examination A broad group of analytical testing methods used to evaluate the properties of a material or component without causing damage to the material or component being examined. See **destructive examination**.

normal conditions of transport As applied by the U.S. Nuclear Regulatory Commission to radioactive material packages, a package design must be evaluated under normal conditions of transport by determining the effect on the package design of a series of conditions and tests. The conditions and tests include specified levels of heat, cold, reduced external pressure, increased external pressure, vibration, water spray, free drop, corner drop, compression, and penetration.

package As applied to radioactive waste transportation, a package is the packaging together with its radioactive contents as presented for transport. See **packaging**.

packaging The assembly of components necessary to ensure compliance with the radioactive material packaging requirements of the U.S. Nuclear Regulatory Commission. Packaging may consist of one or more receptacles, absorbent materials, spacing structures, thermal insulation, radiation shielding, and devices for cooling or absorbing mechanical shocks. The vehicle, tie-down system, and auxiliary equipment may be designated as part of the packaging.

peak-power rod The nuclear fuel rod or rods operating in a nuclear reactor at the highest linear heat rating. See **linear heat rating**.

pellet-cladding bonding A phenomenon in which the fuel pellets inside a fuel rod become chemically and physically bonded to the inside of the fuel cladding during reactor irradiation.

phase field model A mathematical model for solving interfacial problems. Phase field models have mainly been applied to solidification dynamics, but they have also been applied to other situations such as fracture mechanics and hydrogen embrittlement.

physisorbed water Water that is physically bound as an adsorbate by weak forces to the surfaces of solid materials, such as those inside a spent nuclear fuel cask or canister.

Pilling-Bedworth ratio In corrosion science, the Pilling-Bedworth ratio is the ratio of the thickness or volume of an oxide to the thickness or volume of the original, unoxidized metal.

pinch mode loading A stress imparted to a tube or rod in which the stress is imparted at diametrically opposed positions on the outside of the tube, like two fingers pinching a straw. During transport of a spent nuclear fuel rod in a horizontal orientation, large shocks in the vertical direction that may occur in the event of an accident could cause a pinch mode load imparted above and below the rod.

pressure rebound test A test used to determine adequate dryness of a cask or canister holding commercial spent nuclear fuel, whereby a vacuum of at least 4.0×10^{-4} MPa (3 Torr) is drawn in the cask or canister and then, the vacuum pump is isolated. If the pressure inside the cask or canister does not rise above 4.0×10^{-4} MPa (3 Torr) in 30 minutes, the test is successful. Also referred to as a "pressure rise test." See **dryness test**.

proton irradiation A type of out-of-reactor irradiation method that can be used to simulate in-reactor irradiation of fuel or material samples. Proton irradiation can be conducted using a particle beam accelerator.

puncturing As applied to a spent nuclear fuel rod, puncturing is a destructive examination method used to determine the rod internal void volume, pressure, and gas composition. During puncturing, a hole is made in the spent nuclear fuel cladding and the rod internal gases are vented into a sealed, calibrated volume for measurement.

pycnometry The science or technology of measuring the density of fluids or solids.

radial hydrides Zirconium hydride precipitates or platelets in zirconium-alloy cladding that lie in a plane formed by the axial direction and the radial direction in cylindrical coordinates. See **circumferential hydrides**.

radiolysis Chemical decomposition of a compound, like a water molecule, into free radicals when exposed to ionizing radiation.

ready retrieval As applied by the U.S. Nuclear Regulatory Commission to spent nuclear fuel storage, ready retrieval is an operation whereby spent nuclear fuel can be removed from storage by normal means; no special equipment or procedures are required. See **retrievability**.

reprocessing The chemical or electrochemical treatment of spent nuclear fuel that can separate valuable or usable fissile materials, such as uranium and plutonium, from fission products and other waste materials in the fuel. The separated fissile material may be recycled and used in new applications, such as using the recovered uranium in the fabrication of new nuclear fuel.

residual water As applied to spent nuclear fuel in casks or canisters, residual water is any water remaining in a spent nuclear fuel cask or canister after the normal drying process is complete and the cask or canister has passed a dryness test. The three types of residual water are unbound or free water, chemisorbed water, and physisorbed water. See **dryness test**, **chemisorbed water**, and **physisorbed water**.

retrievability As applied by the U.S. Nuclear Regulatory Commission to spent nuclear fuel storage, retrievability is a state or condition of spent nuclear fuel whereby the fuel can be removed from storage for further processing or disposal by normal means; no special equipment or procedures are required. See **ready retrieval**.

rim region A portion of a nuclear fuel pellet located near the outer circumferential surface the pellet that experiences increased physical and chemical changes, during irradiation in a reactor, compared to the inner portions of the pellet. A rim region occurs in high burnup fuel. The rim region is defined by three characteristics: (1) increased plutonium content, (2) very fine-grained structure, and (3) high porosity with pores containing high-pressure fission gas.

ring compression test A destructive examination of a specimen cut from a length of tubing, such as spent nuclear fuel cladding, that is used to assess the ductile behavior of the specimen. In a ring compression test, the specimen is placed under a compressive load and the deformation (or strain) of the specimen is determined as a function of the load. See **ductility**.

rod plenum A volume present at the top or bottom of the fuel pellet column inside a fuel rod to accommodate both the build-up of fission gases as they are released and fuel pellet swelling from entrapped fission gases generated during the fission process.

rod stiffness A property of a fuel rod that refers to the rod's flexural rigidity. Studies have shown that pellet-cladding bonding increases the stiffness and fatigue strength of a spent nuclear fuel rod. See **pellet-cladding bonding**.

safety analysis report A documented assessment of the extent to which a nuclear facility or system can be operated safely with respect to workers, the public, and the environment, including a description of the conditions, safe boundaries, and hazard controls that provide the basis for ensuring safety.

shaker table test A testing method wherein an object, such as a spent nuclear fuel assembly, is mounted on a table that can be shaken in 3 to 6 directions (including rotational directions) with a given input vibration frequency to measure the strain response of the object.

sintering The process of solidifying a pressed agglomerate of powder by heating it to a high temperature (sometimes under pressure) without liquefaction.

sister rod, or sibling rod A spent nuclear fuel rod that has characteristics similar to one that is stored in the High Burnup Dry Storage Research Project test cask. The two potential donor fuel assembly sources for sister rods were (1) assemblies having similar operating histories to those assemblies chosen for storage in the test cask; or (2) actual fuel assemblies selected for storage in the test cask. Sister rods were selected from both types of assemblies noted above.

smectite A type of clay mineral (e.g., montmorillonite) that undergoes reversible expansion on absorbing water and is the principal component of bentonite. Smectite minerals can transform to illite at temperature above 100°C. See **bentonite** and **illite**.

S-N curve A data plot or graph of stress versus the number of cycles to failure obtained from repeatedly bending or flexing a material at different stress levels. This type of curve is used for materials fatigue assessment. See **fatigue lifetime, fatigue failure, and Cyclic Integrated Reversible-Bending Fatigue Tester**.

soak period A period of time, after drying a spent nuclear fuel cask or canister, during which the heat conduction, temperature, and pressure reach a steady state in the cask or canister (neglecting the slow change attributed to radioactive decay).

source term Types and quantities of radioactive or hazardous material released to the environment following a potential accident during storage or transport. In nuclear applications, the source term is used in analyses of the radiological consequences of a potential accident. For geologic disposal, source term means both the inventory of radionuclides in spent nuclear fuel and their release from the fuel during both normal, long-term behavior of the repository, and during low-probability events such as earthquakes or volcanic eruptions.

spacer grid A fuel assembly component that holds fuel rods in place and properly spaced in the assembly while allowing reactor cooling water to pass through them. Spacer grids are made from a material compatible with the cladding materials.

span A segment of a nuclear fuel rod between spacer grids. See **spacer grid**.

spent nuclear fuel pool A water-filled storage and cooling facility for spent nuclear fuel assemblies that have been removed from a reactor.

stress riser As applied to spent nuclear fuel cladding, a stress riser is a localized force on the cladding caused by the impingement of another component or object. For example, fuel pellet fragments may become lodged between a fuel pellet and the cladding and cause an increase in stress on the cladding as the fuel pellet swells during reactor irradiation.

swaging A forging process in which the dimensions of an item are altered using dies into which the item is forced. Swaging is usually a cold working process, but also may be hot worked.

tensile strength The maximum load that a material can support without fracture when being stretched, divided by the original cross-sectional area of the material.

texture The orientation of the metal grains in the crystalline structure of a metal or alloy. Some pressurized water reactor fuel cladding is manufactured by swaging the zirconium alloy to impart a preferred orientation, or texture, to the metal grains. See **swaging**.

thin wall formula A formula used to calculate the hoop stress on tubing, like nuclear fuel cladding, that has a small wall thickness relative to the diameter of the tubing. The thin wall formula is $\sigma(T) = P(T) r/t$ where: $\sigma(T)$ is the hoop stress on the cladding at the internal gas temperature, T; $P(T)$ is the internal pressure in the rod at the internal gas temperature, T; r is the mid-wall radius of the cladding; and t is the cladding thickness.

transport cradle The physical support for a spent nuclear fuel transport cask. The cradle is mounted to the bed of a truck trailer or railcar. Most spent nuclear fuel transport cask types will have their own specially-designed cradles, although some casks may share a common cradle.

transport package see **package**.

type of rock at the Yucca Mountain site that has been investigated as a potential location for a repository.

undamaged spent nuclear fuel Any nuclear fuel rod or nuclear fuel assembly that can meet the pertinent fuel-specific or system-related performance regulations specified by the U.S. Nuclear Regulatory Commission for the transportation package or dry cask storage system. Undamaged spent nuclear fuel rods may contain pinholes or hairline cracks but may not contain gross ruptures. See **damaged spent nuclear fuel**.

vacuum drying A method of drying spent nuclear fuel casks or canisters that relies on reduced pressure relative to atmospheric pressure to evaporate moisture and humid air or purge gas from the cask or canister.

volatile fission products Fission products that can form gaseous species depending on temperature and pressure conditions (e.g., iodine, cesium). See **fission products**.

waste package In the context of radioactive waste disposal, a waste package is the waste form and any containers, shielding, packing, and any absorbent materials immediately surrounding an individual waste container.

water radiolysis See **radiolysis**.

zircaloy Any of a group of alloys of zirconium, tin, and other metals, used chiefly as cladding for nuclear reactor fuel.

zirconium hydride A chemical compound formed in zirconium alloys when hydrogen combines with zirconium metal in the alloy.

ZIRLO® Westinghouse-trademarked fuel cladding alloy, which contains zirconium, tin, and niobium.

APPENDICES

Evaluation of the Department of Energy's Research Program to Examine the Performance of Commercial High Burnup Spent Nuclear Fuel During Extended Storage and Transportation

Appendix A

Characteristics of High Burnup Spent Nuclear Fuel

The Nuclear Waste Policy Act provides the following definition of spent nuclear fuel: “Spent Nuclear Fuel (SNF) means fuel that has been withdrawn from a nuclear reactor following irradiation, the constituent elements of which have not been separated by reprocessing” (U.S. Congress 1982).

The properties of nuclear fuel rods, including fuel pellets and cladding, and the structural components of an SNF assembly change with irradiation dose as the fuel is burned in a reactor. High burnup spent nuclear fuel (HBF)¹ is defined by the NRC as SNF whose burnup exceeds 45 GWd/MTU (NRC 2018). Generally, as burnup increases in the range of 40 to 45 GWd/MTU, there is a gradual increase in the rate of change of some of the properties of the fuel (described below) that may affect its behavior in storage and transportation.

This appendix describes (1) the general physical and chemical characteristics of light water reactor (LWR)² fuel rods and assembly design variations; (2) how burnup changes the physical, chemical, and radiological characteristics of SNF; and (3) how these properties differ between HBF and low burnup SNF (LBF, <45 GWd/MTU).

An extensive review of HBF characteristics is provided in the International Atomic Energy Agency Technical Report entitled “Impact of High Burnup Uranium Oxide and Mixed Plutonium Oxide Water Reactor Fuel on Spent Fuel Management” (IAEA 2011), which can be consulted for more detail.

A.1 General Description of Spent Nuclear Fuel Rods and Assemblies

In the United States, most commercial SNF comes from either pressurized water reactors (PWRs) or boiling water reactors (BWRs).³ The nuclear fuel comprises a column of ceramic

¹ Fuel burnup is a measure of the energy generated in a nuclear reactor per unit initial mass of nuclear fuel and is typically expressed in units of gigawatt-days per metric ton of uranium (GWd/MTU).

² LWRs are reactors that use H₂O as a coolant versus heavy water reactors that use deuterium-oxide (D₂O) as a coolant.

³ A small amount of commercial SNF came from the Fort St. Vrain gas cooled reactor. This type of fuel is not considered in this report.

pellets, composed of sintered⁴ uranium oxide (UO₂) grains⁵ that are enriched up to 5% uranium-235 (U-235). Pellets are anywhere from 1.0-1.5 cm (0.39-0.59 in) long (see Figures A-1 and A-2).

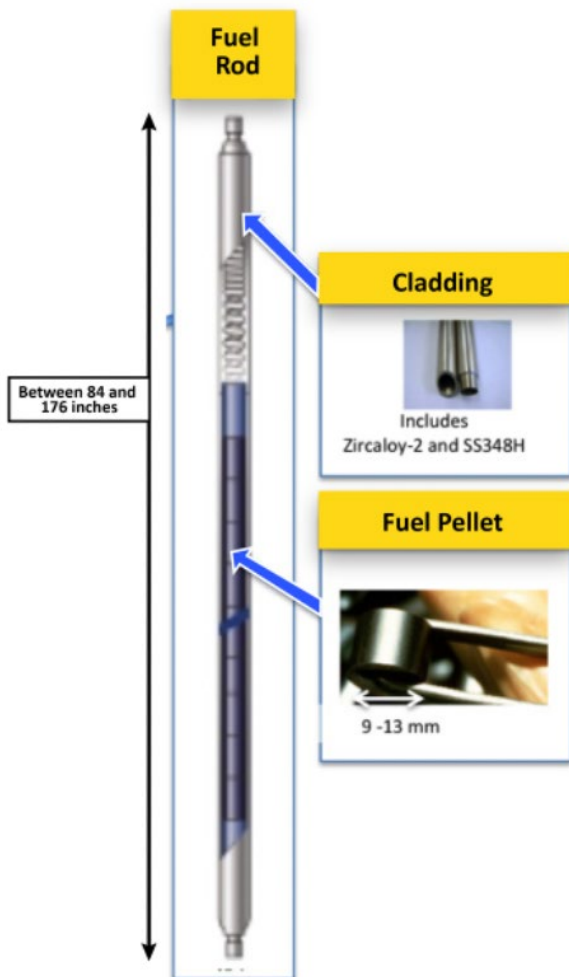


Figure A-1. A simplified figure of one type of BWR fuel rod.

The range of lengths of the fuel, widths of cylindric fuel pellet, and thickness of cladding used for BWR fuel is depicted. The general arrangement of a PWR fuel rod is similar (*modified from Wagner et al. 2012*).

The pellet ends are sometimes dished to allow space for irradiation growth and thermal expansion of the pellet and sometimes have a chamfered (beveled) edge to reduce the pellet-to-cladding mechanical interaction. The pellets are sealed inside zirconium-alloy metal tubes referred to as cladding (Figures A-1 through A-4).

A fuel rod (sometimes called a fuel pin) consists of a column of fuel pellets held in place with a hold-down spring that is sealed by welded end caps inside a cladding tube with sufficient space to accommodate gaseous fission products (also called fission gas) released from the pellets during irradiation (Figures A-1 and A-3). The purpose of the hold-down spring is to ensure that the stack of pellets remain together while allowing for expansion of the fuel pellets during irradiation. A large amount of the older PWR and BWR fuel rod claddings were made from Zircaloy-4 and Zircaloy-2, respectively. While these alloys are still used, newer alloys developed to reduce the corrosion of the cladding are starting to replace Zircaloy-2 and Zircaloy-4 and will eventually become the dominant cladding for HBF. These include ZIRLO[®], M5[®], GNF-Ziron [Global Nuclear Fuels], Low-Tin ZIRLO[®], and Optimized ZIRLO[™] for PWRs, and varieties of Zircaloy-2 for BWRs. Other new types of cladding are under study.

⁴ Sintering is the process of solidifying a pressed agglomerate of UO₂ powder by heating it to a high temperature (sometimes under pressure) without liquefaction. The purpose is to reduce and optimize the final pellet porosity for in-reactor operations.

⁵ Grains are small agglomerates of UO₂ crystals. Almost all materials are composed of such small crystals interspersed with more randomly oriented atoms (termed the intergranular regions).

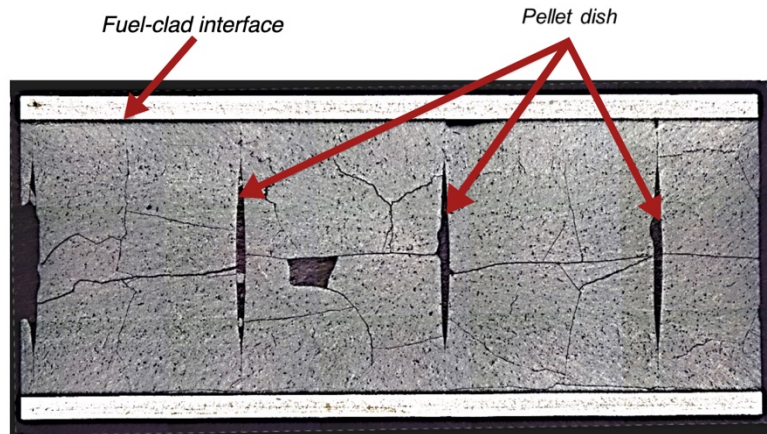


Figure A-2. Cross section of a fuel rod showing dished fuel pellets inside the fuel cladding. Note that the missing pellet fragment is due to the sample preparation (*adapted from Wang et al. 2016*).

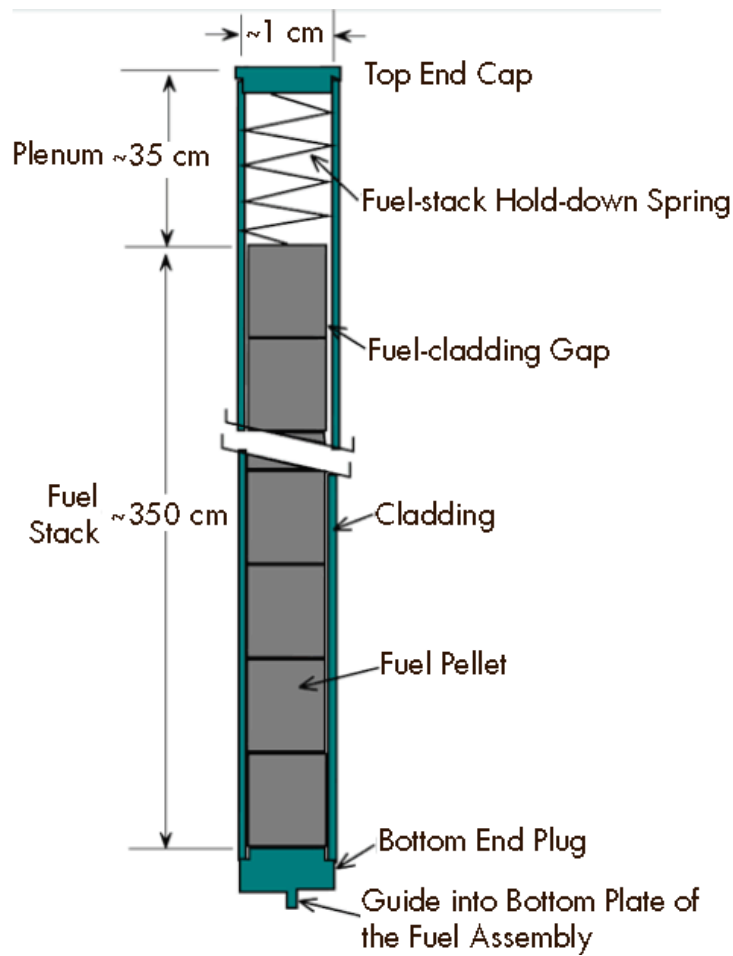


Figure A-3. Schematic of a generic LWR fuel rod (Olander 2009).

Most Zircaloy-2 cladding manufactured today contains a liner of pure zirconium or copper (Westinghouse uses copper in its BWR fuel), which reduces the risk of cladding breaches caused by pellet-cladding mechanical interaction.⁶ Compositions of these alloys are given in Table A-1, and a more complete discussion of the alloys is available from the NRC (Sindelar et al. 2011).

Fuel rods are manufactured with an inner diameter sufficient to provide a small gap or space between the pellets and cladding once the pellets are inserted. The gap initially is filled with helium at various elevated pressures⁷ to increase the thermal conductivity, thereby lowering the fuel operating temperature and reducing the compressive load on the cladding due to the coolant pressure (i.e., the difference in water-side and pellet-side pressures while in the reactor). An additional volume, referred to as the plenum, is present at the top and/or bottom of the fuel rod to accommodate both the buildup of fission gases as they are released and axial fuel pellet growth caused by swelling from entrapped fission gases generated during the fission process (Figures A-1 and A-3).

Table A-1 Compositions of alloys used as nuclear fuel cladding.

Nominal Compositions of Alloys Used as Nuclear Fuel Cladding									
Alloy	Sn (wt%)	Fe (wt%)	Cr (wt%)	Nb (wt%)	Ni (wt%)	O (wt%)	C (wt%)	Si (wt%)	Zr (wt%)
Zr-2 (BWR)	1.5	0.12	0.1		0.05	0.13			Balance
Zr-2(BWR) Improved	1.3	0.17	0.1		0.06	0.13			Balance
Zr-4 (PWR) High Tin	1.55	0.22	0.12			0.12	0.015	0.01	Balance
Zr-4 (PWR) Improved	1.3	0.22	0.12			0.12	0.12	0.01	Balance
M5 [®]		0.04		1		0.14			Balance
ZIRLO [®]	1	0.1		1		0.12			Balance
Optimized ZIRLO [™]	0.7	0.1		1		0.12			Balance
Zircaloy 2 Specification ATSM B811	1.2–1.7	0.07–0.20	0.05–0.15		0.03–0.08	0.09–0.16	0.027 max	0.012 max	Balance
Zircaloy 4 Specification ASTM B811	1.2–1.7	0.18–0.24	0.07–0.13			0.09–0.16	0.027–max	0.012–max	Balance

(Sindelar et al. 2011).

While the length of fuel rods can vary, they are generally about 4.0 m (13 ft; 157 in) long with the pellet stack height (“active fuel zone”, Figure A-4B) generally being 3.7 m (12 ft; 144 in). The fuel rods are held in place in the fuel assemblies by spacer grids (“spacers,” Figures A-4

⁶ Pellet-cladding mechanical interaction refers to stress placed on the cladding by the pellet once it comes into contact with the cladding. The presence of a zirconium liner also affects the distribution of hydrogen dissolved in the cladding metal as discussed in Appendix F.

⁷ The helium fill pressure also influences the hoop stress on the cladding during storage and transportation. Cladding hoop stress and its impact on cladding ductility during transportation are discussed in detail in Chapter 3 and Appendix F.

and A-5) typically made from a zirconium alloy⁸ that is compatible with the fuel cladding and resembles an egg crate (Figure A-5). The spacer grids are designed to hold the fuel rods in place laterally while allowing reactor cooling water to pass through them. Within each position of a spacer grid, the rod is centered by springs and dimples, which can create a localized force on the cladding and cause an additional stress called a stress riser. In addition, the spacer grid springs and dimples can trap debris that can cause the rod cladding to erode or “fret.” To mitigate damage to the rods by debris, most assemblies have a debris filter as part of the bottom-end nozzle (in PWRs) or bottom tie-plate (in BWRs) that screens the incoming coolant water (Figure A-4B). Depending on the fuel manufacturer, the top and bottom spacer grids may differ in design from the mid-span spacer grids in order to provide better structural support at the top and bottom of the assembly.

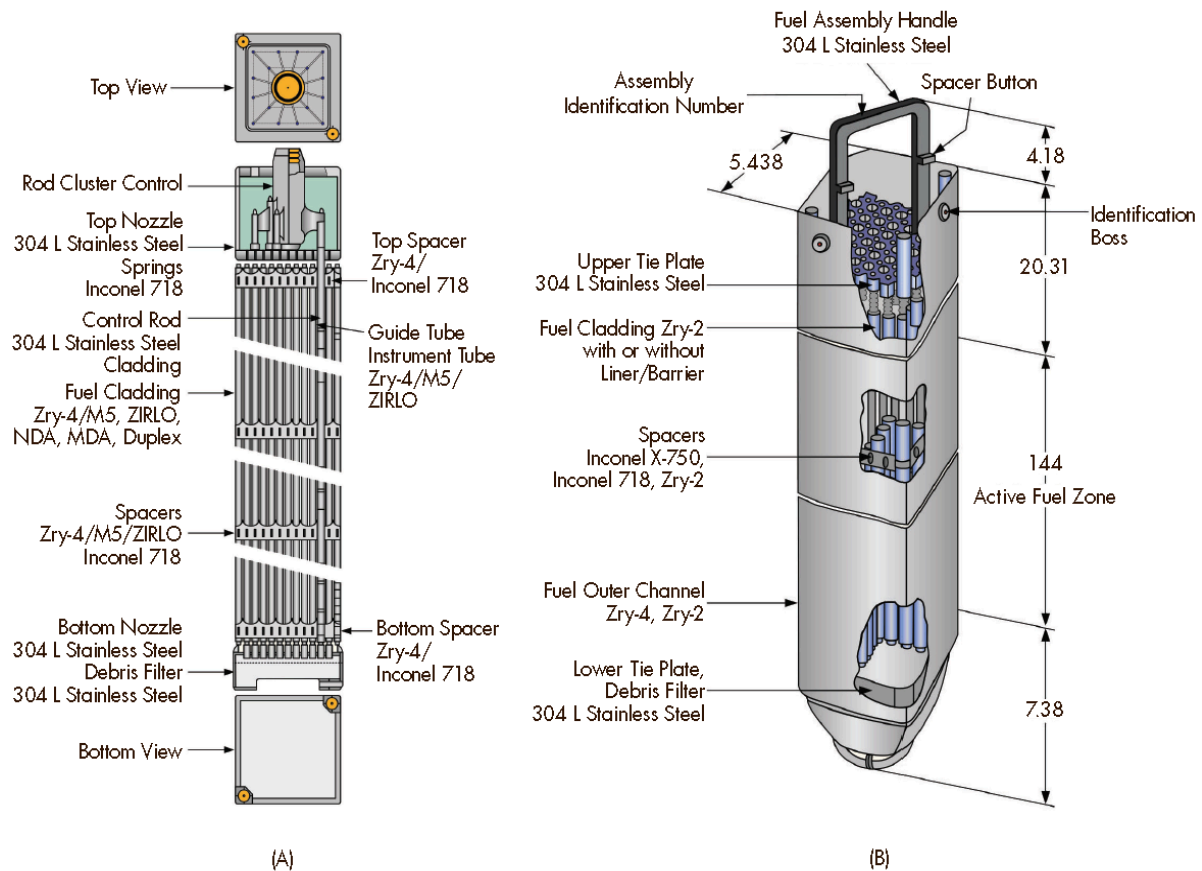


Figure A-4. Schematics of (A) pressurized water reactor and (B) boiling water reactor fuel assemblies

Dimensions are in inches. Provided courtesy of ANT International (*Strasser, Rudling, and Patterson 2014*).

Fuel assemblies also include assembly nozzles (tie plates in BWR fuel) at the top and bottom of the assembly. The nozzles on PWR fuel and the tie plates on BWR fuel have similar functions, such as providing paths for coolant flow and connection points at the top

⁸ Some fuel designs use spacer grids made of nickel-chromium based Inconel[®] metal.

for lifting the assemblies. Fuel and cladding are designed almost exclusively to optimize in-reactor performance. PWR fuel assemblies typically comprise arrays ranging from 14 x 14 to 17 x 17 rods. Figure A-6 depicts a fuel assembly with a 17 x 17 array. The benefits of employing an increased array size are better use of the uranium fissile content and lower pellet and cladding temperatures.

Hence, array sizes have been increasing over time. HBF, which is based on more recent fuel assembly designs, generally comprises arrays of 16 x 16 or 17 x 17 rods.⁹ However, the overall dimensions of the fuel assembly must remain the same to fit in existing reactors. To accommodate a greater number of rods in an array, maintain an optimized water to fuel mass ratio, and retain the same geometric array size, the outer diameter of the fuel pellets and the thickness of the cladding must be decreased.¹⁰

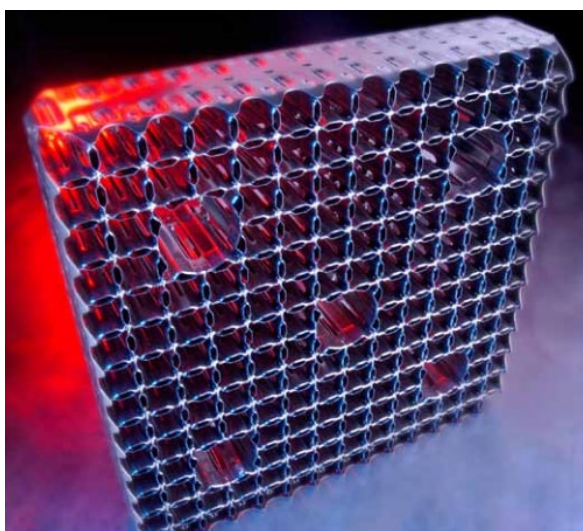


Figure A-5. Example of a spacer grid.

Photo of a spacer grid for an Areva (now Orano) 14 x 14 fuel assembly (photo courtesy Areva; AREVA Inc. 2010).

The initial helium gas fill pressure in the PWR fuel rods generally ranges from 2.1 to 3.5 MPa (300 to 500 psi). In approximately 20 positions of the PWR assembly array, fuel rods are replaced by control rod guide tubes, which also serve to connect the upper and lower nozzles¹¹ of the assemblies (see Figure A-4A for an example of an upper nozzle).

PWR assemblies have “dash pots” at the bottom of the control rod guide tubes to slow the descent of the control rod during its last few centimeters of travel. Most assembly types

⁹ Older PWR fuel assemblies, normally operated to lower burnup and lower linear heat rating used 14 x 14 and 15 x 15 rod arrays.

¹⁰ It is necessary to keep the same assembly size so the new assembly designs can be accommodated by existing reactor core structures, including the upper and lower core plates and the control rod drive mechanisms.

¹¹ In some literature, these are also called end bells.

have drain holes above the bottom of the guide tube to allow water to drain when the control rods are inserted (Figure A-7). This “dash pot” is one place where water may be trapped when the fuel is dried for storage depending on the existence and effectiveness of drain holes (see Appendix E for a detailed discussion of drying).

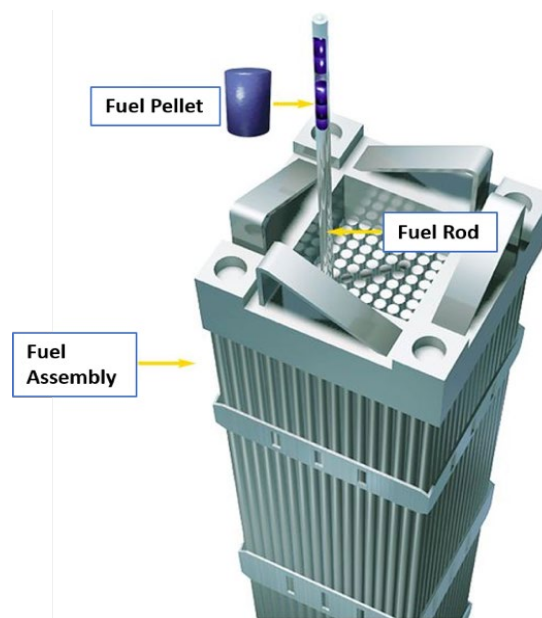


Figure A-6. Simplified schematic of a PWR nuclear fuel rod and fuel assembly.
(Image adapted from: Duke Energy, Nuclear Information Center 2016).

Older BWR fuel assemblies, which achieved lower burnups at higher linear heat ratings, have arrays ranging in size from 6 x 6 to 7 x 7 rods. Like PWR HBF arrays, newer HBF from BWRs generally comprises 8 x 8 to 11 x 11 rods. Also like PWR arrays, as the number of rods in the BWR array increases, it is necessary to reduce the outer diameter of the fuel pellet and rod and the thickness of the cladding to maintain the same geometric array size. The initial helium gas fill pressure in the BWR fuel rods generally ranges from 0.7 to 1.4 MPa (100 to 200 psi), which is lower than in PWR fuel rods because the coolant water pressure is lower.

Unlike the PWR assemblies, the BWR assemblies are held together axially with tie-rods, which are fuel rods slightly longer than standard. These rods have threaded connectors at each end that are bolted to the upper and lower tie plates (Figure A-4B). There are usually 4 to 8 tie-rods per assembly. Each BWR assembly is surrounded by a square, Zircaloy channel (also called a wrapper) that extends the length of the fuel assembly. The channel provides physical hydraulic separation of the fuel assembly from the lower flow resistance space between the fuel assemblies to ensure (1) appropriate axial coolant flow through each assembly (assisted by assembly inlet orifices), and (2) mechanical separation of the fuel assembly from the cruciform control blades and fixed in-core instrumentation to prevent interference. The channels not only improve the fuel assembly performance, but also improve assembly structural stiffening and transmittal of decay heat by radiation to the channel, which acts as a heat sink (Garzarolli et al. 2011).

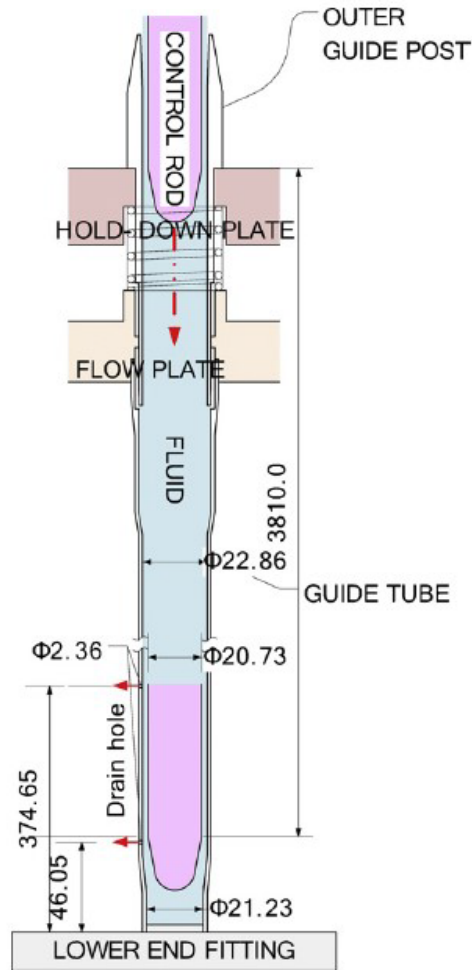


Figure A-7. Control rod guide tube in a PWR assembly showing insertion of a control rod.

The bottom of the schematic shows drain holes where water can escape. Dimensions in mm (*Yoon et al. 2009*).

A.2 Characteristics of High Burnup Fuel Compared to Low Burnup Fuel

The characteristics of the components that comprise a fuel assembly (i.e., pellets, cladding, and structural components) change as burnup increases, which may affect how the SNF and other system components respond during storage, transportation, and disposal. Some of the more rapid changes to the fuel characteristics occur early when the fuel is in the low burnup range, while other changes occur after longer irradiation times, when the fuel reaches high burnup. This section describes the changes that occur as the fuel is irradiated in the reactor.

A.2.1 Radioactive Inventory and Decay Heat

To achieve higher burnup levels, the initial enrichment of U-235 in the fuel must be increased. In contrast to the initial 3% U-235 for lower burnup fuels indicated in Figure A-8,

newer fuels designed to run to high burnup may start with as much as 5% U-235 (Meyer 2007). However, the higher initial enrichment level means that the higher fuel reactivity during early irradiation in the reactor must be counterbalanced to maintain criticality control. This is done by adding to some pellets or separate absorber rods isotopes of boron, erbium, or gadolinium, which have high neutron absorption properties, to absorb the extra neutrons that result from the higher initial enrichment. The added isotopes are converted to less effective neutron-absorbing isotopes as they absorb neutrons, so they are called “burnable absorbers.” An example of this type of modified pellet is the Integral Fuel Burnable Absorber pellet manufactured by Westinghouse. By the time the burnable absorbers are used up, the remaining concentration of U-235 has sufficiently decreased such that reactivity control can be maintained using the reactor control rods or soluble poisons. The reaction between the boron-based neutron absorbers and the neutrons generate alpha particles that then capture electrons to form helium. Hence, the amount of helium gas inside the fuel rods increases as the boron-based burnable neutron absorbers are consumed. As discussed in Appendix F, more helium gas increases the gas pressure inside the fuel rod leading to higher hoop stress on the cladding and potential deleterious effects during storage and transportation.

Figure A-8 illustrates typical changes in the chemical and isotopic composition of LBF in a reactor over time.¹² Such trends, involving increases in rapidly-decaying fission products and in long-lived transuranic radioisotopes, continue as the fuel experiences higher burnups. An increase in burnup results in SNF with increasing concentrations of fission products and actinides (beyond the actinides present in the fresh fuel), the latter being mostly comprised of plutonium (Lovasic and Einziger 2009). In general, HBF has a higher U-235 concentration at the time of discharge from the reactor than LBF because HBF has a higher initial loading of U-235 compared to LBF to compensate for higher levels of fission products and other neutron absorbers that accumulate in the HBF as it is taken to higher burnups during reactor operation. Changes in the radionuclide inventories occur in the fuel pellet (UO₂) matrix, the fuel grain boundaries, and the fission product inventory released to the fuel rod free volume¹³ (see Figure A-3).

In general, nuclear fuel becomes more radioactive and has a higher decay heat generation rate (per ton of uranium) as a function of burnup (Figure A-9). The fission product concentration in the fuel increases almost linearly with burnup. During the first 100 years after discharge from the reactor, the radioactivity and decay heat are mostly due to the radioactive decay of fission products, especially the decay of strontium-90 (half-life of 29 years) to yttrium-90 and of cesium-137 (half-life of 30 years) to barium-137. Thus, increasing burnup results in higher SNF radioactivity and heat load—both of which are relevant to storing, transporting, and disposing of SNF.¹⁴

¹² Although Figure A-8 is for lower burnup fuel, the trend is similar in higher burnup fuel.

¹³ The fuel rod free volume comprises the fuel pellet-cladding gap and the plenum.

¹⁴ After 100 to 200 years, the radioactivity and decay heat from actinides become dominant.

Composition of Conventional Nuclear Fuel (17x17 Westinghouse, 3% enr., 1100 irrad, 33000 MWD/MTU, discharge composition, Origen Arp analysis)

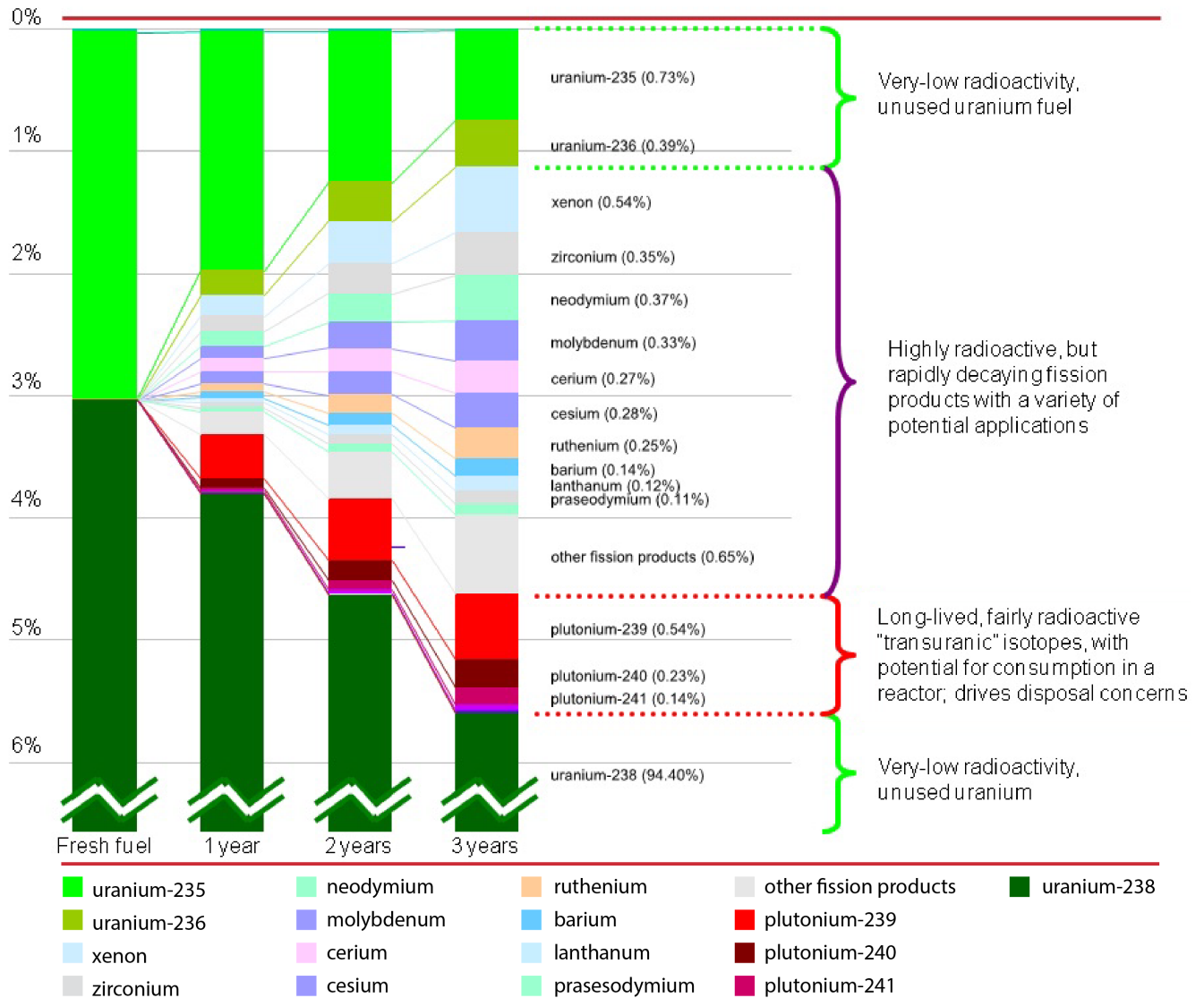


Figure A-8. Percentage radioactive composition of low burnup SNF as a function of irradiation time.

(adapted from Wang 2010).

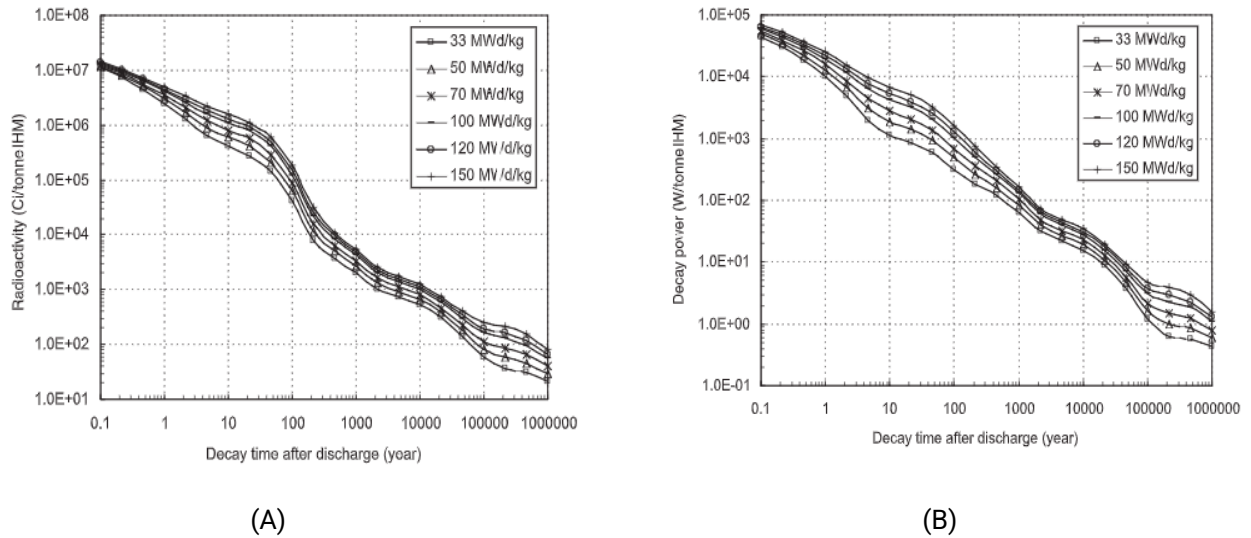


Figure A-9. Spent nuclear fuel (A) radioactivity and (B) decay power.

SNF radioactivity and decay power are shown as a function of local burnup and time after discharge (Xu, Kazimi, and Driscoll 2005).

A.2.2 Fuel Pellet Characteristics

Fuel pellets are formed from an agglomerate of small grains of UO_2 that are pressed together and sintered into a dense (~95% of the theoretical density) solid structure. Pellet lengths range from 1.0 to 1.5 cm (0.39 to 0.59 in) with diameters ranging between 0.7 to 1.0 cm (0.27 to 0.39 in) for PWR fuel and 0.9 to 1.3 cm (0.35 to 0.51 in) for BWR fuel (Figures A-1 and A

A-2). As discussed earlier, the fuel pellet ends are sometimes dished to provide space for the pellet to swell axially (see Figure A-2). Because UO_2 is a poor thermal conductor, the temperature at the center of the pellet is much higher than at the pellet periphery during reactor operation. Large temperature gradients and non-uniform heating rates in the reactor cause uneven thermal expansion, which will cause the fuel pellets to crack and deform (section A.2.2.4, Figure A-10A). As the fuel burnup increases, the fuel pellet becomes more fragmented due to swelling caused by radiation damage¹⁵ and the buildup of gaseous fission products. Near the outer circumferential surfaces of HBF pellets, a highly fractured "rim region" forms (also called the "high burnup structure;" see Figure A-10B and section A.2.2.2). In LWR fuel, the initial pellet-cladding gap will close due to fuel-pellet thermal expansion and swelling combined with creep down (inward deformation) of the cladding due to the higher coolant pressure in the reactor compared to the pressure inside the fuel rod.¹⁶ This phenomenon causes the cladding to develop a bamboo-like shape, but this effect is not usually visible to the human eye (see Figure A-11).

¹⁵ Voids and dislocations in the UO_2 crystalline lattice of the fuel pellet caused by the irradiation process.

¹⁶ Note that for LBF, the pellet-cladding gap will open once the fuel cools in the reactor spent fuel pool because the pellets contract. At high burnups, this is not apparent in photomicrographs of the fuel

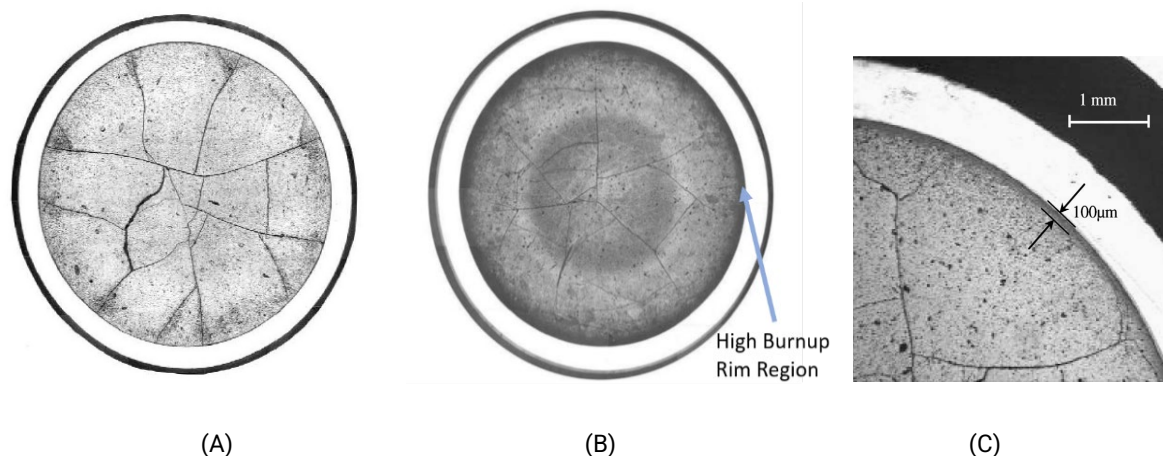


Figure A-10. Cross sections of PWR fuel pellets.

Images of (A) a 35 GWd/MTU (average) PWR fuel pellet (Tsai and Billone 2003); (B) a 67 GWd/MTU (average) PWR fuel pellet, indicating the high burnup rim region near the outer circumference of the fuel pellet (Tsai and Billone 2003); and (C) a 59 GWd/MTU (average) PWR fuel pellet, indicating the high burnup rim region within 100 µm of the outer circumference of the fuel pellet (Fors et al. 2009).

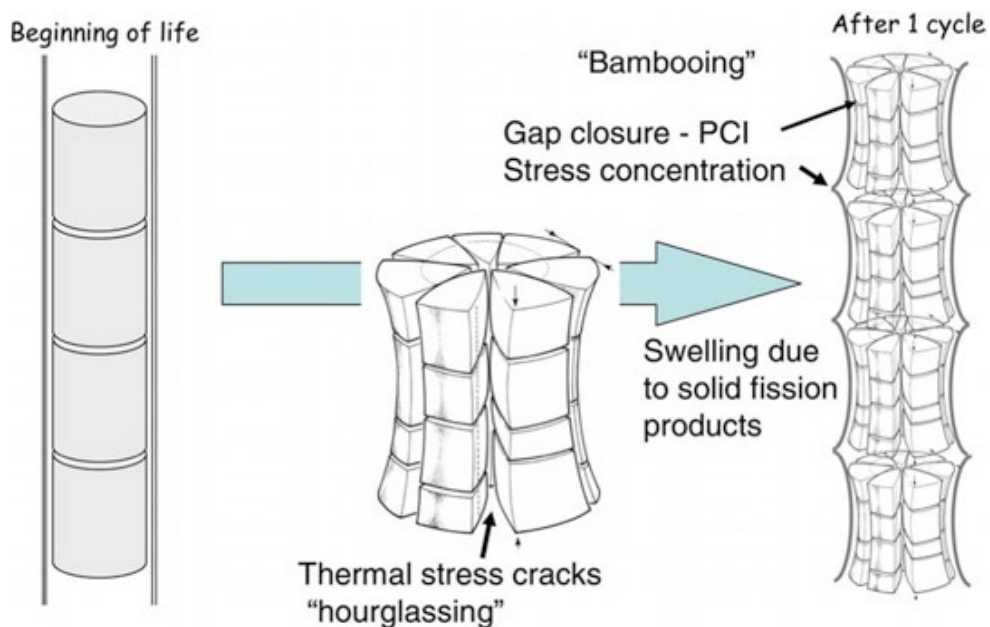


Figure A-11. Exaggerated depiction of “bambooning” deformation of SNF cladding.

“Hourglassing” of fuel pellets and bambooning of SNF cladding are not usually visible to the human eye (Olander 2009).

Note: PCI = pellet cladding interaction

cross-section as the gap volume is distributed in the inter-fragmental space after the pellet breaks into fragments. The fragments have a slight displacement and do not perfectly align, leaving a space between them (Raynaud and Einziger 2015).

Changes to the properties of fuel pellets at higher burnups are important because the altered properties can (1) increase the potential for the fuel cladding to develop cracks because of increased stress caused by pellet swelling and the increased rod internal pressure due to release of fission gas to the rod plenum (Olander 2009), and (2) cause the release of a greater fraction of the radionuclide content in the event of an accident and during long-term geologic disposal (Sanders et al. 1992). The following subsections summarize the effect of higher burnups on pellet grain size (section A.2.2.1), the formation of a pellet rim region where pellet properties have changed (section A.2.2.2), fission gas release (FGR)¹⁷ (section A.2.2.3), and the degree of pellet fracturing (section A.2.2.4).

A.2.2.1 Pellet Grain Size

Newer fuel being taken to higher burnups is manufactured with grain sizes¹⁸ between 8 to 12 micrometers (μm) as compared to older fuel, operated to lower burnups, that had grain sizes in the 15 to 25 μm range. During irradiation, the grains in the central hotter region of the pellet can grow depending on the temperature at which the fuel is operated. Simultaneously, fission gas is produced in the fuel grains and migrates to the grain boundaries where fission gas bubbles form. With continued irradiation, these bubbles line up on the grain boundaries. As the bubbles become interlinked, the fission gas and other volatile products migrate towards the fuel-cladding gap. This phenomenon first occurs within the central portion of the fuel pellet, and the radius at which gas interlinkage occurs increases with increasing burnup for a constant temperature profile. This interlinkage is one of the principal reasons why more fission gas is released as burnup increases. The added fission gas in the pellet-cladding gap contributes to total gas pressure and stress on the cladding during storage and transportation.

A.2.2.2 Pellet Rim Region

The local burnup in a fuel pellet rim region can be 2–3 times higher than the average pellet burnup depending on the specific irradiation conditions (Rondinella and Wiss 2010). This occurs because a greater proportion of neutron captures and fission take place at the pellet circumferential surface since neutrons slow down in the coolant (moderator), becoming more efficient at producing fission in U-235, and since these moderated neutrons are closest to the circumferential surface of the pellet. Therefore, the fission rate, production of transuranic elements, and production of fission products tends to be higher in the pellet rim region. The rim region is defined by three characteristics: (1) increased plutonium content, (2) very fine-grained structure, and (3) high porosity with pores containing high-pressure fission gas. As the fuel burnup increases, these phenomena become more pronounced (Jernkvist and Massih 2002). The thickness of the rim region, as measured by these three parameters, is not always consistent. However, the physical thickness of the restructured

¹⁷ The FGR is the fraction of the fission gas generated during irradiation that is released from the fuel pellets into the internal rod free volume.

¹⁸ In materials science, a grain is an individual crystallite in solids (ASTM International 2017b). The interface separating two grains where the orientation of individual crystallites changes is called a grain boundary. During irradiation of nuclear fuel, fission products and lattice defects are formed in the grains of the fuel and can migrate to the grain boundaries.

rim region increases with increasing burnup.¹⁹ Pellet restructuring and rim region formations are primarily due to accumulating radiation damage. These processes start at a local burnup of about 60–70 GWd/MTU,²⁰ which corresponds to an average pellet burnup of about 40 GWd/MTU (Lovasic and Einziger 2009). Restructuring causes the grain size to reduce, porosity to increase (Figures A-12 and A-13), and fission gas from the UO₂ matrix to become depleted. For steady-state power operation, the majority of the FGR is from the inner portion of the fuel pellet rather than from the rim region (Lozano et al. 1998).

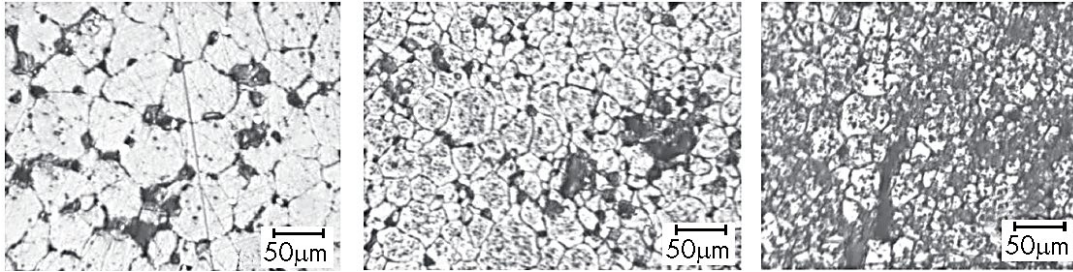


Figure A-12. Etched fuel pellet of H.B. Robinson fuel at a rod average burnup of 67 GWd/MTU.

The images show the decreasing fuel pellet grain size from the center (left) to the edge of the pellet (right) (*images courtesy ANL*). This fuel was irradiated to a high burnup as part of a special demonstration program (*EPRI 2001*).

Above 60 to 80 GWd/MTU local burnup, the UO₂ matrix in the rim region starts to release fission product gases, especially xenon (which is insoluble in the UO₂ matrix), to the open pores (Lösönen 2000; Hanson 2016). The fully restructured region has a typical grain size of 0.2 to 0.3 μm, which is much smaller than that of the original material. Some of the fission product gases released from the UO₂ matrix escape into the free volume of fuel rod, but many are trapped in newly formed, large-sized (~1 μm) pores in the rim region. Reported porosity for the rim region can reach 20% or higher (Spino et al. 2005), compared to about 6% in the bulk material.

Outstanding questions are whether the formation of a rim region is relevant to the performance of the fuel, and whether there are any significant consequences of the potentially changed performance during storage and transportation. If the fuel rod remains undamaged while being stored or transported, the presence of the rim region is of no consequence; however, if the cladding becomes grossly breached, then fuel particulates may be released from the rod, and if the fuel particulates are sufficiently small (<10 μm), they would then remain in Brownian motion in the cask cover gas (i.e., form an aerosol) (Sanders et al. 1992). The extent of this release is uncertain, and work is continuing internationally to quantify and characterize the fuel particulates. Even if fuel is released from the rod to the cask, it is only of concern if the cask system develops a leak. Because the rim

¹⁹ The data presented by Manzel and Walker (2000) on measured rim region thickness versus pellet average burnup up to 100 GWd/MTU are likely the best available data. A correlation based on Manzel and Walker (2002) data was developed and used in the fuel performance model FRAPCON-3 (Berna et al. 1997).

²⁰ The local burnup at the rim region is allowed to be higher than the NRC limit for average peak rod average burnup of 62.5 GWd/MTU.

region in HBF has a different grain structure than that of LBF, it could influence the pellet-cladding bond strength, which in turn could influence fuel rod stiffness and cladding crack formation during pinching.

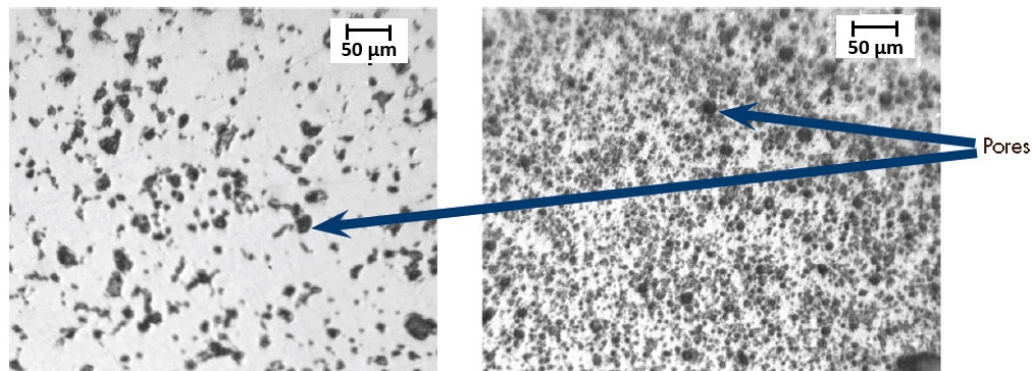


Figure A-13. Porosity at the pellet center (left) and rim region (right) of H.B. Robinson fuel at rod average burnup of 67 GWd/MTU.

(Images courtesy ANL). This fuel was irradiated to a high burnup as part of a special demonstration program (EPRI 2001).

A.2.2.3 Fission Gas Release and Internal Rod Pressure

The FGR of the noble gases xenon and krypton into the fuel-cladding free volume during reactor operations can vary from rod to rod within the same batch of fuel. Fuel rods operating in the reactor at the highest linear heat rating,²¹ (called peak-power rods), can have FGR as high as 25% compared with releases as low as 0.5% for lower power rods, depending on the design and burnup level. In PWR fuel and in newer BWR fuel, the release is typically 1 to 2% at burnups below 35 GWd/MTU. The release of noble fission gases (i.e., xenon and krypton) from the fuel pellet increases with burnup, which leads to higher internal gas pressure in the fuel rod (Figure A-14). The average FGR from high-burnup fuel pellets is between 3 and 7%. The higher value of release (7%) is reported in papers by Manzel and Walker (2000), in which fission gas is plotted versus burnup from fuel rod puncture data. Fractional FGR increases from approximately 7% at 60 GWd/MTU local burnup²² to 28% at 100 GWd/MTU local burnup and this may be due to a combination of the interlinkages of grain boundaries (discussed in section A.2.2.1) and the formation of much smaller UO₂ grains in the rim region (Manzel and Walker 2002). Johnson (2002) gives a detailed discussion of the FGR as a function of fuel type.

²¹ The linear heat rate is defined as the heat generated per unit length in a fuel rod where fuel pellets are loaded. High linear heat rate can cause an increase in the fuel pellet internal stress.

²² Burnup varies both axially and radially within a rod and an assembly. Local burnup is the burnup at the particular location in question.

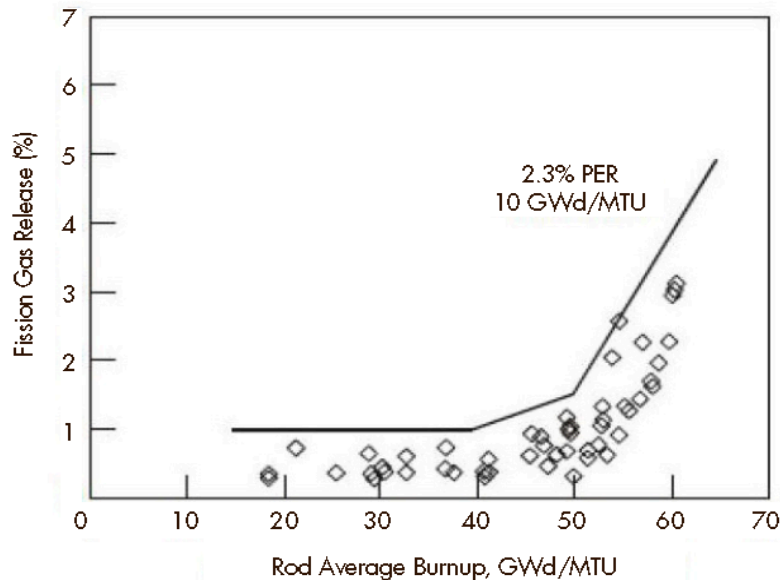


Figure A-14. Fraction of fission gas created that migrates to the free volume in the fuel rod in U.S. PWRs.
(Hanson 2016).

Increased release of xenon and krypton are deleterious because those gases mix with the original helium fill gas in the fuel-cladding gap and reduce the thermal conductivity of the gas in the gap. The reduced thermal conductivity causes the fuel pellet temperature to rise, which in turn could increase FGR from the pellet to the gap and increase the cladding temperature. Assuming the linear power density of the fuel is constant, these synergistic effects could result in higher fuel temperatures and higher than usual FGR as burnup increases (Olander 2009).

Other volatile fission products such as iodine and cesium are also released from the pellet to the interior of the fuel rod. The cesium comes mostly from the hotter grains interior to the pellet, and its release fraction closely tracks that of xenon, the isotopes of which are precursors of cesium isotopes. The small grains in the rim region almost completely retain their cesium, although some may be released at very-high burnup (Manzel and Walker 2002). When there is significant FGR, iodine and cesium generally migrate to the fuel pellet surfaces and to open cracks. These fission gases may be important to consider in the context of disposal, when conducting a repository performance assessment. The cesium and iodine can combine to form cesium iodide, which is not volatile at room temperature. Only at temperatures above 1030°C (1886°F), which is well above anticipated storage, transportation, and disposal temperatures, does cesium iodide volatilize to the point where it will increase the internal pressure in a rod more than 1% (Ewing and Stern 1974).

A.2.2.4 Degree of Pellet Fracturing

Due to thermal gradients in the fuel pellet creating internal stresses, the pellets tend to fragment early in their life (Olander 2009; see Figures A-2 and A-10). These pellet fractures lead to more pathways to release fission gases to the fuel rod void space in the plenum and the gaps. Cross-sectional and longitudinal photomicrograph images of the pellets show that

there can be as many as 20 to 50 large fragments²³ per pellet. To date, there have not been any systematic studies conducted to determine if the fragment size differs between BWR and PWR fuel or if fragment size changes with burnup. Example cross-sections of cracked fuel at 35 and 67 GWd/MTU are shown in Figure A-10. There are more fuel pellet fractures in the HBF than in the LBF. Many small fuel particles (also called fuel fines) collect at the pellet-pellet interfaces as the edges of the pellets erode when the pellets swell and press against each other. At higher burnups, additional circumferential fuel cracks are seen in the fuel rim region adjacent to the cladding. This may lead to more fragmentation when the fuel is subjected to handling or accident stresses.

A.2.3 Pellet-Cladding Gap Closure

LWR fuel has a small initial pellet-cladding gap that varies depending on the manufacturer (section 2.2.2.4 and A.1). During the first few irradiation cycles of LWR fuel, the gap closes due to pellet fracture, fuel pellet swelling, and creep down of the cladding caused by greater exterior coolant pressure. This results in slight ridging in the cladding at the pellet-pellet interfaces, imparting a bamboo shape to the cladding. These ridges cannot be visually observed but are noted when measurements of the rod's diameter (profilometry) are conducted (see Figure A-11 and Figure A-15).

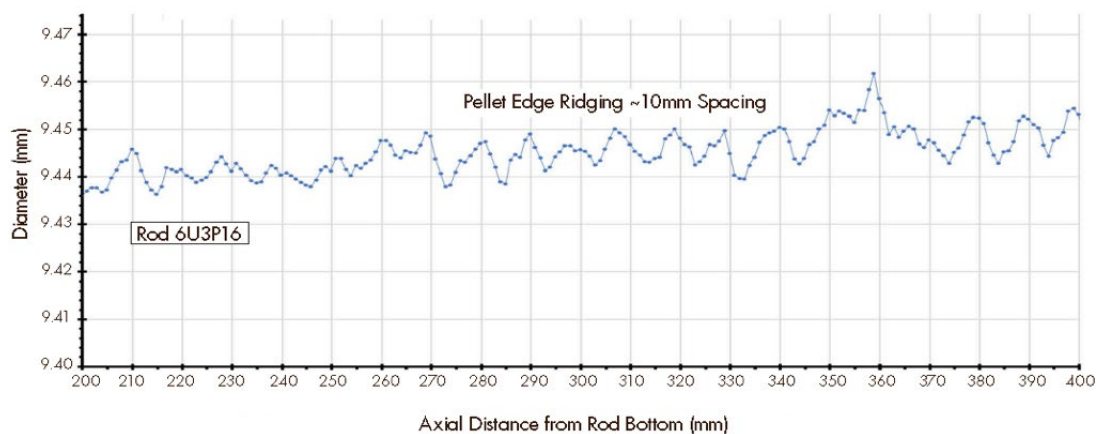


Figure A-15. Profilometry scan of the outer SNF rod surface showing localized ridging at pellet-pellet interfaces.

(adapted from Montgomery et al. 2018).

The pellet-cladding gap is measured from photomicrographs after the fuel has cooled. Due to differential thermal expansion of the fuel and cladding materials, the gap is not the same as it was during reactor operation (i.e., prior to cooling). Photomicrographs of LBF indicate that there are pellet-cladding gaps at room temperature. No such pellet-cladding gaps have been observed in HBF even after the fuel has cooled and differential thermal expansion between the fuel and the cladding should have theoretically opened a gap. This introduces some uncertainty regarding the fraction of the cladding where the gap has closed, and the fuel has chemically bonded to cladding.

²³ A fragment large enough so that it does not fall out of what the NRC defines as a gross breach of the cladding (NRC 2007).

While the pellet-cladding gap is not a cladding property *per se*, the extent to which the pellet-cladding gap has closed has important implications:

- 1) SNF rod stiffness and fatigue strength. Based on the static and fatigue bending tests at Oak Ridge National Laboratory (Wang and Wang 2017; see Appendix H), the pellet-cladding bond increases the stiffness (flexural rigidity) and fatigue strength of an SNF rod. Because HBF experiences greater pellet-cladding bonding, HBF is generally expected to be stiffer and stronger than LBF. A similar conclusion was reached by the NRC staff (NRC 2020).
- 2) SNF rod depressurization in accident conditions. The rate of depressurization²⁴ and the amount of fine fuel particulate released from an SNF rod to the cask atmosphere are key variables to consider in accident analyses. They directly affect the radioactive source term available for release to the environment if the transportation overpack or cask (Figure 1-5) also breaches. The rate of depressurization and loss of particulates if the cladding breaches is partially determined by the pellet-cladding gap size: if there is no gap, the rate of depressurization of the fuel rod may be significantly decreased reducing the potential for radioactive particulate release if the cask containment also fails. There is still some uncertainty regarding the rate of depressurization of HBF rods if they become grossly breached in an accident. However, DOE's examination of sister rods from the High Burnup Dry Storage Research Project included rod depressurization tests. The preliminary results from this testing show a range of times for a punctured rod to fully depressurize (ranging from approximately 5 hours to approximately 22 hours) (Montgomery et al. 2019). Further testing and evaluation are needed to determine the significance of these rod depressurization rates on radioactive material releases in accident conditions.

A.2.4 Cladding Changes with Burnup

Like fuel pellet properties, fuel cladding properties also change with increasing burnup (Olander 2009). As noted earlier, cladding takes on a bamboo-like structure with stress risers²⁵ at the pellet-pellet interface (Figure A-11). Irradiation causes the cladding to harden and the outer surface to oxidize due to the reaction with the coolant water (section A.4.2.2). The oxidized layer has a lower thermal conductivity than the cladding. A layer of Chalk River Unidentified Deposits (CRUD) (section A.2.4.3) may form on top of the oxide, which also reduces the cladding heat transfer capabilities due to the relatively poor thermal conductivity of the CRUD compared to the cladding. Reduction of thermal conductivity will increase the outer cladding surface temperature, thereby increasing the rate of cladding corrosion.

²⁴ The depressurization rate is a measure of how rapidly gas inside the fuel rods (containing both fission gas and fuel particulates) will flow through the crack or hole in the cladding in the event of cladding breach. Faster flow rates through the breach could entrain a higher number of particulates.

²⁵ An increase in stress due to non-uniform deformation of the cladding.

A.2.4.1 Irradiation-Induced Cladding Alterations

As the fuel is irradiated, lattice defects produced in the cladding produce changes in the cladding physical dimensions and mechanical properties in a manner similar to that for the UO₂ pellets discussed earlier. These changes are a function of the radiation dose or burnup.

A.2.4.1.1 Fuel Rod Growth

During irradiation, the length of a rod can increase by as much as 0.6 percent or 2.5 cm (1.0 in) due to void formation in the cladding and cladding creep due to axial swelling of the pellet after the pellet-cladding gap closes causing the cladding to stretch (Jernkvist and Massih 2004). Irradiation-induced rod growth lessens the severity of the deformation of the SNF rod due to shocks in the event of certain accidents, such as a truck or train head-on collision with the SNF in a horizontal configuration. This is because the smaller gap between the top of the rods and the bottom of the top nozzle limits the distance the rod will travel in an accident. Therefore, the rods will have a less severe impact compared to rods traveling a greater distance in a similar accident. The result is a smaller deceleration of the rods and a reduced potential for deformation. The size of this gap decreases with burnup, but the growth is not predictable or systematic and usually only the average rod growth with uncertainties is reported.²⁶

A.2.4.1.2 Mechanical Properties

The mechanical properties of LBF and HBF are important for storage and disposal, but especially so during transportation. For normal conditions of transport, it is important to know the mechanical strength of the fuel under static load conditions and the fatigue strength during normal transportation vibrations. For hypothetical accident conditions during transport, it is important to know flexural rigidity and the ultimate tensile strength of the fuel. In addition to tensile and compressive strength, the degree to which the cladding remains ductile (versus brittle) is important in evaluating the potential for cladding breach during accident conditions. Irradiation causes the mechanical properties of the zirconium alloy cladding to change due to damage in the material from the formation of lattice defects, such as voids, and by corrosion of the outer surface of the cladding. Irradiation can cause an increase in strength, but also a decrease in ductility. The irradiation effects typically saturate within the first few years of fuel operation and do not change significantly with additional burnup (Lovasic and Einziger 2009). Some studies, for example Coleman et al. (2018), suggest that the fuel drying process used when placing fuel in dry storage may cause annealing of radiation defects of the cladding material, which may alleviate some irradiation damage. Other evaluations (Einziger et al. 1982) indicate that annealing could be minimal up to the allowable cladding storage temperatures of 400°C (752°F) (NRC 2003); however, more recent testing by Billone and Burtseva (2016) did demonstrate some annealing at 400°C (752°F). If annealing does occur, it may reduce the amount of radiation damage to the cladding to levels at or below that present in lower burnups fuels.

A.2.4.2 Cladding Corrosion

Cladding corrosion increases continuously with increasing burnup (Motta and Chen 2012). It has been found that the effects of corrosion—including cladding wall thinning, hydriding effects (see section 3.2 and Appendix F), and CRUD deposition (section A.2.4.3)—are more

²⁶ Two rods adjacent to each other can have significantly different irradiation growth.

important than irradiation damage to the mechanical properties of HBF cladding within the context of fuel performance during storage and transportation (Jernkvist and Massih 2002).

A.2.4.2.1 Cladding Wall Thinning

During irradiation in the reactor, cladding oxidation in the coolant can cause thinning of the fuel cladding walls. The extent of cladding oxidation at higher burnup depends on whether standard Zircaloy versus new cladding compositions are used (Table A-1). The Zircaloy corrosion rate begins to increase as burnup increases beyond approximately 40 GWd/MTU and becomes quite appreciable at higher burnup in many cladding alloys. Sabol et al. (1997) reports oxide layer thicknesses on high burnup conventional Zircaloy-4 cladding to be as high as approximately 130 μm . As seen in Table A-2, high burnup PWR rods with low-tin Zircaloy-4 cladding can have oxide thicknesses as high as 115 μm ²⁷ (Hanson 2016; Sabol et al. 1997). The newer alloys, such as M5[®] and Optimized ZIRLO[™], experience significantly less oxidation. Under PWR conditions, non-uniform, but contiguous, oxide corrosion layers are formed. In contrast, under BWR conditions, corrosion initially forms nodules, which eventually merge into a thin, contiguous oxide layer. Since this oxide is porous, its strength is not credited when calculating the stress on the cladding (NRC 2003). Newer cladding compositions—such as M5[®] and ZIRLO[®]—were developed to resist corrosion during extended irradiation (Ishimoto et al. 2000; Meyer 2000). The extent of corrosion of these cladding alloys is considerably less than that of Zircaloy at equivalent burnups. Even though the ZIRLO[®] advanced cladding from Westinghouse was designed to reduce cladding corrosion, in recent years it was found that oxide thicknesses larger than 80 μm were observed when the fuel was irradiated at high linear power ratings (Kaiser, Leech, and Casadei 2000; Knott et al. 2003). Cladding wall thinning due to corrosion in the reactor core water will increase the hoop stress²⁸ on the cladding, possibly affecting the fuel rod performance during storage and transportation.

Table A-2 Oxide growth in micrometers (μm) on PWR cladding as a function of burnup.

Oxide Growth (μm)			
Alloy	35 GWd/MTU	50 GWd/MTU	60 GWd/MTU
Low-tin Zircaloy-4	10–30, average 20	35–100, average 60	60–115, average 95
ZIRLO [®]	5–30, average 15	10–60, average 35	20–100, average 40
Optimized ZIRLO [™]	5–20, average 10	20–40, average 35	20–40, average 30
M5 [®]	5–15, average 10	5–25, average 18	10–30, average 20

(Data from Hanson, 2016).

A.2.4.2.2 Hydriding Effects

Hydrogen is generated during the corrosion process on the outside of the cladding during reactor operation ($\text{Zr} + 2\text{H}_2\text{O} \rightarrow 2\text{H}_2 + \text{ZrO}_2$) and most of the hydrogen is carried away by the coolant water and reacts with other elements such as oxygen. Fifteen to twenty percent of the hydrogen released during cladding corrosion will diffuse into the cladding and increase its hydrogen content; some of the hydrogen will precipitate as zirconium hydride when the temperature decreases after reactor operation. As corrosion progresses, the oxide

²⁷ For comparison, PWR cladding thickness ranges from 560–670 μm , and BWR cladding thickness ranges from 630–860 μm , depending on the assembly design.

²⁸ Hoop stress is a stress in the tangential (azimuthal) direction in a cylinder causing an increase in the cylinder diameter.

thickness on the cladding increases, and the cladding continues to absorb hydrogen.²⁹ Zirconium hydrides are relatively brittle and depending on the orientation of the stresses during storage and transportation versus the orientation of the hydrides, the cladding may behave in a more brittle manner leading to a higher probability of a gross breach – especially during transportation.

Under certain conditions in storage, zirconium hydrides may reorient to a radial direction affecting the ductility of the cladding, which could be important in determining the behavior of the cladding in a hypothetical transportation accident. More detailed information on cladding hydriding and hydride reorientation can be found in Appendix F. High-burnup cladding experiences reduced ductility when there is a large amount of corrosion that introduces a large amount of hydrogen into the cladding (Garde, Smith, and Pirek 1996; Itagaki et al. 2000; Lösönen 2000). The less ductile the cladding is, the more susceptible it is to a gross breach in accident conditions.

Zircaloy-4 and ZIRLO® are metallurgically treated in the manufacturing process to preferentially form circumferential hydrides during irradiation. Similarly, M5® cladding is recrystallized and annealed during manufacturing to improve its in-reactor performance. Zircaloy-2 is not treated and has a random grain texture that remains after irradiation. Some new cladding materials experience less corrosion, which results in less hydrogen diffusion into the cladding.

For example, M5® cladding has less than 100 wppm³⁰ hydrogen even at high burnups, compared to Zircaloy-4 cladding which can have more than 500 wppm hydrogen at high burnups (Mardon, Hoffmann, and Garner 2005; Billone et al. 2014).

A.2.4.3 CRUD Deposition

A layer of CRUD that is formed by corrosion products from the steel components of the primary cooling system in the reactor can accumulate on top of the cladding oxide. CRUD can deposit on the rod as either a tightly adherent layer or as light fluffy particulates that eventually agglomerate. Most of the CRUD on PWR rods is tightly adherent nickel iron oxide ($\text{Ni}_x\text{Fe}_{3-x}\text{O}_4$) that only forms where subcooled boiling occurs, which is about 2/3 up from the bottom of the higher power fuel rods. CRUD on BWR rods is a loosely adherent, fluffy iron oxide (Fe_2O_3). In addition, the diameter of CRUD particles on BWR rods tends to be larger (0.1–10 μm) than the CRUD on PWR rods (0.1–3 μm). The CRUD layer on BWR rods is generally thicker (25–75 μm) and varies by as much as a factor of three along the axial length of the rod. Very limited data indicate that the CRUD thickness is not dependent on burnup (up to about 54 GWd/MTU) (Sandoval et al. 1991; Sanders et al. 1992). If CRUD spalls from the rod, both flakes and particulate from the de-agglomeration of the flakes are found.

CRUD deposits contain neutron-activated ions. The major radioisotopes in CRUD are manganese-54, zinc-65, cobalt-60, and cobalt-58. After the SNF has been out of the reactor for about eight years, the only radioisotope of interest within the CRUD is cobalt-60

²⁹ The rate of absorption of the generated hydrogen decreases with burnup, but the total amount of hydrogen in the cladding increases with burnup since the cladding continues to oxidize.

³⁰ Weight parts per million.

(Sandoval et al. 1991), which has a half-life of about five years. Due to its relatively poor thermal conductivity compared to the cladding, CRUD reduces the cladding's heat-transfer capabilities. If the CRUD and oxide spall,³¹ two adverse situations may develop:

1. The heat-transfer capabilities improve and a cool spot develops at the location where the CRUD spalled. Since hydrogen that is in the cladding migrates towards lower temperatures in zirconium, hydrogen will migrate to the location of the spallation. If there is sufficient hydrogen in the cladding, the hydrogen will precipitate at the cool spot forming a "blister" of zirconium hydride (Figure A-16). Since the hydrides can reduce the ductility of the cladding, this location is a potential cladding breach site.
2. The CRUD may become a source of contamination in the cask when the SNF is removed. CRUD is a source of radioactive particulate that can be released without breaching the fuel rod cladding and presents a risk if the cask system is breached. Note that when the cask from the low burnup demonstration was opened no spalled CRUD was found (Bare and Torgerson 2001).

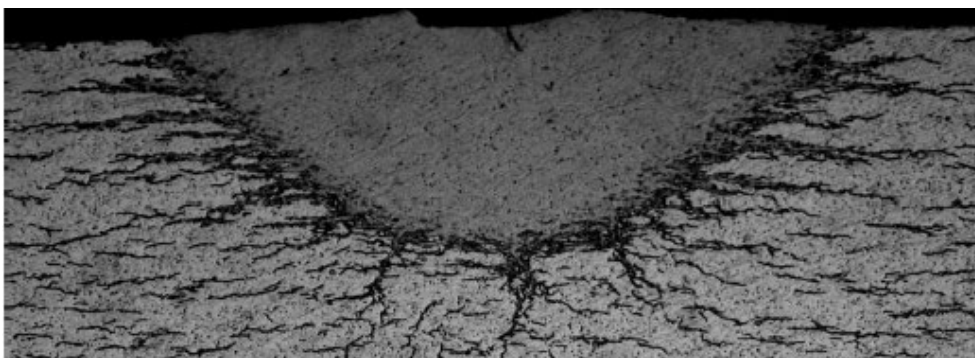


Figure A-16. Example of a hydride blister at the outer diameter of fuel cladding.
(Sindelar et al. 2011).

A comprehensive survey of CRUD behavior up to 1988 can be found in Sandoval et al. (1991).

A.2.4.4 Hoop Stress on the Cladding

Internal rod pressure creates hoop stress on the cladding. The stress on the cladding can be calculated from the thin wall formula $\sigma(T) = P(T) r/t$ where $\sigma(T)$ is the hoop stress on the cladding at the internal gas temperature, T , $P(T)$ is the internal pressure in the rod as a function of temperature, r is the mid-wall radius of the cladding, and t is the cladding thickness. As the cladding oxidizes in the reactor, some of the cladding metal will convert to zirconium oxide, both decreasing the metal-cladding diameter and effective cladding thickness. Based on the measured growth of the oxide layer (Table A-2), the cladding thickness is reduced by between 5 and 13% for low-tin Zircaloy-4 and between 1 and 4% for

³¹ This is only a concern for BWR fuel rods because PWR fuel rods are now stored in borated water, which is slightly acidic and appears to dissolve most of the CRUD on the rods (Einziger and Beyer 2007).

M5® at 60 GWd/MTU (Chung 2000), which will result in increased cladding stress due to a decrease in effective cladding thickness.

The main influence on the cladding stress under static load conditions is the internal gas pressure. The pressure is caused by (1) helium gas, which is used to fill the rod for thermal conductivity and to counteract reactor cooling water pressure on the cladding, and (2) fission gas that is released into the fuel-void volume from the fuel pellets as they are irradiated. There is reasonably good information on FGR as shown in Figure A-14, but this gas release cannot simply be added to the initial gas fill to determine the pressure. During irradiation, the fuel swells and the cladding creeps down on the fuel, which decreases the free rod volume, and the cladding grows axially, which increases the free rod volume. As a result, the volume to accommodate the fuel changes from when the rod was initially manufactured, and the distribution of gas volume between the plenum region and the fuel column changes with burnup.³²

A preferred method for measuring the final gas pressure in a rod is to puncture it during destructive examination in a hot cell. Following puncture, the rod internal gas is expanded into a known volume at a known temperature and the pressure is measured. This process is repeated into a second, larger volume. Using this “double expansion” process allows the original rod internal pressure to be calculated (Desgranges, Faure, and Thouroude 2005). After the pressure measurement, the rod is backfilled to a known pressure with a gas such as helium while measuring the quantity of gas introduced. This allows for a more accurate calculation of the rod internal volume. Data collected on rod internal pressures (EPRI 2013; Machiels et al. 2013) show a steady rise in pressure with burnup.

DOE has been working to enhance the database of fuel rod pressures and volumes as it continues to conduct gas analysis on the sister rods from the High Burnup Dry Storage Research Project cask (section F.5, Appendix G). The temperature of the gas in the rod also affects the rod pressure. The gas in the plenum (Figure A-3), which is located either above or below the fuel column, is at a lower temperature (as much as 100°C (180°F) lower, depending on the SNF type, operating history, and the environment) than the gas in the fuel column. Rondinella et al. (2015) has shown that there is rapid communication between the free volumes of gas in an HBF rod. DOE-sponsored testing on the sister rods at ORNL and PNNL also confirmed gas communication inside HBF rods (Montgomery et al. 2019; Shimskey et al. 2019). Using the ideal gas law, the proper stress can be calculated if the partitioning of volume between the plenum and fuel column and the temperatures of the plenum and fuel column are known; however, neither of these variables are known. One study (Machiels et al. 2013) used the lower temperature of the plenum to calculate the stress, but without correcting for the ratio of gas in the fuel column to that in the plenum.

³² Calculating the internal rod volume post-irradiation is difficult because rods within an assembly can grow axially and the difference in axial growth from rod to rod can be as much as 1%. Adding to the uncertainty in rod internal volume is the variability in cladding creep down, which is a sensitive function of the internal rod pressure, coolant water pressure, cladding temperature, and type of cladding.

A.2.5 Assembly Behavior

Vendors have developed new assembly and rod designs to improve in-reactor neutronics and structural performance (section A.1, Figures A-4 through A-6). For example, newer BWR assemblies use an increased number of rods per assembly (9×9 to 11×11) with a constant assembly cross-section to allow for loading a larger mass of U-235 in the reactor core and improve uranium utilization. In the context of this report, the role of assembly channels (in BWRs) and assembly spacer grids (in PWRs and BWRs) is to keep the rods in a stable configuration during both normal and accident conditions. These assembly components are discussed in more detail below.

A.2.5.1 Boiling Water Reactor Fuel Assembly Channel Deformation

Unlike PWR control rods that are inserted within the fuel assemblies (Figure A-4A), BWRs use control blades inserted between assemblies (Figure A-17). Due to the asymmetric placement of the control blades in a BWR that causes local neutron flux and temperature spatial gradients in the reactor, BWR channels and fuel assemblies may bow. Furthermore, the pressure gradient between the inside and the outside of a BWR channel might cause the assembly to bulge permanently in the reactor. Because the causes of channel deformation are related to irradiation in the reactor, higher burnup can lead to greater channel deformation (Garzarolli et al. 2011).

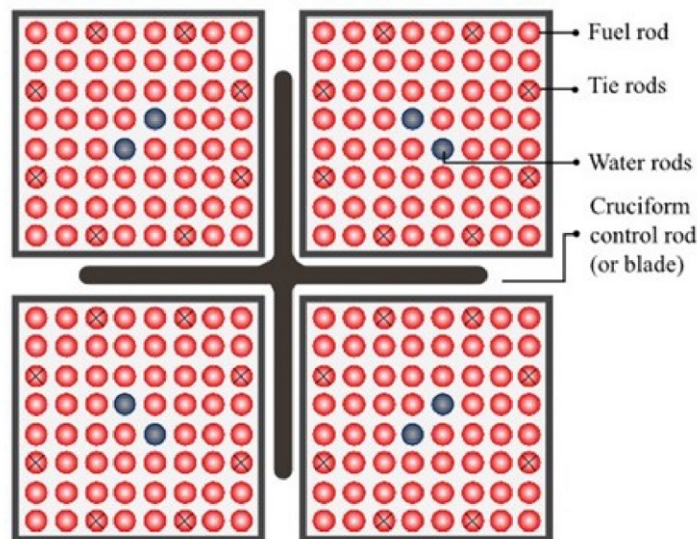


Figure A-17. Simplified depiction of a BWR control blade between four BWR fuel assemblies.

(Courtesy MIT OpenCourseWare: adapted from Buongiorno 2010).

Bow deformation is a major concern, because if it is excessive, there could be difficulty inserting the control blades in BWRs. Bowing tends to increase with burnup but can be limited by relocating the assembly within the core to manage the causes of bowing over different surfaces. There can be other problems with the assembly before the bow reaches about 6 mm (0.25 in) measured at the point of maximum deflection. These problems include adverse changes in coolant flow between bowed assemblies and a corresponding change in local power generation (Andersson, Almberger, and Björnkvis 2004). Garzarolli et

al. (2011) provides an extensive review of the subject. Some BWR fuel manufacturers have developed new fuel designs that may alleviate channel bowing. For example, in 2017, Global Nuclear Fuels (a subsidiary of GE Hitachi Nuclear Energy) completed the NRC-approved process for new fuel product introductions for a new fuel design called GNF3. According to the manufacturer, the new channel material in GNF3 fuel “provides protection against channel distortion, almost completely eliminating the need for additional monitoring, inspections and re-channeling ...” (GE Hitachi Nuclear Energy 2020).

Storing and transporting assemblies that have excessive bow or other deformities can be challenging if the assemblies are too curved to fit in the dry storage slots of the basket. In addition, the bow must be accounted for in structural analysis calculations to determine any potential damage to the rods if the assembly is dropped. The bow must also be properly accounted for in precise heat transfer calculations to determine the cladding temperature.

A.2.5.2 Spacer Grid Behavior

Maintaining the geometric configuration of the rods in an SNF assembly following an accidental drop depends, in part, on the integrity of the spacer grids (see Figure A-5 for an example of a spacer grid). If the spacer grids collapse to varying degrees, the rod spacing can change, which could increase or decrease the probability of a criticality. Experience in the nuclear industry has indicated that spacer grids can become brittle as they are irradiated to high burnups (NRC 2012). The structural performance of grid spacers at high burnups has been evaluated by some vendors and nuclear utilities (Mitsubishi Heavy Industries, Ltd. 2010, Exelon Generation 2014). These evaluations included detailed analyses showing that the high-burnup spacer grids exhibit more brittle behavior than unirradiated spacer grids but continue to support the fuel rods sufficiently to meet the NRC regulations pertaining to reactor operations and SNF storage. At low-burnup, the irradiation damage suffered in the reactor by the spacer grids does not appear to affect the geometric configuration of the fuel rods or assembly (Bare and Torgerson 2001; Einziger et al. 2003).

A.3 References

10 CFR 72. “Licensing Requirements for the Independent Storage of Spent Nuclear Fuel, High-Level Radioactive Waste, and Reactor-Related Greater than Class C Waste.” *Code of Federal Regulations*. Washington, DC: Government Printing Office.

Adamson, R., M. Griffiths, and C. Paterson. 2017. *Irradiation Growth of Zirconium Alloys—A Review*. Advanced Nuclear Technology International. December.

Andersson, T., J. Almberger, and L. Björnkvist. 2004. “A Decade of Assembly Bow Management at Ringhals.” *Proceedings of the 2004 International Meeting on LWR Fuel Performance*. Orlando, Florida. September 19–22.

AREVA Inc. 2010. HTP: Robust Technology for PWR Fuel Assemblies.
https://www.framatome.com/solutions-portfolio/docs/default-source/default-document-library/product-sheets/a0529-p-us-g-en-328-05-18-http.pdf?Status=Master&sfvrsn=60b7ce1d_2

- ASTM International. 2017a. Standard Specification for Wrought Zirconium Alloy Seamless Tubes for Nuclear Reactor Fuel Cladding. ASTM B811–17.
- ASTM International. 2017b. Standard Terminology Relating to Metallography. ASTM E7–17.
- Bare, W.C. and L.D. Torgerson. 2001. Dry Cask Storage Characterization Project—Phase 1: CASTOR V/21 Cask Opening and Examination. NUREG/CR-6745. September.
- Berna, G.A., C.E. Beyer, K.L. Davis, and D.D. Lanning. 1997. FRAPCON-3: A Computer Code for the Calculation of Steady-State, Thermal-Mechanical Behavior of Oxide Fuel Rods for High Burnup. NUREG/CR-6534, Vol. 2. December.
- Billone, M.C., T.A. Burtseva, Z. Han, and Y.Y. Liu. 2014. *Effects of Multiple Drying Cycles on High-Burnup PWR Cladding Alloys*. FCRD-UFD-2014-000052. September 26.
- Billone, M.C. and T.A. Burtseva. 2016. Effects of Lower Drying-Storage Temperature on the Ductility of High-Burnup PWR Cladding. FCRD-UFD-2016-000065. August 30.
- Buongiorno, J. 2010. “BWR Description.” Class lecture, Engineering of Nuclear Systems from Massachusetts Institute of Technology, Cambridge, MA.
https://ocw.mit.edu/courses/nuclear-engineering/22-06-engineering-of-nuclear-systems-fall-2010/lectures-and-readings/MIT22_06F10_lec06b.pdf
- Cheng, B., D. Smith, E. Armstrong, K. Turnage, and G. Bond. 2000. “Water Chemistry and Fuel Performance in LWRs.” *Proceedings of an International Topical Meeting on Light Water Reactor Fuel Performance*. Park City, Utah. April 10–13.
- Chung, H.M. 2000. “Fundamental Metallurgical Aspects of Axial Splitting in Zircaloy Cladding.” *Proceedings of an International Topical Meeting on Light Water Reactor Fuel Performance*. Park City, Utah. April 10–13.
- Coleman, C.E., V.A. Markelov, M. Roth, V. Makarevicius, Z. He, J.K. Chakravarty, A.-M. Alvarez-Holston, L. Ali, L. Ramanathan, and V. Inozemtsev. 2018. “Is Spent Nuclear Fuel Immune from Delayed Hydride Cracking during Dry Storage? An IAEA Coordinated Research Project.” *Zirconium in the Nuclear Industry: 18th International Symposium*. American Society for Testing and Materials STP 1597. pp. 1224–1251.
- Desgranges, L., M. Faure, and A. Thouroude. 2005. “A New Apparatus for Determination of the Free Volume of a Fuel Rod Using the Double Expansion Method.” *Nuclear Technology*, 149:1, 14-21.
- Duke Energy, Nuclear Information Center. 2016. *The Facts About Used Nuclear Fuel*.
<https://nuclear.duke-energy.com/2016/10/05/the-facts-about-used-nuclear-fuel>. October 5.
- Einziger, R.E., S.D. Atkin, D.E. Stellrecht, and V. Pasupathi. 1982. “High Temperature Postirradiation Materials Performance of Spent Pressurized Water Reactor Fuel Rods under Dry Storage Conditions.” *Nuclear Technology*. Vol. 57, pp. 65–80.
- Einziger, R.E., H. Tsai, M.C. Billone, and B.A. Hilton. 2003. “Examination of Spent Pressurized Water Reactor Fuel Rods After 15 Years in Dry Storage.” *Nuclear Technology*. Vol. 144, pp. 186–200.

Einziger, R.E. and C. Beyer. 2007. "Characteristics and Behavior of High-Burnup Fuel That May Affect the Source Terms for Cask Accidents." *Nuclear Technology*. Vol. 159, pp. 134–146.

EPRI (Electrical Power Research Institute). 2001. Design, Operation, and Performance Data for High Burnup PWR Fuel from the H. B. Robinson Plant for Use in the NRC Experimental Program at Argonne National Laboratory. EPRI, Palo Alto, California. 1001558.

EPRI. 2013. End-of-Life Rod Internal Pressures in Spent Pressurized Water Reactor Fuel. EPRI, Palo Alto, California. 3002001949.

Ewing, C.T. and K.H. Stern. 1974. "Equilibrium Vaporization Rates and Vapor Pressures of Solid and Liquid Sodium Chloride, Potassium Chloride, Potassium Bromide, Cesium Iodide, and Lithium Fluoride." *The Journal of Physical Chemistry*. Vol. 78, pp. 1998–2005.

Exelon Generation. 2014. Letter to the NRC re "Request for Supplemental Information - Amendment Request No. 11 to Materials License No. SNM-2505 for the Calvert Cliffs Specific Independent Spent Fuel Storage Installation - Acceptance Review." NRC Accession No. ML14274A498. July 25.

Fors, P., P. Carbol, S. Van Winckel, and K. Spahi. 2009. "Corrosion of high burn-up structured UO₂ fuel in presence of dissolved H₂" *Journal of Nucl. Mater.* 394, 1–8. October.

Garde A.M., G.P. Smith, and R.C. Pirek. 1996. "Effects of Hydride Precipitate Localization and Neutron Fluence on the Ductility of Irradiated Zircaloy-4." *Zirconium in the Nuclear Industry: 11th International Symposium*. American Society for Testing and Materials STP 1295. pp. 407–429.

Garzarolli, F., R. Adamson, P. Rudling, and A. Strasser. 2011. *ZIRAT Special Topic Report: BWR Fuel Channel Distortion*. Advanced Nuclear Technology International. Mölnlycke, Sweden.

GE Hitachi Nuclear Energy. 2020. "GNF3 Fueling The Future." <https://nuclear.gepower.com/fuel-a-plant/products/gnf3>. Website accessed November 3, 2020.

Hanson, B.D. 2016. *High Burnup Fuel, Associated Data Gaps, and Integrated Approach for Addressing the Gaps*. Presentation to the Nuclear Waste Technical Review Board at its February 17, 2016, meeting.

International Atomic Energy Agency. 2011. *Impact of High Burnup Uranium Oxide and Mixed Uranium-Plutonium Oxide Water Reactor Fuel on Spent Fuel Management*. IAEA Nuclear Energy Series No. NF-T-3.8. Vienna: International Atomic Energy Agency.

Ishimoto, S., T. Kubo, R.B. Adamson, Y. Etoh, K. Ito, and Y. Suzawa. 2000. "Development of New Zirconium Alloys for Ultra-High Burnup Fuel." *Proceedings of an International Topical Meeting on Light Water Reactor Fuel Performance*. Park City, Utah. April 10–13.

- Itagaki, N., K. Tsuda, T. Azuma, T. Karasawa, Y. Suzawa, T. Anegawa, and T. Uegata. 2000. "Experience and Development of BWR Fuel Supplied by NFI." *Proceedings of an International Topical Meeting on Light Water Fuel Performance*. Park City, Utah. April 10–13.
- Jernkvist, L.O. and A. Massih. 2002. Analysis of the Effect of UO₂ High Burnup Microstructure on Fission Gas Release. SKI Report 02:56. December.
- Jernkvist, L.O. and A. R. Massih. 2004. *Models for Fuel Rod Behaviour at High Burnup*. SKI Report 2005:41. December.
- Johnson, L.H. and D.F. McGinnes. 2002. *Partitioning of Radionuclides in Swiss Power Reactor Fuels*. NAGRA Technical Report 02-07. August.
- Kaiser, R.S., W.J. Leech, and A.L. Casadei. 2000. "The Fuel Duty Index (FDI)—A New Measure of Fuel Rod Cladding Performance." *Proceedings of an International Topical Meeting on Light Water Reactor Fuel Performance*. Park City, Utah. April 10–13.
- Knott, R.P., R.L. Kesterson, L.G. Hallstadius, M.Y. Young, and B. Johansen. 2003. "Advanced PWR Fuel Designs for High Duty Operation." *Proceedings of the TopFuel 2003—Nuclear Fuel for Today and Tomorrow Conference*. Wuerzburg, Germany. March 16–19.
- Lösönen, P. 2000. "Modelling Steady State Fission Gas Release at High Burnup." *Proceedings of an International Topical Meeting on Light Water Reactor Fuel Performance*. Park City, Utah. April 10–13.
- Lovasic, Z. and R. Einziger. 2009. "International Atomic Energy Agency (IAEA) Activity on Technical Influence of High Burnup UOX and MOX Water Reactor Fuel on Spent Fuel Management—9065." *Proceedings of the WM2009 Conference*. Phoenix, Arizona, March 1–5.
- Lozano, N., L. Desgranges, D. Aymes, and J.C. Niepce. 1998. "High Magnification SEM Observations for Two Types of Granularity in a High Burnup PWR Fuel Rim." *Journal of Nuclear Materials*. Vol. 257, pp. 78–87.
- Machiels, A.J., D.J. Sutherland, J.Y.R. Rashid, and W.F. Lyon. 2013. "Cladding Hoop Stresses in Spent PWR Fuel—Determination of Rod Internal Pressure as Initial Condition for Dry Storage." *Proceedings of the 17th International Symposium on the Packaging and Transportation of Radioactive Materials*. San Francisco, California. August 18–23.
- Manzel, R. and C.T. Walker. 2000. "High Burnup Fuel Microstructure and its Effect on Fuel Rod Performance." *Proceedings of an International Topical Meeting on Light Water Reactor Fuel Performance*. Park City, Utah. April 10–13.
- Manzel, R. and C.T. Walker. 2002. "EPMA and SEM of Fuel Samples from PWR Rods with an Average Burn-up of Around 100 MWd/kgHM." *Journal of Nuclear Materials*. Vol. 301, pp. 170–182.
- Mardon, J.P., P.B. Hoffmann, and G.L. Garner. 2005. "High Burnup Behavior and Licensing of Alloy M5™." *Proceedings of the 2005 International Meeting on LWR Fuel Performance*. Kyoto, Japan. October 2–6.

Meyer, R.O. 2000. "NRC Activities Related to High Burnup, New Cladding Types, and Mixed-Oxide Fuel." *Proceedings of an International Topical Meeting on Light Water Reactor Fuel Performance*. Park City, Utah. April 10–13.

Meyer, M.K. 2007. *High Burnup Fuels*. Presentation at the Global Climate and Energy Project Fission Workshop. Cambridge, Massachusetts. November 29–30.

Mitsubishi Heavy Industries, Ltd. 2010. *Evaluation Results of US-APWR Fuel System Structural Response to Seismic and LOCA Loads*. MUAP-08007-NP (R1), Appendix A, Effect of Irradiation on Grid Spacer Impact Behavior. NRC Accession No. ML102710117. August.

Montgomery, R., B. Bevard, R.N. Morris, J. Goddard, Jr., S.K. Smith, J. Hu, J. Beale, and B. Yoon. 2018. *Sister Rod Nondestructive Examination Final Report*. SFWD-SFWST-2017-000003 Rev. 1. May 16.

Montgomery, R., R.N. Morris, R. Ilgner, B. Roach, J. Wang, Z. Burns, J.T. Dixon, and S.M. Curlin. 2019. *Sister Rod Destructive Examinations (FY19)*. ORNL/SPR-2019/1251 Rev. 1. September 27.

Motta, A.T. and L-Q. Chen. 2012. "Hydride Formation in Zirconium Alloys." *JOM*. Vol. 64, pp. 1403–1408.

NRC (U.S. Nuclear Regulatory Commission). 2003. Spent Fuel Project Office Interim Staff Guidance-11, Revision 3, Cladding Considerations for the Transportation and Storage of Spent Fuel. November.

NRC. 2007. *Division of Spent Fuel Storage and Transportation Interim Staff Guidance-1, Revision 2, Classifying the Condition of Spent Nuclear Fuel for Interim Storage and Transportation Based on Function*. May.

NRC. 2012. *NRC Information Notice 2012-09: Irradiation Effects on Fuel Assembly Spacer Grid Crush Strength*. June 28.

NRC. 2018. *Backgrounder on High Burnup Spent Nuclear Fuel*. <https://www.nrc.gov/reading-rm/doc-collections/fact-sheets/bg-high-burnup-spent-fuel.html>. September.

NRC. 2020. *Dry Storage and Transportation of High Burnup Spent Nuclear Fuel, Final Report*. NUREG 2224. November.

Olander, D. 2009. "Nuclear Fuels—Present and Future." *Journal of Nuclear Materials*. Vol. 389, pp. 1–22.

Raynaud, P.A.C. and R.E. Einziger. 2015. "Cladding Stress During Extended Storage of High Burnup Spent Nuclear Fuel." *Journal of Nuclear Materials*, Vol. 464, pp. 304–312.

Rondinella V.V. and T. Wiss. 2010. "The High Burn-up Structure Nuclear Fuel." *Materials Today*. Vol. 13, pp. 24–32.

Rondinella V.V., D. Papaioannou, R. Nasyrow, W. Goll, and M. Rehm. 2015. "Measurement of Gas Permeability Along the Axis of a Spent Fuel Rod." *Proceedings of the 2015 TopFuel Reactor Fuel Performance Conference*. Zurich, Switzerland. September 13–17.

Sabol, G.P., R.J. Comstock, G. Schoenberger, H. Kunishi, and D.L. Nuhfer. 1997. "In-Reactor Fuel Cladding Corrosion Performance at Higher Burnups and Higher Coolant Temperatures." *Proceedings of an International Topical Meeting on Light Water Reactor Fuel Performance*. Portland, Oregon. March 2–6.

Sanders, T.L., K.D. Seager, Y.R. Rashid, P.R. Barrett, A.P. Malinauskas, R.E. Einziger, H. Jordan, T.A. Duffey, S.H. Sutherland, and P.C. Reardon. 1992. *A Method for Determining the Spent-Fuel Contribution to Transport Cask Containment Requirements*. SAND90-2406. November.

Sandoval, R.P., R.E. Einziger, H. Jordan, A.P. Malinauskas, and W.J. Mings. 1991. *Estimate of CRUD Contribution to Shipping Cask Containment Requirements*. SAND88-1358. January.

Shimskey, R.W., J.R. Allred, R.C. Daniel, M.K. Edwards, J. Geeting, P.J. MacFarlan, L.I. Richmond, T.S. Scott, and B.D. Hanson. 2019. *PNNL Phase 1 Update on Sibling Pin Destructive Examination Results*. PNNL-29179. Pacific Northwest National Laboratory. Richland, Washington. September.

Sindelar, R.L., A.J. Duncan, M.E. Dupont, P.-S. Lam, M.R. Louthan, Jr., and T.E. Skidmore. 2011. *Materials Aging Issues and Aging Management for Extended Storage and Transportation of Spent Nuclear Fuel*. NUREG/CR-7116. November.

Spino, J., J. Rest, W. Goll, and C.T. Walker. 2005. "Matrix Swelling Rate and Cavity Volume Balance of UO₂ Fuels at High Burn-Up." *Journal of Nuclear Materials*. Vol. 346, pp. 131–144.

Strasser, A., P. Rudling, and C. Patterson. 2014. *Fuel Fabrication Process Handbook: Revision I*. Advanced Nuclear Technology International. Mölnlycke, Sweden. May.

Tsai, H. and M.C. Billone. 2003. "Characterization of High-Burnup PWR and BWR Rods, and PWR Rods after Extended Dry-Cask Storage." *Proceedings of the 2002 Nuclear Safety Research Conference*. NUREG/CP-0180. pp. 157–168.

U.S. Congress. 1982. *Nuclear Waste Policy Act of 1982*. 97th Congress, 1st Session. 1982. Washington, DC: Government Printing Office.

Wagner, J.C., J.L. Peterson, D.E. Mueller, J.C. Gehin, A. Worrall, T. Taiwo, M. Nutt, M.A. Williamson, M. Todosow, R. Wigeland, W.G. Halsey, R.P. Omberg, P.N. Swift, and J.T. Carter. 2012. *Categorization of Used Nuclear Fuel Inventory in Support of a Comprehensive National Nuclear Fuel Cycle Strategy*. FCRD-FCT-2012-000232. December.

Wang, B. 2010. *Spent Nuclear Fuel Composition and Brave New Climate's Renewables and Nuclear Power*. <http://www.nextbigfuture.com/2010/06/soent-nuclear-fuel-composition-and.html>. June 26.

Wang, J., H. Wang, H. Jiang, Y. Yan, and B. Bevard. 2016. *CIRFT Testing of High Burnup Used Nuclear Fuel from PWR and BWRs*. Presentation to the Nuclear Waste Technical Review Board at its February 17, 2016, meeting.

Wang, J. and H. Wang. 2017. *Mechanical Fatigue Testing of High-Burnup Fuel for Transportation Applications*. NUREG/CR-7198, Rev. 1. October.

Xu, Z., M.S. Kazimi, and M.J. Driscoll. 2005. "Impact of High Burnup on PWR Spent Fuel Characteristics." *Nuclear Science and Engineering*. Vol.151, pp. 261–273.

Yoon, K.H., J.Y. Kim, K.H. Lee, Y.H. Lee, and H.K. Kim. 2009. "Control rod drop analysis by finite element method using fluid–structure interaction for a pressurized water reactor power plant." *Nuclear Engineering and Design*. Vol. 239, pp. 1857–1861.

Appendix B

Technical Information Needs for the Management of High Burnup Fuel

As a part of its evaluation of Department of Energy (DOE) research programs, the Nuclear Waste Technical Review Board (Board) also evaluated DOE's own assessment of the data needs, or technical information needs, that are to be fulfilled through the research program. The purpose of this appendix is to provide more detail of the Board's evaluation of the technical information needs related to high burnup spent nuclear fuel (HBF).

The performance of HBF during extended storage and subsequent transportation is a subject of interest not only for the United States, but also for other countries with nuclear programs. In response to concerns about HBF performance in storage and transportation, the International Atomic Energy Agency developed a safety case¹ for spent nuclear fuel (SNF) dual purpose casks (IAEA 2013). In addition, the Electric Power Research Institute's (EPRI) Extended Storage Collaboration Program (ESCP) was established to evaluate the future performance of HBF. The ESCP encourages its members to evaluate the technical information, or data, that are needed—and may be currently lacking—to support the development of license applications and safety cases to store SNF for extended periods of time and then transport it. Reports discussing technical information needs² for HBF storage and transportation have been published by the Board (NWTRB 2010), the Nuclear Regulatory Commission (NRC) (NRC 2014a), EPRI (EPRI 2011), and DOE (Hanson, Alsaed, and Stockman 2012; Hanson et al. 2012; Stockman et al. 2014; Alsaed and Hanson 2017; Teague et al. 2019). The ESCP international sub-committee has also developed a technical information needs report (EPRI 2012).

Most of these reports also prioritized the data needed to resolve questions and uncertainties about the performance of HBF during storage and transportation.³ There was general agreement on the issues for which more data were needed, but a diversity of opinions on the priority for obtaining the necessary data. These differences reflected the various mandates and responsibilities of different organizations, which ranged from safe and secure storage to transportation or disposal and required different data to resolve a wide spectrum of questions. The data priorities and needs also vary among utilities and countries due to variations in the types of dry cask storage systems in use, the conditions of those systems, the SNF type, the irradiation conditions (such as burnup), other storage conditions and national policies. For example, the NRC's data priorities were based on addressing regulatory concerns related to dry cask storage systems and SNF degradation, whereas DOE's data priorities were based on when the data were needed and on meeting regulatory requirements. In another example, the technical information need priorities for

¹ The International Atomic Energy Agency safety case documentation is similar to the NRC-required Safety Analysis Report that an applicant must supply when applying for a license or a Certificate of Compliance.

² The technical information need reports are called "gap reports" by some organizations.

³ No prioritization was given in the NWTRB report (NWTRB 2010).

SNF stored in casks filled with air are different than those for SNF stored in casks filled with an inert gas such as helium.

Detailed tables for each organization's data requirements, priorities, as well as a short explanation of any regulatory or operational concerns are provided below, followed by a broader discussion of how technical information needs are prioritized by the various organizations.

B.1 DOE-Identified Technical Information Needs and Priorities

The first DOE evaluation of technical information needs related to HBF was completed in 2012 (Hanson, Alsaed, and Stockman 2012; Hanson et al. 2012). The evaluation was subsequently revised in 2014 (Stockman et al. 2014), 2017 (Alsaed and Hanson 2017), and 2019 (Teague et al. 2019). The 2017 and 2019 updates account for work done by DOE and other entities since the 2014 update.

Recommendations made by other organizations may also affect DOE's priorities for obtaining new data related to SNF. For example, the Blue Ribbon Commission on America's Nuclear Future recommended that DOE establish a consolidated interim storage site for its SNF and proceed with preparation for transportation (BRC 2012). However, it is unclear if DOE's original priorities considered new data that are needed to assess and address degradation that might occur when SNF is stored, transported, and then stored again at a consolidated interim storage site prior to subsequent transportation and disposal.

The need for such data arises from one of the NRC's regulatory requirements: the condition of the SNF must be understood when it is placed into storage. While the condition of the SNF is generally known at the time it is initially placed into wet storage at the reactor site and when it is moved from wet storage to dry storage, the nuclear industry has no plans to inspect the SNF after dry storage or before transportation. There are several reasons for this. For SNF stored inside welded canisters, inspecting the fuel would require the canisters to be cut open, entailing additional work (and cost) for the utilities, additional radiation exposure for nuclear power plant workers, and generation of more radioactive waste from the canister cutting operation. Some, but not all, of these same concerns apply to SNF stored in bolted-lid casks.

However, as noted above, the condition of the SNF needs to be sufficiently well-understood to be accepted for storage at a consolidated interim storage site (if available), even after extended storage at the utility site and then, transportation to a waste repository. Therefore, the licensees and DOE are examining selected samples of HBF (in the High Burnup Dry Storage Research Project; see Appendix G) combined with computer modeling to predict the condition and behavior of the broader population of SNF. To help guide selecting SNF samples, funding research, and developing computer models, DOE evaluates a broad range of technical information needs related to SNF and assigns a priority to each technical information need.

The majority of the DOE-funded research related to HBF is designed to obtain data on the mechanical properties of the HBF. Mechanical property testing is discussed in Appendices A, F, G, and H of this report. Mechanical property data, such as ultimate tensile strength of

HBF cladding, are compared against the dynamic conditions (such as mechanical loads) that HBF may experience during storage and transportation. Computer modeling is used to estimate if the HBF will maintain its integrity given the expected dynamic conditions.

DOE took a systems-engineering approach to identify and prioritize the technical information needs for gaining a better understanding of the characteristics and behavior of HBF and associated storage and transport cask systems. In particular, DOE focused on characteristics and behavior of HBF that may cause or allow acceleration of degradation mechanisms during extended storage and transportation. DOE conducted a risk-based evaluation of the likelihood and consequence of the degradation mechanisms. The risk criteria included subjective evaluations of the factors required to meet NRC's safety requirements for criticality safety, confinement of radioactive materials, and limiting radiation exposure. The identified technical information needs were prioritized into three groups (low, medium, and high) based on four criteria:

1. Whether existing data are sufficient to evaluate the degradation mechanism and its impact on HBF and associated storage and transport cask systems;
2. The likelihood of occurrence of the degradation mechanism during extended storage;
3. Ease of remediation of the degraded system such that it continues to provide its safety function; and
4. The significance of the potential consequences that may result from the degradation mechanism (Hanson et al. 2012).

In this case, DOE considered "consequences" subjectively and primarily in the sense of adverse impacts on the ability of the HBF (and SNF cask systems) to meet NRC safety requirements.

When the technical information needs were revisited in 2014, DOE added a fifth criterion regarding how soon the data are needed (Stockman et al. 2014). The purpose of this criterion was not to change the high, medium or low rankings, but to determine the sequence of allotting resources to obtain the data. For example, a lower priority data need that required a very long lead time to resolve might start earlier than a higher priority data need for which the data could be obtained easily or was not needed until a future date. As more data became available and as programmatic decisions were made, the priorities of some technical information needs were reduced; for example, the high priority technical information need to address the effects of rewetting fuel rods (if they were to be repackaged) was reduced to medium when DOE decided to minimize wet repackaging of SNF (Hanson 2016).

Several HBF technical information needs were added after the 2014 revision due to questions from the NRC regarding the condition of HBF after the initial licensing period (20 years). The NRC questions were prompted by new applications from industry to the NRC, seeking approval of renewed licenses (or certificates of compliance) for storage of SNF, including HBF, beyond 20 years (EPRI 2014; NWTRB 2016). Further guidance from the NRC clarified that data from a suitable demonstration—such as the High Burnup Dry Storage

Research Project (EPRI 2014; NRC 2014b) (discussed in Appendix G)—could be used to support aging management programs, which provide procedures and processes to monitor and address age-related aging mechanisms in SNF dry cask storage systems. The NRC also raised questions about how HBF might behave while being transported after the fuel had been stored for a considerable time. As a result, DOE gave a high priority to continuing the fatigue tests that the NRC had started at the Oak Ridge National Laboratory (ORNL) (Appendix H), and to determining the cyclic stress that HBF may experience while being transported in large casks (Appendix H). Tables B-1, B-2, and B-3 reflect the DOE evaluations of technical information needs.

In its 2014 R&D Plan that also updated the technical information needs (Stockman et al. 2014), DOE noted an ongoing effort to develop computer models that could be used to predict hydride precipitation and reorientation in a zirconium alloy matrix (i.e., at a meso-scale level). When these models are combined with macro-scale models (e.g., the BISON model at the Idaho National Laboratory; see Appendix I) and properly validated, they can be used to “assess hydride effects for different cladding material subjected to a wide range of reactor, pool, and dry storage operational conditions” (Stockman et al. 2014). This type of modeling is referred to as fuel performance modeling and is discussed in more detail in Appendix I. Although DOE support for modeling in the area of fuel performance was continuing in 2014, that support waned in later years, and fuel performance modeling was not discussed in the DOE technical information needs reports of 2017 or 2019.

Table B-1 DOE Summary of Cross-Cutting Technical Information Needs for HBF Cladding.

Cross-Cutting TIN	Importance of R&D 2014/2017/2019	Approaching to Closing TINs and Status
Temperature Profiles	High/High/High	Develop thermal models, calculate temperature profiles as a function of time, and make temperature measurements for representative DCSSs. In Progress
Drying Issues	High/High/High	Perform tests and develop models to better quantify the amount of residual water remaining in a cask or canister after a normal drying cycle. In progress.
Stress Profiles	NA/High/High	Measure cladding strains during various modes of transport and evaluate cladding stresses due to internal rod pressures. Near Completion.
Subcriticality (burnup credit*) and moderator exclusion**)	High/Low/Low	Interact with industry and NRC to develop regulatory guidance and a consistent set of approaches to obtain moderator exclusion exception. Depend on NRC to acquire the data needed, including radio chemical essays and critical experiments, validate the models, and develop the technical bases for full burnup credit. (Little DOE work is currently being done.)
Fuel transfer options	High/Medium/Medium	Investigate the effects of drying and wetting cycles on fuel, cladding, and canister/cask internal components such as baskets and absorbers and define acceptable transfer alternatives. Investigate the need to use dry transfer systems on a regular basis. (Deferred due to no plans for wet transfer.)

(Hanson et al. 2012; Stockman et al. 2014; Alsaed and Hanson 2017; Teague et al. 2019)

* As nuclear fuel is irradiated in a reactor, the fissile material content in the fuel decreases and some neutron absorbing isotopes (aka neutron poisons) are formed. These two factors reduce the probability of a criticality accident involving SNF after it is removed from the reactor. In certain cases, the safety analysis reports that support applications for NRC approval of SNF storage or transportation can take credit for these two factors. This approach is called burnup credit.

** Moderator exclusion is another approach to ensuring criticality safety. In this approach, a case is made, through design or analysis, that no water (a moderator, which, which is necessary for criticality accident to occur) can enter an SNF cask cavity. With no moderator, criticality is precluded.

Table B-2 DOE-Identified Degradation Mechanisms That Could Impact the Characteristics and/or the Performance of Fuel Pellets

Stressor	Degradation Mechanism	Influenced by Extended Storage and/or Higher Burnup	Additional Data Needed to Understand the Mechanism	Importance of R&D
Thermal and Mechanical	Fuel Fragmentation	Yes (Higher burnup)	Yes	Low
Chemical	Restructuring/Swelling	Yes	Yes	Low
	Fission product attack on cladding	Yes	Yes	Low
	Fuel oxidation	Yes	Yes	Low

(Hanson et al. 2012; Stockman et al. 2014; Alsaed and Hanson 2017; Teague et al. 2019)

Table B-3 DOE-identified Degradation Mechanisms That Could Impact the Characteristics and/or Performance of SNF Cladding

Stressor	Degradation Mechanism	Influenced by Extended Storage and/or High Burnup	Additional Data Needed to Understand the Mechanism	Importance of R&D
Thermal	Annealing of radiation damage	Yes	Yes	Low
	Metal fatigue caused by temperature fluctuations	Yes	Yes	Low
	Phase change	No	Yes	Low
Chemical	Emissivity changes	No	Yes	Low
	H ₂ effects: Embrittlement and reorientation	Yes	Yes	High
	H ₂ effects: Delayed hydride cracking	Yes	Yes	Medium
	Wet Corrosion	Yes	Yes	Low
Mechanical	Low temperature creep	TBD	Yes	Low
	Transportation vibration	TBD	Yes	Low

(Hanson, Alsaed, Stockman 2012; Hanson et al. 2012; Stockman et al. 2014; Alsaed and Hanson 2017; Teague et al. 2019)

B.2 NRC-Identified Technical Information Needs and Priorities

The NRC as a regulatory body only does research to address regulatory issues. In other words, the NRC focuses on determining if there is sufficient information available about the components of an SNF cask or canister system to support the issuance of an NRC license or certificate of compliance. The NRC determines that data are needed if either (1) there are insufficient data to determine if a safety question exists, or (2) there are insufficient data to confirm an applicant's position on a subject. As a result, the NRC data needs will be different than those of cask manufacturers, utilities, or Certificate of Compliance holders.

However, the NRC has documented several high priority technical information needs related to degradation mechanisms in SNF and SNF dry cask storage systems (Table B-4).

Table B-4 NRC-identified High Ranking Technical Information Needs^a

Component	Degradation Phenomena ^b	Overall Ranking	Reason for High Ranking
Cladding	Galvanic corrosion	H	This is only high if the drying task indicates that sufficient water to support galvanic corrosion remains in the canister. This may revert to low if sufficient water is not present.
	Stress corrosion cracking	H ^{c,d}	All three mechanisms depend on a source of stress that might come from pellet swelling. If the stress is not present, the mechanisms are not operative. If operative, these mechanisms could cause cladding cracks and increase the source term if an accident were to occur.
	Delayed hydride cracking	H ^{c,d}	
	Low temperature creep	H ^{c,d}	
	Propagation of existing flaws	H	There is little current knowledge of the initial flaw size distribution in High burnup cladding. As a result, it cannot be determined whether the cladding will fail in the long term. Grossly breached cladding affects the radioactive source term if an accident were to occur. More data is needed to increase the knowledge level of this mechanism.
Fuel-cladding Interactions	Fission gas release during accident	H	Both mechanisms result in increased pressure in the canister and potential containment issues. More data is needed to increase the knowledge level of this mechanism.
	Helium release		
	Pellet Swelling	H	Swelling of the pellets may be a significant source of cladding stress together with the rod internal gas. The level of knowledge is low.
	Additional fuel fragmentation	H	Under accident conditions, additional fuel fragmentation will release fission gas and pressurize the rod. Should the cladding also breach, there would be an increased radioactive source term to be contained in the cask or canister system.

Table B-4 NRC-identified High Ranking Technical Information Needs^a (Continued)

Component	Degradation Phenomena ^b	Overall Ranking	Reason for High Ranking
Fuel Assembly hardware	Metal fatigue caused by temperature fluctuations	H	Loss of assembly hardware would put the fuel in an unanalyzed slate for criticality. The extent of the fatigue will depend on the size of the temperature fluctuations determined from the thermal crosscutting task. ^e
	Wet Corrosion and stress corrosion cracking	H	This is only high if the drying task indicates that sufficient water remains in the canister. This may revert to low if sufficient water is not present.
Cross-cutting	Drying	H	Many degradation mechanisms will not be active if two issues are resolved: 1) the canister is dry. There is strong evidence that if the canister is dry using the accepted techniques (Appendix E), ^f and 2) the temperatures in the canister and components are accurate.
	Thermal Calculations	H	

(NRC 2014a)

^a NRC did not consider hydride reorientation research a high priority because it had already done sufficient research to determine that the mechanism was important and that the applicant had to address it in storage or transportation license applications.

^b Additional information on many of these degradation mechanisms, such as source term, pellet swelling, fuel fragmentation, and fission gas release, is available in Appendices A and F in this report.

^c The priority is high only if stress generated from helium swelling of the fuel is shown to be operative; otherwise the priority is low.

^d These rankings may change based on the results of work on pellet swelling.

^e The NRC did not consider metal fatigue of the assembly hardware due to transportation vibration. The reasoning for that omission was not stated.

^f Drying is being evaluated by DOE and other countries (Appendix E).

The NRC did not consider hydride reorientation research a high priority because it had already done sufficient research to determine that the mechanism was important and that the applicant had to address it in storage or transportation license applications. In order to support these future applications for extended storage and transportation, DOE determined that more data are needed to better understand and better characterize hydride reorientation in HBF, which is why the topic is considered a high priority for DOE but not for NRC.

B.3 EPRI/ESCP-Identified Technical Information Needs and Priorities

EPRI reviewed existing reports on technical information needs and then independently prioritized the issues (EPRI 2011). They ranked the need for research and development (R&D) to address the extended storage technical information needs by considering the following factors:

1. The extent to which degradation of each component would affect the ability of the system to meet the safety functions with emphasis on confinement.⁴ EPRI considers the containment provided by the SNF cladding to be a secondary confinement barrier.⁵
2. The need for relevant data that are not included in the reports of past R&D or are not expected to be produced in ongoing research.
3. The lack of proven systems and methods for detecting, inspecting, or mitigating degradation of SNF or associated cask systems affected by the long-term degradation mechanisms being considered.

The EPRI-identified technical information needs and priorities are provided in Table B-5.

B.4 International Technical Information Needs and Priorities

International Atomic Energy Agency standards typically govern transport of SNF that crosses international borders (IAEA 2009; IAEA 2012). However, this is not the case for stored SNF. Each country has its own storage regulations and guidance to meet those regulations. EPRI compiled a report of international technical information needs identified by nine countries (EPRI 2012). The identified technical information needs are country-specific and reflect the data needed to meet regulations in those countries. As a result, a technical information need rated highly for one country may be low for another. Priorities depend on variables such as the type of dry cask storage system capabilities and design, the atmosphere in the storage cask, maximum allowable fuel temperature, requirements to maintain fuel cladding integrity, and the need to encapsulate damaged SNF. There are no technical information needs related to HBF that are common to all nine countries, although there is a strong consensus that more information is needed on drying, monitoring, and hydriding effects. The technical information needs and priorities identified in other countries are provided in Table B-6.

⁴ The official NRC definitions of confinement and containment are as follows: Confinement systems are those systems, including ventilation systems, that act as barriers between areas containing radioactive substances and the environment (10 CFR Part 71). Confinement usually refers to storage systems. Alternatively, a containment system is the assembly of components of the packaging intended to retain the radioactive material during transport (10 CFR Part 72). Containment usually refers to transportation systems. In practice, the terms are used interchangeably.

⁵ This is the same view taken by the NRC.

Table B-5 EPRI-identified Technical Information Needs and Priorities.

	Degradation Issue(s) ^a	Priority	Comments to Support Priority Position
UO ₂ Fuel	High burnup source term	L	Adequate information is available to estimate the gamma, neutron, and decay heat source terms as a function of time.
	Rim effects leading to potentially more particulate release	L	Not an extended storage issue.
	Waterlogged Rods	L	More information is needed to determine how much water is necessary to cause degradation within breached cladding or within the cask or canister. It is possible the amount of water necessary to degrade the fuel is larger than any residual water left behind by current drying protocols
	Air Oxidation	L	Assuming only air contacts the UO ₂ or MOX after 20 years of storage, temperatures will be low enough to keep the oxidation rate low. The incubation period prior to onset of oxidation is also longer for higher burnup fuels.
Cladding	General and localized corrosion	L	Cladding corrosion is insignificant in a dry environment.
	Air Oxidation	L	Cladding corrosion likely is insignificant in a dry environment.
	Delayed Hydride Cracking (DHSC)	L	Additional information is needed to determine if DHC is important at lower temperatures on the time scale of many decades.
	Embrittlement: Hydride reorientation	M	This is not specifically an extended storage issue but will affect cladding properties on all time frames. Additional information for high burnup fuel and advanced claddings (e.g., ZIRLO [®] , M5 [®]) is needed.
	Creep: High temperature	L	High-temperature creep will cease after the first decade or two. Creep is also self-limiting.
	Creep: Low temperature	L	It is unclear whether this mechanism is active. If so, it will also be self-limiting.
	Ductile-to-brittle transition	M	For HBF it is possible the cladding will transition from being ductile at higher temperatures to being more brittle at lower temperatures. The transition temperature range is a function of many parameters such as burnup, cladding morphology, maximum temperatures and pressures experienced by the cladding, and cladding type. Limited data are available about when or at what temperature the cladding may become more brittle. Therefore, it is necessary to do more testing to determine HBF cladding ductility at low temperatures.
	Stress Corrosion Cracking	L	The stresses and temperatures needed to drive this mechanism were evaluated by EPRI (EPRI 2002) and found insufficient to cause cladding breach during dry storage of SNF.
	Helium pressurization	L	The time to generate sufficient additional helium via alpha decay is longer than several centuries.

(EPRI 2011)

M = medium priority, and L = low priority

^a Additional information on many of these degradation mechanisms, such as stress corrosion cracking and ductile-to-brittle transition, as well as terminology, such as high burnup source term, rim effects, and waterlogged rods, is discussed in Appendices A, E, and F of this report.

Table B-6 Technical Information Needs and Priorities Identified by Other Countries

Structure or System Component	Degradation Mechanism	Germany	Hungary	Japan	Republic of Korea (ROK)	Spain	United Kingdom (UK)	United States (DOE)
Cladding	Annealing		M	H	M	M	H	M
	H ₂		H		H	H	H	H
	H ₂ hydride cracking		M		H	M	H	H
	Oxidation	M	M		M	H	H	M
	Creep	M	M		M	M	H	M
	High Burnup Fuel	M						
Pellet	Cracking, Bonding			H	L	M		
Cross-cutting Needs	Monitoring	M	H	H			H	H or M
	Temperature profiles	M	H		H	M	H	H
	Drying issues	M	H		H	M	H	H
	Burnup credit ^a		H					H
	Fuel Transfer Options		H		M	M		H
	Verify fuel condition ^b			H		M	H	
	Examination ^c		H			H		
	Fuel classification ^d					H	H	
“Damaged fuel” definition				H	H	H		

(EPRI 2012)

H = high priority, M = medium priority, and L = low priority

^a The reactivity of the SNF is lowered from its initial unirradiated state due to a decrease in the concentration of fissile material, which is burned in the reactor, and due to the buildup of neutron poisons.

^b Verify fuel condition means that the noted country needs to have a process to verify that SNF cladding has not failed and that integrity of the SNF, when it is loaded into an SNF cask, is maintained (i.e., excessive deformation or degradation of material properties has not been observed).

^c Hungary – fuel storage tube used to isolate the fuel from the atmosphere in the storage vault. United Kingdom – not specified.

^d Fuel classification means that the indicated countries believe that more precise definitions are needed for fuel classifications, such as “normal fuel” and “damaged fuel.”

B.5 Board Evaluation of Technical Information Needs

The Board's 2010 evaluation of SNF storage and transportation assessed the state of knowledge regarding degradation mechanisms for various components of SNF dry cask storage systems but did not provide priorities for each mechanism or component (NWTRB 2010). Instead, the evaluation drew overarching conclusions about the effects of component degradation on storing and transporting SNF. In its 2010 report, the NWTRB identified the following research goals for storing and/or transporting SNF over the long-term:

1. Understanding long-term changes in the mechanical cladding behavior and fuel cladding degradation mechanisms potentially active during extended dry storage, including those that will act on the materials introduced in the last few years for fabrication of HBF;
2. Understanding and modeling the time-dependent conditions that affect aging and degradation processes, such as temperature profiles, in situ material stresses, quantity of residual water, and quantity of helium gas;
3. Modeling age-related degradation of internal components during extended dry storage;
4. Inspecting and monitoring fuel to verify the actual conditions and degradation behavior over time, including techniques for assuring the presence of helium cover gas;
5. Verifying the predicted mechanical performance of fuel after extended dry storage during cask and container handling, normal transportation operations, fuel removal from casks and containers, off-normal occurrences and accident events; and
6. Designing and demonstrating dry-transfer fuel systems to remove fuel canisters following extended dry storage from casks.

B.6 Conclusion

While many of the technical information needs reports described in this Appendix are consistent regarding the overall list of technical information needs, there is no general agreement on the priorities assigned to the technical information needs. Several technical information needs that were assigned a high priority by some organizations were assigned a medium priority by others. For example, technical information needs rated "conditionally high"⁶ by the NRC, such as fuel fragmentation, fission gas release during an accident, galvanic corrosion of the cladding, and inspection and verification of the fuel condition, are not considered high priorities by DOE.

⁶ NRC rates these information needs highly only if work shows that the fuel is not sufficiently dry or that the production of decay helium will provide excessive stress on the cladding (NRC 2014a). Note that, since the NRC technical information need report (NRC 2014a) was issued, work has shown that excessive stresses are not expected (Raynaud and Einziger 2015).

Hydride reorientation was not highly rated by a majority of the evaluations. Each country has different reasons for not giving hydride reorientation a high priority. For example, Japan does not rate it highly because Japanese regulations set a lower limit on maximum cladding temperature during packaging and storage, and this limit serves to preclude the phenomenon of hydride reorientation. The NRC did not rate hydride reorientation as a high priority for gathering new technical information (data), because the NRC has already collected a significant amount of data through research at ORNL and Argonne National Laboratory. These data confirmed that hydride reorientation was an issue to be addressed in applications for licenses and certificates of compliance for storage or transportation of HBF. In order to support these future applications for extended storage and transportation, DOE determined that more data are needed to better understand and better characterize hydride reorientation in HBF, which is why the topic is considered a high priority for DOE but not for NRC.

DOE has made considerable progress in developing and fine-tuning thermal models and structural models that can be used to predict the behavior of SNF in storage and transportation conditions. However, DOE has provided less support to developing fuel performance models—e.g., models that can predict fracture behavior of the fuel cladding in accident conditions. As noted in section B.1, DOE sponsored some work in this area in 2014, but that support has decreased. In 2017, DOE provided funding, through its Nuclear Energy University Program, to a team lead by the Pennsylvania State University for developing computer models that can predict SNF degradation such as hydride reorientation in HBF cladding (see Appendices A and F) and then predict how those degradation mechanisms may affect the mechanical properties of the HBF cladding. The Board notes that this research is drawing to a close, with no follow-on work funded by DOE.

The Board finds that the DOE listing of priority technical information needs is largely consistent with the Board’s previously-published “recommended research needs” for extended storage and transportation of SNF (NWTRB 2010). The Board agrees with the DOE-identified technical information needs and priorities, with one exception; the Board believes the cross-cutting research area of fuel performance modeling should be pursued as a priority effort. The Board considers fuel performance modeling to be an important effort that, when fully developed, will provide valuable computer-based tools for predicting the characteristics and behavior of HBF, including HBF with operating histories and/or cladding types that have not been fully studied and characterized.

B.7 References

10 CFR Part 71. “Packaging and Transportation of Radioactive Material.” *Code of Federal Regulations*. Washington, DC: Government Printing Office.

10 CFR Part 72. “Licensing Requirements for the Independent Storage of Spent Nuclear Fuel, High-Level Radioactive Waste, and Reactor-Related Greater than Class C Waste.” *Code of Federal Regulations*. Washington, DC: Government Printing Office.

Alsaed, H. and B. Hanson. 2017. *Extended Storage and Transportation Gap Analysis Update—5 Year Delta*. Presentation at the Spent Fuel and Waste Science and Technology Annual Group Meeting. Las Vegas, Nevada. May 23.

BRC (Blue Ribbon Commission on America's Nuclear Future). 2012. *Report to the Secretary of Energy*. January 26.

EPRI (Electrical Power Research Institute). 2002. *Technical Bases for Extended Dry Storage of Spent Nuclear Fuel*. EPRI, Palo Alto, California. 1003416.

EPRI. 2011. Extended Storage Collaboration Program (ESCP): Progress Report and Review of Gap Analyses. EPRI, Palo Alto, California. 1022914.

EPRI. 2012. Extended Storage Collaboration Program International Subcommittee Report: International Perspectives on Technical Data Gaps Associated with Extended Storage and Transportation of Used Nuclear Fuel. EPRI, Palo Alto, California. 1026481.

EPRI. 2014. High Burnup Dry Storage Cask Research and Development Project: Final Test Plan. EPRI, Palo Alto, California. DE-NE-0000593.

Hanson, B., H. Alsaed, and C. Stockman. 2012. *Review of Used Nuclear Fuel Storage and Transportation Technical Gap Analyses*. FCRD-USED-2012-000215. July 31.

Hanson, B., H. Alsaed, C. Stockman, D. Enos, R. Meyer, and K. Sorenson. 2012. *Gap Analysis to Support Extended Storage of Used Nuclear Fuel*. FCRD-USED-2011-000136, Rev. 0. January.

Hanson, B.D. 2016. *High Burnup Fuel, Associated Data Gaps, and Integrated Approach for Addressing the Gaps*. Presentation to the Nuclear Waste Technical Review Board at its February 17, 2016 meeting.

IAEA (International Atomic Energy Agency). 2009. *Regulations for the Safe Transport of Radioactive Material (2009 edition)*. IAEA Safety Standard Series No. TS-R-1. Vienna: International Atomic Energy Agency.

IAEA. 2012. Advisory Material for the IAEA Regulations for the Safe Transport of Radioactive Material (2012 edition). Specific Safety Guide No. SSG-26. Vienna: International Atomic Energy Agency.

IAEA. 2013. Methodology for a Safety Case of a Dual Purpose Cask for Storage and Transport of Spent Fuel: Report of WASSC/TRANSSC joint working group 2011-2013. Draft TECDOC. Vienna: International Atomic Energy Agency. <https://www-ns.iaea.org/downloads/rw/waste-safety/disp/dual-purpose-spent-fuel-cask-draft-tecdoc.pdf>

NRC (U.S. Nuclear Regulatory Commission). 2014a. Identification and Prioritization of the Technical Information Needs Affecting Potential Regulation of Extended Storage and Transportation of Spent Nuclear Fuel. May.

NRC. 2014b. Division of Spent Fuel Storage and Transportation Interim Staff Guidance-24, Revision 0, The Use of a Demonstration Program as a Surveillance Tool for Confirmation of Integrity for Continued Storage of High Burnup Fuel Beyond 20 Years. July.

NWTRB (U.S. Nuclear Waste Technical Review Board). 2010. Evaluation of the Technical Basis for Extended Dry Storage and Transportation of Used Nuclear Fuel. December.

NWTRB. 2016. Transcript of February 17, 2016 Winter 2016 Board Meeting. p. 63.

Raynaud, P.A.C. and R.E. Einziger. 2015. "Cladding Stress During Extended Storage of High Burnup Spent Nuclear Fuel." *Journal of Nuclear Materials*, Vol. 464, pp. 304–312.

Stockman, C.T., B.D. Hanson, S.C. Marschman, H.A. Alsaed, and K.B. Sorenson. 2014. *Used Nuclear Fuel Extended Storage and Transportation Research and Development Review and Plan*. FCRD-UFD-2014-000050. August 9.

Teague, M., S. Saltzstein, B. Hanson, K. Sorenson, G. Freeze. 2019. *Gap Analysis to Guide DOE R&D in Supporting Extended Storage and Transportation of Spent Nuclear Fuel: An FY2019 Assessment*. SAND2019-15479R. December 23.

Appendix C

Regulations and Guidance Applicable to Spent Nuclear Fuel

C.1 Introduction

The Nuclear Regulatory Commission (NRC) regulates activities involving civilian nuclear fuel from its production through its final disposal. The regulatory process is designed to ensure that the fuel is used and maintained safely throughout its lifetime. A nuclear utility or equipment vender (applicant) wishing to receive NRC approval of a license or a certificate of compliance to manufacture, irradiate, store, transport, or dispose of fuel must apply to the NRC. The application process requires that the applicant demonstrate compliance with the applicable regulations by submitting a safety analysis report and supporting technical information. The applicable regulations and supporting guidance have been published by the NRC in the Code of Federal Regulations (CFR) and in several other NRC documents as discussed below.

C.2 Nuclear Regulatory Commission Regulations

There are three primary sets of regulations governing spent nuclear fuel (SNF) storage, transportation, and disposal:¹

1. Storing SNF outside the reactor spent fuel pool: Title 10, CFR, Part 72 (10 CFR Part 72), “Licensing Requirements for the Independent Storage of Spent Nuclear Fuel, High-Level Radioactive Waste, and Reactor-Related Greater Than Class C Waste”;
2. Transporting SNF: 10 CFR Part 71, “Packaging and Transportation of Radioactive Material”; and
3. Disposing of SNF:
 - a. Regulation specific to the Yucca Mountain repository: 10 CFR Part 63, “Disposal of High-Level Radioactive Wastes in a Geologic Repository at Yucca Mountain, Nevada” and
 - b. Regulation for all other potential geologic repositories that may accept SNF and high-level radioactive wastes: 10 CFR Part 60, “Disposal of High-Level Radioactive Wastes in Geologic Repositories.”

Throughout these regulations and the associated NRC guidance documents (e.g., Regulatory Guide 7.9 [NRC 2005a]), there is a significant focus on ensuring the presence and

¹ This report focuses on SNF storage after the SNF has been removed from the spent fuel pool at a nuclear power plant site. The NRC regulations applicable to spent fuel pools at nuclear power plant sites are included in 10 CFR Part 50, *Domestic Licensing of Production and Utilization Facilities*, and 10 CFR Part 52, *Licenses, Certifications, and Approvals for Nuclear Power Plants*.

reliability of five key safety functions that are provided by SNF components and dry cask storage systems or packaging (casks, canisters, overpacks, etc.) in which the SNF is held. The five key safety functions are 1) maintain subcriticality; 2) ensure confinement of radioactive materials; 3) provide shielding against radiation; 4) maintain structural integrity of the packaging and SNF, where necessary, and; 5) control temperatures and thermal stresses in the SNF and packaging. Having a good understanding of SNF characteristics and performance during storage, transport, and disposal is necessary to ensure that these key safety functions are operable and remain viable.

The NRC regulations and guidance documents provide applicants and the NRC staff with detailed information on the expected format and content of the safety analysis reports and supporting documentation that demonstrate the safety functions are in place and adequately protecting the public, workers, and the environment. The storage and transportation regulations are discussed in sections C.2.1 and C.2.2, respectively. Disposal regulations bearing on SNF are discussed in Appendix D. NRC guidance documents are described in section C.3.

C.2.1 Spent Nuclear Fuel Storage Regulation: 10 CFR Part 72

The purpose of 10 CFR Part 72 is stated in 10 CFR 72.1: "...establish requirements, procedures, and criteria for the issuance of licenses to receive, transfer, and possess power reactor spent fuel, power reactor-related Greater than Class C (GTCC) waste,² and other radioactive materials associated with spent fuel storage in an independent spent fuel storage installation (ISFSI) and the terms and conditions under which the Commission will issue these licenses."

Within 10 CFR Part 72, specific requirements relevant to the performance of SNF in storage are:

- 10 CFR 72.122(h)(1) "Confinement Barriers and Systems. The spent fuel cladding must be protected during storage against degradation that leads to gross ruptures³ or the fuel must be otherwise confined such that degradation of the fuel during storage will not pose operational safety problems with respect to its removal from storage. This may be accomplished by canning of consolidated fuel rods or unconsolidated assemblies⁴ or other means as appropriate."

² Greater than Class C waste is a low-level radioactive waste category that exceeds the concentration limits of radionuclides established for Class C waste in 10 CFR 61.55.

³ "Gross rupture" is defined in NRC Interim Staff Guidance 1, Revision 2 (NRC 2007): "A breach in spent fuel cladding that is larger than a pinhole leak or a hairline crack."

⁴ "Canning" of SNF is defined in NRC (2007): "Spent fuel that has been classified as damaged for storage must be placed in a can designed for damaged fuel, or in an acceptable alternative. The purpose of a can designed for damaged fuel is to (1) confine gross fuel particles, debris, or damaged assemblies to a known volume within the cask; (2) to demonstrate that compliance with the criticality, shielding, thermal, and structural requirements are met; and (3) permit normal handling and retrieval from the cask."

- 10 CFR 72.122(l) “Retrievability. Storage systems must be designed to allow ready retrieval⁵ of spent fuel, high-level radioactive waste, and reactor-related GTCC waste for further processing or disposal.”

There are other requirements for which SNF properties are important in demonstrating compliance:

- 10 CFR 72.124(a), “Design for Criticality Safety. Spent fuel handling, packaging, transfer, and storage systems must be designed to be maintained subcritical and to ensure that, before a nuclear criticality accident is possible, at least two unlikely, independent, and concurrent or sequential changes have occurred in the conditions essential to nuclear criticality safety. The design of handling, packaging, transfer, and storage systems must ... demonstrate safety for the handling, packaging, transfer and storage conditions and in the nature of the immediate environment under accident conditions.”
- 10 CFR 72.126(a), “Exposure Control. Radiation protection systems must be provided for all areas and operations where onsite personnel may be exposed to radiation or airborne radioactive materials. Structures, systems, and components for which operation, maintenance, and required inspections may involve occupational exposure must be designed, fabricated, located, shielded, controlled, and tested so as to control external and internal radiation exposures to personnel. The design must include means to: ... (6) Shield personnel from radiation exposure.”
- 10 CFR 72.128(a), “Spent Fuel, High-Level Radioactive Waste, and Reactor-Related GTCC Waste Storage and Handling Systems. Spent fuel storage, high-level radioactive waste storage, reactor-related GTCC waste storage and other systems that might contain or handle radioactive materials associated with spent fuel, high-level radioactive waste, or reactor-related GTCC waste, must be designed to ensure adequate safety under normal and accident conditions. These systems must be designed with—
 - 1) A capability to test and monitor components important to safety,
 - 2) Suitable shielding for radioactive protection under normal and accident conditions,
 - 3) Confinement structures and systems,
 - 4) A heat-removal capability having testability and reliability consistent with its importance to safety, and
 - 5) means to minimize the quantity of radioactive wastes generated.”

⁵ “Ready retrieval” means that SNF can be removed from storage by normal means: no special equipment or procedures are required to remove SNF from the storage system.

- 10 CFR 72.240, “Conditions for spent fuel storage cask renewal. ... (c) The application must be accompanied by a safety analysis report (SAR). The SAR must include the following:
 - 1) Design bases information as documented in the most recently updated final safety analysis report (FSAR) as required by § 72.248;
 - 2) Time-limited aging analyses that demonstrate that structures, systems, and components important to safety will continue to perform their intended function for the requested period of extended operation; and
 - 3) A description of the AMP [aging management program] for management of issues associated with aging that could adversely affect structures, systems, and components important to safety.”

C.2.2 Spent Nuclear Fuel Transportation Regulation: 10 CFR Part 71

The NRC regulation 10 CFR Part 71 establishes the requirements for packaging, preparing for shipment, and transporting licensed material, which includes SNF. It provides the requirements for NRC approval of packaging and shipping procedures for fissile material and other licensed material. The following are excerpts from 10 CFR Part 71 for which SNF performance and properties have a role in meeting the regulation.

- 10 CFR 71.33, “Package description. The application must include a description of the proposed package in sufficient detail to identify the package accurately and provide a sufficient basis for evaluation of the package. The description must include—...
 - (b) With respect to the contents of the package—
 - (1) Identification and maximum radioactivity of radioactive constituents;
 - (2) Identification and maximum quantities of fissile constituents;
 - (3) Chemical and physical form;
 - (4) Extent of reflection, the amount and identity of nonfissile materials used as neutron absorbers or moderators, and the atomic ratio of moderator to fissile constituents;
 - (5) Maximum normal operating pressure;
 - (6) Maximum weight;
 - (7) Maximum amount of decay heat;”
- 10 CFR 71.43, “General standards for all packages. ...
 - (d) A package must be made of materials and construction that assure that there will be no significant chemical, galvanic, or other reaction among the packaging components, among package contents, or between the packaging components and the package contents, including the possible reaction resulting from inleakage of water, to the maximum credible extent. Account must be taken of the behavior of materials under irradiation.
 - ...
 - (f) A package must be designed, constructed, and prepared for shipment so that ... there would be no loss or dispersal of radioactive contents, no significant increase in external surface radiation levels, and no substantial reduction in the effectiveness of the packaging. ...

(g) A package must be designed, constructed, and prepared for transport so that in still air at 38°C (100°F) and in the shade, no accessible surface of a package would have a temperature exceeding 50°C (122°F) in a nonexclusive use shipment, or 85°C (185°F) in an exclusive use shipment.”⁶

- 10 CFR 71.47, “External radiation standards for all packages.” This paragraph sets dose rate limits on and around the surface of transport packages.
- 10 CFR 71.51, “Additional requirements for Type B packages.”⁷ This paragraph sets limits on the release of particular radionuclides or the dose rate caused by release of those radionuclides during normal conditions of transport and hypothetical accident conditions.
- 10 CFR 71.55, “General requirements for fissile material packages.

...

(d) A package used for the shipment of fissile material must be so designed and constructed and its contents so limited that under the tests specified in § 71.71 (“Normal conditions of transport”)–

- (1) The contents would be subcritical;
- (2) The geometric form of the package contents would not be substantially altered;
- (3) There would be no leakage of water into the containment system unless, in the evaluation of undamaged packages under § 71.59(a)(1), it has been assumed that moderation is present to such an extent as to cause maximum reactivity consistent with the chemical and physical form of the material;

...

(e) A package used for the shipment of fissile material must be so designed and constructed and its contents so limited that under the tests specified in § 71.73 (“Hypothetical accident conditions”), the package would be subcritical. For this determination, it must be assumed that:

- (1) The fissile material is in the most reactive credible configuration consistent with the damaged condition of the package and the chemical and physical form of the contents;
- (2) Water moderation occurs to the most reactive credible extent consistent with the damaged condition of the package and the chemical and physical form of the contents...”

- 10 CFR 71.71, “Normal conditions of transport.
(a) Evaluation. Evaluation of each package design under normal conditions of transport must include a determination of the effect on that design of the conditions and tests specified in this section.

...

⁶ “Exclusive use” means “sole use by a single consignor of a conveyance...” for radioactive materials, as defined in 49 CFR Part 173, “Shippers—General Requirements For Shipments And Packagings” [within Title 49—Transportation, Subtitle B—Other Regulations Relating to Transportation, Chapter I—Pipeline and Hazardous Materials Safety Administration, Department of Transportation, Subchapter C—Hazardous Materials Regulations].

⁷ All SNF shipments must be made in Type B packages.

(c) Conditions and tests.

...

(5) Vibration. Vibration normally incident to transport.

(6) Water spray. A water spray that simulates exposure to rainfall of approximately 5 cm/h (2 in./h) for at least 1 hour.

(7) Free drop. ...

(8) Corner drop. ...”

- 10 CFR 71.73, “Hypothetical accident conditions. ...
(c) Tests. Tests for hypothetical accident conditions must be conducted as follows:
(1) Free drop. A free drop of the specimen through a distance of 9 m (30 ft) onto a flat, essentially unyielding, horizontal surface, striking a surface in a position for which maximum damage is expected. ...
(4) Thermal. Exposure of the specimen fully engulfed ... in a ... fire ... with an average flame temperature of at least 800°C (1475°F) for a period of 30 minutes ...”

C.3 Nuclear Regulatory Commission Guidance

To assist NRC staff in its review of applications for licenses or certificates of compliance to manufacture, irradiate, store, transport, or dispose of nuclear materials, the NRC issues Regulatory Guides. The NRC general description of a Regulatory Guide is: “The Regulatory Guide series provides guidance to licensees and applicants on implementing specific parts of the NRC’s regulations, techniques used by the NRC staff in evaluating specific problems or postulated accidents, and data needed by the staff in its review of applications for permits or licenses.”⁸ The NRC has published many dozens of these Regulatory Guides. Two key Regulatory Guides applicable to SNF storage and transport are Regulatory Guide 3.48, *Standard Format and Content for the Safety Analysis Report for an Independent Spent Fuel Storage Installation or Monitored Retrievable Storage Installation (Dry Storage)* (NRC 1989) and Regulatory Guide 7.9, *Standard Format and Content of Part 71 Applications for Approval of Packages for Radioactive Material* (NRC 2005a).

In addition, the NRC issues Standard Review Plans (SRPs) and Interim Staff Guidance (ISG) documents to help the NRC staff review the safety analysis reports accompanying an application for a license or a certificate of compliance to store or transport radioactive material, including SNF. These are not regulations, and applicants are not obligated to follow this guidance. However, applicants generally do follow them to streamline the NRC review process. Guidance covering all aspects of a review is covered in an SRP. Occasionally, the guidance is revised to reflect new information on a topic. An ISG provides new information on a topic that is intended to be incorporated eventually into a new SRP or a future revision of an existing SRP, and it carries the same weight as an SRP. The SRPs and ISGs applicable to NRC’s review of applications for storage or transportation of SNF are described below.

C.3.1 Standard Review Plans and Similar Guidance

The NRC SRPs and other guidance that are most directly applicable to SNF are summarized below.

⁸ <https://www.nrc.gov/reading-rm/doc-collections/reg-guides/>

- NUREG-1536, Rev. 1 (NRC 2010), *Standard Review Plan for Spent Fuel Dry Storage Systems at a General License Facility, Final Report*: provides guidance for reviewing applications for a certificate of compliance for a dry cask storage system for use at a general license facility.
- NUREG-1567 (NRC 2000a), *Standard Review Plan for Spent Fuel Dry Storage Facilities, Final Report*: provides guidance for reviewing applications for license approval or renewal for commercial independent spent fuel storage installations. An interim spent fuel storage installation may be co-located with a reactor or may be away from a reactor site. These installations may be designed for the storage of irradiated nuclear fuel and associated radioactive materials.
- NUREG-1617 (NRC 2000b), *Standard Review Plan for Transportation Packages for Spent Nuclear Fuel, Final Report*: provides guidance for the review and approval of applications for packages used to transport SNF under 10 CFR Part 71. The objectives of the SRP are to (1) summarize 10 CFR Part 71 requirements for spent fuel transport package approval, (2) describe the procedures by which NRC staff determines that these requirements have been satisfied, and (3) document the practices used by the staff in reviews of package applications.
- NUREG-1927, Rev 1 (NRC 2016a), *Standard Review Plan for Renewal of Specific Licenses and Certificates of Compliance for Dry Storage of Spent Nuclear Fuel, Final Report*: provides guidance for the safety review of renewal applications for specific licenses of interim spent fuel storage installations and certificates of compliance for dry cask storage systems, as codified in 10 CFR Part 72. The SRP also provides guidance for the review aging management information in a renewal application, including time-limited aging analyses and aging management programs.
- NUREG-2214 (NRC 2019), *Managing Aging Processes In Storage (MAPS) Report, Final Report*: provides guidance for the NRC staff for review of renewal applications for specific licenses of independent spent fuel storage installations and certificates of compliance for dry storage systems, as codified in 10 CFR Part 72. NUREG-2214 evaluates known aging degradation mechanisms to determine if they could affect the ability of dry storage system components to fulfill their safety functions in the 20- to 60-year period of extended operation. The guidance also provides examples of aging management programs that are considered generically acceptable to address the credible aging mechanisms.
- NUREG-2215 (NRC 2020a), *Standard Review Plan for Spent Fuel Dry Storage Systems and Facilities, Final Report*: provides guidance to the NRC staff for reviewing safety analysis reports for (1) a certificate of compliance for a dry storage system for use at a general license facility and (2) a specific license for a dry storage facility that is either an independent spent fuel storage installation or a monitored retrievable storage installation. This SRP does not apply to SNF wet storage facilities (e.g., the GE-Morris facility). NUREG-2215 is a consolidation of existing guidance for staff's use when reviewing applications for licenses and certificates for spent fuel dry storage systems and facilities, and as such, it is not intended to offer new or differing guidance.

- NUREG-2216 (NRC 2020b), *Standard Review Plan for Transportation Packages for Spent Fuel and Radioactive Material, Final Report*: consolidates existing guidance to the NRC staff for reviewing an application for package approval submitted under 10 CFR Part 71. This SRP combines and updates NUREG-1617 (NRC 2000b) and incorporates applicable ISGs.
- NUREG-2224 (NRC 2020c), *Dry Storage and Transportation of High Burnup Spent Nuclear Fuel, Final Report*: expands the technical basis in support of the NRC's guidance on high burnup SNF as it pertains to hydride reorientation in the fuel. NUREG-2224 addresses the technical issues of hydride reorientation and provides a technical assessment of the results from NRC-sponsored research on the effect of hydride reorientation on the mechanical performance of high burnup SNF. NUREG-2224 also provides example approaches for licensing and certification of high burnup SNF for dry storage and transportation.

C.3.2 Interim Staff Guidance Documents

The NRC ISG documents most applicable to SNF, including high burnup SNF, are summarized below [Note: this is not intended to be a complete listing of all ISGs related to SNF storage and transportation. All such ISGs can be found on the NRC website].⁹ Many of the ISGs listed below have been incorporated into other NRC guidance documents, such as Standard Review Plans.

- SFST-ISG-1, Rev. 2 (NRC 2007), *Classifying the Condition of Spent Nuclear Fuel for Interim Storage and Transportation Based on Function*: provides guidance on classifying SNF as either (1) damaged, (2) undamaged, or (3) intact, before interim storage or transportation. This is not a regulation or requirement and can be modified or superseded by an applicant with supportable technical arguments.
- SFST-ISG-2, Rev. 2 (NRC 2016b), *Fuel Retrievability in Spent Fuel Storage Applications*: provides guidance for determining if storage systems to be licensed under 10 CFR Part 72 allow ready retrieval of SNF.
- SFST-ISG-3, Rev. 0, *Post Accident Recovery and Compliance with 10 CFR 72.122(l)*: clarifies that 10 CFR 72.122(l) applies to normal and off-normal design conditions and not to accidents. ISG-3, Rev. 0 suggests that Chapter 11 of NUREG-1536 (NRC 2010) and Chapter 10 and Chapter 15 of [NUREG-1567] (NRC 2000a) should be modified to focus on the identification of all credible accidents affecting public health and safety. Further, the SRPs should eliminate all references to non-credible accidents such as non-mechanistic failures of the confinement boundary.
- SFST-ISG-5, Rev. 1 (NRC 1998), *Confinement Evaluation*: provides NRC staff's recommended approach for performing confinement evaluations for dry cask storage systems, including an evaluation of the measures taken to protect SNF cladding.

⁹ The NRC ISGs related to SNF storage and transportation can be found at this website:

<https://www.nrc.gov/reading-rm/doc-collections/isg/spent-fuel.html>.

- SFST-ISG-8, Rev. 3 (NRC 2012), *Burnup Credit¹⁰ in the Criticality Safety Analyses of PWR Spent Fuel in Transportation and Storage Casks*: provides recommendations to the staff for accepting, on a design-specific basis, a burnup credit approach in the criticality safety analysis of pressurized water reactor SNF storage and transportation systems. The guidance provided in this ISG represents one methodology for demonstrating compliance with the criticality safety requirements in 10 CFR Parts 71 and 72 using burnup credit. Alternative methodologies proposed by applicants and licensees would be considered on a case-by-case basis, using this guidance to the extent practicable.
- SFST-ISG-11, Rev. 3 (NRC 2003a), *Cladding Considerations for the Transportation and Storage of Spent Fuel*: expands the technical basis for cladding temperatures for commercial SNF (including high burnup SNF) in storage and transportation systems. The guidance also specifies the acceptance criteria for limiting SNF reconfiguration in dry cask storage systems.
- SFST-ISG-12, Rev. 1, *Buckling of Irradiated Fuel Under Bottom End Drop Conditions*: provides recommendations regarding analyses of fuel rod buckling performed to demonstrate fuel integrity following a cask drop accident.
- SFST-ISG-15, Rev. 0 (NRC 2001), *Materials Evaluation*: provides specific guidance for the review of materials selected by an applicant for its dry cask storage system or transportation package.
- SFST-ISG-19, Rev. 0 (NRC 2003b), *Moderator Exclusion Under Hypothetical Accident Conditions and Demonstrating Subcriticality of Spent Fuel Under the Requirements of 10 CFR 71.55(e)*: provides review guidance for meeting the fissile material package standards in 10 CFR 71.55(e), which require that a fissile material package be subcritical under hypothetical accident conditions assuming that the fissile material is in the most reactive credible configuration consistent with the damaged condition of the package and the chemical and physical form of the contents, and water moderation occurs to the most reactive credible extent consistent with the damaged condition of the package and the chemical and physical form of the contents.
- SFST-ISG-21 (NRC 2006), *Use of Computational Modeling Software*: supplements guidance in the storage and transport SRPs regarding NRC staff's position on what an acceptable analysis using computational modeling software (CMS) "should include, and what information should be reviewed by the staff when considering a submittal from an applicant using CMS in the design review of a storage cask or transportation package. This ISG applies to both thermal and structural analyses utilizing CMS."
- SFST-ISG-22, Rev. 0 (NRC 2005b), *Potential Rod Splitting Due to Exposure to an Oxidizing Atmosphere During Short-Term Cask Loading Operations in LWR or Other Uranium Oxide Based Fuel*: provides technical review guidance to ensure that

¹⁰ Allowance in the criticality safety analysis for the decrease in fuel reactivity resulting from irradiation of the fuel is termed burnup credit.

operating procedures, technical specification, and associated licensing documentation submitted by applicants, provide a supportable analysis of the potential for cladding splitting, should fuel rods be exposed to an oxidizing gaseous atmosphere.

- ISG-24, Rev. 0 (NRC 2014), *The Use of a Demonstration Program as a Surveillance Tool for Confirmation of Integrity for Continued Storage of High Burnup Fuel Beyond 20 Years*: provides guidance regarding the use of testing programs that may be used to support the application for extension of a license or certificate of compliance for SNF storage.

C.4 References

10 CFR Part 50. "Domestic Licensing of Production and Utilization Facilities." *Code of Federal Regulations*, Washington, DC: Government Printing Office.

10 CFR Part 52. "Licenses, Certifications, and Approvals for Nuclear Power Plants." *Code of Federal Regulations*, Washington, DC: Government Printing Office.

10 CFR Part 60. "Disposal of High-Level Radioactive Wastes in Geologic Repositories." *Code of Federal Regulations*, Washington, DC: Government Printing Office.

10 CFR Part 61. "Licensing Requirements for Land Disposal Of Radioactive Waste." *Code of Federal Regulations*, Washington, DC: Government Printing Office.

10 CFR Part 63. "Disposal of High-Level Radioactive Wastes in a Geologic Repository at Yucca Mountain, Nevada." *Code of Federal Regulations*, Washington, DC: Government Printing Office.

10 CFR Part 71. "Packaging and Transport of Radioactive Material." *Code of Federal Regulations*, Washington, DC: Government Printing Office.

10 CFR Part 72. "Licensing Requirements for the Independent Storage of Spent Nuclear Fuel, High-Level Radioactive Waste, and Reactor-Related Greater than Class C Waste." *Code of Federal Regulations*. Washington, DC: Government Printing Office.

49 CFR Part 173, "Shippers—General Requirements For Shipments And Packagings." *Code of Federal Regulations*, Washington, DC: Government Printing Office.

NRC. 1989. *Office of Nuclear Regulatory Research Regulatory Guide 3.48, Revision 1, Standard Format and Content for the Safety Analysis Report for an Independent Spent Fuel Storage Installation or Monitored Retrievable Storage Installation (Dry Storage)*. August.

NRC. 1998. *Spent Fuel Project Office Interim Staff Guidance-5, Revision 1, Confinement Evaluation*. October.

NRC. 2000a. *Standard Review Plan for Spent Fuel Dry Storage Facilities*. NUREG-1567. March.

NRC. 2000b. *Standard Review Plan for Transportation Packages for Spent Nuclear Fuel*. NUREG-1617. March.

NRC. 2001. *Spent Fuel Project Office Interim Staff Guidance-15, Materials Evaluation*. January.

NRC. 2003a. *Spent Fuel Project Office Interim Staff Guidance-11, Revision 3, Cladding Considerations for the Transportation and Storage of Spent Fuel*. November.

NRC. 2003b. *Spent Fuel Project Office Interim Staff Guidance-19, Moderator Exclusion under Hypothetical Accident Conditions and Demonstrating Subcriticality of Spent Fuel under the Requirements of 10 CFR 71.55(e)*. May.

NRC. 2005a. *Office of Nuclear Regulatory Research Regulatory Guide 7.9, Revision 2, Standard Format and Content of Part 71 Applications for Approval of Packages for Radioactive Material*. March.

NRC. 2005b. *Spent Fuel Project Office Interim Staff Guidance-22, Potential Rod Splitting due to Exposure to an Oxidizing Atmosphere During Short-Term Cask Loading Operations in LWR or Other Uranium Oxide Based Fuel*. May.

NRC. 2006. *Spent Fuel Project Office Interim Staff Guidance-21, Use of Computational Modeling Software*. April.

NRC. 2007. *Division of Spent Fuel Storage and Transportation Interim Staff Guidance-1, Revision 2, Classifying the Condition of Spent Nuclear Fuel for Interim Storage and Transportation Based on Function*. May.

NRC. 2010. *Standard Review Plan for Spent Fuel Dry Storage Systems at a General License Facility*. NUREG-1536, Rev. 1. July.

NRC. 2012. *Division of Spent Fuel Storage and Transportation Interim Staff Guidance-8, Revision 3, Burnup Credit in the Criticality Safety Analyses of PWR Spent Fuel in Transportation and Storage Casks*. September.

NRC. 2014. *Division of Spent Fuel Storage and Transportation Interim Staff Guidance-24, Revision 0, The Use of a Demonstration Program as a Surveillance Tool for Confirmation of Integrity for Continued Storage of High Burnup Fuel Beyond 20 Years*. July.

NRC. 2016a. *Standard Review Plan for Renewal of Specific Licenses and Certificates of Compliance for Dry Storage of Spent Nuclear Fuel*. NUREG-1927, Rev. 1. June.

NRC. 2016b. *Division of Spent Fuel Management Interim Staff Guidance-2, Revision 2, Fuel Retrievability in Spent Fuel Storage Applications*. April.

NRC. 2019. *Managing Aging Processes In Storage (MAPS) Report, Final Report*. NUREG-2214. July.

NRC. 2020a. *Standard Review Plan for Spent Fuel Dry Storage Systems and Facilities, Final Report*. NUREG-2215. April.

NRC. 2020b. *Standard Review Plan for Transportation Packages for Spent Fuel and Radioactive Material, Final Report*. NUREG-2216. August.

NRC. 2020c. *Dry Storage and Transportation of High Burnup Spent Nuclear Fuel, Final Report*. NUREG 2224. November.

Appendix D

Implications of the Trend toward High Fuel Burnups for Geologic Disposal of Spent Nuclear Fuel

High burnup fuel (HBF) (>45 gigawatt-days per metric ton of uranium [GWd/MTU])¹ has higher decay heat, higher radioactivity, and higher concentrations of fission products and actinides compared to low burnup fuel (LBF). However, the only significant effect of disposing of HBF in a geologic repository is higher temperatures in the near field² of the repository and that is the focus of this appendix.

D.1 Thermal Effects

HBF generates more decay heat per unit mass, on average, than LBF, thus disposal of HBF will increase the temperature in the near field of a geologic repository more so than disposal of LBF. The increase in near-field temperature from disposal of HBF will depend on several factors. These factors include the waste package loading [i.e., the number of spent nuclear fuel (SNF) assemblies in the waste package], the characteristics (e.g., thermal conductivity) of the host rock and engineered barrier (i.e., buffer, backfill), the repository design (e.g., spacing of waste packages and disposal drifts, backfilled or unbackfilled drifts), SNF surface storage time, disposal drift ventilation period, and, of course, fuel burnup. For example, Figure D-1, taken from Liljenfeldt et al. (2017), shows calculated temperatures at the waste package surface and at the drift wall of a repository in sedimentary (clay-rich) rock resulting from the emplacement of waste packages that each contain 32 pressurized water reactor SNF assemblies. The assumptions Liljenfeldt et al. (2017) used in the calculations include (i) the SNF is in surface storage for 50 years; (ii) the repository is open and ventilated to remove heat for 100 years after emplacement, after which a low-permeability clay-based backfill is emplaced around the waste packages; (iii) waste package spacing is 20 meters; and (iv) drift spacing is 70 meters. Two values of backfill thermal conductivity (Kth) were used—0.6 W/m-K for a compacted, dehydrated clay and 1.43 W/m-K for hydrated clay. The figure shows that, if the backfill has a thermal conductivity of 0.6 W/m-K, the peak waste package surface temperature can reach approximately 150, 260, and 350°C for SNF burnup levels of 20, 40, and 60 GWd/MTU, respectively. Similarly, the peak drift wall temperature can reach approximately 70, 105, and 135°C from disposal of SNF with burnup levels of 20, 40, and 60 GWd/MTU, respectively. The results also show the peak temperatures are lower if the backfill has a higher thermal conductivity (1.43 W/m-K).

¹ Fuel burnup is a measure of the thermal energy generated in a nuclear reactor per unit mass of nuclear fuel initially loaded in the reactor and is typically expressed in units of gigawatt-days per metric ton of uranium (GWd/MTU). In the U.S., nuclear fuel utilized beyond 45 GWd/MTU is defined by the U.S. Nuclear Regulatory Commission as high burnup fuel.

² “Near field” is the excavated area of a repository near or in contact with the waste packages, including filling or sealing materials, and those parts of the host medium/rock whose characteristics have been or could be altered by the repository or its content (IAEA 2003).

Because temperature is an important driver for many thermal, hydrological, mechanical, and chemical processes, the higher temperatures resulting from disposal of HBF will increase the degree, extent, and significance of coupled thermal–hydrological–mechanical–chemical processes in the repository near field. The thermal effects on engineered and natural barriers may need to be considered in repository performance assessments, or otherwise mitigated through appropriate thermal management, as discussed in Section D.2.

D.1.1 Thermal Effects on Engineered Barriers

The geologic disposal concepts being developed in several countries include the use of a bentonite buffer around the waste package. Bentonite, which is a clay with a high content of smectite minerals, has several properties suitable for isolating radioactive wastes (Wilson et al. 2011). Bentonite swells when contacted by water, which reduces its hydraulic conductivity and imparts self-sealing properties. Its low hydraulic conductivity can limit the amount of potentially corrosive groundwater that comes into contact with the waste package. Furthermore, in the event of radionuclide release from the waste package, the bentonite can limit radionuclide transport to a slow diffusion mechanism rather than a faster convective flow in some geologic environments. Radionuclide sorption on and colloid filtration by the bentonite material also can retard radionuclide transport. Further, bentonite is highly plastic and exhibits significant creep when under stress conditions. Plastic behavior of the bentonite buffer can protect the waste package from damage due to small rock shear movements as well as providing some degree of self-sealing.

Elevated temperatures can alter the mineralogical, hydraulic, and geomechanical properties of bentonite. High temperatures can dry out the bentonite in contact with the waste package and result in a complex sequence of dehydration and rehydration of the bentonite material. The elevated temperatures also can cause mineralogical changes in the bentonite that can degrade its buffer performance, including silica precipitation/cementation and phase transformation of smectite to illite (Jové Colón et al. 2014; Wilson and Bond 2016). Alteration of the smectite clay to illite, which is a non-expanding type of clay mineral, will lower the swelling capacity of the bentonite material and decrease its ability to seal gaps in the engineered barrier system. Clay alteration also will increase the rigidity of the bentonite material, which could reduce its ability to protect the waste package from rock shear movements and promote the formation of fractures in the buffer that could serve as pathways for water movement and radionuclide transport. In addition, higher temperatures could decrease the sorption capability of the bentonite.

Wersin, Johnson, and McKinley (2007) reviewed the performance of bentonite at temperatures greater than 100°C and noted that no significant changes in hydraulic and mechanical properties have been reported in the literature for bentonite exposed to temperatures of at least 120°C under wet conditions. Wersin, Johnson, and McKinley (2007) argue that significant cementation and perhaps also illitization effects occur only above 150°C. But literature data also indicate that the temperature at which the smectite to illite transition occurs depends on several factors, including temperature, time, water/rock ratio, and the concentration of potassium ions in the porewater (Wersin, Johnson, and McKinley 2007; Jové Colón et al. 2014; Wilson and Bond 2016). Because these factors are site specific and significant uncertainty exists in the rate of smectite to illite transformation, geologic disposal concepts that make use of bentonite buffers generally place a temperature limit on the bentonite of 100°C. However, not exceeding this temperature limit

may be a challenge in repository concepts that use clay-based buffer or backfill materials. For example, for the clay-based repository concept illustrated in Figure D-1, the temperature of the backfill in contact with the waste package exceeds the 100°C limit for all combinations of SNF burnup and backfill thermal conductivity, except the combination of low burnup (20 GWd/MTU) and high thermal conductivity (1.43 W/m-K) backfill.

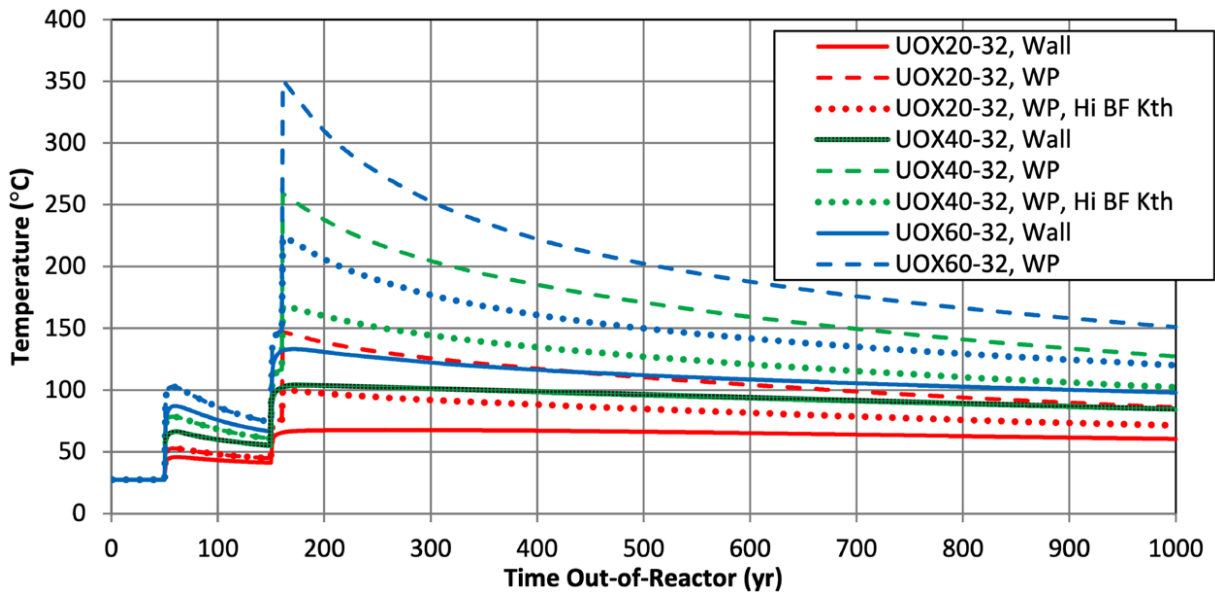


Figure D-1. Calculated temperatures versus time at the surface of waste packages containing 32 pressurized water reactor fuel assemblies and at the drift wall of a repository in sedimentary (clay-rich) rock.

Notes: Figure adapted from Liljenfeldt et al. 2017. The key omits the description of the blue dotted line, which represents the temperature of the waste package holding 32 SNF assemblies with a burnup of 60 GWd/MTU and where the backfill material has a high thermal conductivity.

In addition to thermal effects on bentonite buffer performance resulting from disposal of HBF, the performance of other engineered barriers also could be affected. The degradation rates of engineered materials generally increase with temperature, thus, the higher temperatures that may result from disposal of HBF could lead to higher waste package corrosion and SNF degradation rates.

D.1.2 Thermal Effects on Host Rocks in the Near Field

Elevated temperatures also could affect the properties of the geologic host rock in the near field. In the case of repositories with clay-rich host rocks, heating can modify the structure and composition of the clay mineral components that are considered to be important for retarding radionuclide transport. Considering again the repository concept illustrated in Figure D-1, if a temperature limit of 100°C were proposed for the clay-rich host rock, SNF burnup levels of 40 GWd/MTU or higher would result in peak temperatures greater than 100°C at the drift wall of the clay-rich host rock.

In a salt repository, most of the constituents of the salt body (whether bedded- or dome-type), such as halite, gypsum, and other evaporite minerals, deform slowly through creep

mechanisms when subjected to deviatoric stress (i.e., stress state with different magnitudes in different component directions). The local deformation rate of the salt body could be affected by higher temperatures created by geologic disposal of HBF. Salt deformation may cause changes in the porosity and permeability in the near field of the repository, which could facilitate movement of water (liquid and vapor) around the waste package. Bedded-type salt formations typically have interbedded layers of hydrous clay and sulfate minerals that, upon heating, can dehydrate and release water (Caporuscio et al. 2014). The resulting brines potentially can contact the waste package and cause its corrosion (Hardin et al. 2012), although this is believed to be just a local effect.

In crystalline host rocks such as granite, significant chemical alteration of the host rock due to geologic disposal of HBF is unlikely. However, thermally induced microcracking may degrade near-field in-situ mechanical properties or create flow paths for water movement and radionuclide transport through the geologic barrier. If the host rock is a volcanic rock known as tuff, the potential for near-field chemical alteration would be greater than for granite and would depend on the amount of volcanic glass present in the tuff. Volcanic glass, in the presence of water, is susceptible to alteration to zeolites and clay minerals at rates that increase with temperature. Zeolite and clay minerals can sorb and retard the movement of radionuclides. However, as the formation of zeolites and clays tend to reduce the permeability of the rock, it is possible that water might flow preferentially through the unaltered rock matrix or through rock fractures, if present, and bypass the sorptive minerals. Although thermal effects can be significant in the disposal drifts of a repository, these effects will decrease as distance from the heat source increases. Thus, the performance of the natural barrier—the host rock in the far-field—is unlikely to be affected.

D.2 Thermal Management

Because of concerns about temperature effects on repository performance, maximum temperature limits are imposed on various features of repository designs. For example, for the Finnish repository under construction and for the proposed Swedish repository, it is required that the temperature at the disposal canister surface must not exceed 100°C, in order to avoid mineral transformations in the buffer that could degrade its safety functions (SKB and Posiva Oy 2017). If HBF were to be emplaced in a repository with a similar temperature limit, the heat output of HBF waste packages could be reduced by decreasing the waste package loading or by increasing the time the SNF is allowed to cool by radioactive decay during storage at a surface facility or, after emplacement in a repository, during the pre-closure period when the disposal drift can be ventilated. The potential thermal effects also could be reduced by increasing the waste package spacing in the disposal drifts or by increasing the spacing between the repository drifts, both of which would decrease the temperatures within the repository (Hardin et al. 2012).

Figure D-2 shows the calculated waste package thermal power versus fuel age for a waste package containing 32 pressurized water reactor SNF assemblies having burnup values of 20, 40, or 60 GWd/MTU. The horizontal lines in the figure depict the approximate thermal power limits for the waste package, at emplacement in the repository, for the different disposal concepts that are described in the text boxes in the figure. The points A, B, C, and D depict that a waste package with SNF having a burnup of 40 GWd/MTU would require approximately 40, 50, 150, and 200 years of aging prior to repository closure in the described unsaturated hard rock, salt, argillite, and crystalline repository, respectively. If the

SNF burnup were 60 GWd/MTU, the waste package would have a higher thermal power (shown by the solid black curve), which would require aging times several decades longer than those required for SNF having a 40 GWd/MTU burnup.

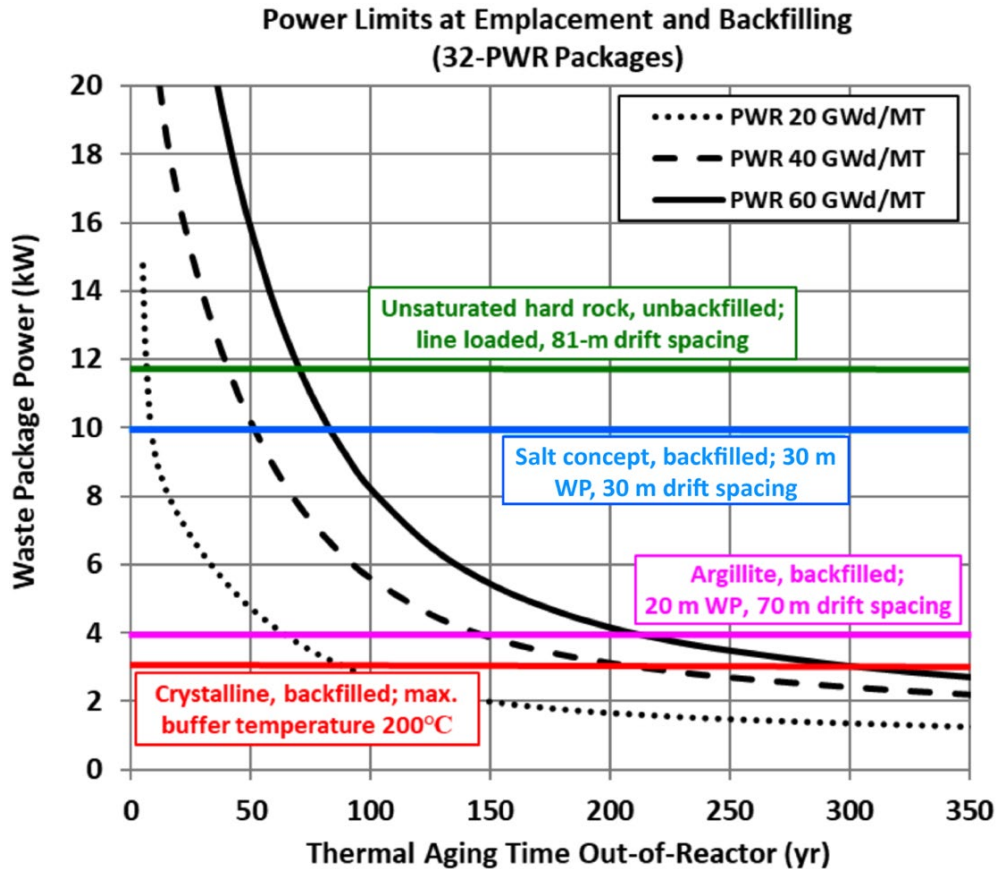


Figure D-2. Calculated thermal power versus age for a waste package containing 32 assemblies of pressurized water reactor SNF.

Note: Figure taken from Hardin (2020; Slide 18) and revised for clarity. The horizontal green, blue, magenta, and red lines depict the approximate thermal power limits for the waste package, at emplacement in the repository, for the different disposal concepts that are described in the text boxes.

D.3 References

Caporuscio, F.A., H. Boukhalfa, M.C. Cheshire, and M. Ding. 2014. *Brine Mitigation Experimental Studies for Salt Repositories*. LA-UR-14-26603. Los Alamos National Laboratory. August 25.

Hardin, E. 2020. *Technical Basis for Engineering Feasibility and Thermal Management*. Presentation to Nuclear Waste Technical Review Board at its July 27, 2020 meeting.

Hardin, E., T. Hadgu, D. Clayton, R. Howard, H. Greenberg, J. Blink, M. Sharma, M. Sutton, J. Carter, M. Dupont, and P. Rodwell. 2012. *Repository Reference Disposal Concepts and Thermal Load Management Analysis*. FCRD-UFD-2012-000219 Rev. 2. November.

IAEA (International Atomic Energy Agency). 2003. *Radioactive Waste Management Glossary: 2003 Edition*. STI/PUB/1155. July.

Jové-Colón, C.F., P.F. Weck, D.H. Sassani, L. Zheng, J. Rutqvist, C.I. Steefel, K. Kim, S. Nakagawa, J. Houseworth, J. Birkholzer, F. Caporuscio, M. Cheshire, M.S. Rearick, M. K. McCarney, M. Zavarin, A. Benedicto, A.B. Kersting, M. Sutton, J. Jerden, K.E. Frey, J.M. Copple, and W. Ebert. 2014. *Evaluation of Used Fuel Disposition in Clay-Bearing Rock*. FCRD-UFD-2014-000056. August.

Liljenfeldt, H., K. Banerjee, J. Clarity, J. Scaglione, R. Jubin, V. Sobes, R. Howard, E. Hardin, L. Price, E. Kalinina, T. Hadgu, A. Ilgen, C. Bryan, J. Carter, T. Severynse, and F. Perry. 2017. *Summary of Investigations on Technical Feasibility of Direct Disposal of Dual-Purpose Canisters*. SFWD-SFWST-2017-000045. September.

SKB (Svensk Kärnbränslehantering AB) and Posiva Oy. 2017. *Safety Functions, Performance Targets and Technical Design Requirements for a KBS-3V Repository: Conclusions and Recommendations from a Joint SKB and Posiva Working Group*. Posiva SKB Report 01. January.

Wersin, P., L.H. Johnson, and I.G. McKinley. 2007. "Performance of the Bentonite Barrier at Temperatures Beyond 100°C: A Critical Review." *Physics and Chemistry of the Earth, Parts A/B/C*. Vol. 32, pp. 780–788.

Wilson, J. and A. Bond. 2016. *Impact of Elevated Temperatures on Bentonite Buffers*. QRS-1384Q-R3 Version 1.2. October.

Wilson, J., D. Savage, A. Bond, S. Watson, R. Pusch, and D. Bennett. 2011. *Bentonite: A Review of Key Properties, Processes and Issues for Consideration in the UK Context*. QRS-1378ZG-1 Version 1.1. February.

Appendix E

Spent Nuclear Fuel Drying

E.1 Introduction

The topic of spent nuclear fuel (SNF) drying and any concerns that may arise due to an incomplete drying process apply to all SNF, regardless of burnup. The need for more information regarding SNF drying has been identified by the numerous technical information needs reports (see Appendix B) as a cross-cutting issue due to uncertainties about the quantity, location, and chemical or physical form of water that may remain after drying. This is important because in SNF degradation analyses, a SNF cask or canister system (also called a dry cask storage system)¹ is assumed to be dry, so that possible degradation mechanisms, such as galvanic action between dissimilar metals enhanced by residual water are not considered. Incomplete drying could also lead to the generation of flammable gases, such as hydrogen, in quantities above acceptable limits. If new issues are identified during further study of the drying process, especially in cask systems holding high burnup SNF (HBF), mechanisms of degradation, such as those mentioned above, may be found to occur earlier and at different rates because HBF generally has a higher decay heat load and ionizing radiation emission than low burnup SNF.

Drying SNF when it is removed from a spent fuel pool is needed to meet the requirements of the Nuclear Regulatory Commission (NRC) in subsequent life-cycle steps, including dry storage and transportation when the fuel has been packaged inside a cask or canister system. By adequately drying the contents of the SNF cask or canister, the main safety concerns arising from the presence of water will be addressed. Those concerns include generation of hydrogen and oxygen gases through radiolysis of water, and moisture-enhanced corrosion of SNF cladding and other mechanical components inside the SNF cask or canister. SNF drying processes and a dryness criterion are discussed in NRC guidance documents (see section E.2.2). However, no specific requirements regarding SNF drying are provided in the NRC regulation for storage, Title 10, Code of Federal Regulations, Part 72 (10 CFR Part 72), “Licensing Requirements for the Independent Storage of Spent Nuclear Fuel and High-Level Waste, and Reactor-Related Greater than Class C Waste” or in the NRC regulation for transportation, 10 CFR Part 71, “Packaging and Transport of Radioactive Materials.”

¹ SNF may be packaged into a welded stainless-steel canister that is then placed into a shielded overpack for storage and, for some designs, transportation. Alternatively, SNF may be packaged into a bolted-lid cask (sometimes called a bare fuel cask) that does not use an internal canister and includes its own shielding. These packaging systems are explained in more detail in section 2.1.2 of this report. For storage applications, some literature refers to both of these types of systems as “dry cask storage systems” and this report uses the same terminology. This report also may use the terms “cask” and “canister” when it is necessary to distinguish between specific types of storage or transportation systems.

E.2 Drying Commercial Spent Nuclear Fuel

E.2.1 Description of the Drying Process

After irradiation in a nuclear reactor, commercial SNF is moved to a spent fuel pool for cooling. If the spent fuel pool has limited storage capacity, which is the case for most nuclear power plant sites in the U.S., the SNF—typically, the older SNF—must be moved to free up more space in the pool. At most nuclear utilities,² the preferred storage option following pool storage is dry storage at a nearby dry storage pad, called an independent spent fuel storage installation.

The process to move SNF from pool storage to dry storage includes several steps: loading the SNF into an SNF cask or canister underwater, placing the lid on the cask or canister, removing the bulk water, performing a vacuum drying or alternative process,³ conducting a dryness test, sealing the cask or canister, and moving the cask or canister using a shielded transporter to the dry storage pad. More details of the vacuum drying process are provided below.

After most of the water in the canister is removed by draining and purging with pressurized helium, the canister is vacuum dried: a vacuum pump is connected to the canister and operated in stages to evaporate the remaining liquid water and remove the resulting water vapor from the canister. During the vacuum drying process, fuel temperatures rise because the internal gas that had provided heat transfer capability via conduction and convection is temporarily absent. The rate of drying is dependent on the level of the vacuum and the temperature at the location of the water inside the canister. The vacuum drying process might require significant amounts of time to achieve the required level of dryness, especially when the cask or canister contains breached SNF rods with water ingress, which can occur if there are pinholes or cracks in the SNF cladding.⁴ The drying process can vary widely from one cask or canister design to another. After vacuum dryness is confirmed (see section E.1.2), helium backfill procedures are implemented, and the canister is sealed shut by welding the drying system ports. The drying process is described in more detail in Miller et al, 2013a and 2013b.

E.2.2 Dryness Criterion for Commercial Spent Nuclear Fuel Packaged in Cask or Canister Systems

As noted above, the NRC regulations do not provide an explicit requirement for the amount of residual water that is allowed to remain in an SNF canister after drying. However, in its guidance to NRC staff for reviews of dry storage license or certificate applications, NUREG-2215 (NRC 2020), the NRC provides the following guidance: “The NRC staff has accepted

² In the past, some SNF was moved from certain nuclear power plant sites to a dedicated spent fuel storage pool at the Morris site in Illinois. In other cases, SNF assemblies from Duke Energy nuclear power plant sites were moved from spent fuel pools with limited pool space to spent fuel pools with available space, such as those at the Shearon Harris Nuclear Power Plant site.

³ Some utilities may use a forced helium dehydration process.

⁴ Reactor cooling water ingress can occur during reactor operation if a fuel rod breaches and depressurizes.

vacuum drying methods comparable to those recommended in PNL-6365” (Knoll and Gilbert 1987). NRC (2020) provides additional detail:

“The [cask or canister] should be drained of as much water as practicable and evacuated to less than or equal to 4.0×10^{-4} MPa (4 millibar, 3.0 mm Hg or Torr). After evacuation, adequate moisture removal should be verified by maintaining a constant pressure over a period of about 30 minutes without vacuum pump operation (or the vacuum pump is running but it is isolated from the cask with its suction vented to atmosphere).”

Nuclear utilities have interpreted, and NRC has accepted in its reviews, that during this dryness test, if the pressure does not rise above 4.0×10^{-4} MPa (3 Torr; $\sim 6 \times 10^{-2}$ psi) in 30 minutes, then the intent of the Knoll and Gilbert (1987) recommendation has been met. This means that the pressure could rise above 4 millibars (3 Torr; $\sim 6 \times 10^{-2}$ psi) after 30 minutes without vacuum pump operation and still meet the intent of Knoll and Gilbert (1987). Since the vacuum pressure at the beginning of the 30-minute time period is not specified, licensees evacuate to various initial pressures below 4.0×10^{-4} MPa (3 Torr; $\sim 6 \times 10^{-2}$ psi) to begin the test. Clearly, the lower the initial vacuum pressure, the longer it takes to exceed the 4.0×10^{-4} MPa (3 Torr; $\sim 6 \times 10^{-2}$ psi) threshold. As an example, the results of the dryness test conducted on the High Burnup Dry Storage Research Project (HDRP; see section E.4.3.2) test cask is shown in Figure E-1.

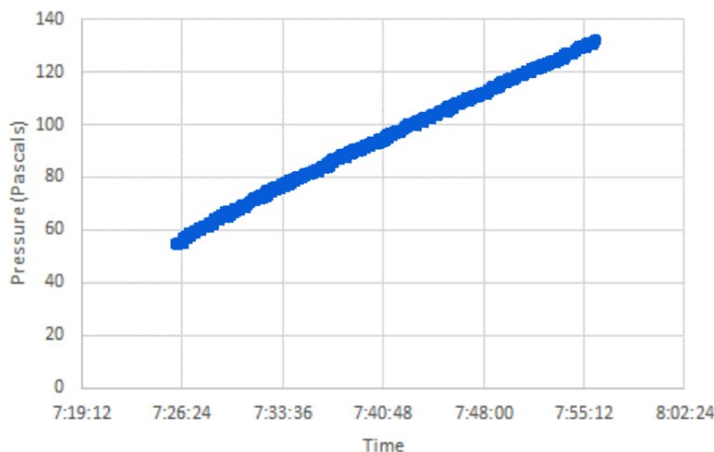


Figure E-1. Results of the HDRP cask dryness test (pressure rebound test).

For reference, 140 Pa = 1.05Torr (0.02psi) (adapted from EPRI 2019).

The basis for the 4.0×10^{-4} MPa (3 Torr; $\sim 6 \times 10^{-2}$ psi) threshold stems from concerns for corrosion of SNF cladding and internal components of SNF canisters. Pacific Northwest National Laboratory (PNNL) evaluated the effects of oxidizing impurities on dry storage of LWR SNF and suggested limiting the maximum quantity of oxidizing gases (e.g., oxygen, carbon dioxide, and carbon monoxide) to no more than 1 gram-mole (or mole) per cask (Knoll and Gilbert 1987). A one-mole limit ensures the concentration of oxidants (such as O_2 , CO_2 , and CO) is below a level at which cladding degradation may be expected. Moisture is one source of oxidizing gases; thus, removal of water is inherent in the vacuum drying process, and levels at or below about 0.43 mole of water (7.74 ml; 0.26 oz of water) evaluated in Knoll and Gilbert (1987) are expected if adequate vacuum drying is performed. According to ASTM C1553-16, *Standard Guide for Drying Behavior of Spent Nuclear Fuel*

(ASTM International 2016): “Quantitative criteria for drying are currently being evaluated and are not yet available for inclusion in this standard. For interim dry storage of commercial SNF some conditions or drying criteria have been adopted. These eliminate enough water to preclude gross damage to fuel cladding during storage. ... An evaluation of dryness must consider the starting system, the types of water, and the water inventory, and then determine if appropriate techniques have been applied through the drying process to ensure that transportation and storage requirements will be met or exceeded.”

In practice, the guidance of ASTM C1553-16 (ASTM International 2016) means that nuclear utilities, when applying to the NRC for a license to store SNF or a Certificate of Compliance to transport SNF, must include an analysis with their application that addresses the amount of residual water remaining in the cask or canister system and the effect of that water. The analysis must demonstrate the SNF and the SNF cask system can meet the NRC requirements for storage (10 CFR Part 72) and transportation (10 CFR Part 71), as applicable (see Appendix C for more detail about the NRC regulations).

The NRC approach to approving SNF canisters for storage or transport is further captured in guidance to the NRC staff. NUREG-1617, *Standard Review Plan for Transportation Packages for Spent Nuclear Fuel, Final Report*, (NRC 2000) Section 7.5.1.2, Loading of Contents, states that “Methods to drain and dry the cask are described, the effectiveness of the proposed methods is discussed, and vacuum drying criteria are specified.”

According to NUREG-1927, Rev. 1, *Standard Review Plan for Renewal of Specific Licenses and Certificates of Compliance for Dry Storage of Spent Nuclear Fuel – Final Report*⁵ (NRC 2016): “... the moisture content in the cask/canister, accounting for measurement uncertainty, should be less than the expected upper bound moisture content per the design-bases drying process.” Integral to this criterion is that the applicant will need to provide the expected upper bound moisture content based on its design-bases drying process.

With regard to controlling flammable gases, such as hydrogen, the NRC similarly provides guidance in one of its standard review plans. NUREG-1609, *Standard Review Plan for Transportation Packages for Radioactive Material*, (NRC 1999), states, “Ensure that the application demonstrates that hydrogen and other flammable gases comprise less than 5% by volume of the total gas inventory within any confined volume.”

E.2.3 Challenges to Removing Residual Water from a Spent Nuclear Fuel Canister

- Jung et al. (2013) notes that Knoll and Gilbert (1987) is not based on experimental data, but on thermodynamic calculations of equilibrium gas pressures. Thus, the small holes or cracks in breached, waterlogged SNF rods that limit the exit of water from inside the rod;
- Bottoms of pressurized water reactor (PWR) control rod guide tubes not having drains, which are shaped like cups and retain water (see section E.4.3.1);

⁵ Table B-3, Example of a High Burnup Fuel Monitoring and Assessment Program – item 6, Acceptance Criteria.

- Boiling water reactor (BWR) water rods; and
- Crevices in the fuel assemblies, such as those created by spacer grids, nozzles, and guide tubes.

PNNL report does not consider issues such as ice formation in occluded areas containing liquid water during vacuum drying. Examples of occluded areas are:

Regarding the first of these occluded areas, if the water temperature inside a breached rod is low enough and the vacuum pressures are low enough, icing could occur in the crack or pinhole of the SNF rod that would prevent dewatering of the waterlogged rod.

Regarding the other occluded areas in the list above, the Board notes that some water always remains in the bottom of the canister after bulk water removal because the siphon tube used to withdraw the majority of the water during the initial stage of draining does not extend all the way to the bottom of the canister. Furthermore, in some canister designs, there are horizontal surfaces that could also hold some water, such as structural spacer disks that do not include drain holes. Some of these occluded areas, such as the bottoms of the PWR control rod guide tubes, are located in a lower temperature region of the canister where the evaporation rate will be lower than that in the hotter portions of the canister. Thus, if care is not taken, some of the canisters may meet the dryness test criterion (limits on pressure rebound) but still contain quantities of water higher than the criteria described in Knoll and Gilbert (1987).

The drying process involves steps to minimize the remaining liquid water and to avoid freezing in occluded areas (ASTM International 2016). To avoid icing due to excessive vacuum conditions, the vacuum pressure is lowered in steps, using hold points to confirm a stable pressure is established at each step. The vacuum is isolated from the rest of the cask/canister and piping/pressure gauge system and the pressure is monitored. Assuming there is no leak in the vacuum piping and connections, a rise in pressure during the hold point would likely indicate slow evaporation of water. If temperatures are low due to low decay heat, then icing is more likely, and evaporation will be slower. Thus, drying for canister systems with low total decay heat may be more susceptible to inadequate drying if sufficient time is not taken during the drying process.

E.3 Potential Effects of Residual Water Remaining in a Spent Nuclear Fuel Cask or Canister

As noted above, neither 10 CFR Part 71 (transport), nor 10 CFR Part 72 (storage) specify the amount of residual water that can be left in a cask or canister after drying. However, both regulations stipulate that, when necessary, special protective environments (e.g., inert gas atmospheres) and specific moisture content and temperature levels must be maintained to prevent deterioration of the SNF and the packaging. Even with acceptable amounts of residual water in the canister after drying, the Board notes that several uncertainties or questions remain about the effects of the residual water:

1. How much hydrogen gas can be generated by radiolysis of the water in the canisters?

- a. can it contribute to a flammable gas mixture in the canister?
 - b. can it be absorbed into the cladding and either change the cladding properties or the cladding response to normal conditions and/or accidents?⁶
 - c. can it be absorbed into the canister materials and affect their mechanical properties?
 - d. can it over-pressurize the canister?
2. Will residual water or water vapor in the canister affect heat transfer from the canister due to the different thermal conductivities of moist helium and dry helium? If so, to what extent?
 3. How much will the cladding oxidize due to residual moisture?
 4. If the SNF cladding is breached, how much will the uranium dioxide (UO₂) fuel pellets oxidize to U₄O₉ which opens the grain boundaries of the fuel pellet or U₃O₈ which degrades the fuel pellet into a small-grained powder due to residual moisture or radiolysis products? In the case of radiolysis products, will the temperature dependence of the oxidation rate change?

See Hurt (2009), Wittman (2013), and Jung et al. (2013) for more information on the effects of water remaining in a canister system. These questions and uncertainties about drying SNF and the amount of residual moisture have led the nuclear industry, the NRC, and DOE to continue to sponsor research on drying. The rest of this Appendix examines a number of these research efforts.

E.4 Research on Spent Nuclear Fuel Drying

E.4.1 Early Drying Tests and Evaluations

Spilker and Fleisch (1986) studied the drying of loaded SNF casks and produced a graph of pressure versus time for a vacuum drying procedure on a Castor-1b cask (Figure E-2). The vacuum drying procedure and dryness check, using a pressure rebound test, were similar to those used by the U.S. nuclear industry. Spilker and Fleisch (1986) indicated that the procedure had to be repeated several times in order to pass the dryness check. The results indicated that stainless steel canisters are more favorable to drying than aluminum canisters probably due to the water of hydration (chemically bound water) for the aluminum, which is energetically difficult to remove by heating (Spilker and Fleisch 1986). This has implications for drying aluminum-based neutron absorber material contained in some cask or canister systems as well as for DOE-managed aluminum-based SNF.

Peehs, Bokelmann, and Fleisch (1986) conducted experiments to test how to dry defective, waterlogged SNF rods in a test container. Under low helium pressure, the rods were heated to 160°C (320°F) for 7 hours, after which the pressure was lowered further, and the

⁶ Credible accidents as specified in 10 CFR 72.236 or as specified in 10 CFR 71.73.

temperature was raised first to 200°C (392°F) and then to 400°C (752°F) for up to 64 hours.⁷ The results indicated that moisture contained in defective fuel rods can safely be removed during canister drying, depending on the type of defect—and if the defective fuel rod temperature approaches 400°C (752°F).⁸

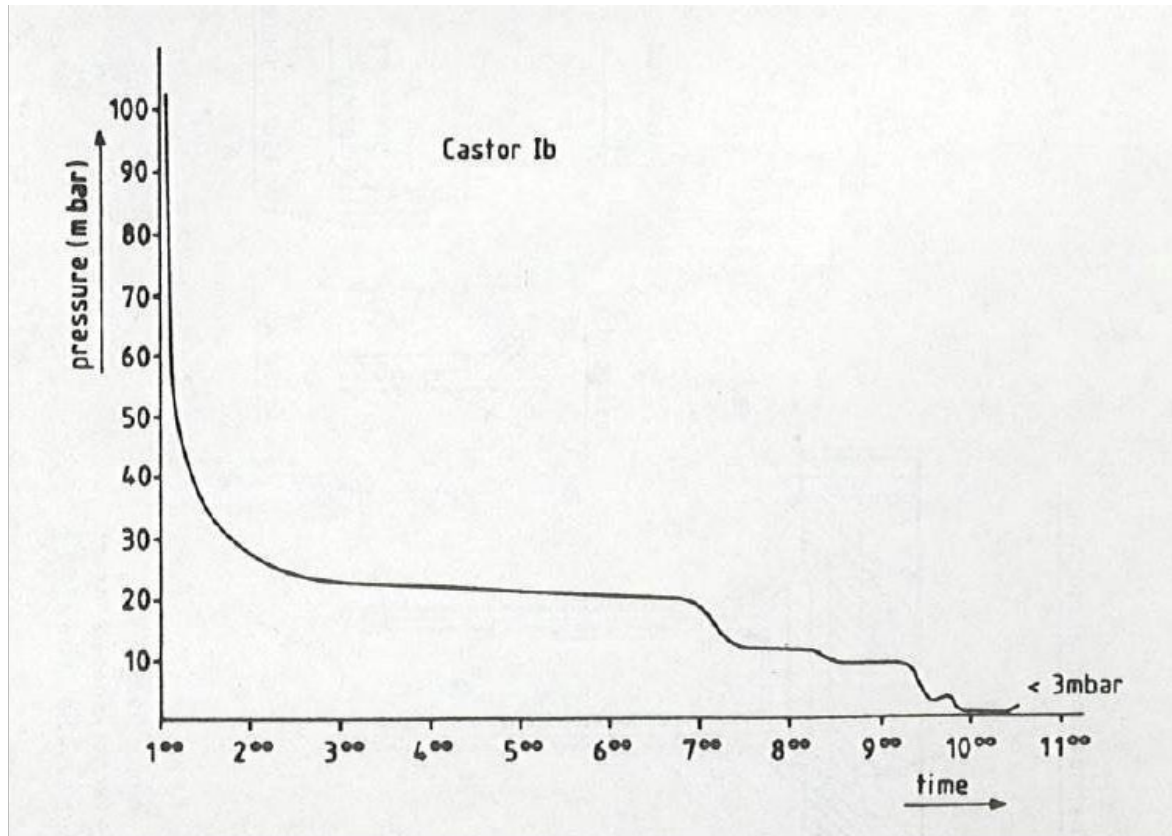


Figure E-2. Pressure versus time during vacuum drying of a Castor Ib SNF cask.
The time scale is in hours (adapted from Spilker and Fleisch 1986).

ASTM International published a standard for drying SNF that addresses the three types of residual water (unbound or free, physisorbed, or chemisorbed)⁹ that might remain in a cask or canister after bulk water removal. This standard, ASTM C1553-16 (ASTM International 2016), makes a number of statements concerning the removal of bound water:

⁷ A detailed temperature-pressure history was not given in the paper.

⁸ See the discussion in Appendix H that implies peak cladding temperature even for high burnup fuel may be well below 400°C (752°F).

⁹ Physisorbed water (adsorbed water) is water that is physically bound (as an adsorbate by weak forces) to internal or external surfaces of solid material. It is expected that most of the physisorbed water will be desorbed in a relatively short time (~30 hours) at a reasonably low temperature (50°C [122°F]) (ASTM International 2016). Chemisorbed water is water that is bound to other species by forces whose energy levels approximate those of a chemical bond and it is not expected to be released at less than 500°C (ASTM International 2016).

- "... removal of bound water¹⁰ will only occur when the threshold energy required to break the specific water-material bonds is applied to the system. For spent nuclear fuel this threshold energy may come from the combination of thermal input from decay heat and forced gas flow and from the ionizing radiation itself." ([ASTM International 2016] Section 4.4.5).
- "The free and most physisorbed water should be removed using a standard drying process" ([ASTM International 2016] Section 7.2.1.2).
- "Dry air at 50°C (122°F) should desorb the superficial physisorbed water layers in 10 to 30 hours [without vacuum]. Less desorption time is required to vacuum dry at 20°C (68°F)" ([ASTM International 2016] Section 6.1.3.2).
- "The water content of hydrated zirconium oxides [i.e., physisorbed water] is small, and the water will not be released below 500°C (932°F)" ([ASTM International 2016] Section 5.6.4).

While several calculations have been made to estimate the amount of chemisorbed water on spent fuel cladding, these calculations involve many assumptions and estimated inputs. Jung et al. (2013) notes that, "there is little data on the potential quantity of chemisorbed water present on the zirconium cladding because of dehydration of hydroxides or their hydrates," which is consistent with the results of Spilker and Fleisch (1986).

In an analysis funded by DOE, Wittman (2013) modeled the radiolysis of water vapor contained in an idealized 4,500 L (1,190 gal) SNF canister after drying. The model included the following inputs and assumptions: the canister was backfilled with helium gas, with and without air infiltration (ranging from 0.0–1.0% by volume); internal canister temperatures were varied between 120 and 300°C (248–572°F); and residual water was varied between 0.1 and 1.0 L (0.03–0.26 gal). A few sensitivity cases were calculated assuming residual water quantities as large as 20 L (5.3 gal). The analysis calculated the amount of hydrogen and corrosive species that might accumulate in a canister over a 300-year period, based on water radiolysis along with coupled kinetics for 111 reactions for 40 gas species (Wittman 2013). This analysis considered water in the vapor space only and did not include physisorbed or chemisorbed water. This work also used a hydrogen flammability limit of 4% by volume versus the 5% guideline used by the NRC (NRC 2009). Although the model was not validated against actual gas measurements from an SNF canister after drying, the sub-model for radiolysis in water vapor was verified and found to be accurate using experimental data collected in Russia and reported in 2007 (see Wittman (2013) for details).

The main results of the analysis are described as follows (Wittman 2013):

1. Significant radiolysis of water vapor requires the presence of residual air to reduce the recombination of hydrogen and oxygen into water.

¹⁰ Bound water means physisorbed water and chemisorbed water.

2. Reactions between residual water (1 L [0.26 gal]) and residual air (1% by volume) at 5 atm (73.5 psi) of backfill pressure result in a hydrogen concentration of 2.3% by volume and all oxygen consumed (0% by volume) at 300 years.
3. Calculations indicate that residual water in the amount of 20 L (5.3 gal) would be required to reach the 4% H₂ flammability limit in 16 years, and between 3 and 4 L [between 0.79 and 1.1 gal] of water would be required to reach the 4% H₂ flammability limit in 300 years. [Note: for comparison, the amount of water remaining in the HDRP test cask after drying was found to be approximately 0.1 L (0.03 gal) (Bryan et al. 2019)].
4. Increased residual air results in greater H₂ and HNO₃ concentrations, but also in the depletion of O₂ because it is more effectively removed by a radiolytically induced reaction with N₂.
5. For less residual water (0.1 L [0.03 gal]) and 1% by volume air in the initial container environment, all radiolytic products are less than 1% by volume.

Because of the idealized nature of the study and the need for many assumptions about the location and form of water remaining in the canister, the results are accompanied by some uncertainty. Wittman (2013) concluded: "While the results of this work indicate ... sufficiently low concentrations (< 4%) of H₂ inside the canister, a more direct comparison of model results with canister data would give greater confidence in model predictions."

E.4.2 Nuclear Regulatory Commission and ASTM Drying Evaluations

The ASTM drying standard (ASTM International 2016) addresses many issues pertaining to drying SNF. The standard addresses drying LWR fuel and other types of SNF, such as research-reactor fuels that have different types of cladding, fuel material such as uranium silicide, and geometries other than a square array of rods. The concerns for both physisorbed and chemisorbed water on the fuel assemblies are discussed in detail. Depending on the cladding type, the standard drying process may not remove all residual water, which means that some oxygen and hydrogen will be generated by radiolysis during extended storage or transport. While there have been studies about drying aluminum fuels (e.g., Large and Sindelar 1997) and other DOE SNF (e.g., Beller 2014) that discuss physisorbed and chemisorbed water, the following discussion concentrates on drying commercial UO₂ SNF clad with zirconium alloy.

In principle, the degree of dryness can be determined if the drying temperature and time, pumping speed, and locations and types of water (e.g., physisorbed, chemisorbed) are known. Locations of residual water will be unique for each cask or canister design. The NRC sponsored three studies, discussed below, to evaluate the potential impacts of water remaining in a SNF cask or canister after drying.

1. The first study (Jung et al. 2013) evaluated the potential impacts of residual water remaining in an SNF storage canister after the drying and helium backfill process. The analyses evaluated potential degradation mechanisms, including oxidation and hydration of SNF, oxidation and hydrogen-absorption-induced damage of cladding, and corrosion of internal structural materials. The evaluation also included the potential for a flammable canister environment resulting from hydrogen and oxygen

generated by radiolytic decomposition of water. The overall conclusions provided by Jung et al. (2013) were:

- a. Degradation of cladding, fuels, and other internal components is not expected to be significant over the analyzed period, up to 300 years of storage time.
- b. With no significant degradation of cladding, fuel, and internal components, criticality safety is not affected.
- c. Regarding the potential for developing a flammable atmosphere inside the canister (i.e., 5 percent by volume hydrogen and a sufficient concentration of an oxidizer, such as oxygen [NRC 1999]), the study found:

“conditions for flammability could be met (in the presence of ignition) for 55 moles [1 L; 0.26 gal] of residual water and 1 atm (14.7 lb/in.²) of backfill pressure and for the two temperature and radiation conditions considered in this study. The data also indicate that the canister environment would meet the conditions of flammability when 17.4 moles [0.3 L; 0.08 gal] of residual water undergoes radiolysis via linear decomposition in 71.62 years, given the low-end SNF and cladding initial temperature condition and 1 atm (14.7 lb/in.²) of backfill pressure. The conditions of flammability are never met when backfill pressure is 5 atm (73.5 lb/in.²) and the residual water amount is 55 moles [1 L; 0.26 gal] or less.”

- d. Other observations of this study were that:
 1. In most scenarios analyzed, cladding oxidation is limited to a few micrometers and consumes most of the produced oxygen;
 2. if there is a SNF rod with breached cladding, exposed UO₂ fuel material could be oxidized to U₃O₈ in hotter parts of the canister when radiolysis of residual water occurs at a sufficiently high rate—if a significant fraction of UO₂ in an SNF rod is oxidized to U₃O₈, swelling of the SNF pellets can rupture the cladding and release SNF particles into the canister and;
 3. significant hydrogen absorption by cladding is unlikely.
2. The second NRC study compiled information on the design and operation of systems currently used by the industry for vacuum drying and on characteristics of fuel assemblies or canisters that could affect the quantity of residual water (Miller et al. 2013a). This study also addressed potential methods to measure the quantity of residual water remaining in the canister following vacuum drying, and it identified locations where liquid water could be trapped in crevices or might be difficult to remove during drying for a range of PWR and BWR fuel assemblies and canister designs. The study concludes by providing a list of recommended parameters, or

factors, to be considered when developing a test plan for measuring residual water in an SNF cask or canister after drying.

3. The third study developed, but did not implement, a conceptual test plan¹¹ to measure the quantity of residual water remaining in an SNF dry storage canister after vacuum drying (Miller et al. 2013b). The information in the study allows the experimenter to (1) identify experimental parameters and test variables related to vacuum drying operational procedures, fuel assembly characteristics, and canister characteristics that must be considered when developing an experimental plan; (2) identify options for test setup and equipment selection to be able to vary the conditions of testing to maximize the data from the tests; and (3) determine an appropriate sequence for experimental drying runs in order to minimize the number of tests that need to be run.

E.4.3 DOE-Sponsored Drying Research

DOE initiated several experimental projects and modeling exercises, which are described below, to gather more information about the effectiveness of the industry standard approach to drying SNF canisters. The research also aims to determine if SNF storage canisters are sufficiently dry to reduce degradation mechanisms including fuel oxidation, cladding corrosion, and hydrogen generation to acceptable levels.

E.4.3.1 Testing at the University of South Carolina

In 2015, DOE funded an Integrated Research Project (IRP) that was jointly conducted by the University of South Carolina (USC), the University of Florida, and Areva (now Orano) to evaluate how well the recommended NRC drying process and other drying processes remove free water from dry storage canisters containing damaged fuel (Knight 2016; Knight et al. 2019). The purpose of the project was to (1) quantify water remaining in an SNF dry storage canister after a typical industry drying operation: vacuum drying and forced helium dehydration (FHD) followed by applying a vacuum to ensure the <3 Torr ($\sim 6 \times 10^2$ psi) for 30 minutes criterion was met; (2) develop a science-based understanding of the canister drying process; (3) evaluate a range of conditions and features likely to be encountered during storage of SNF; and (4) develop computer modeling tools that may allow utilities, vendors, and regulators to estimate the amount of residual water remaining in an SNF canister after drying. A test drying system and fuel assembly inside a surrogate SNF basket were built that allowed known amounts of water to be introduced so that variations of the vacuum drying method could be tested and evaluated (Figure E-3).

¹¹ Parts of the study were incorporated into the Integrated Research Project on SNF drying at the University of South Carolina, which is described in section E.4.3.1.

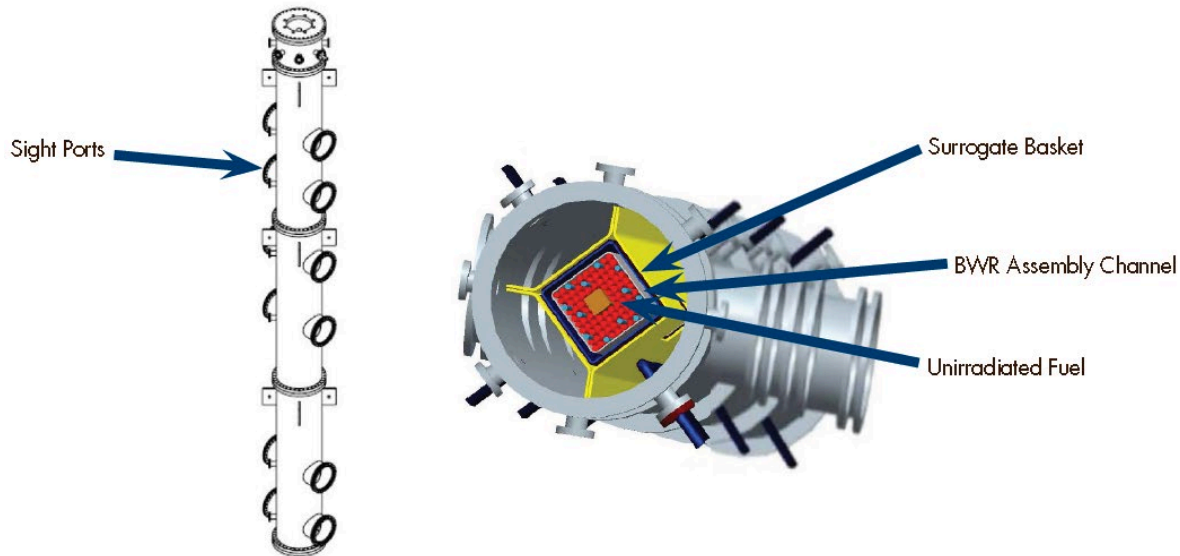


Figure E-3. University of South Carolina SNF drying test chamber.

The schematic shows the various locations of sight ports where water removal from rods or evaporation from surfaces can be observed as well as the major interior components of the system (*Knight 2016*).

Surrogate BWR rods, PWR guide tubes¹² (Figure E-4), breached fuel rods, neutron absorber sheets (i.e., Boral[®]), canister spacer disks, spaces between hardware, and surface areas of rods, hardware, and structures were evaluated and modeled as locations in the canister and assembly components that may retain or absorb water.

The test apparatus included a modified, unirradiated, 10 x 10 array Atrium 10A BWR fuel assembly from Areva (now Orano) having features of both BWR and PWR fuel assemblies. It contained cerium dioxide pellets to simulate UO₂ SNF pellets and used heater rods to simulate decay heat. There were no partial-length fuel rods or empty rod positions, which are typical in a real BWR fuel assembly. Thermocouples and other instrumentation were attached throughout the assembly.

¹²PWR fuel assemblies include control rod guide tubes that can be completely closed at the bottom (in a cup-shaped feature called a dashpot). The dashpots include perforations (drain holes) some distance up from the bottom of the guide tube (the distance varies by PWR fuel design) to allow water to escape when the control rod is inserted into the guide tube. The purpose of the dashpots is to slow the descent of the control rods if they are inserted into the core rapidly. When the canister is drained of free water, some water will remain in the dashpots that do not have drain holes at the bottom. A simple calculation of volume indicates that a large canister containing 37 PWR assemblies could have as much as $9.5 \times 10^{-2} \text{ m}^3$ (25 gal) of water remaining in dashpots (without drain holes at the bottom) prior to vacuum drying.

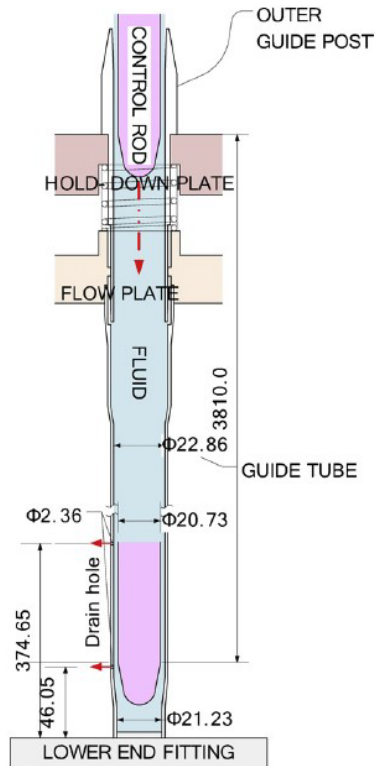


Figure E-4. Example of a control rod guide tube showing the drain holes near the bottom.

Note that not all of the water will drain out of the guide tubes. Dimensions in millimeters (Yoon et al. 2009).

Some of the key components of the surrogate fuel assembly are shown in Figure E-5 (Knight 2016). A test rod position, in one corner of the assembly, accommodated interchangeable test rods that allowed simulation of several fuel assembly design features:

- A breached fuel rod with a perforation at 175 cm (69 in) above the bottom and a Swagelok fitting at top for filling with a measured amount of water;
- A PWR guide tube with a dashpot, simulated by a Zircaloy-4 tube, plugged at bottom, with weep holes at 40 and 43 cm (16 and 17 in) height above the bottom; or
- A BWR water rod, which was a Zircaloy-4 tube, plugged at the bottom, with weep holes at 175 and 178 cm (69 and 70 in) above the bottom.

Figure E-6 is a photograph of a typical view through the vacuum chamber view port showing the surrogate fuel rods and SNF basket with a thermocouple attached.

The temperatures of the simulated fuel rods, heater rods, and inlet and outlet gas were measured with thermocouples and infra-red cameras. In addition, the chamber pressure, gas composition, gas flow rate during the drying process, and water removed as a function of time were measured. A more detailed description of the experimental apparatus and modeling for temperature simulation can be found in Knight et al. (2019).

Testing was conducted to determine how much water remained in breached fuel rods, horizontal surfaces outside the fueled zone, PWR guide tubes, and BWR water rods, after the standard drying procedure was used. Following the dewatering process that removed the bulk of the water at the beginning of a test, a vacuum was applied in stages to lower the system pressure to below 3 Torr ($\sim 6 \times 10^{-2}$ psi).

Ice formation was found for two cases:

1. On a horizontal spacer disk that was external to the SNF basket. This is not surprising since flat surfaces would be expected to retain some water after the majority of the water is removed, but prior to drying; and

2. In the siphon tube in “some” tests. However, these may have been experimental artifacts due to the determination that there was inadequate heating of the bottom of the chamber.¹³

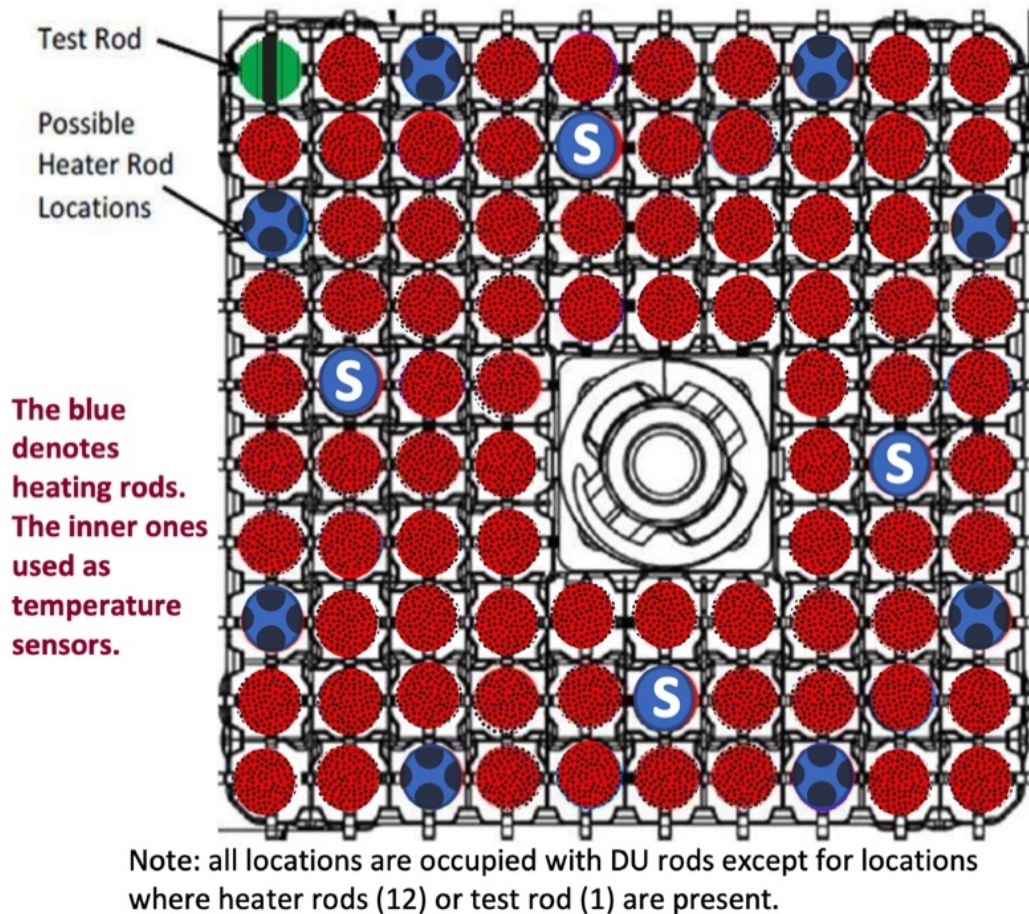


Figure E-5. Illustration of the mock fuel assembly used in the University of South Carolina experiments.

DU = depleted uranium (figure adapted from Knight et al. 2019).

Except for the tests involving a simulated breached rod, the standard drying procedure was followed. In one test containing a breached rod, the system passed the dryness criterion (holding a vacuum below 3 Torr ($\sim 6 \times 10^{-2}$ psi) for 30 minutes with the vacuum pump isolated) but approximately 7 to 12 ml (0.25 to 0.41 oz) of the water remained in the breached rod. The temperature of this test was not stated. As noted above, early tests were found to have inadequate (non-representative) heating in the bottom of the test chamber. After heating tape and insulation were added to the outside of the test chamber, “...the breached rod, with a temperature in the range of 100 to 130°C [212 to 266°F], was dried in almost all tests. In a

¹³ The authors stated that “[o]nce heating tape and insulation was added, complete dryness of the chamber was achieved in every type of FHD and vacuum test” (Knight et al. 2019).

few such tests, a small amount of water was measured in the range of 0.5 to 2 ml [0.02 to 0.07 oz]" (Knight et al. 2019).



Figure E-6. View of the surrogate SNF basket and thermocouple through a viewport.
(Knight et al. 2019).

The IRP team initiated a computer modeling effort to simulate the experimental mockup discussed above. The thermal-hydraulic model, which solved coupled mass, momentum, and energy conservation equations, included phase change from liquid to gas. However, when the IRP final report was published in 2019, the modeling effort had not been completed (Knight 2019).

Because there were no oxide or CRUD¹⁴ layers on the mock SNF rods, the IRP testing only addressed the removal of free water. In an actual SNF dry storage canister, there may be free water as well as physisorbed and chemisorbed water in the cladding oxide and CRUD layers.

Peak test rod temperatures achieved during the IRP testing ranged from 85 to 190°C (185 to 374°F). These temperatures are considerably lower than the NRC's maximum allowed temperature of 400°C (752°F). Because of these temperature limitations, and because of the remaining uncertainties about removing water from breached fuel and removing all physisorbed and chemisorbed water, DOE is planning follow-on testing. In addition to research into drying and storage of a cask loaded with HBF (see section E.4.3.2), DOE has funded the development of instrumentation to be used for moisture measurements in SNF

¹⁴ CRUD is a conglomerate of products resulting from the primary cooling system corroding. If the CRUD gets too thick, it can spall and create cool spots on the cladding. The CRUD has a spinel structure and tends to be very tenacious on PWR cladding but will dissolve in the storage pool water. The CRUD on the BWR has a hematite structure and is very fluffy. CRUD can trap both free water and physisorbed water.

drying simulators (see section E.4.3.3) and analyses of the consequences of water remaining in an SNF cask or canister after drying (section E.4.3.4).

E.4.3.2 High Burnup Dry Storage Research Project Testing

Separately from the DOE IRP, DOE tried to confirm if the standard drying process removes bound water from the Orano TN[®] 32 cask system used in the High Burnup Dry Storage Research Project (HDRP) (EPRI 2014; Bryan et al. 2019). In the demonstration (see Appendix F, Section F.5), free water was drained from the HDRP cask and residual water blown out 14 times. The amount of water expected to be left in the cask after this step was indeterminate, because it was not known how many of the assemblies contained drain holes in the dashpots at the bottom of the control rod tubes instead of about 15 cm (6 in) above the bottom of the tubes.¹⁵ The cask was then pumped down to a low pressure (below 3 Torr [$\sim 6 \times 10^{-2}$ psi]) and isolated from the vacuum pump.

The internal cask pressure did not rise above 3 Torr ($\sim 6 \times 10^{-2}$ psi) after 30 minutes, thus meeting the criterion for being dry as per the recommended procedure (see Figure E-1). However, as can be seen in Figure E-1, the pressure inside the cask was continuing to rise nearly linearly with time after 30 minutes. This condition raises questions about how much water remains in the cask and what internal cask pressure would eventually be reached. The HDRP test plan included gas sampling, described below, that provides data which can help answer these questions.

The HDRP cask was backfilled with helium gas and kept in the fuel loading area for a two-week “soak” period, during which the cask and its contents were allowed to come to thermal equilibrium with the surrounding environment (EPRI 2019). Three gas samples were taken from the cask’s internal vapor space during this period (at 5 hours, 5 days, and 12 days after helium backfilling) and analyzed for krypton-85, oxygen, water vapor, hydrogen, and other gases. The rationale for sampling early but not sampling later when the cask was on the storage pad was that the effects of moisture on fuel degradation will occur during the initial storage period when the system is hottest (Stockman et al. 2015).¹⁶

Results of the three gas samples are published in Bryan et al. (2019) and EPRI (2019). While no krypton-85 was detected, confirming that none of the fuel rods had breached, the following gases were detected at the end of 12 days:

- CO₂: 930 parts per million by volume (ppmv). Bryan et al. (2019) speculate the CO₂ could be caused by residual organic material or vacuum pump oil.

¹⁵ Some dashpots include drain holes at the bottom rather than higher up on the control rod guide tube. The HDRP project documentation did not contain this level of design detail. Six of the HDRP assemblies had poison rod assemblies inserted into the guide tubes to facilitate early transportation. It is possible that these poison rods displaced most of the water in the dashpot, but the poison rods could also potentially block or provide a tortuous path for water to escape from the weep holes.

¹⁶ The original plan was to take gas samples a few times over the 10-year storage on the pad, however, logistical and regulatory concerns changed that plan, so the operator, Dominion Energy, declined to conduct sampling on the storage pad.

- H₂: ~500 ppmv (0.05 vol%). This was speculated to have arisen from either radiolysis, metal corrosion, or direct reduction of water by metals in the cask if anoxic conditions exist. For comparison, NRC guidance suggests the concentration of flammable gases, such as hydrogen, should be less than 5% by volume in an SNF transportation cask (NRC 1999).
- Water vapor: ~17,400 ppmv ± 10% – equivalent to ~100 ml (5.6 moles; 0.03 gal) of water within the entire cask gas phase. The authors also noted that this amount of water was “higher than anticipated” and that measuring water content “proved challenging”. However, Bryan et al. (2019) also concludes that “[i]f the cask gas phase is compositionally homogeneous, then liquid water is not present within the cask, unless trapped in inaccessible locations.” As noted in Section E.2.2, the NRC assumes that if the SNF cask or canister passes the dryness test recommended by Knoll and Gilbert (1987), then the quantity of water remaining should be no more than 0.43 moles (7.74 ml; 0.002 gal) (NRC 2020).

Bryan et al. (2019) described several lessons learned that can be applied to future water vapor sampling efforts. For example, the researchers noted “it is essential that the sample bottles be heated to desorb water adsorbed onto the interior of the bottles” (Bryan et al. 2019). The Board encourages DOE to improve and validate gas sampling methods before attempting to obtain the next set of samples.

Additional measurements of the water vapor content of the cover gas in the cask are not planned again during the 10-year dry-storage period. However, DOE has discussed plans to obtain additional gas samples from the vapor space of the HDRP cask after it is transported to the Idaho National Laboratory for SNF examination or from another commercial SNF cask (Larson 2019). As of December 2020, no specific plans have been made public.

The Board notes that if further testing or further moisture measurements do not provide greater detail regarding the amount of moisture remaining in SNF casks and canisters, other drying methods (e.g., forced helium dehydration) and other methods to evaluate the degree of dryness (e.g., falling rate method)¹⁷ may need to be considered.

E.4.3.3 Sensor Development for Liquid and Gaseous Water Detection

A new sensor technology is being developed by DOE to detect and measure the amount of liquid water inside of a dry cask (Meyer et al. 2019). PNNL has conducted a feasibility study focusing on a typical bare fuel cask, such as the TN[®] 32, utilizing ultrasonic sensors that can be mounted on the exterior of the metal cask system without the need for physical penetration of the confinement boundary. Through several scoping tests performed in 2019, PNNL demonstrated the efficacy of the proposed sensing approach by the generation of ultrasonic waves in the carbon steel plate components of the mockup with enough resolution for sensing water at the bottom of the cask. Based on the results at PNNL,

¹⁷ The falling rate method of dryness test is a method where the system is pumped down to an acceptable vacuum and the pressure in the system is allowed to rise. The time to reach a pre-determined (higher) pressure is measured. The system is subsequently pumped down again, and the process is repeated. The time to reach the predetermined upper pressure is plotted against the number of drying cycles. When the time required to reach the higher pressure is constant, the system is deemed dry (Christensen and Wendt 2001).

additional future work was proposed to optimize sensor designs and determine suitable parameters for a prototype sensor to be tested on an actual full-scale system.

At Sandia National Laboratories, DOE funded a separate effort to develop instrumentation to measure moisture levels in the gaseous phase in a planned SNF drying simulator (Salazar et al. 2020). This effort included the implementation of a mass spectrometer for moisture measurements and demonstrated its functionality during both forced helium dehydration and vacuum drying processes. As of October 2020, DOE had not announced a timeframe for assembling and operating the planned drying simulator.

E.4.3.4 Evaluations of Water Remaining in a Cask or Canister after Drying

DOE continued to fund analyses of the potential consequences of water remaining in an SNF cask or canister after drying, including estimates of the quantities of hydrogen and oxygen generated due to radiolysis of water. For example, d'Entremont, Kesterson, and Sindelar (2020) estimated the generation of hydrogen and oxygen inside the HDRP cask after drying. In this study, it was assumed that no liquid water remained in the HDRP cask and that only water in the form of water vapor, physisorbed water, and chemisorbed water was available and subject to radiolysis. d'Entremont, Kesterson, and Sindelar (2020) evaluated several different gas generation scenarios, based on different assumptions about the locations of residual water (adsorbed on surfaces or in the vapor space) and the possible "replenishment" of surface-adsorbed water from the water vapor in the cask. The results of the calculations of total hydrogen gas generation (at 12 days after drying) were highly variable, ranging from approximately 500 ppmv to approximately 16,000 ppmv hydrogen, depending on the assumptions, noted above, about residual water. For comparison, Bryan et al. (2019) measured approximately 500 ppmv hydrogen in a vapor sample obtained from the HDRP cask 12 days after drying.

Regarding oxygen gas generation, d'Entremont, Kesterson, and Sindelar (2020) concluded that oxygen from radiolytic breakdown of free and surface water is not built up in the canister, and rather is assumed to be consumed by oxidation reactions. Overall, the study found that "[t]hese results illustrate the need for testing to refine understanding of radiolysis rates, etc., in systems closely resembling the SNF-in-canister materials system. ... A laboratory-scale test involving surrogate specimens to represent the materials in the canister is suggested" (d'Entremont, Kesterson, and Sindelar 2020).

E.5 Current State of Drying Research

The Board observes that the existing body of research on SNF drying provides no definitive conclusion regarding the amount of residual free water that could remain in an SNF canister after drying, especially if the canister contains water-logged SNF rods. The research also provides no clear picture of the amount of physisorbed or chemisorbed water that may remain after drying. The questions of what constitutes "dry" and how to determine if a canister is dry drove the development of the ASTM standard guide C1553-16 (ASTM International 2016).

The effectiveness of the NRC-accepted PNNL drying methodology (Knoll and Gilbert 1987) depends on the configuration of the canister, materials in the canister, maximum temperature reached, and pumping speed. Unless these parameters are well known, it is difficult to conclude justifiably that results from one set of parametric studies apply to

another study under different conditions or to all SNF packaging configurations that exist in the nuclear industry. It is also unclear how any residual water remaining in an SNF canister after drying will impact the SNF while being stored for extended periods or while being transported. This uncertainty is highlighted by the results of analyses of water remaining in an SNF cask or canister after drying (see sections E.4.1., E.4.2., and E.4.3.4.), where it can be seen that the effects of residual water can vary substantially, depending on the assumptions and inputs used in the analysis. These types of uncertainties about the drying process are motivating DOE to plan for continued drying research and continued efforts to obtain moisture samples from SNF cask or canister systems after they have been dried (Larson 2019).

E.6 References

10 CFR Part 71. "Packaging and Transportation of Radioactive Material.: *Code of Federal Regulations*. Washington, DC: Government Printing Office.

10 CFR Part 72. "Licensing Requirements for the Independent Storage of Spent Nuclear Fuel, High-Level Radioactive Waste, and Reactor-Related Greater than Class C Waste." *Code of Federal Regulations*. Washington, DC: Government Printing Office.

ASTM International. 2016. *Standard Guide for Drying Behavior of Spent Nuclear Fuel*. ASTM C1553-16. West Conshohocken, Pennsylvania.

Beller, B. 2014. Presentation to the NWTRB: Fuel Drying Activities by the Environmental Management Program at Idaho National Laboratory. Presentation to the Nuclear Waste Technical Review Board at its August 6, 2014 meeting.

Bryan, C.R., R.L. Jarek, C. Flores, and E. Leonard. 2019. *Analysis of Gas Samples Taken from the High Burnup Demonstration Cask*. SAND2019-2281. February.

Christensen, A.B. and K.M. Wendt. 2001. "Drying of Spent Nuclear Fuels and Fuel Debris Dried in a Vacuum Furnace." *Proceedings of the 8th International Conference on Radioactive Waste Management and Environmental Remediation*. Bruges, Belgium. September 30–October 4.

d'Entremont, A.L., R.L. Kesterson, and R.L. Sindelar. 2020. *Evaluation of Hydrogen Generation in High Burnup Demonstration Dry Storage Cask*. SRNL-STI-2020-00268, Revision 0. August 1.

EPRI (Electrical Power Research Institute). 2014. *High Burnup Dry Storage Cask Research and Development Project: Final Test Plan*. EPRI, Palo Alto, California. DE-NE-0000593.

EPRI. 2019. *High Burnup Dry Storage Research Project Cask Loading and Initial Results*. EPRI, Palo Alto, California. 3002015076.

Hurt, W.L. 2009. "Material Interactions on Canister Integrity During Storage and Transport." *Proceedings of a Technical Meeting on Management and Storage of Research Reactor Spent Nuclear Fuel*. Thurso, United Kingdom. October 19–22.

Jung, H., P. Shukla, T. Ahn, L. Tipton, K. Das, X. He, and D. Basu. 2013. *Extended Storage and Transportation: Evaluation of Drying Adequacy*. Center for Nuclear Waste Regulatory Analyses. ADAMS Accession No. ML13169A039.

Knight, T.W. 2016. *Experimental Determination and Modeling of Used Fuel Drying by Vacuum and Gas Circulation for Dry Cask Storage*. Presentation to the Nuclear Waste Technical Review Board at its February 17, 2016 meeting.

Knight, T.W., T. Farouk, J. Khal, E. Roberts, J. Tarbuton, J. Yulenko. 2019. *Experimental Determination and Modeling of Used Fuel Drying by Vacuum and Gas Circulation for Dry Cask Storage: Final Report*. Integrated Research Project Awards, Nuclear Energy University Program, U.S. Department of Energy.

Knoll, R.W. and E.R. Gilbert. 1987. *Evaluation of Cover Gas Impurities and Their Effects on the Dry Storage of LWR Spent Fuel*. PNL-6365. November.

Large, W.S. and R.L. Sindelar. 1997. *Review of Drying Methods for Spent Nuclear Fuel (U)*. WSRC-TR-97-0075 (U). April.

Larson, N. 2019. *DOE High Burnup Demonstration Project*. Presentation to the Nuclear Waste Technical Review Board at its November 19, 2019 meeting.

Meyer, R.M., M.S. Good, J.D. Suter, F. Luzi, B. Glass, and C. Hutchinson. 2019. *Sensor Development for Liquid Water Detection in Dry Storage Casks: FY19 Status*. SFWD-SFWST-M3SF-19PN010201034. September.

Miller, L., D. Basu, K. Das, T. Mintz, R. Pabalan, and G. Walter. 2013a. *Overview of Vacuum Drying Methods and Factors Affecting the Quantity of Residual Water After Drying—Public Version*. Center for Nuclear Waste Regulatory Analyses, San Antonio, Texas. July.

Miller, L., G. Walter, T. Mintz, and T. Wilt. 2013b. *Vacuum Drying Test Plan—Public Version*. Center for Nuclear Waste Regulatory Analyses, San Antonio, Texas. July.

NRC (U.S. Nuclear Regulatory Commission). 1999. *Standard Review Plan for Transportation Packages for Radioactive Material*. NUREG-1609. March.

NRC. 2000. *Standard Review Plan for Transportation Packages for Spent Nuclear Fuel*. NUREG-1617. March.

NRC. 2016. *Standard Review Plan for Renewal of Specific Licenses and Certificates of Compliance for Dry Storage of Spent Nuclear Fuel*. NUREG-1927, Rev. 1. June.

NRC. 2020. *Standard Review Plan for Spent Fuel Dry Storage Systems and Facilities, Final Report*. NUREG-2215. April.

Peehs, M., R. Bokelmann, and J. Fleisch. 1986. "Spent Fuel Dry Storage Performance in Inert Atmosphere." *Proceedings of the Third International Spent Fuel Storage Technology Symposium/Workshop*. Seattle, Washington. April 8–10.

Salazar, A., E.R. Lindgren, R.E. Fasano, R.J.M. Pulido, S.G. Durbin. 2020. *Development of Mockups and Instrumentation for Spent Fuel Drying Tests*. SAND2020-5341R. May.

Spilker, H. and J. Fleisch. 1986. "Dry Storage Demonstrations of Castor I and TN-1300 Casks." *Proceedings of the Third International Spent Fuel Storage Technology Symposium/Workshop*. Seattle, Washington. April 8–10.

Stockman, C.T., H.A. Alsaed, C.R. Bryan, S.C. Marschman, and J.M. Scaglione. 2015. *Evaluation of the Frequency for Gas Sampling for the High Burnup Confirmation Data Project*. FCRD-UFD-2015-000051. May 22.

Wittman, R. 2013. Radiolysis Model Sensitivity Analysis for a Used Fuel Storage Container. FCRD-UFD-2013-000357. September 20.

Yoon, K.H. J.Y. Kim, K.H. Lee, Y.H. Lee, and H.K. Kim. 2009. Control Rod Drop Analysis by Finite Element Method Using Fluid-Structure Interaction for a Pressurized Water Reactor Power Plant. *Nuclear Engineering and Design*. Vol. 239, pp 1857-1861.

Appendix F

Hydrogen Effects in Spent Nuclear Fuel Cladding

F.1 Introduction

The integrity of spent nuclear fuel (SNF) cladding plays an important role in ensuring safety during SNF storage and transport operations, usually in a secondary or “defense in depth” role. The integrity of the cask or canister¹ into which SNF is packaged often provides the primary safety barrier against flooding (which may cause a criticality accident), radiation exposure to nuclear facility workers and the public, and the release of radioactive material. These safety roles are explained in more detail in section 1.2 of the main body of this report. A short recap of the safety functions of SNF cladding is provided here.

One of the Nuclear Regulatory Commission (NRC) requirements is that a bolted-lid transportation cask containing either “bare” SNF or SNF inside a welded steel canister must remain subcritical even if the cask or canister fills with water after a transportation accident (Title 10, Code of Federal Regulations, Part 71 [10 CFR Part 71]). To evaluate the potential for criticality, if such an accident were to occur, it is necessary to perform the criticality calculations assuming the SNF is in its worst credible geometry, creating the worst case relative to criticality. If there is significant SNF reconfiguration, it will be difficult for an applicant to demonstrate to the NRC that the SNF cask or canister will remain subcritical when fully flooded with water. Furthermore, if there is significant cladding damage, more fission gas and radioactive particulates would be released to the cask/canister interior. If the cask/canister also leaked after the accident, there would be a larger amount of radioactive material released to the environment. Hence, it is desirable to keep the amount of SNF and cladding damage during a transportation accident to a minimum.

The primary SNF cladding characteristic governing the potential for cracking or a gross breach of the cladding during transportation is its ductility. More ductile cladding will be better able to withstand the stresses experienced during transportation without a breach; more brittle (i.e., less ductile) cladding will be more susceptible to a breach under sufficiently high loads.

There are two phenomena governing the ductility of any given type of zirconium-alloy cladding: the presence of relatively brittle zirconium hydrides within the cladding and in-reactor irradiation hardening of the cladding, which can also cause brittleness. Both

¹ SNF may be packaged into a welded stainless-steel canister that is then placed into a shielded overpack for storage and, for some designs, transportation. Alternatively, SNF may be packaged into a bolted-lid cask (sometimes called a bare fuel cask) that does not use an internal canister and includes its own shielding. These packaging systems are explained in more detail in section 2.1.2 of this report. For storage applications, some literature refers to both of these types of systems as “dry cask storage systems” and this report uses the same terminology. This report also may use the terms “cask” and “canister” when it is necessary to distinguish between specific types of storage or transportation systems.

increase with increasing fuel burnup,² so, for a given cladding type, they tend to be of more concern in high burnup fuel (HBF). Irradiation hardening cannot increase once the fuel is removed from the reactor, but it may decrease by annealing in certain conditions of SNF drying and dry storage (Einzigler and Kohli 1984; Ribis et al. 2007; Einzigler et al. 2003). Because irradiation hardening of the cladding is not expected to change appreciably during drying, storage, or transportation, it will not be considered further in this appendix.

This appendix discusses hydrogen accumulation in the cladding as well as the formation and behavior of zirconium hydrides in the cladding. Once hydrides have formed in the cladding at a sufficiently high concentration, it is assumed that cladding may be susceptible to cracking, given a tensile stress with an adverse orientation and a sufficiently high magnitude. However, the specific phenomenology of crack initiation and crack growth in the cladding are beyond the scope of this report and will not be discussed.

F.2 Hydrogen Accumulation and Hydride Formation in Nuclear Fuel Cladding

During nuclear reactor operation, nuclear fuel cladding oxidizes in the reactor coolant water at a rate that is a function of cladding temperature, water pH and impurities, both the metallurgical and chemical characteristics of the cladding, and time in the reactor. The oxidation reaction of zirconium metal (Zr) with water (H₂O) to form zirconium oxide (ZrO₂) and hydrogen (H₂) ($Zr + 2H_2O \rightarrow ZrO_2 + 2H_2$) produces a zirconium-oxide layer on the exterior cladding surface. The zirconium alloy cladding becomes thinner as the zirconium converts to oxide. A small fraction of the hydrogen produced in the reaction (15–20%) diffuses through the oxide layer and into the cladding, thereby becoming interspersed in the metal lattice of the cladding.³ The remainder of the hydrogen reacts with other elements in the coolant water, primarily reacting with oxygen to re-form water. Although the rate of hydrogen diffusion decreases as the fuel burnup increases (Lanning, Beyer, and Painter 1997), the total amount of hydrogen in the cladding increases with burnup.

There can be significant differences in the level of oxidation and hydrogen absorption from one cladding type to the next (Motta, Couet, and Comstock 2015) (see also Appendix A, Table A-2). As discussed in more detail below, it is desirable to limit the amount of corrosion and hydrogen absorption in the cladding. Therefore, newer fuel cladding types, such as ZIRLO[®] from Westinghouse and M5[®] from Orano (formerly Areva), have been designed to reduce cladding corrosion and hydrogen absorption. Figure F-1 shows a comparison of the oxide layer thickness (a direct indicator of corrosion and an indirect indicator of hydrogen absorption) as a function of fuel burnup for Zircaloy-4 cladding (an older cladding design) and for M5[®] cladding.

² Fuel burnup is a measure of the energy generated in a nuclear reactor per unit initial mass of nuclear fuel and is typically expressed in units of gigawatt-days per metric ton of uranium (GWd/MTU). In the U.S., the NRC considers SNF with a fuel rod average burnup of greater than 45 GWd/MTU to be high burnup fuel.

³ When hydrogen atoms are interspersed in the metal lattice of the cladding, they are referred to as being in solution.

When the concentration of hydrogen in the cladding reaches the hydrogen solubility limit of the cladding metal at a given temperature, the hydrogen precipitates and forms a separate phase, zirconium hydride (ZrH_2), by the reaction ($Zr + H_2 \rightarrow ZrH_2$).⁴ Zirconium hydride is also referred to as “hydride.” Hydrogen solubility in zirconium alloys decreases with decreasing temperature (see section F.3).

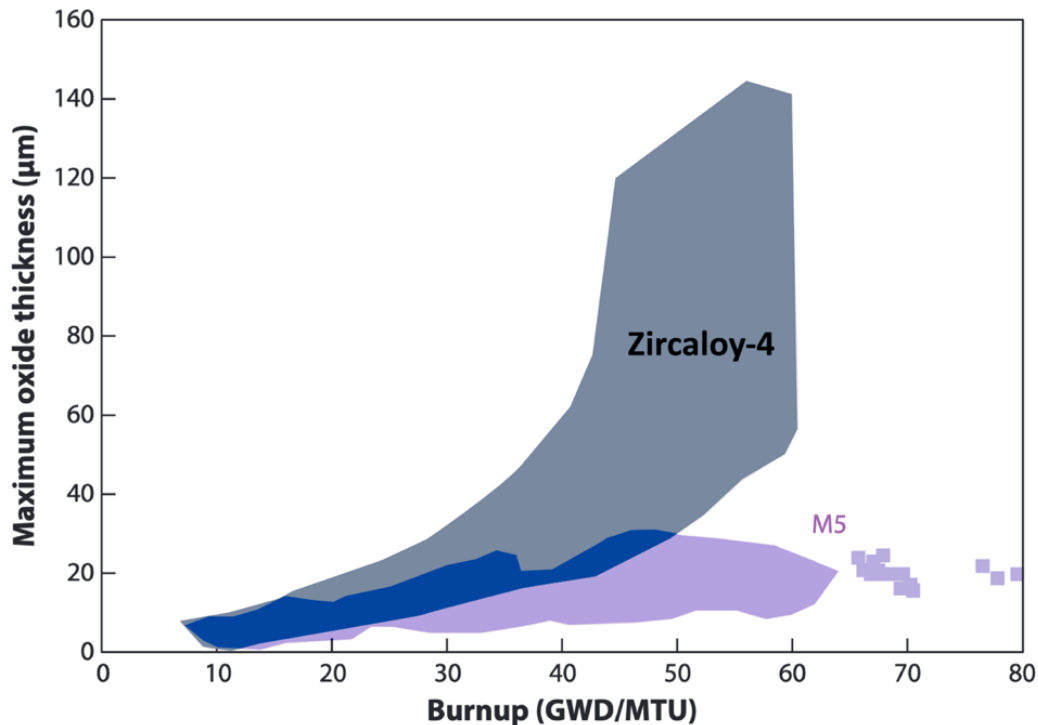


Figure F-1. Oxide layer thickness on Zircaloy-4 and M5[®] cladding.
(adapted from Motta, Couet, and Comstock 2015)

The precipitated hydride phase is in the form of very small platelets that form between the cladding metal grains. Compared to the cladding metal that is ductile, the hydrides within the cladding are relatively brittle (Puls 2018). In a hypothetical accident during SNF storage or transport, if a mechanical load or shock of a sufficient magnitude at an adverse orientation is imparted on the cladding, some of the hydrides might break, possibly leading to cracking and a breach of the cladding. The behavior of the hydrides in HBF cladding and their impact on the mechanical properties of the cladding will be detailed in this appendix.

Some pressurized water reactor (PWR) cladding is manufactured by swaging⁵ zirconium alloy tubing to impart a preferred orientation to the grains (known as “texture”). This texture tends to encourage hydrides that precipitate during reactor operations to be formed as

⁴ The exact chemical composition of hydrides can vary such that, in some literature, the hydride is listed as ZrH_x , where x can vary slightly above or below the value of 2.0.

⁵ Swaging is a forging process in which the dimensions of an item are altered using dies into which the item is forced. Swaging is usually a cold working process, but also may be hot worked. Newer PWR fuel cladding, such as M5[®] are fabricated in a process that includes recrystallization and annealing, which result in a much lower hydrogen uptake during reactor operation.

platelets aligned in a circumferential orientation (i.e., the hydrides are aligned in a plane formed by the circumferential (or azimuthal) direction and the axial direction in cylindrical coordinates). Figure F-2 depicts hydrides (darker color) aligned in a circumferential orientation. In contrast, under certain circumstances (discussed in section F.3) some hydride platelets may align in a radial orientation (i.e., the hydrides are aligned in a plane formed by the radial direction and the axial direction in cylindrical coordinates [like the spokes of a wheel]). These are called radial hydrides and they are depicted in Figures F-3, which is a micrograph of Zircaloy-2 cladding that was irradiated in a boiling water reactor (BWR).

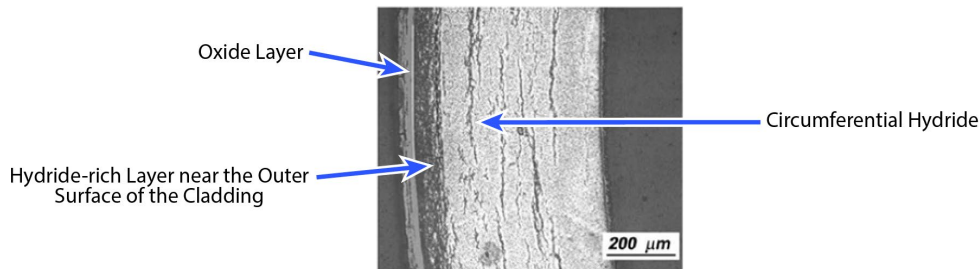


Figure F-2. Hydride distribution and orientation in HBF (approximately 70 GWd/MTU) with ZIRLO® cladding.

The circumferential hydrides are concentrated in a layer near the outer cladding surface. This cladding contains approximately 660 wppm hydrogen. (*adapted from Billone, Burtseva, and Einziger 2013*).

As noted above, hydrogen generated during oxidation diffuses into the cladding. Within the cladding, hydrogen diffuses to cooler regions, like the region near the outer surface that is in contact with the reactor coolant water. Hydrogen solubility also decreases with decreasing temperature, so more hydrides precipitate near the outer, cooler surface of the cladding. When a reactor is cooled down for refueling and the SNF is transferred from the reactor to the spent fuel pool, the cladding temperature drops to 30–75°C (86–167°F). Microstructural examination at room temperature of irradiated PWR fuel removed from the pool shows primarily circumferential hydrides (IAEA [International Atomic Energy Agency] 2015). For the specimen of high burnup ZIRLO® cladding shown in Figure F-2, the hydride rich layer can be seen near the outer surface of the cladding. For this specimen, the hydrogen content in the region of circumferential hydrides is approximately 660 wppm⁶ (Billone, Burtseva, and Einziger 2013).

Unlike PWR fuel cladding, Zircaloy-2 cladding used for BWR fuel has a random grain structure due to use of a different manufacturing technique, and any hydrides that form in BWR fuel cladding just after reactor operation tend to precipitate in random orientations (see Figure F-3). As explained in Appendix A, to reduce fuel pellet-cladding mechanical

⁶ Wppm is the ratio of the weight of the absorbed hydrogen to the weight of the zirconium-alloy cladding available to absorb the hydrogen expressed in parts per million. Most of the time this measurement is made by fusion analysis that melts a relatively thin ring of cladding cut at a particular axial position such that the reported wppm value is an average over the total cladding available at the same rod elevation.

interactions that could lead to a cladding breach in BWR fuel with Zircaloy-2 cladding, a thin layer (or “liner”) of pure zirconium or zirconium alloyed with iron or tin is included at the inner diameter of the cladding during fabrication.⁷ Due to the high solubility of hydrogen in zirconium, a significant fraction of hydrides is found in the zirconium liner (see Figure F-3). However, the zirconium liner in BWR fuel is not of significance with regard to mechanical performance and is not credited for the structural performance of the cladding in NRC safety reviews. There is no liner used in PWR fuel cladding.

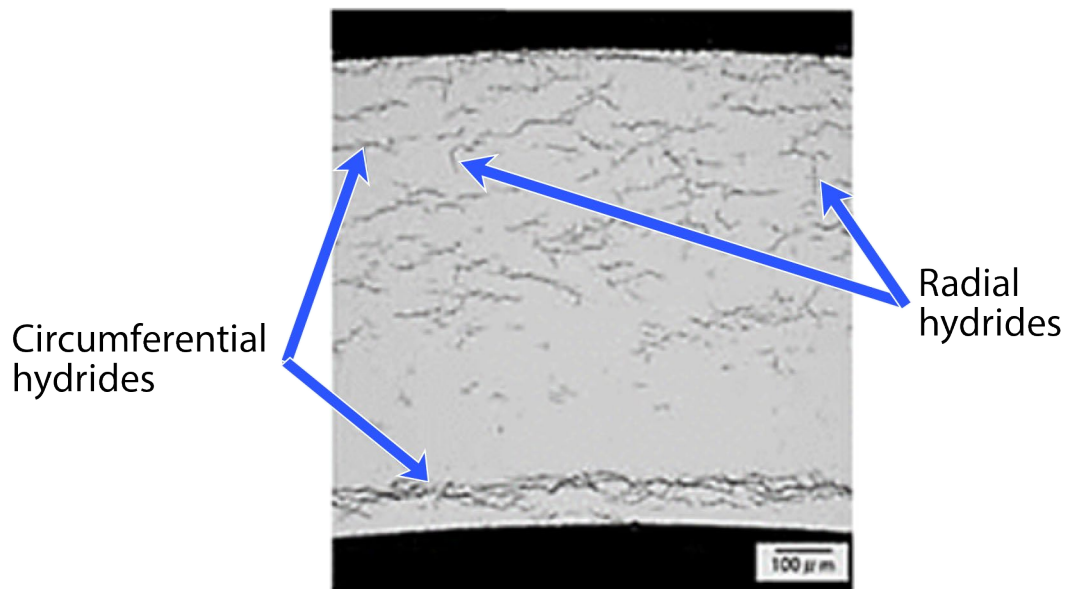


Figure F-3. BWR Zircaloy-2 cladding containing precipitated hydrides.

The sample depicted had a burnup of 50 GWd/MTU and illustrates a random orientation of hydrides (i.e., a mixture of circumferential and radial hydrides). Mainly circumferential hydrides can be seen concentrated in the liner near the inside diameter of the cladding (adapted from Aomi et al. 2008).

No known studies have been conducted to determine whether the orientation of the precipitated hydrides in SNF cladding changes during the cooldown period in the reactor and when the SNF is moved to the spent fuel pool. The hydride structure of both PWR and BWR SNF cladding is assumed to remain essentially unchanged while the SNF is in the spent fuel pool, where the temperature is relatively low and unchanging.

When the radioactive decay heat in the SNF has decreased below the NRC guidelines regarding decay heat, and if storage space is needed in the spent fuel pool, then the SNF is transferred from the pool to a dry cask storage system.

⁷ In some early tests of Zircaloy-2 liners, copper was used as an alternative to zirconium, but it was abandoned after it was found to be less effective than zirconium (Cox 1990).

F.3 Hydride Reorientation

Hydride reorientation is a phenomenon in which some of the hydrides that were initially precipitated in a circumferential orientation in PWR cladding (previously illustrated in Figure F-2) or in a random orientation in BWR cladding (previously illustrated in Figure F-3) realign, under certain conditions, mostly in a radial orientation in the cladding (see Figures F-4 and F-5C) (Einziger and Kohli 1984). The conditions necessary for reorientation include a temperature high enough (e.g., during and shortly after SNF drying) for hydrogen to go back into solution in the zirconium-alloy matrix and a sufficiently high hoop (circumferential) stress in the cladding during cooling. Both Figures F-4 and F-5C show images depicting different extents of hydride reorientation where some of the hydrides have transitioned from a circumferential orientation to a radial orientation. Figure F-6 illustrates hoop stress in the cladding. The details of the reorientation phenomenon are discussed below.

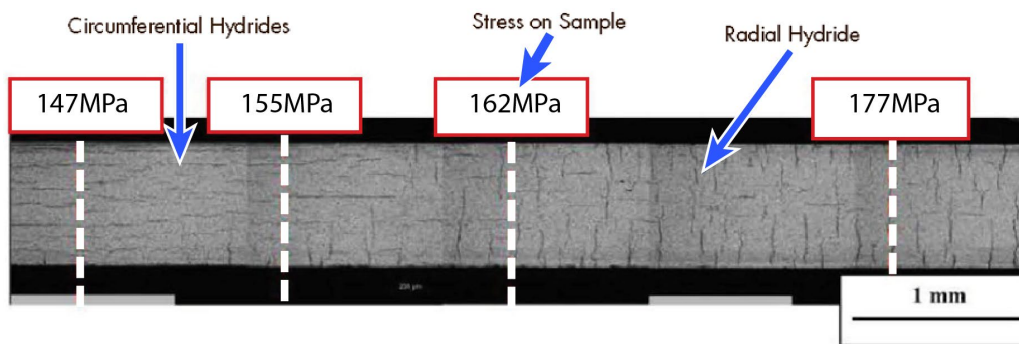


Figure F-4. Influence of applied stress on the extent of hydride reorientation.

Hydride reorientation in a flat-plate, cold-worked, stress-relieved, and annealed Zircaloy-4 tensile sample heated to 500°C (932°F) and cooled to room temperature under different stresses. At lower stresses, the hydrides are primarily circumferential. At higher stresses, the hydrides are primarily radial (*adapted from Cinbiz, Koss, and Motta 2014*).

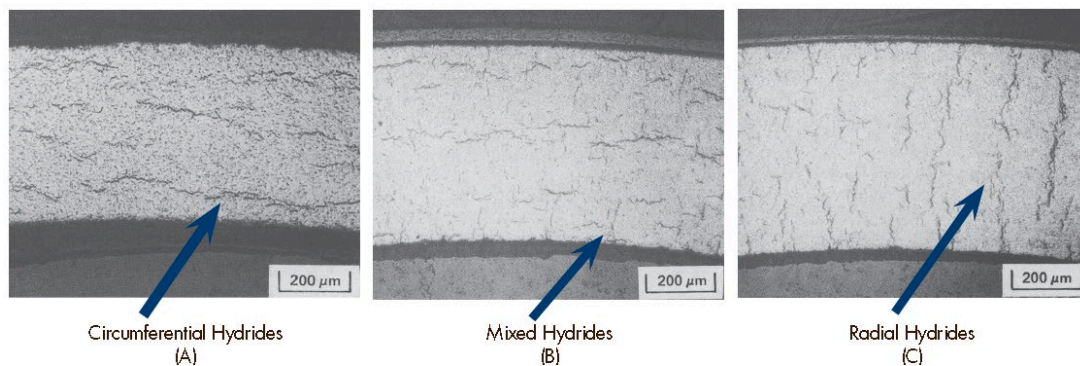


Figure F-5. Hydride reorientation in irradiated Zircaloy-4 cladding at approximately 35 GWd/MTU.

(A) Circumferential hydrides form when there is no hoop stress during cooldown; (B) mixed hydrides and (C) predominately radial hydrides form when there is high hoop stress during cooldown (*Einziger and Kohli 1984*).

As noted earlier, examinations of HBF cladding from fuel that had been removed from a reactor and moved to the spent fuel pool revealed predominantly circumferential hydrides but few or no radial hydrides. It has been postulated that when the cladding is at high temperature in the reactor, the primary coolant water pressure offsets the rod internal pressure such that the net tensile hoop stress on the cladding is insufficient to cause the precipitation of radial hydrides, but circumferential hydrides may form in certain conditions (Electric Power Research Institute [EPRI] 2020).

When the reactor is shut down and cooled down, the coolant water temperature and pressure are reduced in increments. During this phase of operations, as the coolant water pressure is reduced, the net hoop stress on the cladding is increased. However, in this case, the cladding hoop stress– temperature combination during cooling is such that the hydrogen precipitates as circumferential hydrides (EPRI 2020). A detailed discussion of the specific conditions necessary for the formation of radial hydrides is provided below.

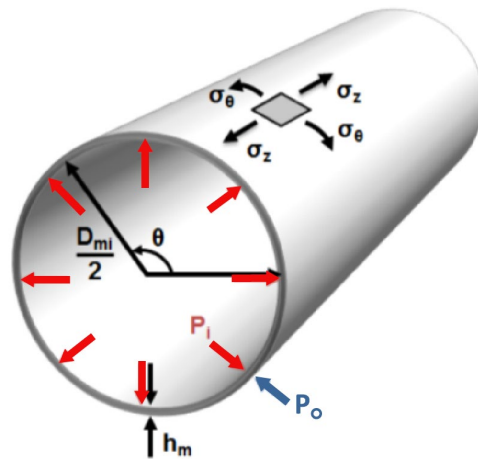


Figure F-6. Fuel cladding segment displaying internal pressure and hoop stress.

The image illustrates hoop stress (σ_θ), longitudinal stress (σ_z), internal pressure (P_i), cladding thickness (h_m), external pressure (P_o), the circumferential coordinate (θ), and inner cladding diameter (D_{mi}) (adapted from NRC 2020).

Hydride reorientation is a complex phenomenon and its occurrence and prevalence in HBF cladding are dependent on a large number of factors (see, for example, Louthan and Marshall 1963; Sindelar, Louthan, and Hanson 2015). These factors fall into two major groups:

1. Inherent fuel and cladding properties:
 - a. differences in mechanical and chemical properties associated with the particular zirconium alloy used in the cladding
 - b. thickness of the cladding
 - c. the presence and type of zirconium liner inside the cladding (in some BWR fuel types)

- d. the presence and type of burnable absorbers in the fuel rod
2. Conditions or environments to which the fuel and cladding are exposed:
- a. cladding manufacturing processes:
 - 1) degree of cold working
 - 2) degree of annealing
 - 3) degree of recrystallization
 - b. in-reactor and spent fuel pool operations:
 - 1) rod linear heat rating and linear power rating
 - 2) rod average burnup and peak burnup (which affects fission gas generation in the fuel contributing to rod internal pressure)
 - 3) rod total neutron fluence (which affects lattice displacements in the cladding alloy, affecting ductility)
 - 4) reactor operating temperature and primary coolant water chemistry (which determine cladding oxidation and subsequent hydrogen absorption in the cladding)
 - 5) length of time in pool storage (which affects the amount of helium gas produced from radioactive decay in the fuel)
 - c. drying and dry storage operations:
 - 1) drying time and process used (e.g., vacuum drying) (which affects maximum cladding temperature and maximum rod internal pressure, contributing to the maximum cladding hoop stress)
 - 2) length of time at maximum temperature and rod internal pressure
 - 3) number of drying cycles
 - 4) cooldown rate after drying

The processes leading to the formation of radial hydrides via hydride reorientation are discussed in this section, as are the dependencies of hydride reorientation on the factors listed above.

Drying Processes and the Dissolution of Existing Hydrides. After the SNF is moved underwater into a storage cask or canister, the bulk of the water is drained from the canister followed by either vacuum drying or forced helium dehydration to remove un-drained free water (i.e., water that is not chemically bound to materials inside the canister). After the

canister is confirmed to be sufficiently dry by passing a dryness test (see Appendix E), it is then backfilled with helium.

When the fuel is dried under a vacuum, it heats up because of radioactive decay and a lack of convective heat transfer. The NRC recommends that the maximum temperature the cladding should be allowed to reach is 400°C (752°F) (NRC 2003) at any time, including during drying and dry storage. The average cladding temperature is much lower than this value, and even the maximum cladding temperature may be substantially lower in many drying and storage situations (Hanson 2018) because of conservatism used by utilities and vendors in their approach to meeting the NRC requirements for transport (see Appendix H). As the temperature of the SNF increases, some of the hydrides disassociate, and the hydrogen goes back into solution in the zirconium alloy as atomic hydrogen (up to the solubility limit in the zirconium alloy).

Post-drying Cooling and Hydride Reorientation. Once the drying process is finished and the canister is backfilled with helium, the cladding temperature may either increase or decrease. The cladding temperature may initially decrease due to the improved heat transfer capacity of the helium gas; it may initially increase after drying if the drying time is insufficient for the cladding to reach thermal equilibrium. Regardless, the cladding will eventually begin to cool as the decay heat decreases. As the cladding temperature drops, the solubility limit for hydrogen decreases and any hydrogen remaining in solution will precipitate to form hydrides once again. If the total hydrogen concentration becomes high during reactor operation (above the solubility limit), as may occur for HBF, then a higher concentration of hydrides will precipitate when the cladding cools after reactor operation. However, as illustrated in Figure F-1, newer fuel claddings have been designed to reduce corrosion and hydrogen pickup during reactor operation.

Importance of hydrogen concentration, temperature, and hoop stress to hydride reorientation. As noted above, there are a large number of variables that can affect the reorientation of circumferential hydrides to radial hydrides. Among the most important of these variables are the hydrogen concentration in the cladding, the maximum cladding temperature attained during drying, and the resulting maximum hoop stress in the cladding (Sindelar, Louthan, and Hanson 2015). The processes of hydride dissolution and reorientation during re-precipitation are best understood by examining the hydrogen dissolution curve and precipitation curve applicable to the specific zirconium alloy of interest. Figure F-7 shows these curves for Zircaloy-4.

The hydrogen solubility curve exhibits a memory effect, referred to as hysteresis, as shown in Figure F-7 (Billone 2016). As the zirconium alloy heats up during initial drying and storage, hydrogen goes into solution up to the solubility limit following the dissolution curve (also called the solvus curve; in blue and purple in Figure F-7). The curve depends on the total neutron fluence that the cladding receives because the neutrons create vacancies in the cladding's crystalline structure that act as hydrogen traps⁸ (Kammenzind 2018).

Depending on the maximum temperature the cladding reaches, all or some of the hydrogen that had precipitated as hydrides when the SNF cooled during reactor shutdown will go back

⁸ Hydrogen traps are defects in the cladding caused by irradiation that attract and hold hydrogen atoms.

into solution in the cladding. If the amount of hydrogen available to go back into solution is greater than the solubility limit at the maximum cladding temperature, then some of the hydrides formed upon initial cooling will remain in the cladding.

Zirconium alloys exhibit a memory effect relative to hydride reprecipitation. As the cladding starts to cool, the hydrogen in solution will exceed the solubility limit. One of two situations may arise depending on whether any hydrides remained in the cladding after the heat-up.

1. If hydrides are present in the cladding, reprecipitation starts as soon as the cladding starts to cool and the amount of hydrogen remaining in solution follows the dissolution curve instead of the precipitation curve. The hydrides that reprecipitate are more likely to precipitate on the existing hydrides such that the orientation of the additional hydrides will be the same as the orientation of the existing hydrides.
2. If there are no existing hydrides, then reprecipitation does not start until the temperature drops to the precipitation curve (in red in Figure F-7). The hysteresis is important because, at a given hydrogen concentration (in wppm in Figure F-7), reprecipitation of hydrides will occur at a lower temperature (and corresponding lower hoop stress) than the temperature at which they dissolved. In this case, since there were no existing hydrides, there is no memory effect, and the hydrides will reprecipitate in either the circumferential or radial orientation, depending on the cladding hoop stress.

Although the same amount of hydrogen will eventually precipitate as hydrides, the ratio of the radial to circumferential hydrides will be affected by the cladding hoop stress, which is a function of the cladding temperature. The existence of a memory effect for zirconium hydride precipitation during cooling means that fewer radial hydrides will precipitate at any given temperature than if the memory effect did not occur.

The location of the precipitation curve in relationship to the dissolution curve depends on whether thermal equilibrium is reached (the steady-state condition is shown in Figure F-7) and if, at maximum cladding temperature, there are still hydrides in the cladding that can act as nucleation sites since precipitation is more likely on preexisting hydrides (Louthan 2014). More undissolved hydrides in the cladding will move the precipitation curve closer to the dissolution curve.

Phenomenological models. Several phenomenological models for hydride behavior in zirconium-alloy cladding have been proposed for predicting the behavior of the cladding. Puls (1985) and Liu, Rashid, and Machiels (2016) proposed models for hydride reorientation, and Courty, Motta, and Hales (2014) adapted the BISON fuel performance model to simulate hydride behavior in Zircaloy-4 cladding. These models describe the general phenomenon of hydride precipitation and reorientation in zirconium-alloy cladding but are often limited to one-dimensional analyses or limited to one cladding type. The Board observes that much work remains to extend the models to multi-dimensional analyses and to the full range of cladding types in use. These modeling challenges are discussed further in section F.5 and in Appendix I.

In summary, the amount of hydride reorientation that occurs depends on many factors, as noted above. Some of the most important factors are the maximum cladding hoop stress

(and temperature), the total amount of hydrogen in the cladding (Colas et al. 2014), the type of zirconium alloy used and how the cladding was manufactured (Sindelar, Louthan, and Hanson 2015), the rate of cooling during drying (Aomi et al. 2008; Burtseva, Yan, and Billone 2010), and the number of heating and cooling cycles during drying (Chu et al. 2007; NRC 2003).

As a general guideline, the likelihood of a particular type of cladding becoming less ductile is a function of the concentration of radial hydrides in that cladding: i.e., the more precipitated radial hydrides in the cladding, the more likely it will experience reduced ductility.

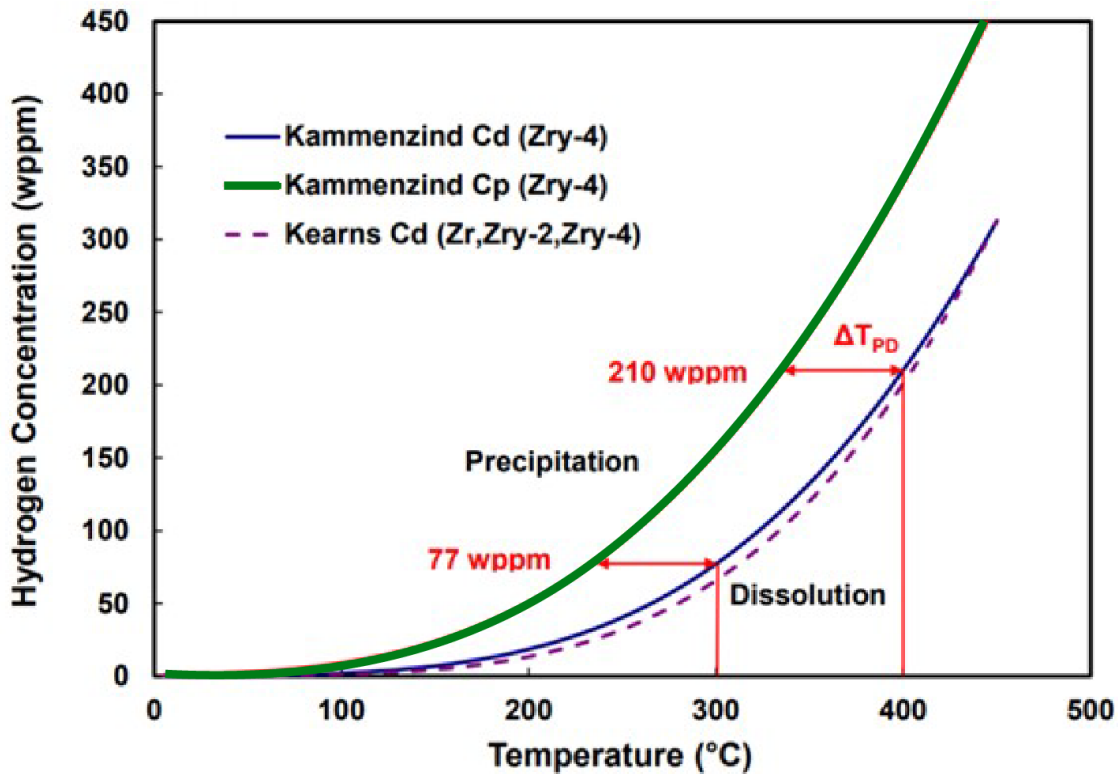


Figure F-7. Steady-state solubility of hydrogen in zirconium and Zircaloy.

Terminal solubility of hydrogen as detected by the onset of hydride precipitation (Cp) during cooling from elevated temperatures (red curve) and by the onset of hydride dissolution (Cd) during heating from low temperatures (blue, and purple dotted curves) (adapted from Billone 2016).

Notes: Zry-4 is Zircaloy-4, Zr is zirconium, Zry-2 is Zircaloy-2, DTPD is the temperature difference between hydrogen precipitation and dissolution.

F.3.1 History of Hydride Reorientation

Hydride reorientation in zirconium alloy tubing was discovered in the early 1960s (Louthan and Marshall 1963). Later, hydride reorientation was found to be an issue for SNF during drying and dry storage when the pressure in some annealed SNF rod segments was lost due to failed welds during rod segment testing at Battelle Columbus Laboratories (Einziger and Kohli 1984). Metallography results of lower burnup cladding that had been heated and then cooled with no cladding hoop stress compared with metallography results from cladding

that had been cooled with high hoop stress indicated that radial hydrides can form in cladding during drying and dry storage if the hoop stress is high enough (Figures F-4 and F-5) (Einziger and Kohli 1984).

Because the potential for hydride reorientation was thought to be eliminated for PWR SNF cladding due to swaging of the cladding during fabrication, and because both circumferential- and random-oriented hydrides but limited radial hydrides had been observed in BWR cladding, hydride reorientation was not initially considered as a degradation mechanism in SNF during dry storage (NRC 2003). The NRC (2003), and others (Peehs, Kaspar, and Steinberg 1986) evaluated several other SNF degradation mechanisms (e.g., creep, oxidation, and diffusion-controlled cavitation growth⁹) (NRC 2003) and determined that SNF could safely be stored with little probability of gross cladding breach if the cladding temperatures were held below 400°C (752°F) under drying and dry storage conditions.

All available data on hydride reorientation in SNF as a function of annealing temperature and applied hoop stress were used by the NRC to support the development of Interim Staff Guidance-11, Revision 3 (ISG-11, Rev. 3; NRC 2003). ISG-11, Rev. 3 sets limitations on SNF drying and storage conditions to preclude hydride reorientation in SNF cladding (ISG-11 specifically addresses low burnup SNF but was written to apply to all SNF, including HBF). Except for special cases, the NRC set a maximum cladding temperature limit of 400°C (752°F). A higher maximum cladding temperature can be used if the applicant can show that the maximum cladding hoop stress is less than 90 MPa (~13,000 psi) for SNF in normal conditions of storage.

All the available data on hydride reorientation were later compiled by Chung (2004), as shown in Figure F-8. Below the hoop stress threshold line in Figure F-8, no hydride reorientation was detected in unirradiated cladding samples. Furthermore, the data in Figure F-8 revealed that hydride reorientation does not occur in low burnup SNF cladding or unirradiated cladding if the cladding hoop stress is held below 90 MPa (~13,000 psi), irrespective of maximum temperature or burnup. At the time Figure F-8 was developed, there were no hydride reorientation data available on HBF cladding at maximum temperatures below 400°C (752°F) and a hoop stress below 90 MPa (~13,000 psi).

The set of data used by Chung (2004) is subject to several caveats that prevent it from definitively predicting if SNF will be susceptible to hydride reorientation. These caveats are primarily due to the varieties of spent fuel claddings, irradiation conditions, and differences in cladding characteristics such as hydrogen content, and internal rod pressures (Appendix A). The data are derived from a variety of cladding compositions used in fuels for both PWRs and BWRs. Due to the different conditions of the claddings when they come out of the reactor, different reorientation behaviors may be expected. Evaluation by the Board staff of the papers underlying the data used by Chung (2004, and references therein) reveals issues, listed below, that limit the usefulness of the Chung (2004) analysis in Figure F-8.

⁹ A mechanism where vacancies in the cladding coalesce and form through-wall cavities in the cladding. While this mechanism has been observed in similar metals like titanium, it has never been observed in zirconium.

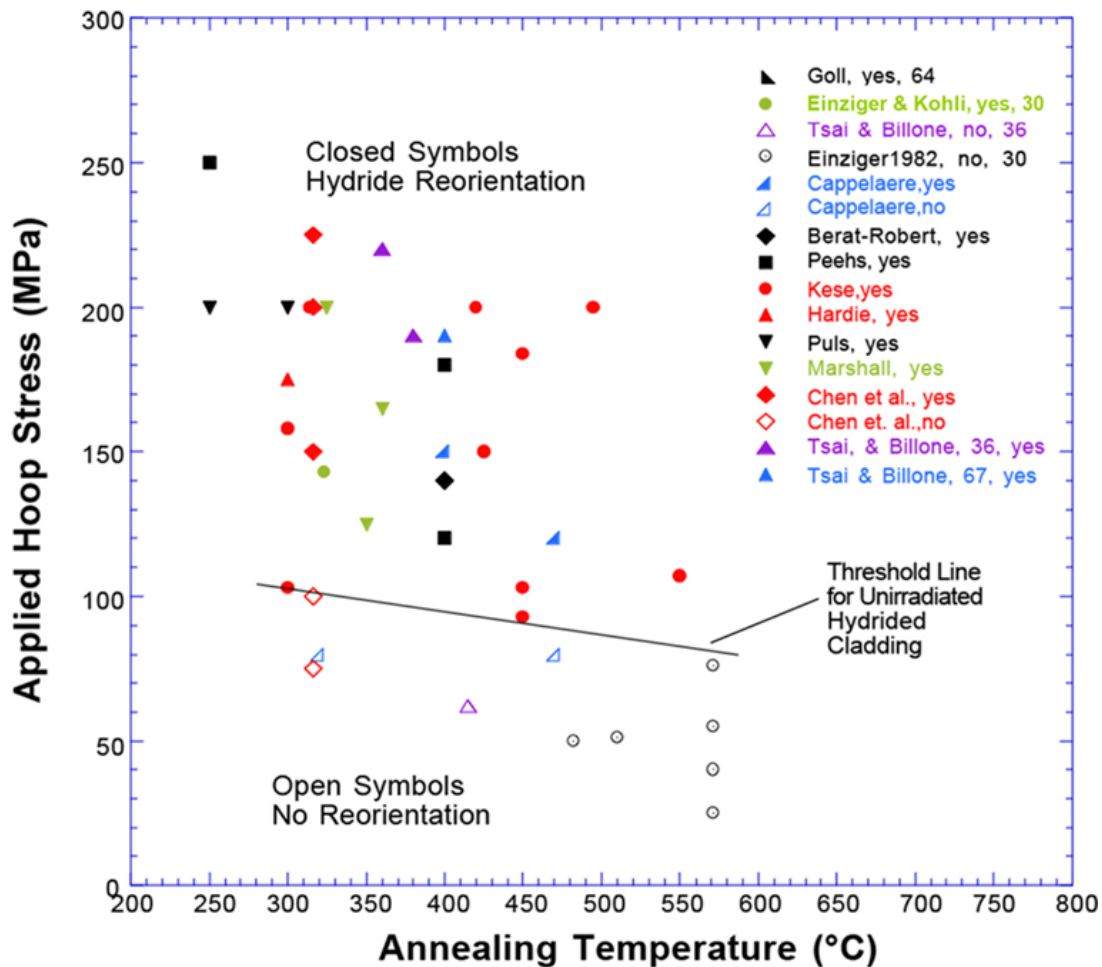


Figure F-8. An early compilation of hydride reorientation data taken on a variety of Zircaloy cladding types.

“Yes” in the legend (and a solid symbol) indicates that hydride reorientation occurred. “No” (and an open symbol) indicates that hydride reorientation did not occur. The number after a citation in the legend indicates the reference number in Chung (2004).

- As shown in later tests (Billone, Burtseva, and Einzigler 2013), the onset of hydride reorientation in irradiated samples cannot be predicted based on the onset determined from testing unirradiated samples. Many of the samples in earlier studies cited by Chung (2000) were unirradiated making it difficult to use the results to determine the behavior of irradiated fuel (see section F.3.4.1).
- Although a few samples had burnups in the range of 30 GWd/MTU, most of the irradiated samples had a burnup below 10 GWd/MTU. Because less hydrogen is generated and absorbed at lower burnup, there are fewer hydrides in the cladding, which is not the case for HBF (>45 GWd/MTU).
- The hydrogen content and its distribution varied considerably between samples, and in some samples the hydrogen content was not even specified.

- The data were nearly always determined from isothermal, isobaric experiments that are not representative of the temperature–stress profile experienced by SNF cladding during drying and dry storage.
- Some of the data were collected on samples subjected to a uniaxial stress, rather than a biaxial stress as found in SNF cladding.¹⁰ Stress on the cladding decreases with temperature. By maintaining a high stress state during cooling, more of the hydrides will precipitate radially in the test samples than in actual cladding in dry storage. For tests conducted in this manner, the minimum stress needed to cause hydride reorientation is lower than that in experiments where the stress on the cladding decreased with temperature.
- The testing methods in the various experiments were not consistent: some tests used pressurized tubes while others used mandrel applied stress. These differences in methodology resulted in different hoop stress states on the samples.
- The cooling rate of the samples varied by an order of magnitude. Slower experimental cooling rates are more representative of actual cooling rates. In laboratory experiments that applied different cooling rates, other cladding characteristics, such as hydride content, which will affect the amount of hydride reorientation, were also different. For all cladding types, more hydrogen diffusion will occur in samples that are cooled slowly than in samples that are cooled at faster rates, which leads to more precipitation of reoriented (radial) hydrides.
- The definition of “reorientation” (i.e., what constitutes a radial hydride) varied among different researchers.
- In many cases, the research did not specify how the stress and temperature at which hydride reorientation occurred was determined.

F.3.2 Research on Hydride Reorientation by Organizations Other than DOE

Building on the earlier work cited in Chung (2004), additional hydride reorientation research related to SNF storage and transportation began in 2002, when the NRC funded Argonne National Laboratory (ANL) to conduct testing (described below) on a variety of HBF cladding types (Billone, Burtseva, and Einziger 2013). In this same time frame, other countries also started to study hydride reorientation (section F.3.2.3).

To fully explore the formation of hydrides, hydride reorientation, and the effects of hydride reorientation on HBF performance (particularly, cladding ductility), the ANL research approach applied four basic steps. First, irradiated and defueled cladding samples were obtained, and their hydrogen contents were measured. If irradiated cladding was not available, unirradiated cladding was used and charged with a known quantity of hydrogen in a laboratory setting. Second, the cladding samples were subjected to a high-temperature (typically greater than 350°C [662°F]), high hoop stress (typically greater than 90 MPa

¹⁰ The cladding of intact fuel rods has a stress biaxiality of 0.5 during drying operations such that the measured effects of stress on hydride reorientation in uniaxial-loaded samples may not provide conservative estimates (Cinbiz, Koss, and Motta 2016).

[13,000 psi]) treatment that, upon cooldown, caused the reorientation of hydrides from a circumferential to a radial orientation (in cladding that contained pre-existing hydrides) or the formation of radial hydrides (in cladding that did not contain pre-existing hydrides). This treatment is called hydride reorientation treatment (HRT). In the third step, short cladding rings were subjected to a series of ring compression tests (RCT) at different temperatures where the amount of cladding deformation (or strain) at failure was determined as a function of compressive load (the point of failure is defined and discussed in section F.3.2.2). Finally, in the fourth step, the measured failure strains were plotted as a function of temperature and a “ductility transition temperature” (DTT) was determined.

The DTT is the temperature demarcating the transition between ductile and brittle behavior of the cladding in a “pinch mode” of loading, like that which may be experienced by HBF cladding in a side-drop accident during transportation. At temperatures below the DTT, the cladding is less ductile and is at risk of experiencing through-wall cracking when subjected to a sufficiently large shock or tensile stress that is oriented perpendicular to the radial hydrides in the cladding (i.e., the pinch mode of loading). The Board notes that the RCT is a scoping test to determine the temperature range where ductility of the HBF cladding decreases. It is not a direct measure of the ductility itself. Therefore, any uncertainties in the RCT results propagate as uncertainties in the temperature range over which the ductility changes, not uncertainties in the cladding ductility itself. The research efforts to study hydride reorientation and its effects are discussed below.

F.3.2.1 Hydride Reorientation Treatment to Simulate Bounding Drying Conditions

As discussed above, the NRC provided guidance for limiting maximum SNF cladding temperature and cladding hoop stress to prevent hydride reorientation from occurring during storage (NRC 2003). The suggested limits were based on the data shown in Figure F-8. However, due to the concerns associated with those data (noted in section F.3.1), the NRC and EPRI initiated a program to study the effects of the aforementioned variables and uncertainties on hydride reorientation (Billone, Burtseva, and Einziger 2013). The goal of the program had been to determine how to prevent hydride reorientation in stored HBF. However, a member of the research team noted that the program suffered from a lack of funding, lack of samples, and operational issues at the ANL hot cells, so the goal shifted to understanding what effects hydride reorientation (if it occurred) would have on the cladding’s structural performance.

The ANL effort included HRTs to induce hydride reorientation in SNF cladding like that which may occur when SNF temperature and internal rod pressure increase during drying or dry storage. Starting with NRC-sponsorship and then transitioning to DOE-sponsorship, the overall program included tests on SNF cladding specimens fabricated from Zircaloy-2, Zircaloy-4, ZIRLO[®], and M5[®]. The study used irradiated, defueled (no UO₂ pellets inside) cladding samples that were re-pressurized and heated for testing. This approach achieves the desired hoop stress at the maximum allowed cladding temperature of 400°C (752°F) during drying (Billone, Burtseva, and Einziger 2013). One test was conducted at 190 MPa (~27,500 psi) and 400°C (752°F),¹¹ and the remaining early tests were done at 110–140

¹¹ This particular test was not intended to be at such a high internal stress. A calculation error was made when determining the room temperature gas pressure to put in the rod to reach the desired cladding hoop stress at 400°C (752°F).

MPa (~16,000–20,000 psi) and 400°C (752°F) to bound all the expected SNF inventory except perhaps SNF with integral burnable absorbers rods containing boron, which are expected to have the highest internal rods pressures of any SNF¹² (Lanning and Beyer 2004; Bratton, Jessee, and Wieselquist 2015; Richmond and Geelhood 2018). Newer measurements of HBF temperatures during drying and storage have revealed lower cladding temperatures than expected (as much as 60°C [108°F] lower; see Appendix G), so the expected cladding hoop stresses are now significantly lower than the hoop stresses used in early ANL tests. This is expected to be the case also for rods containing integral burnable absorbers.

During the HRTs, the samples were first brought to test temperature and then held at that temperature for 1–24 hours.¹³ In early tests, all M5[®] test rodlets were cooled at 5°C/h¹⁴ (9°F/h) down to about 130°C (266°F). Zircaloy-4 and ZIRLO[®] rodlets were cooled at 5°C/h (9°F/h) down to 200°C (392°F). Later, the protocol was changed to cool all rodlets down to 130°C (266°F) at 5°C/h (9°F/h). After the rodlets cooled to the temperatures indicated above, they were cooled further at a rapid rate because most of the hydrogen precipitation had already occurred by 200°C (392°F) (Billone, Burtseva, and Einziger 2013). After HRT, cladding rings of approximately 2–8 mm (0.1–0.3 in) wide (i.e., in the axial direction) were cut from the samples. The sample rings were subjected to metallographic examination to determine the amount of hydride reorientation that occurred. Hydrogen analysis of the sample rings was conducted to determine average hydrogen concentration as well as axial and circumferential variation in hydrogen content. Finally, some of the rings were subjected to RCTs to determine ductile behavior versus temperature (see section F.3.2.2 for a description of the RCTs). The results of HRTs conducted by ANL are well documented (Billone, Burtseva, and Einziger 2013; Billone, Burtseva, and Martin-Rengel 2015; Billone, Burtseva, and Garcia-Infanta 2017; Billone 2019).

F.3.2.2 Ring Compression Tests Simulating the Loads in a Transportation Side Drop Accident

Hydride reorientation, if it occurs, is expected to be of most consequence for cladding performance during a side drop accident when the SNF is being handled or transported in a horizontal configuration (NRC 2020). In such an accident, a fuel rod may be impinged upon or pinched by other rods, assembly structures (e.g., spacer grids), or cask system structures (e.g., the fuel basket). See Figure F-9 for a schematic of the pinch mode of loading. In this case, the maximum tensile stresses will occur at the 12 o'clock and 6 o'clock positions at the inside diameter of the cladding and at the 3 o'clock and 9 o'clock positions at the outside diameter of the cladding (Figure F-9B). In these positions of maximum tensile

¹² Higher pressures are expected in integral burnable absorber rods containing boron because these rods generate helium via an (n, alpha) reaction when irradiated in the reactor.

¹³ 24 hours is shorter than the actual drying time of most SNF, but long enough to stabilize the amount of hydrogen that goes into solution. However, it may not be long enough to get the same amount of cladding annealing that might be expected in an SNF rod that was dried for a day or longer. The temperature is low enough that no substantial cladding creep is expected, which lowers the cladding hoop stress.

¹⁴ This cooldown rate is 3–4 orders of magnitude faster than the expected long-term cooldown after drying and during dry storage. This rate was an experimental limitation due to time considerations.

stress, the stresses are perpendicular to the plane of the radial hydrides and therefore, are more likely to cause breakage of the radial hydrides, potentially leading to cracking and a cladding breach.

The rate at which an actual load is applied, and the magnitude of the load are dependent on the type of accident and the design of the cask or canister system. To investigate the behavior of HBF cladding under pinch mode loadings, the NRC and later, DOE, sponsored ANL to conduct RCTs on various cladding types under a wide range of test conditions.

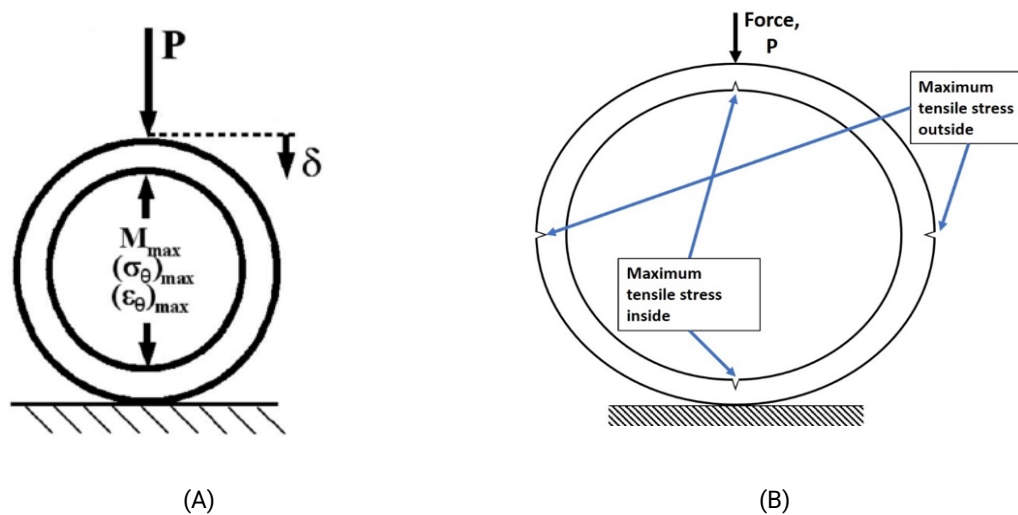


Figure F-9. Pinch load, P , on a cross-section of cladding caused by a hypothetical transportation side drop accident.

(A) The distance the cladding is squeezed (deformation) is δ . The maximum deformation will cause a maximum cladding tensile stress, σ_{max} , and a maximum cladding strain of ϵ_{max} . M_{max} is the maximum bending moment (*Billone, Burtseva, and Martin-Rengel 2015*); (B) shows the locations of the maximum tensile stresses in the cladding.

In the early NRC-sponsored testing, ANL conducted a series of RCTs (Figure F-10) at strain rates of 0.05 mm/s, 5 mm/s, and 50 mm/s (0.02 in/s, 0.2 in/s, 2 in/s) for irradiated M5[®], ZIRLO[®], and Zircaloy-4 cladding from commercial PWR HBF (*Billone, Burtseva, and Liu 2012*). In terms of ductility, there was very little effect of strain rate. This is not surprising as these irradiated zirconium-based alloys are relatively strain-rate insensitive. Earlier impact tests were performed at 2 m/s (6.6 ft/s), but the apparatus was not designed to prevent multiple impacts, which prematurely cracked the cladding. Until an actual SNF cask design is tested in a 9 meter side drop test to determine the strain rate on an HBF rod during impact, assumptions regarding the insensitivity of ductility to strain rates will continue to prevail, and NRC license applicants will be able to use the range of data obtained from existing tests to support their design's safety basis.¹⁵

¹⁵ The strain rates used by industry in their licensing modeling are proprietary.

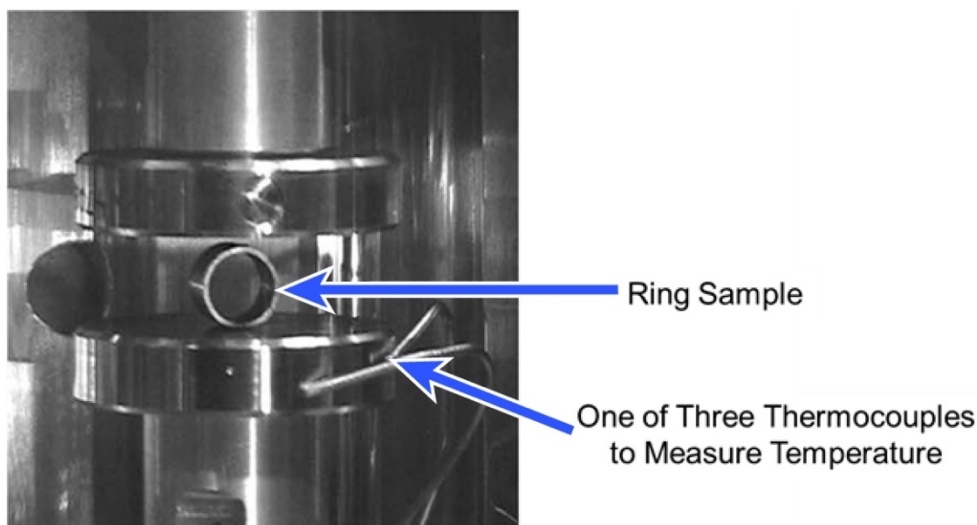


Figure F-10. Ring Compression Test Apparatus.

The ring sample is compressed at a known displacement rate to a maximum change of diameter of 1.7 mm in the compression direction (*adapted from Billone et al. 2008*).

The test apparatus used to conduct RCTs is depicted in Figure F-10 (Billone, Burtseva, and Einziger 2013). The RCTs included unirradiated cladding samples as well as defueled PWR HBF cladding samples that had undergone HRT (see section F.3.2.1) (Billone, Burtseva, and Einziger 2013). Displacement of the cladding test ring diameter in the direction of the applied load was determined as a function of time by means of the constant displacement rate (controlled) and the applied load was measured as a function of time to determine applied load as a function of displacement. Because the cladding samples had been defueled and the fuel pellets were not present to resist cladding compression,¹⁶ the tests used a limited maximum displacement of about 10% offset displacement¹⁷ at room temperature. The ANL testing conducted for the NRC¹⁸ was intended to examine HBF properties under the limiting or worst-case scenario of storage conditions. As a result, this testing program examined cladding that was subjected to HRT at a maximum cladding temperature of 400°C (752°F) and cladding hoop stresses above 90 MPa (~13,000 psi).

The PWR HBF cladding contained hydrogen at concentrations between 300 and 840 wppm. The extensive tests on unirradiated cladding conducted by ANL determined the ranges of hydrogen concentration, cladding hoop stress, and temperature for which radial-hydride-induced degradation (i.e., ductility decrease) would and would not occur; however, when irradiated samples were tested in ranges that were benign for unirradiated cladding,

¹⁶ These tests were originally intended to be performed on fueled samples, but the samples had to be defueled when the ANL hot cells closed, requiring that the tests be conducted in a glove-box facility.

¹⁷ Offset displacement is the total displacement minus the elastic displacement and can be found from examining the load-displacement curves, such as those shown in Figure F-12.

¹⁸ The research sponsored by the NRC was conducted at limiting conditions of temperature and hoop stress, while the follow-on research sponsored by DOE was conducted at both limiting and more typical conditions.

significant ductility decrease was observed (Billone and Liu 2013). The Board notes that there were insufficient data to determine if the differences between the results for unirradiated and irradiated samples were due to a lack of radiation-induced hydrogen traps, differences in the samples' hydrogen profiles, or some other cause. However, this outcome reinforces the view that unirradiated cladding is not an adequate surrogate for irradiated cladding in the context of testing the effects of hydride reorientation. An image of a sample that cracked during an RCT is shown in Figure F-11. It should be noted that this fuel was operated beyond the normal NRC average rod burnup limit of 62 GWd/MTU as part of a special demonstration program (EPRI 2001). The oxide layer on the outside of the cladding (dark grey) is on the far right. The hydrides appear as dark lines within the zirconium cladding.

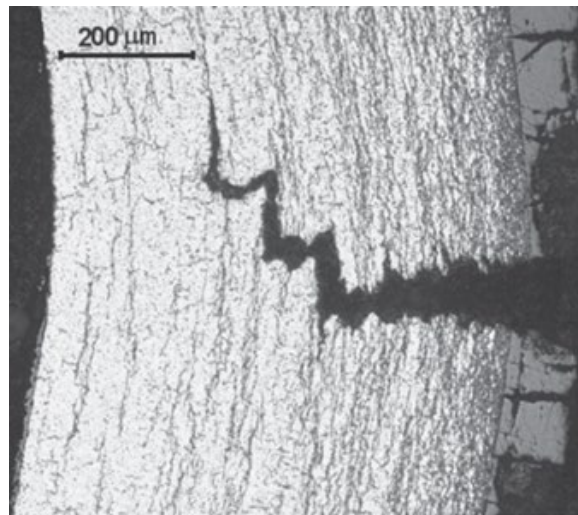


Figure F-11. Example of a cladding sample that cracked during a ring compression test. The specimen was HBF (67 GWd/MTU) Zircaloy-4 after HRT at 400°C (752°F) and 140 MPa (~20,000 psi) (Billone, Burtseva, and Einziger 2013).

For this sample, it can be seen that cracking initiated on the outside of the cladding, at a location of high tensile stress caused by pinching in the RCT apparatus. The crack propagated through the densest concentration of hydrides but stopped near the inside of the cladding where the hydride concentration is lower. The figure also shows that the cracking did not occur solely in the radial direction but followed a path of hydrides that were connected both radially and circumferentially.

A load-displacement curve was generated from each RCT, resulting in the identification of an offset strain.¹⁹ Offset strains from RCTs on several samples of the same cladding over a range of temperatures were then measured, plotted, and used to determine the DTT of the cladding (the temperature at which the cladding began to lose ductility). At ANL, the DTT

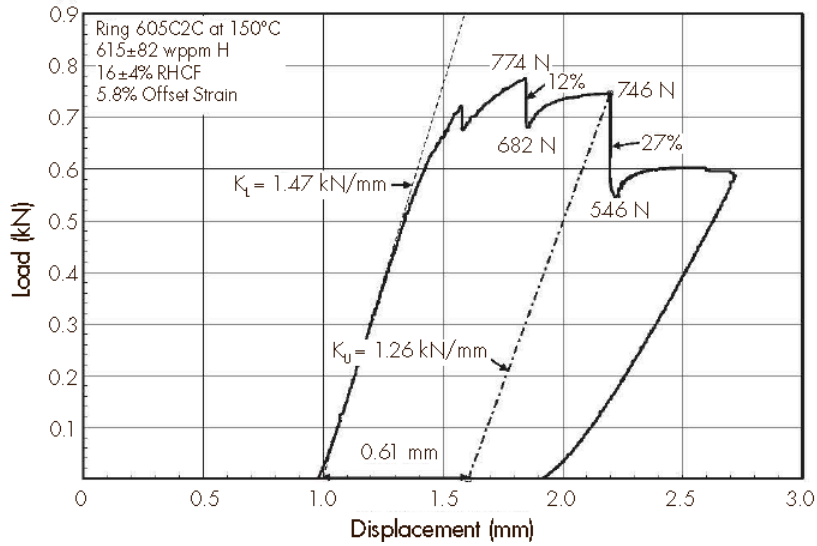
¹⁹ During the compression of the cladding ring in an RCT, the outer diameter change is measured and can be converted to a strain. Part of the change results from elastic strain and the remainder is from inelastic strain. The inelastic strain is the offset strain. It can be determined from the load-displacement curve like that illustrated in Figure F-12B. It is described in ASTM International Standard E8 (ASTM International 2016).

was defined to be the temperature at which an offset strain of less than 2% causes more than a 50% through-wall crack in the cladding during the RCT.

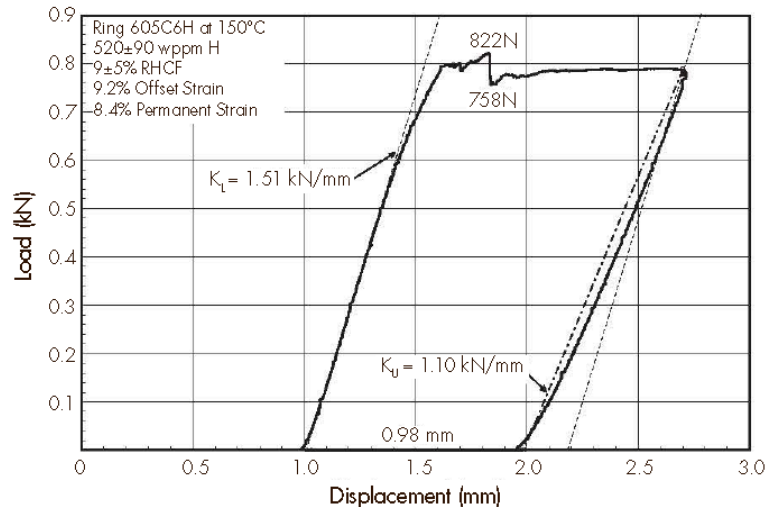
Examples of load-displacement curves for two RCT samples are shown in Figures F-12A and F-12B (Billone, Burtseva, and Einziger 2013). Each of these figures includes, in the upper left corner, information about the cladding sample and conditions under which the RCT was conducted. These are (in order, from left to right and top to bottom): the cladding ring identification number, the RCT temperature, the hydrogen concentration in the cladding, the radial hydride continuity factor (RHCF; explained two paragraphs below), the measured offset strain (as a percentage), and the measured permanent strain (as a percentage).

Figure F-12A shows a cladding sample that did not crack. Note that the small load drop at approximately 1.8 mm of displacement is attributed to a combination of cracking of the oxide layer on the outside of the cladding and possibly cracking in the hydride-rich layer at the outer circumference of the cladding. Figure F-12B shows the load-displacement curve corresponding to a cladding sample that did crack; this is the same sample shown in Figure F-11. Crack propagation is indicated by the sudden drops in load as the displacement increases. The sample that cracked was prepared with a higher initial cladding hoop stress than the sample that did not crack (140 MPa versus 110 MPa [\sim 20,000 psi versus 14,500 psi]). Figure F-12B shows that the sample does not crack all at once but cracks in steps as the ring continues to be compressed. Between each individual cracking event (indicated by a load drop) the remaining intact cladding thickness deforms plastically (indicated by the load rises after each crack) until enough stress has built up again to cause the next crack.

The concept of a radial hydride continuity factor (RHCF) was developed to provide insight regarding why some samples cracked while other samples did not (Burtseva, Yan, and Billone 2010). The history of ring compression testing made it clear that samples with longer grouping of hydrides (continuous sets of overlapping hydride platelets; sometimes called macroscopic hydrides) oriented in the radial direction were more likely to crack than those without such long groupings. RHCF is the ratio of the maximum length of continuous radial hydride to the thickness of the cladding and is often reported as a percentage. The RHCF is determined by examining etched micrographs of the cladding after it has undergone HRT and noting the lengths of the visible, connected radial hydrides. Two radial hydrides connected by a circumferential hydride can be considered as one hydride if they are close to one another. However, in this context, no standardized definition of “close” exists. A discussion of how to determine which hydrides are radial and when the hydrides can be considered continuous can be found in Billone, Burtseva, and Einziger (2013). DOE is currently participating in an ASTM International activity to develop a standard guide for calculating the RHCF.



(A)



(B)

Figure F-12. Load–displacement curves from RCTs on Zircaloy-4 rodlets.

RCTs were conducted on 67 GWD/MTU Zircaloy-4 cladding following HRT at (A) 400°C and 110 MPa (752°F and 16,000 psi) and (B) 400°C and 140 MPa (752°F and 20,000 psi). The sample tested in (A) did not crack and the sample in (B) did crack. Note: KL is the calculated linearized loading force and KU is the calculated linearized unloading force (Billone, Burtseva, and Einziger 2013).

The RCTs were conducted at several temperatures representative of cladding temperatures during transportation, and the offset strain at which a crack extends to greater than 50% wall thickness²⁰ was plotted against the RCT temperature (a typical plot is shown in Figure

²⁰ The total offset strain accumulated prior to a 25% load drop (corresponds to a 50% through-wall crack) is used as the ductility metric. 50% was chosen to ensure that fuel-rod cladding would hold pressure, which indicates the cladding would not experience a gross breach.

F-13) (Billone and Liu 2014; IAEA 2015). An offset strain of less than 2% was chosen as an indication of loss of ductility (Billone, Burtseva, and Einziger 2013). For offset strains $\geq 2\%$, there is high confidence that enough ductility has been retained that cladding with similar properties would not experience a gross breach when subjected to large mechanical shocks, as in a transportation accident. For offset strains $\leq 1\%$ there is high confidence that the sample is brittle and would likely breach when subjected to large mechanical shocks that are perpendicular to the radial hydrides. For offset strains greater than 1% and less than 2%, there is high uncertainty that ductility has been retained.

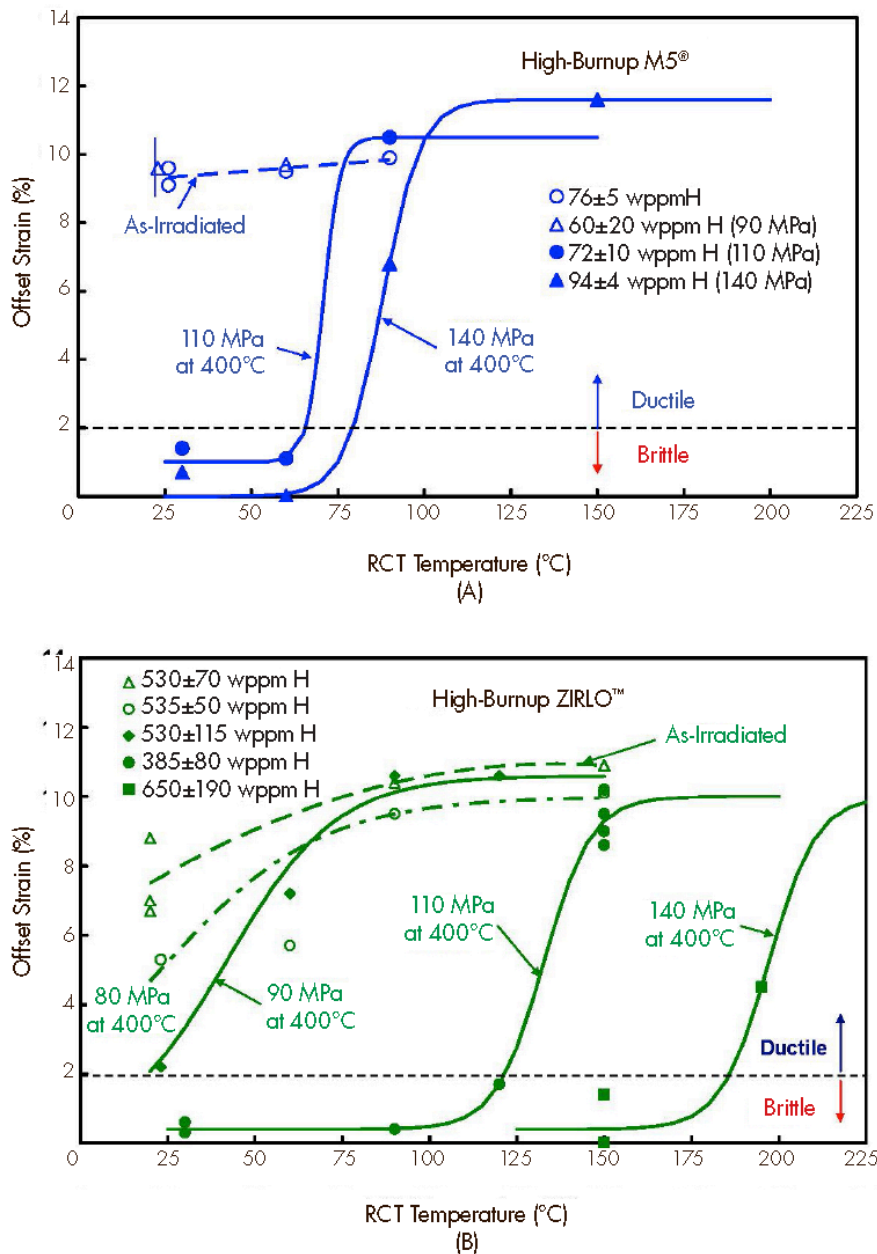


Figure F-13. Effect of maximum cladding hoop stress on cladding ductility. (A) Plots of offset strain versus temperatures for HBF M5® cladding. (B) Plots of offset strain versus temperature for HBF ZIRLO® cladding (Billone et al. 2013).

For a given cladding type with a given operational history (i.e., a single curve in Figure F-13), Figure F-13 clearly shows that the offset strain at which the sample showed greater than 50% through-wall cracking decreases with decreasing RCT temperature. The RCT temperature at which the offset strain drops below 2% is called the ductility transition temperature or DTT (Billone, Burtseva, and Einziger 2013).²¹

While hydride reorientation may occur during drying and storage of HBF, the effect of hydrides on cladding performance is a function of cladding temperature during transportation. If transport occurs at low temperature after extended storage, any hydride reorientation that occurred as a result of the drying process might result in a cladding breach in the event of an accident: “Depending on the concentration of hydrogen in the cladding and the size, distribution, orientation, and location of ZrH₂, the spent fuel cladding could become less ductile with decreasing storage temperatures such that the stresses on the cladding when applied at high strain rates could cause fracture of the cladding under transportation accident conditions” (Gruss, Brown, and Hodges 2003).

Figure F-13 depicts RCT results for as-irradiated cladding samples (no HRT) and cladding samples subjected to HRT at 400°C (752°F) and various hoop stresses (as indicated in Figure F-13) and then cooled at 5°C/hour (9°F/hour) with decreasing pressure and stress (Billone 2016; Billone et al. 2013). Figure F-13A represents high burnup M5[®] cladding (72 GWd/MTU for the as-irradiated sample and 68 GWd/MTU for the other three samples), while Figure F-13B represents high burnup ZIRLO[®] cladding (68 GWd/MTU for all samples). Although the DTT values for the two cladding types are different, there are two clear trends: 1) DTT increases with increasing hydrogen concentration (and thus, increasing hydride concentration); and 2) DTT increases with increasing hoop stress applied during HRT.

The ring compression test is a scoping test to determine the temperature range where ductility of the HBF cladding decreases. It is not a direct measure of the ductility itself. Therefore, any uncertainties in the RCT results propagate as uncertainties in the temperature range over which the ductility changes, not uncertainties in the cladding ductility itself. The RCTs at ANL were conducted using a specific range of forces; however, the actual loads the HBF could experience in a side drop accident depend on the exact nature of the accident and the energy absorbed by the SNF transportation cask system. In addition, any energy transmitted to the rods depends on the integrity of the spacer grids, guide tubes, and end nozzles in the fuel assembly. Without knowing the relationship between the actual force profile the cladding might experience in an accident and the forces applied in the tests, there remains significant uncertainty about the relevance of the experimental conditions that lead to cladding cracking and thus, the extent to which hydride reorientation should be of concern.

²¹ Previously, the DTT had been called the ductile-brittle transition temperature (DBTT). Typically, DBTT is interpreted by metallurgists to mean that most materials subjected to tensile stress fail below the DBTT and do not fail above the DBTT. Since there are no data to imply this absolute transition will be the case with irradiated cladding material, DBTT has been dropped in some circles. The term DBTT, applied to irradiated cladding, may be found in older and international literature.

F.3.2.3 International Research

By the early 2000s, hydride reorientation research was also being conducted in Japan, Korea, Taiwan, Germany, France, Switzerland, Canada, India, Sweden, and Spain. Many of these countries are still working to determine the effects of hydride reorientation and identify storage and transportation conditions under which hydride reorientation is not an issue. Unfortunately, because there was no consistent methodical attempt at the start of this research to standardize sample conditions and testing protocols, it is difficult to compare hydride reorientation testing results among countries. This international work was evaluated and considered when DOE established, as a high priority, the need to study hydride reorientation in HBF (Hanson et al. 2012).

Three conferences dedicated to the hydride reorientation phenomena have been convened.

1. A symposium sponsored by ASTM International in Anaheim, California, in 2007.
2. A workshop sponsored by Gesellschaft für Anlagen-und Reaktorsicherheit in Hanover, Germany in 2008. No proceedings were published.²²
3. In June 2014, ASTM International held a workshop in Jackson, Wyoming, to address some of the outstanding and sometimes conflicting information on hydride reorientation and its ramifications. In addition to presenting results from the various international testing programs, the workshop included discussions of parameters that affect hydride reorientation, the pros and cons of various types of testing methods for hydride reorientation and DTT, methods to quantify the degree of hydride reorientation, and standards needed to resolve the differences in results from the various testing programs. The information from that workshop was analyzed by three participants who produced a white paper evaluating the information and suggesting further work required to resolve uncertainties (Sindelar, Louthan, and Hanson 2015).

An extensive analysis of the worldwide work being done on hydride reorientation comprised a significant part of an IAEA report (IAEA 2015) that determined there are still many outstanding issues that need to be resolved (see section F.3.4).

To date, non-DOE research, both international and domestic, has qualitatively shown that:

1. The higher the hoop stress on the cladding due to the internal rod pressure, the more likely it is that hydride reorientation will occur (Burtseva, Yan, and Billone 2010). Much of the ANL hydride reorientation research has been conducted with cladding hoop stresses greater than those expected in normal rods (now expected to be below 90 MPa [\sim 13,000 psi] at maximum temperature) (Billone 2018) and at levels that should bound the higher hoop stresses that might be expected in integral burnable absorbers rods containing boron. The publicly available data on the post-

²² Gesellschaft für Anlagen-und Reaktorsicherheit Project and Workshop on Behavior of LWR [light water reactor] Spent Nuclear Fuel under Transport Accident Conditions, December 4–5, 2008, Hannover, Germany.

irradiation internal rod pressure are somewhat limited, as most of these data are proprietary (EPRI 2013; Billone and Liu 2014).

2. The extent and consequences of hydride reorientation depend on several factors, including the type of cladding material, the manufacturing technique, the maximum temperature the cladding reaches, the maximum hoop stress in the cladding, the cooling rate, and possibly the number of drying cycles (Aomi et al. 2008).
3. Unirradiated Zircaloy cladding charged with hydrogen is a poor surrogate for SNF cladding for determining hydride reorientation effects, particularly if hydrogen is uniformly distributed throughout the unirradiated cladding (Sindelar, Louthan, and Hanson 2015).
4. Lined BWR cladding, such as that shown in Figure F-3, behaves differently than PWR cladding with respect to hydride reorientation by preferentially absorbing hydrogen in the pure zirconium liner (Valance et al. 2015).
5. Testing has produced mixed results regarding the effect of multiple drying cycles on the amount of hydride reorientation (Kammenzind et al. 2000; Chu et al. 2007; Billone, Burtseva, and Martin-Rengel 2015). The Paul Scherrer Institute in Switzerland found that increasing the number of thermal cycles from one to three at a maximum temperature of 420°C (788°F)²³ promotes additional hydride reorientation (IAEA 2015). In contrast, ANL conducted thermal cycling (three cycles) between 400 and 300°C (752 and 572°F) prior to cooling the samples to 200°C (392°F) at a peak hoop stress of about 90 MPa (~13,000 psi) and found no appreciable change in hydride reorientation and cladding ductility (Billone, Burtseva, and Martin-Rengel 2015).

Based on the ANL work, the NRC observed, “the results suggest that multiple drying cycles have no effect on the length of radial hydrides or the DTT at [90 MPa (~13,000 psi)]” (NRC 2020). Furthermore, DOE has not identified a technical information need that warrants more research on multiple drying cycles (Teague et al. 2019).

F.3.3 DOE Research to Examine the Effects of Hydride Reorientation

In 2012, DOE identified two high-priority technical information needs regarding the behavior of cladding hydrides during storage and transportation (Hanson et al. 2012; see Appendix B for more information on DOE’s technical information needs). The first high priority issue was the potential for hydride reorientation and the effect of hydride reorientation on the structural performance of the cladding during transportation. The second issue was whether DHC is an active degradation mechanism during storage. In later assessments of technical information needs, DOE determined that DHC could be downgraded to medium and then to low priority (e.g., see Teague et al. 2019). The reasons for this downgrade are discussed in section F.4.2.

The DOE research program on hydride reorientation includes several research projects and the focus and level of effort is periodically reassessed based on experimental results and on

²³ The report of testing in Switzerland (IAEA 2015) did not mention the temperature at the low end of the cycle.

new evaluations of the technical information needs (Saltzstein et al. 2017). Completed and ongoing research efforts at ANL, Oak Ridge National Laboratory (ORNL), Pacific Northwest National Laboratory (PNNL), and SNL are discussed below.

At ANL, DOE continued to fund the HRT and RCT program started by the NRC. DOE's research expanded the original range of NRC testing to include a greater range of cladding hoop stresses that are more relevant to actual HBF; lower reorientation temperatures (350°C [662°F]) that are more typical of actual maximum drying and storage temperatures; the effect of possible multiple drying cycles; and testing of more cladding types (Billone, Burtseva, and Martin-Rengel 2015; Billone and Burtseva 2016; Billone 2019; Billone and Burtseva 2020).

DOE also continued the NRC-initiated effort to conduct static bend tests and fatigue tests of HBF cladding samples at ORNL using the Cyclic Integrated Reversible-Bending Fatigue Tester (CIRFT). These tests include BWR cladding, cladding with induced hydride reorientation, and fueled cladding—with fuel pellets still inside the cladding (Wang et al. 2015; Wang et al. 2016; Wang et al. 2017). The static and cyclic bend testing at ORNL is expected to provide more data about the performance of HBF during normal conditions of transport and in certain postulated accident conditions during transport. See Appendix H for more details about the CIRFT testing. ORNL continues to test HBF cladding segments in the CIRFT as part of a broader DOE research program on HBF, which is described below.

Under contract to DOE and in cooperation with EPRI, SNL has managed the High Burnup Dry Storage Research Project (HDRP),²⁴ which is a broad, coordinated effort to study the behavior of HBF during drying, storage, and transport operations (EPRI 2014; Saltzstein et al. 2017). The aspects of the HDRP relevant to HBF and hydride reorientation include non-destructive and destructive examinations of HBF rods and CIRFT research at ORNL, HBF rod examinations and internal gas pressure measurements at PNNL, and HRTs and RCTs of defueled HBF cladding segments at ANL. More details about the HDRP can be found in Appendix G.

Much of the work associated with the HDRP continues, particularly destructive examinations of the HDRP sister rods. Key trends and results from DOE-sponsored research on hydride reorientation are discussed in the following subsections. Based on the testing and data collected as of early 2019, DOE published a preliminary conclusion regarding hydride reorientation in HBF (Teague et al. 2019):

“With the exception of confirmatory testing being conducted under the sister rod test program, the TIN [technical information need] (or data gap) related to hydride reorientation is essentially closed. Results of the RCTs, HDRP testing, and SNF cask transport tests, examined as integrated effects from actual temperature, actual hoop stress, and realistic external loads, indicate that risks associated with hydride reorientation and embrittlement to cladding integrity

²⁴ The HDRP has been referred to by different names, depending on the organization reporting on the project. For example, some DOE reports refer to the project as the High Burnup Spent Fuel Data Project.

of SNF are low for current fuel designs, burnups, and reactor operational limits [in] the United States.”

F.3.3.1 Testing at Lower Maximum Hoop Stresses

The NRC-sponsored program at ANL included HRTs conducted at hoop stresses primarily above 100 MPa in order to bound the hoop stresses expected in the nation’s HBF population, including HBF rods with integral burnable absorbers. More recent evaluations of the expected hoop stress in HBF cladding indicate that the hoop stress may be significantly lower than 100 MPa (Billone and Burtseva 2016). ANL performed additional cladding HRTs at hoop stresses as low as 80 MPa (~11,600 psi) and then completed RCTs on those cladding specimens. Billone (2018) concluded that significant hydride reorientation could occur in ZIRLO® and Zircaloy-4 cladding only if cladding hoop stress at maximum temperature is greater than 80 MPa (~11,600 psi).

In 2019, ORNL and PNNL measured rod internal pressures in HBF “sister rods”²⁵ from the HDRP, which included M5®, ZIRLO®, Zircaloy-4, and low-tin Zircaloy-4 cladding types. These measurements confirmed that the rod internal pressures were below 5 MPa (725 psi) at 25°C (77°F) and consistent with rod internal pressures measured in other HBF rods in the past (Montgomery et al. 2019, Shimskey et al. 2019). For comparison, a rod internal pressure of 5 MPa (725 psi) at 25°C (77°F) is equivalent to a hoop stress of approximately 81 MPa (~11,700 psi) at 400°C (752°F), neglecting the change in rod free volume with temperature. Researchers at ANL noted that “[e]xtrapolation of 5 MPa (725 psi) to drying-storage temperatures, and accounting for the fuel rod external pressure during storage, suggests that peak hoop stresses will be too low to cause radial-hydride-induced embrittlement” (Billone and Burtseva 2020). The Board notes that this conclusion applies to the HDRP sister rods and does not include other HBF with integral burnable absorber rods containing boron.

As of December 2020, the sister rod destructive examinations continue at ORNL and ANL and will include HBF rod segments that experienced lower maximum temperatures and pressures as well as those that were experimentally heated at ORNL to 400°C (752°F) (and experienced higher cladding hoop stresses) (Montgomery et al. 2019). The ongoing testing is expected to include static bend tests, cyclic fatigue tests, RCTs, axial tension tests, and microhardness tests.

As discussed in Section F.3.1, Chung (2004) compiled data on low burnup SNF suggesting that hydride reorientation can be precluded if the maximum cladding hoop stress is maintained below 90 MPa (~13,000 psi). However, as observed by ANL, certain HBF cladding types may be susceptible to hydride reorientation after experiencing a maximum cladding hoop stress that is less than 90 MPa (~13,000 psi). For example, some ZIRLO® cladding specimens experienced hydride reorientation after HRT at 400°C (725°F) and 89 MPa (~12,900 psi) (Billone, Burtseva, and Martin-Rengel 2015) and some M5® cladding specimens experienced hydride reorientation after HRT at 350°C (662°F) and 89 MPa

²⁵ A sister rod is a rod that has similar characteristics to one that is stored in the HDRP test cask. There were two potential fuel assembly types that could be donors for sister rods: (1) assemblies having similar operating histories to those assemblies chosen for storage in the HDRP test cask; or (2) actual fuel assemblies selected for storage in the cask. See Appendix G for more details.

(~12,900 psi) (Billone and Burtseva 2016). Although these two examples include hoop stress values that are close to 90 MPa (~13,000 psi) (within experimental uncertainty), limited data are available on the formation of radial hydrides in various cladding types with various operating histories in these lower ranges of hoop stress. The Board observes that until more testing is done on more HBF cladding types with more varied operating histories, considerable uncertainty will remain regarding the lower limits of cladding hoop stress that will contribute to hydride reorientation.

However, the Board notes two points that mitigate the concern regarding hydride reorientation at lower hoop stresses. First, as noted above, the body of DOE research to date indicates a low likelihood of radial hydride formation in HBF. Second, DOE testing of surrogate SNF assemblies in normal conditions of transport indicates low levels of loading on the cladding such that the probability of a cladding breach is low, even if radial hydrides are present in the cladding.

F.3.3.2 Testing at Lower Maximum Temperatures

As part of the HDRP, PNNL, among others, developed a detailed thermal model for SNF dry cask storage systems. The PNNL model accounts for the actual burnup and associated best-estimate decay heats for SNF rods, rather than bounding, or worst-case values, that are used in license applications. The SNF cladding temperatures predicted using best-estimate inputs are significantly lower than the temperatures estimated in license applications (Hanson 2016). For example, industry calculations for the maximum cladding temperatures used in licensing the HDRP cask (see Appendix G) predicted peak cladding temperatures of 350°C (662°F), while the PNNL model predicted peak cladding temperatures of approximately 270°C (518°F) (Hanson 2016). The PNNL thermal model, as well as other industry thermal models, were validated using temperatures measured in the HDRP cask during and after vacuum drying (see Appendix G).

The Board notes that the lower temperatures found in the HDRP cask do not imply that all casks or canisters will have fuel with a maximum cladding temperature at or below 270°C (518°F), because the maximum temperature depends on several factors, such as fuel burnup, cooling time, cask or canister design, and the drying process used. However, the HDRP thermal modeling results indicate that actual maximum cladding temperatures may be systematically lower than those predicted in licensing basis documents. The lower cladding temperatures measured in the HDRP cask provided the impetus for DOE to test for hydride reorientation at lower temperatures.

At ANL, HRTs were conducted on samples of high burnup ZIRLO® (hydrogen concentration of 350–650 wppm) at hoop stresses of about 88 MPa (~12,800 psi) and maximum cladding temperatures of 350°C (662°F) and 400°C (752°F) (Billone, Burtseva, and Martin-Rengel 2015). The length of the resulting radial hydrides and the DTT were approximately the same in both cases. However, the DTT rose from approximately 25°C (77°F) following HRT at a cladding temperature of 400°C (752°F) at a peak hoop stress of about 88 MPa (~12,800 psi) to approximately 120°C (248°F) following HRT at a cladding temperature of 350°C (662°F) and peak hoop stresses of 93–94 MPa (~13,500–13,600 psi) (Billone, Burtseva, and Martin-Rengel 2015). These results were unexpected because significantly less hydrogen goes into solution at 350°C (662°F) than at 400°C (752°F) (about 120 wppm at 350°C [662°F] compared to about 200 wppm at 400°C [752°F]). Therefore, there is less hydrogen available

to form radial hydrides when the cladding cools, less reduction of ductility, and a lower expected DTT.

To explore this unexpected result further, ANL conducted additional HRTs at 350°C followed by RCTs on high burnup ZIRLO® cladding (Billone 2019; Billone and Burtseva 2020). The test results show that the ductility and DTT for ZIRLO® are highly sensitive to the peak cladding hoop stress in the range of 90±5 MPa at 350°C (~13,000±725 psi at 662°F) during HRT. To illustrate, following HRTs at a maximum temperature of 350°C and a hoop stress of 87 MPa (~12,600 psi), a series of RCTs showed the DTT to be approximately 28°C (82°F); in contrast, following HRTs at a maximum temperature of 350°C (662°F) and a hoop stress of 95 MPa (13,800 psi), a series of RCTs showed the DTT to be 138±5°C (280±41°F) (Billone 2019).

At ORNL, HDRP sister rod testing, including non-destructive examinations, destructive examinations, static bend tests, and cyclic fatigue tests have been and continue to be conducted (Montgomery et al. 2018, Montgomery et al. 2019, Montgomery and Bevard 2020). All 25 HBF sister rods experienced relatively low temperatures when they were removed from their respective SNF assemblies, loaded in a transport cask, dried, and transported to ORNL (EPRI 2019). However, three sister rods were subjected to a full-rod heat treatment at ORNL to achieve a maximum temperature of approximately 400°C (752°F) in order to simulate the maximum cladding temperature allowed by the NRC. This will allow a comparison of the effects of high cladding temperature versus lower cladding temperature on the characteristics of HBF cladding. As of December 2020, some early results of the sister rod destructive examinations had been reported (Montgomery et al. 2019, Montgomery and Bevard 2020).

The Board notes that the results of the HDRP so far indicate that SNF cladding temperatures in dry cask storage systems are likely to be much lower than the cladding temperatures postulated in applications to the NRC for approval of SNF storage or transportation, and the lower cladding temperatures mean there will be less hydride reorientation.

However, as indicated by recent research at ANL on ZIRLO® cladding, hydride reorientation may be significant even when the cladding is subjected to lower maximum temperatures (i.e., 350°C [662°F] versus 400°C [752°F]). This is because other factors—in this case, cladding hoop stress—can play an important role in the formation of radial hydrides. A similar situation is observed in M5® cladding, where more radial hydrides are formed after HRT at 350°C (662°F) than are formed after HRT at 400°C (752°F) (Billone and Burtseva 2016; also see section F.3.3.4). In this case, the recrystallized-annealed microstructure of M5® cladding may be an important factor, as well as differences in hydrogen concentrations in the samples (i.e., the former sample [HRT at 350°C (662°F)] had a hydrogen concentration of 80±7 wppm and the latter sample [HRT at 400°C (752°F)] had a hydrogen concentration of 58±15 wppm).

Given the large number of factors that can affect the formation of hydrides and the occurrence of hydride reorientation (see the list of factors in section F.2), no simple generalizations can be made about when hydride reorientation may occur. Limiting HBF cladding temperatures to a maximum temperature of 400°C (752°F) is no guarantee, by itself, that hydride reorientation will be precluded. Unless and until extensive testing is done to examine all cladding types, subjected to a wide range of operating conditions, including

lower maximum cladding temperatures, some uncertainty remains about the formation and extent of hydride reorientation.

F.3.3.3 Testing Fueled versus Defueled Cladding Samples

Conducting tests on defueled cladding samples (with no fuel pellets inside) is less hazardous and less expensive than doing the same tests on fueled cladding. For these reasons, some of the testing on HBF cladding is done using defueled cladding. There are additional pros and cons for testing with defueled cladding as well as implications for how the test results may be interpreted when considering HBF behavior during normal conditions of transport and in hypothetical accident conditions, like a side drop accident. These issues are discussed in more detail below.

Testing relevant to normal conditions of transport.

At ORNL, a test device called the CIRFT is used in the static bending mode to measure the flexural rigidity of SNF cladding (see Appendix H for more details about testing with the CIRFT). The flexural rigidity is an important measure of the cladding's resistance to cracking or fracture that could be caused by a shock load such as that which may be experienced in a drop during handling.²⁶ When used in the cyclic mode, the CIRFT can determine the fatigue strength (or fatigue lifetime) of SNF cladding. The fatigue strength of the cladding is important to know when considering the cumulative vibration loads that may occur over the course of a long trip, such as a cross-country transport.

CIRFT testing at ORNL on fueled cladding has shown that “the interface bonding efficiency at the pellet-pellet and pellet-cladding interfaces can significantly dictate the SNF system dynamic performance” (Jiang, Wang, and Wang 2016). If there is full pellet-pellet bonding and pellet-cladding bonding, the fuel pellets can carry most of the bending moment, thereby increasing the fuel rod's flexural rigidity and its resistance to fracturing under large applied tensile stresses. To further examine this issue, ORNL conducted additional CIRFT static bend tests with the fueled cladding. The results from the tests indicate that the fuel pellets do strengthen the pellet-cladding composite system by a factor of about two if the pellet-cladding bond is maintained (Wang and Wang 2017). However, CIRFT results have also shown that, at the dished ends of the pellets, the pellet-pellet bonds are easily broken under cyclic bending loading (Jiang, Wang, and Wang 2016). More details about testing HBF to assess the effect of transportation loads can be found in Appendix H.

The effect of bonding of surrogate stainless-steel pellets to surrogate unirradiated copper cladding has also been studied (Zargar, Medina, and Ibarra 2017). The results obtained on the vibration response of surrogate copper cladding indicate that bonding (using epoxy) of the pellets to the cladding results in a total rod flexural rigidity equal to the rigidity of the copper cladding plus up to 15% of the flexural rigidity of the pellets. For the case of the pellets and the cladding simply in contact (but not bonded with epoxy), the contribution of the steel pellets to the total rod flexural rigidity is negligible.

²⁶ The NRC's regulation on SNF transportation, 10 CFR Part 71, includes a 30-cm (1-ft) drop of a package containing SNF as part of normal conditions of transport that should be addressed in a transportation safety analysis report.

The Board observes that NRC- and DOE-sponsored research indicates the pellet-pellet bonding and pellet-cladding bonding add strength to the fuel pellet-cladding composite system. However, the extent of the pellet-pellet bonding and the pellet-cladding bonding, both circumferentially and axially, in a given fuel rod is difficult to predict or measure. Additionally, the persistence of the pellet-pellet and pellet-cladding bonds throughout a fuel rod's lifecycle (e.g., cooling, loading, vacuum drying, transporting) is not known. Unfortunately, determining the extent and persistence of the bonding would require detailed, time-consuming, and expensive non-destructive examinations of each type of fuel irradiated under different conditions.

The Board notes also that fatigue strength and flexural rigidity test results using defueled cladding may be considered by some to be unrealistic or too conservative because the cladding lacks the composite strength imparted to the cladding by the fuel pellets, which are often strongly bound to the cladding in HBF. However, if the performance of the cladding without the additional strength provided by the pellets is adequate in making a case for safe transportation, then continued testing of defueled HBF cladding can be considered to be acceptable.

Testing relevant to hypothetical accident conditions.

As discussed in section F.3.2.2, RCTs are used to examine the ductility of HBF cladding in a pinch mode of loading, which hypothetically could occur in a side-drop accident during transportation. At ANL, RCTs have been completed on defueled cladding. However, testing defueled cladding does not account for the presence of the fuel pellets inside the cladding, which will physically limit the amount of deformation the cladding can experience in the pinch mode of loading as discussed below. At ANL, the maximum compression allowed during RCTs was 10% offset displacement, which, in many cases, equaled approximately 1.7 mm (Billone, Burtseva, and Garcia-Infanta 2017; see section F.3.2.2).

At ORNL, HDRP sister rod destructive examinations continue, and among the tests completed in 2020 were RCTs on cladding segments that still contained fuel pellets (Montgomery and Bevard 2020). The RCTs were conducted on specimens representing all four cladding types in the HDRP (M5[®], ZIRLO[®], Zircaloy-4, and low-tin Zircaloy-4) but ORNL found that cladding type had little effect on the RCTs results. Based on preliminary RCT data,²⁷ ORNL reported that “[t]he load-bearing capability of the fueled specimen is about eight times higher than that of a defueled cladding specimen” (Montgomery and Bevard 2020), again confirming that the fuel pellets add load-bearing strength to the pellet-cladding composite system.

To further examine the behavior of HBF cladding in the pinch mode of failure, it is useful to consider the geometry of a fuel rod. Nuclear fuel rods are manufactured with a gap between the fuel pellets and the inside of the cladding (Olander 2009). During irradiation in a reactor, several phenomena occur affecting the size and the nature of this gap. Over time, the fuel pellets accumulate fission product gases and swell, reducing the size of the pellet-cladding gap. At the same time, the coolant pressure on the outside of the cladding compresses the cladding, assisted by radiation creep, further reducing the gap. For HBF, there is often

²⁷ ORNL reported that the RCT data published in Montgomery and Bevard (2020) had not yet been corrected for “machine compliance,” i.e., deformations associated with the load frame, load cell, and grips in the RCT device.

complete closure of the gap and significant bonding of the pellets and the cladding (Olander 2009). Conversely, the fuel pellets crack due to thermal stresses during reactor operation, creating void spaces filled with fission product gases. Finally, fuel assembly movements during core refueling and subsequent operations can result in changes to the fuel pellet power level, temperature profile, and thermal expansion, further affecting the size of the pellet-cladding gap. All these effects, which will vary in degree depending on the fuel type, tend to leave some void space at different locations inside the fuel rod.

The Board offers a simple analysis of the size of the pellet-cladding gap and its implications for the onset of a cladding crack. As the cladding compresses during an RCT or during a side drop resulting in pinch mode loading, the diameter of the cladding will be reduced until the pellet-cladding gap, if it still exists, closes and the pellet fragments are compressed together. At this point, the cladding can compress no further. If the RCTs using defueled cladding show that the development of the first cladding crack requires more compression of the cladding than is possible with the fuel pellets present, then real HBF rods (with fuel pellets) will not develop cracks during the side drop accident. Two measurements are needed to estimate whether cladding compression in a pinch mode accident may lead to cracking:

1. *The amount of cladding compression needed before a crack develops.* This can be determined by observing when the first significant crack appears in an RCT load versus displacement plot, such as the one shown in Figure F-12B. In this case—Zircaloy-4 HBF cladding with a high concentration of radial hydrides—the displacement necessary to crack the cladding is approximately 800 μm . The exact amount of displacement or compression needed to cause a cladding crack will vary from cladding type to cladding type and will depend on many other conditions (burnup, corrosion [and subsequent hydrogen absorption], maximum cladding temperature, maximum cladding hoop stress, etc.).
2. *The gap or spacing available for the cladding to compress.* The pellet-cladding gap in HBF is expected to be small or non-existent. However, as a worst-case, hypothetical condition for this analysis, the gap can be estimated based on the as-manufactured dimensions of the fuel rod. For typical PWR fuel, the gap size is approximately 80 μm (Buongiorno 2010). An alternative method for estimating the available space inside the fuel rod is to assume the pellet-cladding gap has closed and determine the total amount of fuel fragment spacing by applying the FRAPCON model to HBF fuel. Using the FRAPCON model, Raynaud and Einziger (2015) estimated that after five years in dry storage, the inter-fragment space would be equivalent to a gap of 40–80 μm , assuming an evenly-spaced gap around the circumference of the fuel rod.

One source of uncertainty for this latter estimate arises from the characteristics of very high-burnup fuel. In very high burnup fuel rods (i.e., fuel rods with burnups near the maximum allowed rod-average burnup of 62 GWd/MTU), the fine-grain structure of the rim region at the outer surfaces of the fuel pellets (see Appendix A) may result in the pellets having a lower compressive-load-bearing capacity than pellets in lower-burnup fuel rods. With less resistance from the pellets to compressive loading, the cladding of these very high burnup fuel rods may continue to compress after the cladding contacts the pellet. However, as noted above, a competing effect is the fact

that at higher fuel burnups, the pellet-cladding gap is likely to be small or non-existent.

So, based on these measurements and estimates, the largest available gap between the pellet and the cladding is approximately 80 μm . This applies to the pellet-cladding gap in one radial direction. Therefore, the full size of the gap, when considering the full circumference of the fuel rod, can be approximately 160 μm . This analysis shows that the compression needed to cause the first crack during the RCT of Zircaloy-4 HBF cladding—a compression (displacement) of 800 μm —is more than four times the displacement possible in HBF cladding containing fuel pellets (160 μm). In this example, it can be concluded that it is very unlikely that HBF with Zircaloy-4 cladding would crack in a pinch mode accident. However, given the large number of variables affecting HBF cladding, this conclusion could vary considerably from fuel type to fuel type.

This simplified analysis shows that conducting RCTs with defueled cladding is likely to provide conservative results relative to the ductility of HBF cladding and the performance of HBF cladding in hypothetical accident conditions that include a side drop with pinch mode loading on the cladding.

F.3.3.4 Testing Additional Cladding Types

PWR SNF with M5[®] Cladding. Niobium-bearing zirconium alloys containing less than 1 wt.% tin typically have lower hydrogen contents after irradiation than other PWR cladding alloys since they corrode less in the reactor. M5[®] cladding, which has no tin and a recrystallized-annealed microstructure, experiences particularly low in-reactor corrosion (oxide layers are typically thinner than 15 μm) and low hydrogen content (less than 130 wppm). As a result, if there is sufficient hoop stress at the maximum cladding temperature, all the hydrogen in the cladding circumferential hydrides will go into solution and will be available to precipitate as radial hydrides as the cladding cools (Figure F-14) (Billone 2016).

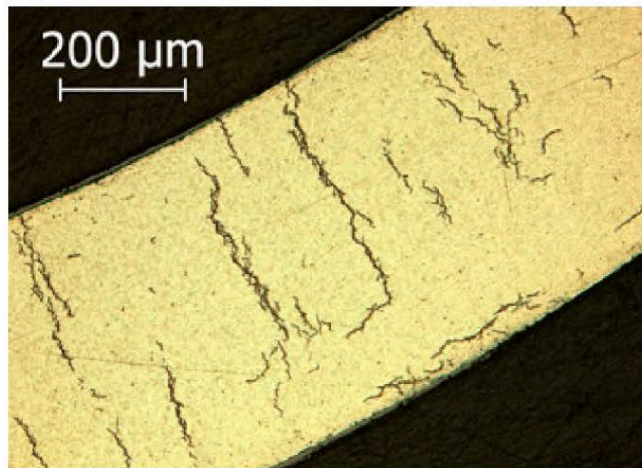


Figure F-14. Micrograph of radial hydrides in M5[®] cladding.

These radial hydrides formed in high burnup (68 GWd/MTU) M5[®] cladding after being subjected to 111 MPa (16,199 psi) hoop stress at 400°C (752°F). The sample contains 72 \pm 10 wppm hydrogen (Billone *et al* 2013).

The DOE-sponsored research at ANL expanded the scope of the HRT and RCT efforts to include cladding types not tested under the NRC-sponsored program (Billone, Burtseva, and Liu 2012). As part of that work, ANL conducted testing on M5® cladding samples over a range of maximum temperatures and maximum cladding hoop stresses.

In one particular M5® cladding sample, when tested at a hoop stress of 90 MPa (~13,000 psi) and a maximum cladding temperature of 400°C (752°F) during HRT, hydride reorientation had no effect on the ductility (open triangle symbols in Figure F-15). However, for another M5® cladding sample tested at a maximum cladding temperature of 350°C (662°F) and 89 MPa (~12,900 psi) hoop stress during HRT (red line in Figure F-15), there was a reduction in cladding ductility caused by the hydride reorientation. Billone, Burtseva, and Garcia-Infanta (2017) suggested that the difference in cladding behavior between these two samples may be caused by differences in the degree of continuity of the radial hydrides and differences in total hydrogen content (i.e., the former sample [HRT at 400°C (752°F)] had a hydrogen concentration of 58 ± 15 wppm and the latter sample [HRT at 350°C (662°F)] had a hydrogen concentration of 80 ± 7 wppm). ANL continues to conduct HRTs, metallographic examinations, and RCTs on HDRP sister rod cladding segments, including segments made of M5® (Billone and Burtseva 2020).

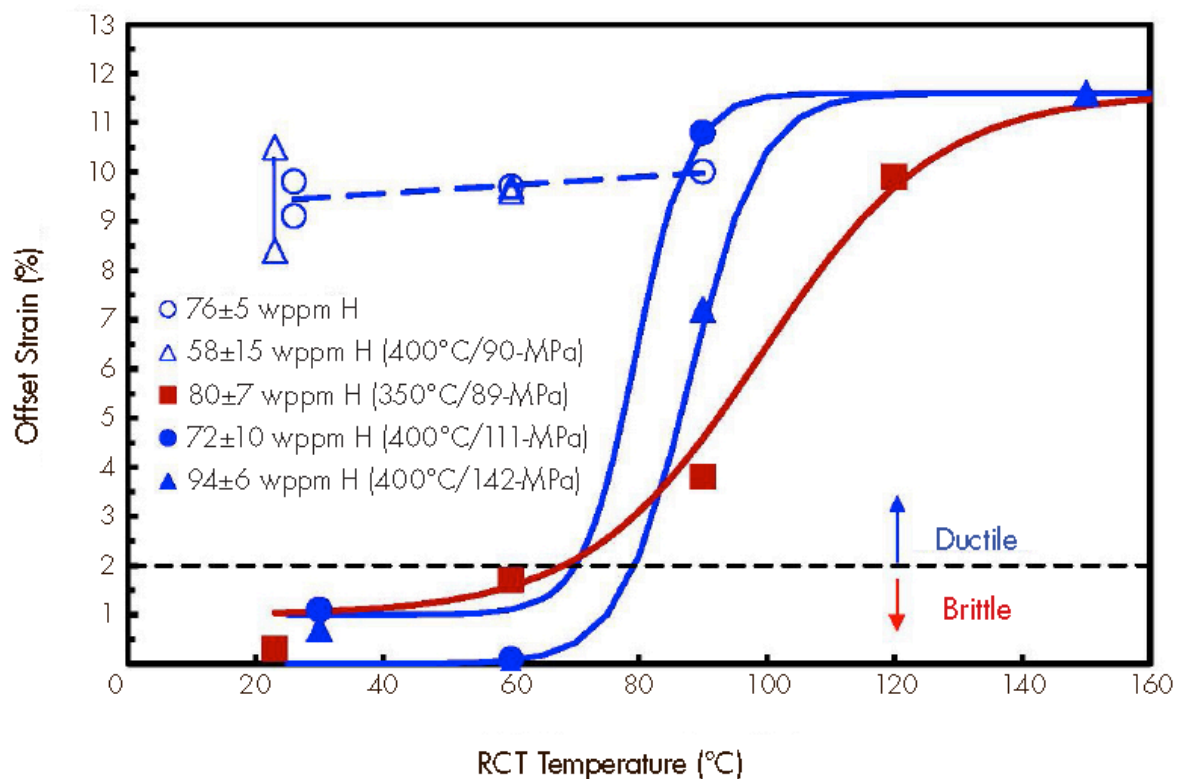


Figure F-15. RCT ductility curves for high burnup M5® cladding.

The burnup of the cladding was 72 GWd/MTU. The open blue circles (no loss of ductility) indicate data obtained from RCTs on cladding that was not subjected to HRT. The open blue triangles (no loss of ductility) indicate data obtained from RCTs on cladding that was subjected to HRT at 400°C (752°F) and 90 MPa (~13,000 psi) but had a low hydrogen concentration (58 ± 15 wppm). Solid symbols represent cladding that experienced a reduction in ductility after HRT at the indicated temperatures and hoop stresses. (Billone and Burtseva 2016).

BWR SNF Cladding. Research on hydride reorientation in BWR SNF cladding is limited because internal rod pressures and thus, cladding hoop stresses, are about half of those in PWR SNF cladding.²⁸ For this reason, there has not been as much concern about hydride reorientation in BWR SNF cladding.

Observations of hydride reorientation tests on BWR SNF cladding with liners indicate that soluble hydrogen diffused from the Zircaloy cladding into the zirconium liner at the inner diameter of the cladding. This diffusion depleted hydrogen from the part of the cladding that would be susceptible to reduced ductility due to radial hydrides (see Figure F-16) (Aomi et al. 2008; Valance et al. 2015). The micrographs in Figure F-16 show the results of the hydrogen migration to the zirconium liner for each of two different heat treatments for BWR SNF. Type B treatments were held at 400°C (752°F) for 1.25 hours and were then cooled under constant stress of 80 MPa (11,600 psi). Type C SS (storage scenario) treatments were held at a constant temperature of 400°C (752°F) for 10 days at a stress of 80 MPa (11,600 psi), and then the stress was programmed to decrease linearly with absolute temperature while the sample cooled. In both the Type B and Type C SS scenarios, the cooling rates used were much faster than cooling rates experienced during SNF dry storage. More hydrogen migrated to the liner during the slower Type C SS treatment (Auzoux et al. 2017). It should be noted that the zirconium liner in BWR fuel is not credited for the structural performance of the cladding in NRC safety reviews.

At ORNL, CIRFT tests, in the cyclic mode, were used to measure the fatigue lifetime of BWR HBF with Zircaloy-2 cladding, and the results were compared to PWR HBF with Zircaloy-4 and M5[®] cladding (Wang et al. 2015). The researchers noted, “detailed examination revealed that, at same stress level, the [BWR] fuel showed a longer fatigue lifetime than the other two SNFs between 10⁴ and 10⁶ cycles” (Wang et al. 2016).

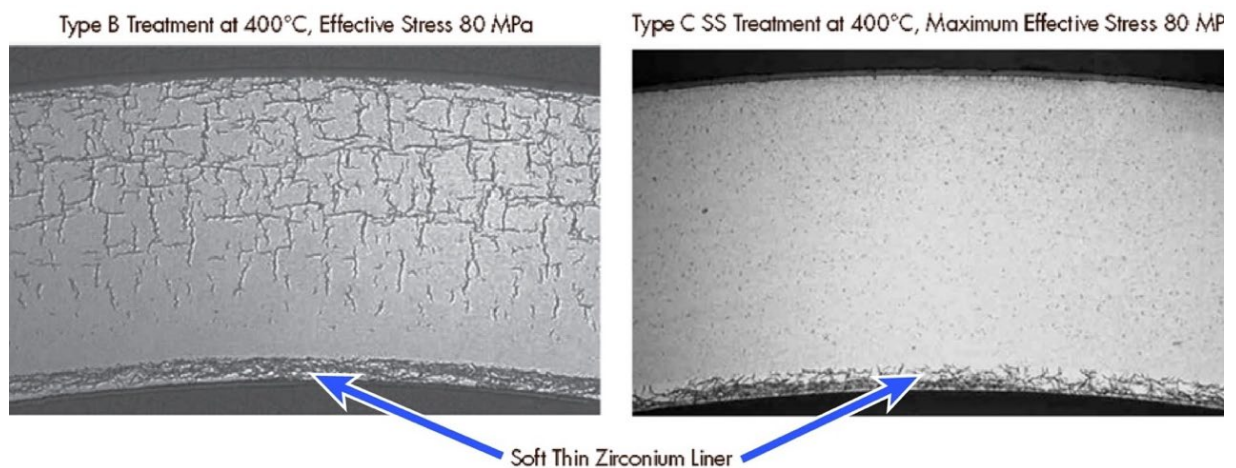


Figure F-16. Micrographs of irradiated BWR SNF cladding with a zirconium liner.

These cladding samples consist of Zircaloy-2 coextruded with a thin inner liner of zirconium. The images show the results of hydrogen migration to the zirconium liner (*adapted from Auzoux et al. 2017*).

²⁸ The lower pressure in BWR SNF rods is due to lower fill-gas pressures and thicker cladding.

The Board observes that BWR HBF that includes cladding with a zirconium liner appears to be less likely to be affected by hydride reorientation than cladding without a liner. However, given that data on hydride reorientation effects in BWR cladding are limited, it is premature to draw broad conclusions about the behavior of BWR HBF cladding when subjected to conditions that might cause hydride reorientation.

There are considerable differences among various PWR SNF cladding alloys and alloy textures (created during the manufacturing process) in terms of the extent of hydride reorientation, experimentally determined DTTs, and whether the DTT increases or decreases with changes in the maximum temperature and stress (Sindelar, Louthan, and Hanson 2015; Billone 2018; Billone 2019; Billone and Burtseva 2020). As noted above in the M5[®] cladding example, other factors, such as hydrogen concentration in the cladding, also affect the ductility of the cladding. The causes of these differences have not been completely determined and DOE continues to sponsor relevant research, including further testing on the HBF sister rods that are part of the HDRP.

Generally, the large number of factors that influence hydride reorientation in HBF cladding make it difficult, if not impossible, to draw general conclusions about the ductility (or fracture behavior) of one type of cladding based on testing conducted on other types of cladding. Similarly, it is difficult to predict the behavior of one type of cladding with a given operational history based on testing of the same cladding type with a different operational history.

The Board acknowledges that valuable data are being collected on PWR HBF cladding during the DOE-sponsored HDRP. However, the HDRP does not include BWR cladding, cladding from integral burnable absorber rods containing boron, or newer fuel claddings, such as GNF-Ziron²⁹ or chrome-coated claddings that are being tested for use in U.S. commercial reactors. The Board does note the positive trend in newer cladding designs, such as M5[®], to improve (reduce) cladding corrosion in the reactor, thus reducing the amount of hydrogen absorption in the cladding, which in turn, reduces the formation of hydrides and reduces the probability of hydride reorientation.

F.3.4 Additional Challenges to Conducting Research on Hydride Reorientation

There are several other challenges related to testing the effects of hydrogen reorientation that are described in subsections F.3.4.1 to F.3.4.3.³⁰ below.

F.3.4.1 Testing Unirradiated Samples

Using unirradiated or lightly irradiated cladding samples for testing has many advantages over using irradiated samples, such as reduced cost, less dose exposure to the experimenters, and less need for shielded facilities. Because studying hydride reorientation on unirradiated cladding material is less expensive than testing irradiated samples, more

²⁹ GNF-Ziron cladding is manufactured by Global Nuclear Fuels.

³⁰ These effects are discussed in much more detail in the IAEA SPAR-III report (IAEA 2015), the Proceedings from the 2nd ASTM International workshop on hydride reorientation (Sindelar, Louthan, and Hanson 2015), and the critical analysis of those proceedings by Louthan for the Nuclear Waste Technical Review Board (Board) contained in this appendix.

tests can be conducted, which allows more data to be collected, which, in turn, provides better confidence in the results of statistical analyses.

Before using unirradiated cladding materials in tests, the samples must first be infused with hydrogen to a pre-determined level to simulate the hydrogen content of irradiated cladding. While there are several ways to do this,³¹ none has been successful in replicating the hydride structure of cladding found in irradiated SNF (e.g., the hydride rich layer near the outer surface of the cladding). Also, as noted earlier, irradiation causes hydrogen traps that shift the hydrogen solubility-temperature curves, which has not yet been replicated in the hydrogen-infused, unirradiated cladding samples. Another important factor is the “softness” (i.e., high-ductility/low-yield-stress) of unirradiated cladding compared to irradiated cladding. Hydrided cladding that has been irradiated will behave in a more brittle manner than hydrided cladding that is unirradiated because of irradiation hardening of the alloy matrix in the irradiated cladding.

For example, DOE funded PNNL to try to create a hydride rich layer in unirradiated cladding. PNNL was successful in producing a hydride rich layer, but the sample did not contain hydrogen traps (Shimskey and MacFarlan 2014).

The presence or absence of a hydride rich layer has ramifications for the testing of cladding segments using HRT and RCTs:

1. In irradiated cladding samples, the hydride rich layer is important because it may have small cracks that act as initiation points for larger cracks that propagate further into the cladding metal.
2. Hydride behavior and its ramifications will differ if (a) the precipitated hydrides are equally distributed throughout the sample (as is the case in most unirradiated samples charged with hydrogen), or (b) the hydrides are concentrated near the outer surface of the cladding with limited hydrides in the remainder of the cladding as is common in irradiated cladding. After the hydrides are dissolved at high temperature during drying, the reprecipitation and possible reorientation of hydrides upon cooling can be very different for cases (a) and (b) above, depending on the maximum temperatures and hoop stresses reached and the total hydrogen concentrations (this is discussed in detail in section F.3).

During both the ASTM 18th International Symposium on Zirconium in the Nuclear Industry meeting (Comstock and Motta 2018) and the American Nuclear Society Embedded Topical Meeting on Nuclear Fuels and Structural Materials (American Nuclear Society 2016), participants discussed alternate methods (other than in-reactor irradiation) to irradiate samples for testing, such as proton irradiation.³² Proton irradiation should create samples that emit a lower radiation dose, making the samples easier to handle. The dose rate from the proton-irradiated target will be lower than that of a reactor-irradiated sample because the proton beam can be directed only at a limited area of the entire sample. Furthermore, the

³¹ Methods for infusing cladding with hydrogen are described in the proceedings of the ASTM International workshop (Sindelar, Louthan, and Hanson 2015) and the IAEA review (IAEA 2015).

³² The discussion occurred during the question and answer period and is not documented in the proceedings.

overall activation of a proton-irradiated sample can be minimized since the penetrating strength of the proton is a function of proton energy, which can be controlled and reduced as needed (Was 2010). However, samples with lower activation are not good surrogates for in-reactor irradiated samples because they have lower levels of radiation-induced damage in the material matrix. A discussion with proton irradiation experts at the ASTM International symposium indicated that it might take 5–10 years of experimentation to confirm if proton irradiation adequately simulates neutron irradiation effects. It is not clear if proton irradiation could produce samples representative of reactor-irradiated materials.³³ A critical, outstanding issue is that any alternative method used to simulate an irradiated sample must be capable of producing hydrogen traps throughout the surrogate sample while not highly activating the cladding, which would then require hot cell testing and reduce the benefit of using the alternative method.

Further, studies demonstrate that unirradiated zirconium alloys treated to produce a uniform distribution of hydrides across the cladding thickness are a poor substitute for irradiated cladding (Billone, Burtseva, and Einziger 2013). During reactor operations, hydrogen tends to migrate to lower temperature regions, which are found at the outer diameter of the cladding and where a buildup of hydrides occurs. Using unirradiated cladding material with a hydride structure like that of irradiated cladding could be a valid surrogate (Billone, Burtseva, and Einziger 2013) for testing.

Taking advantage of any economies associated with using unirradiated samples in tests requires that any differences between using irradiated and unirradiated samples be resolved. In addition, models capable of accurately accounting for differences in hydride reorientation behavior between irradiated and unirradiated samples must be developed. Unfortunately, validating such models may be cost prohibitive because considerable testing of irradiated cladding will be required (see the Louthan white paper in section F.5).

F.3.4.2 Hydride Reorientation Treatment Protocol

Test protocols for inducing hydride reorientation in cladding samples (HRT) vary from lab to lab and include some processes that do not recreate precisely the conditions experienced by HBF when natural hydride reorientation occurs. These differences in the laboratory procedures are discussed in more detail below.

The first step in any hydride reorientation test is to raise the temperature of the cladding to dissolve the existing hydrides. Once the cladding temperature reaches the desired maximum in a laboratory setting, it is maintained for a 1–2 hours hold time. This hold time may be significantly shorter than the time that HBF experiences maximum temperatures during and after drying. However, as discussed in Billone, Burtseva, and Einziger (2013), dissolution of hydrides is very rapid, so the rate limiting step for equilibrium is hydrogen diffusion. Diffusion calculations were performed assuming ZIRLO[®] cladding at 400°C (752°F) for the extreme case of all hydrogen initially concentrated at the outer surface of the

³³ Almost all out-of-reactor irradiation effects studies use electrons, protons, or alpha particles. Many colleagues at the 18th International Symposium on Zirconium in the Nuclear Industry thought there was insufficient information to determine if proton irradiation could duplicate the effects of neutron irradiation. Additional information can be found in several papers in the proceedings of the ASTM International symposium (Comstock and Motta 2018).

cladding. For cladding with a wall thickness of 0.57 mm (0.02 in), the time to reach 93% equilibrium of hydrogen concentration across the wall is less than 30 minutes. Therefore, 1–2 hour at 400°C (752°F) is more than adequate hold time to simulate the longer hold time in the actual drying process.

After the hold period at maximum temperature, a cooling rate of 5°C/hour (9°F/hour) or greater typically is used for experimental expedience (e.g., see Billone et al. 2013). However, actual cooling rates during dry storage of SNF can be 3 to 4 orders of magnitude slower. It is not clear whether the migration pattern and migration rate (i.e., diffusion rate) of hydrogen to existing hydride sites, grain boundaries, and BWR liner material (see Appendix A) will be the same as in HBF in storage that cools at a much slower rate. This difference introduces uncertainties regarding the hydride structure in cladding treated in the laboratory compared to the hydride structure in HBF cladding that is cooled slowly in storage.

Hydrides only reorient if a sufficient hoop stress is placed on the cladding while it is being cooled from a sufficiently high temperature. During HRT, the hoop stress is usually applied by (1) internal pressure in the cladding sample or (2) a mandrel (or equivalent) that stresses the cladding from the inside by expanding it. Both methods have advantages and disadvantages. For example, the pressurized cladding method subjects the cladding sample to a stress that is uniform around the circumference of cladding but is variable from the inside diameter to the outside diameter of the cladding. This is more representative of the stress experienced by cladding during the drying process. Pressurization is a better approach if the samples will then be cut for RCTs. Alternatively, the expanding mandrel test places a varying stress both around the sample circumference and throughout the cladding thickness. This type of test is best to determine how the hydride reorientation varies with the applied stress but does not produce appropriate samples for RCT. In both cases, the stress distribution can be determined using finite element analysis.

Unfortunately, the results from the various HRTs and RCTs are not always consistent. Furthermore, as noted in the Proceedings of the 2014 ASTM International Workshop on Hydrides in Zirconium Alloy Cladding (Sindelar, Louthan, and Hanson 2015), there are no standardized procedures for conducting HRTs.

F.3.4.3 Quantifying Hydride Reorientation

Quantifying hydride characteristics in HBF cladding often is done using a range of microscopic methods. As-irradiated or post-HRT cladding samples are cut, usually after defueling, and placed in a metallurgical mount. The cladding cross section is then polished and chemically etched to highlight the hydride structure. Etching samples to bring out the detail of the hydrides requires skill in technique and execution: “At present, metallographic preparation techniques and the matrices used to characterize hydride orientations vary from site to site. Even characterizations on samples prepared using automatic polishers and image analysis equipment may differ because of etching magnifications” (section F.5; Louthan 2014). Once etching is complete, the sample surface can be examined using different microscopic techniques. Optical microscopy is capable of revealing large hydrides, which may or may not have been widened by the etching procedure (see Figures F-2, -3, -5, -6, -11, -14, -16 and -17 for examples of etched sample cross-sections). Alternatively, scanning electron microscopy can elucidate details of smaller hydrides surrounding the larger hydrides. The most commonly used method is optical microscopy.

Macroscopic hydrides (sometimes called hydride stacks) were thought to be formed by small hydride particles or discs rotating and aligning themselves end to end during the cooling process. Simulations and further studies, however, suggest that this is not energetically possible. Motta et al. (2019) report that “The elastic stress field surrounding these nanoscale hydride discs favors precipitation of other hydride particles nearby. This coupling leads to ‘mesoscale’ hydride particles that are composed of many nanoscale hydrides arranged in a ‘deck of cards’ configuration within a single crystal...” Transmission electron microscopy can resolve microscopic hydride platelets as opposed to hydride stacks (Colas et al. 2014).

While automated methods exist to quantify visible hydrides, the criteria for counting them must be specified. Depending on the cladding hoop stress at the time of maximum cladding temperature and hydrogen content in the cladding, many cladding samples contain some fraction of hydrides that are not fully radial or fully circumferential. For these hydrides, one criterion used is to designate any hydride that is within ± 45 degrees of the radial direction as a radial hydride (Aomi et al. 2008).

The RHCF, which is based on the ratio of the maximum radial hydride length to the thickness of the cladding, may also be effective in quantifying hydride reorientation in samples (Burtseva, Yan, and Billone 2010). If the total hydrogen in the cladding is above the solubility limit at the reorientation temperature, then there will be residual circumferential hydrides that may break up the continuity of the radial hydrides into a checkerboard pattern (Figure F-17A). In this case, the RHCF may be quite small. If the same amount of hydrogen goes into solution, but is below the solubility limit, then very long radial hydrides form (with sufficiently high hoop stress) since there are no remaining circumferential hydrides to break up the radial hydrides.

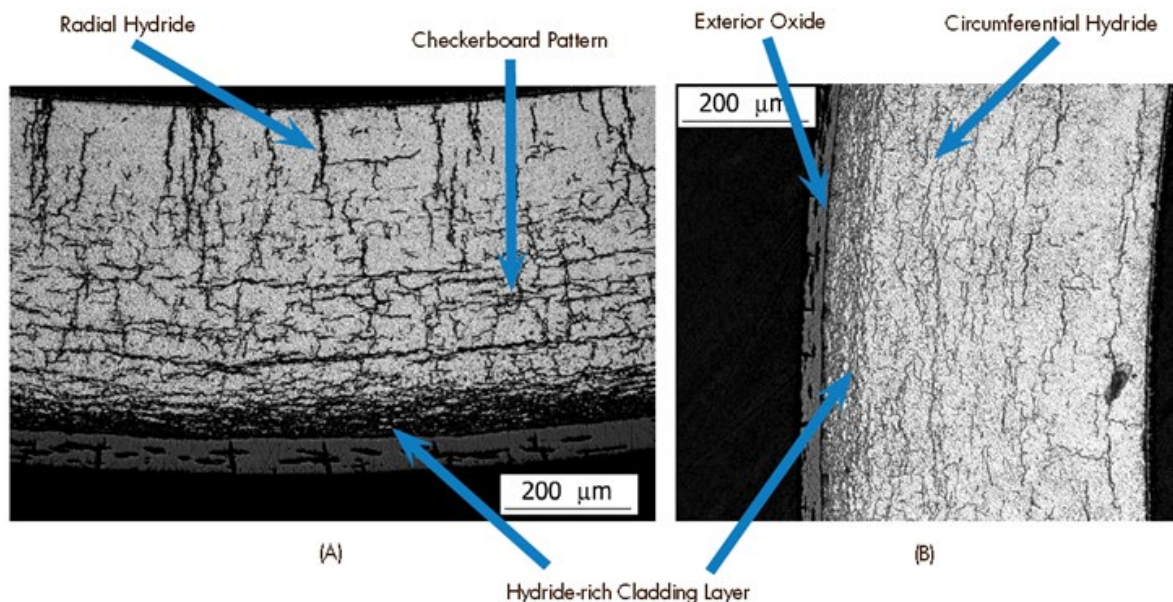


Figure F-17. Micrographs of cladding after HRT showing the orientation of hydrides.

(A) 70 GWd/MTU ZIRLO® rodlet that was subjected to an HRT hoop stress of 140 MPa (20,300 psi), showing a “checkerboard” pattern comprising both radial and circumferential hydrides. (B) 70 GWd/MTU ZIRLO® rodlet that was subjected to an HRT hoop stress of 110 MPa (~16,000 psi), showing that mostly circumferential hydrides were formed (Burtseva, Yan, and Billone 2010).

Other factors affecting the amount of hydride reorientation are the grain structure within the base metal of the cladding and spatial variations of hydrogen concentrations within the cladding. Hydride precipitation can be affected by the grain structure in the cladding in such a way that the hydrides are not always contiguous.

Additionally, measurements of HBF cladding have shown that there can be significant axial and circumferential hydrogen gradients in the cladding (Geelhood and Beyer 2011). This high degree of variability in hydrogen concentration will affect the formation and orientation of hydrides significantly.

In summary, comparing the degree of hydride reorientation among different studies is difficult when different test methods and hydride metrics are used. Standardizing the test methods, the quantification of hydrides, and the characterization of reorientation would be helpful in interpreting the data. These issues are being addressed, in part, in the development of a new, draft ASTM International standard on HRT and RCT of zirconium-alloy SNF cladding.

F.4 Delayed Hydride Cracking

The presence of hydrides in SNF cladding with sufficiently high tensile stress can lead to another failure mechanism called delayed hydride cracking (DHC; a detailed description of DHC is provided in section F.4.1). DHC is dependent on many factors including the cladding alloy composition, cladding manufacturing processes, and the operational life cycle, including burnup, operational temperatures, and cladding temperatures during the drying process. Although DHC has not been found in commercial SNF cladding in the United States, it is a known failure mechanism in other zirconium alloys used in reactor cores. For example, DHC has been observed under certain conditions in pressure tubes of zirconium-2.5% niobium alloy used in Canada Deuterium Uranium and Reaktor Bolshoy Moshchnosti Kanalnyy (RBMK)³⁴ reactors (IAEA 2004). DHC has also been observed in tests of Zircaloy-2 pressure tubing (not fuel cladding) like that used in the Hanford N-reactor (Huang and Mills 1991).³⁵

In DOE's early assessment of technical information needs related to HBF (Hanson et al. 2012), a high priority was assigned to advancing research on DHC and, more specifically, research to determine (1) the extent of DHC in SNF cladding during extended storage and (2) if it is active, determine the rate at which DHC-induced cracks progress. Subsequently, cladding tensile stresses calculated by the NRC (and discussed below) were found to be

³⁴ The Canada Deuterium Uranium reactor is a heavy water moderated reactor using fuel consisting of uranium oxide in a zirconium-2.5% niobium cladding. Reaktor Bolshoy Moshchnosti Kanalnyy (RBMK) is a "High Power Channel-type Reactor" that is graphite-moderated. This power reactor was designed and built by the Soviet Union.

³⁵ Based on the discovery of DHC in zirconium-2.5% niobium alloys used in the Canada Deuterium Uranium reactors, there were concerns that DHC may affect ZIRLO[®] or M5[®] claddings, which are both zirconium-1% niobium alloys. Similarly, due to the discovery of DHC in Zircaloy-2 pressure tubing at Hanford, concerns arose regarding the possibility of DHC in Zircaloy-2 cladding used for BWR fuel cladding. Differences in irradiation conditions, lower niobium contents in ZIRLO[®] and M5[®] cladding, or structural difference, such as the presence of a zirconium liner in Zircaloy-2 cladding, may be why DHC has not been found in these cladding materials.

insufficient to activate DHC, with the result that this issue was downgraded to a low priority in DOE's later updates to its assessment of technical information needs (Teague et al. 2019).

F.4.1 Delayed Hydride Cracking Mechanism

DHC is a time-dependent mechanism generally thought to occur when hydrogen that is dissolved in SNF cladding diffuses to a crack tip and precipitates as zirconium hydride. The hydride then grows and fractures, which extends the crack into the base metal of the cladding. If there is a sufficiently high and sustained tensile stress, the crack can propagate easily into fresh metal, and the cycle begins again until a crack penetrates through the cladding. Canada Deuterium Uranium reactor pressure tubing that failed by DHC was found to contain residual tensile stresses of 350 MPa (~50,700 psi), which had been induced during manufacturing (IAEA 2004). The DHC process continues if there is sufficient stress to promote hydrogen diffusion and sufficient hydrogen to precipitate (Puls 2009; McRae, Coleman, and Leitch 2010). DHC traditionally has been ruled out as a possible mechanism for cladding degradation during extended storage because, as the fuel temperature decreases, the stress also decreases and becomes insufficient to propagate cracks—unless the initial crack length is a substantial fraction of the cladding wall thickness (EPRI 2002; DOE 2004). A number of reviews of the DHC mechanism in dry storage have been published (Huang and Mills 1991; IAEA 2004; NWTRB 2010; Sindelar et al. 2011; EPRI 2011; Hanson et al. 2012).

In Puls' model (2009), the high tensile stress results from the cladding manufacturing process and externally applied stresses. However, in a newer DHC model, the stress at the crack tip results from a phase transition in the zirconium hydride (from the δ phase to the γ phase) due to material density changes, which is expected to occur as the cladding cools below 180°C (356°F) (Kim 2009). A significant portion of the cladding in the LBF demonstration at Idaho National Laboratory went through this transition temperature, but no cladding breaches due to DHC or any other mechanism occurred (Einziger et al. 2003). This may be due to a lack of hydrogen in LBF cladding, a lack of large enough initial cracks, or both. To date, there have been no papers published that present experimental data to definitively confirm or disprove Kim's model.

F.4.2 Estimating Cladding Hoop Stress During Storage

Although the internal rod pressure following irradiation may be too low to drive DHC, swelling of the fuel pellets (caused by a buildup of fission product gases and helium production from alpha decay) has been proposed as another source for cladding hoop stress (Ahn, Rondinella, and Wiss 2013). To assess this, the NRC performed an analytical study to predict cladding hoop stress over a 300-year dry storage period for a 10 x 10 array of BWR fuel and 17 x 17 array of PWR fuel, both with burnups of 65 GWd/MTU (Raynaud and Einziger 2015).

As part of this study, radioactive fission gas production in the fuel rod during storage was predicted using the ORIGEN model (Bowman and Gauld 2010) and realistic fission gas release fractions were derived from the literature. Additionally, calculations were made assuming both 0% and 100% helium gas release to evaluate the effects of maximum gap gas pressure and maximum pellet swelling. The NRC's steady-state fuel performance model FRAPCON-3.5 (Geelhood and Luscher 2014) was modified to account for the fuel-pellet

swelling, helium gas production, and gas release during storage to produce circumferential average cladding hoop stress predictions of many different assembly types over a 300-year period. The calculations showed that the resulting stresses, for both PWR and BWR fuel, decreased during 300 years of storage due to the decreasing temperature of the system. These calculations also predicted hoop stresses on HBF cladding during the drying process to be about 50 MPa (~7,200 psi) or less. Similar stresses were predicted by others (EPRI 2013; Bratton, Jessee, and Wieselquist 2015; Billone, Burtseva, and Garcia-Infanta 2017; Richmond and Geelhood 2018).

The potential for DHC was also assessed by calculating the critical crack size required to trigger this failure mechanism. The critical crack size for DHC to occur was calculated to be over 50% of the cladding thickness for all SNF fuel rod types after five years of dry storage, and it increased to 60–65% of the cladding thickness by 300 years of dry storage for all the cases modelled (Raynaud and Einziger 2015). The DHC critical crack size exceeds any realistic crack size that is expected to exist in HBF cladding after being irradiated or any crack size observed by the authors (Raynaud and Einziger 2015; EPRI 2013). It was concluded that, unless the cladding crack length is a significant fraction of the cladding thickness, there will be insufficient stress to propagate a crack by DHC (Raynaud and Einziger 2015; Coleman et al. 2018). Based on these results, DHC is not realistically expected to occur during a 300-year period of dry storage.

F.5 Louthan Recommendations White Paper

Based on papers presented at an ASTM International workshop in Jackson, Wyoming, in June 2014, M. R. (Mac) Louthan was funded by DOE to assist in developing a white paper evaluating the results of the workshop and to make recommendations for standards development regarding the effects of hydride reorientation on SNF storage and transportation (Sindelar, Louthan, and Hanson 2015). Louthan presented the results of this work at the Board's public meeting on HBF held in Knoxville, Tennessee, on February 17, 2016 (Louthan 2016). During that presentation, Louthan described the information presented at the 2014 ASTM International workshop, the methodology used to evaluate the information, and recommendations for useful standards to determine the effects of hydride reorientation on storing and transporting SNF.

The recommendations in the ASTM International workshop white paper were reached by three methods of consensus: (1) discussions with presenters during and after meeting, (2) drafts of a white paper that were circulated and revised based on reviewers' comments, and (3) discussions after publication of the initial draft white paper soliciting any needed changes.

As a consultant to the Board, Louthan documented further analysis of the workshop recommendations and presented them in "Selective Implementation of Recommendations from 2nd ASTM International Workshop on Hydrides in Zirconium Alloy Claddings Priorities, and Consequences." This paper, which is included below, describes the value of having standards when conducting hydride reorientation work, identifies which standards were the most important, and discusses the consequences of not developing standards. Louthan and several Board and staff members met on May 25, 2016, to clarify several statements in the paper that Louthan prepared. This meeting provided additional information for the Board to

use in evaluating DOE's program focused on hydride issues in storing and transporting SNF and in developing Board recommendations on improvements needed in the DOE program.

Selective Implementation of Recommendations from 2nd ASTM International Workshop on Hydrides in Zirconium Alloy Cladding Priorities and Consequences

M. R. Louthan, Jr.

Abstract

The Nuclear Waste Technical Review Board asked for an assessment of the potential consequences of selective implementation of the recommendations from the 2nd ASTM International Workshop on Hydrides in Zirconium Alloy Cladding (Sindelar, Louthan, and Hanson 2015). The resources required for full implementation are so extensive that selective implementation is the only practical approach. The recommendations were made to demonstrate the need to cooperation and collaboration throughout the nuclear industry, including academic and National Laboratory participants and were focused on practical implications of hydride reorientation in the cladding of used nuclear fuels during the long term, dry storage. This paper summarizes the recommendations, demonstrates the large number of variables associated with the reorientation process and prioritizes an approach to selective implementation. The general processes associated with hydride reorientation have been extensively studied and are well known; however, application of developed technical bases to a specific assembly, from a specific irradiation and dried under a specific set of conditions is difficult, if not impossible, because of the large number of variables potentially involved. The preponderance of evidence associated with long term storage of spent nuclear fuels is that such storage is successful. This success, coupled with the already existing scientific data base, suggests that increased scientific understanding of hydride reorientation processes and/or further demonstration of short (10 to 20 years) term successful dry storage of selected fuels are unlikely to improve our ability to either predict future behaviors or increase the certainty that we can mitigate the potential for hydride embrittlement during the long-term storage of used nuclear fuels.

Introduction

The 2nd ASTM International Workshop on Hydrides in Zirconium Alloy Cladding demonstrated the need for standardizing laboratory practices and programs to quantify and predict the effects of hydrogen and hydrides on the behavior of used nuclear fuel rods and assemblies during long term storage (Sindelar, Louthan, and Hanson 2015). Differences in fuel claddings, reactor service, pool storage conditions, drying operations and canister designs, loadings and storage conditions combine to demonstrate that a significant quantity of work is required before the behavior of specific rods or assemblies can be extrapolated into the distant future. However, information and understanding of hydrogen/hydride effects on used nuclear fuel elements is not lacking and generic behaviors can be postulated with reasonable accuracy.

Predictive difficulties arise for specific system predictions because there is no model cladding alloy and behaviors vary with alloy chemistry and microstructure, thermomechanical history and other material/service conditions. A summary of the recommendations from the Workshop was presented to the Nuclear Waste Technical Review Board on February 17, 2016 (Louthan 2016). The Board subsequently requested a summary of the consequences if selected portions of the recommended work were not attempted. This report outlines the anticipated consequences of following only selected

portions of the Workshop recommendations and suggests a path forward to maximize the return on investment from programmatic evaluations of the effects of hydrogen/hydrides on the long-term behavior of zirconium alloy clad used fuels during dry storage, transfer and disposition.

Workshop Recommendations

The data and analyses presented at the Workshop demonstrated the need for coordination and cooperation among nuclear facilities engaged in evaluating the effects of hydrogen and hydrides on the performance of zirconium alloy fuel cladding and used nuclear fuel assemblies during long term storage. The Workshop recommendations presented to the Board included:

- 1) Develop standards for characterization and testing of used fuel cladding and cladding alloys,
- 2) Integration of efforts -get everyone on the same page by creating multi-site testing and analysis teams,
- 3) Develop and verify protocol to use non-irradiated alloy testing to predict irradiated alloy behavior,
- 4) Recognize and attempt to understand alloy to alloy differences (there is no model alloy or assembly), and
- 5) Establish ductile-to-brittle transition temperatures that are relevant to fuel handling situations.

These, or very similar, recommendations are published in SRNL-STI-2015-00256 (Sindelar, Louthan, and Hanson 2015) and represent consensus concerns discussed in the Workshop. The resources required to fully implement these recommendations are extensive and require long term programmatic commitments. Additionally, the level of success achieved during implementation of the recommendations will depend on the extent of information exchange and cooperation among research laboratories, reactor operators, fuel and cladding manufacturers and regulatory organizations.

Implementation Goal

The recommendations outlined above were made to help guide technical programming activities, maximize the potential for information exchange among practitioners serving the nuclear industry and maximize the benefits derived from the associated programs. The potentially adverse impacts of hydrogen and hydrides on the long-term performance of irradiated zirconium alloy cladding on used nuclear fuel rods are known to depend on multiple factors, including: alloy chemistry, cladding manufacturing process, irradiation history, post irradiation history, fuel drying treatments, applied and residual stresses and other manufacture and service variables. Fuel rod cladding integrity will, to a large extent, determine assembly performance during long term storage and during subsequent handling and transfer operations.

The basic concern being addressed, either directly or indirectly, in laboratory and large-scale test programs on hydrogen containing zirconium based nuclear fuel cladding alloys primarily relate to the effects of radially oriented hydrides on the mechanical behavior of such claddings. The processes that lead to radial hydride orientations and to the resulting

loss of ductility during mechanical loadings are relatively well understood in a general sense. However, application and extrapolation of the general understanding to specific, untested situations is fraught with difficulties. These difficulties, as will be discussed later, are broadly associated with the very large number of material and service variables that impact hydride reorientation and embrittlement processes.

Hydride Reorientation and Embrittlement

The elevated temperatures (about 590K in pressurized water reactors) associated with exposure of zirconium alloy clad fuels to nuclear reactor service cause the outer surface of the cladding to react with the water ($\text{Zr} + 2\text{H}_2\text{O} \rightarrow \text{ZrO}_2 + 4\text{H}$) to form an oxide film. The cladding will also absorb some of the hydrogen generated by the reaction.

Hydrogen absorption is endothermic; thus, the absorbed hydrogen will be retained in the cladding throughout subsequent storage, drying and transfer operations. The cooling water temperature at the clad surface is about 550K at the bottom of a PWR core and about 590K near the top of an assembly. The temperature of the cladding will increase radially and because the oxide film on the clad surface inhibits heat transfer and the clad temperature just beneath the oxide film will exceed the cooling water temperature. The solubility of hydrogen in zirconium alloys increases exponentially with increasing temperature, going from near zero at room temperature to about 100 ppm at 625K. When the absorbed hydrogen concentration just beneath the oxide film approaches 100 ppm (the exact hydrogen concentration required depends on the temperature just beneath the oxide film), hydrides begin to precipitate in the zirconium lattice. The heat of transport of hydrogen in zirconium alloys is positive; therefore, hydrogen will diffuse toward the cooler (outer) surface of the cladding because of the thermal gradient across the cladding. The pressure of the cooling water is maintained at about 15.5 MPa to prevent boiling. After the irradiation cycle is completed some of the fuel assemblies are transferred to a fuel storage pool. Transfer of a used fuel assembly from a reactor to a spent fuel storage pool requires that the surface temperatures of the fuel cladding be below 373K to avoid boiling at the clad-water interface when water pressure is reduced to atmospheric. The hydrogen solubility in zirconium alloys at 373K is generally less than 5 ppm, thus virtually all the absorbed hydrogen that did not precipitate during service precipitates as the fuel cooled, under pressure, to the temperatures required for pool storage. Shutdown schedules for reactors vary but for economic reasons are as short as possible and generally require at least several weeks. The as-irradiated hydride morphology is expected to remain essentially unchanged throughout pool storage. There is limited evidence that the hydride morphology may be altered by room temperature plastic deformation; however, the large strains required for such alteration do not occur during pool storage.

Circumferentially oriented hydrides are typical in as-irradiated cladding alloys, regardless of the alloy chemistry or fabrication process. Early work demonstrated that the stress acting on zirconium alloy claddings influenced the hydride orientation and that the hydride orientation influenced the mechanical properties of the cladding. Radial hydride orientations in fuel cladding led to significant embrittlement while circumferential hydrides had minimal impact on mechanical properties. Cladding manufacturing processes were therefore designed to maximize the tendency for circumferential hydride orientations. Radial hydride orientations in test samples were produced by heating the hydrogen containing samples to dissolve existing hydrides, applying a tensile stress to the heated sample and allowing the

hydrides to precipitate as the samples cooled to room temperature while under stress. The extent to which radial hydrides formed depended on the magnitude of the tensile stress. Circumferential hydrides were formed when the cladding was under a compressive stress during hydride precipitation. Thermal treatments to dissolve and reprecipitate hydrides in test material maintained under a controlled stress are termed a hydride reorientation tests (HRT). The results from such tests are used to evaluate the potential for hydride reorientation during the drying operations required to transfer fuel assemblies from pool storage to storage in a dry storage canister and to estimate behaviors during the subsequent long-term storage in the canister.

The decay heat load in a fuel rod decreases with time but, in the absence of water cooling, may raise the fuel cladding temperatures to levels sufficient to dissolve precipitated hydrides. The fraction of the hydrides dissolved will depend on the hydrogen content in the cladding, the hydride distribution across the cladding wall and the temperature reached during the drying operation. Regulatory guidelines limit the temperature to 673K, but most drying and dry storage temperatures are significantly below the regulatory limit. The decay heat load inside the dried canister will continue to decrease with storage time, lowering the fuel cladding temperatures and causing the dissolved hydrogen to reprecipitate during dry storage.

The cladding stresses during the reprecipitation process differ significantly from the stresses associated with hydride precipitation in as-irradiated cladding. The water pressure acting on the fuel cladding exceeds the fuel rod internal pressure thus placing the cladding in circumferential compression and favoring circumferential hydride precipitation. The pressure inside a dry storage canister is below the fuel rod internal pressure, thus the cladding will be in tension during the hydride reprecipitation process and radial hydride precipitation will be favored.

The potential for reprecipitation of radial hydrides in the cladding of used nuclear fuels in dry storage canisters leads to two basic concerns:

- (A) The development of a hydride morphology that embrittles the cladding to the extent that cladding fracture (overload, fatigue, impact, etc.) during handling and transfer operations is likely, and
- (B) The precipitation of a hydride at a stress concentration, fracture of the precipitated hydride, intensification of the stress because of the fracture and sequential precipitation/fracture/intensification processes that lead to a through wall crack that compromises the cladding integrity. This process is termed delayed hydride cracking (DHC). Delayed hydride cracking was not discussed at the Workshop but is mentioned in this report because the challenges in predicting DHC are similar to challenges in predicting whether hydride reorientation will lead to the development of brittle hydride morphologies. Understanding the magnitude of these challenges requires an appreciation for the variables that impact the hydride reorientation process.

Variables Impacting Hydride Reorientation

The early stress orientation (reorientation) studies demonstrated that:

- 1) Hydrides tend to precipitate perpendicular to a tensile stress and parallel to a compressive stress (This effect was termed stress orientation.),
- 2) A critical stress is necessary to cause stress orientation and the magnitude of the critical stress varies with alloy, crystallographic texture (fuel tube fabrication technique) and local conditions,
- 3) The room temperature tensile properties of the samples depended on the hydrogen content in the sample and the hydride orientation relative to the stress axis,
- 4) Hydride precipitation processes were influenced by the presence of other hydride as indicated by the tendency for an end to end alignment of the hydride packets.

Subsequent studies confirmed the early work, especially the behavioral variations among cladding alloys. Work also demonstrated that the response of any given cladding alloy to mechanical loadings, including tensile, impact, bend, fatigue and creep behaviors is influenced by the hydrogen and hydride content in the cladding and by the orientation of the hydrides relative to the major stress axis. Numerous tests with irradiated and non-irradiated materials including cladding, sheet and plate have further demonstrated that:

- 5) The basal plane is the hydride habit plane in zirconium based alloys and that optical microscopy (the typical hydride characterization technique) generally does not resolve the individual hydrides within a packet,
- 6) The punching of dislocations generally accompanies hydride precipitation and that the energy required for such punching gives rise to a hysteresis in the solubility versus temperature curve,
- 7) The susceptibility of a given alloy to stress orientation during a hydride reorientation test depends on the hydrogen content, reorientation test temperature, stress level and stress state. Tests with non-irradiated alloys have demonstrated that the threshold stress required for reorientation decreases significantly with increasing stress biaxiality ratio (The stress biaxiality ratio for many reorientation tests has been near zero while the ratio in the cladding of as-irradiated fuel rods is 0.5.),
- 8) Under a given set of HRT conditions, the susceptibility to stress orientation increases as the number of reorientation test cycles increases, especially if the reorientation test temperature is too low to dissolve all the existing hydrides. However, if the HRT does not dissolve all the non-oriented hydrides, the tendency for reorientation is decreased regardless of the number of reorientation cycles,
- 9) Stress [re]orientation is generally promoted by slow cooling, and
- 10) Irradiation impacts the strength and ductility of the fuel cladding, alters the dislocation structure, impacts the stress reorientation process and may significantly lower the critical stress for hydride reorientation.

None of these observations are truly independent. For example, the observation (Observation 3) that the tensile properties depend on the hydrogen content and the hydride orientation relative to the stress axis is influenced by the tendency of the hydride packets to

align end to end (Observation 4). A greater tendency for end to end alignment increases the tendency for embrittlement. Additionally, the tendency for end-to-end alignment increases as the cooling rate decreases (Observation 9) however, if the HRT does not dissolve all the hydrides the existing hydrides impact both the reorientation process and the end-to-end alignment (Observation 8). Furthermore, if the hydrides are characterized by optical microscopy individual hydrides may not be resolved (Observation 5) and the measurements of hydride orientations may actually be measurements of the orientation of a hydride packet and the orientation of individual hydrides is not determined.

The determination of mechanical properties relevant to either assessing or predicting the behavior of fuel claddings and/or fuel assemblies is also fraught with difficulties. Observation 10 suggests that mechanical property measurements should be made on irradiated cladding alloys to be relevant to predicting cladding and fuel behaviors during post irradiation handling, storage and transport. Observation 7 demonstrates that the relevant reorientation tests on irradiated cladding samples should be made on samples tested so that the longitudinal to circumferential stress ratio was 0.5. The vast majority of hydride reorientation studies ignore either Observation 10 or 7 or both. Additionally, as will be discussed later, many mechanical tests used to evaluate the effects of hydrogen and hydrides on cladding alloys are not standardized and tests with non-irradiated alloys generally evaluate the effects of hydride morphologies that are not typical of the morphology in irradiated claddings.

Accurately predicting the behavior of a specific cladding, on a specific fuel rod is further complicated by the differences in temperatures and neutron fluxes along the rod length. These differences lead to as irradiated differences in oxide film thickness, hydrogen content and irradiation induced microstructural changes along the rod length. These differences will cause local differences in hydride reorientation processes during drying and may result in different mechanical properties at the bottom, middle and top of a fuel rod. Therefore, even for a single rod, projecting the long-term mechanical behavior into the distant future is not straightforward.

Discussions at the Jackson Hole Workshop noted the multiple influences of material, service, and test variables mentioned above and described numerous other important influences on the hydride reorientation process. Integration of these multiple variables into a cohesive model that successfully describes hydride reorientation and its impact on the long-term behavior of a specific zirconium based nuclear fuel cladding on a specific rod in a specific assembly is a daunting task. The recommendations from that workshop were designed to aid in the understanding and integration of those influences. In the roughly two years since the Workshop it has become apparent, at least to this author, that increased scientific understanding of hydride reorientation processes and/or further demonstration of short (10 to 20 years) term successful dry storage of selected fuels are unlikely to improve our ability to either predict future behaviors or increase the certainty that we can mitigate the potential for hydride embrittlement during the long-term storage of used nuclear fuels. Reasons for this conclusion are discussed in the last section of this report.

Consequences of Selective Implementation of Recommendations

The probable consequences of not following the five Workshop recommendations presented to the Board (develop standards for characterization and testing of used fuel

cladding and cladding alloys, integration of efforts by creating multi-site testing and analysis teams, develop and verify protocol to use non-irradiated alloy test data to predict irradiated alloy behavior, recognize and attempt to understand alloy to alloy differences, and establish ductile-to-brittle transition temperatures that are relevant to fuel handling situations) are:

- 1) The development and use of standards was recommended to facilitate information exchange among practitioners in the nuclear industry. At present, metallographic preparation techniques and the matrices used to characterize hydride orientations vary from site to site. Even characterizations on samples prepared using automatic polishers and image analysis equipment may differ because of in etching, magnifications and evaluated hydride matrix. Information exchange is enhanced if similar samples prepared at different sites have similar microstructural appearances when examined in an optical microscope or shown in a micrograph. Similarly, several different matrices are currently used to characterize the hydride orientation in a microstructure. Although these matrices are related and can be correlated, information sharing would be enhanced if a single matrix were used throughout the nuclear industry. The consequences of not following this recommendation are minimal. However, it is likely that benefits to multiple site information exchange far outweigh the cost of reworking the existing Annex 2 of ASTM Standard B811 (ASTM 2002) so that practitioners in this field recognize the benefits of adhering to standard metallographic preparation practices and use recommended matrices to describe hydride orientations. The impetus for developing this standard should come from the practitioners, thus the priority for any single organization to fund this task is low.
- 2) The creation of multisite testing and analysis teams was recommended to minimize the duplication of effort, to promote data exchange between sites before a task is accomplished and to develop increased cooperation among individuals and sites working on the same program. The potential benefits of multisite programs can be seen in two independent investigations presented at the Workshop. One investigation described the influence of stress biaxiality on the threshold stress for hydride reorientation in non-irradiated materials, showing (as described in Observation 7) that the threshold stress decreased with increasing biaxiality while another investigation with irradiated cladding alloys used uniaxial stresses (stress biaxiality near zero) during the hydride reorientation studies. The cladding of intact fuel rods has a stress biaxiality of 0.5 during cooling from drying operations thus the measured effects of stress on hydride reorientation in the uniaxially loaded samples may not provide conservative estimates. Reasons for the program independence include the testing of non-irradiated materials at an academic institute and the testing of irradiated materials in shielded facilities at a National Laboratory. However, regardless of the reasons for independence, a multisite testing and analysis team may have integrated the programmatic goals and provided more applicable research results. Duplication of efforts was also apparent from the Workshop presentations when two independent programs described experimental techniques to develop a hydride distribution and morphology in non-irradiated cladding alloys that simulated the distributions and morphology observed in as-irradiated claddings. The potential benefits of multisite cooperation are numerous although benefits may also be derived through competition and the goals of university investigations may differ significantly for the goals of an operating nuclear

reactor site or even a National Laboratory. The consequences of not creating multisite testing and analysis teams is continuing along established funding paths that have been relatively successful but, through integration of efforts, could provide increased scientific understanding for a similar expenditure of resources.

Investigators typically enjoy programmatic independence and to some extent would resist its loss, unless they were the program lead and investigator resistance may minimize the benefits of multisite programs. Therefore, there is a high priority for partial implementation of this recommendation using a fraction of the funding resources while the priority for full scale implementation is very low.

- 3) The recommendation to develop and verify protocols that provide techniques to use test data from non-irradiated cladding alloys to predict behavior after irradiation was made recognizing that resources required to implement such a program are enormous and would necessitate resource sharing with other irradiation effects studies. Even very limited implementation such as demonstrating that the critical or threshold stress for hydride reorientation measured in a newly developed alloy is duplicated in the same alloy irradiated as fuel rod cladding requires multiple, long term tests: irradiation, pool storage and drying prior to any metallographic examination or mechanical property determination. Such implementation is therefore impractical over short time frames. However, to begin to implement the recommendation cladding alloys on irradiated, pool stored fuels must be selected and non-irradiated companion cladding tubes (hopefully) from the same production lots be tested and compared to the test results from the irradiated fuel cladding. Detailed test plans and procedures for the comparative tests should be evaluated and approved by qualified personnel from multiple sites. Implementation of the test program coupled with analytical correlations among the test results should establish the validity and value of testing non-irradiated cladding alloys to predict the post irradiation behavior. Unfortunately, the correlations, at best, may be only applicable to the alloy tested. Much of the data necessary for such correlations may have been obtained across the nuclear industry but is not readily available for analysis and projection. The resources necessary and the time required to implement this portion of the recommendation may be practical for a limited number of alloys. The consequences of failing to initiate action on this recommendation are continued compartmentalization of data into irradiated and non- irradiated materials studies and the resulting limits to the utility of non-irradiated material tests to predicting the long-term behavior of fuel cladding. The priority for developing (or making available) correlations between the behaviors of non-irradiated and irradiated cladding alloys is relatively high but should only be attempted in concert with the release of related proprietary information.

The Nelson curves, used by the petrochemical industry, demonstrate a value to industry wide use of proprietary data. Competing industries are typically reluctant to share information because of the potential loss of a competitive advantage. However, when failure occurs in pressurized hydrogen containing system, the material of construction, the temperature of operation and the hydrogen partial pressure in the failed system are shared industry wide. The result of such sharing is a curve, for numerous alloys, that uses the failure data to define regions of safe operation as a function of temperature and pressure for that alloy. Cooperation is the key to the Nelson curve development. Similar cooperation within the nuclear industry

could lead to emergent correlations of post-reactor material performance with pre-reactor material testing.

- 4) The fact that behavior variations are common among cladding alloys is widely recognized and accepted throughout the nuclear industry. Alloy development programs have been designed to improve the mechanical properties, corrosion resistance and in-reactor performance of zirconium-based alloys. However, there is also a tendency to discuss hydrogen/hydride induced degradation of zirconium-based alloy claddings in general rather than specific terms. Results reported at the Workshop demonstrated that the reorientation behavior of the M5 cladding alloy differed significantly from the behavior of ZIRLO® claddings. However, these same studies showed that the M5 cladding picked up far less hydrogen during irradiation than the ZIRLO® cladding thus the difference in reorientation behavior may be associated with differences in hydrogen content rather than fundamental differences in a susceptibility to hydride reorientation. The recommendation that we recognize and attempt to account for alloy to alloy differences in behavior was made in an attempt to promote multi-variable analyses: alloy chemistry, microstructure, hydrogen content, HRT temperature, cooling rate and other test and material variables including irradiation and post irradiation storage and transfer conditions. The consequence of not following this recommendation is a continuation along the current path where the typical investigation controls and discusses only a fraction of the variables that are known to impact the reorientation process. This limitation reduces the value of the test program and minimizes the ability to fully understand the reorientation process. A high priority should be placed on encouraging all investigators to report and control as many test variables as practical. Implementation of this approach should require minimal additional resources and will ultimately provide a data base that can readily be mined for correlations and understanding.
- 5) The recommendation to establish ductile-to-brittle transformation temperatures that are relevant to fuel handling and transfer situations (including off normal behaviors such as assembly drops) was made because ring compression tests of irradiated samples are currently being used to establish (recommend) a transformation temperature. The relevance of the onset of brittle behavior in an empty ring of cladding cut from an irradiated fuel rod to the behavior of the same cladding on an intact fuel rod has not been established. Additionally, the mechanical response of non-irradiated fuel cladding tested in a pinch mode (the ring compression test) differs significantly from the behavior of the same cladding when tested in a bend mode. The impact of hydride reorientation on the test results also varies with test technique. Regulatory use of ductile-to-brittle transformation temperatures established by ring compression testing may place unnecessary restrictions on fuel handling processes or, even worse, not restrict handling processes when such restrictions are necessary. The relevance of small sample tests to actual spent fuel handling, transfer and accident situations may be established through an understanding of fuel rod behavior in the assembly, and finite element analysis of the cladding stresses and strains associated with the situation and an analysis of how those stresses and strains are duplicated in the small sample test. Implementation of this recommendation has the highest priority of any recommendation made, basically because of the potential that data from the ring compression test may be

used to restrict fuel handling operations before any relevance is established. The consequences of not implementing this recommendation may be minimal but could include improper restrictions on the drying handling and transfer of spent nuclear fuel assemblies.

The discussions in this report do not include substantial portions of the available literature that further demonstrate that hydride reorientation is well understood in a general sense but that the variables impacting reorientation are extensive and have not been fully integrated. As previously mentioned, the generic behaviors of irradiated fuels can be postulated with reasonable accuracy while the specific behaviors may vary significantly. Predictive difficulties arise for specific system because there is no model cladding alloy and behaviors vary with alloy chemistry and microstructure, thermo-mechanical history and other material/service conditions. However, the industry has demonstrated successful dry storage for decades and this success indicates that hydride reorientation is not an overwhelming problem and may not be a problem at all.

Conclusion

Review of recommendations from the 2nd ASTM International Workshop on Hydrides in Zirconium Alloy Cladding suggests that the most pressing concern is implementation of the recommendation to develop ductile-to-brittle transformation temperature that are relevant to assembly handling and transfer operations. Application of finite element analysis techniques is the suggested approach to developing this relevance. However, the lack of dry storage problems, the extensive number of variables known to impact hydride reorientation and large differences in cladding alloys, assembly irradiations and pool and dry storage conditions combine to suggest that increased scientific understanding of hydride reorientation processes and/or further demonstration of short (10 to 20 years) term successful dry storage of selected fuels are unlikely to improve our ability to either predict future behaviors or increase the certainty that we can mitigate the potential for hydride embrittlement during the long term storage of used nuclear fuels.

F.6 References

10 CFR Part 71. "Packaging and Transportation of Radioactive Material." *Code of Federal Regulations*. Washington, DC: Government Printing Office.

Ahn, T., V. Rondinella, and T. Wiss. 2013. "Potential Stress on Cladding Imposed by the Matrix Swelling from Alpha Decay in High Burnup Spent Nuclear Fuel." *Proceedings of the 2013 International High-Level Radioactive Waste Management Conference*. Albuquerque, New Mexico. April 28–May 2.

American Nuclear Society. 2016. *Transactions of the American Nuclear Society and Embedded Topical Meeting Nuclear Fuels and Structural Materials*. New Orleans, Louisiana. June 12–16.

Aomi, M., T. Baba, T. Miyashita, K. Kamimura, T. Yasuda, Y. Shinohara, and T. Takeda. 2008. "Evaluation of Hydride Reorientation and Mechanical Properties for High-Burnup Fuel-Cladding Tubes in Interim Dry Storage." *Journal of ASTM International*. Vol. 5. pp 1–21.

ASTM International. 2002. Standard Specification for Wrought Zirconium Alloy Seamless Tubes for Nuclear Reactor Fuel Cladding. ASTM B811–02.

ASTM International. 2016. *Standard Test Methods for Tension Testing of Metallic Materials*. ASTM E8/E8M-16ae1.

Auzoux, Q., P. Bouffieux, A. Machiels, S. Yagnik, B. Bourdilliau, C. Mallet, N. Mozzani, and K. Colas. 2017. "Hydride Reorientation and its Impact on Ambient Temperature Mechanical Properties of High Burn-up Irradiated and Unirradiated Recrystallized Zircaloy-2 Nuclear Fuel Cladding with an Inner Liner." *Journal of Nuclear Materials*. Vol. 494, pp. 114–126.

Billone, M. 2016. *Update on Testing to Evaluate Radial Hydrides*. Presentation to the Nuclear Waste Technical Review Board at its February 17, 2016 meeting.

Billone, M.C. 2018. *SNF Cladding Hydride Reorientation Research*. Presentation to the Nuclear Waste Technical Review Board at its October 24, 2018 meeting.

Billone, M.C. 2019. *Ductility of High-Burnup-Fuel ZIRLO™ following Drying and Storage*. M2SF-19AN010201011. ANL-19/14. June 30.

Billone, M. and Y. Liu. 2013. Ductile-to-Brittle Transition Temperatures for High-Burnup PWR Cladding Alloys. Presentation to the Nuclear Waste Technical Review Board at its November 20, 2013 meeting.

Billone, M.C. and Y.Y. Liu. 2014. *End-of-Life Internal Pressures for High-Burnup PWR Fuel Rods*. Presentation at the 2nd Zirconium Alloy Cladding/Hydride Workshop. Jackson Hole, Wyoming. June 10–12.

Billone, M.C. and T.A. Burtseva. 2016. Effects of Lower Drying-Storage Temperature on the Ductility of High-Burnup PWR Cladding. FCRD-UDF-2016-000065. August 30.

Billone, M.C. and T.A. Burtseva. 2020. *Preliminary Destructive Examination Results for Sibling Pin Cladding*. ANL-19/53, Rev. 2. Argonne National Laboratory. Lemont, Illinois. February 28.

Billone, M., Y. Yan, T. Burtseva, and R. Daum. 2008. *Cladding Embrittlement During Postulated Loss-of-Coolant Accidents*. NUREG/CR-6967. ANL-07/04. Argonne National Laboratory. Lemont, Illinois. July.

Billone, M.C., T.A. Burtseva, and R.E. Einziger. 2013. "Ductile-to-Brittle Transition Temperature for High-Burnup Cladding Alloys Exposed to Simulated Drying-Storage Conditions." *Journal of Nuclear Materials*. Vol. 433, pp. 431–448.

Billone, M.C., T.A. Burtseva, and J.M. Garcia-Infanta. 2017. *Effects of Radial Hydrides on PWR Cladding Ductility following Drying and Storage*. SFWD-SFWST-2017-000001. September 13.

Billone, M.C., T.A. Burtseva, and M.A. Martin-Rengel. 2015. *Effects of Lower Drying-Storage Temperatures on the DBTT of High-Burnup PWR Cladding*. FCRD-UFD-2015-000008. August 28.

Billone, M.C., T.A. Burtseva, and Y.Y. Liu. 2012. *Baseline Studies for Ring Compression Testing of High-Burnup Fuel Cladding*. FCRD-USED-2013-000040. November 23.

Billone, M.C., T.A. Burtseva, Z. Han, and Y.Y. Liu. 2013. *Embrittlement and DBTT of High-Burnup PWR Fuel Cladding Alloys*. FCRD-UFD-2013-000401. September 30.

Bowman, S.M. and I.C. Gauld. 2010. *OrigenArp Primer: How to Perform Isotopic Depletion and Decay Calculations with SCALE/ORIGEN*. ORNL/TM-2010/43. April.

Bratton, R.N., M.A. Jessee, and W.A. Wieselquist. 2015. *Rod Internal Pressure Quantification and Distribution Analysis Using FRAPCON*. FCRD-UFD-2015-000636. September 30.

Buongiorno, J. 2010. "PWR Description." Class lecture, Engineering of Nuclear Systems from Massachusetts Institute of Technology, Cambridge, MA.
https://ocw.mit.edu/courses/nuclear-engineering/22-06-engineering-of-nuclear-systems-fall-2010/lectures-and-readings/MIT22_06F10_lec06a.pdf.

Burtseva, T.A., Y. Yan, and M.C. Billone. 2010. *Radial-Hydride-Induced Embrittlement of High-Burnup ZIRLO Cladding Exposed to Simulated Drying Conditions*. ML101620301. June 20.

Chu, H.C., S.K. Wu, K.F. Chien, and R.C. Kuo. 2007. "Effect of Radial Hydrides on the Axial and Hoop Mechanical Properties of Zircaloy-4 cladding." *Journal of Nuclear Materials*. Vol. 362, pp. 93–103.

Chung, H.M. 2000. "Fundamental Metallurgical Aspects of Axial Splitting in Zircaloy Cladding." *Proceedings of an International Topical Meeting on Light Water Reactor Fuel Performance*. Park City, Utah. April 10–13.

Chung, H.M. 2004. "Understanding Hydride- and Hydrogen-Related Processes in High-Burnup Cladding in Spent-Fuel-Storage and Accident Situations." *Proceedings of an International Topical Meeting on Light Water Reactor Fuel Performance*. Orlando, Florida. September 19–22.

Cinbiz, M.N., D.A. Koss, and A.T. Motta. 2016. "The Influence of Stress State on the Reorientation of Hydrides in a Zirconium Alloy." *Journal of Nuclear Materials*. Vol. 477, pp. 157–164.

Colas, K., J-C. Brachet, P. Bossis, C. Raepsaet, S. Allegre, O. Rabouille, D. Hamon, J-L. Béchade, C. Cappelaere, and D. Gilbon. 2014. *Characterization Techniques to Quantify Hydrogen Content, Hydride Morphology and Orientation on Unirradiated and Irradiated Zirconium Alloy Cladding*. Presentation at the 2nd ASTM International Zirconium Alloy Cladding/Hydride Workshop. Jackson Hole, Wyoming. June 10–12.

Coleman, C.E., V.A. Markelov, M. Roth, V. Makarevicius, Z. He, J.K. Chakravarty, A.-M. Alvarez-Holston, L. Ali, L. Ramanathan, and V. Inozemtsev. 2018. "Is Spent Nuclear Fuel Immune from Delayed Hydride Cracking during Dry Storage? An IAEA Coordinated Research Project." *Zirconium in the Nuclear Industry: 18th International Symposium*. STP 1597. ASTM International. pp. 1224–1251.

Comstock, R.J. and A.T. Motta (editors). 2018. *Zirconium in the Nuclear Industry: 18th International Symposium*. STP 1597. ASTM International.

Cox, B. 1990. "Pellet-Clad Interaction (PCI) Failures of Zirconium Alloy Fuel Cladding - A Review." *Journal of Nuclear Materials* 172 (1990) 249-292.

Department of Energy. 2004. *Clad Degradation—FEPs Screening Arguments*. ANL-WIS-MD-000008, REV 02. October.

Einzig, R.E. and R. Kohli. 1984. "Low-Temperature Rupture Behavior of Zircaloy-Clad Pressurized Water Reactor Spent Fuel Rods Under Dry Storage Conditions." *Nuclear Technology*. Vol. 67, pp. 107–123.

Einzig, R.E., H. Tsai, M.C. Billone, and B.A. Hilton. 2003. "Examination of Spent Pressurized Water Reactor Fuel Rods After 15 Years in Dry Storage." *Nuclear Technology*. Vol. 144, pp. 186–200.

EPRI [Electrical Power Research Institute]. 2001. *Design, Operation, and Performance Data for High Burnup PWR Fuel from the H. B. Robinson Plant for Use in the NRC Experimental Program at Argonne National Laboratory*. EPRI, Palo Alto, California. 1001558

EPRI. 2002. *Technical Bases for Extended Dry Storage of Spent Nuclear Fuel*. EPRI, Palo Alto, California. 1003416.

EPRI. 2011. *Delayed Hydride Cracking Considerations Relevant to Spent Nuclear Fuel Storage*. EPRI, Palo Alto, California. 1022921.

EPRI. 2013. *End-of-Life Rod Internal Pressures in Spent Pressurized Water Reactor Fuel*. EPRI, Palo Alto, California. 3002001949.

EPRI. 2014. *High Burnup Dry Storage Cask Research and Development Project: Final Test Plan*. EPRI, Palo Alto, California. February 27.

EPRI. 2019. *High Burnup Dry Storage Research Project Cask Loading and Initial Results*. EPRI, Palo Alto, California. 3002015076.

EPRI. 2020. *Effect of Hydride Reorientation in Spent Fuel Cladding—Status from Twenty Years of Research*. EPRI, Palo Alto, California. 3002016033.

- Geelhood, K. and C. Beyer. 2011. "Hydrogen Pickup Models for Zircaloy-2, Zircaloy-4, M5™ and ZIRLO™." Paper T2-011. 2011 Water Reactor Fuel Performance Meeting, Chengdu, China, Sept. 11–14.
- Geelhood, K.J. and W.G. Luscher. 2014. FRAPCON-3.5: A Computer Code for the Calculation of Steady-State, Thermal-Mechanical Behavior of Oxide Fuel Rods for High Burnup. NUREG/CR-7022, Vol. 1, Rev. 1. October.
- Gruss, K.A., C.L. Brown, and M.W. Hodges. 2003. "U.S. Nuclear Regulatory Commission Acceptance Criteria and Cladding Considerations for the Dry Storage and Transportation of Spent Fuel." *Proceedings of the TopFuel 2003—Nuclear Fuel for Today and Tomorrow Conference*. Wuerzburg, Germany. March 16–19.
- Hanson, B. 2016. *Peak Cladding Temperatures: Conservative Licensing Approach vs. Actual*. Presentation at the 2016 Nuclear Energy Institute Used Fuel Management Conference. Orlando, Florida. May 3–5.
- Hanson, B. 2018. *High Burnup Spent Fuel Data Project & Thermal Modeling and Analysis*. Presentation to the Nuclear Waste Technical Review Board at its October 24, 2018 meeting.
- Hanson, B., H. Alsaed, C. Stockman, D. Enos, R. Meyer, and K. Sorenson. 2012. *Gap Analysis to Support Extended Storage of Used Nuclear Fuel*. FCRD-USED-2011-000136, Rev. 0. January.
- Huang F.H. and W. Mills. 1991. "Delayed Hydride Cracking Behavior for ZIRCALOY-2 Tubing." *Metallurgical Transactions A*. Vol. 22, pp. 2049-2060.
- IAEA [International Atomic Energy Agency]. 2004. *Delayed Hydride Cracking in Zirconium Alloys in Pressure Tube Nuclear Reactors: Final Report of a Coordinated Research Project 1998-2002*. IAEA-TECDOC-1410. Vienna: International Atomic Energy Agency.
- IAEA. 2015. *Spent Fuel Performance Assessment and Research: Final Report of a Coordinated Research Project on Spent Fuel Performance Assessment and Research (SPAR-III) 2009–2014*. IAEA-TECDOC Series No. 1771. Vienna: International Atomic Energy Agency.
- Jiang, H., J. Wang, and H. Wang. 2016. "The Impact of Interface Bonding Efficiency on High-Burnup Spent Nuclear Fuel Dynamic Performance." *Nuclear Engineering and Design*. Vol. 309, pp. 40–52.
- Jernkvist, L.O. and A.R. Massih. 2007. "A numerical model for delayed hydride cracking of zirconium alloy cladding tubes." *Transactions, SMiRT 19*. Toronto, Canada. August.
- Kammenzind, B.F. 2018. "Hydrogen Trapping at Neutron Irradiation Produced Defects in Recrystallized Alpha Annealed Zircaloy-4." *Zirconium in the Nuclear Industry: 18th International Symposium*. STP 1597. ASTM International. pp 1167–1191.
- Kammenzind, B.F., B.M. Berquist, R. Bajaj, P.H. Kreyns, and D.G. Franklin. 2000. "The Long-Range Migration of Hydrogen Through Zircaloy in Response to Tensile and Compressive Stress Gradients." *Zirconium in the Nuclear Industry: 12th International Symposium*. American Society for Testing and Materials STP 1354. pp. 196–233.

Kim, Y.S. 2009. "Hydride Reorientation and Delayed Hydride Cracking of Spent Fuel Rods in Dry Storage." *Metallurgical and Materials Transactions A*. Vol. 40A, pp. 2867–2875.

Lanning, D.D., C.E. Beyer, and C.L. Painter. 1997. *FRAPCON-3: Modifications to Fuel Rod Material Properties and Performance Models for High-Burnup Application*. NUREG/CR-6534. December.

Lanning D.D. and C.E. Beyer. 2004. *Estimated Maximum Cladding Stresses for Bounding PWR Fuel Rods During Short Term Operations for Dry Cask Storage*. PNNL. January.

Liu, W., J. Rashid, and A. Machiels. 2016. "A Hydride Reorientation Model for Irradiated Zirconium Alloy Cladding." *Proceedings of the 2016 TopFuel Reactor Fuel Performance Conference*. Boise, Idaho. September 11–15.

Louthan, M.R. Jr. 2014. "Old Data and New Knowledge." Presentation at the 2nd ASTM International Workshop on Hydrides in Zirconium Alloy Cladding. Jackson, Wyoming. June 10–12.

Louthan, M.R. Jr. 2016. *Hydride Reorientation Occurrence and Effects: Summary of the Findings of the June 2014 Jackson, WY Workshop Used Fuel Disposition Campaign Published in SRNL-STI-2015-00256*. Presentation to the Nuclear Waste Technical Review Board at its February 17, 2016 meeting.

Louthan, M.R. Jr. and R.P Marshall. 1963. "Control of Hydride Orientation in Zircaloy." *Journal of Nuclear Materials* 9, No. 2 (1963) 170–184

McRae G.A., C.E. Coleman, and B.W. Leitch. 2010. "The First Step for Delayed Hydride Cracking in Zirconium Alloys." *Journal of Nuclear Materials*. Vol. 396, pp. 130–143.

Montgomery, R. and B. Bevard. 2020. *Sister Rod Destructive Examinations (FY20)* ORNL/SPR-2020/1798. November 30.

Montgomery, R., B. Bevard, R.N. Morris, J. Goddard, Jr., S.K. Smith, J. Hu, J. Beale, and B. Yoon. 2018. *Sister Rod Nondestructive Examination Final Report*. SFWD-SFWST-2017-000003, Rev. 1. May 16.

Montgomery, R., R.N. Morris, R. Ilgner, B. Roach, J. Wang, Z. Burns, J.T. Dixon, and S.M. Curlin. 2019. *Sister Rod Destructive Examinations (FY19)*. ORNL/SPR-2019/1251, Rev. 1. September 27.

Motta, A.T., A. Couet, and R.J. Comstock. 2015. "Corrosion of Zirconium Alloys Used for Nuclear Fuel Cladding." *Annu. Rev. Mater. Res.* 2015. 45:311–343.

Motta, A.T., L. Capolungo L. Chen, M.N. Cinbiz M.R. Daymond D.A. Koss, E. Lacroix, G. Pastore, P.A. Simon, M.R. Tonks, B.D. Wirth, M.A. Zikry. 2019. "Hydrogen in zirconium alloys: A review." *Journal of Nuclear Materials* 518 (2019) 440–460.

NRC [U.S. Nuclear Regulatory Commission]. 2003. *Spent Fuel Project Office Interim Staff Guidance-11, Revision 3, Cladding Considerations for the Transportation and Storage of Spent Fuel*. November.

- NRC. 2020. Dry Storage and Transportation of High Burnup Spent Nuclear Fuel. NUREG-2224. November.
- NWTRB [U.S. Nuclear Waste Technical Review Board]. 2010. *Evaluation of the Technical Basis for Extended Dry Storage and Transportation of Used Nuclear Fuel*. December.
- Peehs, M., G. Kaspar, and E. Steinberg. 1986. "Experimentally Based Spent Fuel Dry Storage Performance Criteria." *Proceedings of the Third International Spent Fuel Storage Technology Symposium/Workshop*. Seattle, Washington. April 8–10.
- Puls, M.P. 1985. "Effect of Stress on Hydride Reorientation in Zirconium Alloys." *Proceedings of the International Symposium on Solid-Defect Interaction*. Kingston, Ontario. August.
- Puls M.P. 2009. "Review of the Thermodynamic Basis for Models of Delayed Hydride Cracking Rate in Zirconium Alloys." *Journal of Nuclear Materials*. Vol. 393, pp. 350–367.
- Puls, M.P. 2018. *The Effect of Hydrogen and Hydrides on the Integrity of Zirconium Alloy Components*. Advanced Nuclear Technology International. Tollerød, Sweden. April.
- Raynaud, P.A.C. and R.E. Einziger. 2015. "Cladding Stress During Extended Storage of High Burnup Spent Nuclear Fuel." *Journal of Nuclear Materials*. Vol. 464, pp. 304–312.
- Ribis, J., F. Onimus, J-L. Béchade, S. Doriot, C. Cappelaere, C. Lemaignan, A. Barbu, and O. Rabouille. 2008. "Experimental and Modelling Approach of Irradiation Defects Recovery in Zirconium Alloys: Impact of an Applied Stress." *Journal of ASTM International*. Vol. 5, pp. 1–21.
- Richmond, D.J. and K.J. Geelhood. 2018. "FRAPCON Analysis of Cladding Performance during Dry Storage Operations." *Nuclear Engineering and Technology* 50 (2018) 306–312. March.
- Saltzstein, S.J., K. Sorenson, B. Hanson, M. Billone, J. Scaglione, R. Montgomery, and B. Bevard. 2017. *EPRI/DOE High Burnup Fuel Sister Pin Test Plan Simplification & Visualization*. SAND2017-7597. July.
- Shimskey, R. and P. MacFarlan. 2014. *Hydriding of Unirradiated Samples*. Presentation at the 2nd ASTM International Zirconium Alloy Cladding/Hydride Workshop. Jackson Hole, Wyoming. June 10–12.
- Shimskey, R., P. Jensen, P. MacFarlan, L. Lin, and B. Hanson. 2016. "Mechanical Testing of Hydrided Fuel Cladding." *Proceedings of the 2016 TopFuel Reactor Fuel Performance Conference*. Boise, Idaho. September 11–15.
- Shimskey, R.W., J.R. Allred, R.C. Daniel, M.K. Edwards, J. Geeting, P.J. MacFarlan, L.I. Richmond, T.S. Scott, and B.D. Hanson. 2019. *Phase 1 Update on Sibling Pin Destructive Examination Results*. PNNL-29179. September.
- Sindelar, R.L., A.J. Duncan, M.E. Dupont, P.-S. Lam, M.R. Louthan, Jr., and T.E. Skidmore. 2011. *Materials Aging Issues and Aging Management for Extended Storage and Transportation of Spent Nuclear Fuel*. NUREG/CR-7116. November.

Sindelar, R.L., M.R. Louthan, Jr., and B.D. Hanson. 2015. *White Paper Summary of 2nd ASTM International Workshop on Hydrides in Zirconium Alloy Cladding, June 10–12, 2014, Jackson, WY*. FCRD-UFD-2015-000533. May 29.

Teague, M., S. Saltzstein, B. Hanson, K. Sorenson, and G. Freeze. 2019. *Gap Analysis to Guide DOE R&D in Supporting Extended Storage and Transportation of Spent Nuclear Fuel: An FY2019 Assessment*. SAND2019-15479R. December.

Valance, S., M. Zemek, J. Bertsch, and C. Hellwig. 2015. "Hydrogen Relocation Kinetics Within Zircaloy Cladding Tubes." *Proceedings of the 2015 TopFuel Reactor Fuel Performance Conference*. Zurich, Switzerland. September 13–17.

Wang, J.-A., H. Wang, H. Jiang, Y. Yan, and B. Bevard. *FY 2015 Status Report: CIRFT Testing of High-Burnup Used Nuclear Fuel Rods from Pressurized Water Reactor and Boiling Water Reactor Environments*. ORNL/SPR-2015/313. Oak Ridge National Laboratory. September 4.

Wang, J.-A., H. Wang, B. B. Bevard, J. M. Scaglione. 2016. *FY 2016 Status Report: CIRFT Testing Data Analyses and Updated Curvature Measurements*. ORNL/SPR-2016/276. Oak Ridge National Laboratory, July 24.

Wang, J.-A., H. Wang, B. Bevard, and J. Scaglione. *FY 2017 Status Report: CIRFT Data Update and Data Analyses for Spent Nuclear Fuel Vibration Reliability Study*. ORNL/SR-2017/291. July 18.

Wang, J. and H. Wang. 2017. *Mechanical Fatigue Testing of High-Burnup Fuel for Transportation Applications*. NUREG/CR-7198, Rev. 1. October.

Was, G.S. 2010. *Fundamentals of Radiation Materials Science: Metals and Alloys*. Second Edition. Springer-Verlag Berlin Heidelberg.

Yagnik, S.K., R-C Kuo, Y.R. Rashid, A.J. Machiels, and R.L. Yang. 2004. "Effect of Hydrides on the Mechanical Properties of Zircaloy-4." *Proceedings of the 2004 International Meeting on LWR Fuel Performance*. Orlando, Florida. September 19–22. pp. 191–199.

Zargar, S., R.A. Medina, and L. Ibarra. 2017. "Effect of Pellet-Cladding Bonding on the Vibration of Surrogate Fuel Rods." *Proceedings of the 2017 International High-Level Radioactive Waste Management Meeting*. Charlotte, North Carolina. April 9–13.

Appendix G

Spent Nuclear Fuel Performance under Normal Conditions of Dry Storage

G.1 Background

Several decades ago, it was thought that commercial spent nuclear fuel (SNF) being discharged from reactors would be processed and its constituent elements (e.g., uranium, plutonium) would be recycled. The operators of commercial reactors assumed that the SNF would only be stored at the reactor site for a few years prior to off-site shipment for reprocessing. Thus, many spent fuel pools adjacent to the reactors had an original capacity for storing SNF for five to ten years, after which the SNF would be shipped for processing to make room for newly discharged SNF.

In the U.S., there is no ultimate disposition pathway (i.e., disposal at a deep geologic repository) operating to allow removal of commercial SNF away from nuclear power plant sites. In other countries (e.g., Finland and Sweden), some progress on planning for disposal of nuclear waste, including SNF, is being made. However, as of October 2020, no geologic disposal facility for commercial SNF is operational anywhere in the world. Another possible option in the U.S. is to ship the SNF to a consolidated interim storage facility, but that option is also not yet available.¹ As the spent fuel pools within the reactor buildings reach capacity, one or both of the following approaches to managing the longer-term but still temporary storage of SNF have been adopted: physically modify the SNF storage racks in the spent fuel pools to increase the amount of SNF that can be stored and package and dry the SNF for removal from the spent fuel pool and move it to a dry storage pad at the nuclear power plant site. Both options are used in the U.S., with expanding the spent fuel pool typically being the first option. At-reactor storage of SNF may be as short as one to two years, as is sometimes done in France, or as long as multiple decades—perhaps as long as a century—in many countries that have no immediate options for ultimate disposition of the SNF via reprocessing or geologic disposal.

The dry storage systems in use in the U.S. have licenses or certificates of compliance from the U.S. Nuclear Regulatory Commission (NRC) for 20, 40, or 60 years, depending on the system. Users of dry storage systems with licenses/certificates for 60 years have had to conduct evaluations, via updated Safety Analysis Reports, to demonstrate that all safety functions (see Appendix C) can be maintained for the longer storage period. The Safety Analysis Reports address long-term degradation processes that may affect those safety functions. Among the issues requiring analysis is the long-term change in SNF properties.

¹ There are two independent, private efforts underway to develop consolidated interim storage facilities – one in west Texas and another in southeast New Mexico. As of October 2020, applications for both sites were being reviewed by the Nuclear Regulatory Commission.

The U.S. inventory of high burnup fuel (HBF)² is diverse and comprises assemblies of various designs, cladding compositions, manufacturing processes, in-reactor power histories, levels of burnup, and linear heat generation rates³ (these factors affect HBF characteristics in different ways; see Appendix A). SNF is stored in a variety of dry cask storage system⁴ designs having varying heat loads and therefore different cladding maximum temperatures. These variations will cause the fuel cladding in storage to be exposed to a variety of oxidation and hydride conditions and experience different stress levels (see Appendix A). Short-term testing has shown that hydride levels and stress conditions in the HBF cladding may affect the cladding's integrity (Peehs, Bokelmann and Fleisch 1986; Peehs, Kaspar, and Steinberg 1986) (see Appendix F for a more detailed discussion).

Ideally, it would be useful to reopen one or more of the dry cask storage systems that have been in operation for many decades to examine the SNF directly. In the U.S., this was done once at the Idaho National Laboratory (INL) in the 1999–2001 timeframe (Bare and Torgerson 2001; Einziger et al. 2003). This examination effort is described in more detail in section G.4.1. However, during the time of the INL study, almost no HBF existed. Therefore, to understand better the characteristic and behavior of HBF, the NRC, DOE, and the nuclear industry have decided that it would be best to directly examine HBF that has been in storage for several years. In conjunction with this effort, DOE is also developing computer models that can predict the characteristics and behavior of HBF and these models can be validated using data collected in the HBF examination program.

G.2 Department of Energy High Burnup Dry Storage Research Project

In fiscal year (FY) 2013, the Department of Energy (DOE) contracted with the Electric Power Research Institute (EPRI) to conduct the High Burnup Dry Storage Research Project (HDRP)—a long-term project to generate data and validate computer models that can predict HBF performance, inform future dry cask storage cask designs, support license renewals and new licenses for HBF storage, and support transportation licensing for HBF (EPRI 2014). The focus of the testing is to obtain data about the long-term behavior of HBF in dry storage systems typical of SNF in storage today and in the future.

² Fuel burnup is a measure of the energy generated in a nuclear reactor per unit initial mass of nuclear fuel and is typically expressed in units of gigawatt-days per metric ton of uranium (GWd/MTU). In the United States, nuclear fuel utilized beyond 45 GWd/MTU is defined by the NRC as HBF.

³ The linear heat generation rate is a parameter of interest during reactor operations and is defined as the heat generated per unit length in the fueled portion of a fuel rod.

⁴ SNF may be packaged into a welded stainless-steel canister that is then placed into a shielded overpack for storage or transportation. Alternatively, SNF may be packaged into a bolted-lid cask (sometimes called a bare fuel cask) that includes its own shielding. These packaging systems are explained in more detail in section 2.1.2 of this report. For storage applications, some literature refers to both of these types of systems as “dry cask storage systems.” In this appendix, the terms “cask,” or “canister” (or both), or “dry cask storage system” are used, where most appropriate.

G.2.1 High Burnup Dry Storage Research Project Long-term Testing Program

A specially designed Orano (formerly AREVA) TN[®]-32 cask with a modified lid for diagnostic monitoring of the fuel temperature and internal cask gas composition is being used for the test (Figure G-1) at the North Anna Nuclear Generating Station in Virginia. Originally, the cask was only licensed to store low burnup fuel (LBF). A license amendment request to allow storage of HBF and to modify the cask for monitoring was approved by the NRC in late 2017. Approval for gas monitoring before and after transportation of the cask may be requested in separate license amendments. Loading of the Orano TN[®]-32 cask and completion of the drying process were done in November 2017. These activities were accompanied by measurements of cask internal temperatures and analysis of cask internal gas composition.



Figure G-1. TN[®]-32 cask manufactured by AREVA (now Orano).
(Hanson 2016a).

The Orano TN[®]-32 cask lid (Figure G-2), which was specially modified for the HDRP, has drain and fill port penetrations that were sealed with double O-ring bolted cover plates after the cask was dried. The lid includes seven penetrations to allow thermocouple lances to be placed in the guide tubes of fuel assemblies at various radial locations within the cask. Each lance comprises nine thermocouples placed at various axial elevations in the cask to continuously monitor the temperature inside the cask (Figure G-3). The temperatures measured in the guide tubes have been related to the cladding temperature using thermal models (see section G.3). Computer model estimates of the maximum cladding temperature expected, based on the initial set of SNF assemblies chosen for the test, was 315°C (599°F) (Hanson 2018). This was significantly lower than the NRC maximum cladding temperature limit of 400°C (752°F) (NRC 2003). At this lower predicted temperature, many

of the HDRP objectives would not be met, such as the ability to study the extent of hydride reorientation in the HBF cladding (see Appendix F).

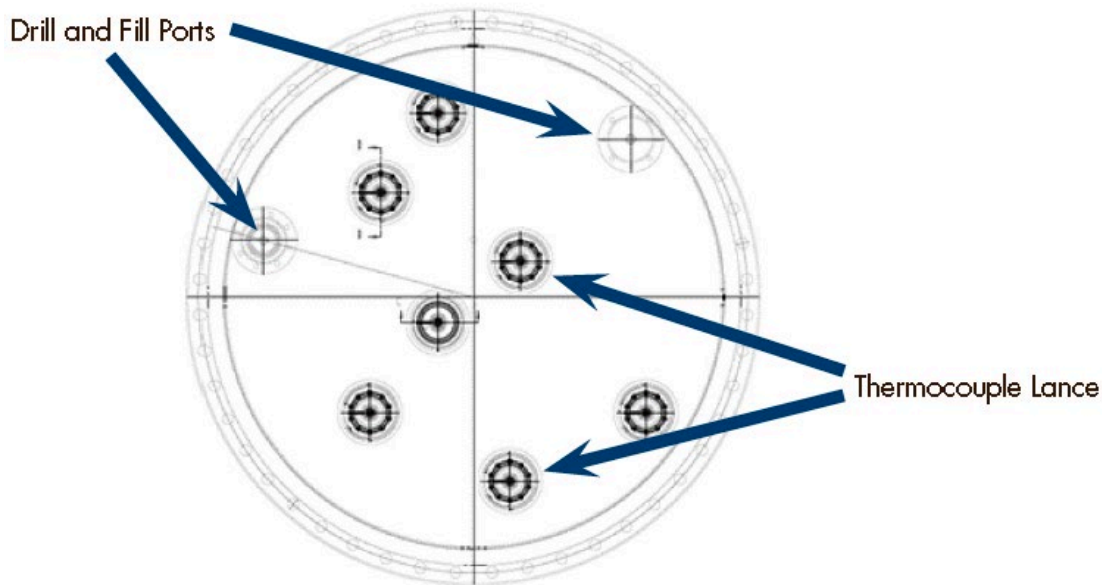


Figure G-2. Penetration locations for thermocouple lances in the modified lid for the AREVA TN®-32 HDRP storage cask
(adapted from Hanson 2018).

To raise the maximum cladding temperature, a second set of assemblies cooled for a shorter period was chosen for the test; however, the cask loading configuration for these assemblies would have resulted in the calculated neutron shield temperature exceeding its temperature limit ($\sim 140^{\circ}\text{C}$ [284°F]) and this configuration would not have been allowed by the NRC. Therefore, a new (and final) group of SNF assemblies was chosen for the test. This cooler set of SNF assemblies, which was calculated to not exceed the neutron shield temperature limit, was predicted to have a maximum fuel cladding temperature of 271°C (520°F) during storage (Hanson 2018). Although the expected cladding temperatures would not approach 400°C as hoped and not all of the project's original objectives would be met, DOE and EPRI decided to continue the demonstration since:

- a significant amount of data would be obtained from measuring cask temperatures and cover gas composition and conducting examinations of the HDRP sister rods (to establish a pre-storage baseline—see section G.2.2) and the HDRP test rods after storage and transport; and
- the demonstration would provide an excellent means of benchmarking the thermal models that were being developed to predict realistic dry cask component temperatures (see section G.3).

DOE made the final selection of 32 pressurized water reactor (PWR) HBF assemblies from the North Anna Nuclear Generating Station and those assemblies were loaded into the HDRP test cask in 2017. The 32 assemblies are described in Figure G-4 (Hanson 2018).

The fuel burnup of these assemblies is between 50 and 55.5 GWd/MTU, which is at the higher end of the burnup range of most spent fuel assemblies in the U.S. The SNF rods in these assemblies include ZIRLO®, Zircaloy-4, low tin Zircaloy-4, and M5® cladding.

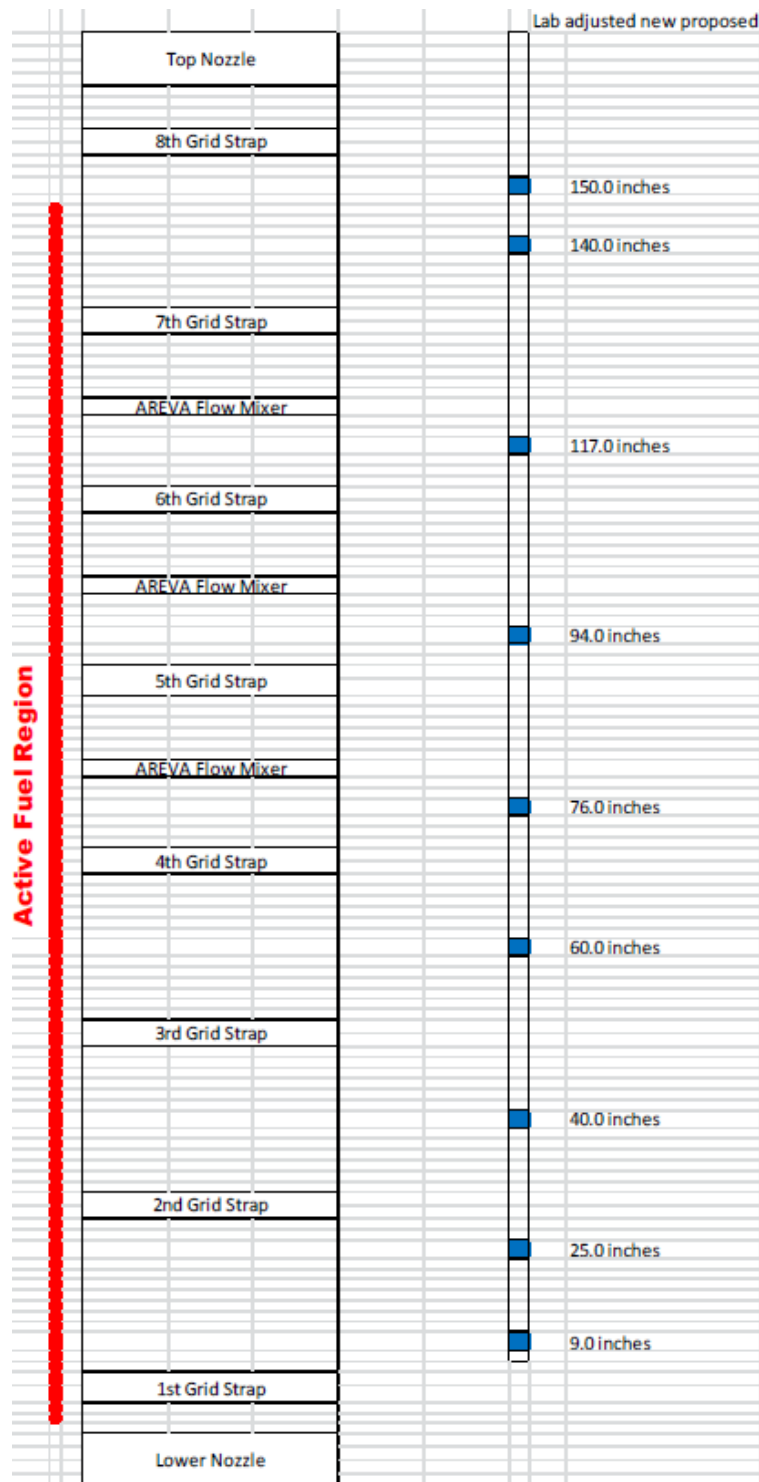


Figure G-3. Axial locations for thermocouples in the HDRP storage cask.

The thermocouples are indicated by the blue boxes in the right side of the figure. (Hanson 2018).

	1 6T0 Zirlo, 54.2 GWd 4.25%, 3cy, 11yr 907/727 W	2 (TC Lance) 3K7 M5, 53.4 GWd 4.55%, 3cy, 8yr 983/749 W	3 3T6 Zirlo, 54.3 GWd 4.25%, 3cy, 11yr 909/729 W	4 6F2 Zirlo, 51.9 GWd 4.25%, 3cy, 13yr 793/653 W	Drain Port
5 3F6 Zirlo, 52.1 GWd 4.25%, 3cy, 13yr 795/653 W	6 (TC Lance) 30A M5, 52.0 GWd 4.55%, 3cy, 6yr 1039/746 W	7 22B M5, 51.2 GWd 4.55%, 3cy, 5yr 1170/754 W	8 20B M5, 50.5 GWd 4.55%, 3cy, 5yr 1149/741 W	9 5K6 M5, 53.3 GWd 4.55%, 3cy, 8yr 977/745 W	10 5D5 Zirlo, 55.5 GWd 4.2%, 3cy, 17yr 806/668 W
11 Vent Port 5D9 Zirlo, 54.6 GWd 4.2%, 3cy, 17yr 795/660 W	12 28B M5, 51.0 GWd 4.55%, 3cy, 5yr 1162/750 W	13 F40 Zirc-4, 50.6 GWd 3.59%, 3cy, 30yr 463/397 W	14 (TC Lance) 57A M5, 52.2 GWd 4.55%, 3cy, 6yr 1047/752 W	15 30B M5, 50.6 GWd 4.55%, 3cy, 5yr 1152/744 W	16 3K4 M5, 51.8 GWd 4.55%, 3cy, 8yr 944/718 W
17 5K7 M5, 53.3 GWd 4.55%, 3cy, 8yr 979/746 W	18 50B M5, 50.9 GWd 4.55%, 3cy, 5yr 1159/747 W	19 (TC Lance) 3U9 Zirlo, 53.1 GWd 4.45%, 3cy, 10yr 918/724 W	20 0A4 Low-Sn Zy-4, 50 GWd 4.0%, 2cy, 22yr 641/541 W	21 15B M5, 51.0 GWd 4.55%, 3cy, 5yr 1163/750 W	22 6K4 M5, 51.9 GWd 4.55%, 3cy, 8yr 944/717 W
23 3T2 Zirlo, 55.1 GWd 4.25%, 3cy, 11yr 929/744 W	24 (TC Lance) 3U4 Zirlo, 52.9 GWd 4.45%, 3cy, 10yr 912/719 W	25 56B M5, 51.0 GWd 4.55%, 3cy, 5yr 1161/749 W	26 54B M5, 51.3 GWd 4.55%, 3cy, 5yr 1162/759 W	27 6V0 M5, 53.5 GWd 4.4%, 3cy, 8yr 989/756 W	28 (TC Lance) 3U6 Zirlo, 53.0 GWd 4.45%, 3cy, 10yr 915/721 W
	29 4V4 M5, 51.2 GWd 4.40%, 3cy, 8yr 915/709 W	30 5K1 M5, 53.0 GWd 4.55%, 3cy, 8yr 970/740 W	31 (TC Lance) 5T9 Zirlo, 54.9 GWd 4.25%, 3cy, 11yr 922/738 W	32 4F1 Zirlo, 52.3 GWd 4.25%, 3cy, 13yr 798/656 W	

Figure G-4. Final loading map for the HDRP cask.

Each square represents a basket cell with a cell identifier in the upper left corner and characteristics of the loaded fuel assembly listed in order, from top to bottom and left to right: (1) presence of a thermocouple lance (i.e., TC Lance); (2) assembly identifier number; (3) cladding material; (4) assembly average burnup (GWd); (5) initial enrichment (uranium-235 weight percent); (6) number of cycles operated in the reactor (cy); (7) cooling period since discharge at the cask loading date; and (8) best estimate predicted decay heat at the time of loading and at the end of a 10-year storage period (*adapted from Saltzstein et al. 2017*).

After drying the cask using standard nuclear industry procedures and backfilling it with helium, the gas inside the cask was intermittently monitored for water, fission gases, hydrogen, and oxygen for two weeks in the cask preparation bay at the North Anna Nuclear Generating Station (Hanson 2018). The cask was then transferred to the dry storage pad at North Anna where the internal cask gases may not be monitored again until just prior to transporting the cask to a facility where it will be opened for post-test examination.⁵ The timing and duration of the initial gas sampling was based on assumptions that (1) the drying

⁵ The gas sampling before and after transport can show whether any rods failed during storage or transportation, but only post-test examination of unfailed rods can provide any information of the potential rate of degradation.

criterion would be met within a day or so, and (2) there would be no fuel breaches as the temperature and cladding stress drop (Stockman, Alsaed, and Bryan 2015). Results of the gas samples taken 5 hours, 5 days, and 12 days after completion of drying are available in Bryan et al. (2019) and EPRI (2020). Gas sample analysis determined no fuel failures (no krypton-85 detected), small amounts of hydrogen (<500 ppmv) and oxygen (<200 ppmv), and a maximum estimated 5.6 moles of water (17,400 ppmv; or approximately 100 ml, if the water vapor were condensed) in the entire gas phase. Bryan et al. (2019) observed that, given the relatively high temperatures in the cask and the measured level of moisture, “it is unlikely that there is any free water in the cask, unless it is trapped in an inaccessible location (e.g., within a rod) and is slowly bleeding out.” Bryan et al. (2019) also noted that “[m]easuring water content proved challenging,” and so, there was an uncertainty range of $\pm 10\%$ on the water content measurement.

The maximum measured transient temperature during drying for the HDRP test was 237°C, measured in Cell 14 of the HDRP cask basket (see Figure G-4 for the cell locations). The maximum measured steady-state temperature after drying was 229°C (444°F), also in Cell 14 (Figure G-5) (Hanson 2018).

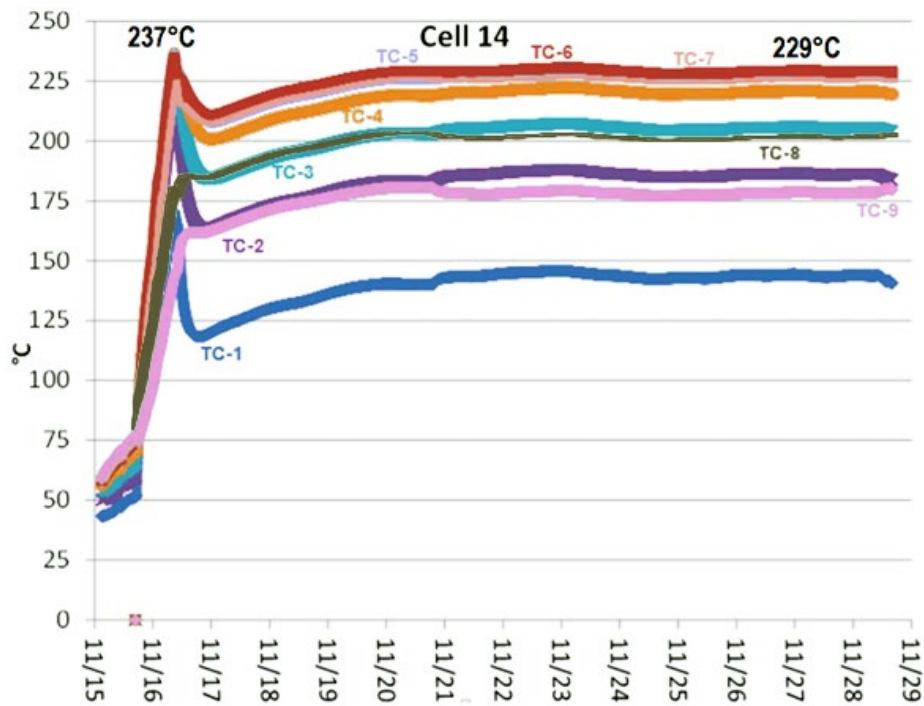


Figure G-5. Measured temperatures in the hottest assembly during and after drying of the HDRP cask

Thermocouple (TC)-1 is near the bottom of the assembly and TC-9 is near the top of the assembly (see Figure G-3) (adapted from Hanson 2018).

Although no further near-term gas sampling is planned, temperature monitoring of the HDRP test cask will continue during its nominal ten-year storage period at the North Anna Nuclear Generating Station (See Appendix E for a discussion of drying and gas sampling and section G.3 for a discussion of temperature measurements).

The demonstration is currently planned to run for ten years, after which DOE plans to transport the cask to the CPP-603 facility at INL.⁶ There, some test rods will be extracted, moved to a hot cell facility, and examined for comparison with the sister rods (EPRI 2014) (see next section for a description of the sister rods) to determine if there are any differences in the characteristics between the test rods and the sister rods and to assess the accuracy of the predictions from short-term testing and fuel performance models. DOE expects that characterizing the test rods extracted from the HDRP will include the same nondestructive and destructive examinations as those conducted on the sister rods (Saltzstein et al. 2017).

G.2.2 Sister Rod Testing

To be able to detect and evaluate any changes to HBF properties after years of dry storage, it is essential to know the properties of the HBF before it is placed into storage. In FY 2015, DOE chose 25 “sister rods” to be examined to establish the pre-storage HBF baseline. A sister rod is a rod that has similar characteristics to one that is stored in the HDRP cask. There were two potential fuel assembly types that could be donors for sister rods and some of each type were used: (1) assemblies having similar operating histories to those assemblies chosen for storage in the Orano TN[®]-32 cask; or (2) actual fuel assemblies selected for storage in the cask. EPRI (2019) includes a detailed description of the selected sister rods. Prior to loading the HDRP cask, the sister rods representing all the cladding types in the HDRP cask (M5[®], ZIRLO[®], Zircaloy-4, and low-tin Zircaloy-4), were shipped to Oak Ridge National Laboratory (ORNL) for examination. The test plan for these rods includes non-destructive examinations of all rods at ORNL, followed by destructive examinations of selected rods, with the work divided among ORNL, Pacific Northwest National Laboratory (PNNL), and Argonne National Laboratory (ANL) (Saltzstein et al. 2017). More details of the sister rods examinations are provided below.

The main goals for examining and testing the sister rods are listed below in order of priority (Saltzstein et al. 2017).

Priority 1: Determine the characteristics, material properties, and fuel rod performance of the sister rods to provide a baseline of the condition of the HBF when it was loaded into the HDRP cask. Once the cask is transported and opened, the test rods will be examined and compared to the sister rods. The results of the comparison will indicate whether HBF performs as predicted by existing models.

Priority 2: Determine the characteristics, material properties, and performance of the sister rods after applying elevated temperatures matching the bounding maximum cladding temperature expected for SNF currently in storage or expected to be placed in dry storage.⁷

⁶ At present, only CPP-603 at INL has been demonstrated to be able to accept the cask for unloading but does not have the capabilities to examine the HBF rods after they are unloaded. The rods would have to be transferred to another facility.

⁷ The maximum temperature of SNF cladding in dry storage currently or in the future is unknown. NRC guidance (NRC 2003) suggests that the maximum cladding temperature should be maintained

Priority 3: Because it is not practical to test all fuel types under all conditions, data will be obtained that supports modeling to predict fuel performance under a range of scenarios associated with extended interim storage and Hanson et al. (2016) provides a detailed description of the sister rods.

The test plan for the non-destructive examinations includes (1) visual inspection; (2) profilometry (for diameter variation) and length measurements; (3) eddy current testing to measure the thickness of any oxide layer present on the outer surface of the fuel rod cladding and, by inference, the hydrogen content in the cladding;⁸ and (4) gamma-scanning to determine the pellet-pellet interfaces, location of the spacer grid relative to the bottom of the rods⁹ and the general burnup profile of all 25 sister rods (Saltzstein et al. 2017).

The non-destructive examinations were completed in 2017 (Montgomery et al. 2018). Visual examination of the sister rod cladding detected no end cap weld failures or gross breaches. The examination did reveal some shallow grid-to-rod fretting,¹⁰ buildup of Chalk River Unidentified Deposits (CRUD, see Appendix A), oxide spalling, and long, shallow axial scratches (most likely caused by insertion and removal of the rods from the fuel assemblies). Gamma scans showed the location of the spacer grids, pellet-pellet interfaces and some small pellet-pellet gaps, but nothing unexpected. The profilometry indicated no significant ovality that might affect the extent of the pellet-cladding bonding (Montgomery et al. 2018). The oxide layer thickness could not be determined from the profilometry due to a buildup of CRUD on the SNF rod surface (Saltzstein et al. 2017). Eventually, this will be accounted for when the CRUD and oxide thicknesses are measured during DEs (Montgomery et al. 2018).

Destructive examination of the sister rods will be done in two phases, with the plans for Phase 2 being informed by the results from Phase 1. The Phase 1 testing includes (Montgomery et al. 2019):

- Full-length fuel rod heat treatments of three sister rods (one ZIRLO[®], one M5[®], and one Zircaloy-4).

below 400°C (752°F). Storage license applicants generally perform thermal calculations that assume the SNF is emitting the maximum decay heat allowable. The applicants' thermal models are designed to ensure that the maximum cladding temperatures are not underestimated. Furthermore, few, if any, of the NRC-approved dry cask storage systems have been loaded with the maximum allowable decay heat. Hence, at most, only a few of the more than 2,000 dry storage systems are likely to have had peak cladding temperatures as high as 400°C.

⁸ Hydrogen analysis will be done during destructive examination (when the cladding is punctured and sectioned) (Saltzstein et al. 2017).

⁹ The exact location of the spacer grids on any particular rod will vary. The location of the spacer grid on the rod can be determined by a dip in the gamma activity when gamma scans along the length of the rods are performed.

¹⁰ Grid-to-rod fretting is partial gouging of the outside surface of the fuel cladding due to rubbing of the spacer grids on the cladding during normal grid and rod vibrations during reactor operation.

- Rough segmenting of the rods for allocation of segments to the various destructive examinations and labs. Segments are stored in aluminum capsules, in air, until the time of the test.
- Defueling of selected segments: Some segments are defueled to prepare them for cladding only destructive examinations; other segments are defueled to gather samples for fuel isotopic and burnup measurements. Aerosolized particles released from the segments where fracture occurs during testing (e.g., four-point bend) will be captured for analysis.
- Rod internal pressure measurement, rod void volume measurement, collection of fission gas specimens, gas transmission tests,¹¹ and fuel isotopics and burnup measurements.
- Metallography.
- Cladding total hydrogen measurements.
- Cyclic integrated reversible-bending fatigue tests in static, dynamic, and cumulative test modes.
- Four-point bend tests.
- Axial tension testing.
- Microhardness tests.
- Ring compression tests (RCTs).
- Burst tests.

Most of the tests will be conducted with fueled cladding (i.e., with pellets still inside the cladding) but a few tests, such as the ring compression tests at ANL, will be conducted on defueled cladding. See Montgomery et al. (2019) and Montgomery and Bevard (2020) for a detailed description of the test plan and test results (as of September 2020).

At ORNL, three full-length sister rods were heated to 400°C—the NRC-allowed maximum cladding temperature that an HBF rod may experience—to provide cladding that has experienced the bounding temperatures for separate effects testing. ORNL, PNNL, and ANL are conducting destructive examination testing and characterization that includes mechanical tests on both heated and unheated rod segments. If the Phase 1 tests of cladding heated to 400°C show a change in mechanical properties because of radial hydride

¹¹ The gas transmission tests are also called gas communication tests. These are tests to determine the rate that the internal gas can flow from one end of the rod to the other through the column of fuel pellets. This information is useful to determine the degassing flow rate immediately after a hypothetical cladding breach and then, the potential for entrainment of small fuel particles through the cladding breach (see Appendix F).

formation, then other untested sister rods, being held in reserve, may be tested to further explore this phenomenon (Montgomery et al. 2019).

For all sister rods (both heated and unheated) undergoing destructive examination, the testing began with puncturing the rod cladding to determine the initial (prior to drying and storage) rod void volume and the rod internal pressure. Eight of the 25 sister rods were punctured at ORNL and the results were reported in Montgomery et al. (2019). Ten rods were punctured at PNNL Shimskey et al. (2019). The results are summarized below.

Montgomery et al. (2019) reported ORNL measurements of rod void volume and rod internal pressure. The measured rod pressures, in the range of 3.2 to 4.7 MPa (460 to 680 psi), were consistent with pressures in the publicly available database of HBF rod pressures. As expected, the fission gas partial pressure increased with the rod average fuel burnup. All measured rod void volumes, in the range of 10 to 13 ml [0.34 to 0.44 fl oz], were on the lower side of the publicly available database of void volumes. Based on the measurements of void volume and rod internal pressure, the ORNL analysts identified no significant differences between heat-treated rods and non-heat-treated rods for ZIRLO® and M5® cladding types. ORNL found that the rod internal pressure of the heat-treated Zircaloy-4 rod was approximately 4.8 MPa (700 psi). This pressure is higher than historically-recorded, average rod internal pressures of similar rods (approximately 3.7 MPa [540 psi]). However, this rod was a lead test rod operated for four cycles in the reactor and had a rod-average burnup of 60 GWd/MTU. It should be noted that there is only one heat-treated Zircaloy-4 sister rod, allowing only one data point for rod internal pressure. ORNL concluded “it is not clear whether there was an effect related to the heat treatments on the Zirc[aloy]-4-clad rod” (Montgomery et al. 2019).

ORNL also reported the results of its gas transmission tests. Montgomery et al. (2019) concluded, “[g]as transmission and depressurization testing of eight [HBF] rods revealed that gas communication from one end of the pellet stack to the other is unobstructed, but slow at room temperature. The time constants derived were in the minutes to hours, depending on the starting pressure. Thus, one can expect gas equilibrium in the fuel rod over several hours, rather than in minutes or seconds.”

PNNL analysts found that the rod internal pressures measured for ten sister rods at PNNL were also consistent, within experimental uncertainty, with publicly-available PWR rod internal pressures (Billone and Burtseva 2020). Shimskey et al. (2019) reported preliminary gas transmission test results to evaluate and quantify fuel particulate release during rod depressurization done at PNNL. Based on measurements of cesium-134, cesium-137, and europium-154 activities, total aerosol released from the fuel was in the range of 10^{-8} to 10^{-7} kg of oxide fuel particulate per kg oxide fuel in a rod. The release amount was in line with previous measurements of particulate release noted in Hanson et al. (2008). PNNL also plans to conduct burst testing of sister rod cladding samples and to perform metallographic imaging of sections of cladding.

Both ORNL and PNNL measured the concentrations of krypton, xenon, and helium in the gas collected when the sister rods were punctured. They also determined the xenon-to-krypton

ratio¹² for each punctured rod (Montgomery et al. 2019; Shimskey et al. 2019). Montgomery et al. (2019) reported that the ORNL and PNNL data for krypton concentration versus fission gas partial pressure are consistent except for one Zircaloy-4 rod that had a higher krypton concentration, which may be explained by that rod having a different power history: “The source of higher fission gas release will be investigated once more detailed information on the measured rod burnup and predicted rod fission gas production are available” (Montgomery et al. 2019).

Both ORNL and PNNL measured the xenon-to-krypton ratio in the gas collected from the sister rods. It was found that for both unheated and heated sister rods, the xenon-to krypton ratio was consistent, within experimental uncertainty, with published data for PWR and similar fuels (Montgomery et al. 2019).

G.3 Modeling of Temperature Profiles in Spent Nuclear Fuel and Spent Nuclear Fuel Cask Systems

A critical variable used to determine many cladding properties and the rate of cladding degradation is the cladding’s temperature history, which is discussed in detail in Appendix F. The NRC’s NUREG-2215, Section 5.4.4, Analytical Methods, Models, and Calculations, provides guidance to NRC reviewers on thermal models:

“The computer codes used in the thermal evaluation should be well verified and validated The applicant should provide acceptable basis (e.g., benchmark efforts that mimic heat transfer and flow characteristics for the proposed design and that includes well defined boundary conditions and high-quality data for validation purposes, published results that include the range of applicability of the computer codes and highlight the specific features relevant to storage container design) for the accuracy of the selected computer code or codes and justification for the code’s use in the proposed evaluation.” (NRC 2020)

Conservative thermal models that ensure maximum cladding temperatures are not underestimated are typically used by utilities and cask manufacturers to predict SNF cladding temperatures. The model predictions are used to demonstrate that the cladding temperatures will not exceed the NRC-suggested maximum cladding temperature 400°C (725°F) (NRC 2003). 400°C was set by the NRC as an acceptable maximum temperature to prevent unacceptable amounts of cladding creep and hydride reorientation, which were postulated to be the primary mechanisms responsible for cladding breaches.¹³ To ensure the cladding temperature remains below 400°C, validated models must predict cladding temperatures that do not exceed 400°C, even when modeling and measurement

¹² Different fissile isotopes (e.g., uranium-235, plutonium-239, plutonium-241) produce xenon and krypton in different proportions when they fission. Determining the xenon-to-krypton ratio can provide some information about the location of the fission gas release in the fuel pellet because, for HBF, there are higher concentrations of plutonium isotopes near the outer surface of the fuel pellet (Jernkvist and Massih 2002).

¹³ See section 3.2 and Appendix F for detailed discussions on hydride reorientation.

uncertainties are considered. The risk of the cladding temperatures rising above 400°C diminishes over time as the cladding cools after being stored for extended periods.

DOE's current research program aims, among other things, to develop models that realistically calculate temperatures, including uncertainties, of the SNF and components used in storage and transportation of SNF for a broad range of SNF, including HBF.

G.3.1 Thermal Model Development and Use

U.S. efforts to develop models in the public domain to predict cladding temperatures include those by NRC (Das, Basu, and Walter 2014; Solis and Zigh 2016), PNNL for the DOE (Adkins et al. 2013; Cuta et al. 2013; Michener et al. 2015), and UN-Reno (Hadj-Nacer et al. 2015). The NRC is developing thermal models that predict temperatures inside a fuel canister and from the outer canister surface to the overpack outer surface for horizontal (Das, Basu, and Walter 2014) and vertical configurations (Hall, Zigh, and Solis 2019).¹⁴ PNNL is modeling temperature profiles in a variety of different storage systems from the fuel-cladding interface to the storage and transportation overpack. The UN-Reno studies deal mainly with the heat transfer effects in a very low-pressure atmosphere, consistent with the SNF vacuum drying process (Appendix E). While fuel manufacturers are also improving their thermal models, these models are proprietary and usually over-predict the temperatures. Other countries are also developing thermal models to be applied to SNF dry cask storage systems. For example, Japan is developing new thermal models that will be benchmarked against calibrated heater rods in a two-assembly test storage cask, but no details of the model have been released (Yamamoto et al. 2015).

G.3.1.1 Pacific Northwest National Laboratory Model

The heart of the PNNL model development for DOE is the COBRA-SFS computer model that can predict temperature profiles in SNF dry cask storage systems. Although originally developed to model the axial- and radial-temperature profiles from fuel cladding inside of a bolted-lid storage cask to the inside of the cask wall, the COBRA-SFS model has evolved. It can now be coupled with a computational fluid dynamics model (e.g., STAR-CCM+), which can be used to model air flow and temperature profiles along the exterior of a welded canister stored inside a concrete storage module (e.g., the AREVA-TN NUHOMS™ system [Suffield et al. 2012], a Holtec HI-STORM system [Cuta and Adkins 2014], or a NAC MAGNASTOR® system [Fort et al. 2016]). COBRA-SFS models every fuel rod and channel as well as all the details of the fuel basket and other cask or canister internals. Conditions of CRUD and variable oxide layers on the cladding surface can be accounted for by adjusting the emissivity of the outer surface of the cladding. The COBRA-SFS model assumes that the

¹⁴ Discussions of thermal models other than those developed for DOE, such as those developed by the NRC, are outside the scope of this report.

cask or canister is dry; therefore, any effects of two-phase (residual water and cover gas) gas flow¹⁵ or residual water are not simulated.¹⁶

The COBRA-SFS model does not predict temperature distributions of the fuel rod from the exterior cladding surface inward to the fuel-pellet matrix itself; therefore, the model is unable to predict hydrogen behavior in cladding caused either by temperature gradients across the cladding or stress from rod internal pressure. Instead, COBRA-SFS uses the decay heat produced by the fuel in the rods as an input parameter. The COBRA-SFS model, coupled with STAR-CCM+,¹⁷ can be used to predict the temperatures of various components of the dry cask storage system from the cladding surface to the outside of the overpack. These temperature predictions were done for the HDRP Orano TN[®]-32 cask (Fort et al. 2019a), as discussed below.

Due to the detail and accuracy of both the COBRA-SFS model and the planned use of best-estimate input parameters, the temperature predictions are intended to be more realistic and less conservative than those made by the nuclear industry's proprietary models.¹⁸ In their model, PNNL specifically removed five conservative assumptions typically used by the industry to ensure the maximum cladding temperature is not underestimated. The PNNL approach includes the following modifications:

1. Removing known conservatisms in the model (such as neglecting the contribution of thermal convection to transfer heat in the basket region) (Fort et al. 2019a).
2. Using more-realistic ambient temperatures: Title 10, Code of Federal Regulations, Part 71, "Packaging and Transportation of Radioactive Material," section 71.71(b) states that, under normal conditions of transport, the cask system must be able to tolerate an ambient temperature range of -29°C (-20°F) to +38°C (100°F). The industry uses 38°C (100°F) ambient to calculate temperatures. As the ambient exterior air temperature is decreased in the model, it appears that the maximum cladding temperature decreases by approximately the same amount (10 CFR Part 71). During the 12-day period after the HDRP cask was dried, the ambient temperatures exterior to the cask ranged from approximately 10°C (50°F) to approximately 28°C (82°F) (EPRI 2020).

¹⁵ In this case, two-phase flow means concurrent flow of both cover gas (usually helium) and water vapor.

¹⁶ The amount of water remaining in a dry cask storage system after drying has not been definitively determined. DOE continues to conduct research to investigate this question. Some testing results regarding moisture content after drying are discussed in Appendix E.

¹⁷ Note that these are two separate and distinct models. The strength of COBRA-SFS is to calculate detailed cladding temperatures along the length of each fuel rod. The strength of STAR-CCM+, which uses the k-effective porous media approach typical in computational fluid dynamics models, is its effectiveness at predicting the natural circulation air flow in the annulus between the canister and overpack, from which the temperature profile on the canister's outer wall is predicted.

¹⁸ The industry's computer models are proprietary, but the assumptions made when exercising the models are generally given in the safety analysis reports supporting license applications.

3. Using actual drying times and profiles: The industry assumes that the cladding temperature reaches a steady state during the drying process even though the actual drying times can vary significantly (Carver 2015) and are usually shorter than the time needed to reach steady state (Hanson 2016b). This is important because the time during which the cladding temperature is at a maximum will control how much hydrogen can re-dissolve in the cladding and then re-precipitate as the SNF cools (see Appendix F).
4. Using actual cask loadings (characteristics of the SNF in the cask) instead of design-basis loadings: When a safety analysis report for a storage or transportation license is submitted to the NRC, it contains a design-basis loading specifying the maximum burnup, maximum enrichment, and minimum cooling time allowed to calculate the maximum cladding temperature. The actual SNF loaded into a cask has, on average, lower burnups, lower enrichments, and longer cooling than indicated in the design basis. The PNNL model incorporates actual rod-by-rod heat loads as opposed to the design-basis heat loads used by industry.
5. Using “best estimate” decay heat calculations rather than the conservative NRC standard: Industry usually adheres to the strict NRC guidelines (Gauld and Murphy 2010) to estimate decay heat loads when calculating temperatures. When compared to measured decay heats, the NRC method overpredicts PWR SNF decay heat by a minimum of 6.8% and an average of 12.5% and boiling water reactor (BWR) SNF decay heat by a minimum of 3.7% and an average of 22% (Hanson 2016b). The decay heat information can be calculated from DOE’s database of fuel information¹⁹ (Scaglione et al. 2014).

When actual decay heats, expected at the time of the HDRP cask loading, were calculated (i.e., removing conservatisms as described in points four and five above), the predicted maximum cladding temperature in the HDRP cask decreased substantially from 315 to 271°C (599 to 520°F). Further details of the HDRP modeling effort are included in section G.3.2.3.

G.3.1.2 University of Nevada-Reno Model

DOE funded a Nuclear Energy University Program project at the University of Nevada-Reno (UN-Reno) to develop computational fluid dynamic simulations that accurately predict SNF peak cladding temperatures during drying (Hadj-Nacer et al. 2015; Trujillo 2017). The difference between the PNNL model and the UN-Reno model is that the UN-Reno model builds on the ANSYS/Fluent computational fluid dynamics package,²⁰ and it includes a rarefied-gas thermal resistance²¹ parameter at the cladding boundary; however, the model has not been benchmarked against the data from instrumented tests at INL or any other

¹⁹ The Used Nuclear Fuel-Storage, Transportation, and Disposal Analysis Resource and Data System [UNF ST&DARDS] database.

²⁰ This software package is widely used by some reviewers during NRC reviews of applicants’ thermal calculations to ensure the applicants have used bounding temperatures.

²¹ The effect of including this parameter is a notable difference between the temperature of the cladding and the nearby gas at low gas pressure, as would be seen during vacuum drying. DOE does not model this surface layer.

actual loaded SNF storage system. Since the rarefied gas issue has been raised, Sandia National Laboratories (SNL) has conducted tests on mockups using assemblies containing heater rods that show the rarefied-gas mechanism is not operative in dry cask storage systems (Durbin et al. 2017; Zigh et al. 2017).

G.3.2 Benchmarking the Thermal Models

To benchmark, or validate, the DOE-funded models, three separate experiments have been conducted, two of which are proceeding with multiple organizations conducting independent model development. The experiments are described below.

G.3.2.1 Pacific Northwest National Laboratory Modeling of a Low Burnup Spent Nuclear Fuel Demonstration Cask

The COBRA-SFS model was benchmarked against all temperature data collected during the dry-cask storage project at INL for LBF in vertical, direct-loaded casks (McKinnon and Deloach 1993). The INL cask project included SNF of various compositions, different types of fuel baskets, six different dry-storage casks, different heat loads, and different internal cooling flow conditions. As part of the benchmarking process, the model predicted 78 rod cladding surface temperatures under different conditions that compared favorably to the actual measured SNF temperatures. McKinnon and Deloach (1993) reports that “[c]ode predictions of dry storage system temperatures within 25°C (77°F) can be obtained.” McKinnon and Deloach (1993) attribute the difference between predicted temperature and measured temperature to several uncertainties, including component emissivity and system geometries, especially gap widths between components in the cask system.

G.3.2.2 Sandia National Laboratories Dry Cask Simulator Experiments and Models

SNL conducted tests on a scale model of an SNF dry storage system employing a steel canister inside a concrete overpack (Durbin and Lindgren 2018), called the “Dry Cask Simulator” (DCS). The researchers determined that the DCS “... was shown to have similarity with prototypic systems through dimensional analysis. The data were collected over a broad parameter set including simulated decay power and internal helium pressure.” (Durbin and Lindgren 2018)

The purpose of the DCS testing was to produce high-quality data to be used to validate thermal models for predicting temperatures in SNF dry cask storage systems. The DCS was built to study the thermal-hydraulic response of fuel under a variety of heat loads, internal vessel pressures, and external configurations.

The general design of the DCS is shown in Figure G-6. An existing electrically heated but otherwise prototypic BWR Incoloy-clad test assembly was deployed inside of a representative storage basket and cylindrical pressure vessel that represents a vertical canister system. The symmetric single assembly geometry with well-controlled boundary conditions simplified interpretation of results. Two different arrangements of ducting were used to mimic conditions for aboveground and belowground storage configurations for vertical, dry cask storage systems with canisters. Transverse and axial temperature profiles were measured throughout the test assembly. The induced air mass flow rate was measured for both the aboveground and belowground configurations. In addition, the impact of cross-wind conditions on the belowground configuration was quantified.

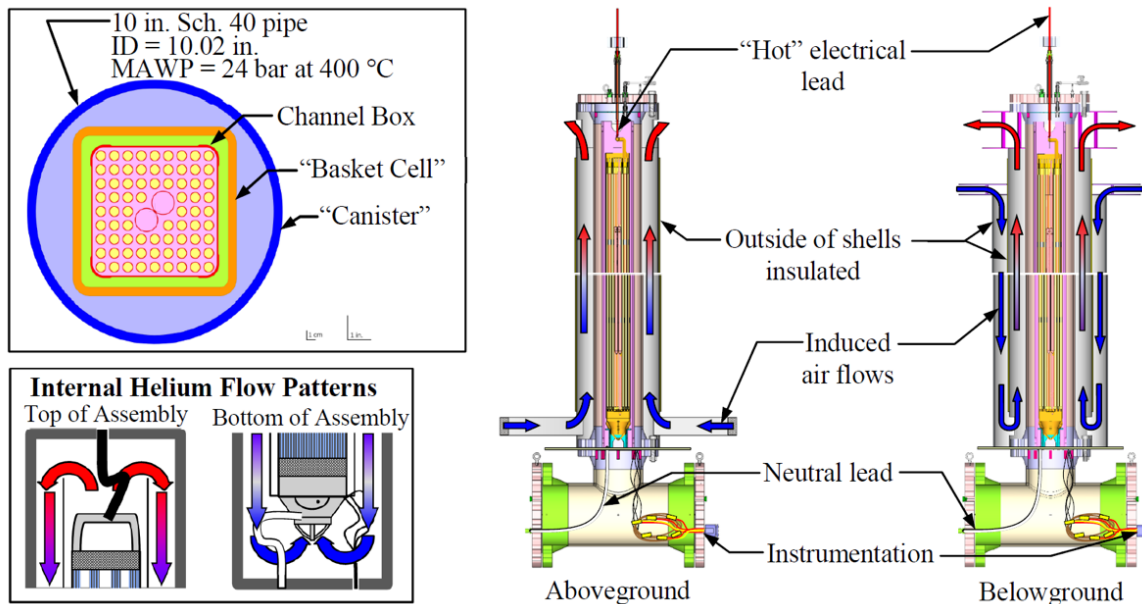


Figure G-6. General layout of the SNL Dry Cask Simulator.

The schematics show a plan view (upper left), the internal helium flow (lower left), and the external air flow for the above-ground (middle) and below-ground (right) configurations.

Note: MAWP is the maximum allowable working pressure (*Durbin and Lindgren 2018*).

More than 40 separate data sets were collected and analyzed. Fourteen data sets for the aboveground configuration were recorded for simulated decay heat loads and internal pressures ranging from 0.5 to 5.0 kW and 0.3 to 800 kPa (0.04 to 116 psi) absolute, respectively. Another fourteen data sets were collected for the belowground configuration starting at ambient conditions and concluding with thermal-hydraulic steady state. Additionally, several tests were conducted using a wind machine to simulate different air turbulence conditions on the outside of the DCS (*Durbin and Lindgren 2018*).

DOE sponsored SNL to coordinate an exercise to compare computer model predictions against the temperature and air flow rates measured in the DCS in the aboveground, vertical position (*Pulido et al. 2020*). Five modeling institutions—NRC, PNNL (two models), Centro de Investigaciones Energéticas, MedioAmbientales y Tecnológicas (CIEMAT, Spain), and Empresa Nacional del Uranio, S.A., S.M.E. (ENUSA, Spain) in collaboration with Universidad Politécnica de Madrid (UPM, Spain)—were granted access to the input parameters listed in *Lindgren and Durbin (2017)* and results from the DCS tests reported in *Durbin and Lindgren (2018)*. With this information, each institution was tasked to calculate minimum, average, and maximum fuel axial temperature profiles for the fuel region as well as the axial temperature profiles of the DCS structures (*Pulido et al. 2020*).

The modeling results are reported in *Pulido et al. (2020)*. The six models represented the DCS fuel assembly in different ways. Two models used computational fluid dynamics tools to explicitly represent the fuel rods and spacers in detail; three used a porous media model, where the fuel is homogenized into a simplified volume with corresponding inertial and frictional loss coefficients; and one used an explicit subchannel model, where the fuel is divided into a number of flow paths or channels. The peak cladding temperature is typically

the most important target variable for cask performance, and all models predicted the peak cladding temperature within 5% root-mean-square error. Based on the results of the modeling exercise, Pulido et al. (2020) concluded that models using a “porous media fuel representation can achieve modeling calculation results of peak cladding temperatures, average fuel temperatures, transverse temperatures, and air mass flow rates that are comparable to explicit fuel representation modeling results.”

The Board notes that the SNL testing includes features not included in the HDRP, like a surrogate BWR assembly and a surrogate welded SNF canister. However, the SNL testing does not include other SNF assembly components such as control rod assemblies or discrete burnable absorber rods,²² which could affect conductive and convective heat transfer inside the SNF cask or canister.

G.3.2.3 High Burnup Dry Storage Research Project Temperature Measurements and Modeling

To assess the accuracy of various thermal models in predicting dry cask storage system temperatures, DOE, in cooperation with EPRI, planned to benchmark four models against the temperatures measured during and after the drying process performed on the full-scale HDRP Orano TN[®]-32 cask (EPRI 2014). Once validated against actual temperature measurements, these models can be used to generate time- and space-dependent temperature profiles for use in conjunction with other models to predict hydride formation, corrosion rates, creep rates, and other factors that affect the integrity of the fuel and its packaging. The Orano TN[®]-32 cask was modified to accommodate seven thermocouple lances as described in section G.2.1. Spatial temperature profiles from all seven thermocouple lances recorded when the HDRP test cask reached steady state after drying are shown in Figure G-7.

EPRI coordinated a double-blind round-robin exercise where four modeling teams adapted their thermal models to predict the temperatures in the HDRP cask at the point in time when the temperatures reached a quasi-steady-state (i.e., neglecting reduction of decay heat due to radioactive decay) after the drying process. The teams and models were (EPRI 2020):

- NRC, using ANSYS Fluent (simulation 1 [S1])
- PNNL, using STAR-CCM+ (simulation 2 [S2])
- PNNL, using COBRA-SFS (simulation 3 [S3])
- AREVA (now Orano), using ANSYS APDL²³ (simulation 4 [S4])

²² Control rod assemblies (also called Rod Cluster Control Assemblies or Rod Control Cluster Assemblies), comprise several rods containing neutron absorbers connected by a common structure or “spider.” The control rods are used for core reactivity and axial power shape control by insertion of the rods into some of the control rod guide tubes in some of the fuel assemblies. Similarly, a bank of connected discrete burnable absorber rods, which contain neutron absorber materials but no fuel, may be inserted into some of the guide tubes in some fuel assemblies to control the reactivity of the reactor core.

²³ APDL is the Ansys Mechanical Parametric Design Language offered by Ansys, Inc.

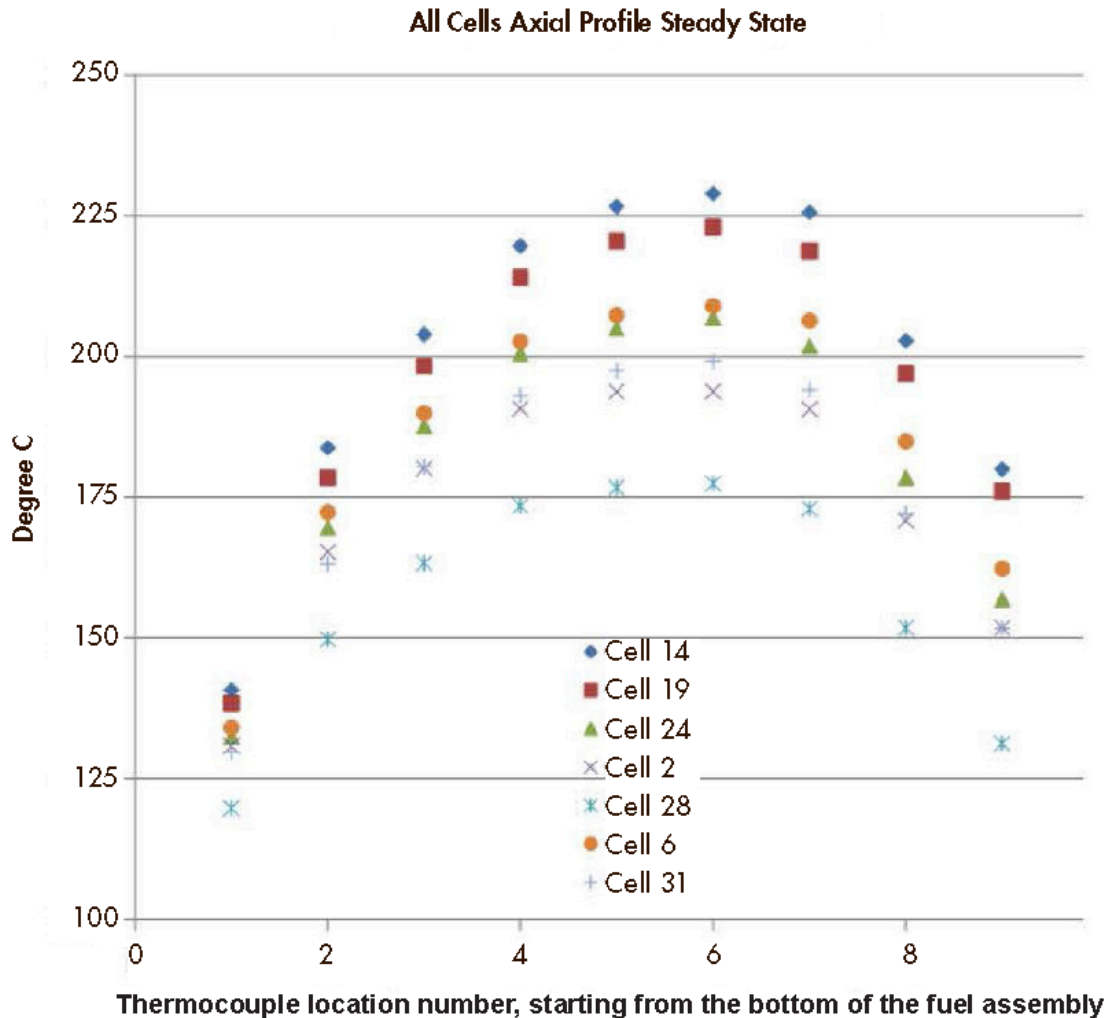


Figure G-7. Peak temperature measurements during the HDRP drying process. Temperatures are shown for each of the seven thermocouple lances and reflect the axial and radial variation of the temperature within the cask. Each symbol represents one radial location (or basket cell) within the cask (*Hanson 2018*).

Each modeling team was given the same initial information about the cask construction, dimensions, and fuel parameters such as cooling times, burnups, and decay heats. The measured temperatures in the hottest assembly (in basket cell 14) during the drying process are shown in Figure G-5. The measured temperatures from all seven thermocouple lances at the time of the peak temperature (after drying) are shown in Figure G-7 (Csonotos et al. 2018). All of the models over-predicted the actual temperatures in nearly all cask locations (see Figure G-8).

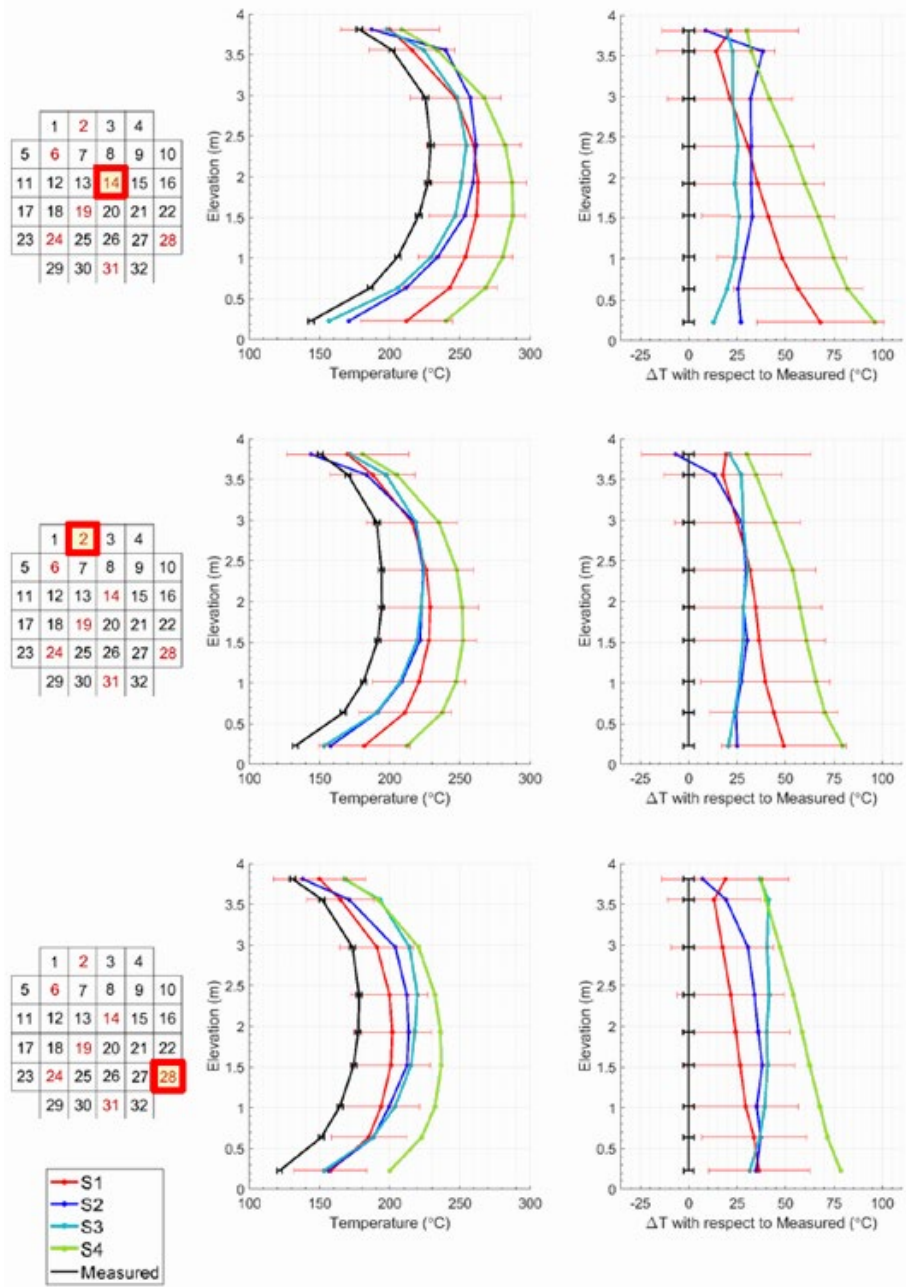


Figure G-8. Model-predicted temperatures, measured temperatures, and temperature differences (ΔT) in three locations in the HDRP cask.

Axial temperature profiles and ΔT s are shown for cells 14, 2, and 28 in the cask. The models are indicated as follows: S1 – ANSYS Fluent; S2 – STAR CCM+; S3 – COBRA-SFS; S4 – ANSYS APDL. The uncertainty bars shown in all figures apply to model S1 only (*adapted from Csontos et al. 2018*).

The PNNL modeling results from simulations performed with COBRA-SFS and STAR-CCM+ are described in Fort et al. (2019a). Examples of the temperature predictions from these two models are shown in Figure G-8 for three different cell locations in the Orano TN[®]-32 cask. To further refine and benchmark the models, PNNL conducted model runs to predict Orano

TN[®]-32 cask temperatures during the transient conditions during the drying process (Fort et al. 2019b). The COBRA-SFS temperature predictions for Cell 14 during the vacuum drying process are shown in Figure G-9.

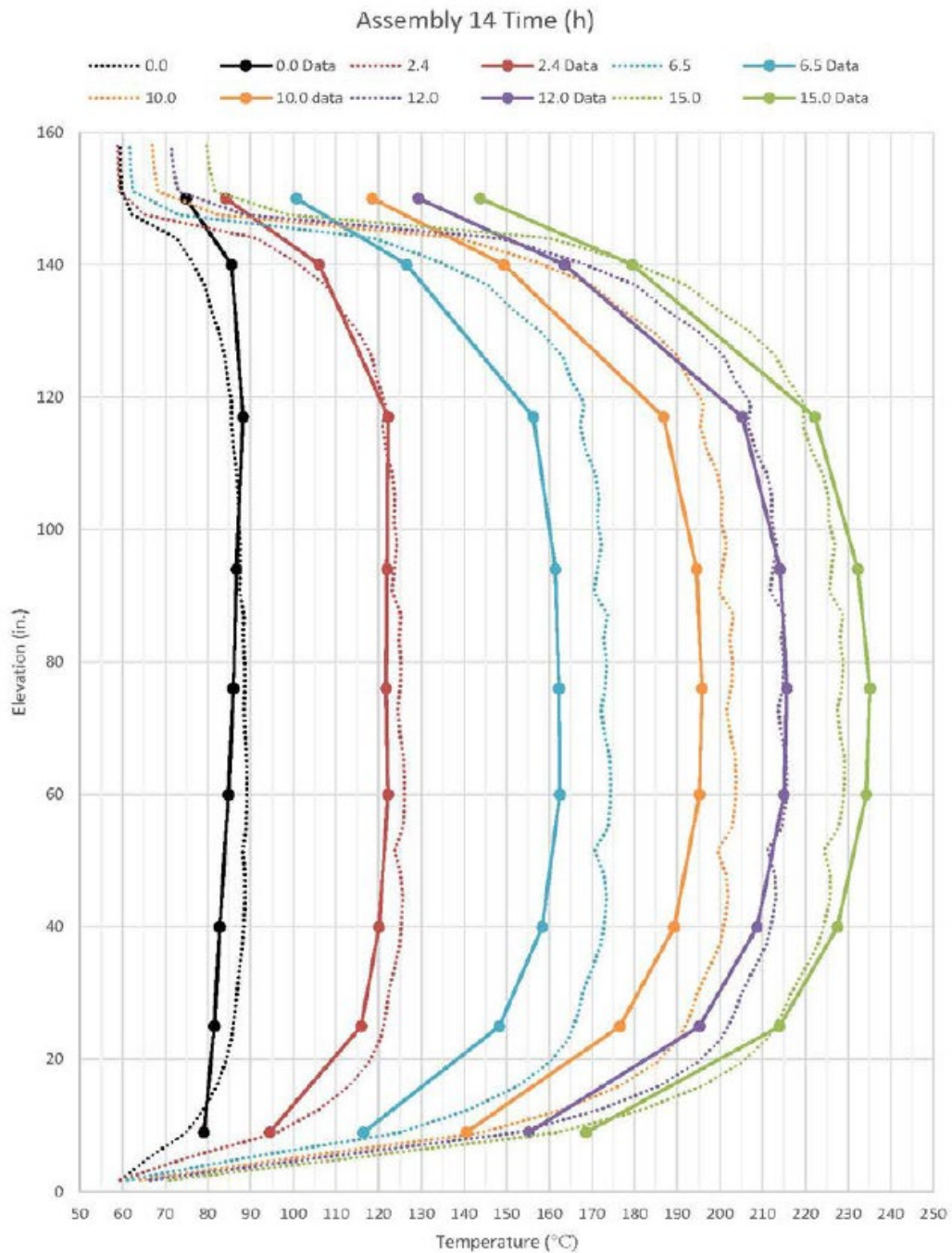


Figure G-9. COBRA-SFS simulation of the temperature time-history compared to thermocouple data for Assembly 14 (Cell 14) in the HDRP test cask.

Elevation is shown relative to cask cavity. The time period covered is 15 hours during the cask vacuum drying process. Dotted and solid lines are the model and measured results, respectively. (Fort et al. 2019b).

The thermal model predictions tended to be 20–40°C higher than the measured cladding temperatures (Fort et al. 2019a). The NRC team noted that its model (ANSYS Fluent) “over-predicted the experimental measurements everywhere, and by more than 60°C (110°F) in some locations.” (Hall, Zigh, and Solis 2019).

The modeling teams postulated that one cause of the model overpredictions could be the closing of the physical gap between the internal SNF basket and the cask rails that center the basket, caused by differential thermal expansion of the different materials used. A smaller gap (or a closed gap) in this part of the cask system would permit a greater amount of conductive heat transfer, lowering the temperatures throughout the cask. However, as part of the modeling input parameters, the modeling teams all used an evenly-spaced open gap around the full circumference of the SNF basket, which is expected at ambient (unloaded) conditions, per the design specifications of the Orano TN[®]-32 cask (Fort et al. 2019b).

To test this theory, some of the modeling teams conducted an analysis in which the size of this gap was reduced in steps and the model predictions re-performed at each step (Fort et al. 2019; Hall, Zigh, and Solis 2019). As the gap size was reduced, the difference between the predicted and measured temperatures lessened, as expected. For example, PNNL ran its COBRA-SFS model three times with the gap size reduced to 3.8 mm (0.15 in), 2.5 mm (0.10 in), and 1.3 mm (0.05 in) and found that the difference between the predicted and measured maximum cladding temperature was reduced by 5, 12, and 20°C, respectively (Fort et al. 2019).

The NRC modeling team also calculated the modeling uncertainty in accordance with the ASME standard on validation of computational fluid dynamics models (ASME 2009). They found that the validation uncertainty (a combination of the numerical uncertainty, the input uncertainty, and the experimental uncertainty) for the peak cladding temperature prediction was 63°C (145°F). Given this high level of validation uncertainty, the NRC team concluded:

“... this experiment cannot be classified as a CFD [computational fluid dynamics] grade experiment. Cask vendors have been submitting applications [with temperature] margins in the range of about 10–20°C from the ISG-11 temperature limit of 400°C. In order to be useful as a demonstration of the accuracy of the CFD modeling process or to improve the model’s capabilities, the validation uncertainty should be less than this 10–20°C margin.” (Hall, Zigh, and Solis 2019)

All modeling teams involved in the HDRP thermal modeling effort recognized that the size of the uncertainty in predicting temperatures of a real SNF dry cask storage system is an issue that needs to be addressed. DOE, EPRI, NRC, and international groups participating the EPRI Extended Storage Collaboration Program Thermal Subcommittee continue to work together to understand and address these uncertainties. Part of this work included an expert elicitation process to assess computer-based thermal modeling of SNF dry cask storage systems. This process identified several “phenomena that could immediately realize a significant reduction in bias or uncertainty compared to typical existing practice” (EPRI 2020). The phenomena or areas most directly related to SNF drying and storage and presenting the largest sources of uncertainty or bias included assumptions about ambient

air temperature, cooling assumptions during loading and drying, and decay heat estimates. The expert panel recommended further research in several of these areas (EPRI 2020).

G.4 Past Spent Nuclear Fuel Demonstration Programs

The HDRP is a follow-up to a past demonstration conducted at the INL on LBF discussed in sections G.1 and G.3.2.1. Additional dry storage demonstrations of uranium oxide (UO₂) fuel with zirconium-based claddings have been conducted or are planned in Canada, Japan, and Germany (IAEA [International Atomic Energy Agency] 2019). While these demonstrations differ in size, storage conditions, and pre- and post-test fuel characterization, they all show that conclusions drawn from short-term testing could be extrapolated to long-term performance of LWR fuel under actual service conditions. Brief descriptions of the salient points from these demonstrations are provided below. These demonstrations provide lessons learned about the information that can be derived and the problems that arise (e.g., effects of lack of pre-characterization, internal cover gas control, etc.).

G.4.1 Low Burnup Fuel Performance Demonstration

Starting in 1984, a monitored dry-storage demonstration program sponsored by the NRC and EPRI²⁴ was conducted at the Idaho National Environmental and Engineering Laboratory, now INL. Five dry storage casks instrumented with thermocouples were loaded with LBF²⁵ from PWRs to determine the thermal characteristics of the casks. Another dry-storage cask (REA-2023) containing LBF²⁶ from BWRs was instrumented with thermocouples and stored at the General Electric–Hitachi facility in Morris, Illinois. The bare fuel (uncanistered) casks were evacuated, dried, and either backfilled with nitrogen or helium or left in a vacuum, and the temperature was measured in various control rod guide tubes in a variety of assembly locations in the cask while the casks were placed in horizontal and vertical configurations (McKinnon and Deloach 1993; McKinnon and Doherty 1997). Temperature and dose measurements were made frequently during the initial test period, which ran for about two years and then, less frequently once the cask was moved to the storage pad. The SNF was characterized visually and/or by sipping²⁷ to determine the integrity of the rod cladding prior to loading it into the casks. No breached rods were put into the instrumented CASTOR-V/21 cask holding 21 LBF PWR assemblies when it was loaded in September 1985 (McKinnon and Doherty 1997). The CASTOR-V/21 was the only cask from which SNF was removed and examined. The casks still remain on a storage pad at INL. A complete description of the tests is provided by McKinnon and Deloach (1993).

The cover gas in the casks was monitored and analyzed during the storage period to determine changes in its composition and for krypton-85, which is an indicator of a

²⁴ DOE contributed indirectly by providing the hot cell examination space and support services. DOE was not involved in any programmatic decisions.

²⁵ The burnup of the fuel in the PWR demonstrations ranged from 24 to 35 GWd/MTU.

²⁶ No burnup information was reported for the BWR fuel demonstration although extensive calorimetry was done on this fuel.

²⁷ Sipping is the process of placing a gas-gathering device over an assembly and collecting and analyzing any gas released by the assembly to determine if any radioactive gas is leaking from a rod.

breached SNF rod. After 15 years of storage in a dry helium atmosphere, where the maximum measured cladding temperature of 420°C (788°F) was reached for a short time and then, decreased with the decreasing decay heat, the CASTOR-V/21 cask was opened to examine the condition of the interior components, seals, and SNF. The other casks in the initial 1985 demonstration have not been opened for SNF inspection. Prior to the demonstration, it was unknown whether the CRUD on the SNF rods would flake off as the rods cooled; however, the demonstration showed very little flaking of CRUD from the outside surface of the SNF rod cladding, which is a positive result should a cask or canister have to be reopened or if a transportation cask containing bare SNF is intended to be reused.²⁸

A number of SNF rods were removed from the CASTOR-V/21 cask to measure radiation levels, the physical dimensions and properties of the rods, and fission product gases. Measurements taken by rod puncturing indicated no additional fission gas had been released. Profilometry measurements indicated that no discernable cladding creep had occurred during testing or storage, based on a comparison to the profilometry results from similar “sibling” SNF rods that did not undergo high temperature testing. A deficiency in this demonstration was not characterizing the rods prior to testing, leading to uncertainty in the interpretation of the results. Full accounts of the post-demonstration observations can be found in EPRI (2002) and Einziger et al. (2003). The main conclusions that could be drawn from this demonstration were that no cladding creep or breach occurred even though the temperature of the SNF exceeded 400°C.

G.4.2 Canada Deuterium Uranium Reactor Spent Nuclear Fuel Demonstration

The Whiteshell Nuclear Research Establishment in Whiteshell Canada conducted a three-part demonstration to study the long-term behavior of Canada Deuterium Uranium reactor SNF. A variety of CANLUB²⁹ and non-CANLUB SNF assemblies were used in the demonstration, which included intact and breached Canada Deuterium Uranium SNF.³⁰ Fuel burnups, which depend on the initial fuel enrichment, did not exceed ~20 GWd/MTU. The casks were equipped to monitor both the cladding temperatures and the composition of the cask cover gas. Three experiments with different parameters were conducted: one demonstration was conducted in dry air at ~55°C (131°F), the second was in dry air at 150°C (302°F), and the third was in a moisture-saturated atmosphere at 150°C (302°F). Periodically, the casks were opened to examine the SNF.

The initial demonstration used an air atmosphere in a sealed system to demonstrate the ability to store defective SNF in air temperatures below 150°C. The results seemed very promising until it was found early in the demonstration that the oxygen in the system was depleted, which meant the results did not represent long-term storage conditions in an

²⁸ Flaking CRUD is the major source of contamination in the pool or hot cell if no breached SNF is present.

²⁹ This is a Canadian-designed fuel rod using relatively low-enriched (up to ~2%) or natural UO₂ pellets in a Zircaloy-4 cladding. CANLUB fuel has a thin coating of graphite on the inner surface of the cladding.

³⁰ The defected Canada Deuterium Uranium SNF was intentionally damaged by drilling holes in the cladding.

unlimited air atmosphere. However, the results are very useful if SNF is stored in a sealed-air atmosphere (Wasywich, Taylor and Frost 1993; Wasywich et al 1993).

After approximately six years, no measurable SNF cladding degradation was detected, and no changes were observed visually in any of the rods. Profilometry on selected intact and defected rods indicated that no significant creep had occurred. A few rods were removed for destructive examination, which included metallography and ceramography: no degradation or additional failure of the intact rods was detected. A major objective of this program was to investigate the long-term oxidation of the SNF rods with exposed UO_2 fuel material in a moist-air atmosphere: the results of those tests indicated that some of the fuel material had oxidized from UO_2 to U_4O_9 in the defected rods. Only trace amounts of surface oxidation to the lower density U_3O_8 was observed. This is important since the density of U_3O_8 is approximately 36% lower than UO_2 . The expansion of the oxide fuel material could put stress on the cladding such that additional cladding splitting could occur in the axial direction. The extent of the fuel material oxidation depended on the linear heat-generation rate at which the fuel operated in the reactor. No dependence on the fuel burnup, which was in the 8–10 GWd/MTU range, or temperature of the fuel, which was held below 150°C (302°F) in an air atmosphere, was mentioned. The cladding did not appear to bulge from the strain of the oxidizing fuel material, which is not unsurprising given that the oxygen was depleted. Furthermore, no handling problems were reported. As of 1989, the SNF had been stored for 11 years (Wasywich and Frost 1989).³¹ Additional information on the results of these demonstrations can be found in He et al. (2011).

G.4.3 Japanese Spent Nuclear Fuel Performance Demonstrations

A demonstration was conducted in Japan with five BWR Mixed Oxide Fuel SNF rods and one PWR UO_2 SNF rod stored for 20 years after discharge (Sasahara and Matsumura 2008). The BWR Mixed Oxide Fuel SNF rods had a burnup of ~20 GWd/MTHM and the PWR UO_2 SNF rod had a burnup of ~58 MWd/MTU. Three of the BWR Mixed Oxide Fuel SNF rods were stored wet in a spent fuel pool, and two were cut into segments and stored dry. In all cases, the SNF rods were stored with other SNF rods providing the additional heat necessary to bring the test rods up to realistic storage temperatures. Before the BWR Mixed Oxide Fuel SNF rods were stored, sibling SNF rods were studied using visual inspection, gas measurements, pellet and cladding ceramography and metallography, and pycnometry³² to form a baseline for comparison. Similar examinations were conducted on the PWR UO_2 SNF rods that had been stored for 20 years. No substantial change in either the BWR Mixed Oxide Fuel or PWR UO_2 SNF was observed. One major deficiency in this demonstration was that the temperature of the rods was not measured at the time the rods were put into storage or during storage. Full details of this demonstration can be found in Sasahara and Matsumura (2008). Further details on this demonstration are given in He et al. (2011).

G.4.4 German Spent Nuclear Fuel Demonstrations

In the early 1980s, Kraftwerk Union Aktiengesellschaft (now KWU), and Deutsche Gesellschaft für Wiederaufarbeitung conducted full-scale, dry storage cask demonstrations with 10 PWR and 15 BWR LBF rods of undocumented burnup from the Research Center at

³¹ This project was eventually discontinued, and no further reports on the results have been found.

³² Pycnometry is a method used to determine pellet density.

Ispra, Italy (Peehs, Bokelmann, and Fleisch 1986). All the rods were non-destructively characterized before the demonstration. Tests lasted up to 17 months in a dry, oxygen-free atmosphere. The isothermal storage temperature was raised incrementally approximately every 6 months from 400 to 430 to 450°C (725 to 806 to 842°F) (Peehs, Kaspar, and Steinberg 1986). Visual, rod diameter, and eddy current examinations that were conducted before and after the testing confirmed the integrity of the rods. The main conclusions were that there were no rod breaches, although small amounts of tritium, hydrogen, and tritiated water were found in the cask atmosphere, and the cladding creep after all temperature changes was cumulatively less than 1%.³³

Additionally, experimental data from integrated demonstrations of SNF dry storage in a CASTOR 1C cask at Wurgassen by Deutsche Gesellschaft für Wiederaufarbeitung for 22 months was compared to the empirical models developed based on single-effects testing to develop dry storage SNF performance criteria (Peehs, Kaspar, and Steinberg 1986). Effects investigated were thermal creep, zircaloy cladding oxidation, iodine-stress-corrosion cracking, and propagation of any cracks that developed. The authors state that the German TRAB³⁴ model is able to predict the SNF characteristics listed above at well known storage conditions (Peehs, Kaspar, and Steinberg 1986). Peehs, Bokelmann, and Fleisch (1986) describes shorter-term tests by KWU and Deutsche Gesellschaft für Wiederaufarbeitung using PWR assemblies fitted with thermocouples and containing SNF rods of varying design at an average burnup of 40 GWd/MTU. The assemblies were tested in a special dry storage box in the Obrigheim reactor pool. The tests were run with maximum cladding temperatures of 300 and 400°C (572 and 752°F). Gas analyses indicated that no rod breaches occurred even after the rods were quenched from 210°C (410°F) to pool temperature in 120 seconds.

Fleisch and Peehs (1986) reported the results of SNF dry storage demonstrations in an inert atmosphere using three models of CASTOR bare-fuel casks and more than 3000 PWR and BWR SNF rods at the German Wurgassen reactor. The rod burnups ranged between 6–30 GWd/MTU. The demonstrations lasted between 24 and 30 months, and the maximum temperatures ranged from 250 to 430°C (482 to 806°F). Pre- and post-demonstration NDEs were conducted on select SNF rods to determine rod integrity and cladding creep. During the tests, the temperature distribution inside the cask was monitored and the inert cover gas was sampled for krypton-85 and tritium. The demonstrations showed that there was no significant cladding creep and no indication of rod failure. Additional information can be found in Fleisch and Peehs (1986).

G.5 Planned or Ongoing International Demonstration Programs

G.5.1 Japan

Japan is storing its SNF, uncanistered, in metal, dual-purpose, dry-storage casks for a maximum 50 years until it is to be reprocessed (Yamamoto et al. 2015). The Central

³³ Germany has a regulatory limit on the cladding creep allowed in dry storage of no more than 1%. This was based on in-reactor performance of the cladding where the creep was limited to ensure there was sufficient cooling flow.

³⁴ The TRAB model is a coupled neutronics-thermal hydraulics model for transient and accident analyses of HBF in the reactor.

Research Institute of Electric Power Industry in Japan has done extensive short-term experimentation to determine the conditions (e.g., maximum temperature, cover gas type and impurity level, and vibration levels) that will affect cladding integrity (Namba et al. 2013). Based on this information and international experience, the Japanese will set the conditions for storage and transportation so that cladding integrity is maintained.

To ensure that only intact SNF rods are being transported after storage, three Japanese electric utility companies are conducting a long-term storage test of PWR SNF assemblies to confirm that the integrity of the SNF has been maintained. In this test, the utilities installed a compact, dry-test container in a research facility pool used to store two PWR SNF assemblies. The test on the first assembly (burnup of ~42 GWd/MTU) started in 2016 and will last for 35 years. In 2026, the second assembly (burnup of ~55 GWd/MTU) will be added and stored for 10 years. The cladding of the SNF in the first assembly is made from Zircaloy-4. The cladding on the SNF in the second assembly will be ZIRLO®. The assemblies will be visually inspected, and no leaking SNF will be used in the test. The assemblies will be stored in a helium atmosphere with a 10% moisture content. The maximum cladding temperature will be calculated using precalibrated thermal codes and is expected to be approximately 230°C (446°F). Samples of the cask internal gas will be drawn and analyzed every five years to determine if SNF cladding has maintained its integrity. Once the test has concluded, visual examination and rod puncturing to determine the rod internal pressure will be conducted (Fukuda 2019). This test is anticipated to provide benchmarking for a model to predict the performance of other SNF types and cask types without having to conduct full-size demonstrations.

G.5.2 Republic of Korea SNF Performance Demonstration

The Korea Atomic Energy Research Institute plans to conduct an SNF storage demonstration to analyze how SNF degrades under dry storage conditions by focusing on creep effects and material property changes including hydriding effects (Kook, Yang, and Koo 2017). The test will use six Zircaloy-4 PWR SNF rods irradiated to between 43–53 GWd/MTU rod average burnup that will be contained in a sealed stainless steel vessel that is vacuum dried, backfilled with helium, and placed in a pool for shielding purposes. The vessel will contain 12 thermal heaters surrounding the SNF rods to maintain the outer temperature of the SNF cladding between 300–400°C (572–752°F). The system will be instrumented to measure the rod temperature continuously. After three years of storage, the rods will be removed and measured for any rod cladding creep. Pre-demonstration characterization, including destructive examination to identify hydrides on six sister rods neighboring the demonstration rods while in the assembly, has been completed (Kook, Yang, and Koo 2017), but no results have been reported as of Fall 2020. The program is currently on hold due to licensing issues.

G.6 Comparison of Demonstrations

Demonstration programs conducted in the United States, Canada, Japan, Germany, and the Republic of Korea were compared to identify commonalities and lessons learned. Aside from the demonstrations in Canada that used Canada Deuterium Uranium SNF, SNF from LWRs was used in all other cited demonstrations. There are some commonalities between the Canada Deuterium Uranium fuel and the LWR fuel, such as Zircaloy-4 cladding, UO₂ fuel pellets, and possible breached fuel in storage. Note that Canada Deuterium Uranium fuel

rarely has burnups more than 20 GWd/MTU. The burnup of the fuel used in these demonstrations was much lower than typically used in LWRs, so the results from the Canadian demonstrations should only be applied to LWR fuel after considerable evaluation of the differences in burnup level. Therefore, the Canadian demonstration was included because some of the results (e.g., oxidation rate and breached fuel behavior) may also be applicable to LWR SNF.

Since the demonstrations discussed were, are, or will be run independently by different countries, the programs were not designed to be complementary to each other. For example, in some demonstrations, the SNF was loaded dry, and in others, it was loaded wet, so the SNF—some of which was breached—had to be dried. Some of the demonstrations were conducted in a dry or moist air atmosphere, although most were conducted with a helium atmosphere.³⁵ A systematic evaluation of the cumulative conditions or results from the demonstrations has not yet been made.

Almost all of the demonstrations were coupled with some degree of pre-characterization of the SNF to establish a baseline for comparison of the SNF behavior during storage, but most of the characterizations were non-destructive examinations because they are easier and cheaper to do. The exception was the U.S. demonstration, for which the test fuel was destructively examined. All the demonstrations had temperature and cover gas monitoring. Common to all the demonstrations was an intensive, post-demonstration characterization of the SNF.

Only one of the early demonstrations (Peehs, Kaspar, and Steinberg 1986; in Germany) tried to analyze the data in terms of a predictive computer model. Until recently, few other countries used either fundamental or empirical models to determine how the results of a demonstration could be applied to the spectrum of SNF conditions that will need to be managed (e.g., cladding type, burnup, range of storage conditions associated with atmosphere, temperature, and humidity). The demonstrations do show the benefit of good pre-test SNF characterization, temperature measurements, and cover gas analyses to obtaining meaningful data from demonstration programs.

There was no indication in the reports describing the work above that a comparison of measured temperatures and expected temperatures was conducted. Ongoing progress on international demonstrations is being provided by the EPRI Extended Storage Collaboration Project International sub-committee and the IAEA, through its Spent Fuel Performance Assessment Research program.

G.7 References

10 CFR Part 71. "Packaging and Transportation of Radioactive Material." *Code of Federal Regulations*. Washington, DC: Government Printing Office.

³⁵ In the lab, 99.9999% pure helium typically is used. The purity of the fill gas was not specified in the demonstrations, but it is probably not this pure. The atmosphere in tests conducted in laboratory grade helium are probably not completely representative of the moisture level in a "dried" cask due to residual moisture (e.g., physisorbed and/or chemisorbed water) remaining after the drying process is completed.

Adkins, H.E., Jr., J.A. Fort, S.R. Suffield, J.M. Cuta, and B.A. Collins. 2013. "Thermal Modeling Studies for Active Storage Modules in the Calvert Cliffs ISFSI." *Proceedings of the 2013 International High-Level Radioactive Waste Management Conference*. Albuquerque, New Mexico. April 28–May 2.

ASME (American Society of Mechanical Engineers). 2009. Standard for Verification and Validation in Computational Fluid Dynamics and Heat Transfer. ASME V&V 20-2009.

Bare, W.C. and L.D. Torgerson. 2001. Dry Cask Storage Characterization Project—Phase 1: CASTOR V/21 Cask Opening and Examination. NUREG/CR-6745. September.

Billone, M.C. and T.A. Burtseva. 2020. *Preliminary Destructive Examination Results for Sibling Pin Cladding*. ANL-19/53, Rev. 2. February 28.

Bryan, C.R., R.L. Jarek, C. Flores, and E. Leonard. 2019. *Analysis of Gas Samples Taken from the High Burnup Demonstration Cask*. SAND2019-2281. February.

Carver, G.C. 2015. *Drying Process Efficiency for Used Fuel Storage Campaigns*. Presentation at the 2015 Nuclear Energy Institute Used Fuel Management Conference. Orlando, Florida. May 5–7.

Csontos, A., K. Waldrop, S. Durbin, B. Hanson, J. Broussard, and G. Lenci. 2018. "Spent Fuel Dry Storage Cask Thermal Modeling Round Robin." *Proceedings of the 2018 TopFuel Reactor Fuel Performance Conference, Prague, Czech Republic*. September 30–October 4.

Cuta, J.M., S.R. Suffield, J.A. Fort, and H.E. Adkins. 2013. *Thermal Performance Sensitivity Studies in Support of Material Modeling for Extended Storage of Used Nuclear Fuel*. FCRD-UFD-2013-000257. September 27.

Cuta, J.M. and H.E. Atkins. 2014. Preliminary Thermal Modeling of HI-STORM 100 Storage Modules at Diablo Canyon Power Plant ISFSI. FCRD-UFD-2014-000505. April 17.

Das, K., D. Basu, and G. Walter. 2014. *Thermal Analysis of Horizontal Storage Casks for Extended Storage Applications*. NUREG/CR-7191. December.

Durbin, S.G. and E.R. Lindgren. 2018. *Thermal-Hydraulic Experiments Using a Dry Cask Simulator*. NUREG/CR-7250. October.

Durbin, S.G., E.R. Lindgren, A. Zigh, and J. Solis. 2017. "Thermal-Hydraulic Results for the Aboveground Configuration of a Dry Cask Simulator." *Transactions of the 2017 American Nuclear Society Annual Meeting*. San Francisco, California. June 11–15.

Einzigler, R.E., H. Tsai, M.C. Billone, and B.A. Hilton. 2003. "Examination of Spent Pressurized Water Reactor Fuel Rods After 15 Years in Dry Storage." *Nuclear Technology*. Vol. 144, pp. 186–200.

EPRI (Electric Power Research Institute). 2002. *Dry Cask Storage Characterization Project*. EPRI, Palo Alto, California. 1002882.

EPRI. 2014. *High Burnup Dry Storage Cask Research and Development Project: Final Test Plan*. EPRI, Palo Alto, California. DE-NE-0000593.

EPRI. 2019. *High Burnup Dry Storage Research Project Cask Loading and Initial Results*. EPRI, Palo Alto, California. 3002015076.

EPRI. 2020. High-Burnup Used Fuel Dry Storage System Thermal Modeling Benchmark: Round Robin Results. EPRI, Palo Alto, California. 3002013124.

Fleisch, J. and M. Peehs. 1986. "Analysis of Spent Fuel Behaviour in Dry Storage Cask Demonstrations in the FRG." *Proceedings of the Third International Spent Fuel Storage Technology Symposium/Workshop*. Seattle, Washington. April 8–10.

Fort, J.A., T.E. Michener, S.R. Suffield, and D.J. Richmond. 2016. *Thermal Modeling of a Loaded Magnastor Storage System at Catawba Nuclear Station*. FCRD-UFD-2016-000068. September 29.

Fort, J.A., D.J. Richmond, B.J. Cuta, and S.R. Suffield. 2019a. *Thermal Modeling of the TN-32B Cask for the High Burnup Spent Fuel Data Project*. PNNL-28915. July 30.

Fort, J.A., D.J. Richmond, B.J. Jensen, and S.R. Suffield. 2019b. *High-Burnup Demonstration: Thermal Modeling of TN-32B Vacuum Drying and ISFSI Transients*. SFWD-SFWST-M2SF-19N010203027. PNNL-29058. September 20.

Fukuda, S.-I. 2019. "Annex VI: Demonstration Test Program for Long-Term Dry Storage of PWR Spent Fuel." *Demonstrating Performance of Spent Fuel and Related Storage System Components During Very Long Term Storage*. IAEA-TECDOC-1878. Vienna: International Atomic Energy Agency.

Gauld I.C. and B.D. Murphy. 2010. *Technical Basis for a Proposed Expansion of Regulatory Guide 3.54—Decay Heat Generation in an Independent Spent Fuel Storage Installation*. NUREG/CR-6999. February.

Hadj-Nacer, M., T. Manzo, M. Ho, I. Graur, and M. Greiner. 2015. "Phenomena Affecting Used Nuclear Fuel Cladding Temperatures During Vacuum Drying Operations." *Proceedings of the 2015 International High-Level Radioactive Waste Management Meeting*. Charleston, South Carolina. April 12–16.

Hall, K., G. Zigh, and J. Solis. 2019. *CFD Validation of Vertical Dry Cask Storage System*. NUREG/CR-7260. May.

Hanson, B.D., W. Wu, R.C. Daniel, P.J. MacFarlan, A.M. Casella, R.W. Shimskey, R.S. Wittman. 2008. *Fuel-In-Air FY07 Summary Report*. PNNL-17275, Rev. 1. September.

Hanson, B.D. 2016a. *High Burnup Spent Fuel Data Project*. Presentation to the Nuclear Waste Technical Review Board at its February 17, 2016 meeting.

Hanson, B. 2016b. *Peak Cladding Temperatures: Conservative Licensing Approach vs. Actual*. Presentation at the 2016 Nuclear Energy Institute Used Fuel Management Conference. Orlando, Florida. May 3–5.

Hanson, B.D., S.C. Marschman, M.C. Billone, J. Scaglione, K.B. Sorenson, and S.J. Saltzstein. 2016. *High Burnup Spent Fuel Data Project Sister Rod Test Plan Overview*. FCRD-UFD-2016-000063. April 29.

- Hanson, B. 2018. *High Burnup Spent Fuel Data Project & Thermal Modeling and Analysis*. Presentation to the Nuclear Waste Technical Review Board at its October 24, 2018 meeting.
- He, X., L. Tipton, Y. Pan, H. Jung, J. Tait, R. Einziger, H. Gonzalez. 2011. *Development and Evaluation of Cask Demonstration Programs*. Prepared for U.S. Nuclear Regulatory Commission Contract NRC-02-07-006.
- IAEA (International Atomic Energy Agency). 2019. *Demonstrating Performance of Spent Fuel and Related Storage System Components during Very Long Term Storage*. IAEA-TECDOC-1878. Vienna: International Atomic Energy Agency.
- Jernkvist, L.O. and A. Massih. 2002. Analysis of the Effect of UO₂ High Burnup Microstructure on Fission Gas Release. SKI Report 02:56. December.
- Kook, D., J. Yang, and Y. Koo. 2017. "PWR Spent Nuclear Fuel Research Status for Dry Storage and Transportation in Korea." 2017 Water Reactor Fuel Performance Meeting. 2017 Water Reactor Fuel Performance Meeting. Jeju Island, Korea. September 10–14.
- Lindgren, E.R. and S.G. Durbin. 2017. *Materials and Dimensional Reference Handbook for the Boiling Water Reactor Dry Cask Simulator*. SAND2017-13058R. November.
- McKinnon, M.A. and V.A. Deloach. 1993. *Spent Nuclear Fuel Storage—Performance Tests and Demonstrations*. PNL-8451. April.
- McKinnon, M.A. and A.L. Doherty. 1997. *Spent Nuclear Fuel Integrity During Dry Storage—Performance Tests and Demonstrations*. PNNL-11576. June.
- Michener, T.E., J.M. Cuta, D.R. Rector, and H.E. Adkins, Jr. 2015. *COBRA-SFS: A Thermal-Hydraulic Analysis Code for Spent Fuel Storage and Transportation Casks, Cycle 4*. PNNL-24841. October.
- Montgomery, R. and B. Bevard. 2020. *Sister Rod Destructive Examinations (FY20)* ORNL/SPR-2020/1798. November 30.
- Montgomery, R., B. Bevard, R.N. Morris, J. Goddard, Jr., S.K. Smith, J. Hu, J. Beale, and B. Yoon. 2018. *Sister Rod Nondestructive Examination Final Report*. SFWD-SFWST-2017-000003, Rev. 1. May 16.
- Montgomery, R., R.N. Morris, R. Ilgner, B. Roach, J. Wang, Z. Burns, J.T. Dixon, and S.M. Curlin. 2019. *Sister Rod Destructive Examinations (FY19)*. ORNL/SPR-2019/1251, Rev. 1. September 27.
- Namba, K., M. Wataru, K. Shirai, and T. Saegusa. 2013. "Evaluation of Sealing Performance of Metal Gaskets Used in Dual Purpose Metal Cask Under Normal Transport Condition Considering Ageing of Metal Gaskets Under Long-Term Storage." *Proceedings of the 17th International Symposium on the Packaging and Transportation of Radioactive Materials*. San Francisco, California. August 18–23.
- NRC (U.S. Nuclear Regulatory Commission). 2003. *Spent Fuel Project Office Interim Staff Guidance-11, Revision 3, Cladding Considerations for the Transportation and Storage of Spent Fuel*. November.

NRC. 2020. *Standard Review Plan for Spent Fuel Dry Storage Systems and Facilities*. NUREG-2215, April.

Peehs, M., R. Bokelmann, and J. Fleisch. 1986. "Spent Fuel Dry Storage Performance in Inert Atmosphere." *Proceedings of the Third International Spent Fuel Storage Technology Symposium/Workshop*. Seattle, Washington. April 8–10.

Peehs, M., G. Kaspar, and E. Steinberg. 1986. "Experimentally Based Spent Fuel Dry Storage Performance Criteria." *Proceedings of the Third International Spent Fuel Storage Technology Symposium/Workshop*. Seattle, Washington. April 8–10.

Pulido, R.J.M., E.R. Lindgren, S.G. Durbin, A. Zigh, J. Solis, S.R. Suffield, D.J. Richmond, J.A. Fort, L.E. Herranz, F. FERIA, J. Penalva, M. Lloret, M. Galbán, J. Benavides, and G. Jiménez. 2020. *Modeling Validation Exercises Using the Dry Cask Simulator*. SAND2019-6079R. January.

Saltzstein, S.J., K. Sorenson, B. Hanson, R. Shimskey, N. Klymyshyn, R. Webster, P. Jensen, P. MacFarlan, M. Billone, J. Scaglione, R. Montgomery, and B. Bevard. 2017. *EPRI/DOE High Burnup Fuel Sister Rod Test Plan Simplification & Visualization*. SAND2017-1031R. September 15.

Sasahara, A. and T. Matsumura. 2008. "Post-irradiation Examinations Focused on Fuel Integrity of Spent BWR-MOX and PWR-UO₂ Fuels Stored for 20 years." *Nuclear Engineering and Design*. Vol. 238, pp. 1250–1259.

Scaglione, J.M., J.L. Peterson, K. Banerjee, K.R. Robb, and R.A. LeFebre. 2014. "Integrated Data and Analysis System for Commercial Used Nuclear Fuel Safety Assessments—14657." *Proceedings of the WM2014 Conference*. Phoenix, Arizona. March 2–6.

Shimskey, R.W., J.R. Allred, R.C. Daniel, M.K. Edwards, J. Geeting, P.J. MacFarlan, L.I. Richmond, T.S. Scott, and B.D. Hanson. 2019. *Phase 1 Update on Sibling Pin Destructive Examination Results*. PNNL-29179. September.

Solis, J. and G. Zigh. 2016. *Impact of Variation in Environmental Conditions on the Thermal Performance of Dry Storage Casks: Final Report*. NUREG-2174. March.

Stockman, C.T., H.A. Alsaed, and C.R. Bryan. 2015. *Draft Evaluation of the Frequency for Gas Sampling for the High Burnup Confirmatory Data Project*. FCRD-UFD-2015-000509. March 26.

Suffield, S.R., J.A. Fort, H.E. Adkins, J.M. Cuta, B.A. Collins, and E.R. Siciliano. 2012. *Thermal Modeling of NUHOMS HSM-15 and HSM-1 Storage Modules at Calvert Cliffs Nuclear Power Station ISFSI*. PNNL-21788. October.

Trujillo, C. 2017. "Computational Fluid Dynamics Thermal Simulations of a Nuclear Fuel Canister During Drying." Master's thesis, University of Nevada, Reno.

Wasywich, K.M. and C.R. Frost. 1989. "Update on the Canadian Experimental Program to Evaluate Used-Fuel Integrity Under Dry-Storage Conditions." *Proceedings of the Second International Conference on CANDU Fuel*. Pembroke, Canada. October 1–5.

Wasywich, K.M., W.H. Hocking, D.W. Shoesmith, and P. Taylor. 1993. "Differences in Oxidation Behavior of Used CANDU Fuel During Prolonged Storage in Moisture-Saturated Air and Dry Air at 150°C." *Nuclear Technology*. Vol. 104, pp. 309–329.

Wasywich K.M., P. Taylor, and C.R. Frost. 1993. "The Canadian Long-term Experimental Used Fuel Storage Program." *Proceedings of the 1993 International Conference on Nuclear Waste Management and Environmental Remediation, Vol 1*. Prague, Czech Republic. September 5–11.

Yamamoto, M., T. Fujimoto, K. Shigemune, H. Matsuo, T. Matsuoka, and D. Ishiko. 2015. "Demonstration Test Program for Long-Term Dry Storage of PWR Spent Fuel." *Proceedings of an International Conference on Management of Spent Fuel from Nuclear Power Reactors*. Vienna, Austria. May 31–June 4.

Zigh, A., S. Gonzalez, J. Solis, S.G. Durbin, and E.R. Lindgren. 2017. "Validation of the Computational Fluid Dynamics Method using the Aboveground Configuration of the Dry Cask Simulator." *Transactions of the 2017 American Nuclear Society Annual Meeting*. San Francisco, California. June 11–15.

Appendix H

Spent Nuclear Fuel Performance under Normal Conditions of Transport

H.1 Introduction

In order to transport radioactive materials, including spent nuclear fuel (SNF), the material owner or transporter must meet the requirements of the Department of Transportation as well as the requirements specified by the U.S. Nuclear Regulatory Commission (NRC) in Title 10, Code of Federal Regulations, Part 71, “Packaging and Transportation of Radioactive Material” (10 CFR Part 71). Within 10 CFR Part 71, section 71.71 specifies the requirements to be met during “normal conditions of transport” (NCT).

During NCT, SNF, including high burnup fuel (HBF),¹ packaged inside a cask or canister system² will experience a variety of vibration and shock loads that will induce strain in the HBF rods. The mechanical loads experienced during NCT are quite different than the high-energy “shocks” caused by hypothetical accident conditions during transport, which are characterized by high accelerations that may cause “pinch-mode” failure of the rods (see Appendix F for a more detailed discussion). The loads experienced during NCT are expected to include:

- Repeated vibrations during normal transportation due to uneven road or rail conditions or wave motion and rough seas for shipment by water;
- Lower energy “shocks” due to:
 - Normal handling of the loaded transportation cask as it is being transferred (see section H.4) between modes of transport that may include setting the cask down on hard surfaces; and
 - Bumps or crossings in the road or rail causing somewhat higher energy shocks. These shocks may occur hundreds of times during a 2,000 mile trip,

¹ Fuel burnup is a measure of the energy generated in a nuclear reactor per unit mass of initial nuclear fuel and is typically expressed in units of gigawatt-days per metric ton of uranium (GWd/MTU). In the U.S., high burnup spent nuclear fuel is defined by the NRC as SNF whose burnup exceeds 45 GWd/MTU.

² SNF may be packaged into a welded stainless-steel canister that is then placed into a shielded overpack for storage and, for some designs, transportation. Alternatively, SNF may be packaged into a bolted-lid cask (sometimes called a bare fuel cask) that does not use an internal canister and includes its own shielding. These packaging systems are explained in more detail in section 2.1.2 of this report. For storage applications, some literature refers to both of these types of systems as “dry cask storage systems” and this report uses the same terminology. This report also may use the terms “cask” and “canister” when it is necessary to distinguish between specific types of storage or transportation systems.

compared to the vibration events, which occur more than ten million times during a 2,000 mile trip.

Repeated vibrations at magnitudes exceeding the fatigue limit of a metal can lead to “fatigue” failure of the metal, including SNF cladding. Fatigue failure is a function of the number of vibrations and the cumulative stress history of the metal. Transportation casks containing commercial SNF are transported horizontally. Therefore, the SNF assemblies are laying on their sides. Normal shock and vibration will impart mostly vertical vibrations on the rods, which will flex between the SNF assembly upper and lower end fittings and between the spacer grids (see Figure H-1). Note that the assembly spacer grids were designed to improve in-reactor performance of the fuel, physically support the fuel rods in certain reactor accident conditions, and support transport of unirradiated fuel from the fuel fabrication plant to the nuclear power plant. The characteristics and behavior of HBF rods that are important when considering these vibration and shock loads during NCT are the main subjects of this appendix.

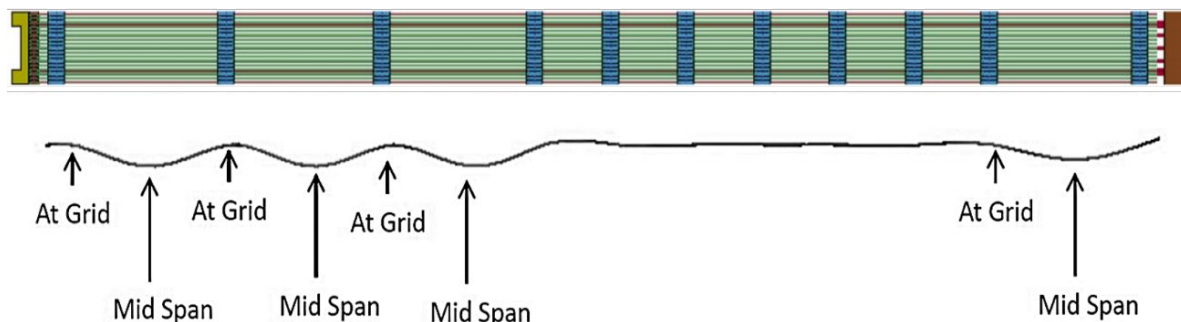


Figure H-1. Model of an SNF assembly in a horizontal position during transport.

The thin line under the assembly is an exaggerated view of how the SNF rods might flex in the vertical (up and down) direction during vibrations and bumps experienced during NCT.

A “grid” is a spacer grid in the assembly and a “span” is a segment of SNF rod between spacer grids. The locations of the spacer grids are typical of a Westinghouse pressurized water reactor assembly (*adapted from McConnell et al. 2018*).

H.2 Department of Energy (DOE) Research Related to Spent Nuclear Fuel Transportation

To evaluate the behavior of HBF during transport, a structural evaluation of the HBF rods under transport conditions (i.e., with relevant temperatures, vibrations, and shocks) must be conducted.

This evaluation requires an understanding of the mechanical properties of the HBF rods and cladding, which will depend, in part, on the amount of hydride reorientation that occurs in the cladding during the HBF drying process (see Appendices E and F). There is evidence that hydride reorientation can occur in HBF cladding under certain conditions of high cladding temperature and high cladding hoop stress (NRC 2003). Theoretically, even if hydride reorientation does occur, neither radial nor circumferential hydrides are expected to affect the performance of fuel rods during NCT because, during NCT, the principal bending stress

on the cladding is parallel to the hydrides.³ To explore the effects of hydride reorientation on the bending and fatigue behavior of HBF cladding in conditions simulating NCT, the NRC sponsored research at the Oak Ridge National Laboratory (ORNL) (Wang and Wang 2017). Building on the NRC-sponsored work, DOE funded Sandia National Laboratories (SNL), Pacific Northwest National Laboratories (PNNL), and ORNL to conduct a broad range of experiments and computer modeling of HBF under NCT.

To ensure that future shipments of HBF will meet the requirements for SNF transportation stipulated in 10 CFR 71.55, DOE has undertaken a multistep research program (Sorenson et al. 2016, Teague et al. 2019) that is summarized as follows:

1. Determine the number of vibration cycles necessary to cause HBF rods to breach as a function of (a) the vibration strain amplitude on the SNF rod, (b) the cladding composition, (c) the fuel burnup, and (d) the previous drying and storage conditions.
2. Determine if the presence of hydrides in HBF cladding has any effect of the number of cycles to failure of the cladding.
3. Determine the magnitude of the vibrations and frequency of vibrations at each magnitude that the HBF rods and assemblies may experience while being transported via road, rail, barge, and ocean-going ship.
4. Determine if pellet-cladding and pellet-pellet bonding that can occur in HBF rods⁴ will change the response of the rod to applied vibration and drop loads.
5. Determine the cladding strains that HBF rods experience during actual transport.
6. Develop and benchmark a computer-based structural model that relates the vibration load that a truck or railcar experiences to the strain amplitude that HBF rods (and cladding) may experience after the load has been transmitted through the transport platform (of the truck or railcar), the transport cradle, the transportation cask, the SNF canister (if used), the SNF basket, and finally HBF assembly components (see Figure H-2)⁵.

³ Circumferential and radial hydrides in HBF cladding are aligned in a manner that is less susceptible to fracture when subjected to a stress that is oriented parallel to the hydrides. They are more susceptible to fracture when subjected to a stress that is oriented perpendicular to the hydrides (see Appendix F).

⁴ Pellet-cladding bonding is a phenomenon in which the fuel pellets inside a fuel rod become chemically and physically attached to the inside of the fuel cladding during reactor irradiation. Similarly, pellet-pellet bonding is the chemical and physical attachment of the end of one pellet to another where they meet inside the cladding. More details about these phenomena are provided in Appendix A and Appendix F.

⁵ A transport cradle is the physical support onto which an SNF transportation cask is mounted for transport by truck or rail (or barge). The cask cradle stabilizes the cask and positions the cask so that the cask impact limiters, which are larger in diameter than the cask, are not in contact with the truck or rail car.

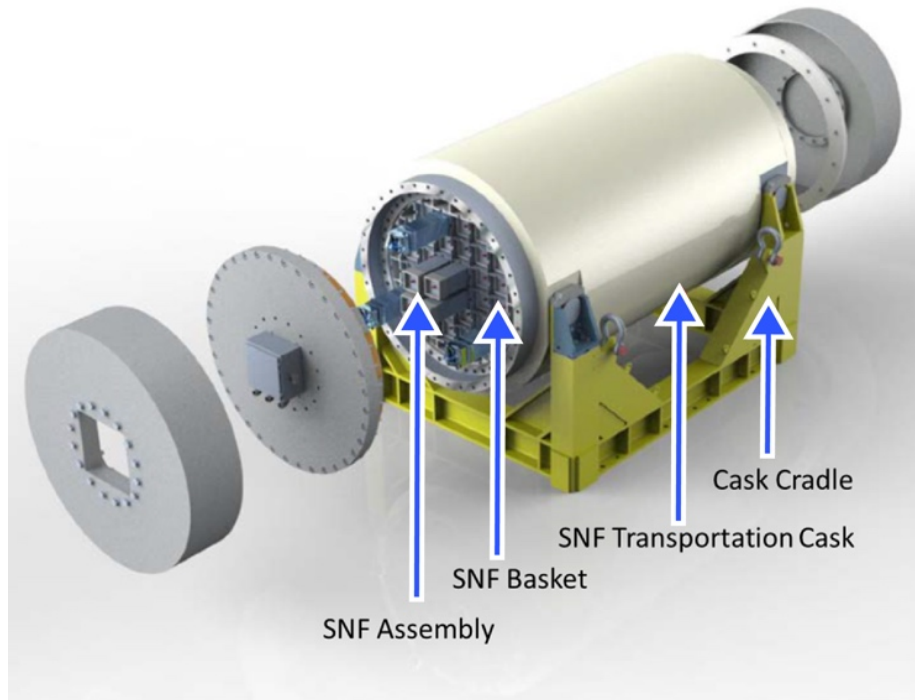


Figure H-2. Schematic of an SNF transportation cask and cask cradle.

In this bolted-lid transportation cask design (the ENUN-32P, manufactured by Equipos Nucleares Société Anonyme of Spain), there is an SNF basket, but no SNF canister. To accommodate transport testing, this design includes lids that were modified to include instrumentation and uses smaller-than-normal diameter impact limiters (*adapted from McConnell et al. 2018*).

H.3 Measuring High Burnup Fuel Cladding Properties Relevant to Normal Conditions of Transport

The NRC-sponsored testing program at ORNL was started “to determine the ability of high burnup (>45 GWd/MTU) spent nuclear fuel (SNF) to maintain its integrity under conditions relevant to storage and transportation” (Wang and Wang 2017). Starting in 2011, ORNL developed a laboratory testing system composed of a U-frame apparatus equipped with load cells to impose pure bending loads on SNF rod specimens and measure the in-situ curvature of the specimens during bending. The system was also designed to operate in a cyclic mode to measure the number of bending cycles to failure for SNF rod specimens; i.e., determine the fatigue lifetime of the specimens (Wang and Wang 2017). This system is called the Cyclic Integrated Reversible-Bending Fatigue Tester (CIRFT; see Figure H-3). ORNL conducted an extensive amount of design evaluation and calibration work to develop the CIRFT to minimize irrelevant experimental artifacts. DOE began funding the CIRFT program in fiscal year 2014 (Wang et al. 2015).

Early in the ORNL testing program, static bend tests using the CIRFT were conducted on pressurized water reactor (PWR) Zircaloy-4 cladding specimens with burnups in the range of 64–67 GWd/MTU (Wang and Wang 2017). It should be noted that this fuel was operated

beyond the NRC permitted average rod burnup limit of 62 GWd/MTU as part of a special demonstration program (Electric Power Research Institute 2001).

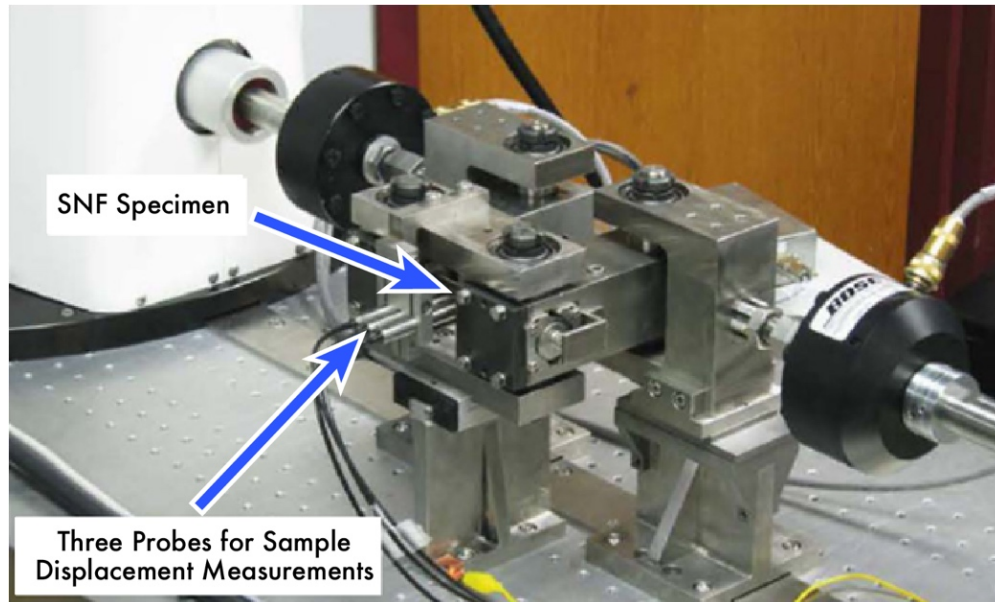


Figure H-3. The Cyclic Integrated Reversible-bending Fatigue Tester, or CIRFT.

The components of the CIRFT apparatus relevant to the fatigue testing are identified. A complete description of the apparatus can be found in Wang et al. (*figure adapted from Wang et al. 2017*).

Key observations from the static testing were:

- The static CIRFT results indicate a significant increase in the flexural rigidity⁶ of a fueled SNF rod compared to the flexural rigidity in a calculated response for only cladding (i.e., defueled cladding) This indicates that the presence of the pellets helps to increase the resistance of cladding to flexing and therefore failure.
- The HBF rods in the as-irradiated state (with no other treatments) survived static unidirectional bending to a maximum curvature of 2.2–2.5 m⁻¹. The maximum equivalent strain was 1.2–1.3%.
- The HBF rods in the as-irradiated state (with no other treatments) exhibited a multi-stage flexural response, with the two linear stages followed by a nonlinear stage. The flexural rigidity at the initial stage was 63–78 N·m². The flexural rigidity at the second stage was 55–61 N·m².
- Most HBF rods in the as-irradiated condition (with no other treatments) subjected to static unidirectional loading followed by fatigue testing fractured at a location coincident with the pellet-to-pellet interface, as validated by the post-test

⁶ Flexural rigidity is a measure of a structure's resistance to bending. For a cylindrical rod, flexural rigidity is $E \times I = \Delta M / \Delta \kappa$, where E is the elastic modulus, I is the area moment of inertia, M is bending moment, and κ is the curvature of the bending rod.

examinations showing pellet end faces in most of the fracture surfaces (Wang and Wang 2017).

In fiscal year 2015, ORNL performed static bend tests of fueled boiling-water reactor (BWR) HBF with Zircaloy-2 cladding and burnups in the range of 54–57 GWd/MTU (Wang et al. 2016a). The test specimens did not fracture after loading to a maximum moment of 85 N·m and a maximum curvature of 4 m^{-1} . Subsequent cyclic testing of Zircaloy-2 cladding indicated that the flexural rigidity ranged from 30 to 50 N·m² (Wang et al. 2015).

The data collected during static bend tests provide useful information about the strength properties of HBF cladding. These data are used to set the range of stress amplitudes applied in fatigue testing of HBF cladding (see section H.4) and as inputs for computer modeling of the behavior of cladding during NCT (see section H.6).

H.4 Determining the Fatigue Lifetime of High Burnup Fuel

At a given vibration amplitude, HBF can tolerate some number of vibration cycles prior to failure. The number of vibration cycles to failure is called the fatigue lifetime. One common method of measuring the fatigue lifetime of a material is to repeatedly bend or flex the material at the same stress level until it fails and record the number of cycles at failure. The test is repeated on new specimens at different stress levels and all the results are plotted on a graph of strain versus the number of cycles to failure (ϵ -N curve) or stress versus the number of cycles to failure (S-N curve). This type of plot is also called a fatigue curve. O'Donnell and Langer (1964) were the first to take experimental data to populate an S-N curve for irradiated Zircaloy. This method of determining the fatigue lifetime of HBF is discussed in section H.4.1. Another method of calculating the fatigue lifetime of HBF is to record all shock and vibration loads that the cladding experiences during loading, handling, transportation, etc., and calculate the amount of cladding damage each shock and vibration load causes. This “damage fraction” of each load is then summed over the lifetime of the cladding to determine the accumulated fatigue damage. When the accumulated fatigue damage is equal to or greater than 1.0, then, in theory, the cladding will fracture (breach). This approach to determining the fatigue lifetime of HBF is discussed in section H.4.3.

H.4.1 Determining the Fatigue Curves for High Burnup Fuel

DOE continued the work started by the NRC to determine the number of cycles to failure as a function of the vibration amplitude (or stress) and cladding type for HBF. ORNL used the CIRFT to generate fatigue curves for a variety of HBF cladding types, including fueled and defueled cladding, and as-irradiated cladding (no treatment) and cladding that was subjected to hydride reorientation treatment (see Appendix F for more details about this treatment). The testing was also used to better understand the effects of pellet-pellet interactions, and pellet-cladding interactions (including pellet-cladding bonding) on the behavior of the overall pellet-cladding composite system (Jiang, Wang, and Wang 2016).

Fatigue testing of fueled, as-irradiated (no additional treatments) HBF samples.

In the first set of cyclic fatigue tests sponsored by DOE, ORNL tested HBF from four nuclear power plant sites, comprising three cladding types (Wang et al. 2015):

1. PWR HBF (64–67 GWd/MTU) with Zircaloy-4 cladding from the H.B. Robinson nuclear power plant site;

2. PWR HBF (60–63 GWd/MTU) with M5[®] cladding from the North Anna nuclear power plant site;
3. PWR HBF (40–49 GWd/MTU) with M5[®] cladding from the Catawba nuclear power plant site;⁷ and
4. BWR HBF (50–57 GWd/MTU) with Zircaloy-2 cladding from the Limerick nuclear power plant site.

The test results were published (Wang et al. 2015) and presented at the Board’s February 2016 public meeting (Wang et al. 2016a). Unlike the ring compression tests that were conducted at Argonne National Laboratory on samples that had been defueled (see Appendix F), the cyclic fatigue tests at ORNL were conducted on HBF rod segments that contained fuel pellets to evaluate the effects of the fuel-cladding and pellet-pellet bonds. The data collected from this testing and from additional CIRFT testing discussed below provide important baseline information regarding HBF rod flexural rigidity and fatigue strength. DOE compares the loads applied during the HBF CIRFT testing to the loads measured during shaker table and transportation testing to evaluate the performance of HBF and predict the likelihood of HBF cladding failure (gross breach). As defined by the NRC, a gross breach is “a breach in the spent fuel cladding that is larger than either a pinhole leak or a hairline crack and allows the release of particulate matter from the spent fuel rod” (NRC 2020).

The fatigue curves produced from the testing described above are shown in Figure H-4. During the fatigue testing at ORNL, “failure” occurs when the SNF rod sample fractures and breaks into two pieces. ORNL observations based on this testing (Wang et al. 2016a) were:

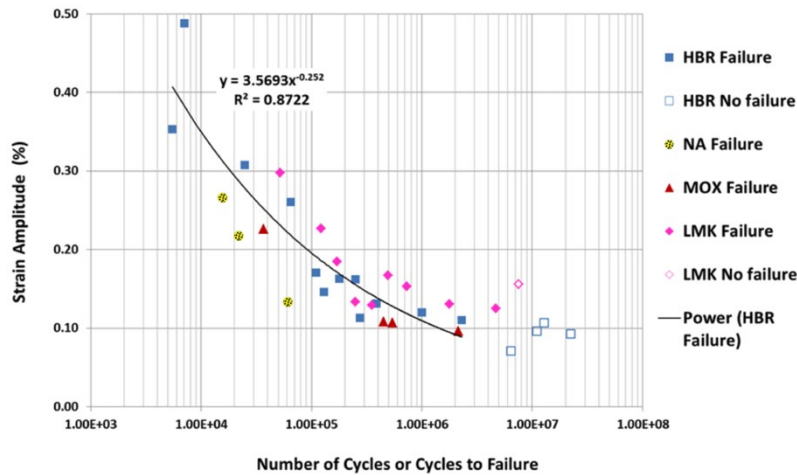
1. The fuel pellets provide strength (flexural rigidity) to the pellet-cladding composite system. The amount of additional strength added depends on the amount of bonding⁸ of the pellet to the cladding.
2. Fractures (“failures” in Figure H-4) in the cladding occur primarily at a location corresponding to a pellet-pellet interface.
3. For the samples that fractured, the fuel pellets retain their shape (dishing and chamfering are evident)⁹ and do not undergo further fragmentation beyond what has occurred in the reactor—a very small amount of fuel particulates are released.

⁷ The Catawba PWR HBF was loaded with fuel pellets made of mixed-oxide (MOX; a mixture of oxides of plutonium and uranium) as opposed to the more common fuel pellets made of uranium-dioxide.

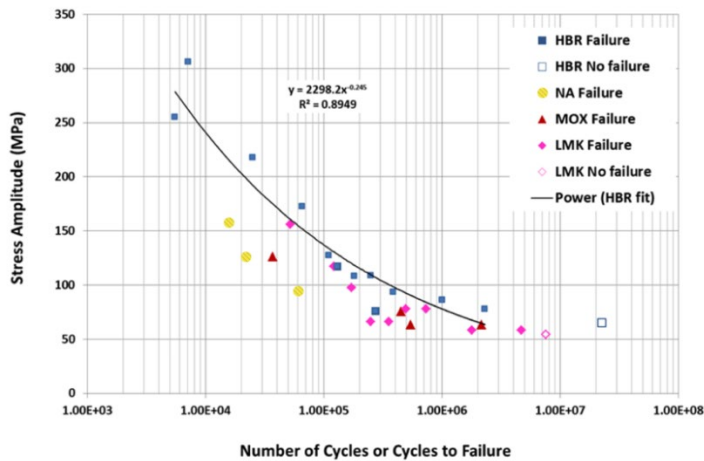
⁸ Bonding of the fuel pellets to the cladding occurs in HBF but, due to thermal cycling both in the reactor and during storage and due to the mismatch of the respective thermal expansion coefficients, the strength of this bond will vary significantly from fuel type to fuel type and the bond may not persist over time (Wang et al. 2017).

⁹ The ends of each pellet have a depression called a dish that allows for pellet axial growth during irradiation (see Figure A-2 for an example). Chamfering is the modification or trimming of the sharp, circular edges of the fuel pellet so there is less local stress riser at the corresponding location in the cladding when the cladding creeps down on the pellet due to reactor coolant pressure. This is where the cladding in some of the CIRFT tests fractured.

4. Considering the complexity and non-uniformity of the HBF pellet-cladding composite system, it is significant that the strain to failure data for the HBF were characterized by a curve expected of “standard uniform materials” (Wang et al. 2016).¹⁰
5. At very low cladding strains, less than approximately 0.1 percent (Figure H-4A) or low stresses and less than approximately 55 MPa (8,000 lbs./in²) (Figure H-4B), HBF fuel exhibited an endurance limit (i.e., it did not fail) of greater than 10⁷ cycles.



(A)



(B)

Figure H-4. Fatigue curves for several as-irradiated HBF samples.

The graphs show (A) strain amplitude versus number of cycles to failure (ϵ -N curve) for HBF rod segments and (B) stress amplitude versus number of cycles to failure (S-N curve) for HBF rod segments (*adapted from Wang et al. 2015*).

¹⁰ Although Wang et al. (2016) did not define “standard uniform materials,” the context of the report implies that they meant a homogenous, metal test specimen.

Notes:

HBR = H.B. Robinson (Zircaloy-4 cladding)

NA = North Anna (M5[®] cladding)

MOX = mixed oxide fuel; Catawba (M5[®] cladding)

LMK = Limerick (Zircaloy-2 cladding)

Power = power law curve fit to the indicated data points

Fatigue testing of HBF samples that were subjected to hydride reorientation treatment.

In the next phase of its testing, ORNL subjected three rodlets (i.e., axial sections of a rod) from an H.B. Robinson HBF rod to a hydride reorientation treatment to provide samples with radial hydrides for CIRFT fatigue testing (Wang and Wang 2017).¹¹ The purpose was to determine if the presence of radial hydrides affected the fatigue lifetime of the cladding. These specimens were subjected to the same CIRFT experimental conditions as the cladding samples without reoriented hydrides (Figure H-5).

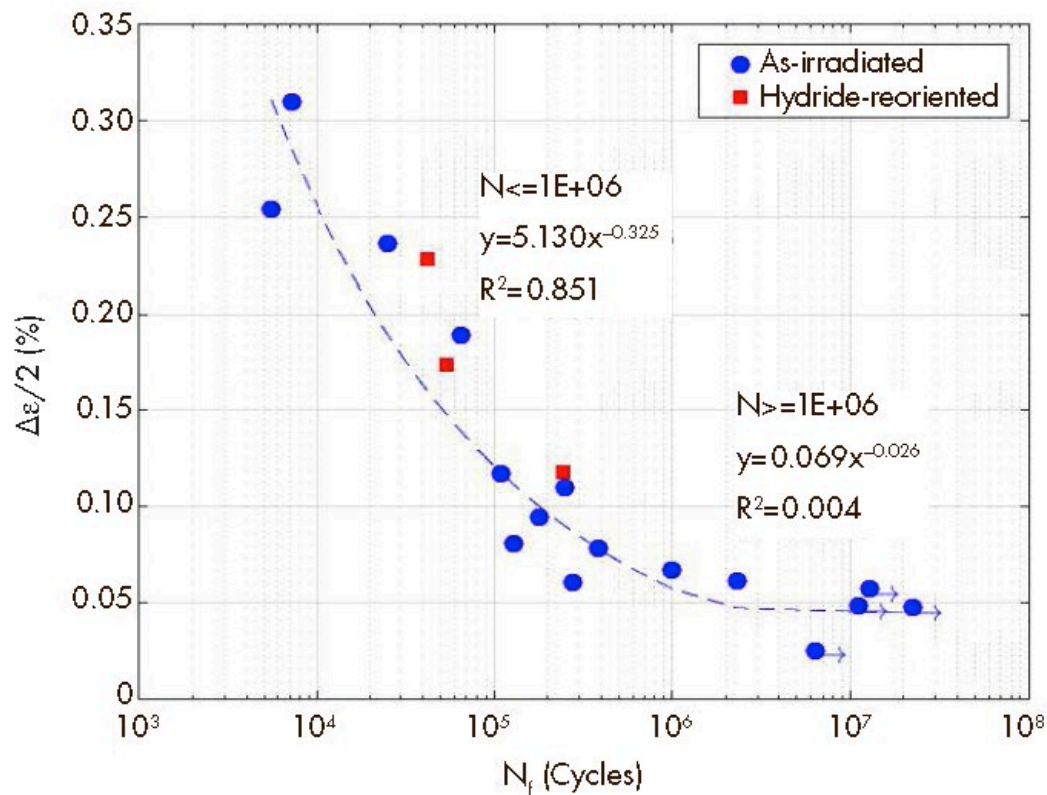


Figure H-5. Equivalent strain amplitudes ($\Delta\epsilon/2$; a measure of strain) as a function of the number of cycles to failure.

The curve fitting is extended to include data points without failure; the markers with arrows indicate that the tests were stopped without cladding failure (Wang and Wang 2017).

¹¹ Hydride reorientation treatment is designed to change the orientation of zirconium hydrides in the cladding from a circumferential to a radial orientation. Radial hydrides are more susceptible to brittle fracture when subjected to a tensile stress that is applied in an orientation perpendicular to the plane of the radial hydrides. See Appendix F for a more detailed description of hydride reorientation.

Based on these fatigue tests, ORNL reported that samples subjected to hydride reorientation treatment had lower flexural rigidity compared to as-irradiated samples (without hydride reorientation treatment). The reduced flexural rigidity of hydride-reoriented samples resulted in an increase in strain amplitude at failure compared to as-irradiated samples. However, the results for all sample types (with and without hydride reorientation) fall within the range of experimental uncertainty. Furthermore, ORNL noted that the reduction in flexural rigidity may indicate that the hydride reoriented samples have a different pellet-cladding composite system when compared to the as-irradiated sample; thus using the hydride reoriented sample strain amplitude versus the failure frequency trend for comparison to as-irradiated samples may be misleading (Wang and Wang 2017).

The Board notes that there are too few cyclic fatigue tests of hydride-reoriented cladding at low strain amplitude to conclude that it will perform any better or worse than cladding without reoriented hydrides when subjected to vibration loads under NCT.

During fatigue testing, cladding specimens without reoriented hydrides primarily experienced guillotine fractures¹² at locations in the cladding corresponding to pellet-pellet interfaces, as shown in Figure H-6. One H.B. Robinson cladding sample with radial hydrides fractured at 45 degrees (diagonally) to the cladding axis,¹³ which is more typical of low burnup SNF cladding. It is not clear whether the change in fracture mode in this sample was due to the presence of radial hydrides or some artifact of the hydride reorientation treatment process that may have significantly affected the pellet-cladding bond. According to ORNL, examination of this H.B. Robinson sample revealed that the crack initiated at a location near a pellet-pellet interface, but the crack propagation was in a mixed-mode (tensile + shear) failure mechanism. The postmortem examination of this sample also indicated that a large area of the pellet-cladding bond was disrupted (Wang et al. 2017).

¹² A guillotine fracture occurs in a plane that is perpendicular to the rod axis.

¹³ This sample underwent a hydride reorientation treatment that included five heating-cooling cycles and was conducted at a significantly higher temperature (400°C [752°F]) and cladding hoop stress (140 MPa [20,300 psi]) than usually seen by HBF rods. After the treatment, the sample was cooled quickly at 60°C/hour (108°F/hour) (the implications of these treatment parameters are discussed in Appendix F).

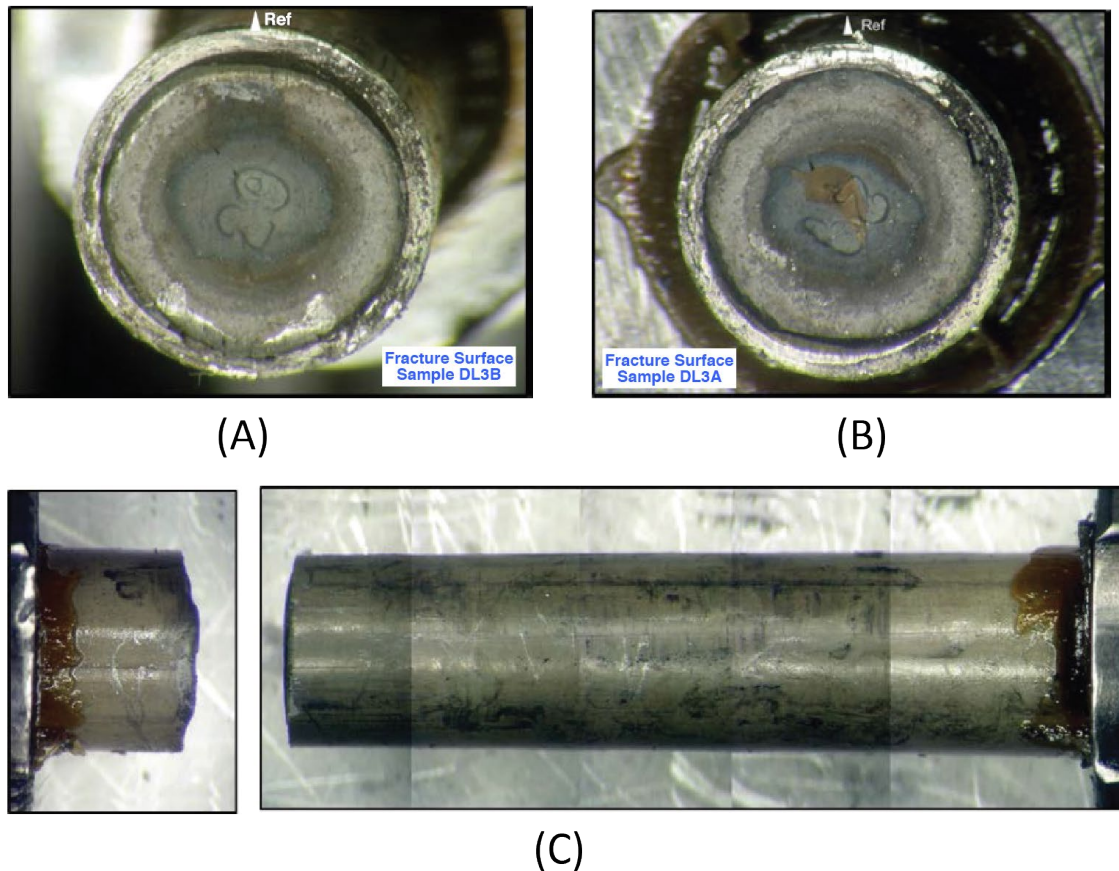


Figure H-6. Example of an HBF test specimen after failure in the CIRFT.

This H.B. Robinson HBF (66.5 GWd/MTU) test specimen fractured at the pellet-pellet interface. In (A) and (B) showing the two pieces of the test specimen after fracturing, the ends of the pellets are clearly visible. (C) is a view of the whole specimen after fracture (adapted from Wang and Wang 2017).

Fatigue testing of HBF after a 30 cm (1 ft) drop.

For commercial SNF packaged in a large transportation cask (greater than 15,000 kg [33,100 lb.]), road vibrations and bumps as well as drops of less than or equal to 30 cm (1 ft) onto an unyielding surface are considered by the NRC to be normal conditions of transport (10 CFR 71). ORNL conducted a study of the combined effect of a transient shock followed by harmonic vibration on HBF cladding (Wang et al. 2016b). BWR HBF rod specimens (Zircaloy-2 cladding) and PWR HBF rod specimens (M5[®] cladding loaded with MOX fuel) were each dropped twice in a horizontal position from heights ranging from 0.3 m (1 ft) to 0.61 m (2 ft) and then subjected to fatigue lifetime testing (see Figure H-7).

The effects of the drops on the HBF rod specimens are highlighted in the lower right corner of Figure H-7; the fatigue lifetimes before and after the drops are indicated by red vertical lines and a pink arrow pointing from the pre-drop fatigue lifetime to the post-drop fatigue lifetime. The red triangles correspond to M5[®] cladding loaded with MOX fuel and the pink diamonds correspond to Zircaloy-2 cladding.

It should be noted that these laboratory drop conditions were more extreme than the conditions the HBF would experience during NCT because the laboratory conditions did not include an SNF canister, transportation overpack, or impact limiters, all of which would absorb or attenuate some of the drop load.

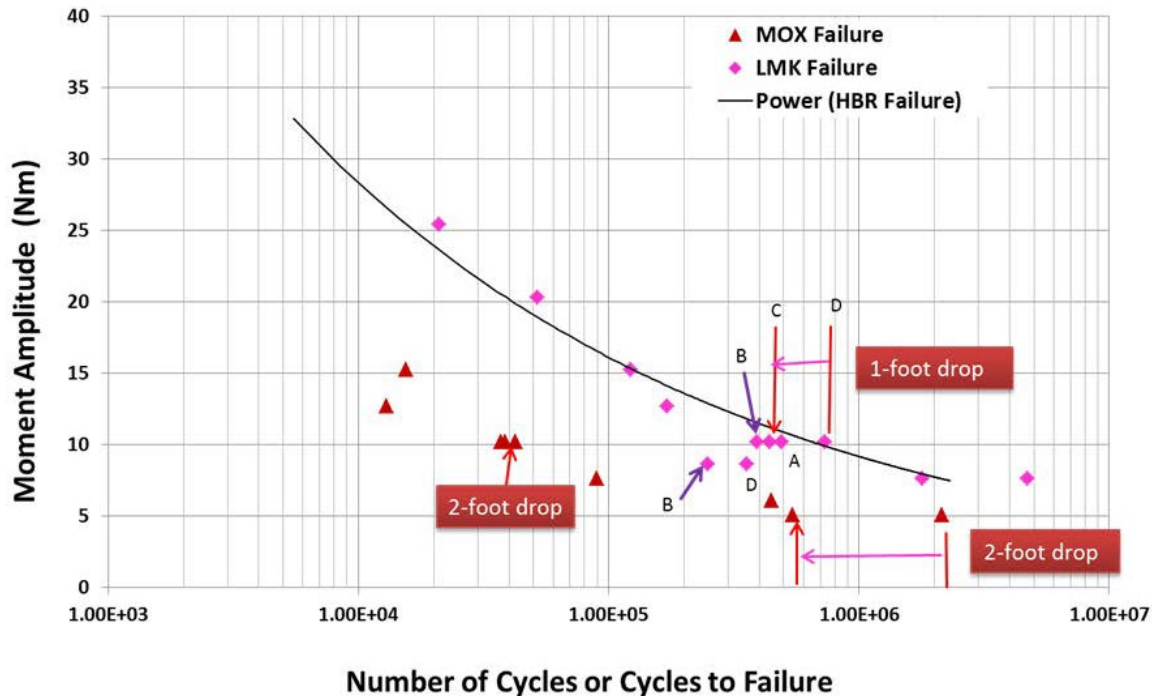


Figure H-7. Fatigue curves for HBF rod specimens following transient shocks.

CIRFT results for PWR HBF with M5[®] cladding and MOX fuel pellets are indicated by red triangles. CIRFT results for BWR HBF with Zircaloy-2 cladding (from the Limerick [LMK] nuclear power plant) are indicated by pink diamonds. The black curve represents a power curve fit to the data (equation not provided by authors). The letters A, B, C, and D refer to specific rodlets cut from the Zircaloy-2 HBF rod (see Wang et al. 2016b for more details).

ORNL found that the Zircaloy-2 rods that were dropped from 0.3 m (1 ft) and then tested in the CIRFT, showed a 50% reduction in fatigue lifetime. M5[®] rods that were dropped 0.610 m (2 ft) and tested in the CIRFT showed a 73% reduction in fatigue lifetime (Wang et al. 2016b). Note that a drop of 0.61 m (2 ft) is beyond the range of conditions considered to be NCT.

To further examine the effects of a transient shock followed by cyclic loading on HBF, ORNL conducted finite element analyses of the drop scenarios described above. For the case of PWR HBF with Zircaloy-4 cladding dropped from a height of 0.3 m (1 ft) onto a steel block, the finite element analysis found that the maximum stress on the cladding was 525 MPa (~76,000 psi) and occurs on the inner surface of the cladding wall due to impact-induced bending. This stress is less than the Zircaloy-4 yield stress of 906 MPa (~131,000 psi), and ORNL concluded, “[n]evertheless, residual stress contours remain in the cladding after the impact event and will eventually reduce the fatigue lifetime of the sample, as validated by the CIRFT evaluations...” (Wang et al. 2016b).

Fatigue testing of HBF as part of the High Burnup Dry Storage Research Project (HDRP).

The DOE-sponsored research on the fatigue lifetime of HBF has continued in the HDRP that is a joint effort between DOE and the Electric Power Research Institute (see Appendix G for more details about the HDRP). As part of the HDRP, PWR HBF rods, called “sister rods”¹⁴ clad in Zircaloy-4, low-tin Zircaloy-4, ZIRLO®, and M5® were made available to ORNL for examination (Montgomery et al. 2019). ORNL has been performing a variety of tests, including fatigue testing using the CIRFT, on the HDRP sister rods, both in the as-irradiated condition and after full-rod heat treatment to 400°C (752°F) (to simulate the maximum cladding temperature suggested by the NRC during or after the SNF drying proces).

Results from the fatigue testing are provided in Montgomery et al. (2019) and Montgomery and Bevard (2020) and show that heat treatment of the HBF rods appears to cause a slightly shorter fatigue lifetime compared to the baseline HBF without heat treatment but the results are within the range of experimental uncertainty. ZIRLO® and M5® clad specimens that were heat treated and tested in the CIRFT exhibited lower flexural rigidity than the corresponding baseline specimens (Montgomery and Bevard 2020). ORNL also plans to investigate the impact of pellet-pellet gaps on the fatigue lifetime of the rod specimens. The flexural rigidity measurements for the sister rods were consistent with previously tested PWR HBF specimens and the flexural rigidity did not appear to change appreciably with higher burnups (Montgomery et al. 2019).

H.4.2 Determining the Vibration Spectrum Experienced by High Burnup Fuel During Normal Conditions of Transport

DOE has sponsored a long-running research program, managed by SNL, to determine the vibration spectrum (magnitudes and frequencies) that may be experienced by SNF, including HBF, during NCT (Sorenson et al. 2016). Over the course of the program, SNL has used several methods to induce vibration loads and shocks and measure the resulting accelerations and strains experienced by the SNF cladding. These methods include transport by legal-weight truck, heavy-haul truck, barge, ocean-going ship and rail. SNL also used shaker table testing of surrogate SNF and computer-based structural modeling to assist in the analyses. Each of the test efforts are discussed below.

H.4.2.1 Legal-Weight Truck Transport Testing

SNL conducted transport tests using a legal-weight truck to determine the number of vibration cycles and the amount of strain that SNF cladding experiences under typical road conditions (McConnell et al. 2014). As part of the test, an unirradiated 17 x 17 PWR assembly containing surrogate rods with copper cladding (except for one rod with unirradiated Zircaloy-4 cladding) filled with lead rope in lieu of pellets was driven over a 40.2-mile route with a range of road surface conditions. The weight of a lead rope-filled test rod is nearly the same as the weight of a normal fuel rod filled with uranium dioxide pellets. The Zircaloy-4 rod was instrumented with strain gages at four axial and three azimuthal locations, and uniaxial accelerometers were placed at various axial locations of the rod including at a spacer grid location. Accelerometers were placed on the basket and the truck bed. The assembly was placed in a surrogate PWR basket with the same internal dimensions as an actual PWR truck cask basket. The assembly/basket test unit was bolted

¹⁴ A sister rod is an HBF rod with characteristics similar to an HBF rod stored in the HDRP cask. See Appendix G for a more detailed explanation of how sister rods were selected.

to concrete blocks that simulated the mass of an actual truck cask. The concrete blocks were securely attached to a trailer (Figure H-8).

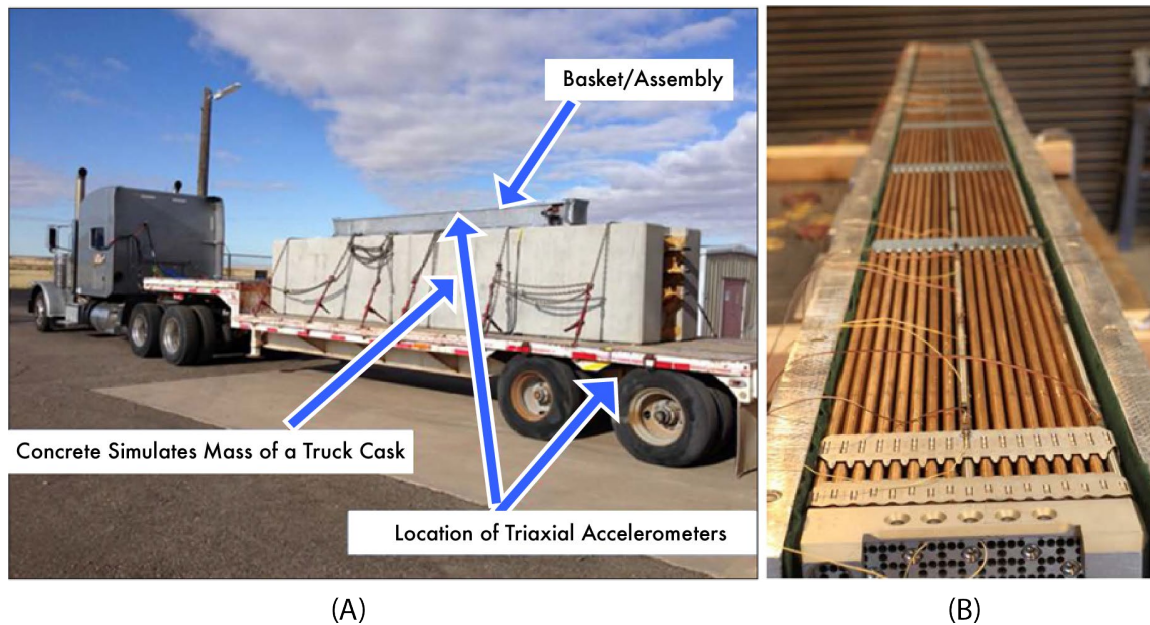


Figure H-8. Truck, surrogate cask components, and surrogate assembly used during measurements of the vibration and shock spectrum for truck transport.

(A) Legal weight truck carrying a surrogate SNF assembly mounted atop concrete slabs that were used to simulate an SNF transportation cask and (B) a surrogate SNF assembly inside the surrogate SNF basket (*adapted from McConnell et al. 2014*).

The maximum cladding strain measured during the truck transport test was 143 micro-strain (also reported as 143 $\mu\text{m}/\text{m}$ or 143 $\mu\text{in}/\text{in}$). This strain is far below the yield point for irradiated Zircaloy-4, which is approximately 9,000 micro-strain (McConnell et al. 2014).

There were significant tradeoffs or compromises made for the SNL truck transport test, and the tradeoffs may affect how the test results are interpreted and applied (McConnell et al. 2014). The tradeoffs included using less-expensive equipment to reduce costs (e.g., using concrete blocks to simulate the weight of a transport overpack), using available transport components to reduce costs and reduce test preparation time, and using unirradiated components to eliminate concerns about worker risks due to radioactive contamination and radiation dose.

The Board notes that the surrogate SNF assembly used in these experiments has many differences compared to actual SNF. For instance, these experiments did not account for any changes in mechanical behavior of the SNF cladding that would occur due to hydride reorientation or irradiation hardening in the cladding. Furthermore, using lead rope instead of irradiated fuel pellets did not allow the experiment to address pellet-pellet interactions or pellet-cladding bonding that would be expected in irradiated SNF. Finally, none of these tests included actual transportation casks, which will change the shocks and vibrations experienced by the fuel assembly during transport. DOE tried to address the uncertainties resulting from these approximations by using different pellet surrogates in shaker table

tests (McConnell et al. 2015) to gather data about vibration loads and strains for the various surrogate configurations (see section H.4.2.2).

H.4.2.2. Shaker Table Testing

SNL conducted shaker table tests on two different shaker tables: one had a single degree of freedom (single-axis; vertical) and the other had six degrees of freedom (six-axis; X, Y, Z lateral motion and X, Y, Z rotational motion) (McConnell 2016).

Testing on the single-axis shaker table.

The first shaker table tests were conducted in 2013, prior to the over-the-road truck tests described above. The purpose of the shaker table test with one degree of freedom was “to better understand fuel rod response to normal conditions of truck transport (NCT) for loadings as defined by 10 CFR 71.71 in order to estimate the ability of aged, used nuclear fuel to withstand these conditions” (McConnell et al. 2013).

The surrogate SNF assembly used in the single-axis shaker table test was like the one used in the truck test described previously, except there were three Zircaloy-4 clad rods containing lead rope instead of one. The assembly was placed in an aluminum basket with the same internal dimensions and approximate weight as the aluminum basket used in the NAC International Legal Weight Truck cask. Accelerometers were placed on the test rod cladding at spacer grid locations and between spacer grids to measure stresses on the cladding. The surrogate SNF basket was fitted with three accelerometers at the top, bottom, and mid assembly locations. Strain gages were attached to various positions on the assembly (McConnell et al. 2013). SNL determined the frequency and magnitude range of the vibration and shock accelerations to be applied by the shaker table by referencing previous truck transport testing sponsored by the NRC (Magnuson 1977; Magnuson 1978). The maximum strains measured on the surrogate SNF cladding during the single-axis shaker table testing was 213 micro-strain; again, well below the yield strain of Zircaloy-4 cladding (McConnell et al. 2013).

Testing on the six-axis shaker table.

After completing the over-the-road truck tests with a surrogate SNF assembly, SNL utilized a six-axis shaker table owned by Dynamic Certification Laboratories, LLC to do additional testing. This testing expanded the scope of parameters tested to include vibrations and shocks typical of rail transport and to include a wider range of surrogate materials as discussed below (McConnell et al. 2015). Figure H-9 provides a comparison of the SNL road tests and shaker table tests.

For the six-axis shaker table testing, the surrogate SNF assembly was populated with copper rods filled with lead rod (“rope”) except for three Zircaloy-4-clad rods that were filled with lead rope, lead pellets, and molybdenum pellets, respectively. The different materials and different configurations were used to determine if there would be a difference in the response of the Zircaloy-4 rods filled with different surrogate fuel materials (McConnell et al. 2015). In this test, the strain gages on the cladding straddled pellet-pellet gaps (inside the cladding). The shaker table imparted vibration and shock loads typical of either truck or rail transport. The amplitude and frequency of the truck transport loads mimicked the loads measured during the SNL over-the-road truck tests. The rail transport loads were set to mimic the loads measured on a railcar platform by Transportation Technology Center, Inc., a rail testing company in Pueblo, Colorado (McConnell et al. 2015). The maximum strain

measured on the surrogate SNF cladding when simulating truck transport was 301 micro-strain.



SNL Shaker	Over-the-Road Truck Test	DCL Multi-axis Shaker
<p>Truck NCT shock and vibration: Loadings taken from NUREG/CR-0128, "Shock and Vibration Environments for a Large Shipping Container During Truck Transport"</p> <ul style="list-style-type: none"> • Simulated mass of an assembly and truck basket • Vertical accelerations only • 6 vibration / 5 shock tests • ≥ 3 Hz to 2000 Hz 	<p>Over-the-road truck test:</p> <ul style="list-style-type: none"> • Simulated over-the-road test to compare strains with the shaker table tests • Simulated mass of a truck cask • Conducted test over 40 miles to simulate various road conditions and speeds 	<p>Multi-axis (6) shaker tests:</p> <ul style="list-style-type: none"> • Truck NCT shock and vibration: NUREG/CR-0128 • Rail NCT shock and vibration: constructed load vibration and shock data from TTCI to simulate railcar-deck loading expected on the S-2043 rail car • Filled lead pellets and Mo pellets into two Zircaloy rods to better simulate fuel • Six degrees shaker table motion • 5 truck shock / 5 truck vibration • 5 rail shock / 5 rail vibration • rail coupling shock • <1 Hz to 100 Hz

Figure H-9. SNL shaker table and truck transport test comparison. (McConnell 2016)

Notes:

DCL = Dynamic Certification Laboratories, LLC

TTCI = Transportation Technology Center, Inc.

S-2043 = Association of American Railroads Standard S-2043, "Performance Specification for Trains Used to Carry High-Level Radioactive Material"

The maximum strain measured on the surrogate SNF cladding when simulating rail transport was 241 micro-strain. These strains are well below the yield strain of irradiated Zircaloy-4 cladding, which is approximately 9000 micro-strain (McConnell et al. 2015). Figure H-10 provides a comparison of maximum strains measured during the various SNL tests and the yield strains of irradiated and unirradiated Zircaloy-4 cladding.

Based on the six-axis shaker table testing, SNL concluded that "all of the strains for these three rod types (lead shot, lead rope, and molybdenum pellets) are so low and so similar as to make any statement that there was a difference in strains measured on the rods futile. The conclusion is that for these tests, the use of lead or molybdenum (higher stiffness than lead) pellets or the use of lead "rope" to simulate fuel pellets has no effect on the measured strains" (McConnell et al. 2015). The Board notes, however, that other characteristics of real, irradiated HBF cladding were not examined in this testing. These cladding characteristics include irradiation embrittlement, hydride reorientation, pellet-pellet bonding, and pellet-cladding bonding.

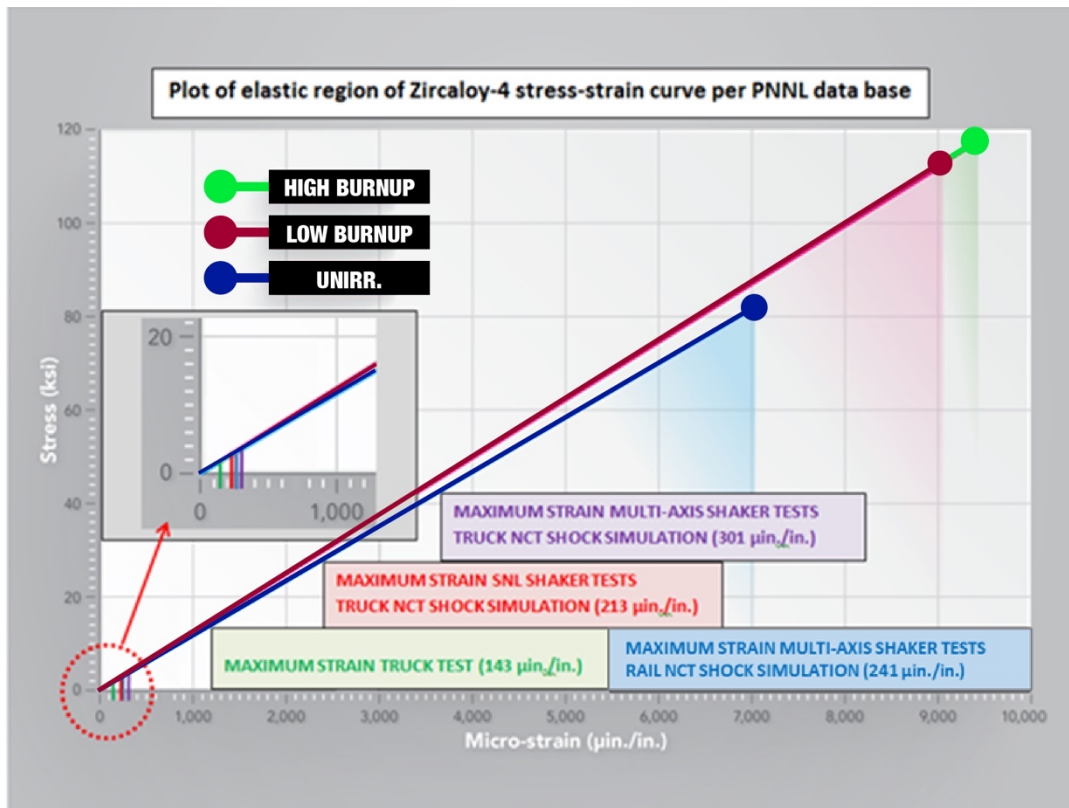


Figure H-10. Maximum strains measured by SNL during transport testing of surrogate Zircaloy-4 rods.

The maximum strains measured during NCT (all less than 310 $\mu\text{in./in.}$) are shown in the left-side inset; the color-code is given in the text boxes in the figure. These strains are shown in contrast to the elastic regions and yield strains (ranging from 7,000–9,400 $\mu\text{in./in.}$) of unirradiated, low burnup, and high burnup Zircaloy-4 rods (*adapted from McConnell 2016*).

H.4.2.3 The Multimodal Transportation Test

DOE and SNL, in cooperation with Korea’s Radioactive Waste Agency (KORAD), the Korea Atomic Energy Research Institute, and two Spanish companies, Equipos Nucleares Société Anonyme (ENSA), and Empresa Nacional de Residuos Radiactivos, S.A (ENRESA), conducted a multimodal transportation test (MMTT) using a real ENSA SNF transportation cask (the ENUN-32P; a cask designed to hold 32 PWR SNF assemblies). The ENSA cask was transported sequentially by heavy-haul truck, barge, ocean-going ship, and rail from Spain to Pueblo, Colorado. Three surrogate, unirradiated, instrumented PWR assemblies were placed in the cask along with 29 concrete “dummy” assemblies (McConnell et al. 2018). The surrogate assemblies are listed below along with their contributors.

- SNL: This Westinghouse 17 x 17 PWR assembly, which was also used in the SNL shaker table tests, contained three Zircaloy-4 clad rods (one rod contained lead pellets, the second contained molybdenum pellets, and the third contained lead rope). The remaining rods were copper clad and contained lead rope. The assembly was instrumented with 18 strain gages and five accelerometers.

- ENRESA: The Spaniards supplied an assembly of the Westinghouse 17 x 17 PWR design with ZIRLO® clad fuel rods containing lead pellets. The assembly was instrumented with 18 strain gages and five accelerometers.
- KORAD: The Koreans supplied an assembly of the 17 x 17 PWR design with ZIRLO® clad fuel rods containing lead pellets. The assembly was instrumented with one strain gage and three accelerometers.

The locations of the instrumentation mounted on the SNL assembly are shown in Figure H-11.

A similar arrangement of instrumentation was used on the ENRESA assembly. The KORAD assembly included the strain gage and one accelerometer at a common location on one fuel rod and two accelerometers on the assembly top nozzle. Lead or molybdenum is used to simulate fuel pellets instead of uranium dioxide because the regulations were such that the project would not have been feasible within budget constraints. The remaining 29 spaces in the 32-position SNF basket were filled with concrete “dummy assemblies” with the same mass as real assemblies. The SNF basket, cask, and cask cradle were also fitted with triaxial accelerometers. Computer-based structural modeling was used to identify the most conservative locations in the cask for the surrogate assemblies in order to obtain the largest accelerations and strains.

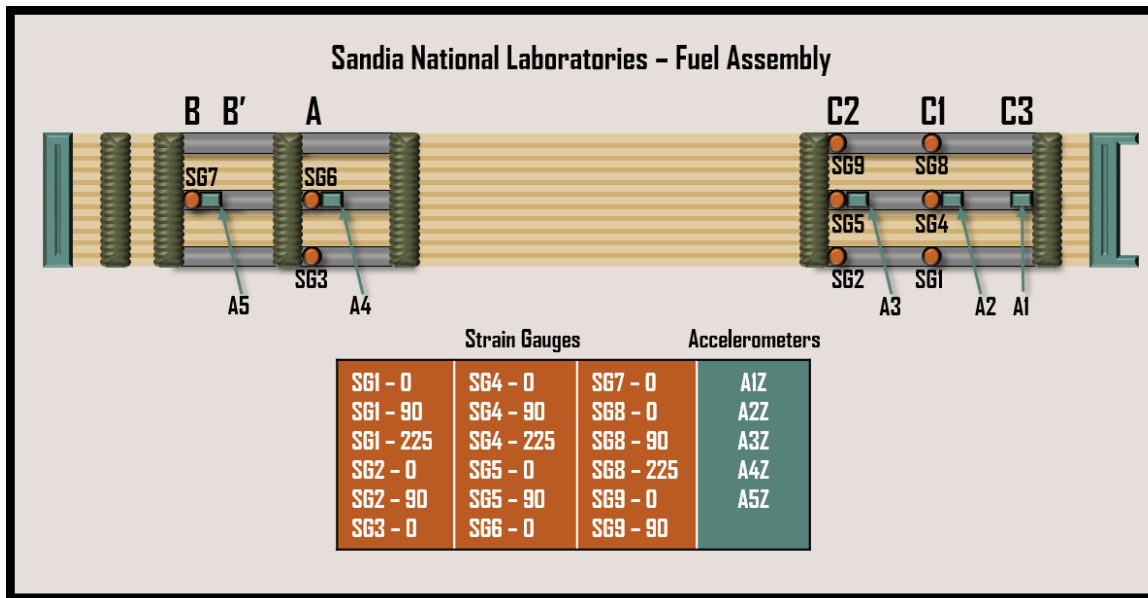


Figure H-11. Instrumentation configuration on the SNL assembly for the MMTT.

Strain gages are indicated by “SG” and accelerometers are indicated by “A.” The indicators A, B, B’, C1, C2, and C3 shown above the SNL assembly are axial position reference points. “Z” after the accelerometer designator indicates measurement in the Z-axis, which is the vertical direction (McConnell et al. 2018).

The cask and test assemblies were shipped from Spain to the Transportation Technology Center (TTC) in Pueblo, Colorado where they underwent testing over various controlled track conditions. The cask left Maliaño, Spain in June 2017, and arrived in Pueblo, Colorado in

July 2017, after having traveled by heavy-haul truck, barge (coastal freight carrier), ship, and rail. The trip included the following legs (McConnell et al. 2018):

- Heavy-haul truck from Maliaño, Spain, to Santander, Spain: 2 days and approximately 400 km (250 mi)
- Coastal freight carrier from Santander, Spain, to Zeebrugge, Belgium: 4 days and approximately 1,500 km (930 mi)
- Ocean-going ship from Zeebrugge, Belgium to Baltimore, Maryland: 14 days and approximately 7,800 km (4,200 nautical miles)
- Rail transport from Baltimore, Maryland, to Pueblo, Colorado: 7 days and approximately 3,050 km (1,900 miles)

Data (e.g., strain, acceleration, and temperature) were collected during all transport legs and intermodal transfers from truck to barge, barge to ship, and ship to rail (Kalinina et al. 2018). Eight different tests encompassing 125 separate events including road crossings and track switches were conducted over nine days at the TTC (Kalinina et al. 2018). Complete details of the test, instrumentation, data acquisition system, and cask design are given in the initial report of the MMTT results (McConnell et al. 2018). The cask was returned to Spain without full-time monitoring, and the demonstration concluded in October 2017.

Analysis of the ENSA cask truck test (Kalinina et al. 2018) indicates that the maximum cladding strains detected ($16 \mu\text{m/m}$) were less than those detected in the DOE/SNL truck test ($143 \mu\text{m/m}$), or either of the DOE/SNL shaker table tests ($241\text{--}301 \mu\text{m/m}$). The maximum cladding strain detected during the transoceanic shipping was less than $20 \mu\text{m/m}$, and during the cross-country rail trip, the maximum strain was $36 \mu\text{m/m}$ (Kalinina et al. 2018). The maximum strain measured on a fuel rod during the MMTT ($99 \mu\text{m/m}$; measured in the rail coupling tests) is about two orders of magnitude lower than the yield strain of irradiated zirconium alloy cladding ($9,000 \mu\text{m/m}$; (Kalinina et al. 2018). DOE sponsored extensive data analyses, computer-based structural modeling (see section H.4), and parametric studies using the acceleration and strain data collected during the MMTT (Kalinina et al. 2018; Klymyshyn et al. 2018; Klymyshyn et al. 2019).

Although several parametric studies were conducted in an attempt to understand the non-prototypic conditions and responses introduced by the use of surrogate materials in the MMTT (Klymyshyn et al. 2019), the Board notes that uncertainties remain about the behavior of HBF during NCT. These uncertainties arise from the limited data available on the characteristics of actual, irradiated HBF and how the characteristics of HBF compare to those of surrogate materials. However, the Board also notes that DOE continues to sponsor testing of the HDRP sister rods (see section H.4.1), which will provide more data about the characteristics of HBF and, presumably, reduce the level of uncertainty.

H.4.3 Determining Fatigue Lifetime Using Accumulated Fatigue Damage

In typical transport cases, HBF cladding will not see vibration loads with uniform frequencies and amplitudes. Due to variations in the condition of the road or rail transport, there will be variations in the frequency and amplitude of the vibration loads. There will also be occasional bumps or shocks during transport; for example, the SNF transportation cask

may experience a small shock when moved by a crane from one transport conveyance to another. However, the fatigue testing conducted with the CIRFT at ORNL determines the fatigue lifetime of a specimen when subjected to a cyclic load with a preset (unchanging) frequency and a preset (unchanging) amplitude (see section H.4.1). The Board notes that the CIRFT cannot impart a separate shock load on a specimen during cyclic testing. Because real transport conditions are variable, it is useful to examine the fatigue lifetime of HBF cladding by examining the full range of vibration and shock loads that occur and to consider the cumulative effect of these loads. This can be done by recording the number of fatigue cycles by the method recommended in ASTM Standard E1049, *Standard Practices for Cycle Counting in Fatigue Analysis* (ASTM International 2017) and calculating an accumulated fatigue damage fraction. This calculation is done by recording the strain cycles, applying knowledge of the fatigue lifetime curve for the HBF cladding in question, and applying Miner's Rule,¹⁵ shown in Equation [1]:

For failure, Miner's Rule states:

$$\Sigma i = n_i/N_i = n_1/N_1 + n_2/N_2 + n_3/N_3 + \dots = 1 \quad \text{Equation [1]}$$

where:

n_i = number of strain cycles at strain level i

N_i = number of strain cycles to produce failure at strain level i .

The number of cycles at a given strain level (n_i in equation [1]) is measured during transport. The number of cycles necessary to cause failure at a given strain level (N_i in equation [1]) can be found on the fatigue lifetime curve, like the one depicted in Figure H-4A. The ratio of these two values (n_i/N_i) is the damage fraction at that strain level. When the accumulated fatigue damage, which is the integration of these individual damage fractions, equals one, then the cladding will theoretically breach from fatigue.

From equation [1], one notes that Miner's Rule assumes a simple additive effect of damage caused by fatigue. Although Miner's Rule is well-established in fatigue assessment, it is known to overpredict fatigue lifetime in certain cases when compared to experimental data (see, for example, Baek, Cho, and Joo 2008). The NRC (2020) addressed the uncertainty in Miner's Rule in the context of estimating the fatigue lifetime of HBF during NCT, and the NRC suggested "[t]o account for uncertainty in using a simple linear damage rule to describe the accumulated fatigue damage in [high burnup] fuel, the right side of [Equation [1]] should be set equal to 0.7" (NRC 2020).

After the MMTT, the accumulated fatigue damage for the surrogate SNF cladding during rail transport was calculated (Klymyshyn et al. 2018). Figure H-12 shows the total amount of cladding fatigue damage calculated for the westbound MMTT rail journey from Baltimore, Maryland to Pueblo, Colorado. For strains measured by any given strain gage mounted on surrogate SNF cladding, the accumulated fatigue damage was less than 1×10^{-10} ; i.e., ten

¹⁵ A more detailed description of Miner's Rule is provided in NRC (2020).

orders of magnitude below the amount of accumulated fatigue damage necessary for cladding failure.

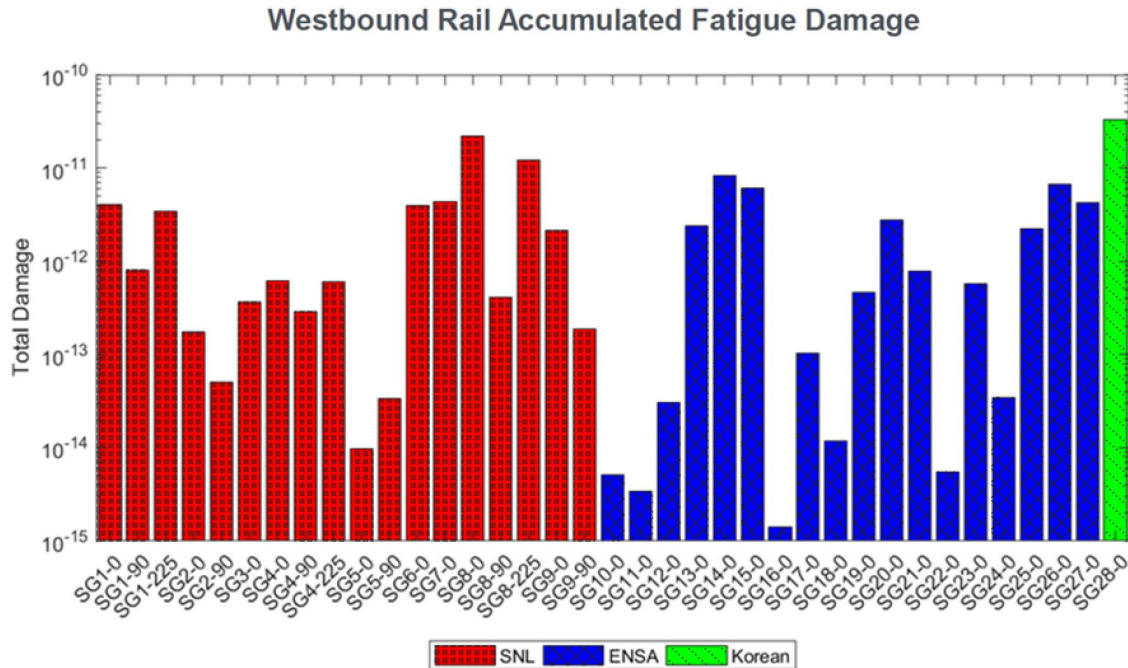


Figure H-12. Accumulated fatigue damage for each strain gage during the MMTT. Each bar in the graphic depicts the accumulated fatigue damage calculated from the strains recorded by one strain gage (SG) mounted on a surrogate SNF rod during the westbound portion of the MMTT rail transport (adapted from Klymyshyn et al. 2018).

H.5 30 cm Drop Tests

Before 2018, the DOE-sponsored transportation testing examined SNF behavior in a wide range of conditions that may be expected during NCT. However, those tests were focused on vibration loads but not on the response of SNF to a free drop that may be expected during SNF handling and other operations during NCT. The NRC transportation regulation, 10 CFR 71, requires that the effects of a free drop on an SNF transport package¹⁶ be evaluated. For all commercial SNF packaged in a transportable cask or canister in the U.S. (i.e., packages that have a mass greater than 15,000 kg [33,100 lbs.]), 10 CFR 71.71(c)(7) requires an evaluation of the effects on the package of a 0.3 m (30 cm; 1 ft) free drop.¹⁷ See Appendix C for more details about the NRC regulations applicable to SNF transportation.

To explore the effects of a 30 cm (1 ft) drop on SNF and SNF transportation casks, DOE has sponsored a series of drop tests. The goals of the drop tests are to measure accelerations

¹⁶ In 10 CFR 71.4, “package” is defined as “the packaging together with its radioactive contents as presented for transport.”

¹⁷ In 10 CFR 71.71(c)(7), the free drop test height depends on the total package weight. For example, packages smaller than an SNF transport cask and that weigh less than or equal to 5,000 kg (11,000 lbs.) have a free drop test height of 1.2 m (4 ft).

and strains on surrogate fuel assemblies, and to determine whether the fuel rods can maintain their integrity inside a cask when dropped from a height of 30 cm (1 ft).

Due to the difficulty and cost of obtaining a full-scale SNF transportation cask with impact limiters for testing, DOE planned three separate steps for drop tests with surrogate and 1/3-scale components:

1. 30 cm (1 ft) drop tests of a 1/3-scale cask holding 1/3-scale dummy SNF assemblies (completed in 2018)
2. 30 cm (1 ft) drop tests of a single, full-scale dummy assembly (completed in 2019)
3. 30 cm (1 ft) drop tests of a single, full-scale surrogate assembly (completed in two parts in 2019 and 2020)

Drop Test—Step One. The goal of the first step, a 30 cm (1 ft) drop test of the 1/3 scale cask was to obtain acceleration data on the cask and on the 1/3 scale dummy assemblies¹⁸ (Figure H-13; Kalinina et al. 2019). The 1/3 scale cask and associated hardware were provided by ENSA of Spain and were scale models of the same cask used in the MMTT campaign. The test was conducted at the BAM facility (Germany) in December 2018. Accelerometers were placed on the dummy assemblies, the fuel basket, and on the external surface of the cask. The locations of the accelerometers were based on structural analysis model results for the 1/3 scale ENSA ENUN-32 cask. Two drop tests were conducted with two different configurations: first test with a normal horizontal transport configuration and second test, rotated 45 degrees around the longitudinal axis, to quantify the variation of the impact response due to a change in basket orientation.

The data gathered from the 1/3 scale drop test revealed that the peak accelerations on the dummy assemblies varied significantly depending on their location within the cask. The maximum acceleration was about 2.4 times higher than the minimum. The maximum accelerations and their spatial distributions were similar for both drops with different SNF basket orientations. As expected, amplifications of the acceleration pulses from the cask to the assemblies were observed. To accurately represent the expected accelerations on the full-scale dummy assembly, the measured accelerations and strains were adjusted by applying appropriate scaling factors (Kalinina et al. 2019).

¹⁸ The dummy assemblies used for the drop tests were hollow steel blocks with the same mass as the fuel assemblies (Kalinina et al. 2019).



Figure H-13. Photo of the 1/3 Scale ENSA ENUN-32 cask with impact limiters.
(Kalinina et al. 2019)

Drop Test—Step Two. The goal of the second step, a 30 cm (1 ft) drop test of a full-scale dummy assembly, was to determine the drop conditions under which the observed acceleration pulse would be similar to the acceleration pulse measured and then scaled up from the 1/3-scale drop test (Figure H-14; Kalinina et al. 2019).

The full-scale dummy assembly used in the second test was made of machined carbon-steel (Figure H-14A). For this drop test, the dummy assembly was placed inside a full-scale, dummy SNF basket “tube” that mimicked one cell of a PWR SNF basket (Figure H-14B). Felt pads attached to the bottom of the basket tube were used as a shock absorbing material to mimic the behavior of the SNF transportation cask and impact limiters (see Figure H-15). The felt pads were adjustable to allow for fine-tuning of the impact accelerations experienced by the dummy SNF assembly. The full-scale dummy assembly was instrumented with accelerometers and strain gages. The drop test was conducted in June 2019 at the SNL drop tower in Albuquerque, New Mexico (Kalinina et al. 2019).



(A)



(B)

Figure H-14. Full-Scale Dummy Assembly and Basket Tube for SNL Drop Tests.

(A) Full-scale dummy assembly machined from carbon-steel and (B) a surrogate basket tube that mimics one cell of a PWR SNF basket (*adapted from Kalinina et al. 2019*).



Figure H-15. Full-Scale Dummy Assembly Drop Test Setup.

(Kalinina et al. 2019)

SNL conducted four drop tests with the dummy assembly, in iterative steps, to obtain the desired acceleration pulses, which accurately recreate the accelerations measured (and

then scaled) during the 1/3-scale drop test. After each iteration, the acceleration pulse amplitudes, durations, and shapes were examined and adjustments were made to the surrogate assembly configuration by adjusting felt pads that were mounted to the bottom (contact points) of the assembly. The adjustments were made by increasing or reducing the felt pad area (length) and its thickness.

The felt pad configuration used in the last drop of the 2019 testing was used for the 30 cm (1 ft) drop test of the full-scale surrogate assembly conducted later in 2019 and 2020.

Drop Test—Step Three. SNL conducted the Step Three drop tests in June 2019 with an old surrogate SNF assembly and in May 2020 with a new surrogate SNF assembly. In both cases, the surrogate assembly was placed inside a surrogate SNF basket cell for the drop testing. The surrogate assembly used in the 2019 drop test was the same surrogate PWR assembly used in the MMTT; i.e., a Westinghouse 17 x 17 PWR assembly design. The surrogate fuel rods included copper tubes with lead rope (to simulate fuel pellets) in all positions except three, which held Zircaloy-4 rods, one with lead rope, one with lead pellets, and one with molybdenum pellets (Kalinina et al. 2020). The surrogate assembly used in the 2020 drop test included new assembly components (e.g., guide tubes and spacer grids) but the copper and Zircaloy-4 rods were reused. For both the 2019 drop test and the 2020 drop test, the assemblies and rods were instrumented with 18 strain gages and five accelerometers in the same arrangement as that used for the MMTT (see section H.2.4.3).

Kalinina et al. (2020) reported the results of the Step Three drop tests. Regarding adjustment of the acceleration pulses using felt pads, SNL concluded “[t]he acceleration pulses observed on the surrogate assembly during the test were in good agreement with the expected pulses. This confirmed that during the 30 cm drop the surrogate assembly experienced the same conditions as it would if it was dropped in the cask with the impact limiters” (Kalinina et al. 2020). The maximum strain measured on a surrogate fuel rod in the 2019 drop test was 1,736 $\mu\text{m}/\text{m}$ and the maximum strain measured on a surrogate fuel rod in the 2020 drop test was 1,723 $\mu\text{m}/\text{m}$. For comparison, the yield strain of irradiated Zircaloy cladding is approximately 9,000 $\mu\text{m}/\text{m}$. Based on these results, SNL concluded that “[t]he major conclusion that can be drawn from the 30 cm drop test is that the fuel rods will maintain their integrity after being dropped 30 cm or less” (Kalinina et al. 2020).

Although some confidence is gained in the ability of HBF rods to maintain their integrity during NCT based on the 30 cm (1 ft) drop testing, the Board notes that these experiments did not account for any changes in mechanical behavior of the HBF cladding that would occur due to hydride reorientation or irradiation hardening in the cladding. These factors add some uncertainty to the testing results.

H.6 Structural Modeling

Under DOE sponsorship, PNNL developed a suite of modeling tools to predict the vibration or impulse load transmitted from the truck or railcar to the SNF during transport based on the characteristics of the cask, basket, and the configuration of the SNF (Adkins et al. 2013). The suite of models was further refined at PNNL to be applied to the MMTT (Klymyshyn et

al. 2018). The basic components of the coupled models are the LS-DYNA^{®19} dynamic analysis model (to model SNF rods), the ANSYS mechanical model²⁰ (to model the fuel basket, canister [if used], transportation cask, and cask cradle), and the NUCARS^{®21} model (to model the railcar and track features, including transmission of the loads to the cask cradle). The overall suite of models can be assembled as needed to model different fuel, cask, and railcar combinations.

The suite of models uses, as inputs, the structural parameters of the individual components of the complete transportation package (e.g., the configuration of the railcar, cask cradle, SNF cask, SNF canister [if used], SNF basket, SNF assembly, and the fuel rods). The suite of models then calculates and applies the transmissibility of the vibration or impulse loads from one physical component to another until it calculates the final load and strain on an individual fuel rod. No feedback is included in the coupling of the models. DOE's goal is that, eventually, the suite of models can be used to predict the vibration or impulse loads transmitted to the fuel for a variety of fuel types, SNF canisters, and transportation overpacks. Early versions of the modeling suite were adjusted using data from the SNL shaker table tests and truck transportation tests. However, these tests included only dummy weights to represent the cask cradle, cask, and SNF basket, so they represent a rudimentary benchmarking effort. A complete description of the suite of models is available in Adkins et al. (2013). With proper input data about the characteristics of the components, it is expected the suite of models will be able to predict the behavior of many different types of actual SNF in several transportation systems. The controlling parameter in the calculations of strain on the fuel rod is the flexural rigidity of the rod (see section H.3). The suite of models accounts for different SNF types by modifying the flexural rigidity value. Parametric studies of flexural rigidity were used to demonstrate that the strain (for a given acceleration load) does not vary greatly, even over large ranges of flexural rigidity and thus, over a large range of SNF types (Klymyshyn et al. 2019).

PNNL used the data collected during the MMTT to conduct a more accurate and more detailed benchmarking of the suite of models. As a result of this effort, PNNL concluded that "the dynamic response of the [SNF transport] systems is complex enough that finite element modeling is needed to calculate the strains in the fuel rod cladding. There is no simple, linear transfer function that can provide a convincing estimate of strains from fundamental data such as cask mass and train speed" (Klymyshyn et al. 2018). Furthermore, PNNL concluded "[t]he finite element models [provide] a reasonable basis for estimating cladding strains from railcar dynamics models" (Klymyshyn et al. 2018).

Further analyses of the use of surrogates and the use of other transportation cask systems were completed and the results were published by PNNL (Klymyshyn et al. 2019). For this analysis, PNNL modified the suite of models to represent the seventeen different SNF

¹⁹ LS-DYNA[®] is a registered trademark of Livermore Software Technology Corporation. Information on the code can be found at: <https://www.oasys-software.com/dyna/software/ls-dyna/>.

²⁰ The ANSYS family of computer programs is produced by ANSYS, Inc. Information on the ANSYS structural code can be found on a fact sheet at: <https://www.ansys.com/products/structures/ansys-mechanical>.

²¹ NUCARS[®] is a registered trademark of Transportation Technology Center, Inc. Information about NUCARS[®] can be found at: <http://nucars.aar.com/about.php>.

transportation casks that are approved for use by the NRC (or designed for transport, but not yet approved). PNNL also modeled the use of the new commercial SNF railcar being developed by DOE (called the Atlas railcar; Schwab et al. 2017). The suite of models then predicted the cask motion in response to track conditions and a bounding set of train speeds. In addition, the fuel rod flexural rigidity was varied between low (no bonding between fuel pellets and cladding) and high (perfect bonding between fuel pellets and cladding). Through these parametric studies, PNNL was able to study the full range of cask and SNF dynamic responses that may be anticipated during transport of SNF (and HBF) by rail. Major findings from the study (Klymyshyn et al. 2019) are summarized below.

- Because the loads and strains on the cladding estimated for various designs of SNF packages were so low as to be negligible, no further structural dynamic analysis of SNF under normal conditions of rail transport is necessary.
- The fuel rod structural dynamic analysis results for Atlas railcar configurations demonstrates that the fuel cladding strains remain low throughout a broad range of transport package variations, and the MMTT configuration provided a more conservative shock and vibration environment for the fuel rods and assemblies because the MMTT utilized a railcar that was not compliant with the AAR Standard S-2043. Compliance with S-2043 is expected to reduce the acceleration and shock loads on the rail cargo.
- SNF in welded canister systems could experience loads that are four to six times higher than SNF in a bolted-lid fuel cask (like the ENSA cask used in the MMTT) but the potentially higher strains are still not significant when compared to the fuel cladding failure limit or the fuel cladding fatigue limits for irradiated cladding.
- Changes in spacer grid configuration, BWR fuel rod geometry, fuel rod stiffness, and the localized cladding strain effects caused by fuel pellets were all too insignificant to be of concern during NCT shock and vibration loading.
- The presence of fuel pellets inside the cladding was found to be inconsequential for shock and vibration under NCT, but worth studying for SNF package drop scenarios such as the 30 cm (1 ft) drop (see section H.5).

Although the DOE modeling analyses and parametric studies indicate that there is a large margin of safety between the low acceleration loads experienced by the fuel cladding during NCT and the relatively high yield stresses of the cladding, the Board observes that more confidence in the modeling tools can be gained by validating the models against the transportation of real, irradiated HBF. This is because the testing to date has not included validation of the models against HBF cladding with hydride reorientation, irradiation hardening of the cladding, or irradiation hardening of other assembly components such as spacer grids and guide tubes.

H.7 References

10 CFR Part 71. "Packaging and Transportation of Radioactive Material." *Code of Federal Regulations*. Washington, DC: Government Printing Office.

Adkins, H., K. Geelhood, B. Koeppel, J. Coleman, J. Bignell, G. Flores, J-A. Wang, S. Sanborn, R. Spears, N. Klymyshyn. 2013. *Used Nuclear Fuel Loading and Structural Performance Under Normal Conditions of Transport – Demonstration of Approach and Results on Used Fuel Performance Characterization*. FCRD-UFD-2013-000325. September 30.

ASTM International. 2017. *Standard Practices for Cycle Counting in Fatigue Analysis*. ASTM E1049-85(2017). West Conshohocken, Pennsylvania.

Baek, S.H., S.S. Cho, and W. S. Joo. 2008. "Fatigue Life Prediction Based on the Rainflow Cycle Counting Method for the End Beam of a Freight Car Bogie." *International Journal of Automotive Technology*, Vol. 9, No. 1, pp. 95–101.

Electrical Power Research Institute. 2001. *Design, Operation, and Performance Data for High Burnup PWR Fuel from the H. B. Robinson Plant for Use in the NRC Experimental Program at Argonne National Laboratory*. EPRI, Palo Alto, California. 1001558.

Jiang, H., J-A. J. Wang, and H. Wang. 2016. "The Impact of Interface Bonding Efficiency on High-Burnup Spent Nuclear Fuel Dynamic Performance." *Nuclear Engineering and Design*. Vol. 309, pp. 40–52.

Kalinina, E.A., C. Wright, L. Lujan, N. Gordon, S.J. Saltzstein, and K.M. Norman. 2018. *Data Analysis of ENSA/DOE Rail Cask Tests*. SFWD-SFWST-2018-000494. November 19.

Kalinina, E., D. Ammerman, C. Grey, M. Arviso, C. Wright, L. Lujan, G. Flores, and S. Saltzstein. 2019. *30 cm Drop Tests*. SAND2019-15256 R. December 17.

Kalinina, E., D. Ammerman, C. Grey, G. Flores, L. Lujan. S. Saltzstein, and D. Michel. 2020. *Surrogate Assembly 30 cm Drop Test*. SAND2020-10498R. September 28.

Klymyshyn, N.A., P. Ivanusa, K. Kadooka, C. Spitz, P. J. Jensen, S.B. Ross, B.D. Hanson, D. Garcia, J. Smith, and S. Lewis. 2018. *Modeling and Analysis of the ENSA/DOE Multimodal Transportation Campaign*. M2SF-18PN010202014. September 28.

Klymyshyn, N.A., P. Ivanusa, K. Kadooka, C. Spitz, E.D. Irick, P.J. Jensen, S.B. Ross, and B.D. Hanson. 2019. *Structural Dynamic Analysis of Spent Nuclear Fuel*. SFWD-SFWST-M2SF-19PN010202014. September 30.

Magnuson, C.F. 1977. *Shock and Vibration Environments for Large Shipping Container During Truck Transport (Part I)*. SAND77-1110. September.

Magnuson, C.F. 1978. *Shock and Vibration Environments for A Large Shipping Container During Truck Transport (Part II)*. SAND78-0337. May.

McConnell, P. 2016. *Sandia Shaker Table and Over-the-Road Vibration Studies*. Presentation to the Nuclear Waste Technical Review Board at its February 17 meeting.

McConnell, P., G. Flores, R. Wauneka, G. Koenig, D. Ammerman, J. Bignell, S. Saltzstein, and K. Sorenson. 2013. *Fuel Assembly Shaker Test for Determining Loads on a PWR Assembly under Surrogate Normal Conditions of Truck Transport*. FCRD-UFD-2013-000190, Rev. 0.1. December 1.

- McConnell, P., R. Wauneka, S. Saltzstein, and K. Sorenson. 2014. *Normal Conditions of Transport Truck Test of a Surrogate Fuel Assembly*. FCRD-UFD-2014-000066, Rev. 0.1. December 15.
- McConnell, P., G. Koenig, W. Uncapher, C. Grey, C. Engelhardt, S. Saltzstein, and K. Sorenson. 2015. *Surrogate Fuel Assembly Multi-Axis Shaker Tests to Simulate Normal Conditions of Rail and Truck Transportation*. FCRD-UFD-2015-000128, Rev. 0. September 11.
- McConnell, P., S. Ross, C. Grey, W. Uncapher, M. Arviso, R.G. Garmendia, I.F. Pérez, A. Palacio, G. Calleja, D. Garrido, A.R. Casas, L.G. García, W. Chilton, D. Ammerman, J. Walz, S. Gershon, S. Saltzstein, K. Sorenson, N. Klymyshyn, B. Hanson, R. Peña, and R. Walker. 2018. *Rail-Cask Tests: Normal-Conditions-of-Transport Tests of Surrogate PWR Fuel Assemblies in an ENSA ENUN 32P Cask*. SFSW-SFWST-2017-000004. January 16.
- Montgomery, R. and B. Bevard. 2020. *Sister Rod Destructive Examinations (FY20)* ORNL/SPR-2020/1798. November 30.
- Montgomery, R., R.N. Morris, R. Ilgner, B. Roach, J.-A. Wang, Z. Burns, J.T. Dixon, and S.M. Curlin. 2019. *Sister Rod Destructive Examinations (FY19): Spent Fuel and Waste Disposition*. ORNL/SPR-2019/1251, Rev. 1. September 27.
- NRC [U.S. Nuclear Regulatory Commission]. 2003. *Spent Fuel Project Office Interim Staff Guidance-11, Revision 3, Cladding Considerations for the Transportation and Storage of Spent Fuel*. November.
- NRC. 2020. *Dry Storage and Transportation of High Burnup Spent Nuclear Fuel, Final Report*. NUREG-2224. November.
- O'Donnell, W.J. and B.F. Langer. 1964. "Fatigue Design Basis for Zircaloy Components." *Nuclear Science and Engineering*. Vol. 20, pp. 1–12.
- Schwab, P., M. Feldman, B. Reich, S. Maheras, and S. Dam. 2017. "Update on Development of a U.S. Rail Transport Capability for Spent Nuclear Fuel and High-Level Waste." Paper 17138. WM2017 Conference, Phoenix, AZ. Waste Management Symposia. March 5–9.
- Sorenson, K., B. Hanson, S. Saltzstein, and N. Larson. 2016. *Closing the Technical Data Gaps Associated with the Storage and Transportation of High Burnup Spent Fuel*. Presentation at the 2016 Nuclear Energy Institute Used Fuel Management Conference. Orlando, Florida. May 3–5.
- Teague, M., S. Saltzstein, B. Hanson, K. Sorenson, G. Freeze. 2019. *Gap Analysis to Guide DOE R&D in Supporting Extended Storage and Transportation of Spent Nuclear Fuel: An FY2019 Assessment*. SAND2019-15479R. December 23.
- Wang, J.-A. and H. Wang. 2017. *Mechanical Fatigue Testing of High-Burnup Fuel for Transportation Applications*. NUREG/CR-7198, Rev. 1. October.
- Wang, J., H. Wang, H. Jiang, Y. Yan, and B.B. Bevard. 2015. *FY 2015 Status Report: CIRFT Testing of High-Burnup Used Nuclear Fuel Rods from Pressurized Water Reactor and Boiling Water Reactor Environments*. M2-FCRD-UFD-2015-000101. September 4.

Wang, J.-A., H. Wang, H. Jiang, Y. Yan, and B. Bevard. 2016a. *CIRFT Testing of High Burnup Used Nuclear Fuel from PWR and BWRs*. Presentation to the Nuclear Waste Technical Review Board at its February 17, 2016, meeting.

Wang, J.-A., H. Wang, H. Jiang, Y. Yan, B.B. Bevard, and J.M. Scaglione. 2016b. *FY 2016 Status Report: Documentation of All CIRFT Data Including Hydride Reorientation Tests*. ORNL/SR-2016/424. September 14.

Wang, J.-A., H. Wang, B.B. Bevard, and J.M. Scaglione. 2017. *FY 2017 Status Report: CIRFT Data Update and Data Analyses for Spent Nuclear Fuel Vibration Reliability Study*. ORNL/SR-2017/291. August 8.

Appendix I

Fuel Performance Modeling

I.1 Overview

Experimentally determining how high burnup fuel (HBF) and its associated cladding alloys perform while being stored or transported would entail a long and expensive undertaking due to several factors. These factors include, but are not limited to, the wide range of possible cladding alloys used, the range of temperatures and burnup it experienced while in the reactor, and the range of temperatures and other external conditions it was exposed to post-irradiation. Therefore, using modeling informed by experimental data to predict HBF performance is preferred over attempting to test all HBF types under all possible operating conditions. To predict HBF performance while in storage or during transport, model inputs including storage and transport cask thermal-hydraulics, solid mechanics,¹ structural analysis, and material behavior must be integrated successfully. The range of spatial scales for the models spans from micro-scale (e.g., electronic and atomic structures) to meso-scale (e.g., behavior of hydrides and grains) to macro-scale (e.g., fuel rods and assemblies). Similarly, model time scales range from femtoseconds (typical time step for molecular dynamics associated with the fission process) to decades (anticipated time in dry storage). To accommodate the wide range of spatial and temporal scales associated with modeling HBF's behavior, different models are required—in many cases, the lower-scale spatial (i.e., micro- and meso-scale) and time scale models generate data used as input for the upper-scale spatial (i.e., macro-scale) and time scale models.

Section 3.3.2 of the main report and Appendix G present descriptions and evaluations of the thermal-hydraulic modeling capabilities for spent nuclear fuel (SNF) casks or canisters and their contents, with a focus on the model's ability to accurately predict the surface temperatures of the fuel rod cladding during drying, in storage, and during transport. Section 3.4.2 of the main report and Appendix H present descriptions and evaluations of the structural response modeling capabilities for a transportation cask and its contents with a focus on the model's ability to predict how the individual fuel rods mechanically respond to normal conditions of transport.

The material properties of SNF materials after irradiation are needed to analyze the structure of an individual SNF rod. These material properties are provided by a fuel performance model, which consists of a thermo-mechanical model integrated with various material models to predict material properties of the cladding and fuel as a function of irradiation and thermal-hydraulic history and current conditions. Reactor core simulators, consisting of radiation transport and thermal-hydraulic core models, provide the reactor operating history data for the SNF. Post-irradiation history data for the SNF during drying, storage, and transportation is provided by the cask or canister thermal-hydraulic model. This section discusses Department of Energy (DOE)-sponsored research and development (R&D) to develop a fuel performance model capability focused on analyzing fuel behavior during

¹ The fuel performance model solves a coupled thermal-hydraulics/solid mechanics problem. Solid mechanics is employed when structural analysis techniques are inadequate (e.g., fuel pellet deformation).

reactor operations (which is needed to understand the initial condition of the fuel to be managed in the backend of the fuel cycle), drying, storage, and transportation.

Several fuel performance models have been developed and validated, and some are considered mature enough to be used in support of licensing applications submitted to the Nuclear Regulatory Commission (NRC). They include models developed by:

1. Individual fuel vendors for their proprietary use, e.g.:
 - Westinghouse's Performance Analysis and Design Model [PAD5] (Crede et al. 2013)
 - Framatome's GALILEO (Framatome Inc. 2018)
 - The United Kingdom's ENIGMA (Rossiter 2011)
 - GE Nuclear's GSTRM (GE Nuclear Energy 1991)
2. Electric Power Research Institute (EPRI) for its members' proprietary use:
 - FALCON (EPRI 2002)
3. NRC for internal use and use by its contractors:
 - FRAPCON (Geelhood et al. 2015)
 - FRAPTRAN (Geelhood et al. 2016)
 - DOE's Office of Nuclear Energy:
 - BISON (Hales et al. 2014)

The primary focus of these fuel performance models is to assess in-reactor fuel performance for normal and accident conditions, not on assessing fuel performance throughout the post-irradiation life cycle of drying, storage, and transporting. That said, accurately predicting the in-reactor fuel performance during normal conditions is a necessary prerequisite for post-irradiation models because the fuel properties at the start of the post-irradiation process determine how the fuel properties will evolve over time, under different conditions.

To predict fuel performance, an extensive collection of physical and material models, which may consist of algebraic, ordinary, and partial differential equations, and associated feedback paths, along with specified external conditions (e.g., flux, power, and coolant temperature and pressure) are required (Figure I-1).

Table I-1 presents the physical and material models currently incorporated into BISON that are used to predict fuel performance. The irradiated material properties of the cladding may be quite sensitive to the specific alloy used for the fuel cladding. In most cases, the irradiated material properties are obtained from models that are developed by fitting experimental data with the mathematical form of a material model based on either a

fundamental understanding of the physics or empirical curve fitting. More recently, lower-scale (e.g., micro-scale or meso-scale) models conjoined with experimental data have been used to develop macro-scale material models—such as the fission gas release (FGR) model—that are used in fuel performance models. The need for experimental data implies that it may not be possible to apply the fuel performance models to understand newer cladding alloys—such as M5[®]—because proprietary restrictions limit open access to the experimental data and the resulting developed material models.

Table I-1 Physical and material models in the BISON fuel performance model

Fuel Rod Behavior	Dependencies That are Modeled
Oxide Fuel Behavior	<ul style="list-style-type: none"> • Temperature/burnup dependent conductivity • Heat generation with radial and axial profiles (provided by reactor physics models) • Thermal expansion • Solid and gaseous fission product swelling • Densification • Thermal and irradiation creep • Fracture via relocation or smeared² cracking • Fission gas release (two-stage physics) <ul style="list-style-type: none"> ○ transient (ramp) release ○ grain growth and grain-boundary sweeping ○ thermal release
Cladding Behavior	<ul style="list-style-type: none"> • Thermal expansion • Thermal and irradiation creep • Irradiation growth • Gamma heating (provided by reactor physics models) • Combined creep and plasticity • Hydrogen pickup, diffusion, precipitation, and dissolution <ul style="list-style-type: none"> ○ Waterside corrosion
Gap/Plenum Behavior	<ul style="list-style-type: none"> • Gap heat transfer • Mechanical contact • Plenum pressure as a function of <ul style="list-style-type: none"> ○ evolving gas volume (from mechanics) ○ gas mixture (from fission gas release model) ○ gas temperature approximation

(Hales et al. 2014)

The properties of the fuel at the end of irradiation that are most influential in predicting post-irradiation fuel performance include the following:

- internal rod pressure
- fuel rod geometry changes
- pellet-cladding gap size or degree of bonding
- hydrogen content and its spatial distribution
- zirconium hydride (hydride) spatial distribution and orientation
- cladding-oxide thickness

² Rather than treating cracks explicitly, their effect on various properties is treated implicitly.

- decay heat loading

In addition, the following model inputs are required to predict post-irradiation fuel performance:

- pellet-cladding bonding strength
- fuel and cladding thermal expansion coefficients
- Fickian and Soret diffusion coefficients for hydrogen
- hydrogen precipitation and dissolution properties
- initial hydride orientation upon precipitation
- elastic, plastic, and fracture properties of the cladding
- thermal creep rate properties
- fuel cyclic fatigue properties

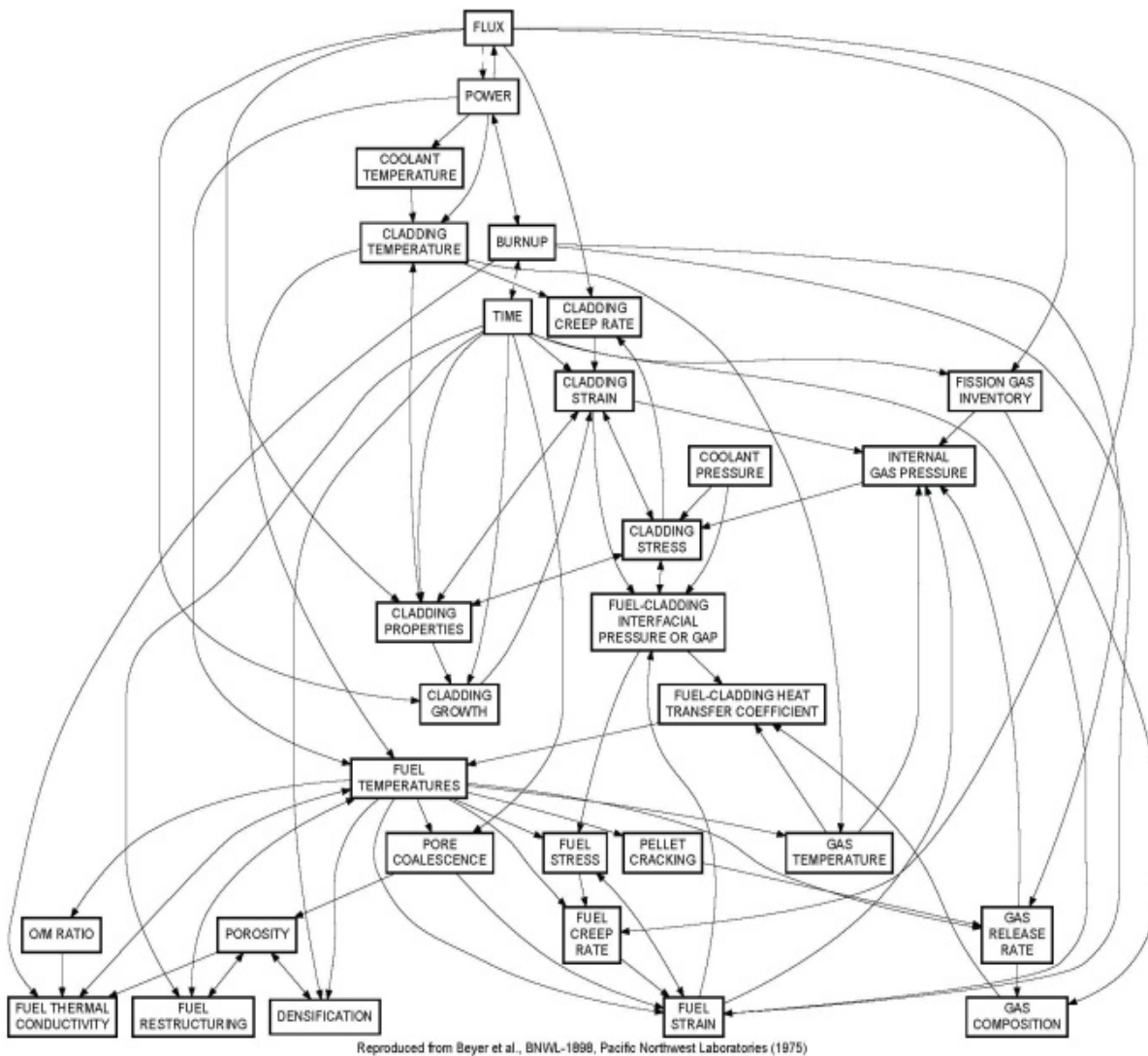


Figure I-1. Desired attributes of a fuel performance model.
(Beyer et al. 1975)

Several of these properties are dependent upon material temperature, stress state and in-core irradiation, and thermal-hydraulic history.

1.2 Evaluation

The DOE-sponsored BISON model has been developed at the Idaho National Laboratory (INL) under the Nuclear Energy Advanced Modeling and Simulation program and the Consortium for Advanced Simulation of Light Water Reactors (the Consortium) energy innovation hub. For Light Water Reactor (LWR) fuel, the material models that are incorporated in BISON are based on Zircaloy-4 alloys because considerable experimental data and models are publicly available for it. BISON is constructed so that material models for other cladding alloys (e.g., M5[®] and ZIRLO[®]) could also be developed and incorporated if the experimental data required to develop and validate the material models were made available. Using the MOOSE [Multiphysics Object Oriented Simulation Environment] (Gaston et al. 2009) finite element method and the Jacobian-Free Newton-Krylov multiphysics solution approach so that multiprocessors/cores can be utilized, BISON solves the thermo-mechanical model of a fuel rod or fuel rod segment in either one-dimensional (1-D), 1.5-D,³ 2-D [(r, z) or (r, theta)], or 3-D geometry using the material models provided. The Consortium's Science Council is an independent body of experts that periodically review the Consortium's science and technology R&D programs. They rendered the opinion that BISON's prediction capabilities for normal, in-reactor conditions and Zircaloy-4 cladding are comparable to those of fuel performance models currently used in fuel design and licensing⁴ based on validation and model-to-model comparisons (Perez et al. 2015; Williamson et al. 2016). BISON prediction comparisons with the Westinghouse Electric Company PAD model are presented in Consortium proprietary reports; however, comparisons with the EPRI FALCON model are public (Capps et al. 2013; Mervin et al. 2015). The Science Council also concluded that BISON has enhanced potential for performance improvements in predicting in-core fuel behavior due to its 3-D capability and strong multiphysics coupling solution algorithm, both of which are lacking in other fuel performance models. The implication is that BISON should be able to provide the initial conditions required to evaluate post-irradiation fuel performance for SNF with Zircaloy-4 cladding and could be expanded to evaluate fuel performance for other cladding alloys, once their material models are developed.

For post-irradiation fuel performance modeling, BISON does contain models for fuel and cladding thermal expansion coefficients; Fickian and Soret diffusion coefficients; hydrogen precipitation and dissolution properties; cladding alloy elastic, plastic and fracture properties; and thermal creep rate properties for Zircaloy-4 cladding. BISON's ability to predict hydrogen dissolution and precipitation is summarized in Courty, Motta, and Hales (2014), and its ability to model hydride spatial concentrations (in two dimensions) during prototypical drying conditions is presented in Stafford (2015). Some preliminary work has

³ In a 1.5D model, one aspect or parameter of a problem is modeled in one dimension, while another aspect or parameter of the same problem is modeled in two dimensions.

⁴ Comparisons have been made against experimental data, and with FALCON and PAD, model predictions were validated using proprietary data collected by EPRI and Westinghouse. Comparisons against the proprietary models were done under Consortium funding and are not publicly available.

also been completed on a hydride damage model (Casagrande et al. 2017). Despite this, validation of these models for post-irradiation conditions is limited, and material models for pellet-cladding bonding strength, hydride orientation upon precipitation, effective macro-scale cladding elastic, plastic and fracture attributes, and cladding-failure models with and without cyclic fatigue are being considered because they either are non-existent or need to be improved. Further, for cladding alloy materials, models only exist for Zircaloy-4.

Improving and extending BISON's prediction capabilities to predict post-irradiation fuel performance accurately during drying, storage, and transportation is possible, but to make progress, material models must be developed utilizing experimental data that are limited or are yet to be obtained. Starting in 2018, DOE began to obtain experimental data on the chemical and mechanical characteristics of HBF "sister rods" as part of the High Burnup Dry Storage Research Project (see Appendix G). These sister rods were packaged and dried using typical industry processes and included fuel types with Zircaloy-4, low-tin Zircaloy-4, ZIRLO[®], and M5[®] cladding. The BISON model is being modified to develop and incorporate the material models that are important for post-irradiation assessment. The material models have received limited support to date through the Nuclear Energy Advanced Modeling and Simulation program and INL Laboratory Directed Research and Development. The only recent support is a Nuclear Energy University Program-sponsored Integrated Research Project (Motta et al. 2017) as discussed below.

Modeling pellet-cladding bonding presents both a mathematical-solution challenge and a material model challenge. Since the mathematical algorithms are state-of-the-art, the remainder of this paragraph addresses the material model challenges. While there are macro-scale models available to predict hydride orientation upon precipitation as a function of temperature, stress state, and radiation damage, they have not yet been incorporated into BISON (Rashid and Machiels 2015). Hydrides introduce a local heterogeneity in the cladding material, which can affect its elastic and plastic behavior and the onset of cladding fracture. Hydrides tend to concentrate in the colder, outer-cladding region near the cladding-oxide interface and in the cladding adjacent to pellet-pellet interfaces due to Soret diffusion. Azimuthal (circumferential) dependence has also been observed. The heterogeneous structure of the hydrides makes it difficult to predict which elastic and plastic properties of the cladding should be used for structural analyses in cases where the hydrides are orientated normal to a component of the stress.

To address cladding breach (i.e., through wall crack propagation), two modeling approaches may be employed. One approach uses a cladding failure model that accounts for stress, hydride orientation and density, radiation damage, and temperature, which can all be predicted at the macro-scale level of a fuel performance model. Currently, the BISON model takes this first approach by incorporating a preliminary cladding failure model, without considering the cyclic fatigue effect. An alternative approach is to use a model that explicitly addresses the heterogeneous structure of hydrides. One example of this approach determined the extent of fatigue damage during transportation utilizing MARMOT, an INL computer model that models at the meso-scale (Tonks et al. 2012) and BISON, in which the spatial position, orientation, and density of hydrides were explicitly represented and accounted for pellet-pellet contact and pellet chamfer (Chakraborty et al. 2015). In this work, spatially-dependent, equivalent, elastic, moduli values were employed that were determined by weighing elastic moduli of the cladding alloy and hydride by the volume fraction of each. A fatigue damage model was also used, and two pellet geometries were analyzed with

spatial displacements provided by an assembly-beam model prediction. This same study also completed a structural analysis of the cladding using the ABACUS finite element model to analyze a vibrating fuel rod with a focus of the analysis on the effects of pellet-cladding bonding and pellet-pellet bonding and debonding. Elastic properties were spatially altered based on the material damage induced by cyclic vibrations. The main focus of this work was to gain insights on what influences cladding breach. Chakraborty et al. (2015) concluded that “experimental test should be performed to gather appropriate material properties for the numerical model runs and to validate numerical models,” implying additional work will need to be completed before the models developed can be used with confidence to predict cladding breach.

Rashid et al. (2009) developed another cladding failure model that addressed any heterogeneities by representing cladding alloy and hydrides as spatially distinct; used separate elastic, plastic, and fracture properties for the cladding alloy and for the hydrides; and balanced the forces at the alloy-hydride interface. The Board notes that, because the material models being used in Rashid et al. (2009) are unaltered from what is normally employed, and because the new material models developed are based on measured homogeneous material properties, there is some confidence that the models have not been tuned specifically to predict heterogeneous behavior. This observation, along with the limited validation that has been completed, does support the conclusion that the modeling approach taken is likely sound. The heterogeneous model proposed by Rashid et al. (2009) has been incorporated into BISON and used to complete sensitivity analyses for various input parameters. The same model could also be used to independently develop a cladding breach model.

R&D is also occurring at the meso-scale using INL’s MARMOT model to improve macro-scale models used in BISON, completed either via one-way (MARMOT to BISON) or iterative coupling (BISON to MARMOT to BISON). MARMOT solves the phase-field equations coupled to a thermo-mechanical model using MOOSE. Many material properties are dependent upon the cladding material’s microstructure, so MARMOT solves for evolving cladding material microstructure as a function of stress, temperature and irradiation, from which it can calculate several fuel material properties including thermal conductivity, creep, swelling, and FGR. MARMOT has also been used to determine the phase field for hydride formation/dissolution (Bair, Zaeem, and Schwen 2017), from which it can supply the density of hydride for each orientation to BISON. The Board notes that micro-scale models (Density Functional Theory and Molecular Dynamics) have also been employed to predict fundamental properties of hydrogen and hydrides in cladding, such as hydrogen solubility and dissolution; hydrogen diffusion; and hydride-nucleation behavior, which is used to inform meso-scale or macro-scale models. Modeling work at the micro-scale does help predict material properties for materials that have limited experimental data.

In 2017, DOE awarded an Integrated Research Program (IRP) grant to an integrated team led by Pennsylvania State University (Motta et al. 2017). Several other universities, DOE national laboratories and industry are partners on this IRP. The IRP has the following three main thrust areas, all in support of developing the capability to predict the behavior and effect on the mechanical properties of the hydrogen formed as a result of fuel cladding oxidation:

1. Migration and redistribution of hydrogen
2. Precipitation and dissolution of hydride particles

3. The impact of hydride microstructure on mechanical properties of the cladding

The research plan calls for a combination of mainly single effect experiments on unirradiated cladding material of different alloys, and modeling at both the meso- and macro-scale levels. Both unirradiated and irradiated experimental data are being employed to develop the associated material models. Part of the validation plan is to compare predicted material properties with those properties being measured for the sister rods of the DOE's High Burnup Dry Storage Research Project (see Appendix G). Under numerous sources of sponsorship including the IRP, a meso-scale phase-field model for hydride formation in polycrystalline metals has been developed, with application to δ -hydride in zirconium alloys (Heo et al. 2019). Experimental determination of zirconium hydride precipitation and dissolution in zirconium alloy has also been reported (Lacroix, Motta, and Almer 2018), providing more insight into hysteresis between the terminal solid solubility for precipitation and dissolution and the thermodynamic solubility limit. Under IRP sponsorship, a comprehensive review paper on hydrogen behavior in zirconium alloys, indicating current knowledge and areas where additional knowledge is required, has been written (Motta et al. 2019). The final report is not yet available for this IRP, so it is too early to assess the research being conducted. However, if successful, the capabilities developed should substantially advance the capability to predict fuel performance during storage and transportation. The Board notes that, to have any practical impact, work must proceed to incorporate the improved material models into fuel performance models such as BISON and meso-scale models such as MARMOT.

I.3 References

- Bair, J., M.A. Zaeem, and D. Schwen. 2017. "Formation Path of δ Hydrides in Zirconium by Multiphase Field Modeling." *Acta Materialia*. Volume 123, pp. 235–244.
- Beyer, C.E., C.R. Hann, D.D. Lanning, F.E. Panisko, and L.J. Parchen. 1975. *GAPCON-THERMAL-2: A Computer Program for Calculating the Thermal Behavior of an Oxide Fuel Rod*. BNWL-1898. November.
- Capps, N., D. Sutherland, W. Liu, R. Montgomery, J. Hales, C. Stanek, and B.D. Wirth. 2013. "Verification and Benchmarking of Peregrine Against Halden Fuel Rod Data and FALCON." *Proceedings of the LWR Fuel Performance Meeting (Top Fuel 2013)*. Charlotte, North Carolina. September 15-19.
- Casagrande, A., D.S. Stafford, G. Pastore, R.L. Williamson, B.W. Spencer, and J.D. Hales. 2017. *UFD Proof-of-Concept Demonstration*. M2MS-17IN0201012. June.
- Chakraborty, P., P. Sabharwall, K. Sener, A.H. Varma, R.E. Spears, and J. Coleman. 2015. *Modeling and Simulation of Used Nuclear Fuel During Transportation with Consideration of Hydride Effects and Cyclic Fatigue*. FCRD-UFD-2015-000273, Rev. 0. September 30.
- Courty, O., A.T. Motta, and J.D. Hales. 2014. "Modeling and Simulation of Hydrogen Behavior in Zircaloy-4 Fuel Cladding." *Journal of Nuclear Materials*. Volume 452, pp. 311–320.
- Crede, T.M., P.J. Kersting, O. Linsuaín, Y. Long, G. Pan, A.J. Petrarca, D.T. Rumschlag, P. Schueren, H. Schutte, and R.E. Sears. 2013. *Westinghouse Performance Analysis and Design Model (PAD5)*. WCAP-17642-NP, Revision 0. October.

- EPRI (Electric Power Research Institute). 2002. *Fuel Performance Analysis Capability in FALCON*. EPRI, Palo Alto, California. 1002866.
- Framatome, Inc. 2018. *GALILEO Fuel Rod Thermal-Mechanical Methodology for Pressurized Water Reactors: Topical Report*. ANP-10323NP, Revision 1. June.
- Gaston, D., C. Newman, G. Hansen, and D. Lebrun-Grandié. 2009. "MOOSE: A Parallel Computational Framework for Coupled Systems of Nonlinear Equations." *Nuclear Engineering and Design*. Volume 239, pp. 1768–1778.
- Geelhood, K.J., W.G. Luscher, P.A. Raynaud, and I.E. Porter. 2015. *FRAPCON-4.0: A Computer Code for the Calculation of Steady-State, Thermal-Mechanical Behavior of Oxide Fuel Rods for High Burnup*. PNNL-19418, Vol.1, Rev. 2. September.
- Geelhood, K.J., W.G. Luscher, J.M. Cuta, and I.E. Porter. 2016. *FRAPTRAN-2.0: A Computer Code for the Transient Analysis of Oxide Fuel Rods*. PNNL-19400, Vol. 1, Rev. 2. May.
- GE Nuclear Energy. 1991. *Fuel Rod Thermal-Mechanical Analysis Methodology (GSTRM)*. NEDO-31959. April.
- Hales, J.D., K.A. Gamble, B.W. Spencer, S.R. Novascone, G. Pastore, W. Liu, D.S. Stafford, R.L. Williamson, D.M. Perez, and R.J. Gardner. 2014. *BISON User's Manual: BISON Release 1.1*. INL/MIS-13-30307, Rev. 2. October.
- Heo, T.W., K.B. Colas, A.T. Motta, and L-Q. Chen. 2019. "A Phase-Field Model for Hydride Formation in Polycrystalline Metals: Application to δ -Hydride in Zirconium Alloys." *Acta Materialia*. Volume 181, pp. 262–277.
- Lacroix, E., A.T. Motta, and J.D. Almer. 2018. "Experimental Determination of Zirconium Hydride Precipitation and Dissolution in Zirconium Alloy." *Journal of Nuclear Materials*. Vol. 509, pp. 162–167.
- Mervin, B.T., M.L. Pytel, D.F. Hussey, and S.M. Hess. 2015. *Pellet-Cladding Mechanical Interaction Analyses Using VERA*. CASL-U-2015-0150-000. April 1.
- Motta, A., N. Brown, L-Q. Chen, D. Koss, R. Kunz, M. Tonks, M. Zikry, T. Downar, A. Manera, V. Petrov, V. Seker, B. Wirth, G. Pastore, K. Terrani, M.N. Cinbiz, C. Tomé, Z. Karoutas, D. Mitchell, J. Romero, M. Daymond, M. Preuss, and E. Mader. 2017. *Development of a Mechanistic Hydride Behavior Model for Spent Fuel Cladding Storage and Transportation: IRP-FC-1: Modeling of Spent Fuel Cladding in Storage and Transportation Environments*. FY2017 Integrated Research Project Awards, Nuclear Energy University Program, U.S. Department of Energy.
- Motta, A.T., L. Capolungo, L-Q. Chen, M.N. Cinbiz, M.R. Daymond, D.A. Koss, E. Lacroix, G. Pastore, P-C.A. Simon, M.R. Tonks, B.D. Wirth, and M.A. Zikry. 2019. "Hydrogen in Zirconium Alloys: A Review." *Journal of Nuclear Materials*. Vol. 518, pp. 440–460.
- Perez, D.M., R.W. Williamson, S.R. Novascone, R.J. Gardner, K.A. Gamble, A.T. Rice, G. Pastore, J.D. Hales, and B.W. Spencer. 2015. *Assessment of BISON: A Nuclear Fuel Performance Analysis Code, BISON Release 1.2*. INL/MIS-13-30314, Rev. 2. September.

- Rashid, J., M. Rashid, A. Machiels, and R. Dunham. 2009. "A New Material Constitutive Model for Predicting Cladding Failure." *Proceedings of the 2009 TopFuel Reactor Fuel Performance Conference*. Paris, France. September 6–10.
- Rashid, J. and A. Machiels. 2015. "A Sufficiency Criterion for Spent Fuel in Dry Storage Subjected to Transportation Accident Conditions." *Proceedings of the 2015 International High-Level Radioactive Waste Management Meeting*. Charleston, South Carolina. April 12–16.
- Rossiter, G. 2011. "Development of the ENIGMA Fuel Performance Code for Whole Core Analysis and Dry Storage Assessments." *Nuclear Engineering and Technology*. Volume 43, pp. 489–498.
- Stafford, D.S. 2015. "Multidimensional Simulations of Hydrides During Fuel Rod Lifecycle." *Journal of Nuclear Materials*. Volume 466, pp. 362–372.
- Tonks, M.R., D. Gaston, P.C. Millett, D. Andrs, and P. Talbot. 2012. "An Object-Oriented Finite Element Framework for Multiphysics Phase Field Simulations." *Computational Materials Science*. Volume 51, pp. 20–29.
- Williamson, R.L., K.A. Gamble, D.M. Perez, S.R. Novascone, G. Pastore, R.J. Gardner, J.D. Hales, W. Liu, and A. Mai. 2016. "Validating the BISON fuel performance code to integral LWR experiments." *Nuclear Engineering and Design*. Volume 301, pp. 232–244.



**United States
Nuclear Waste Technical Review Board**

2300 Clarendon Boulevard
Suite 1300
Arlington, VA 22201

(703) 235-4473
www.nwtrb.gov